ВЕСТНИК ТРАНСПЛАНТОЛОГИИ И ИСКУССТВЕННЫХ ОРГАНОВ

VESTNIK TRANSPLANTOLOGII I ISKUSSTVENNYKH ORGANOV

RUSSIAN JOURNAL OF TRANSPLANTOLOGY AND ARTIFICIAL ORGANS

УЧРЕДИТЕЛЬ: ОБЩЕРОССИЙСКАЯ ОБЩЕСТВЕННАЯ ОРГАНИЗАЦИЯ ТРАНСПЛАНТОЛОГОВ «РОССИЙСКОЕ ТРАНСПЛАНТОЛОГИЧЕСКОЕ ОБЩЕСТВО»

THE OFFICIAL JOURNAL OF ALL-RUSSIAN PUBLIC ORGANIZATION OF TRANSPLANTOLOGISTS "RUSSIAN TRANSPLANT SOCIETY"

2025. Том XXVII. № 3

2025. Vol. XXVII. № 3

Научно-практический журнал основан в 1999 г.
Регистр. № 018616

Scientific and Practical Journal was founded in 1999
Reg. № 018616

Журнал «Вестник трансплантологии и искусственных органов» включен ВАК РФ в перечень российских рецензируемых научных изданий, в которых должны быть опубликованы результаты диссертационных работ

Журнал «Вестник трансплантологии и искусственных органов» включен ФГБУ «НМИЦ ТИО им. ак. В.И. Шумакова» Минздрава России в перечень российских рецензируемых научных изданий, в которых должны быть опубликованы основные результаты исследований в рамках диссертаций, представляемых к защите в диссертационный совет ФГБУ «НМИЦ ТИО им. ак. В.И. Шумакова» Минздрава России

Журнал «Вестник трансплантологии и искусственных органов» индексируется в Scopus и размещен на платформе Web of Science Core Collection: Emerging Science Citation Index

"Russian Journal of Transplantology and Artificial Organs" is included in the list of leading peer-reviewed scientific publication editions, produced in the Russian Federation and is recommended for publication of primary results of dissertation research

"Russian Journal of transplantology and artificial organs" is included by the Federal State Budgetary Institution "Shumakov National Medical Research Center of Transplantology and Artificial Organs" of the Ministry of Health of Russia in the list of Russian peer-reviewed scientific publications in which the main results of research should be published within the framework of dissertations submitted for defense to the dissertation council of Shumakov National Medical Research Center of Transplantology and Artificial Organs

"Russian Journal of Transplantology and Artificial Organs" is indexed in Scopus and in the Emerging Science Citation Index of the Web of Science Core Collection

ISSN 1995-1191

Адрес для корреспонденции:

Россия, 123182, Москва, ул. Щукинская, 1
Тел./факс +7 (499) 193 87 62
E-mail: vestniktranspl@gmail.com
Интернет-сайт журнала: https://journal.transpl.ru
Научная электронная библиотека: https://elibrary.ru

Address for correspondence:

1, Shchukinskaya st., Moscow 123182, Russia
Tel./Fax +7 (499) 193 87 62
E-mail: vestniktranspl@gmail.com
Journal's web site: https://journal.transpl.ru
Scientific eLibrary: https://elibrary.ru

Подписной индекс в каталоге почты России – ПН380

СОДЕРЖАНИЕ

CONTENTS

ПАМЯТИ УЧИТЕЛЕЙ: ВКЛАД ОСНОВОПОЛОЖНИКОВ ОТЕЧЕСТВЕННОЙ ТРАНСПЛАНТОЛОГИИ В ДЕЛО ВЕЛИКОЙ ПОБЕДЫ

IN MEMORY OF TEACHERS: HONORING THE FOUNDERS OF RUSSIAN TRANSPLANTOLOGY AND THEIR EXTRAORDINARY CONTRIBUTIONS TO THE GREAT VICTORY

2025 год ознаменован важной датой – 80-летием Победы в Великой Отечественной войне. Мы чтим подвиг героев, проявивших невероятную отвагу, истинный патриотизм, небывалую стойкость и благородство духа. И сегодня мы отдаем дань памяти тем, кто, сохраняя жизни раненых, внес неоценимый вклад в дело Великой Победы, – врачам, отважно сражавшимся за жизнь и здоровье наших солдат, проявляя при этом беспримерное мужество и самоотверженность. Среди них – основоположники отечественной трансплантологии В.П. Демихов и Б.В. Петровский. В рамках VII Российского национального конгресса «Трансплантация и донорство органов» (с международным участием) состоится торжественная акция «Памяти учителей», посвященная их вкладу в дело Великой Победы.

Владимир Петрович Демихов (1916–1998 гг.) окончил университет с красным дипломом в августе 1940 года и сразу же был призван в армию. В июле 1941 года В.П. Демихов в звании младшего лейтенанта получил назначение на должность лаборанта в 57-ю патологоанатомическую лабораторию 30-й армии, а затем служил в 11-й гвардейской армии. В августе 1945 года, с окончанием боевых действий в Европе, его перевели на Дальний Восток. В.П. Демихов дошел до Берлина, был в Маньчжурии.

Вскоре после демобилизации Владимир Петрович сделал первую в мире трансплантацию сердечно-легочного комплекса собаке. Следующими этапами стали пересадка в грудную клетку собаки изолированных сердца и легкого, а затем пересадка печени собаке. Первым в мире он разработал и по своей методике провел на собаке маммарно-коронарное шунтирование; собака (по кличке Дамка) жила семь лет.

В.П. Демихов был удостоен ордена Отечественной войны II степени и нескольких медалей, в том числе «За боевые заслуги», «За отвагу», «За победу над Японией», за научные достижения награжден Государственной премией (1988 г.), премией Правительства Российской Федерации (1997 г.), орденом «За заслуги перед Отечеством»

The year 2025 marks a significant milestone, the 80th anniversary of the Victory in the Great Patriotic War. On this solemn occasion, we honor the heroes whose incredible courage, true patriotism, extraordinary fortitude, and nobility of spirit secured our freedom.

Equally deserving of tribute are the military doctors and medical personnel who, through their skill, unparalleled bravery and selflessness, saved the lives of countless wounded soldiers, making an invaluable contribution to the Great Victory. Among these outstanding physicians were the founders of Russian transplantology, Vladimir Demikhov and Boris Petrovsky.

As part of the 7th Russian National Congress themed "Transplantation and Organ Donation" (with international participation), a commemorative event titled "In Memory of Teachers" will be held to honor their legacy and extraordinary contributions to the Great Victory.

Vladimir Demikhov graduated from university with honors in August 1940 and was immediately drafted into the army. By July 1941, holding the rank of second lieutenant, he was assigned as a laboratory assistant in the 57th Pathological Anatomy Laboratory of the 30th Army, later serving in the 11th Guards Army. He participated in the Great Patriotic War, reaching Berlin. He was later transferred to the Far East, where he served in Manchuria.

Shortly after demobilization, Vladimir Demikhov achieved a historic breakthrough in experimental surgery, performing the world's first heart–lung transplant on a dog. He then successfully completed a series of pioneering operations, including the transplantation of an isolated heart and lung into a dog's chest and a liver transplant. Demikhov was also the first in the world to develop and perform a mammary-coronary bypass procedure in a dog. His dog, worldwide known as "Dog Damka", lived for 7 years after this operation.

Vladimir Demikhov was a decorated veteran of the Great Patriotic War, honored with the Order of the Patriotic War, 2nd Class, as well as the medals "For Military Merit", "For Courage", and "For Victory over Japan". His pioneering contributions to experimental and clinical transplantology earned him prestigious civilian recognition, including the USSR State Prize (1988), the State Prize of the Russian Federation (1997), and the Order "For Merit to the Fatherland", 3rd Class.

III степени. Памятник В.П. Демихову установлен в здании НМИЦ трансплантологии и искусственных органов им. ак. В.И. Шумакова.

Борис Васильевич Петровский (1908–2004 гг.) был призван на службу в армию в 1939 году в качестве ведущего хирурга и заместителя начальника полевого госпиталя. В 1941–1944 годах военврач Б.В. Петровский – ведущий хирург эвакогоспиталей в действующей армии. Во время тяжелых сражений на подступах к Москве, на Волоколамском направлении, Борис Васильевич спас жизнь многим десяткам тяжелораненых, проявив высокоэффективные образцы работы, отдавая свою кровь для переливания раненым в случае необходимости. За время войны Б.В. Петровский провел более 800 операций, в том числе при ранениях подключичной и сонной артерий, артерии позвоночника, гнойных перикардитах, абсцессах и др., награжден боевыми орденами и медалями – орденом Красной Звезды, двумя орденами Отечественной войны II степени и др. Впоследствии свой бесценный опыт военных лет он отразил в 19-м томе многотомного научного труда «Опыт советской медицины в Великой Отечественной войне 1941–1945 гг.». Докторская диссертация Б.В. Петровского была издана в виде монографии «Хирургическое лечение ранений сосудов» (1949 г.).

Много лет Борис Васильевич возглавлял Всесоюзный НИИ клинической и экспериментальной хирургии Минздрава РСФСР (ныне Российский национальный центр хирургии имени академика Б.В. Петровского РАН); возглавлял Министерство здравоохранения СССР (1965–1980 гг.); осуществил в 1965 году первую в Советском Союзе успешную трансплантацию почки.

Б.В. Петровский был удостоен звания Героя Социалистического Труда (1968), Ленинской премии (1960), Государственной премии СССР (1971), орденов Ленина (1961, 1965, 1968, 1978), «За заслуги перед Отечеством» II степени (1998), Святого Андрея Первозванного (2003) и других орденов и медалей.

Врачи, фельдшеры, медицинские сестры и санитары внесли неоценимый вклад в общую победу над фашизмом, делая все возможное и невозможное для спасения раненых и больных. Более 22 млн человек прошли через госпитали в 1941–1945 годах. Всего на фронтах и в тыловых госпиталях трудились свыше 200 тыс. врачей, 500 тыс. человек среднего медперсонала. Бесценный опыт, приобретенный в годы войны медицинским персоналом, и сегодня дает свои плоды: современная хирургия в существенной степени базируется на этом опыте. Вечная память и слава героям, подарившим нам мир и свободу, а также возможность жить, трудиться, любить и беречь свою Родину.

С уважением,
главный редактор журнала
«Вестник трансплантологии
и искусственных органов»
академик РАН С.В. Готье

In recognition of his extraordinary legacy, a monument to Vladimir Petrovich Demikhov now stands at the Shumakov National Medical Research Center of Transplantology and Artificial Organs, serving as a lasting tribute to this organ transplantation pioneer.

Boris Petrovsky (1908–2004) was drafted into the army in 1939 as a leading surgeon and deputy head of a field hospital. From 1941 to 1944, he served as chief surgeon of evacuation hospitals in the active army. During the fierce battles of Moscow, particularly in the Volokolamsk direction, he saved the lives of dozens of severely wounded soldiers. His dedication went beyond duty – he not only demonstrated highly effective surgical techniques but also personally donated blood for transfusions when necessary.

Over the course of the war, Boris performed more than 800 operations, including procedures for injuries to the subclavian and carotid arteries, spinal arteries, purulent pericarditis, abscesses, and others. For his valor and outstanding medical service, he was awarded combat orders and medals, including the Order of the Red Star and two Orders of the Patriotic War, 2nd Class.

His invaluable wartime experience was later documented in the 19th volume of the multi-volume scientific work "The Experience of Soviet Medicine During the Great Patriotic War of 1941–1945". This later formed the basis of his doctoral dissertation, published as a monograph entitled "Surgical Treatment of Vascular Injuries" (1949).

For many years, Boris Petrovsky headed the All-Union Research Institute of Clinical and Experimental Surgery, which is now the Petrovsky National Research Centre of Surgery. He served as the USSR Minister of Health from 1965 to 1980. In 1965, he performed the first successful kidney transplant in the Soviet Union.

Boris Vasilyevich Petrovsky's outstanding contributions were recognized with numerous high state awards, including the title of Hero of Socialist Labor (1968), the Lenin Prize (1960), the USSR State Prize (1971), four Orders of Lenin (1961, 1965, 1968, 1978), the Order of Merit for the Fatherland, 2nd Class (1998), and the Order of St. Andrew the Apostle the First Called (2003), along with many other orders and medals.

Doctors, paramedics, nurses, and orderlies made an immeasurable contribution to the overall victory over fascism, performing incredible feats of courage and compassion as they fought for the lives of the wounded and sick. Between 1941 and 1945, more than 22 million people passed through hospitals, where over 200,000 doctors and 500,000 medical staff served tirelessly on the front lines and in rear hospitals. The invaluable experience gained by these wartime medical personnel continues to influence modern medicine, as many principles of contemporary surgery and emergency care are rooted in the lessons of that era.

Eternal memory and glory to the heroes who gave us peace and freedom – and with it, the priceless opportunity to live, work, love, and defend our Motherland.

Sincerely,
Sergey Gautier,
Fellow, Russian Academy of Sciences
Editor-in-chief, Russian Journal
of Transplantology and Artificial Organs

DOI: 10.15825/1995-1191-2025-3-8-32

ORGAN DONATION AND TRANSPLANTATION IN THE RUSSIAN FEDERATION IN 2024

17th Report from the Registry of the Russian Transplant Society

S.V. Gautier[1, 2], *S.M. Khomyakov*[1, 2]

[1] Shumakov National Medical Research Center of Transplantology and Artificial Organs, Moscow, Russian Federation

[2] Sechenov University, Moscow, Russian Federation

Objective: to assess the current status and development trends in organ donation and transplantation in the Russian Federation based on data from the year 2024. **Materials and methods.** A survey was conducted among transplant center directors. The Russian Ministry of Health's information accounting system was used for data verification. Comparative analysis was carried out to evaluate trends over time, differences across regions of the Russian Federation, and variations among transplant centers. **Results.** Based on data retrieved from the National Registry in 2024, there were 49 kidney transplant programs, 38 liver transplant programs, and 21 heart transplant programs operating in the Russian Federation. The donor activity rate was 6.7 per million population (p.m.p.). Multi-organ procurement accounted for 78.5% of cases, with an average of 3.0 organs retrieved per effective donor. A total of 3,307 organ transplants were performed in 2024, including 1,943 kidney transplants, 894 liver transplants, and 426 heart transplants. This represents an 8.2% increase in organ transplants compared to 2023. In Moscow, organ donation activity reached 31.6 p.m.p. A total of 12 transplant centers operated in Moscow and Moscow Oblast, collectively performing 54.0% of all kidney transplants and 67.3% of all extrarenal transplants nationwide. The number of patients living with transplanted organs in the Russian Federation exceeds 155.1 p.m.p. **Conclusion.** The network of transplant centers in the Russian Federation continues to expand, with three new transplant programs launched in 2024. Over the past year, both the number of effective donors and the volume of organ transplants have increased. The resource potential of medical institutions has not yet been fully utilized, allowing for further growth in transplant activity. Moscow remains the central driver of transplant medicine in Russia. Shumakov National Medical Research Center of Transplantology and Artificial Organs and its branch account for 27.1% of all organ transplants performed nationally. Successful regional transplant programs are also underway in the Republic of Tatarstan, Kemerovo Oblast (Kuzbass), St. Petersburg and Leningrad Oblast, Novosibirsk Oblast, and Krasnoyarsk Krai. Notably, the Russian Federation places a strong priority on providing pediatric transplant care.

Keywords: organ donation, kidney, liver, heart, lung transplantation, transplant center, waiting list, registry, Shumakov National Medical Research Center of Transplantology and Artificial Organs.

INTRODUCTION

The National Registry tracks the current status and trends in organ donation and transplantation in Russia under the auspices of a dedicated transplantology commission that was established in collaboration between the Russian Ministry of Health and the Russian Transplant Society. Previous reports have been published in 2009–2024 [1–15].

Since 2016, the registry has served as a mechanism for quality assurance and for ensuring the completeness of data collection within the national information system used to register donated human organs and tissues, donors, and recipients. The system operates under executive order No. 355n of the Russian Ministry of Health, dated June 8, 2016.

Apart from statistical data for the reporting period, the Registry's annual reports include a systematic analysis with an assessment of the current status of transplant care in the Russian Federation, as well as trends and prospects for future advancements in this branch of healthcare.

Since 2019, the National Registry has also been used to monitor the implementation of the departmental target program "Organ Donation and Transplantation in the Russian Federation", approved by Order No. 365 of the Russian Ministry of Health on June 4, 2019 (since 2022 – a set of procedural measures).

Beginning in 2024, the work of the transplant registry has been coordinated with annual monitoring in the field of nephrology conducted by the Center for the Improvement of Medical Care in Nephrology at Shumakov

Corresponding author: Sergey Khomyakov. Address: 1, Schukinskaya str., Moscow, 123182, Russian Federation. Phone: (903) 150-89-55. E-mail: profkom_transpl@mail.ru

National Medical Research Center of Transplantology and Artificial Organs, Moscow.

Registry data are collected through standardized questionnaires completed by designated representatives at all transplant centers in the Russian Federation. The collected information is subjected to comparative analysis across different time periods, individual regions, transplant centers, and in relation to international registry data.

The working group extends its gratitude to all regular and new participants who contributed data to the Registry, as well as to the Ministry of Health of the Russian Federation and the Central Research Institute for Health Organization and Informatization for their ongoing support.

TRANSPLANT CENTERS

In the Russian Federation, transplant centers are currently operating across 38 federal subjects, also referred to as regions (Fig. 1).

In order to comply with the regional principle in assessing the status and trends in transplant care and organ donation in the federal subjects of the Russian Federation, the activities of the Shumakov National Medical Research Center of Transplantology and Artificial Organs, Moscow (hereinafter referred to as "Shumakov Center") and its Volzhsky branch are presented in the Registry separately as for two transplant centers.

In 2024, kidney transplants (KT) were performed in 49 centers, liver transplants (LiT) in 38 centers, heart transplants (HT) in 21 centers, pancreas transplants (PaT) in 3 centers, and lung transplants (LuT) in 3 centers.

Overall, transplant procedures were carried out in 61 medical facilities, including:

20 federal institutions, among them 14 institutions under the Russian Ministry of Health, 2 institutions under the Russian Ministry of Science and Higher Education, 3 institutions under the Federal Medical and Biological Agency, and 1 institution under the Russian Ministry of Defense; 41 institutions were operated by the federal subjects of the Russian Federation.

In 2024, a new transplant center began operating in the Donetsk People's Republic at Kalinin Regional Clinical Hospital, where two living-donor KT were successfully performed.

Across the Russian Federation, a total of 3,307 organ transplants were carried out, including 281 procedures for children (Tables 1 and 2). This represents an 8.2% increase (+250 transplants) compared to 2023.

Table 1

Summary of organ donation and transplantation in the Russian Federation, 2024

Indicator	Number (units)
Organ donation	
Total number of organ donors	1365
Deceased donors	975
Living (related) donors	390
Organ transplantation	
Total number of organs transplanted	3307
share of pediatric transplants	281
Kidney	1943
from deceased donors	1720
from living-related donors	223
share of pediatric transplants	124
Liver	894
from deceased donor	727
from living-related donors	167
share of pediatric transplants	132
Heart	424
share of pediatric transplants	25
Heart-lung	2
Lungs	33
Pancreas	10
Small intestine	1

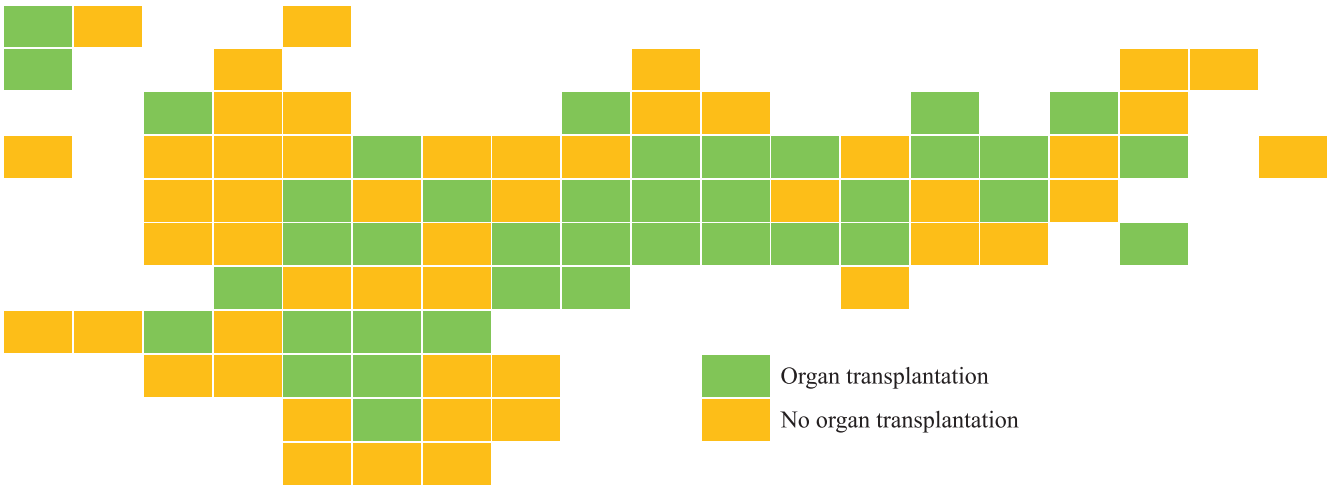

Fig. 1. Geographic spread of organ transplant centers in the Russian Federation in 2024

Table 2

Transplant activity in the Russian Federation, 2024

#	Federal District	Federal subject	Medical institutions	**Total**	**Kidney (total)**	Kidney (deceased-donor)	Kidney (living related)	**Liver (total)**	Liver (deceased-donor)	Liver (living related)	**Heart**	**Pancreas**	**Lungs**	**Heart-lungs**	**Small intestine**
1	2	3	4	5	6	7	8	9	10	11	12	13	14	15	16
1.1	Central Federal District	Moscow	Shumakov National Medical Research Center of Transplantology and Artificial Organs	**794**	**303**	197	106	**187**	83	104	**277**	**5**	**20**	**2**	**0**
1.2	Volga Federal District	Volgograd Oblast	Branch of Shumakov National Medical Research Center of Transplantology and Artificial Organs	**101**	**70**	49	21	**14**	14	0	**17**	**0**	**0**	**0**	**0**
2	Central Federal District	Moscow	Lopatkin Research Institute of Urology and Interventional Radiology, a branch of the National Medical Research Center for Radiology	**82**	**82**	77	5	**0**	0	0	**0**	**0**	**0**	**0**	**0**
3	Central Federal District	Moscow	Russian Children's Clinical Hospital	**31**	**30**	26	4	**1**	0	1	**0**	**0**	**0**	**0**	**0**
4	Central Federal District	Moscow	Petrovsky National Research Centre of Surgery	**25**	**15**	6	9	**10**	0	10	**0**	**0**	**0**	**0**	**0**
5	Central Federal District	Moscow	Burnazyan Federal Medical and Biophysical Center	**55**	**16**	10	6	**39**	14	25	**0**	**0**	**0**	**0**	**0**
6	Central Federal District	Moscow	Bakulev Scientific Center of Cardiovascular Surgery	**2**	**0**	0	0	**0**	0	0	**2**	**0**	**0**	**0**	**0**
7	Central Federal District	Moscow	National Medical Research Center for Children's Health	**20**	**20**	13	7	**0**	0	0	**0**	**0**	**0**	**0**	**0**
	Central Federal District	Moscow	Blokhin National Medical Research Center of Oncology	**2**	**0**	0	0	**2**	2	0	**0**	**0**	**0**	**0**	**0**
8	Central Federal District	Moscow	Botkin Hospital	**224**	**147**	147	0	**68**	68	0	**9**	**0**	**0**	**0**	**0**
9	Central Federal District	Moscow	Sklifosovsky Research Institute of Emergency Care	**419**	**265**	265	0	**135**	133	2	**4**	**3**	**11**	**0**	**1**
10	Central Federal District	Moscow	Moscow Clinical Scientific Center	**100**	**19**	19	0	**81**	81	0	**0**	**0**	**0**	**0**	**0**
11	Central Federal District	Moscow	Vladimirsky Moscow Regional Research and Clinical Institute	**90**	**60**	60	0	**30**	30	0	**0**	**0**	**0**	**0**	**0**

Continuation of Table 2

1	2	3	4	5	6	7	8	9	10	11	12	13	14	15	16
12	Central Federal District	Moscow Oblast	Federal Clinical Center for High Medical Technologies, Federal Biomedical Agency (No. 119)	**22**	**22**	22	0	**0**	0	0	**0**	**0**	**0**	**0**	**0**
13	Central Federal District	Belgorod Oblast	St. Joasaphus Belgorod Regional Clinical Hospital	**12**	**8**	8	0	**3**	3	0	**1**	**0**	**0**	**0**	**0**
14	Central Federal District	Voronezh Oblast	Voronezh Regional Clinical Hospital No. 1	**9**	**8**	8	0	**0**	0	0	**1**	**0**	**0**	**0**	**0**
15	Central Federal District	Tula Oblast	Tula Regional Clinical Hospital	**3**	**3**	3	0	**0**	0	0	**0**	**0**	**0**	**0**	**0**
16	Central Federal District	Ryazan Oblast	Ryazan Regional Clinical Hospital	**18**	**16**	16	0	**2**	2	0	**0**	**0**	**0**	**0**	**0**
17	Northwestern Federal District	St. Petersburg	Granov Russian Research Center of Radiology and Surgical Technologies	**22**	**0**	0	0	**22**	22	0	**0**	**0**	**0**	**0**	**0**
18	Northwestern Federal District	St. Petersburg	Almazov National Medical Research Centre	**38**	**0**	0	0	**0**	0	0	**38**	**0**	**0**	**0**	**0**
19	Northwestern Federal District	St. Petersburg	Pavlov University	**25**	**14**	12	2	**11**	11	0	**0**	**0**	**0**	**0**	**0**
20	Northwestern Federal District	St. Petersburg	St. Petersburg Research Institute of Emergency Medicine	**80**	**60**	60	0	**20**	20	0	**0**	**0**	**0**	**0**	**0**
21	Northwestern Federal District	St. Petersburg	Mariinskaya Hospital	**33**	**33**	33	0	**0**	0	0	**0**	**0**	**0**	**0**	**0**
22	Northwestern Federal District	St. Petersburg	St. Luke's Clinical Hospital	**36**	**36**	35	1	**0**	0	0	**0**	**0**	**0**	**0**	**0**
23	Northwestern Federal District	St. Petersburg	Kirov Military Medical Academy	**16**	**0**	0	0	**16**	16	0	**0**	**0**	**0**	**0**	**0**
24	Northwestern Federal District	St. Petersburg	Leningrad Regional Clinical Hospital	**37**	**35**	35	0	**2**	2	0	**0**	**0**	**0**	**0**	**0**
25	Northwestern Federal District	Arkhangelsk Oblast	Volosevich First City Clinical Hospital	**8**	**6**	6	0	**2**	2	0	**0**	**0**	**0**	**0**	**0**
26	Southern Federal District	Krasnodar Krai	Ochapovsky Regional Clinical Hospital No. 1	**24**	**14**	14	0	**8**	6	2	**0**	**0**	**2**	**0**	**0**

Continuation of Table 2

1	2	3	4	5	6	7	8	9	10	11	12	13	14	15	16
27	Southern Federal District	Volgograd Oblast	Volzhsky Regional Center of Urology	**4**	**4**	0	4	**0**	0	0	**0**	**0**	**0**	**0**	**0**
28	Southern Federal District	Rostov Oblast	Rostov Regional Clinical Hospital	**66**	**40**	40	0	**20**	20	0	**4**	**2**	**0**	**0**	**0**
29	North Caucasian Federal District	Stavropol Krai	Stavropol Regional Clinical Hospital	**17**	**13**	13	0	**4**	4	0	**0**	**0**	**0**	**0**	**0**
30	Volga Federal District	Samara Oblast	Samara State Medical University	**61**	**55**	53	2	**5**	5	0	**1**	**0**	**0**	**0**	**0**
31	Volga Federal District	Saratov Oblast	Saratov State Medical University	**6**	**6**	0	6	**0**	0	0	**0**	**0**	**0**	**0**	**0**
32	Volga Federal District	Saratov Oblast	Regional Clinical Hospital	**8**	**8**	8	0	**0**	0	0	**0**	**0**	**0**	**0**	**0**
33	Volga Federal District	Nizhny Novgorod Oblast	Volga Regional Medical Center	**30**	**19**	14	5	**11**	9	2	**0**	**0**	**0**	**0**	**0**
34	Volga Federal District	Nizhny Novgorod Oblast	Research Institute – Korolev Specialized Cardiac Surgery Clinical Hospital	**1**	**0**	0	0	**0**	0	0	**1**	**0**	**0**	**0**	**0**
35	Volga Federal District	Republic of Tatarstan	Republican Clinical Hospital	**155**	**99**	98	1	**56**	56	0	**0**	**0**	**0**	**0**	**0**
36	Volga Federal District	Republic of Tatarstan	Interregional Clinical Diagnostic Center	**17**	**0**	0	0	**0**	0	0	**17**	**0**	**0**	**0**	**0**
37	Volga Federal District	Republic of Tatarstan	Children's Republican Clinical Hospital	**1**	**1**	1	0	**0**	0	0	**0**	**0**	**0**	**0**	**0**
38	Volga Federal District	Republic of Tatarstan	Emergency Care Hospital	**6**	**0**	0	0	**0**	0	0	**6**	**0**	**0**	**0**	**0**
39	Volga Federal District	Republic of Bashkortostan	Kuvatov Republican Clinical Hospital	**45**	**38**	38	0	**7**	7	0	**0**	**0**	**0**	**0**	**0**
40	Volga Federal District	Republic of Bashkortostan	Republican Cardiology Clinic	**5**	**0**	0	0	**0**	0	0	**5**	**0**	**0**	**0**	**0**
41	Volga Federal District	Perm Krai	Sukhanov Federal Center for Cardiovascular Surgery	**2**	**0**	0	0	**0**	0	0	**2**	**0**	**0**	**0**	**0**
42	Volga Federal District	Perm Krai	Perm Regional Clinical Hospital	**8**	**8**	6	2	**0**	0	0	**0**	**0**	**0**	**0**	**0**
43	Volga Federal District	Orenburg Oblast	Orenburg Regional Clinical Center for Surgery and Traumatology	**35**	**35**	20	15	**0**	0	0	**0**	**0**	**0**	**0**	**0**
44	Ural Federal District	Sverdlovsk Oblast	Sverdlovsk Regional Clinical Hospital No. 1	**49**	**33**	33	0	**13**	13	0	**3**	**0**	**0**	**0**	**0**

End of Table 2

1	2	3	4	5	6	7	8	9	10	11	12	13	14	15	16
45	Ural Federal District	Chelyabinsk Oblast	Chelyabinsk Regional Clinical Hospital	**37**	**24**	24	0	**10**	10	0	**3**	**0**	**0**	**0**	**0**
46	Ural Federal District	Tyumen Oblast	Regional Clinical Hospital No. 1	**35**	**29**	29	0	**3**	3	0	**3**	**0**	**0**	**0**	**0**
47	Ural Federal District	Khanty-Mansi Autonomous Okrug–Yugra	District Clinical Hospital	**20**	**14**	11	3	**6**	6	0	**0**	**0**	**0**	**0**	**0**
48	Siberian Federal District	Novosibirsk Oblast	Meshalkin National Medical Research Center	**10**	**0**	0	0	**0**	0	0	**10**	**0**	**0**	**0**	**0**
49	Siberian Federal District	Novosibirsk Oblast	State Novosibirsk Regional Clinical Hospital	**89**	**42**	33	9	**47**	29	18	**0**	**0**	**0**	**0**	**0**
50	Siberian Federal District	Kemerovo Oblast (Kuzbass)	Research Institute for Complex Issues of Cardiovascular Diseases	**10**	**0**	0	0	**0**	0	0	**10**	**0**	**0**	**0**	**0**
51	Siberian Federal District	Kemerovo Oblast (Kuzbass)	Belyaev Kemerovo Regional Clinical Hospital	**82**	**71**	68	3	**11**	11	0	**0**	**0**	**0**	**0**	**0**
52	Siberian Federal District	Kemerovo Oblast (Kuzbass)	Kuzbass Cardiology Center	**1**	**0**	0	0	**1**	1	0	**0**	**0**	**0**	**0**	**0**
53	Siberian Federal District	Irkutsk Oblast	Irkutsk Regional Clinical Hospital	**53**	**32**	31	1	**21**	19	2	**0**	**0**	**0**	**0**	**0**
54	Siberian Federal District	Altai Krai	Altai Regional Clinical Hospital	**14**	**14**	14	0	**0**	0	0	**0**	**0**	**0**	**0**	**0**
55	Siberian Federal District	Krasnoyarsk Krai	Federal Siberian Research and Clinical Center	**18**	**17**	11	6	**1**	1	0	**0**	**0**	**0**	**0**	**0**
56	Siberian Federal District	Krasnoyarsk Krai	Krasnoyarsk Clinical Hospital	**50**	**26**	26	0	**14**	14	0	**10**	**0**	**0**	**0**	**0**
57	Far Eastern Federal District	Republic of Sakha (Yakutia)	Republican Hospital No. 1 – Nikolaev National Center of Medicine	**4**	**2**	2	0	**2**	1	1	**0**	**0**	**0**	**0**	**0**
58	Far Eastern Federal District	Republic of Buryatia	Semashko Republican Clinical Hospital	**6**	**6**	3	3	**0**	0	0	**0**	**0**	**0**	**0**	**0**
59	Far Eastern Federal District	Primorsky Krai	Primorsky Regional Clinical Hospital No. 1	**20**	**14**	14	0	**6**	6	0	**0**	**0**	**0**	**0**	**0**
60	Far Eastern Federal District	Khabarovsk Krai	Regional Clinical Hospital No. 1”	**14**	**11**	9	2	**3**	3	0	**0**	**0**	**0**	**0**	**0**
Total				**3307**	**1943**	**1720**	**223**	**894**	**727**	**167**	**424**	**10**	**33**	**2**	**1**

In 2024, the number of organ transplants performed each month ranged from 131 in January to 397 in November, with an average of 276 procedures per month (Fig. 2). Over the same period, the monthly distribution by organ type was as follows: 78–224 KT, 35–104 LiT, and 18–48 HT.

Based on data obtained from the Federal Registry for High-Tech Medical Care, in 2024 a total of 3,069 organ transplants (92.8%) were performed using funds from the compulsory medical insurance system allocated for high-tech medical care in transplantation (2023 – 2,683, 87.8%), Fig. 3. Another 238 transplants (7.2%) were financed from the budgets of the federal subjects of the Russian Federation and from the federal budget (2023 – 374, 12.2%).

Thus, the growth in the number of organ transplants in 2024 became possible, among other factors, due to an adequate increase in compulsory medical insurance funding for high-tech transplant care.

Since 2010, when this indicator was first included in the Registry, the absolute number of organ transplants financed through funds allocated for high-tech medical care has increased 3.9-fold, while their share in overall transplant activity has risen by 34.5%.

The financial cost standards per unit of high-tech medical care in transplantation for 2024 were approved by

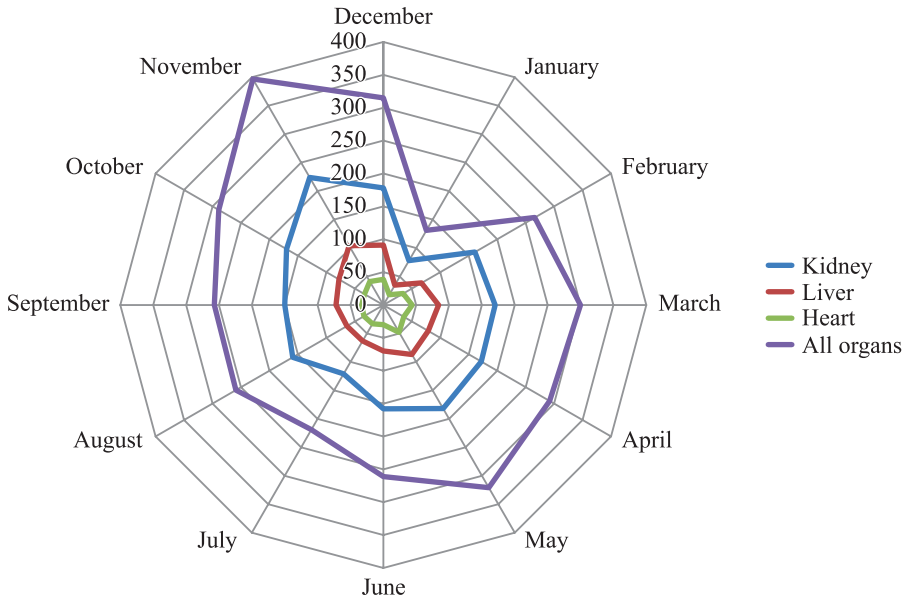

Fig. 2. Monthly distribution of organ transplants in the Russian Federation, 2024

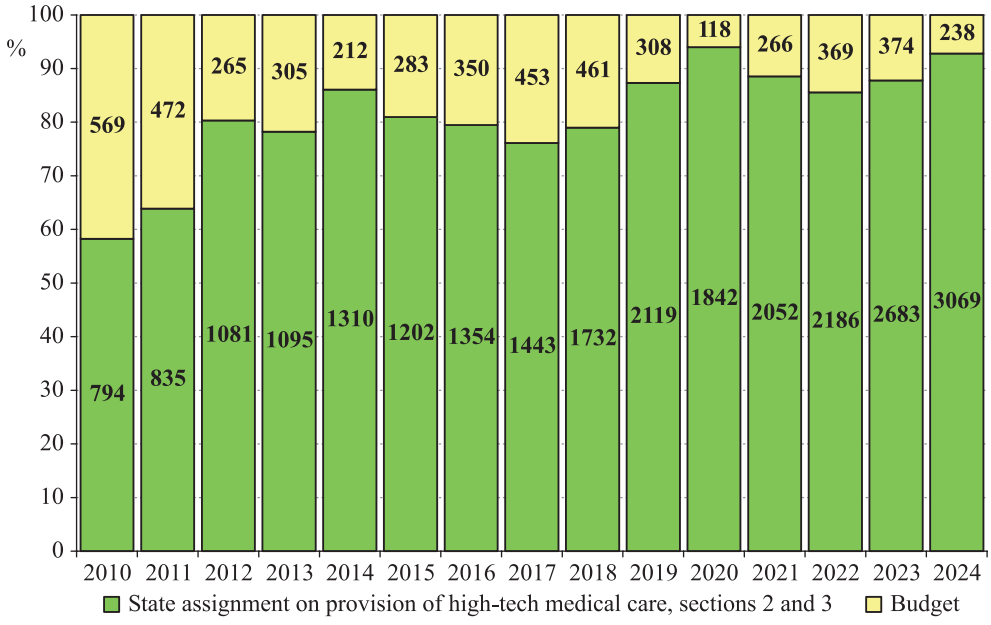

Fig. 3. Funding for organ transplantation in the Russian Federation, 2010–2023

the Government of the Russian Federation on December 28, 2023 via Resolution No. 2497.

ORGAN DONATION

In 2024, donor programs were active in 33 federal subjects of the Russian Federation. During the year, 975 effective deceased donors were recorded, corresponding to 6.7 per million population (p.m.p.); Table 3. This represents an increase of 6.3% (+58 donors) compared to 2023.

The age distribution of effective deceased organ donors is presented in Fig. 4. Among donors, 61.7% were male and 38.3% were female.

In 2024, donor activity per capita in regions implementing donor programs (population: 101.7 million) was 9.6 p.m.p. (Tables 4, 5).

Moscow posted the highest (DA) – 31.6 p.m.p. (compared to 29.1 in 2023). In both the Republic of Tatarstan and Kemerovo Oblast (Kuzbass), the rate reached 14.8 p.m.p. In five more federal subjects – St. Petersburg and Leningrad Oblast, Ryazan Oblast, Tyumen Oblast, and Novosibirsk Oblast – DA also exceeded 10.0 p.m.p.

An increase in DA was observed in 20 regions, with the most notable growth in Moscow (+39 effective donors). Conversely, a decline was noted in 11 regions, including ≥25% reductions in Krasnodar Krai, Perm Krai, and Tula Oblast. However, given the consistently low DA in these regions, the overall national indicator was not affected.

In 2024, Moscow and Moscow Oblast accounted for 46.7% (455) of effective donors (423, or 46.1%, in 2023). Thus, 55.2% of the national increase in DA was attribu-

Table 3

Key indicators of deceased organ donation activity in the Russian Federation, 2024

#	Federal District	Federal Subject	Medical institutions	Population (million)	Number of active donor bases	Donors (absolute, per million population)		including brain-dead donors (absolute, %)		including multi-organ donors (absolute, %)	
1	2	3	4	5	6	7	8	9	10	11	12
1	Central Federal District	Moscow	Botkin Hospital	13.3	20	420	31.6	397	94.5	364	86.7
2	Central Federal District	Moscow Oblast	Vladimirsky Moscow Regional Research and Clinical Institute	8.8	16	35	4.0	35	100.0	33	94.3
3	Central Federal District	Belgorod Oblast	St. Joasaph Belgorod Regional Clinical Hospital	1.5	1	4	2.7	4	100.0	3	75.0
4	Central Federal District	Voronezh Oblast	Voronezh Regional Clinical Hospital No. 1	2.3	4	6	2.6	6	100.0	2	33.3
5	Central Federal District	Tula Oblast	Tula Regional Clinical Hospital	1.5	1	3	2.0	3	100.0	3	100.0
6	Central Federal District	Ryazan Oblast	Ryazan Regional Clinical Hospital	1.1	1	12	10.9	12	100.0	8	66.7
7	Northwestern Federal District	St. Petersburg	St. Petersburg Research Institute of Emergency Medicine	5.6	9	71	12.7	71	100.0	67	94.4
8	Northwestern Federal District	Leningrad Oblast	Leningrad Regional Clinical Hospital	2.1	1	21	10.0	21	100.0	18	85.7
9	Northwestern Federal District	Arkhangelsk Oblast	Volosevich First City Clinical Hospital	0.9	2	8	8.9	8	100.0	6	75.0
10	Southern Federal District	Krasnodar Krai	Ochapovsky Regional Clinical Hospital No. 1	5.8	1	7	1.2	7	100.0	5	71.4
11	Southern Federal District	Volgograd Oblast	Volzhsky Branch of Shumakov National Medical Research Center of Transplantology and Artificial Organs	2.4	4	16	6.7	16	100.0	14	87.5
12	Southern Federal District	Rostov Oblast	Rostov Regional Clinical Hospital	4.1	1	28	6.8	28	100.0	20	71.4
13	North Caucasian Federal District	Stavropol Krai	Stavropol Regional Clinical Hospital	2.9	1	10	3.4	10	100.0	7	70.0
14	Volga Federal District	Samara Oblast	Samara State Medical University	3.1	4	30	9.7	27	90.0	5	16.7

End of Table 3

1	2	3	4	5	6	7	8	9	10	11	12
15	Volga Federal District	Saratov Oblast	Regional Clinical Hospital	2.4	1	7	2.9	6	85.7	6	85.7
16	Volga Federal District	Nizhny Novgorod Oblast	Volga Regional Medical Center	3.0	4	8	2.7	8	100.0	7	87.5
17	Volga Federal District	Republic of Tatarstan	Republican Clinical Hospital	4.0	4	59	14.8	58	98.3	54	91.5
18	Volga Federal District	Republic of Bashkortostan	Kuvatov Republican Clinical Hospital	4.0	6	19	4.8	19	100.0	8	42.1
19	Volga Federal District	Orenburg Oblast	Orenburg Regional Clinical Center for Surgery and Traumatology	1.8	3	10	5.6	10	100.0	10	100.0
20	Volga Federal District	Perm Krai	Perm Regional Clinical Hospital	2.5	2	3	1.2	3	100.0	3	100.0
21	Ural Federal District	Sverdlovsk Oblast	Sverdlovsk Regional Clinical Hospital No. 1	4.2	5	19	4.5	19	100.0	15	78.9
22	Ural Federal District	Chelyabinsk Oblast	Chelyabinsk Regional Clinical Hospital	3.4	1	16	4.7	16	100.0	11	68.8
23	Ural Federal District	Tyumen Oblast	Regional Clinical Hospital No. 1	1.6	3	17	10.6	14	82.4	5	29.4
24	Ural Federal District	Khanty-Mansi Autonomous Okrug–Yugra	District Clinical Hospital	1.8	3	6	3.3	6	100.0	6	100.0
25	Siberian Federal District	Novosibirsk Oblast	State Novosibirsk Regional Clinical Hospital	2.8	10	28	10.0	27	96.4	22	78.6
26	Siberian Federal District	Kemerovo Oblast (Kuzbass)	Belyaev Kuzbass Regional Clinical Hospital	2.5	11	37	14.8	24	64.9	16	43.2
27	Siberian Federal District	Irkutsk Oblast	Irkutsk Regional Clinical Hospital	2.3	3	20	8.7	20	100.0	18	90.0
28	Siberian Federal District	Altai Krai	Altai Regional Clinical Hospital	2.1	1	7	3.3	7	100.0	1	14.3
29	Siberian Federal District	Krasnoyarsk Krai	Krasnoyarsk Regional Clinical Hospital	2.8	4	21	7.5	21	100.0	15	71.4
30	Far Eastern Federal District	Primorsky Krai	Primorsky Regional Clinical Hospital No. 1	1.8	1	10	5.6	10	100.0	3	30.0
31	Far Eastern Federal District	Khabarovsk Krai	Sergeev District Clinical Hospital	1.3	2	7	5.4	7	100.0	2	28.6
32	Far Eastern Federal District	Republic of Sakha	Republican Hospital No. 1 – Nikolaev National Center of Medicine	1.0	1	2	2.0	2	100.0	1	50.0
33	Far Eastern Federal District	Republic of Buryatia	Semashko Republican Clinical Hospital	1.0	1	1	1.0	1	100.0	0	0.0
34	–	Departmental program of the Federal Biomedical Agency of the Russian Federation	Burnazyan Federal Medical and Biophysical Center	-	1	2	–	2	100.0	2	100.0
35	–	Departmental program of the Federal Biomedical Agency of the Russian Federation	Federal Siberian Research and Clinical Center	-	2	5	–	5	100.0	5	100.0
			Total	**146.0**	**135**	**975**	**6.7**	**930**	**95.4**	**765**	**78.5**

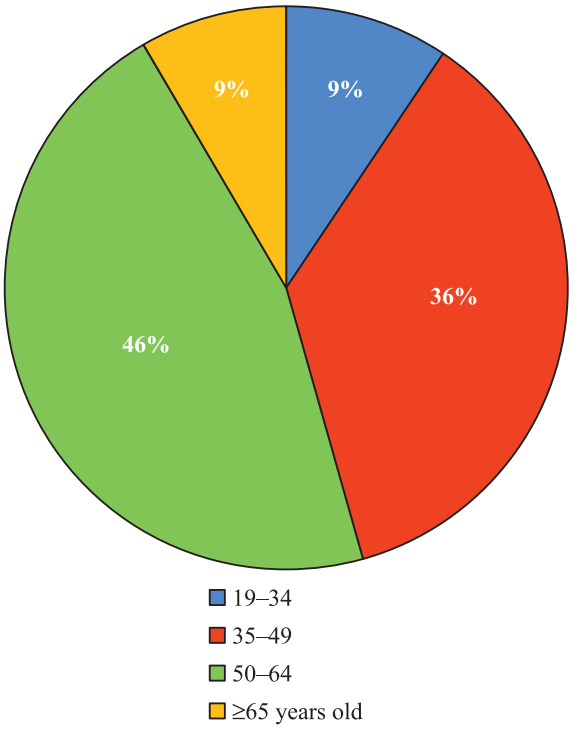

Fig. 4. Age distribution of effective organ donors in the Russian Federation, 2024

table to the Moscow agglomeration, while the remaining 44.8% came from other regions.

In 2024, 930 effective donors were diagnosed with brain death, representing 95.4% of the total donor pool (Fig. 5). In 26 regions of the Russian Federation, centers worked exclusively with brain-death donors. Only Kemerovo Oblast (Kuzbass) reported a percentage below 80% (64.9%).

A total of 765 multi-organ procurements were performed, accounting for 78.5% of all procurements (708, or 77.2%, in 2023). In 21 regions, multi-organ procurements represented ≥70% of donor procedures. Moscow and Moscow Oblast contributed 397 multi-organ donors, or 51.9% of the national total (362, or 51.1%, in 2023).

The average number of organs retrieved per deceased donor in 2024 was 3.0 (compared to 2.9 in 2023). The utilization rate of donor kidneys remained stable at 88.2% (88.3% in 2023).

In addition, 390 organ removals from living related donors (kidneys and partial livers) were performed in 2024, representing 28.6% of all 1,365 procurements (357, or 28.0%, in 2023).

Table 4

Regional ranking by donor activity in 2024

#	Federal Subject	Population in 2024 (million)	Donor count (per million population)	
			2024	2023
1	Moscow	13.3	31.6	29.1
2	Republic of Tatarstan	4.0	14.8	17.0
3	Kemerovo Oblast (Kuzbass)	2.5	14.8	13.5
4	St. Petersburg	5.6	12.7	11.1
5	Ryazan Oblast	1.1	10.9	8.2
6	Tyumen Oblast	1.6	10.6	10.6
7	Novosibirsk Oblast	2.8	10.0	9.6
8	Leningrad Oblast	2.1	10.0	9.0
9	Samara Oblast	3.1	9.7	8.7
10	Arkhangelsk Oblast	0.9	8.9	3.0
11	Irkutsk Oblast	2.3	8.7	11.3
12	Krasnoyarsk Krai*	2.8	7.5	4.6
13	Rostov Oblast	4.1	6.8	5.7
14	Volgograd Oblast	2.4	6.7	6.0
15	Orenburg Oblast	1.8	5.6	6.1
16	Primorsky Krai	1.8	5.6	3.9
17	Khabarovsk Krai	1.3	5.4	5.4
18	Republic of Bashkortostan	4.0	4.8	4.9
19	Chelyabinsk Oblast	3.4	4.7	3.8
20	Sverdlovsk Oblast	4.2	4.5	4.3
21	Moscow Oblast	8.8	4.0	4.9
22	Stavropol Krai	2.9	3.4	0.7
23	Altai Krai	2.1	3.3	4.3
24	Khanty-Mansi Autonomous Okrug – Yugra	1.8	3.3	2.9
25	Saratov Oblast	2.4	2.9	3.8
26	Nizhny Novgorod Oblast	3.0	2.7	2.9
27	Belgorod Oblast	1.5	2.7	2.0
28	Voronezh Oblast	2.3	2.6	1.7
29	Tula Oblast	1.5	2.0	3.3
30	Republic of Sakha	1.0	2.0	–
31	Krasnodar Krai	5.8	1.2	2.2
32	Perm Krai	2.5	1.2	1.2
33	Republic of Buryatia	1.0	1.0	–
	Russia (85 federal subjects of the Russian Federation)**	146.0	6.7	6.3
	Russia (33 federal subjects of the Russian Federation)	101.7	9.6	

* – Excluding the donor program of the Federal Scientific Center of the Federal Medical and Biological Agency, Krasnoyarsk.

** – Deceased-organ donation will not be carried out in the new territories until the special military operation is completed.

Table 5

Number of deceased (effective) organ donors from 2006 to 2024

#	Region	2006	2007		2008		2009		2010		2011		2012		2013		2014		2015		2016		2017		2018		2019		2020		2021		2022		2023		2024	
		Donor count	Donor count	Year-over-year change (abs.)	Donor count	Year-over-year change (abs.)	Donor count	Year-over-year change (abs.)	Donor count	Year-over-year change (abs.)	Donor count	Year-over-year change (abs.)	Donor count	Year-over-year change (abs.)	Donor count	Year-over-year change (abs.)	Donor count	Year-over-year change (abs.)	Donor count	Year-over-year change (abs.)	Donor count	Year-over-year change (abs.)	Donor count	Year-over-year change (abs.)	Donor count	Year-over-year change (abs.)	Donor count	Year-over-year change (abs.)	Donor count	Year-over-year change (abs.)	Donor count	Year-over-year change (abs.)	Donor count	Year-over-year change (abs.)	Donor count	Year-over-year change (abs.)
1	2	3	4	5	6	7	8	9	10	11	12	13	14	15	16	17	18	19	20	21	22	23	24	25	26	27	28	29	30	31	32	33	34	35	36	37	38	39
1	Moscow	87	126	+39	135	+9	136	+1	151	+15	135	–16	111	–24	125	+14	151	+26	142	–9	183	+41	195	+12	218	+23	277	+59	263	–14	298	+35	332	+34	381	+49	420	+39
2	Moscow Oblast	24	45	+21	59	+14	52	–7	71	+19	82	+11	61	–21	56	–5	51	–5	44	–7	39	–5	75	+36	68	–7	41	–27	21	–20	36	+15	30	–6	42	+12	35	–7
3	Belgorod Oblast		2	+2	3	+1	2	–1	5	+3	6	+1	3	–3	1	–2	2	+1	5	+3	4	–1	4	0	4	0	4	0	2	–2	2	0	5	+3	3	–2	4	+1
4	Voronezh Oblast	6	2	–4	8	+6	2	–6	0	–2	1	+1	6	+5	6	0	5	–1	7	+2	4	–3	1	–3	8	+7	8	0	4	–4	3	–1	3	0	4	+1	6	+2
5	Tula Oblast																										2	+2	3	+1	4	+1	3	–1	5	+2	3	–2
6	Ryazan Oblast																								2	+2	13	+11	6	–7	11	+5	7	–4	9	+2	12	+3
7	Ivanovo Oblast																														1	+1	0	–1	2	+2	0	–2
8	Krasnodar Krai						3	+3	39	+36	52	+13	42	–10	41	–1	23	–18	25	+2	24	–1	19	–5	20	+1	23	+3	13	–10	13	0	17	+4	13	–4	7	–6
9	Volgograd Oblast	5	0	–5	11	+11	15	+4	16	+1	17	+1	19	+2	15	–2	18	+3	8	–10	8	0	9	+1	9	0	10	+1	10	0	10	0	8	–2	15	+7	16	+1
10	Rostov Oblast																		1	+1	7	+6	13	+6	19	+6	21	+2	18	–3	21	+3	21	0	24	+3	28	+4
11	Stavropol Krai																								2	+2	3	+1	13	+10	5	–8	3	–2	2	–1	10	+8
12	St. Peters-burg	30	45	+15	47	+2	47	0	41	–6	34	–7	22	–12	13	–9	23	+10	31	+8	29	–2	31	+2	34	+3	53	+19	25	–28	25	0	43	+18	62	+19	71	+9
13	Leningrad Oblast	12	8	–4	11	+3	11	0	13	+2	10	–3	10	0	10	0	9	–1	7	–2	12	+5	11	–1	15	+4	7	–8	11	+4	12	+1	17	+5	18	+1	21	+3
14	Arkhangelsk Oblast																								5	+5	5	0	1	–4	1	0	3	+2	3	0	8	+5
15	Novosibirsk Oblast	17	11	–6	18	+7	29	+11	35	+6	25	–10	20	–4	17	–3	11	–6	14	+3	9	–5	14	+5	17	+3	23	+6	15	–8	15	0	19	+4	27	+8	28	+1
16	Kemerovo Oblast	16	13	–3	18	+5	18	0	22	+4	12	–10	26	+14	26	0	31	+5	28	–3	34	+6	22	–12	30	+8	40	+10	27	–13	28	+1	41	+13	35	–6	37	+2
17	Irkutsk Oblast				4	+4	6	+2	10	+4	9	–1	8	–1	6	–2	9	+3	4	–5	3	–1	2	–1	7	+5	16	+9	16	0	8	–8	15	+7	26	+11	20	–6
18	Omsk Oblast	10	15	+5	13	–2	19	+6	19	0	14	–5	11	–3	14	+3	16	+2	11	–5	4	–7	4	0	3	–1	2	–1	2	0	0	–2	0	0	0	0	0	0
19	Altai Krai														3	+3	5	+2	4	–1	4	0	8	+4	8	0	8	0	9	+1	7	–2	10	+3	9	–1	7	–2
20	Krasnoyarsk Krai																3	+3	6	+3	18	+12	27	+9	16	Note	13	–3	10	–3	12	+2	10	–2	13	+3	21	+8

End of Table 5

1	2	3	4	5	6	7	8	9	10	11	12	13	14	15	16	17	18	19	20	21	22	23	24	25	26	27	28	29	30	31	32	33	34	35	36	37	38	39
21	Sverdlovsk Oblast	14	13	–1	12	–1	13	+1	14	+1	15	+1	14	–1	18	+4	23	+5	18	–5	15	–3	22	+7	24	+2	24	0	6	–18	14	+8	10	–4	18	+8	19	+1
22	Chelyabinsk Oblast								6	+6	2	–4	7	+5	6	–1	10	+4	9	–1	11	+2	8	–3	4	–4	4	0	3	–1	3	0	9	+6	13	+4	16	+3
23	Tyumen Oblast																						4	+4	13	+9	13	0	5	–8	8	+3	16	+8	17	+1	17	0
24	Khanty-Mansi Autonomous Okrug – Yugra																						3	+3	4	+1	5	+1	3	–2	2	–1	3	+1	5	+2	6	+1
25	Samara Oblast	4	17	+13	24	+7	18	–6	20	+2	21	+1	19	–2	21	+2	20	–1	18	–2	26	+8	28	+2	23	–5	25	+2	24	–1	24	0	23	–1	27	+4	30	+3
26	Saratov Oblast														4	+4	7	+3	7	0	7	0	7	0	8	+1	10	+2	0	–10	6	+6	7	+1	9	+2	7	–2
27	Nizhny Novgorod Oblast						7	+7	11	+4	12	+1	10	–2	8	–2	12	+4	10	–2	11	+1	10	–1	12	+2	12	0	5	–7	7	+2	7	0	9	+2	8	–1
28	Republic of Tatarstan		3	+3	1	–2	3	+2	12	+9	16	+4	9	+7	6	–3	6	0	4	–2	1	–3	3	+2	4	+1	15	+11	21	+6	35	+14	52	+17	68	+16	59	–9
29	Republic of Bashkorto-stan								2	+2	7	+5	14	+7	18	+4	19	+1	14	+5	20	+6	22	+2	20	–2	24	+4	18	–6	21	+3	20	–1	20	0	19	–1
30	Orenburg Oblast																		3	+3	8	+5	9	+1	8	–1	11	+3	1	–10	4	+3	5	+1	11	+6	10	–1
31	The Republic of Sakha (Yakutia)																				2	+2	4	+2	4	0	3	–1	0	–3	0	0	1	+1	0	–1	2	+2
32	Primorsky Krai																														3	+3	7	+4	7	0	10	+3
33	Perm Krai																																1	+1	3	+2	3	0
34	Khabarovsk Krai																																		7	+7	7	0
35	Republic of Buryatia																																				1	+1
36	Burnasyan Federal Medical and Biophysical Center, Moscow														6	+6	11	+5	14	+3	16	+2	9	–7	5	–4	1	–4	1	0	3	+2	2	–1	1	–1	2	+1
37	Burnasyan Federal Medical and Biophysical Center, Krasnoyarsk																								24	Note	16	–8	8	–8	10	+2	13	+3	9	–4	5	–4
	TOTAL in the Russian Federation	**225**	**300**	**+75**	**364**	**+64**	**381**	**+17**	**487**	**+106**	**470**	**–17**	**412**	**–58**	**420**	**+8**	**465**	**+45**	**434**	**–31**	**499**	**+53**	**565**	**+78**	**639**	**+74**	**732**	**+93**	**564**	**–168**	**652**	**+88**	**763**	**+111**	**917**	**+154**	**975**	**+58**

Note. The donor activity of Federal Siberian Research and Clinical Center in Krasnoyarsk is presented as a separate program.

KIDNEY TRANSPLANTATION

In 2024, a total of 1,943 kidney transplants (KT) were performed in the Russian Federation (Fig. 6), representing a 6.9% increase (+126) compared to 2023. KT were carried out across 49 centers nationwide. Of these, 1,720 transplants were from deceased donors, while 223 were from living related donors (Fig. 6).

Activity levels varied across centers: 10 centers performed >50 operations per year, 10 centers performed between 30–49, 11 centers performed between 15–29, and 19 centers (38.8%) carried out fewer than 15 transplants annually.

Table 6 and Fig. 7 present the centers with the highest transplant volumes in 2024. The ranking highlights the strong performance of leading Moscow-based transplant programs, supported by effective coordination of the Moscow Coordinating Center for Organ Donation.

Overall, Moscow and Moscow Oblast accounted for 1,049 KT (53.4% of the national total – 1,943).

Kidney transplant centers outside Moscow also demonstrated growth in 2024, with notable increases in activity in St. Petersburg, Volgograd Oblast, Orenburg Oblast, Stavropol Krai, Novosibirsk Oblast, Kemerovo Oblast (Kuzbass), and Krasnoyarsk Krai, among others.

In 2024, 23 centers (46.9%) performed KT from living related donors, totaling 223 procedures. However, only six centers carried out seven or more such operations: Shumakov National Medical Research Center of Transplantology and Artificial Organs (106) and its branch (21), Orenburg Regional Clinical Center for Surgery and Traumatology (15), Petrovsky National Research

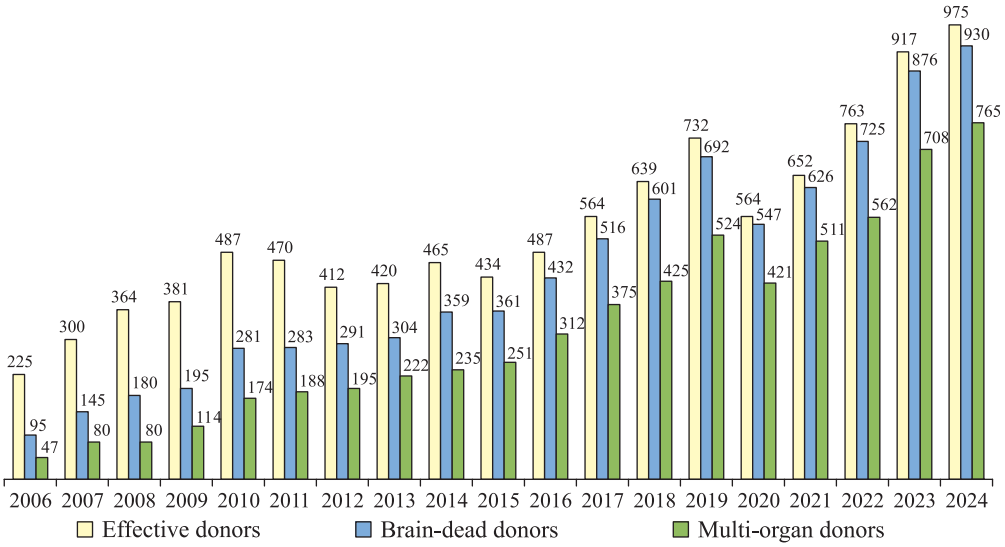

Fig. 5. Structure of effective organ donors in the Russian Federation (2006–2024)

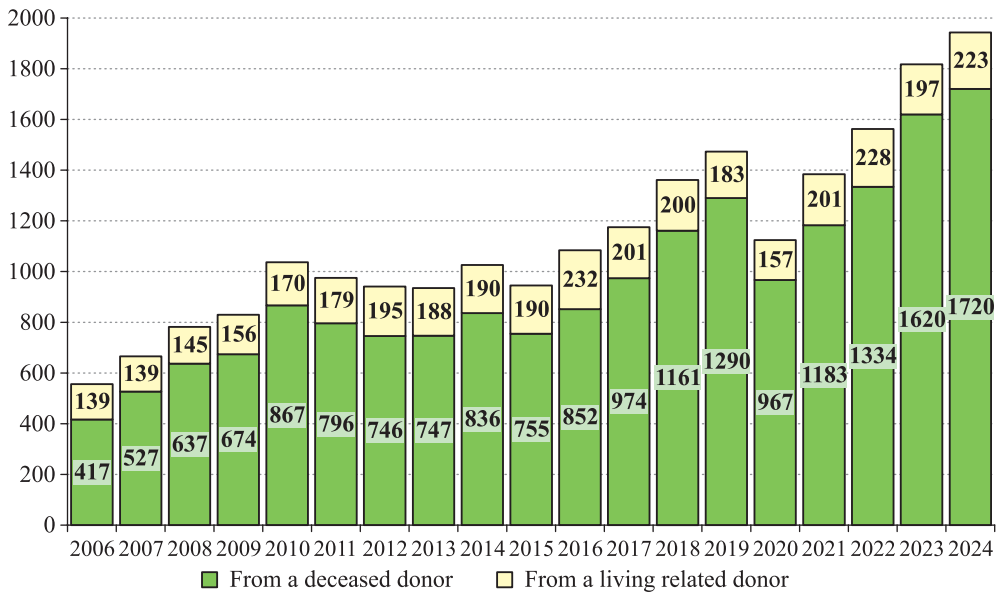

Fig. 6. Trends in kidney transplantation in the Russian Federation (2006–2024)

Centre of Surgery (9), State Novosibirsk Regional Clinical Hospital (9), and National Medical Research Center for Children's Health (7).

Altogether, the Shumakov Center and its branch accounted for 127 operations (56.9% of all related KT in the country). On average, living donor KT represented 11.5% of all KT in 2024, compared with 10.8% in 2023.

Pediatric KT (recipients under 17 years) were performed in 11 centers, totaling 124 procedures. The leading centers were: Shumakov Center and its branch (66), Russian Children's Clinical Hospital (30), and National Medical Research Center for Children's Health (20) (Fig. 8).

EXTRARENAL ORGAN TRANSPLANTATION

In 2024, 426 heart transplants (HT) were performed in the Russian Federation, including 25 pediatric transplants and 2 combined heart–lung transplants carried out

Table 6

Leading kidney transplant centers in the Russian Federation, 2024

Rank	Medical institutions	Number of kidney transplants in 2024
1	Shumakov National Medical Research Center of Transplantology and Artificial Organs, Moscow	303
2	Sklifosovsky Research Institute for Emergency Medicine, Moscow	265
3	Botkin Hospital, Moscow	147
4	Republican Clinical Hospital, Kazan	99
5	Lopatkin Research Institute of Urology and Interventional Radiology – a branch of the National Medical Research Radiological Center, Moscow	82
6	Belyaev Kuzbass Regional Clinical Hospital, Kemerovo	71
7	Volzhsky Branch of Shumakov National Medical Research Center of Transplantology and Artificial Organs, Volzhsky	70
8	St. Petersburg Research Institute of Emergency Medicine, St. Petersburg	60
9	Vladimirsky Moscow Regional Research and Clinical Institute, Moscow	60
10	Samara State Medical University, Samara	55
	TOTAL	**1212**
	62.4% of the total number of kidney transplants in the Russian Federation (1943)	

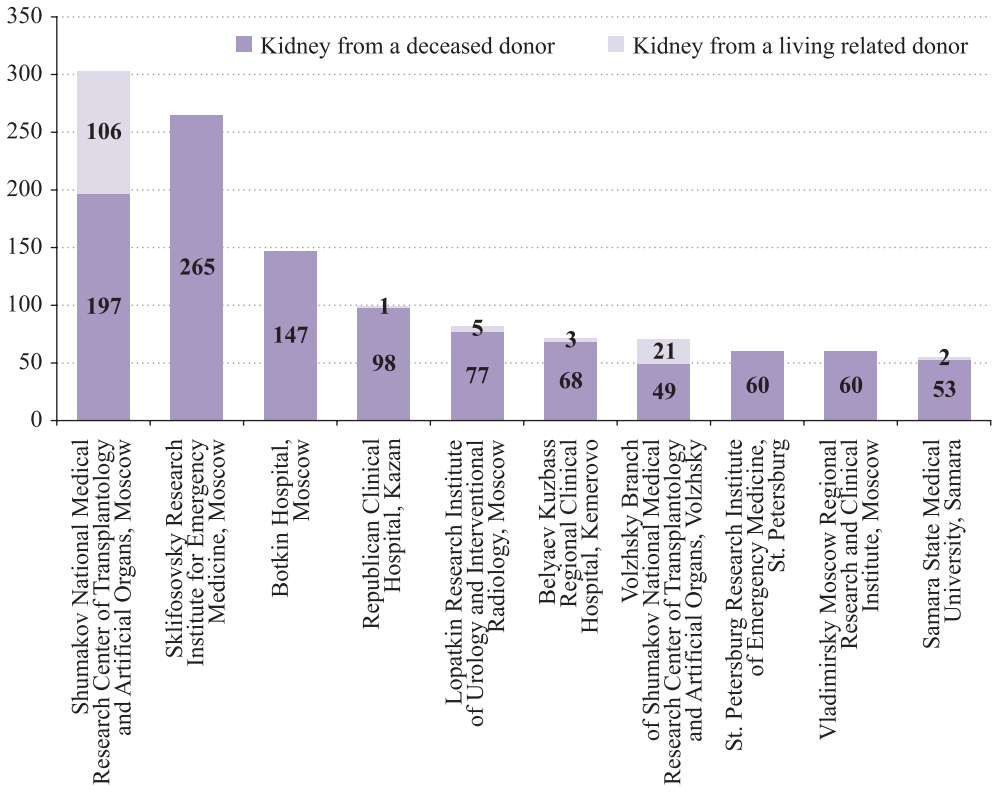

Fig. 7. Leading kidney transplant centers in the Russian Federation, 2024

at Shumakov Center. Compared to 2023, the number of HT increased by 9.8% (+38 procedures).

Heart transplants were carried out across 21 centers, with a new program launched in Naberezhnye Chelny, Republic of Tatarstan (Emergency Medical Care Hospital).

The Shumakov Center in Moscow remains the leading institution, performing 279 HT, along with 17 in its Volzhsky branch, representing 69.5% of all procedures nationwide (426 in total, including 2 heart–lung and 21 pediatric transplants). The program at this center continues to define the overall level of accessibility to heart transplantation in Russia. Other centers performing ≥10 HT in 2024 included Almazov National Medical Research Centre, St. Petersburg (38, Interregional Clinical Diagnostic Center in Kazan (17), Volzhsky Branch of Shumakov Center (17), Meshalkin National Medical Research Center in Novosibirsk (10), Clinical Hospital No. 1 in Krasnoyarsk (10), and the Research Institute for Complex Issues of Cardiovascular Diseases in Kemerovo (10).

In 2024, three additional transplant centers performed between 5 and 9 heart transplants: Botkin Hospital (9), Emergency Medical Center at Naberezhnye Chelny (6), and the Ufa Regional Clinical Hospital (5). The remaining 11 centers (52.4%) carried out fewer than 5 heart transplants each.

There was continued growth in activity at several leading programs: in St. Petersburg, the number of heart transplants rose from 33 to 38, and at the Volzhsky branch of Shumakov Center, the number increased from 12 to 17.

Table 7 and Fig. 9 present the thoracic organ transplant centers with the highest number of heart-lung transplants in 2024.

In 2024, 25 pediatric HT were performed in four centers (*vs* 17 in 2023): Shumakov Center (21), Bakulev National Medical Research Center for Cardiovascular Surgery (1), Almazov National Medical Research Centre (2), and Meshalkin National Medical Research Center (1).

In 2024, 33 lung transplants were performed in three centers (*vs* 19 in 2023): Shumakov Center (20), Sklifosovsky Research Institute of Emergency Care (11), and Regional Clinical Hospital No. 1 Krasnodar (2).

In addition, two more heart-lung transplants were performed at Shumakov Center.

In 2024, a total of 894 liver transplants (LiV) were performed in the Russian Federation, including 132 pediatric transplants. Procedures were carried out across 38 centers, representing a 7.8% increase (+65) compared with 2023 (829).

Two new programs for deceased-donor LiV were launched in 2024: Volosevich First City Clinical Hospital, Arkhangelsk, and Novokuznetsk branch of Barbarash Kuzbass Clinical Cardiological Center, Novokuznetsk.

The distribution of activity among centers highlights significant concentration in leading programs. Two centers performed ≥100 LiV: Shumakov Center (187) and Sklifosovsky Research Institute for Emergency Medicine (135). Four centers performed ≥40 LiV: A.S. Loginov Moscow Clinical Scientific Center (81), Botkin Hospital (68), Regional Clinical Hospital, Kazan (56), and Novosibirsk Regional Clinical Hospital (47).

Seven centers performed between 15 and 40 LiV, while the remaining 25 centers (65.8%) conducted fewer than 15 LiV per year.

Table 8 and Fig. 10 present the transplant centers that performed the highest number of LiV in 2024. The ranking underscores the leadership of the major Moscow

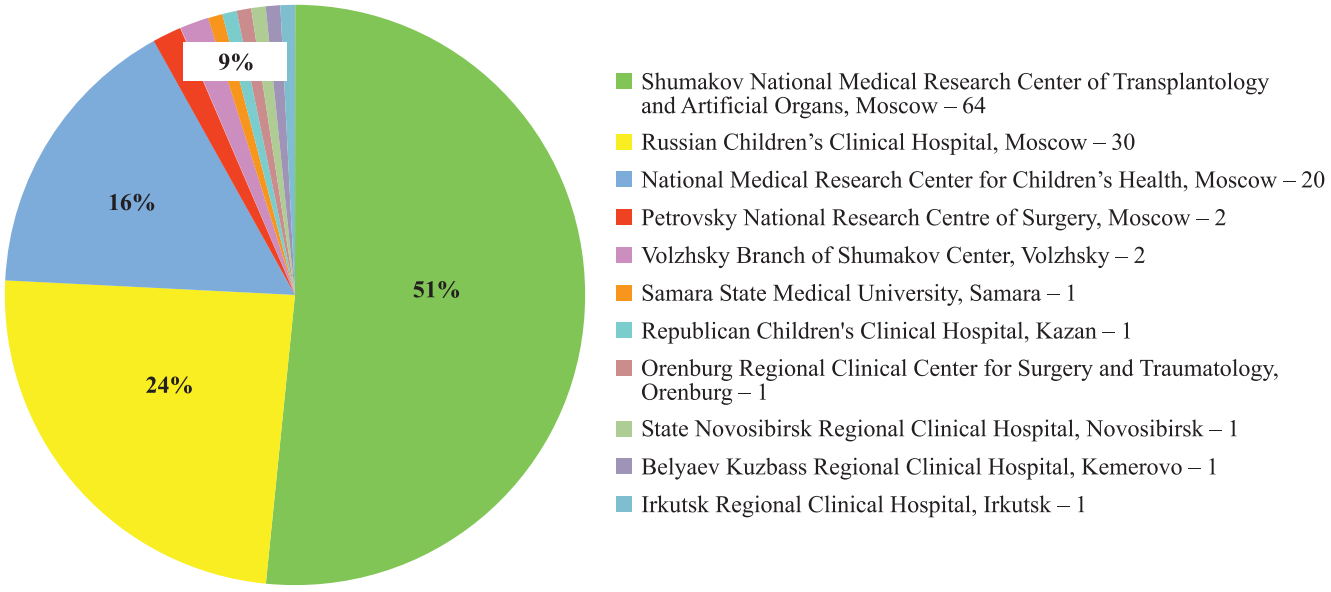

Fig. 8. Pediatric kidney transplantation in the Russian Federation, 2024

programs, reflecting the effective work of the Moscow Coordination Center for Organ Donation and the use of advanced techniques, including living donor partial liver transplantation. Positive dynamics were also observed in the development of transplant programs in St. Petersburg, Novosibirsk Oblast, and Kemerovo Oblast (Kuzbass), while Shumakov Center continues to play a leading role in pediatric living-donor LiV.

In 2024, related living-donor LiV were performed at 10 centers (26.3%), with a total of 167 operations. Only four centers conducted ≥10 procedures per year: Shumakov Center (104), Burnazyan Federal Medical and Biophysical Center (25) Novosibirsk Regional Clinical Hospital (18), and Petrovsky National Research Centre of Surgery (10).

Overall, 62.3% of all related liver transplants in Russia were carried out at Shumakov Center. The average share of living donor LiV in 2024 was 18.7% of all liver transplants, slightly lower than in 2023 (19.3%).

Table 7

Leading heart transplant centers in the Russian Federation, 2024

Rank	Medical institutions	Number of heart transplants in 2024
1	Shumakov National Medical Research Center of Transplantology and Artificial Organs, Moscow	279
2	Almazov National Medical Research Centre, St. Petersburg	38
3	Volzhsky Branch of Shumakov National Medical Research Center of Transplantology and Artificial Organs, Volzhsky	17
4	Interregional Clinical and Diagnostic Center, Kazan	17
5	Research Institute for Complex Issues of Cardiovascular Diseases, Kemerovo	10
6	Meshalkin National Medical Research Center, Novosibirsk	10
7	Krasnoyarsk Regional Clinical Hospital, Krasnoyarsk	10
8	Botkin Hospital, Moscow	9
9	Emergency Care Medical Center, Naberezhnye Chelny	6
10	Republican Cardiological Center, Ufa	5
	TOTAL	**401**
	94.1% of the total number of heart transplants performed in the Russian Federation (426)	

* – including 2 heart-lung transplants.

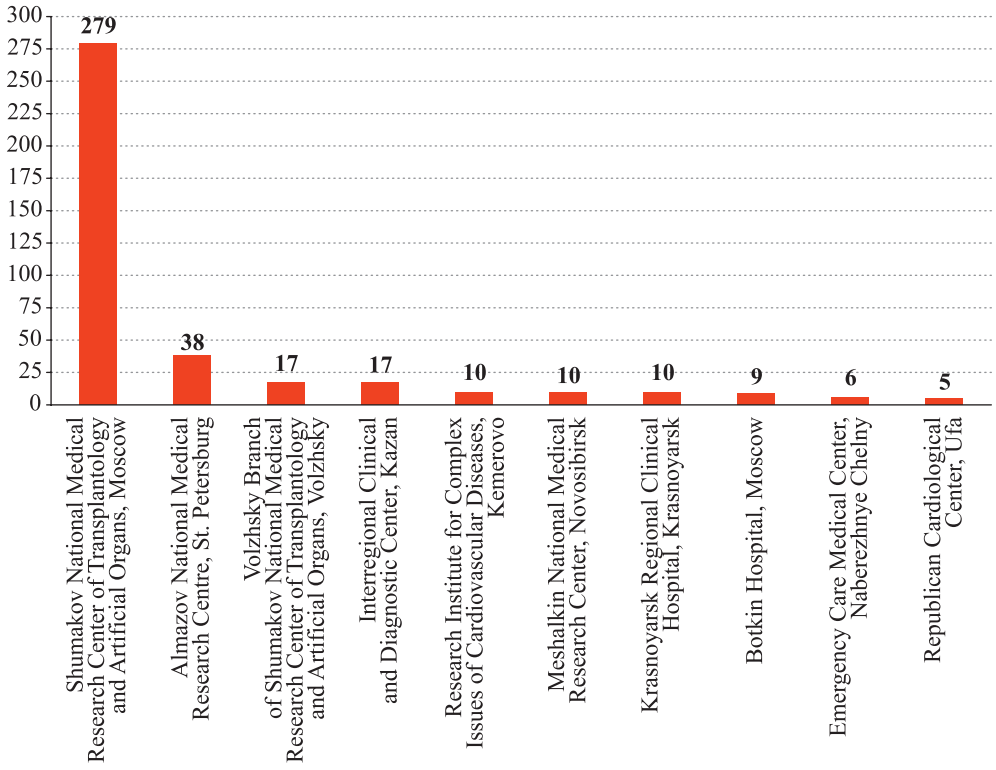

Fig. 9. Leading heart transplant centers in the Russian Federation, 2024

In 2024, a total of 132 pediatric LiV were performed, primarily in younger children. These were carried out in five centers: Shumakov Center (113), Volzhsky branch of the Shumakov Center (2), Russian Children's Clinical Hospital (1), Petrovsky National Research Centre of Surgery (10), and Novosibirsk Regional Clinical Hospital (6).

The Shumakov Center and its branch accounted for 87.1% of all pediatric LiV in 2024. The pediatric program at this center continues to define the overall availability and accessibility of this type of transplant care in the Russian Federation.

Pancreas transplants (PaT) were performed at three centers: Shumakov Center (5), Sklifosovsky Research Institute of Emergency Care (3), and Rostov Regional Clinical Hospital, Rostov-on-Don (2). In total, 10 PaT were carried out in 2024 (3 in 2023), all in combination with a kidney transplant. In addition, the Sklifosovsky Research Institute of Emergency Care performed one small bowel transplant.

Table 8

Leading liver transplant centers in the Russian Federation, 2024

Rank	Medical institutions	Number of liver transplants in 2024
1	Shumakov National Medical Research Center of Transplantology and Artificial Organs, Moscow	187
2	Sklifosovsky Research Institute for Emergency Medicine, Moscow	135
3	Loginov Moscow Clinical Research Center, Moscow	81
4	Botkin Hospital, Moscow	68
5	Republican Clinical Hospital, Kazan	56
6	State Novosibirsk Regional Clinical Hospital, Novosibirsk	47
7	Burnasyan Federal Medical and Biophysical Center, Moscow	39
8	Vladimirsky Moscow Regional Research and Clinical Institute, Moscow	30
9	Russian Research Center for Radiology and Surgical Technologies, St. Petersburg	22
10	Irkutsk Regional Clinical Hospital, Irkutsk	21
	TOTAL	**686**
	76.7% of the total number of liver transplants performed in the Russian Federation (894)	

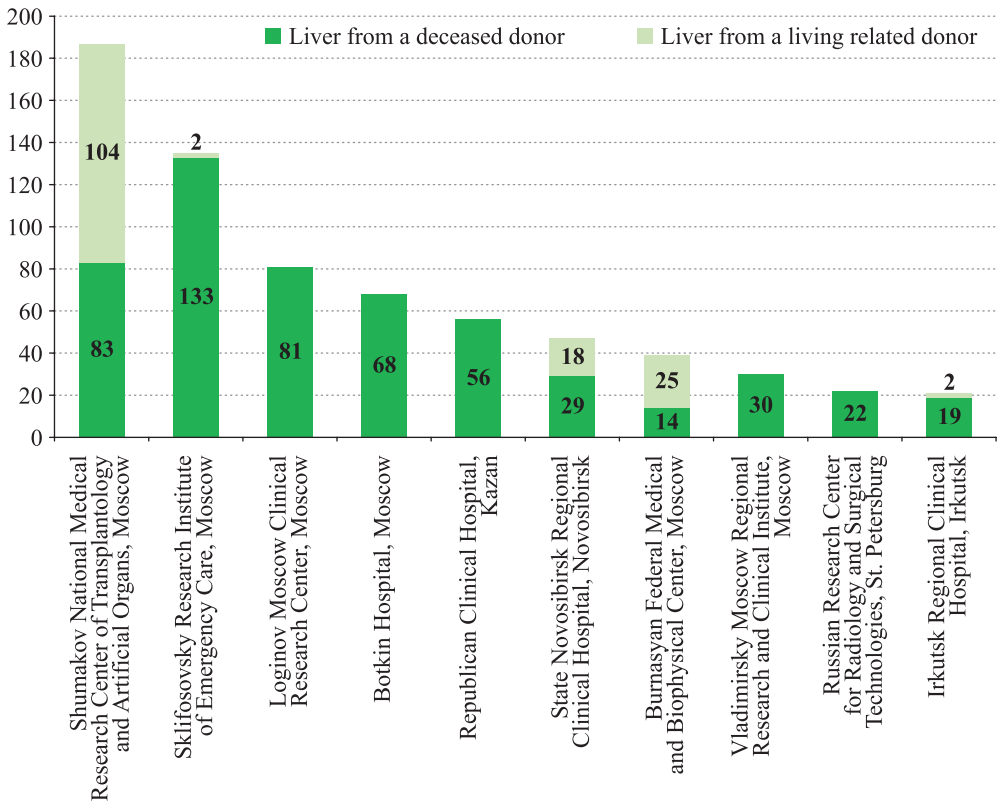

Fig. 10. Leading liver transplant centers in the Russian Federation, 2024

The total number of extra-renal transplants in 2024 reached 1,364, representing 41.2% of all transplants (3,307), compared with 1,240 (40.6%) in 2023. The Moscow agglomeration accounted for 918 procedures (67.3%) of these extra-renal transplants.

Since the beginning of the observation period in 2006, the number of extra-renal organ transplants in Russia has increased by 1,258 procedures, representing a 12.9-fold growth (Figs. 11 and 12).

Table 9 presents the dynamics of organ transplantation in the Russian Federation for the period 2006–2024.

ORGAN TRANSPLANT RECIPIENTS

As of December 2024, the number of patients living with transplanted organs in the Russian Federation was estimated at 22,750 (Table 10). Over the past ten years of follow-up, this number has increased 2.6-fold. The distribution by organ type is as follows: kidney transplants – 15,162 patients (103.8 p.m.p.), liver transplants – 5,150 patients (35.3 p.m.p.), and heart transplants – 2,332 patients (16.0 p.m.p.).

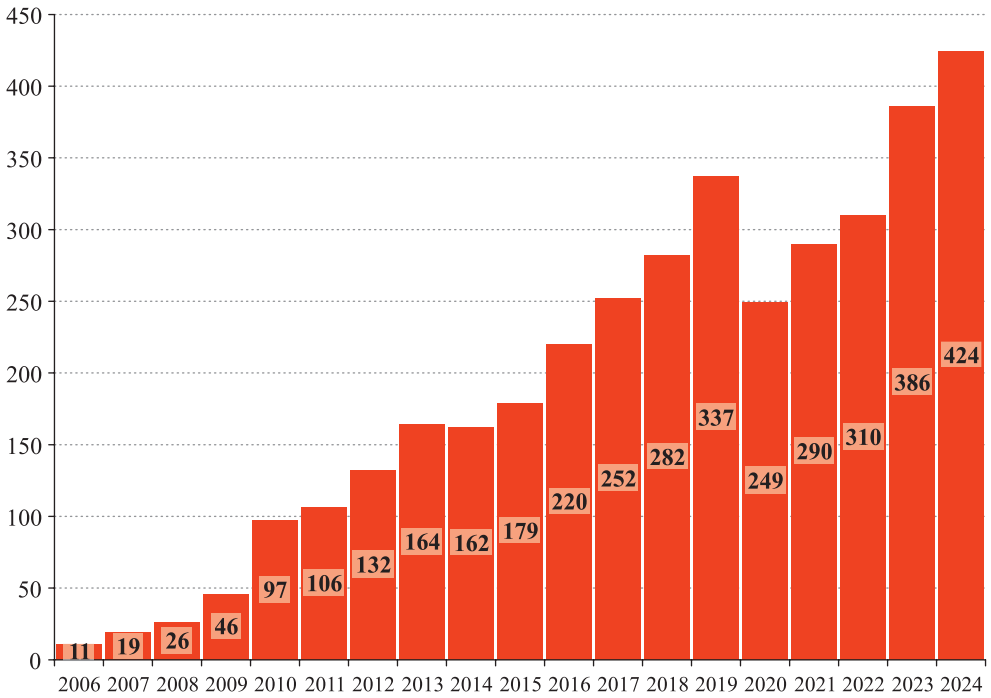

Fig. 11. Heart transplantation in the Russian Federation (2006–2024)

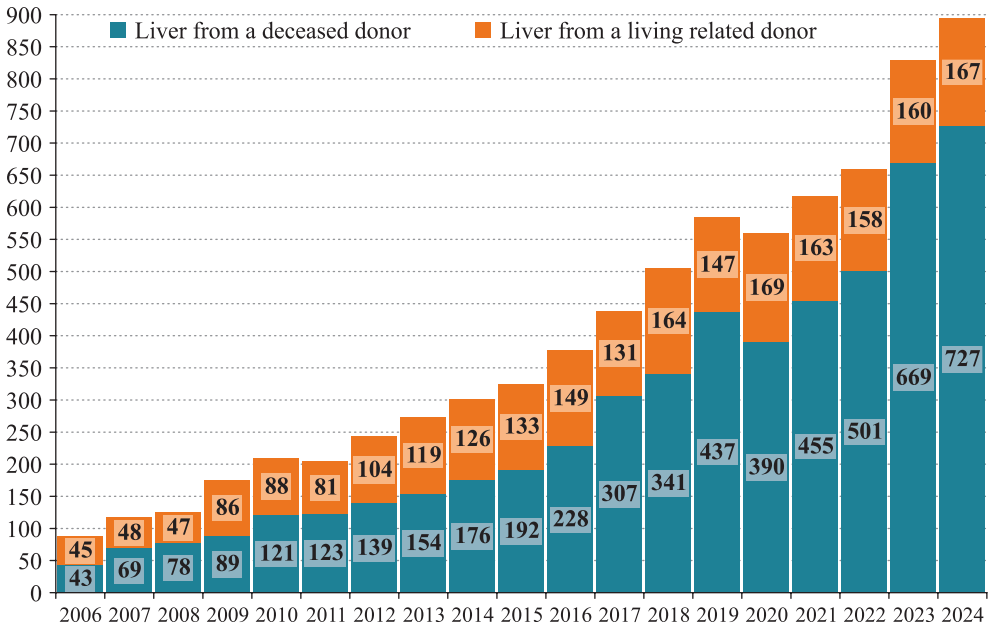

Fig. 12. Liver transplantation in the Russian Federation (2006–2024)

Table 9

Trends in organ transplantation in the Russian Federation, 2006–2024

#	Organ	2006	2007		2008		2009		2010		2011		2012		2013		2014		2015		2016		2017		2018		2019		2020		2021		2022		2023		2024	
		Absolute number	Absolute number	Year-over-year change	Absolute number	Year-over-year change	Absolute number	Year-over-year change	Absolute number	Year-over-year change	Absolute number	Year-over-year change	Absolute number	Year-over-year change	Absolute number	Year-over-year change	Absolute number	Year-over-year change	Absolute number	Year-over-year change	Absolute number	Year-over-year change	Absolute number	Year-over-year change	Absolute number	Year-over-year change	Absolute number	Year-over-year change	Absolute number	Year-over-year change	Absolute number	Year-over-year change	Absolute number	Year-over-year change	Absolute number	Year-over-year change
1	Total number of kidneys transplanted	556	666	+110	782	+116	830	+48	1037	+207	975	–62	941	–34	935	–6	1026	+91	945	–81	1084	+139	1175	+91	1361	+186	1473	+112	1124	–349	1382	+258	1562	+180	1817	+255	1943	+126
2	*from deceased donors*	417	527	+110	637	+110	666	+29	867	+201	796	–71	746	–50	747	+1	836	+89	755	–81	852	+97	974	+122	1161	+187	1290	+129	967	–323	1183	+216	1334	+151	1620	+286	1720	+100
3	*from living-related donors*	139	139	0	145	+6	156	+11	170	+14	179	+9	195	+16	188	–7	190	+2	190	0	232	+42	201	–31	200	–1	183	–17	157	–26	201	+44	228	+27	197	–31	223	+26
4	Total number of livers transplanted	88	117	+29	125	+8	175	+50	209	+34	204	–5	243	+39	272	+29	302	+30	325	+23	378	+53	438	+60	505	+67	584	+79	559	–25	618	+59	659	+41	829	+170	894	+65
5	*from deceased donors*	43	69	+26	78	+9	89	+11	121	+32	123	+2	139	+16	154	+15	176	+22	192	+16	229	+37	307	+78	341	+34	437	+96	390	–47	455	+65	501	+46	669	+168	727	+58
6	*from living-related donors*	45	48	+3	47	–1	86	+39	88	+2	81	–7	104	+23	119	+15	126	+7	133	+7	149	+16	131	–18	164	+33	147	–17	169	+22	163	–6	158	–5	160	+2	167	+7
7	Heart	11	19	+8	26	+7	46	+20	97	+51	106	+9	132	+26	164	+32	162	–2	179	+17	220	+41	252	32	282	+30	335	+53	249	–86	290	+41	308	+18	386	+78	424	+38
8	Pancreas	6	11	+5	9	–2	8	–1	19	+11	14	–5	23	+9	14	–9	19	+5	12	–7	6	–6	6	0	17	+11	10	–7	16	+6	10	–6	10	0	3	–7	10	+7
9	Lungs	1	0	–1	0	0	1	+1	1	0	6	+5	5	–1	10	+5	12	+2	14	+2	16	+2	25	+9	25	0	23	–2	9	–14	13	+4	14	+1	19	+5	33	+14
10	Heart-lung										2	+2	2	0	1	–1	0	–1	0	0	0	0	0	0	3	+3	2	–1	2	0	2	0	1	–1	2	+1	2	0
11	Small intestine														1	+1	1	0	0	–1	0	0	0	0	0	0	0	0	1	+1	1	0	0	–1	1	+1	1	0
	Total	662	813	+151	942	+129	1060	+118	1363	+303	1307	–56	1345	+38	1400	+55	1522	+122	1485	–37	1704	+219	1896	+192	2193	+297	2427	+234	1960	–467	2318	+358	2555	+237	3057	+502	3307	+250

Table 10

Annual number of organ transplant recipients in the Russian Federation, 2013–2024

ICD-10 code	Annual Number of organ transplant recipients, persons																				
	2013	2014		2015		2016		2017		2018		2019		2020		2021*		2022*		2023*		2024*	
		abs.	change (%)	abs.	change (%)	abs.	change (%)	abs.	change (%)	abs.	change (%)	abs.	change (%)	abs.	change (%)	abs.	change (%)	abs.	change (%)	abs.	change (%)	abs.	change (%)
Z94.0 Kidney transplant status	6651	7502	12.8	8164	8.8	9063	11.0	9658	6.6	10,851	12.4	11,880	9.5	12,563	5.7	12,969	–	13,514	–	14,258	–	15,162	–
Z94.1 Heart transplant status	416	520	25.0	639	22.9	803	25.7	952	18.6	1164	22.3	1355	16.4	1524	12.5	1687	–	1855	–	2084	–	2332	–
Z94.2 Lung transplant status	2	3	50.0	4	33.3	5	25.0	8	60.0	28	250.0	26	–7.1	24	–7.7	–	–	–	–	–	–	–	–
Z94.4 Liver transplant status	1150	1406	22.3	1649	17.3	1948	18.1	2152	10.5	2632	22.3	3032	15.2	3489	15.1	3820	–	4165	–	4644	–	5150	–
Z94.8 Other transplanted organ and tissue status (bone marrow, intestines, pancreas)	334	467	39.8	654	40.0	808	23.5	909	12.5	1135	24.9	1344	18.4	1497	11.4	–	–	–	–	–	–		–
TOTAL	8553	9898	15.7	11,110	12.2	12,627	13.7	13,679	8.3	15,810	15.6	17,637	11.6	19,097	8.3	–	–	–	–	–	–		–

* – The number of organ transplant recipients is estimated as it is calculated from the figures of the previous year based on data on the number of organ transplants in 2021-2024 and data on average patient survival.

CONCLUSION

In 2024, the number of organ transplants in the Russian Federation increased by 8.2% (+250) compared to the record year of 2023, consolidating the achievements of previous years. By organ type, kidney transplants increased by 6.9% (+126), heart transplants increased by 7.8% (+38), liver transplants increased by 25.8% (+65). The number of effective post-mortem donors also rose by 6.3% (+58) compared to 2023.

In 2024, the primary goals and trends in the development of organ donation and transplantation across the various regions in the Russian Federation remained consistent and highly relevant:

– expansion of the geographic footprint and increase in the number of transplant centers;
– efficient identification of patients in need of transplantation and their inclusion in the waiting list, supported by the use of information systems and registries;
– increase in the number of deceased organ donors in line with available donor resources, with justified expansion of donor criteria and a higher proportion of multi-organ donors;
– increase in the number of organ transplants to meet the actual needs of the population, including the introduction of extra-renal transplant technologies;
– a focus on providing transplant care to the pediatric population;
– 100.0% coverage of medical screening, including medication support and laboratory monitoring, for transplant recipients.

Current trends also include the accumulation of positive experience and wider adoption of advanced practices, such as the use of perfusion systems for rehabilitating organs from suboptimal donors and the application of long-term mechanical circulatory support systems as a bridge to heart transplantation in children.

In 2024, several new organ transplant programs were launched:

At Emergency Medical Center (Naberezhnye Chelny, Republic of Tatarstan), 6 heart transplants were performed.

At Republican Clinical Hospital (Kazan, Republic of Tatarstan), a deceased-donor kidney transplant was performed on a child.

At Volosevich First City Clinical Hospital (Arkhangelsk, Arkhangelsk Oblast), 2 deceased-donor liver transplants were performed.

At the Novokuznetsk branch of Barbarash Kuzbass Clinical Cardiological Center (Novokuznetsk, Kemerovo Oblast – Kuzbass), 1 deceased-donor liver transplant was performed.

Moscow remains the undisputed leader in terms of organ donation and transplantation in the Russian Federation, consistently demonstrating donor and transplant activity at a level comparable to global standards. Among the regions, the Republic of Tatarstan, Kemerovo Oblast (Kuzbass), St. Petersburg and Leningrad Oblast, Novosibirsk Oblast, Krasnoyarsk Krai, and the Volzhsky branch of Shumakov Center (Volzhsky, Volgograd Oblast) also demonstrate high activity.

Shumakov Center and its branch in Volzhsky together account for 27.1% of all organ transplants performed in the country, 56.9% of related kidney transplants, 69.5% of heart transplants, and 62.3% of related liver transplants.

The Shumakov Center also houses a specialized unit for improving medical care in the field of nephrology. Its priority tasks include timely identification of patients requiring kidney transplantation, harmonization of renal replacement therapy modalities, and enhancement of long-term monitoring of kidney recipients. This nephrology monitoring program is closely integrated with the national transplant registry.

Further increasing donor activity remains a priority task for most regions in the Russian Federation where organ donation and transplantation are organized. Achieving this goal requires oversight by regional health authorities and adequate financial support for medical activities related to organ donation.

In 2024, the average proportion of effective brain-dead organ donors in the Russian Federation exceeded 95.0%, while that of multi-organ donors was above 75.0%. These indicators reflect the efficient use of donor resources in most regions actively engaged in organ donation activities.

Overall, the number of organ transplants in the Russian Federation continues to grow steadily. The existing capacity of medical institutions performing donor and recipient surgeries provides a solid foundation for further expansion of transplant care, provided that adequate funding, systematic work with the waiting list, and sustained support for donor programs are ensured.

The authors declare no conflict of interest.

REFERENCES

1. Organ donation and transplantation in Russian Federation in 2009. *Transplantology 2009: results and prospects*. Vol. I / Ed. by S.V. Gautier. M.–Tver: Triada, 2010: 8–20.
2. Organ donation and transplantation in Russian Federation in 2006–2010. *Transplantology: results and prospects*. Vol. II. 2010 / Ed. by S.V. Gautier. M.–Tver: Triada, 2011: 18–32.
3. Organ donation and transplantation in Russian Federation in 2011 (IV report of National Registry). *Transplantology: results and prospects*. Vol. III. 2011 / Ed. by S.V. Gautier. M.–Tver: Triada, 2012: 14–37.
4. Organ donation and transplantation in Russian Federation in 2012. (V report of National Registry). *Transplantology: results and prospects*. Vol. IV. 2012 / Ed. by S.V. Gautier. M.–Tver: Triada, 2013: 8–28.

5. Organ donation and transplantation in Russian Federation in 2013 (VI report of National Registry). *Transplantology: results and prospects*. Vol. V. 2013 / Ed. by S.V. Gautier. M.–Tver: Triada, 2014: 32–57.
6. Organ donation and transplantation in Russian Federation in 2014 (VII report of National Registry). *Transplantology: results and prospects*. Vol. VI. 2014 / Ed. by S.V. Gautier. M.–Tver: Triada, 2015: 44–75.
7. Organ donation and transplantation in Russian Federation in 2015 (VIII report of National Registry). *Transplantology: results and prospects*. Vol. VII. 2015 / Ed. by S.V. Gautier. M.–Tver: Triada, 2016: 38–71.
8. Organ donation and transplantation in Russian Federation in 2016 (IX report of National Registry). *Transplantology: results and prospects*. Vol. VIII. 2016 / Ed. by S.V. Gautier. M.–Tver: Triada, 2017: 33–66.
9. Organ donation and transplantation in Russian Federation in 2017 (X report of National Registry). *Transplantology: results and prospects*. Vol. IX. 2017 / Ed. by S.V. Gautier. M.–Tver: Triada, 2018: 26–63.
10. Organ donation and transplantation in Russian Federation in 2018 (XI report of National Registry). *Transplantology: results and prospects*. Vol. X. 2018 / Ed. by S.V. Gautier. M.–Tver: Triada, 2019: 46–85.
11. Organ donation and transplantation in Russian Federation in 2019 (XII report of National Registry). *Transplantology: results and prospects*. Vol. XI. 2019 / Ed. by S.V. Gautier. M.–Tver: Triada, 2020: 52–93.
12. Organ donation and transplantation in Russian Federation in 2020 (XIII report of National Registry). *Transplantology: results and prospects*. Vol. XII. 2020 / Ed. by S.V. Gautier. M.–Tver: Triada, 2021: 22–63.
13. Organ donation and transplantation in Russian Federation in 2021 (XIV report of National Registry). *Transplantology: results and prospects*. Vol. XIII. 2021 / Ed. by S.V. Gautier. M.–Tver: Triada, 2022: 38–72.
14. Organ donation and transplantation in Russian Federation in 2022 (XV report of National Registry). *Transplantology: results and prospects*. Vol. XIV. 2022 / Ed. by S.V. Gautier. M.–Tver: Triada, 2023: 25–59.
15. Organ donation and transplantation in Russian Federation in 2023 (XVI report of National Registry). *Transplantology: results and prospects*. Vol. XV. 2023 / Ed. by S.V. Gautier. M.–Tver: Triada, 2024: 35–70.

The article was submitted to the journal on 15.07.2025

DOI: 10.15825/1995-1191-2025-3-33-45

EVOLUTION OF PEDIATRIC LIVER TRANSPLANT: FROM INCEPTION TO MODERN PRACTICE

A.R. Monakhov[1, 2], S.V. Gautier[1, 2], O.M. Tsirulnikova[1, 2]

[1] Shumakov National Medical Research Center of Transplantology and Artificial Organs, Moscow, Russian Federation

[2] Sechenov University, Moscow, Russian Federation

This article explores the historical development of pediatric liver transplantation (LT), tracing its evolution from the first experimental procedures to modern high-tech approaches. Throughout its history, LT in children has been a catalyst for innovation and novel surgical techniques. The earliest attempts at pediatric LT faced numerous technical and immunological challenges and were associated with extremely high mortality rates. A major breakthrough occurred in the 1980s with the introduction of cyclosporine A. During this period, pioneering advances such as reduced-size grafts, split-liver transplantation, and the first successful living-related donor procedures marked a new era. The 1990s witnessed further progress in surgical techniques, introduction of tacrolimus, and the development of right-lobe living donor transplantation. These innovations not only expanded the donor pool significantly but also improved surgical outcomes. Entering the 21st century, the field experienced further breakthroughs with the implementation of ABO-incompatible transplantation and the adoption of MELD and PELD scoring systems for organ allocation. In addition, the integration of minimally invasive laparoscopic and robot-assisted approaches reduced donor morbidity and improved postoperative recovery. Today, pediatric LT is recognized not only as a life-saving treatment for end-stage liver failure in children but also as a driving force of innovation in modern transplant practice. The article underscores the importance of continuous refinement of surgical techniques and personalization of immunosuppressive regimens as key strategies to improve long-term survival and enhance the quality of life in pediatric LT recipients.

Keywords: pediatric liver transplantation, history, innovations, donation, immunosuppression.

INTRODUCTION

The development of liver transplantation (LT), one of the landmark achievements of 20th-century medicine, is inextricably linked to pediatric practice. In many respects, pediatric LT not only adapted technologies from adult surgery but also served as a true catalyst for innovation in this complex field. It is remarkable that the very first attempts at human LT – marked by both tragic failures and the first glimmers of hope – were carried out in children [1, 2]. This fact lent a special ethical and dramatic dimension to the discipline, as it was about saving the lives of young patients for whom other treatment methods had been exhausted.

Unlike other areas of surgery and transplantology, where pioneering procedures were initially performed on adults and only later extended to children, LT from the outset accounted for the unique anatomical, physiological, and nosological characteristics of the pediatric population [3]. The urgent need to treat children with end-stage liver disease largely determined the key directions of transplant hepatology.

The challenge of adapting adult donor organs to small recipients spurred the development of groundbreaking surgical techniques. The introduction of the reduced-size liver graft, first applied in children, represented a major breakthrough that laid the foundation for wider clinical use [4, 5]. This pioneering concept subsequently gave rise to further advances such as split-liver transplantation, enabling a single donor organ to serve both an adult and a child, and living-related donor liver fragment transplantation, which has revolutionized therapeutic strategies not only in pediatrics but also in adult practice [6, 7].

Moreover, in-depth study of the unique features of the pediatric immune system – its plasticity and capacity for tolerance – led to the development of protocols for LT across ABO-incompatible barriers, thereby further expanding the therapeutic options available for saving young patients [8, 9]. Thus, throughout its history, pediatric LT has not been a passive recipient of advances in "adult" medicine but has acted as a powerful engine of progress, driving the search for unconventional solutions and broadening the overall horizons of transplantation. Some of the most important historical milestones along this path will be discussed below.

Corresponding author: Artem Monakhov. Address: 1, Shchukinskaya str., Moscow, 123182, Russian Federation. Phone: (906) 078-16-21. E-mail: a.r.monakhov@gmail.com

EXPERIMENTAL PERIOD AND EARLIEST ATTEMPTS (1950s–1970s)

The historical development of LT in the 1950s–1970s was an intense and often dramatic era, characterized by a shift from bold but largely unsuccessful experimental interventions to the gradual accumulation of knowledge, refinement of surgical techniques, deeper understanding of immune mechanisms, and emergence of the first pharmacological approaches to immunosuppression. This formative stage laid the groundwork for modern transplantology and eventually led to the recognition of LT not merely as an experimental endeavor, but as an effective, life-saving treatment for patients – including children – with end-stage liver disease [10, 11].

A crucial step forward was the extensive series of animal experiments, primarily in dogs, which enabled researchers to refine the fundamental surgical steps of the procedure, study the physiological changes in recipients, and clarify the basic principles governing the function of transplanted organs. Among the pioneers, Thomas Starzl – later known as the "father of transplantology" in Western literature – conducted groundbreaking experiments in Denver, where he developed and standardized the technique of orthotopic LT. His work established the essential stages of hepatectomy in the recipient, followed by implantation of the donor liver with meticulous reconstruction of vascular anastomoses [12].

In parallel, the innovative contributions of our compatriot Vladimir Petrovich Demikhov earned him recognition as the founding father of experimental transplantology. His wide-ranging research, which included pioneering experiments on the head, heart, lungs, kidneys, esophagus, and limbs, as well as creation of artificial circulatory systems, gained worldwide recognition. Importantly, Demikhov also devoted significant attention to LT. In the 1950s, he explored the feasibility of heterotopic LT and even combined LT with other organs such as the adrenal glands and pancreas, investigating their interactions and the potential role of the liver in modulating immune responses [13, 14]. This work significantly enriched the experimental foundation of the field and spurred further scientific exploration in this direction.

The earliest attempts at LT in humans were fraught with immense challenges. Surgeons faced massive, uncontrollable bleeding, driven both by the technical complexity of the procedure and by the severe coagulopathy inherent in patients with liver failure. Transplant rejection, poorly understood at the time, led to rapid graft failure, while postoperative infections, exacerbated by inadequate immunosuppressive therapy, further contributed to the high mortality rates.

A historic milestone was reached in 1963, when Thomas Starzl performed the world's first orthotopic liver transplant in a human. The recipient was a three-year-old child with cirrhosis caused by biliary atresia [1, 12]. Although the surgery itself was technically successful, the child succumbed in the early postoperative period to massive hemorrhage and severe coagulopathy. This case, followed by several other unsuccessful attempts, prompted a temporary moratorium on liver transplants.

Yet, Starzl and his team persisted. On July 23, 1967, they carried out what is regarded as the first successful LT. Once again, the recipient was a child, a one-and-a-half-year-old girl with an extensive malignant liver tumor, most likely hepatoblastoma [12, 15, 16]. Remarkably, she survived for 400 days before dying from recurrence and systemic spread of the cancer. This case proved for the first time that a transplanted liver could function long-term and sustain the recipient's life.

The tragic fate of this little patient, whose portrait reportedly hung above Starzl's bed until his final days, became a symbol of both the formidable obstacles and the extraordinary perseverance of the pioneers of transplantology.

In parallel with their American colleagues, European surgeons were also making early attempts at LT. In 1968, in Cambridge, UK, Sir Roy Calne, another iconic pioneer in the field, performed a liver transplant on a 10-month-old child with biliary atresia. Tragically, the patient died intraoperatively from cardiac arrest [3, 17]. A year later, in Brussels, Jean-Bernard Otte – who would go on to become one of Europe's foremost pediatric transplantologists – carried out a liver transplant in a 15-month-old child with biliary atresia. The patient survived for seven weeks before succumbing to massive bleeding triggered by graft biopsy [3].

By the early 1970s, a modest body of clinical experience in LT had been gathered worldwide, though the outcomes were overwhelmingly negative. One-year survival rates, particularly in pediatric patients, rarely exceeded 30–40% [3, 18]. Still, these pioneering efforts, often undertaken in children because of the absence of therapeutic alternatives, laid the groundwork for future progress. They underscored the critical challenges that needed to be overcome: refinement of surgical techniques, development of effective and safer immunosuppressive strategies, optimization of perioperative care, and prevention of postoperative complications.

However, a transformative breakthrough came in 1972, when Jean-François Borel and Hartmann Stähelin, working at the Swiss pharmaceutical company Sandoz, accidentally discovered cyclosporine A. This substance, isolated from the fungus *Tolypocladium inflatum*, was found to possess highly selective immunosuppressive properties [19, 20]. This event was a turning point, paving the way for new achievements in the following decade.

THE ERA OF CYCLOSPORINE AND THE EMERGENCE OF CLINICAL TRANSPLANTATION (1980s)

The early 1980s ushered in a transformative era for LT and for clinical transplantology as a whole. The decisive breakthrough came with the introduction of cyclosporine A into clinical practice – the first immunosuppressant that was both effective and relatively selective. For the first time, physicians had a drug that could reliably control rejection, dramatically improving both short-term but also long-term graft outcomes [20, 21].

The clinical application of cyclosporine began with Roy Calne's pioneering work in Cambridge on kidney transplantation, where the problem of rejection was particularly acute. The success of these early trials quickly extended to LT, where the benefits proved equally striking [20]. The impact was so profound that, in 1983, the U.S. National Institutes of Health (NIH) convened a consensus conference and formally recognized LT as a clinically valid and effective treatment for end-stage liver disease [22, 23].

This decision was a major milestone, paving the way for wider use of the method, standardization of approaches, and creation of specialized transplant centers.

Paediatric LT during this period faced a set of unique challenges that required innovative solutions. One of the most pressing issues remained the shortage of appropriately sized donor organs, which contributed to persistently high mortality rates among children on waiting lists [3, 24]. The technical complexity of performing transplantation on young patients – with their delicate anatomical structures and limited abdominal cavities – added further obstacles.

Nevertheless, it was the need to save children's lives that continued to stimulate surgical thinking. The concept of reduced-size LT, first pioneered in the late 1970s by Henri Bismuth and others, began to find wider and more consistent application in the 1980s, particularly as outcomes improved in the cyclosporine era [4, 5, 25]. This made it possible to use part of an adult donor's liver for transplantation into a child and somewhat alleviate the growing problem.

Another important achievement, driven by the urgent needs of pediatric recipients, was the first successful split LT, performed in 1988 in Hanover by a German team led by Rudolf Pichlmayr [6, 26]. This groundbreaking procedure made it possible to divide a single donor liver into two functionally independent grafts and transplant them into two recipients – most often an adult and a child. The success of split transplantation was underpinned by advances in the study of segmental liver anatomy, refinement of precision parenchymal transection techniques, and significant improvements in organ preservation methods. Following the Hanover breakthrough, split LT was soon reproduced with success in other leading European centers, notably in Paris and Brussels, which further confirmed the feasibility and promise of the approach [27].

Soviet transplantologists also played a significant role in advancing this field. The experimental and later clinical studies of Evsey Galperin and Valery Shumakov, particularly in the area of heterotopic transplantation of the left hepatic lobe, stimulated scientific discussion and attracted the attention of the international transplant community [28, 29].

The late 1980s witnessed another transformative event in liver transplantation, one that was particularly crucial for pediatric patients: the first successful attempts to transplant a fragment of the liver from a living related donor. The idea of using part of a living donor's liver to save a child in the face of a critical shortage of cadaveric organs had long been considered, but its realization required not only advanced surgical expertise, but also remarkable courage and the resolution of complex ethical issues.

The first clinical attempt was made in Brazil by Silvano Raia and his colleagues in 1988 (according to some sources, in 1987), when a mother donated the left lateral sector of her liver to her child. Sadly, the recipient died in the early postoperative period [30, 31].

A true breakthrough came in 1989 in Sydney (Australia), when Professor Russell Strong and his team performed the world's first successful living-donor LT, transplanting the left lateral lobe from a mother to her young son [7, 32]. The case was widely publicized, causing a sensation in the medical community and marking the start of a new chapter in the history of LT.

Almost simultaneously, also in 1989, a team in Chicago (USA) led by Christoph Broelsch – already experienced in reduced-size and split LT – launched the first structured program of living-related donor LT in children [33, 34]. After returning to Germany, Professor Broelsch and his team continued to successfully develop all these areas.

Thus, the era of cyclosporine not only radically improved transplant outcomes overall, but also gave rise to a series of innovations, many of them driven by the urgent need to improve care for children with end-stage liver disease. Once again, pediatric transplantation became a catalyst for progress, stimulating the development and refinement of techniques such as reduced-size LT, split transplantation, and ultimately living-related donor transplantation. On the wave of these achievements, the young science of clinical transplantology entered the next decade poised for rapid expansion.

TECHNICAL ACHIEVEMENTS AND INNOVATIONS IN TRANSPLANTATION (1990s)

The 1990s marked another qualitative leap in the development of LT, a period that not only significantly

reduced mortality among patients on waiting lists, but also brought substantial improvements in both short-term and long-term survival rates, particularly in the most challenging group: young children [35, 36].

By this time, the fundamental principles and core surgical approaches to LT had gained broad recognition and clinical acceptance. In most developed countries, the legislative framework regulating organ donation had been consolidated, and the criteria for determining brain death had been standardized, both of which were critical steps in expanding the pool of deceased donors [37].

At the same time, surgical hepatology advanced rapidly, supported by the introduction of new imaging technologies, significant improvements in instruments for parenchymal dissection, and a deeper understanding of the segmental anatomy of the liver.

These achievements directly facilitated the further refinement and broader adoption of techniques for reducing graft size and, most importantly, split LT. During the 1990s, transplant surgeons began to actively implement *in situ* division of the liver from deceased donors, that is, splitting the organ directly within the body while maintaining blood flow. This approach significantly minimized warm ischemia of the graft fragments and improved their functional quality [38, 39].

Importantly, these complex operations were no longer isolated, experimental procedures but began to be performed in series at leading transplant centers worldwide. This shift enabled more systematic analysis of outcomes for different types of grafts, accumulation of collective experience, and, ultimately, standardization of surgical approaches and further improvement of results [40]. As before, pediatric recipients were the main beneficiaries, since split transplantation allowed optimal use of a single donor organ to save two lives – most often an adult and a child, or two children.

At the same time, advances in precision parenchymal transection, including the use of ultrasonic dissectors, argon plasma coagulation, and other innovative technologies, as well as a deeper understanding of the variability of biliary and vascular anatomy, made it possible not only to refine transplantation of left-sided liver fragments (the left lateral segment or left lobe) – pioneered in the late 1980s by S. Raia and R. Strong – but also to take the next, even bolder step.

After carefully analyzing the not entirely successful but innovative attempt by Japanese surgeon Y. Yamaoka in 1994 to transplant the right lobe of the liver from a living related donor to an adult patient [41], as well as the controversial experience of Lo Chung Mau in Hong Kong [42], several countries began intensive preparations for introducing this fundamentally new and technically demanding variant of partial LT, living donor right lobe transplantation.

This operation required surgeons to possess not only extensive expertise in liver resection but also the utmost precision and responsibility, as the risks to healthy donors undergoing right-sided hemihepatectomy were considerably higher than in left-lobe donation.

In 1997, within just a few months of each other, the first successful living donor right lobe liver transplants were carried out: in Moscow by a team led by Sergey Gautier at Petrovsky National Research Centre of Surgery, and shortly thereafter in Denver (USA) by a team under Michael Wachs. Paradoxically, history repeated itself here as well – the recipient in the Moscow pair was a minor teenager with autoimmune hepatitis [43, 44]. In Europe, the technique of transplanting the right lobe from a living donor began to be actively used around 1998, largely due to the efforts of Professor Christoph Broelsch and his team, who, after returning to Essen (Germany), continued their pioneering work [46].

In addition to revolutionary surgical innovations, the 1990s also marked a turning point in immunosuppressive therapy. A new, highly potent calcineurin inhibitor – tacrolimus (FK506), developed by Japanese researchers – was increasingly and confidently integrated into clinical practice. Multiple studies demonstrated its superiority over cyclosporine in preventing and treating rejection, and today tacrolimus remains the cornerstone of most modern LT protocols [47, 48].

Tacrolimus provided more reliable and selective control of the rejection response, which in many cases allowed for a reduction in glucocorticosteroid dosages or even their complete withdrawal. This was particularly important for pediatric patients, as it significantly reduced the risk of steroid-associated complications that could impair growth and development [49].

Equally transformative was the introduction, in the mid-1990s, of a new class of immunosuppressants – mycophenolic acid derivatives, especially mycophenolate mofetil, approved by the FDA in 1995. When combined with calcineurin inhibitors, these agents enhanced efficacy while enabling the almost complete elimination of older, more toxic cytostatics such as azathioprine from immunosuppression regimens [50, 51].

In addition, the 1990s witnessed major progress in the prevention and management of infectious complications, which had long remained one of the leading causes of morbidity and mortality after LT. Of particular importance was the development and implementation of effective strategies for the prevention and early treatment of cytomegalovirus (CMV) infection. These strategies relied on regular monitoring of viral load – using either pp65 antigenemia assays or CMV DNA detection by PCR – followed by the timely initiation of antiviral therapy with ganciclovir or foscarnet once viral replication was detected [52, 53]. This approach significantly reduced the incidence of CMV disease and improved transplant outcomes, especially in seronegative recipients receiving grafts from seropositive donors.

Thus, the 1990s became not only a period of consolidation of the achievements of the preceding decades but also an era of remarkable innovation, which firmly established LT as a standard, highly effective therapeutic option. Once again, pediatric transplantology played a key role, driving the search for and implementation of the most advanced technologies and approaches.

THE MODERN ERA: FROM THE 2000s TO THE PRESENT DAY

Pediatric LT entered the modern era as a highly effective therapeutic method with broad clinical applications. Yet, despite these successes, by the beginning of the 21st century a number of pressing challenges had accumulated. These ranged from the limited availability of care, concentrated in a relatively small number of highly specialized centers, to the absence of clear and equitable policies for allocation of deceased donor organs. The shortage of suitable grafts became increasingly acute as the number of children requiring transplantation steadily grew [56].

Over the past 25 years, the global volume of pediatric LT has risen substantially. While the United States and Western European countries have retained their roles as traditional leaders, several new regions have emerged on the world stage, demonstrating impressive results. China, Russia, Turkey, Japan, South Korea, Iran, and India have established large transplant programs, including dedicated pediatric centers, which are now performing LT at a high international standard [57, 58].

Of particular note is the pediatric liver transplant program at Shumakov National Medical Research Center of Transplantology and Artificial Organs in Moscow, developed under the leadership of Sergey Gautier. Today, the center performs more than 110 pediatric liver transplants annually, accounting for up to 95% of all liver transplants in minor recipients nationwide. With this volume and expertise, the clinic has secured its place among the world leaders in pediatric LT.

Improving the allocation of donor organs

One of the most important directions in optimizing the use of scarce donor organs in the early 2000s was the development of objective, standardized systems for assessing disease severity in patients on the waiting list and for determining transplant priority. In the United States, the Model for End-Stage Liver Disease (MELD) was introduced in 2002 in response to rising mortality among patients awaiting transplantation and the urgent need for a more equitable system of organ distribution [59, 60]. This score was calculated from objective laboratory values – bilirubin, INR, and creatinine.

Almost simultaneously, an adapted version, the Pediatric End-Stage Liver Disease (PELD) score, was developed for children under 12 years of age. In addition to laboratory parameters, PELD incorporated factors particularly relevant to the pediatric population, such as growth failure, serum albumin levels, and age [61].

The introduction of the MELD/PELD allocation system had an immediate positive impact: in the United States, mortality among children on the waiting list declined significantly, especially among the youngest and most vulnerable patients for whom delays were most critical [62, 63]. Following this success, MELD- and PELD-based allocation principles – or national modifications thereof – were subsequently adopted in many other countries and regions. This global trend has contributed to greater transparency and medical objectivity in the allocation of liver grafts [59].

In parallel with the introduction of objective scoring systems for assessing the severity of conditions, specific organizational measures were adopted to prioritize pediatric patients on waiting lists. Many national and regional allocation frameworks incorporated special rules or quotas ensuring that donor organs of suitable size and optimal quality were first offered to children [64, 65]. This approach was grounded in the recognition that alternative treatment options for young patients are often absent, and delays in transplantation carry a particularly high risk of irreversible complications or death. Pediatric candidates often receive additional points to their calculated MELD/PELD score or have priority access to organs from young donors.

Another important aspect of optimizing the donor pool has been the wider adoption of split-LT. In response to the severe shortage of suitable organs, several countries have introduced policies mandating consideration of splitting a donor liver for two recipients whenever possible. For example, in Italy, regulations require split transplantation if the donor is under 60 years of age and the organ is of adequate quality.

Thanks to this targeted policy and the active involvement of transplant centers, Italy has accumulated one of the world's largest experiences: between 1993 and 2019, more than 1,700 split procedures were performed. Analysis of these cases has shown steady improvement in outcomes for both adult and pediatric recipients as clinical experience expanded and surgical techniques were refined [66, 67]. This experience clearly demonstrates that the systematic use of split technology, particularly *in situ* splitting, is an effective way to expand the donor pool for children.

Ways to expand the donor pool

In addition to improving allocation systems and actively implementing split transplantation, a crucial strategy that has significantly shaped the landscape of modern pediatric LT has been the development of living-donor liver transplantation (LDLT) programs. This approach has become especially prominent in Asia and the Middle East, where the majority of pediatric liver transplants are now performed using living related donors [68, 69].

Japan provides the clearest example: over 98% of pediatric LT are performed with grafts from living donors. This dominance reflects both cultural attitudes toward organ donation and long-standing legal restrictions on the removal of organs from deceased children – until 2010, Japanese law prohibited postmortem organ donation from individuals under 15 years of age [70]. A similar pattern is observed in South Korea, where the scarcity of deceased donor organs has been successfully offset by widespread reliance on living donors. As a result, South Korea reports some of the best outcomes worldwide for both waitlist survival and post-transplant outcomes [68].

In contrast, in North America and Western Europe, transplantation still relies primarily on deceased donor organs. This is possible due to the existence of robust organizational networks such as Eurotransplant and UNOS, combined with a high level of public trust in postmortem organ donation programs [68, 71]. Nevertheless, even in these regions, LDLT remains an important and much-in-demand resource, particularly for children. In the United States, for example, several hundred pediatric LDLTs are performed annually, usually in emergency situations or when no suitable deceased donor is available [71].

Legislative differences between countries also have a significant impact on the availability of donor organs. In most European nations, the prevailing model is the opt-out system, under which every citizen is regarded as a potential organ donor after death unless they have formally registered their refusal. This approach has consistently been shown to increase the number of postmortem donors [72]. By contrast, many Asian countries as well as the United States adhere to an opt-in system, where explicit consent from the donor during their lifetime – or, in many cases, from the family after death – is required. This reliance on voluntary consent, combined with cultural and religious barriers, often limits the effectiveness of postmortem donation programs [72].

To mitigate organ shortages in certain European Union countries, efforts have gone beyond national measures such as the mandatory consideration of split transplantation. An important complementary strategy has been the establishment of international organ exchange systems, notably Eurotransplant and Scandiatransplant These mechanisms are particularly valuable in urgent cases, such as acute liver failure or transplantation for highly sensitized patients [72, 73].

ABO-incompatible liver transplantation

Overcoming the immunological barrier posed by ABO blood group incompatibility has become another significant achievement in modern transplantology, particularly in pediatric practice, where identifying a donor who is both size- and blood group–compatible can be extremely challenging. In its early stages, ABO-incompatible liver transplantation (ABOi LT) was regarded as an exceptionally high-risk procedure. The incidence of hyperacute antibody-mediated rejection, along with increased rate of vascular complications (hepatic artery thrombosis) and biliary complications, led to discouraging outcomes [74, 75].

A turning point came in the 2000s with the introduction of desensitization protocols that significantly improved ABOi LT results. These strategies included plasmapheresis to remove circulating anti-ABO antibodies, use of rituximab (a monoclonal antibody against CD20-positive B cells), immunoadsorption of specific antibodies, and intravenous administration of high doses of human immunoglobulin (IVIG), with splenectomy applied selectively in some cases [76, 77]. Together, these interventions allowed for effective reduction of isoagglutinin titers to safe levels, thereby minimizing the risk of antibody-mediated rejection. As a result, ABOi LT has become a clinically viable and effective option, particularly under conditions of acute donor organ shortage or when urgent transplantation is necessary [78].

Current protocols for ABOi LT differ between transplant centers and are often tailored to the recipient's baseline anti-ABO antibody titers. Nevertheless, they share a common principle: the simultaneous use of strategies to (1) reduce circulating isoagglutinins, (2) suppress their further production, and (3) modulate the B-cell response. One example is the titer-dependent approach described by Gelbart et al. (2018) for pediatric recipients. In patients with high baseline isoagglutinin titers (≥1:32), enhanced immunosuppressive was used, consisting of pre- and post-transplant plasmapheresis, rituximab (375 mg/m^2), and IVIG (1 g/kg) [79].

Extensive clinical experience has also been accumulated in Russia, particularly at Shumakov National Medical Research Center of Transplantology and Artificial Organs, where a proprietary protocol was developed. In this protocol, an anti-ABO antibody titer of 1:8 is considered borderline. Key interventions include transfusion of AB(IV) fresh frozen plasma (which lacks anti-A and anti-B antibodies), administration of rituximab, and plasmapheresis sessions [80]. Importantly, outcomes with this protocol have been comparable to those of ABO-compatible transplantation, including similar rates of vascular and biliary complications.

Across all protocols, regular monitoring of antibody titers before and after transplantation remains a cornerstone of patient management, enabling timely adjustments to therapy in response to changes in the immune response [77, 79].

Once again, it was the urgent need to save the lives of children in a critical situation for whom no ABO-compatible donor could be found that catalyzed the development and refinement of these complex and resource-intensive technologies.

Surgical aspects and modern challenges

Despite remarkable progress, pediatric LT entered the 21st century with several unresolved surgical problems and new challenges. One of the most pressing issues, particularly in infants under one year of age, is large-for-size syndrome. This condition, essentially a variant of abdominal compartment syndrome, can have severe consequences, including respiratory failure due to elevation of the diaphragm, reduced graft perfusion caused by vascular compression, and impaired visceral blood flow in general [81, 82]. To prevent and manage this syndrome, various surgical strategies have been proposed. Among them are the use of monosegmental grafts (e.g., isolated segment II or III) and hyper-reduced grafts, in which additional resection of a standard left lateral section is performed. However, this approach presents major limitations. The technical difficulty of creating adequate vascular and biliary anastomoses in very small grafts remains a challenge, as does the significantly increased wound surface area, which predisposes to bleeding and infectious complications [83].

Portal vein hypoplasia, commonly found in children with biliary atresia (the leading indication for pediatric LT), represents another major surgical challenge. Successful reconstruction of portal blood flow is crucial for both graft function and long-term patient survival.

To address this problem, transplant surgeons have developed a range of complex reconstructive techniques. Hwang et al. (2013) described a successful method involving the use of a vascular interposition graft, such as a segment of the donor's iliac vein, in an infant with severe portal vein hypoplasia [84]. Later, Namgoong et al. (2021) proposed several alternative strategies, including venous homograft interposition with an inverted T- or Y-shaped incision to create a wider anastomosis; longitudinal incision of the recipient's native portal vein to increase the diameter of the anastomosis; or the use of the recipient's portal vein branches to create a vascular "patch" (patch plasty), compensating for the size discrepancy between donor and recipient vessels [85].

All of these approaches aim to ensure adequate laminar blood flow into the graft and to minimize the risk of portal vein thrombosis, which remains a serious complication in pediatric transplantation, with reported incidence rates of up to 9% [85].

Retransplantation poses another major surgical challenge, particularly when performed long after the initial LT. Indications for repeat transplantation include irreversible chronic graft dysfunction resulting from chronic rejection, unresolvable vascular or biliary complications, or recurrence of the underlying disease in the graft. These procedures are technically demanding for several reasons: severe adhesions within the abdominal cavity, distorted vascular and biliary anatomy, and frequently the absence of clear anatomical planes for safe dissection.

All this is associated with a high risk of massive intraoperative blood loss, injury to surrounding organs and structures, and a greater incidence of postoperative complications [86, 87].

PROMISING TECHNOLOGIES AND FUTURE DIRECTIONS

By the late 2010s and early 2020s, several promising technologies initially tested in experimental settings began entering clinical practice, including pediatric LT. A key development has been the rapid advancement of dynamic *ex vivo* organ perfusion techniques. MacConmara et al. (2020) demonstrated that normothermic machine perfusion (NMP) can improve the viability of grafts obtained from "suboptimal" donors – such as those with expanded criteria or following circulatory death – and enables safe *ex situ* liver splitting while maintaining high functional activity in both grafts [88]. Similarly, Boteon et al. (2022) reported that NMP not only increases the utilization of marginal organs, including those from donors after circulatory death, but also facilitates split transplantation with consistently high-quality outcomes for pediatric recipients [89].

An additional advantage of NMP-assisted splitting is its ability to combine the benefits of *in situ* and *ex situ* approaches: precise identification of vascular and biliary structures in a perfused organ, safer and more controlled parenchymal division under optimal visualization, and elimination of bleeding risks in the donor. However, the high costs of equipment and disposables, the risk of biliary complications – particularly when using marginal grafts – and a range of organizational and institutional barriers currently limit the widespread adoption of this promising technology, requiring further research and experience [90].

Significant technological breakthroughs have also transformed the field of LDLT. In 2002, Professor Daniel Cherqui and his team in France performed the first fully laparoscopic left lateral sectorectomy from a living donor for transplantation into a child [91]. Since then, the adoption of minimally invasive donor hepatectomy has gradually expanded – initially approached with great caution, but by the early 2020s already widely and confidently implemented in many centers. Both purely laparoscopic and robot-assisted procedures are now performed with increasing frequency [92, 93, 94].

The introduction of minimally invasive approaches has been associated with substantial benefits for donors, including reduced intraoperative blood loss, less postoperative pain, shorter hospitalization, and faster recovery. With growing experience, operative times have approached those of traditional open surgery, without increasing the incidence of donor-specific complications [95].

Moreover, to date, several leading transplant programs worldwide have pushed the boundaries further by performing fully robot-assisted and even fully laparoscopic recipient operations, including pediatric cases. Early reports from these pioneering procedures have already been published [96, 97].

This fully minimally invasive transplant strategy remains confined to a few highly specialized centers. It is associated with significant challenges, such as high costs for equipment and consumables, and a significant amount of time to perform the surgical intervention itself and the need for dedicated training for the entire surgical team [98].

CONCLUSION AND HISTORICAL LESSONS

Pediatric LT has undergone an extraordinary evolution, transforming from an experimental intervention with unpredictable results into a standardized, highly effective therapy for life-threatening liver diseases in children. A unique feature of this trajectory is that pediatric transplantation has not only adopted advances from the broader field of medicine but has consistently served as a driver of innovation, propelling the discipline of transplantology forward.

The very first attempts at clinical LT in humans – including the earliest relatively successful procedure, which extended a child's life by several months – were performed in pediatric patients [4, 14]. The introduction and widespread adoption of reduced-size and split-LT were motivated primarily by the urgent needs of children facing a critical shortage of donor organs [23, 38]. Similarly, the development of LDLT, including technically demanding right-lobe grafting, was driven by the need to save children for whom no other treatment options were available [29, 43].

Overcoming the barrier of ABO incompatibility, once considered insurmountable, was likewise pioneered in pediatric populations, expanding the boundaries of what was possible for children previously deemed untreatable [77, 79]. Even the most recent advances, such as minimally invasive donor hepatectomy and recipient surgery, are increasingly being applied and refined within the pediatric setting [91, 96].

This pattern is particularly striking when compared with most other areas of surgery and transplantation, where innovations are typically developed, validated, and implemented first in adults, and only later adapted for pediatric use once safety and efficacy are established.

The modern era can by no means be considered a stage in which the challenges of pediatric LT have been definitively resolved. On the contrary, as experience accumulates and the method becomes more widely adopted for the treatment of terminally ill children, new problems and unresolved questions continue to emerge. The most obvious and pressing among them is the ongoing search for strategies to further improve not only short-term but, more importantly, long-term transplant outcomes. The steadily growing cohort of patients who have successfully passed the threshold of the second and even third decade after surgery has shifted the focus of clinicians and researchers beyond simple measures of graft and patient survival to broader issues such as quality of life, cognitive development, and full social and professional integration of former recipients [99, 100].

Today, the development and implementation of personalized immunosuppression protocols, guided by individual biomarkers and designed to minimize side effects while ensuring reliable protection against rejection, are already shaping a new standard of care. Parallel efforts are directed toward targeted prevention and treatment of specific post-transplant complications, particularly vascular and biliary disorders. The issue of infectious safety has become especially urgent in the context of continuously evolving pathogenic microorganisms and the rapid global spread of pan-resistant flora. At the same time, reducing the long-term cumulative risks of chronic immunosuppressive therapy – including nephrotoxicity, arterial hypertension, diabetes mellitus, dyslipidemia, and the increased likelihood of malignant neoplasms – remains a serious clinical challenge, one that demands a multidisciplinary approach and the development of innovative therapeutic strategies.

The authors declare no conflict of interest.

REFERENCES

1. *Starzl TE, Marchioro TL, Von Kaulla KN, Hermann G, Brittain RS, Waddell WR*. Homotransplantation of the liver in humans. *Surg Gynecol Obstet*. 1963 Dec; 117: 659–676.
2. *Starzl TE, Groth CG, Brettschneider L, Penn I, Fulginiti VA, Moon JB et al*. Orthotopic homotransplantation of the human liver. *Ann Surg*. 1968 Sep; 168 (3): 392–415.
3. *Otte JB*. History of pediatric liver transplantation. Where are we coming from? Where do we stand? *Pediatr Transplant*. 2002; 6 (4): 312–320.
4. *Bismuth H, Houssin D.* Reduced-sized orthotopic liver graft in hepatic transplantation in children. *Surgery*. 1984; 96 (3): 367–370.
5. *Broelsch CE, Emond JC, Thistlethwaite JR, Whittington PF, Zucker AR, Baker AL et al*. Liver transplantation, including the concept of reduced-size liver transplants in children. *Ann Surg*. 1988; 208 (4): 410–420.
6. *Pichlmayr R, Ringe B, Gubernatis G, Hauss J, Bunzendahl H*. Transplantation of a donor liver to 2 recipients (splitting transplantation) – a new method in the further development of segmental liver transplantation. *Langenbecks Arch Chir*. 1988; 373 (2): 127–130.
7. *Strong RW, Lynch SV, Ong TH, Matsunami H, Koido Y, Balderson GA*. Successful liver transplantation from a living donor to her son. *N Engl J Med*. 1990; 322 (21): 1505–1507.
8. *Alexandre GP, Squifflet JP, De Bruyere M, Latinne D, Reding R, Gianello P et al*. Present experiences in a

series of 26 AB0-incompatible living donor renal allografts. *Transplant Proc*. 1987; 19 (1 Pt 1): 748–750.
9. *Tokunaga Y, Tanaka K, Fujita S et al.* Living donor liver transplantation across AB0 incompatibility. *Transplant Proc*. 1999; 31 (1–2): 450–452.
10. *Mazza G, De Coppi P, Gissen P et al*. The history of liver transplantation. *Pediatr Surg Int*. 2020; 36 (10): 1137–1145.
11. *Bishop GA, Bowen DG, Bertolino P*. The liver: a special case for transplantation tolerance. *Nat Rev Immunol*. 2007; 7 (6): 440–451.
12. *Starzl TE*. The saga of liver transplantation, with particular reference to children. *J Pediatr Surg*. 1993; 28 (11): 1469–1478.
13. *Demikhov VP.* Peresadka zhiznenno vazhnykh organov v eksperimente. M.: Medgiz, 1960; 260.
14. *Glyantsev SP.* Vladimir Petrovich Demikhov (k 100-letiyu so dnya rozhdeniya). Vestnik transplantologii i iskusstvennykh organov. 2016; (3): 66–77.
15. *Starzl TE, Iwatsuki S, Todo S et al*. Historical perspective of liver transplantation at Children's Hospital of Pittsburgh. *J Japan Surg Soc*. 1990; 91 (10): 1759–1765.
16. *Fung JJ, Abu-Elmagd K, Jain A et al*. A long-term analysis of 3000 liver transplantations at the University of Pittsburgh: a triumph of clinical and basic science. *Ann Surg*. 1997; 226 (4): 429–440.
17. *Calne RY.* A new lease on life: the history of transplantation. *Transpl Immunol*. 2004; 13 (4): 259–263.
18. *Esquivel CO, Iwatsuki S, Gordon RD, Marsh WW Jr, Koneru B, Makowka L et al*. Liver transplantation for biliary atresia. Long-term follow-up of 85 patients. *Gastroenterology*. 1987; 93 (5): 1117–1120.
19. *Borel JF*. Ciclosporin and its future. *Clin Transplant*. 1990: 1–8.
20. *Calne RY, White DJ, Thiru S, Evans DB, McMaster P, Dunn DC et al*. Cyclosporin A in patients receiving renal allografts from cadaver donors. *Lancet*. 1978; 2 (8104-5): 1323–1327.
21. *Starzl TE, Klintmalm GB, Porter KA, Iwatsuki S, Schröter GP*. Liver transplantation with use of cyclosporin A and prednisone. N Engl J Med. 1981; 305 (5): 266–269.
22. National Institutes of Health Consensus Development Conference Statement: liver transplantation – June 20–23, 1983. *Hepatology*. 1984; 4 (1 Suppl): 107S–110S.
23. *Starzl TE, Iwatsuki S, Shaw BW Jr, Gordon RD, Esquivel CO*. Immunosuppression and other nonsurgical factors in the improved results of liver transplantation. *Semin Liver Dis*. 1985; 5 (4): 334–343.
24. *Goss JA, Shackleton CR, McDiarmid SV et al*. Long-term results of pediatric liver transplantation: an analysis of 569 transplants. *Ann Surg*. 1998; 228 (3): 411–420.
25. *Broelsch CE, Emond JC, Whitington PF, Thistlethwaite JR, Baker AL, Lichtor JL*. Application of reduced-size liver transplants as split grafts, auxiliary orthotopic grafts, and living related segmental transplants. *Ann Surg*. 1990; 212 (3): 368–375.
26. *Broelsch CE, Whitington PF, Emond JC, Heffron TG, Thistlethwaite JR, Stevens L et al*. Liver transplantation in children from living related donors. Surgical techniques and results. *Ann Surg*. 1991; 214 (4): 428–437.
27. *Tanaka K, Uemoto S, Tokunaga Y, Fujita S, Sano K, Nishizawa T et al*. Surgical techniques and innovations in living related liver transplantation. *Ann Surg*. 1993; 217 (1): 82–91.
28. *Makuuchi M, Kawarazaki H, Iwanaka T, Kamada N, Takayama T, Kumon M*. Living related liver transplantation. *Surg Today*. 1992; 22 (4): 297–300.
29. *Hashikura Y, Makuuchi M, Kawasaki S, Matsunami H, Ikegami T, Nakazawa Y et al*. Successful living-related partial liver transplantation to an adult patient. *Lancet*. 1994; 343 (8907): 1233–1234.
30. *Yamaoka Y, Washida M, Honda K, Tanaka K, Mori K, Shimahara Y et al*. Liver transplantation using a right lobe graft from a living related donor. *Transplantation*. 1994; 57 (7): 1127–1130.
31. *Lo CM, Fan ST, Liu CL, Wei WI, Lo RJ, Lai CL et al*. Adult-to-adult living donor liver transplantation using extended right lobe grafts. *Ann Surg*. 1997; 226 (3): 261–269.
32. *Rogiers X, Malago M, Gawad K, Jauch KW, Olausson M, Knoefel WT et al*. *In situ* splitting of cadaveric livers. The ultimate expansion of a limited donor pool. *Ann Surg*. 1996; 224 (3): 331–339.
33. *Azoulay D, Astarcioglu I, Bismuth H, Castaing D, Majno P, Adam R, Johann M*. Split-liver transplantation. The Paul Brousse policy. *Ann Surg*. 1996; 224 (6): 737–746.
34. *Busuttil RW, Goss JA*. Split liver transplantation. *Ann Surg*. 1999; 229 (3): 313–321.
35. *Raia S, Nery JR, Mies S*. Liver transplantation from live donors. *Lancet*. 1989; 2 (8661): 497.
36. *Ozawa K, Uemoto S, Tanaka K, Kumada K, Yamaoka Y, Kobayashi N et al*. An appraisal of pediatric liver transplantation from living relatives. Initial clinical experiences in 20 pediatric liver transplantations from living relatives as donors. *Ann Surg*. 1992; 216 (5): 547–553.
37. *Inomata Y, Tanaka K, Uemoto S, Ozaki N, Okajima H, Yamaoka Y*. Living donor liver transplantation: an 8-year experience with 379 consecutive cases. *Transplant Proc*. 1999; 31 (1–2): 381.
38. *Emond JC, Whitington PF, Thistlethwaite JR, Cherqui D, Alonso EA, Woodle IS et al*. Transplantation of two patients with one liver. Analysis of a preliminary experience with 'split-liver' grafting. *Ann Surg*. 1990; 212 (1): 14–22.
39. *Bismuth H, Morino M, Castaing D, Gillon MC, Descorps Declere A, Saliba F, Samuel D*. Emergency orthotopic liver transplantation in two patients using one donor liver. *Br J Surg*. 1989; 76 (7): 722–724.
40. *Otte JB, de Ville de Goyet J, Alberti D, Balladur P, de Hemptinne B*. The concept and technique of the split liver in clinical transplantation. *Surgery*. 1990; 107 (6): 605–612.
41. *Broelsch CE, Emond JC, Whitington PF, Thistlethwaite JR, Baker AL, Lichtor JL*. Application of reduced-size liver transplants as split grafts, auxiliary orthotopic grafts, and living related segmental transplants. *Ann Surg*. 1990; 212 (3): 368–375.

42. *Otte JB, de Ville de Goyet J, Sokal E, Alberti D, Moulin D, de Hemptinne B et al*. Size reduction of the donor liver is a safe way to alleviate the shortage of size-matched organs in pediatric liver transplantation. *Ann Surg*. 1990; 211 (2): 146–157.
43. *Kawasaki S, Makuuchi M, Matsunami H, Hashikura Y, Ikegami T, Nakazawa Y et al*. Living related liver transplantation in adults. *Ann Surg*. 1998; 227 (2): 269–274.
44. *Marcos A, Fisher RA, Ham JM, Shiffman ML, Sanyal AJ, Luketic VA et al*. Right lobe living donor liver transplantation. *Transplantation*. 1999; 68 (6): 798–803.
45. *Wiesner RH, McDiarmid SV, Kamath PS, Edwards EB, Malinchoc M, Kremers WK et al*. MELD and PELD: application of survival models to liver allocation. *Liver Transpl*. 2001; 7 (7): 567–580.
46. *McDiarmid SV, Anand R, Lindblad AS; Principal Investigators and Institutions of the Studies of Pediatric Liver Transplantation (SPLIT) Research Group*. Development of a pediatric end-stage liver disease score to predict poor outcome in children awaiting liver transplantation. *Transplantation*. 2002; 74 (2): 173–181.
47. *Freeman RB Jr, Wiesner RH, Harper A, McDiarmid SV, Lake J, Edwards E et al*. UNOS/OPTN Liver Disease Severity Score, UNOS/OPTN Liver and Intestine, and UNOS/OPTN Pediatric Transplantation Committees. The new liver allocation system: moving toward evidence-based transplantation policy. *Liver Transpl*. 2002; 8 (9): 851–858.
48. *Merion RM, Schaubel DE, Dykstra DM, Freeman RB, Port FK, Wolfe RA*. The survival benefit of liver transplantation. *Am J Transplant*. 2005; 5 (2): 307–313.
49. *Feng S, Goodrich NP, Bragg-Gresham JL, Dykstra DM, Punch JD, DebRoy MA et al*. Characteristics associated with liver graft failure: the concept of a donor risk index. *Am J Transplant*. 2006; 6 (4): 783–790.
50. *Schaubel DE, Sima CS, Goodrich NP, Feng S, Merion RM*. The survival benefit of deceased donor liver transplantation as a function of candidate disease severity and donor quality. *Am J Transplant*. 2008; 8 (2): 419–425.
51. *Rana A, Pallister ZS, Halazun K, Cotton RT, Guiteau JJ, Nalty CC et al*. Pediatric liver transplant center volume and the likelihood of transplantation. *Pediatrics*. 2015; 136 (1): e99–e107.
52. *Kasahara M, Umeshita K, Inomata Y, Uemoto S; Japanese Liver Transplantation Society* Long-term outcomes of pediatric living donor liver transplantation in Japan: an analysis of more than 2200 cases listed in the registry of the Japanese Liver Transplantation Society. *Am J Transplant*. 2013; 13 (7): 1830–1839.
53. *Otte JB, Reding R, de Ville de Goyet J, Sokal E, Lerut J, Janssen M et al*. Experience with living related liver transplantation in 63 children. *Acta Gastroenterol Belg*. 1999; 62 (3): 355–362.
54. *Spada M, Riva S, Maggiore G, Cintorino D, Gridelli B*. Pediatric liver transplantation. *World J Gastroenterol*. 2009; 15 (6): 648–674.
55. *Hackl C, Schlitt HJ, Melter M, Knoppke B, Loss M*. Current developments in pediatric liver transplantation. *World J Hepatol*. 2015; 7 (11): 1509–1520.
56. *Emre S, Umman V*. Split liver transplantation: an overview. *Transplant Proc*. 2011; 43 (3): 884–887.
57. *Lauterio A, Di Sandro S, Concone G, De Carlis R, Giacomoni A, De Carlis L*. Current status and perspectives in split liver transplantation. *World J Gastroenterol*. 2015; 21 (39): 11003–11015.
58. *Cardillo M, De Fazio N, Pedotti P, De Feo T, Fassati LR, Mazzaferro V et al*. NITp Liver Transplantation Working Group. Split and whole liver transplantation outcomes: a comparative cohort study. *Liver Transpl*. 2006; 12 (3): 402–410.
59. *Renz JF, Emond JC, Yersiz H, Ascher NL, Busuttil RW*. Split-liver transplantation in the United States: outcomes of a national survey. *Ann Surg*. 2004; 239 (2): 172–181.
60. *Vagefi PA, Parekh J, Ascher NL, Roberts JP, Freise CE*. Outcomes with split liver transplantation in 106 recipients: the University of California, San Francisco, experience from 1993 to 2010. Arch Surg. 2011; 146 (9): 1052–1059.
61. *Doyle MB, Maynard E, Lin Y, Vachharajani N, Shenoy S, Anderson C et al*. Outcomes with split liver transplantation are equivalent to those with whole organ transplantation. *J Am Coll Surg*. 2013; 217 (1): 102–112.
62. *Cauley RP, Vakili K, Fullington N, Potanos K, Graham DA, Finkelstein JA, Kim HB*. Deceased-donor split-liver transplantation in adult recipients: is the learning curve over? *J Am Coll Surg*. 2013; 217 (4): 672–684.e1.
63. *Maggi U, De Feo TM, Andorno E, Cillo U, De Carlis L, Colledan M et al*. Liver Transplantation Nord Italia Transplant program (NITp) Working Group. Fifteen years and 382 extended right grafts from deceased donors: a multicenter study on donor and recipient outcomes. *Liver Transpl*. 2015; 21 (4): 500–508.
64. *Lauterio A, Di Sandro S, De Carlis R, Ferla F, Buscemi V, De Carlis L*. Current status and perspectives in split liver transplantation. *World J Gastroenterol*. 2019; 25 (43): 6347–6355.
65. Eurotransplant Manual. Chapter 5: ET Liver Allocation System (ELAS). Version 9.0. 2021. URL: https://www.eurotransplant.org/wp-content/uploads/2021/03/H5-Liver.pdf (date of access: 14.05.2025).
66. Organ Procurement and Transplantation Network (OPTN) Policies. Policy 9: Allocation of Livers and Liver-Intestines. 2022. URL: https://optn.transplant.hrsa.gov/media/eavh5bf3/optn_policies.pdf (date of access: 14.05.2025).
67. *Lauterio A, Di Sandro S, Gruttadauria S, Spada M, Di Benedetto F, Baccarani U et al*. Donor pool expansion in liver transplantation. *Transplant Proc*. 2019; 51 (1): 9–16.
68. *Kasahara M, Sakamoto S, Umeshita K*. Current status of living donor liver transplantation in Asia. *Transplantation*. 2024; 108 (1): 35–43.
69. *Lee SG*. A complete survey of living donor liver transplantation in Korea. *J Korean Med Sci*. 2015; 30 (12): 1731–1738.
70. *Toida C, Mogushi K, Hoshino K et al*. Current status and future prospects of pediatric organ transplantation in Japan. *Pediatr Transplant*. 2016; 20 (6): 756–765.

71. Organ Procurement and Transplantation Network (OPTN) and Scientific Registry of Transplant Recipients (SRTR). OPTN/SRTR 2022 Annual Data Report: Liver. *Am J Transplant*. 2024; 24 (2S): S1–S74.
72. *Silva HT Jr, Felipe CR, Ferreira GF*. Organ donation and transplantation: a global perspective. *Nephrol Dial Transplant*. 2025; 40 (1): 21–29.
73. *Cohen J, Stolk E, Wouters O et al*. The impact of presumed consent legislation on deceased organ donation: a systematic review and meta-analysis of controlled studies. *BMJ Open*. 2016; 6 (5): e010229.
74. *Alexandre GP, Squifflet JP, De Bruyere M et al*. Present experiences in a series of 26 AB0-incompatible living donor renal allografts. *Transplant Proc*. 1987; 19 (1 Pt 1): 700–702.
75. *Tanabe M, Kawachi S, Obara H et al*. Current progress in AB0-incompatible liver transplantation. *Eur J Clin Invest*. 2010; 40 (5): 457–464.
76. *Egawa H, Teramukai S, Haga H et al*. Impact of rituximab on immunity in AB0-incompatible living donor liver transplantation. *Transplantation*. 2014; 97 (1): 65–72.
77. *Song GW, Lee SG, Hwang S et al*. AB0-incompatible adult living donor liver transplantation: a new era. *Liver Transpl*. 2016; 22 (2): 179–196.
78. *Lee CF, Cheng CH, Wang YC et al*. Outcomes of AB0-incompatible pediatric living donor liver transplantation: A systematic review and meta-analysis. *Pediatr Transplant*. 2020; 24 (3): e13683.
79. *Gelbart M, Hawthorne K, Wright M et al*. AB0-incompatible deceased donor pediatric liver transplantation: Novel titer-based management protocol and outcomes. *Pediatr Transplant*. 2018; 22 (5): e13216.
80. *Gautier SV, Monakhov AR, Tsirulnikova OM et al*. AB0-Incompatible Liver Transplantation in Children: Single Center Experience. *Transplantation*. 2020; 104 (S3): S550.
81. *Emre S, Umman V*. Large-for-size syndrome in pediatric liver transplantation: A comprehensive review. *Pediatr Transplant*. 2019; 23 (7): e13561.
82. *Kiuchi T, Kasahara M, Uryuhara K et al*. Impact of graft-size mismatching on pediatric living-donor liver transplantation. *Transplantation*. 2000; 69 (1): 127–132.
83. *Miller CM, Nakaji K, Molmenti EP et al*. The reduced-size liver transplant. Techniques and applications. *Transplantation*. 1993; 56 (3): 561–566.
84. *Hwang S, Lee SG, Kim KH et al*. Surgical reconstruction of portal vein hypoplasia in pediatric living donor liver transplantation. *Liver Transpl*. 2013; 19 (5): 534–541.
85. *Namgoong JM, Hwang S, Park GC et al*. Portal vein reconstruction techniques in pediatric living donor liver transplantation for biliary atresia with portal vein hypoplasia: A pictorial essay. *Korean J Radiol*. 2021; 22 (1): 85–95.
86. *Azoulay D, Linhares MM, Huguet E et al*. Decision for retransplantation of the liver: an experienced-based approach. *Ann Surg*. 2002; 236 (6): 713–721.
87. *Mehrabi A, Fonouni H, Schemmer P et al*. Retransplantation of the liver: a single-center experience of 150 patients. *Clin Transplant*. 2008; 22 (3): 347–359.
88. *MacConmara M, Hobeika L, Vachharajani N et al*. Normothermic machine perfusion: The future of liver preservation. *Curr Transplant Rep*. 2020; 7 (1): 38–46.
89. *Boteon YL, Laing RW, Schlegel A et al*. Combined Hypothermic and Normothermic Machine Perfusion for Enhanced Organ Preservation in Liver Transplantation. *Liver Transpl*. 2022; 28 (3): 518–529.
90. *Watson CJE, Kosmoliaptsis V, Randle LV et al*. Normothermic machine perfusion in liver transplantation: a randomized clinical trial. *JAMA Surg*. 2019; 154 (6): 481–489.
91. *Cherqui D, Soubrane O, Husson E et al*. Laparoscopic living donor hepatectomy for liver transplantation in children. *Lancet*. 2002; 359 (9304): 392–396.
92. *Soubrane O, Perdigao F, Goumard C et al*. Laparoscopic living donor left lateral sectionectomy: a new standard practice for pediatric transplantation. *Ann Surg*. 2015; 261 (6): 1071–1076.
93. *Kim KH, Kang SH, Jung DH et al*. Initial experiences with 100 cases of purely laparoscopic living-donor hepatectomy. *Br J Surg*. 2017; 104 (12): 1648–1657.
94. *Broering DC, Elsheikh Y, Nagy K et al*. Robotic-assisted versus laparoscopic live donor hepatectomy: a systematic review and meta-analysis. *Updates Surg*. 2021; 73 (6): 2035–2045.
95. *Rhu J, Choi GS, Kim JM et al*. Feasibility of totally laparoscopic living donor hepatectomy for adult-to-adult living donor liver transplantation: A prospective pilot study. *Am J Transplant*. 2018; 18 (5): 1249–1255.
96. *Suh KS, Hong SK, Yi NJ et al*. Pure laparoscopic living donor hepatectomy and recipient hepatectomy for pediatric liver transplantation. *Liver Transpl*. 2018; 24 (10): 1443–1448.
97. *Rela M, Kaliamoorthy I, Reddy MS*. Robotic-assisted pediatric liver transplantation: The next frontier? *Pediatr Transplant*. 2021; 25 (1): e13871.
98. *Giulianotti PC, Addeo P, Bianco FM*. Robotic liver surgery: a systematic review. *J Hepatobiliary Pancreat Sci*. 2011; 18 (1): 1–10.
99. *Fredericks EM, Bucuvalas JC, Alonso EM et al*. Patient-reported outcomes in pediatric liver transplant recipients: A systematic review. *Liver Transpl*. 2016; 22 (8): 1149–1169.
100. *Annunziato RA, Bucuvalas JC, Stuber ML*. Health-related quality of life in pediatric liver transplant recipients: a meta-analysis. *Pediatr Transplant*. 2008; 12 (1): 70–77.

The article was submitted to the journal on 11.07.2025

DOI: 10.15825/1995-1191-2025-3-46-54

IMPLEMENTATION OF ENHANCED RECOVERY AFTER SURGERY (ERAS) PROTOCOLS IN LIVER TRANSPLANTATION

K.O. Semash, T.A. Dzhanbekov, M.M. Nasyrov, D.R. Sabirov
National Children's Medical Center, Tashkent, Republic of Uzbekistan

Background. Liver transplantation (LT) is one of the most complex surgical procedures, presenting significant challenges in preoperative preparation, intraoperative management, and postoperative rehabilitation. These complexities make it demanding both technically and logistically. The introduction of enhanced recovery after surgery (ERAS) protocols has revolutionized perioperative care across numerous surgical disciplines, leading to improved patient outcomes and reduced healthcare costs. However, the application of ERAS protocols in LT remains limited and inconsistent, with considerable variation in implementation strategies across institutions. **Objective:** to summarize current knowledge and assess an overview of implementation and outcomes of ERAS protocols in LT recipients. **Materials and methods.** A structured literature search was conducted using the keywords "ERAS" and "liver transplantation" across major scientific databases. The review included a range of relevant publications, including review articles, clinical trials, observational studies, and case-control studies. **Conclusion.** ERAS protocols in LT are designed to optimize postoperative recovery, improve clinical outcomes, and minimize the risk of complications. Given the complexity and individuality of each LT case, ERAS pathways must be carefully tailored to the recipient's clinical condition, donor characteristics, and intraoperative variables.

Keywords: liver transplantation, rehabilitation, enhanced recovery after surgery, ERAS.

INTRODUCTION

Perioperative management of liver transplantation (LT) has advanced significantly in recent decades, resulting in improved patient outcomes, reduced morbidity and mortality, and enhanced quality of life [1]. Despite these achievements, the global burden of chronic liver diseases, responsible for approximately 2 million deaths worldwide annually, continues to rise [2]. As indications for LT expand, the demand for this procedure is projected to grow by 10% over the next decade, while the total cost of care is expected to rise by 50% over the next 20 years [3]. These trends underscore the need to implement enhanced recovery after surgery (ERAS) protocols in LT to accommodate the growing patient population and manage escalating healthcare costs.

The ERAS concept emerged in the 1990s [4], facilitated by advancements in minimally invasive surgical techniques, introduction of short-acting anesthetics and muscle relaxants, and the use of regional anesthesia [5]. ERAS represents a comprehensive, evidence-based, multimodal perioperative care program designed to attenuate the body's response to surgery, thereby reducing perioperative and postoperative complications. This approach facilitates shorter hospital stays without increasing readmission rates [6]. The efficacy of ERAS protocols has been well-documented across multiple surgical fields, including colorectal surgery, gynecology, and hepatobiliary surgery [7–11]. A dedicated ERAS protocol for LT was developed in 2022 [12], which was adapted and optimized from a previously developed hepatobiliary surgery protocol [13].

LT poses unique challenges for implementation of ERAS protocols due to several factors, including the severity of preoperative patient conditions [14], presence of hepatic encephalopathy [15], prolonged surgery time, high demand for perioperative blood product transfusions [16], and the need for postoperative immunosuppressive therapy [17]. These complexities have contributed to the limited adoption of ERAS protocols in LT, with most centers relying on individualized approaches that demonstrate variable success rates.

This review examines the core components of ERAS protocols in LT and highlights the key barriers to their implementation. A systematic literature search was conducted using the keywords "ERAS" and "liver transplantation". The review includes relevant clinical evidence, encompassing review papers, clinical trials, observational studies, and case-control studies.

WHICH LIVER RECIPIENTS CAN BE INCLUDED IN THE ERAS PROTOCOL?

Although ERAS protocols are increasingly adopted in liver transplant programs, patient selection criteria remain heterogeneous across centers. Nonetheless, several general considerations can help identify candidates most likely to benefit from ERAS implementation:

Corresponding author: Konstantin Semash. Address: 294, Parkenskaya str., Yashnobod District, Tashkent, 100171, Uzbekistan. Phone: +998 (94) 090-89-05. E-mail: mail@doctorsemash.com

Patient readiness and commitment

Successful participation in ERAS requires active patient involvement, including preoperative education and adherence to postoperative instructions. While hepatic encephalopathy may pose challenges, patients with grade 1–2 encephalopathy can generally be included in ERAS protocols [12]. The social and psychological support available to the patient is often underestimated. These factors must be carefully assessed before surgery.

Functional and nutritional status

Sarcopenia and cachexia should be ruled out, and proactive measures must be taken to optimize the patient's nutritional status [17]. Multimodal prehabilitation has emerged as an effective strategy for enhancing the physiological reserves of LT recipients [18].

Absence of cardiopulmonary dysfunction

K Severe cardiopulmonary dysfunction can significantly complicate ERAS implementation due to increased risk of perioperative complications, challenges in the administration of infusion therapy, specific requirements for anesthetic support, and reduced exercise tolerance, which can directly affect surgical outcomes [12]. Whenever feasible, ERAS protocols should be adapted to each patient's needs and risks to optimize outcomes.

Satisfactory graft function

Graft function is a critical determinant of successful LT and directly impacts the feasibility of accelerated postoperative recovery [18]. A graft with low steatosis (<30%), an adequate graft-to-recipient weight ratio (GRWR >0.8), high-quality preservation, and implantation using meticulous surgical techniques forms the foundation for favorable outcomes [18–21]. Postoperatively, adequate graft function should be evidenced by the resolution of metabolic acidosis, normalization of liver enzyme levels, and improvement in both functional and cognitive status [20].

In general, most ERAS principles can be safely applied to most LT recipients, except for patients presenting with acute liver failure. Implementation of ERAS protocols has improved postoperative outcomes in all surgical specialties [12]. The ERAS protocol can be modified or adapted to the patient's clinical condition and tailored to the requirements of the surgical team and attending physicians [12].

ACCELERATED RECOVERY IN LIVER TRANSPLANT RECIPIENTS

Building on the success of ERAS protocols in other surgical specialties, many transplant centers are now incorporating elements of accelerated recovery into perioperative patient management, even during the early stages of their LT programs [22]. Short-term complications – such as ventilator-associated pneumonia, acute kidney injury, postoperative ileus, and biliary complications – are known to worsen graft survival and increase morbidity and mortality [23–28]. Integrating ERAS principles has been shown to reduce the incidence of these early postoperative complications, thereby improving overall liver transplant outcomes [12].

Preoperative preparation

Preoperative evaluation for LT should involve a comprehensive assessment of the patient's comorbidities, both related and unrelated to liver failure. Most patients with chronic liver disease (CLD) are physically weakened by the time of transplantation. Sarcopenia and weakness are observed in approximately 50% of candidates preparing for surgery [29]. Optimizing the patient's nutritional status before surgery is a critical step in reducing postoperative complications and accelerating recovery.

Risk stratification can be supported by validated tools, including the Karnofsky Performance Status Index [30], the Frailty Index [31], and muscle mass indices derived from computed tomography (CT) imaging [32]. The European Association for the Study of the Liver (EASL) recognizes that patients with CLD often face a dual burden of malnutrition and obesity [33].

Although three randomized controlled trials evaluating preoperative nutritional interventions found no significant differences in short-term outcomes between intervention and control groups [34–36], targeted preoperative strategies remain promising. These include vitamin D supplementation and ensuring adequate caloric and protein intake, which may improve postoperative outcomes [36].

Preoperative optimization of the patient's clinical status is crucial in improving surgical outcomes [12]. This process requires the coordinated efforts of a multidisciplinary team, including surgeons, anesthesiologists, hepatologists, and other relevant specialists [12]. Signs of decompensated cirrhosis should be identified and corrected whenever possible before surgery to reduce perioperative risks [18]. Notably, current evidence does not support correction of coagulopathy before surgery unless the patient shows clinical signs of coagulation disorders [12].

Cardiopulmonary screening is particularly important in preoperative assessment of LT recipients. Beyond common cardiovascular conditions such as ischemic heart disease and valvular pathologies, these patients often present with diastolic dysfunction and electrophysiological abnormalities, which may significantly increase perioperative risk under the stress of transplantation [18]. Ultrasound evaluation of the pleural cavities is also recommended to detect hepatic hydrothorax, which commonly develops secondary to impaired liver synthetic function. Management of hydrothorax typically includes

diuretic therapy, correction of protein disorders, and, if necessary, thoracentesis or drainage.

Special attention should be directed toward identifying and managing infections. Prophylactic antibiotics are indicated for bacterial infections, while antiviral therapy is recommended for hepatitis B, C, and D. In the context of rising antibiotic resistance, screening for multidrug-resistant organisms, including carbapenem-resistant *Enterobacteriaceae*, should be an essential component of preoperative evaluation [18].

Renal function assessment is equally critical. Evaluation should include markers of kidney injury, such as cystatin C, NGAL, and KIM-1 (if available), in combination with ultrasound examination and glomerular filtration rate (GFR) estimation using creatinine clearance. In some patients, judicious fluid expansion combined with splanchnic vasoconstrictor therapy may be effective [12, 18].

Psychosocial assessment is a critical component of preoperative preparation, as depression affects 17%–57% of liver transplant candidates and anxiety disorders occur in 19%–55% [37]. Psychological counseling has been shown to improve short-term postoperative outcomes, primarily by enhancing adherence to the treatment plan, which reduces the risk of graft rejection [38]. Additionally, abstinence from alcohol and smoking is strongly recommended [38].

Preoperative fasting requirements for these patients are generally similar to those for other major surgical procedures: six hours for solid food and two hours for liquids. Prolonged fasting is discouraged. There is no strong evidence for or against preoperative carbohydrate loading in liver transplant recipients [12].

Intraoperative measures

Anesthetic measures

An optimal anesthetic regimen is critical for accelerating postoperative recovery and improving short-term outcomes following LT. The primary objectives of intraoperative anesthesia are facilitating early extubation, providing effective postoperative analgesia, and minimizing the risk of respiratory depression. LT recipients typically require lower doses of anesthetic agents than the general surgical population [12].

Intraoperative monitoring of anesthetic depth, using tools such as the bispectral index (BIS) or equivalent monitors, allows for precise titration of inhalation anesthetics and opioids. Short-acting opioids, when used in dose-optimized regimens, have been shown to facilitate rapid recovery. Evidence suggests that dose reduction strategies improve recovery outcomes regardless of the opioid chosen [12].

Traditionally, benzylisoquinoline muscle relaxants have been the agents of choice for LT due to their extrahepatic metabolism [39]. However, the introduction of sugammadex [40] has made vecuronium or rocuronium suitable alternatives.

Regional anesthesia techniques, particularly neuraxial approaches, were previously used with caution due to the high risk of coagulopathy in patients with chronic liver disease. Recently, there has been renewed interest in regional anesthesia in this patient group due to its potential advantages in terms of reducing opioid consumption, improving hemodynamic stability, and alleviating postoperative pain [41, 42]. In some centers, transversus abdominis plane (TAP) blocks are now routinely used in liver recipients without significant coagulation disorders. TAP blocks provide high-quality intraoperative analgesia and facilitate early extubation [41].

Adequate intraoperative volume management is critical for preventing postoperative complications in LT. Sustained hypervolemia and elevated central venous pressure (CVP) should be avoided [12]. The assessment of volemia should rely on dynamic and minimally invasive cardiac output monitoring and adjusted tailored to the patient's needs and the experience of the anesthesiology team. Empirical correction of coagulopathy should be avoided; instead, blood substitutes should be prescribed based on viscoelastic tests and clinical assessment [43].

Every patient who has undergone LT should be assessed for early extubation ideally within 3–8 hours postoperatively. The decision should be individualized, based on the patient's clinical condition and the availability of close postoperative monitoring. Numerous studies have shown that early extubation after LT improves short-term outcomes [44].

Although there are no strict recommendations regarding contraindications for early extubation, several factors are considered relative exclusions for early extubation in many centers: need for high-volume blood transfusion (>2 units/hour), severe vasoplegia, severe preoperative hepatic encephalopathy, acute liver failure, preoperative mechanical ventilation, concerns about graft function, such as persistent hyperlactatemia [44].

Surgical measures

Surgical techniques should be optimized to reduce operating time, minimize blood loss, and decrease cold ischemia time [12]. Routine use of veno-venous bypass is generally not recommended [45]. However, the creation of a temporary portocaval shunt may be indicated in cases where prolonged interruption of hepatic blood flow is anticipated.

Organ perfusion techniques are critical for protecting the liver graft during the phases of explantation, preservation, and reperfusion. Mechanical perfusion methods also help prevent ischemic reperfusion syndrome and early transplant dysfunction [46, 47]. Whenever feasible, such methods should be considered for all deceased donor grafts, particularly expanded-criteria donors [46].

In cases of massive intraoperative hemorrhage, the use of autologous blood reinfusion systems may be appropriate [48].

Postoperative rehabilitation of liver recipients

Postoperative management of LT recipients is a highly complex and multidisciplinary process aimed at optimizing graft function, preventing complications, and facilitating recovery [12]. Successful care requires continuous monitoring of liver graft function, tailored immunosuppressive therapy, and timely detection and management of vascular, biliary, and infectious complications, while supporting the patient's overall physical rehabilitation.

A multidisciplinary team – including transplant surgeons, anesthesiologists, hepatologists, infectious disease specialists, physical therapists, and dietitians – plays a critical role in ensuring optimal postoperative outcomes.

The implementation of ERAS protocols in LT remains challenging due to a number of factors, such as optimization of infusion therapy, selection of immunosuppression regimens, complex multimodal anesthesia, early removal of catheters and postoperative drains.

Patients with end-stage liver disease have increased susceptibility to infections, which directly affects the effectiveness of accelerated recovery protocols [12]. In addition to these clinical challenges, entrenched surgical and postoperative practices ("clinical dogmas") in some transplant centers may slow the adoption of ERAS protocols [11–13]. These factors will be discussed further below.

ERAS protocols have traditionally emphasized the careful management of fluid therapy, particularly the prevention of hypervolemia. Despite this, many transplant centers continue to favor relative hypervolemia in the early postoperative period to mitigate the risk of vascular complications that may be triggered by hypovolemia [49]. However, recent evidence challenges this approach, indicating that a positive cumulative fluid balance is associated with an increased risk of hepatic artery thrombosis [50]. Notably, even attempts to maintain normovolemia may inadvertently result in fluid overload in this patient population [50]. In light of these findings, some researchers advocate for routine echocardiographic assessment of all liver transplant recipients upon admission to guide and individualize infusion therapy [12, 50].

Unlike other surgeries, post-op pain management in LT recipients is often underestimated, largely due to the standard practices of delayed extubation and delayed mobilization [12]. However, adoption of ERAS protocols requires a multimodal analgesic regimen that not only improves patient comfort but also facilitates early mobilization and accelerates overall recovery [11–13]. Importantly, the requirement for postoperative opioids in LT patients is generally significantly lower than in other surgical populations, particularly in those with high MELD scores and severe hypoalbuminemia [51]. While some centers recommend paracetamol as a first-line analgesic in the postoperative setting [51], others contraindicate its use in LT patients [22]. Moreover, the use of subcostal TAP blocks has been shown to effectively reduce morphine consumption and facilitate earlier weaning from mechanical ventilation [52].

Early removal of catheters and surgical drains remains a significant challenge in LT recipients, largely influenced by the severity of the patient's condition and graft function. Factors such as ongoing bleeding, the need for vasopressor support, management of biliary complications, and postoperative lymphorrhea. However, evidence suggests that LT patients are at high risk of catheter-associated infections, which can negatively impact short-term outcomes [53]. To mitigate this risk, strict adherence to aseptic and antiseptic protocols is essential, along with the use of central venous catheters coated with antimicrobial agents [12]. Although current literature lacks clear consensus or guidelines regarding the optimal timing for catheter and drain removal, early removal may be justified if the patient's condition is stable.

LT recipients are particularly vulnerable to postoperative infections due to the combined effects of pre-existing immunodeficiency and immunosuppressive therapy. Infections not only increase the risk of sepsis but may also contribute to graft dysfunction. Opportunistic pathogens, especially cytomegalovirus (CMV), can lead to significant complications, including vascular and biliary damage. Antibiotic prophylaxis against bacterial infections should be guided by local antimicrobial resistance patterns. Prevention of CMV infection is largely dependent on the serological compatibility between donor and recipient [53]. In some transplant centers, in addition to serological tests, polymerase chain reaction (PCR) testing for CMV is mandatory [22]. Antifungal prophylaxis is also strongly recommended for liver recipients identified as high-risk for invasive fungal infections [54].

Early initiation of enteral nutrition and early patient mobilization are critical components of any enhanced recovery protocols following LT [12]. These measures are particularly important for patients with chronic liver disease, who often present with pre-existing nutritional deficiencies and reduced physical function [12, 55]. In some centers, nasogastric tubes are removed during the immediate postoperative period, sometimes while the patient is still coming out of anesthesia. However, caution is advised in patients with hepaticojejunostomy, where early removal may compromise adequate intestinal decompression.

Oral feeding can be initiated within 12 to 24 hours after transplantation. Parenteral nutrition should be reserved for cases in which enteral feeding fails to meet the patient's caloric and nutritional needs [55]. Early mobilization should begin as soon as clinically feasible

[11–13]. Particular emphasis should also be placed on respiratory physiotherapy and exercises, which play a vital role in preventing pulmonary complications.

Length of hospital stay following LT is widely recognized as a key indicator of treatment quality and effectiveness. A review of six studies assessing optimal discharge timing revealed that, under specific conditions, patients can be safely discharged as early as postoperative day 8 [56–61]. This early discharge is generally appropriate for low-risk patients and in transplant centers equipped with robust outpatient monitoring and follow-up systems.

To support earlier discharge and ensure long-term success, transplant centers are encouraged to implement comprehensive patient education programs. These programs should focus on raising patient awareness of the need to adhere to immunosuppression regimens and awareness of potential complications. In addition, systematic clinical audits have been shown to enhance adherence to medical recommendations and contribute to improved clinical outcomes across transplant populations [62].

IS IT POSSIBLE TO APPLY ERAS PROTOCOLS IN PEDIATRIC LIVER TRANSPLANTATION?

Traditionally, pediatric LT recipients were placed on mechanical ventilation for several days postoperatively. The primary reasons for this prolonged ventilation included a higher GRWR and a greater incidence of vascular complications [63, 64]. However, advances in surgical techniques – such as graft size reduction and monosegmental transplantation – along with improvements in anesthesiology and pediatric intensive care, have enabled some centers to adopt early extubation practices after pediatric LT [65].

Although no meta-analyses have yet evaluated the overall effectiveness of ERAS protocols in this specific patient population, multiple reports in the literature indicate that early extubation is associated with a reduced length of stay in the intensive care unit (ICU) [65].

Fullington et al. [66] reported a series of observations involving 84 pediatric patients who underwent LT. Over the last three years of their study, the authors documented a twofold increase in the number of intraoperative extubations, which correlated with improved short-term outcomes, namely, a reduced length of stay in the ICU and a lower frequency of reintubations. However, the publication did not provide detailed descriptions of the specific surgical or anesthetic techniques employed in their center.

A later report by Sahinturk et al. [67] found that early extubation was achieved in 48% of pediatric liver recipients, also demonstrating a decrease in the length of stay in the ICU. The authors presented a series of cases involving 16 patients under two years of age who were extubated immediately after LT. In all cases, a right-sided TAP block was combined with a bilateral rectus abdominis block after wound closure, resulting in reduced postoperative opioid consumption [68].

ERAS protocols in LT can be effectively adapted for pediatric patients. Recent advances in pediatric anesthesiology, such as adoption of myofascial blocks, together with improvements in pediatric intensive care, have contributed to shorter durations of postoperative ventilation. Additional measures that may further support the successful implementation of ERAS in pediatric transplantation include optimized preoperative nutritional support, use of bedside ultrasound for postoperative monitoring, and active parental participation in the child's care [65].

CONCLUSION

Although many centers remain unfamiliar with, or have yet to adopt, ERAS protocols, their introduction has the potential to improve perioperative outcomes in LT significantly. This procedure presents unique challenges and risks that can hinder implementation of ERAS protocols; however, perioperative teams can develop tailored accelerated recovery strategies that align with institutional resources and individual patient needs. The success of any transplant program – including ERAS integration – relies on a multidisciplinary approach supported by a skilled, collaborative team. Ultimately, application of enhanced recovery protocols reduces early postoperative complications and ultimately improves overall treatment outcomes.

The authors declare no conflict of interest.

REFERENCES

1. *Meirelles Júnior RF, Salvalaggio P, Rezende MB et al.* Liver transplantation: history, outcomes and perspectives. *Einstein (Sao Paulo)*. 2015; 13 (1): 149–152. https://doi.org/10.1590/S1679-45082015RW3164.
2. *Asrani SK, Devarbhavi H, Eaton J, Kamath PS.* Burden of liver diseases in the world. *J Hepatol*. 2019; 70 (1): 151–171. https://doi.org/10.1016/j.jhep.2018.09.014.
3. *Habka D, Mann D, Landes R, Soto-Gutierrez A.* Future economics of liver transplantation: a 20-year cost modeling forecast and the prospect of bioengineering autologous liver grafts. *PLoS One*. 2015; 10 (7): e0131764. https://doi.org/10.1371/journal.pone.0131764.
4. *Taurchini M, Del Naja C, Tancredi A.* Enhanced recovery after surgery: a patient centered process. *J Vis Surg*. 2018; 4: 40. https://doi.org/10.21037/jovs.2018.01.20.
5. *Pache B, Hübner M, Jurt J, Demartines N, Grass F.* Minimally invasive surgery and enhanced recovery after surgery: the ideal combination? *J Surg Oncol*. 2017; 116 (5): 613–616. https://doi.org/10.1002/jso.24787.
6. *Brown JK, Singh K, Dumitru R, Chan E, Kim MP.* The benefits of enhanced recovery after surgery programs and their application in cardiothoracic surgery. *Methodist Debakey Cardiovasc J*. 2018; 14 (2): 77–88. https://doi.org/10.14797/mdcj-14-2-77.

7. *Cavallaro P, Bordeianou L.* Implementation of an ERAS pathway in colorectal surgery. *Clin Colon Rectal Surg*. 2019; 32 (2): 102–108. https://doi.org/10.1055/s-0038-1676474.
8. *Moorthy K, Halliday L.* Guide to enhanced recovery for cancer patients undergoing surgery: ERAS and oesophagectomy. *Ann Surg Oncol*. 2022; 29 (1): 224–228. https://doi.org/10.1245/s10434-021-10384-5.
9. *Santiago AE, Filho ALDS, Cândido EB et al.* Perioperative management in gynecological surgery based on the ERAS program. *Rev Bras Ginecol Obstet*. 2022; 44 (2): 202–210. https://doi.org/10.1055/s-0042-1743401.
10. *Agarwal V, Divatia JV*. Enhanced recovery after surgery in liver resection: current concepts and controversies. *Korean J Anesthesiol*. 2019; 72 (2): 119–129. https://doi.org/10.4097/kja.d.19.00010.
11. *Joliat GR, Kobayashi K, Hasegawa K, Thomson JE, Padbury R, Scott M et al*. Guidelines for Perioperative Care for Liver Surgery: Enhanced Recovery After Surgery (ERAS) Society Recommendations 2022. *World J Surg*. 2023 Jan; 47 (1): 11–34. https://doi.org/10.1007/s00268-022-06732-5.
12. *Brustia R, Monsel A, Skurzak S, Schiffer E, Carrier FM, Patrono D et al*. Guidelines for Perioperative Care for Liver Transplantation: Enhanced Recovery After Surgery (ERAS) Recommendations. *Transplantation*. 2022 Mar 1; 106 (3): 552–561. https://doi.org/10.1097/TP.0000000000003808.
13. *Melloul E, Hübner M, Scott M, Snowden C, Prentis J, Dejong CH et al*. Guidelines for Perioperative Care for Liver Surgery: Enhanced Recovery After Surgery (ERAS) Society Recommendations. *World J Surg*. 2016 Oct; 40 (10): 2425–2440. https://doi.org/10.1007/s00268-016-3700-1.
14. *Tandon P, Montano-Loza AJ, Lai JC, Dasarathy S, Merli M.* Sarcopenia and frailty in decompensated cirrhosis. *J Hepatol*. 2021; 75 Suppl 1 (Suppl 1): S147–S162. https://doi.org/10.1016/j.jhep.2021.01.025.
15. *Denk A, Müller K, Schlosser S et al.* Liver diseases as a novel risk factor for delirium in the ICU – Delirium and hepatic encephalopathy are two distinct entities. *PLoS One*. 2022; 17 (11): e0276914. https://doi.org/10.1371/journal.pone.0276914.
16. *Devi AS.* Transfusion practice in orthotopic liver transplantation. *Indian J Crit Care Med*. 2009; 13 (3): 120–128. https://doi.org/10.4103/0972-5229.58536.
17. *Montgomery J, Englesbe M.* Sarcopenia in liver transplantation. *Curr Transplant Rep*. 2019; 6 (1): 7–15. https://doi.org/10.1007/s40472-019-0223-3.
18. *Jetten WD, Hogenbirk RNM, Van Meeteren NLU et al.* Physical effects, safety and feasibility of prehabilitation in patients awaiting orthotopic liver transplantation, a systematic review. *Transpl Int*. 2022; 35: 10330. https://doi.org/10.3389/ti.2022.10330.
19. *Chae MS, Kim Y, Lee N et al.* Graft regeneration and functional recovery in patients with early allograft dysfunction after living-donor liver transplantation. *Ann Transplant*. 2018; 23: 481–490. https://doi.org/10.12659/aot.909112.
20. *Duan X, Yan L, Shen Y, Zhang M, Bai X, Liang T.* Outcomes of liver transplantation using moderately steatotic liver from donation after cardiac death (DCD). *Ann Transl Med*. 2020; 8 (18): 1188. https://doi.org/10.21037/atm-20-5888.
21. *Mohapatra N, Gurumoorthy Subramanya Bharathy K, Kumar Sinha P et al.* Three-dimensional volumetric assessment of graft volume in living donor liver transplantation: does it minimise errors of estimation? *J Clin Exp Hepatol*. 2020; 10 (1): 1–8. https://doi.org/10.1016/j.jceh.2019.03.006.
22. *Semash K, Dzhanbekov T, Akbarov M, Mirolimov M, Usmonov A, Razzokov N et al*. Implementation of a living donor liver transplantation program in the Republic of Uzbekistan: a report of the first 40 cases. *Clin Transplant Res.* 2024; 38: 116–127. https://doi.org/10.4285/ctr.24.0013.
23. *Ben-Haim M, Emre S, Fishbein TM et al.* Critical graft size in adult-to-adult living donor liver transplantation: impact of the recipient's disease. *Liver Transpl*. 2001; 7 (11): 948–953. https://doi.org/10.1053/jlts.2001.29033.
24. *Siniscalchi A, Aurini L, Benini B et al.* Ventilator associated pneumonia following liver transplantation: etiology, risk factors and outcome. *World J Transplant*. 2016; 6 (2): 389–395. https://doi.org/10.5500/wjt.v6.i2.389.
25. *Durand F, Francoz C, Asrani SK et al.* Acute kidney injury after liver transplantation. Transplantation. 2018; 102 (10): 1636–1649. https://doi.org/10.1097/tp.0000000000002305.
26. *Bai R, An R, Han K et al.* Prognosis of liver transplantation: does postoperative ileus matter? *BMC Gastroenterol*. 2021; 21 (1): 444. https://doi.org/10.1186/s12876-021-02026-7.
27. *Boeva I, Karagyozov PI, Tishkov I.* Post-liver transplant biliary complications: current knowledge and therapeutic advances. *World J Hepatol*. 2021; 13 (1): 66–79. https://doi.org/10.4254/wjh.v13.i1.66.
28. *Semash KO*. Post-liver transplant biliary complications. *Russian Journal of Transplantology and Artificial Organs*. 2024; 26 (3): 72–90. (In Russ.). https://doi.org/10.15825/1995-1191-2024-3-72-90.
29. *Montgomery J, Englesbe M.* Sarcopenia in liver transplantation. *Curr Transplant Rep*. 2019; 6 (1): 7–15. https://doi.org/10.1007/s40472-019-0223-3.
30. *Thuluvath PJ, Thuluvath AJ, Savva Y*. Karnofsky performance status before and after liver transplantation predicts graft and patient survival. *J Hepatol*. 2018; 69 (4): 818–825. https://doi.org/10.1016/j.jhep.2018.05.025.
31. *Lai JC, Sonnenday CJ, Tapper EB et al.* Frailty in liver transplantation: an expert opinion statement from the American Society of Transplantation Liver and Intestinal Community of Practice. *Am J Transplant*. 2019; 19 (7): 1896–1906. https://doi.org/10.1111/ajt.15392.
32. *Shafaat O, Liu Y, Jackson KR et al.* Association between abdominal CT measurements of body composition before deceased donor liver transplant with posttransplant outcomes. *Radiology*. 2023; 306 (3): e212403. https://doi.org/10.1148/radiol.212403.

33. European Association for the Study of the Liver. EASL Clinical Practice Guidelines on nutrition in chronic liver disease. *J Hepatol*. 2019 Jan; 70 (1): 172–193. https://doi.org/10.1016/j.jhep.2018.06.024.
34. *Le Cornu KA, McKiernan FJ, Kapadia SA, Neuberger JM*. A prospective randomized study of preoperative nutritional supplementation in patients awaiting elective orthotopic liver transplantation. *Transplantation*. 2000; 69 (7): 1364–1369. https://doi.org/10.1097/00007890-200004150-00026.
35. *Victor DW 3rd, Zanetto A, Montano-Loza AJ et al.* The role of preoperative optimization of the nutritional status on the improvement of short-term outcomes after liver transplantation? A review of the literature and expert panel recommendations. *Clin Transplant*. 2022; 36 (10): e14647. https://doi.org/10.1111/ctr.14647.
36. *Bahari H, Aliakbarian M, Norouzy A, Mansourian M, Akhavan-Rezayat K, Khadem-Rezaiyan M et al*. Assessment of the nutritional status of patients before, one, and three months after liver transplantation: A multi-center longitudinal study. *Clin Nutr ESPEN*. 2023 Feb; 53: 244–250. https://doi.org/10.1016/j.clnesp.2022.12.027.
37. *Kimura H, Kishi S, Narita H et al.* Comorbid psychiatric disorders and long-term survival after liver transplantation in transplant facilities with a psychiatric consultation-liaison team: a multicenter retrospective study. *BMC Gastroenterol*. 2023; 23: 106. https://doi.org/10.1186/s12876-023-02735-1.
38. *Matthews LA, Lucey MR*. Psychosocial evaluation in liver transplantation for patients with alcohol-related liver disease. *Clin Liver Dis (Hoboken)*. 2022; 19 (1): 17–20. https://doi.org/10.1002/cld.1160.
39. *Adeyinka A, Layer DA.* Neuromuscular Blocking Agents. 2024 Jun 8. In: StatPearls [Internet]. Treasure Island (FL): StatPearls Publishing; 2024 Jan. PMID: 30725853.
40. *Deana C, Barbariol F, D'Incà S, Pompei L, Rocca GD*. Sugammadex versus neostigmine after rocuronium continuous infusion in patients undergoing liver transplantation. *BMC Anesthesiol*. 2020; 20 (1): 70. https://doi.org/10.1186/s12871-020-00986-z.
41. *Milan ZB, Duncan B, Rewari V, Kocarev M, Collin R.* Subcostal transversus abdominis plane block for postoperative analgesia in liver transplant recipients. *Transplant Proc*. 2011; 43 (7): 2687–2690. https://doi.org/10.1016/j.transproceed.2011.06.059.
42. *Hausken J, Haugaa H, Hagness M et al.* Thoracic epidural analgesia for postoperative pain management in liver transplantation: a 10-year study on 685 liver transplant recipients. *Transplant Direct*. 2021; 7 (2): e648. https://doi.org/10.1097/txd.0000000000001101.
43. *Park SY.* Viscoelastic coagulation test for liver transplantation. *Anesth Pain Med (Seoul)*. 2020; 15 (2): 143–151. https://doi.org/10.17085/apm.2020.15.2.143.
44. *Tinguely P, Badenoch A, Krzanicki D et al.* The role of early extubation on short-term outcomes after liver transplantation: a systematic review, meta-analysis and expert recommendations. *Clin Transplant*. 2022; 36 (10): e14642. https://doi.org/10.1111/ctr.14642.
45. *Fonouni H, Mehrabi A, Soleimani M et al.* The need for venovenous bypass in liver transplantation. *HPB (Oxford)*. 2008; 10 (3): 196–203. https://doi.org/10.1080/13651820801953031.
46. *Semash K, Salimov U, Dzhanbekov T, Sabirov D.* Liver Graft Machine Perfusion: From History Perspective to Modern Approaches in Transplant Surgery. *Exp Clin Transplant*. 2024 Jul; 22 (7): 497–508. https://doi.org/10.6002/ect.2024.0137.
47. *Schlegel A, Muller X, Dutkowski P*. Machine perfusion strategies in liver transplantation. *Hepatobiliary Surg Nutr*. 2019; 8 (5): 490–501. https://doi.org/10.21037/hbsn.2019.04.04.
48. *Pinto MA, Chedid MF, Sekine L et al.* Intraoperative cell salvage with autologous transfusion in liver transplantation. *World J Gastrointest Surg*. 2019; 11 (1): 11–8. https://doi.org/10.4240/wjgs.v11.i1.11.
49. *Semash KO, Dzhanbekov TA, Akbarov MM*. Vascular complications after liver transplantation: contemporary approaches to detection and treatment. A literature review. *Russian Journal of Transplantology and Artificial Organs*. 2023; 25 (4): 46–72. https://doi.org/10.15825/1995-1191-2023-4-46-72.
50. *Larivière J, Giard JM, Zuo RM, Massicotte L, Chassé M, Carrier FM.* Association between intraoperative fluid balance, vasopressors and graft complications in liver transplantation: a cohort study. *PLoS One*. 2021; 16 (7): e0254455. https://doi.org/10.1371/journal.pone.0254455.
51. *Castellani Nicolini N, Belfiore J, Biancofiore G.* Multimodal pain management of liver transplantation: what is new? *OBM Transplant*. 2023; 7 (4): 198. https://dx.doi.org/10.21926/obm.transplant.2304198.
52. *Assefi M, Trillaud E, Vezinet C et al*. Subcostal transversus abdominis plane block for postoperative analgesia in liver transplant recipients: a before-and-after study. *Reg Anesth Pain Med*. 2023; 48 (7): 352–358. https://doi.org/10.1136/rapm-2022-103705.
53. *Russell TA, Fritschel E, Do J et al.* Minimizing central line-associated bloodstream infections in a high-acuity liver transplant intensive care unit. *Am J Infect Control*. 2019; 47 (3): 305–312. https://doi.org/10.1016/j.ajic.2018.08.006.
54. *Evans JD, Morris PJ, Knight SR.* Antifungal prophylaxis in liver transplantation: a systematic review and network meta-analysis. *Am J Transplant*. 2014; 14 (12): 2765–2776. https://doi.org/10.1111/ajt.12925.
55. *Yirui L, Yin W, Juan L, Yanpei C*. The clinical effect of early enteral nutrition in liver-transplanted patients: a systematic review and meta-analysis. *Clin Res Hepatol Gastroenterol*. 2021; 45 (3): 101594. https://doi.org/10.1016/j.clinre.2020.101594.
56. *Tanaka T, Reichman TW, Olmos A et al*. When is the optimal time to discharge patients after liver transplantation concerning short-term outcomes? A systematic review of the literature and expert panel recommendations. *Clin Transplant*. 2022; 36 (10): e14685. https://doi.org/10.1111/ctr.14685.
57. *Verma S, Das LK, Naganathan SK*. Super-fast-track discharge of liver transplant recipients. *Korean J*

Transplant. 2023; 37: 76–78. https://doi.org/10.4285/kjt.23.0002.
58. *Brett KE, Ritchie LJ, Ertel E, Bennett A, Knoll GA*. Quality metrics in solid organ transplantation: a systematic review. *Transplantation*. 2018; 102: e308–e330. https://doi.org/10.1097/tp.0000000000002149.
59. *Rodríguez-Laiz GP, Melgar-Requena P, Alcázar-López CF et al.* Fast-track liver transplantation: six-year prospective cohort study with an enhanced recovery after surgery (ERAS) protocol. *World J Surg*. 2021; 45: 1262–1271. https://doi.org/10.1007/s00268-021-05963-2.
60. *Rodríguez Laiz GP, Melgar Requena P, Alcázar López C et al.* Fast track liver transplantation: lessons learned after 10 years running a prospective cohort study with an ERAS-like protocol. *J Liver Transplant*. 2023; 10: 100151. https://doi.org/10.1016/j.liver.2023.10015.
61. *Rodríguez-Laiz GP, Melgar-Requena P, Alcázar-López CF et al.* ERAS in liver transplantation: a decade running a comprehensive fast-track liver transplant protocol. *Transplantation*. 2021; 106 (9S): S14. https://doi.org/ 10.1097/01.tp.0000885280.16539.35.
62. *López-Púa Y, Navasa M, Trilla A et al.* Implementation of a quality management system in a liver transplant programme. *BMJ Open Qual*. 2023; 12 (3): e002440. https://doi.org/10.1136/bmjoq-2023-002440.
63. *Avolio AW, Gaspari R, Teofili L et al.* Postoperative respiratory failure in liver transplantation: risk factors and effect on prognosis. *PLoS One*. 2019; 14 (2): e0211678. https://doi.org/10.1371/journal.pone.0211678.
64. *Semash K, Dzhanbekov T.* Large-for-size syndrome prophylaxis in infant liver recipients with low body mass. *World J Transplant* 2025; 15 (1): 99452. https://doi.org/10.5500/wjt.v15.i1.99452.
65. *Kitajima T, Sakamoto S, Sasaki K et al.* Impact of graft thickness reduction of left lateral segment on outcomes following pediatric living donor liver transplantation. *Am J Transplant*. 2018; 18 (9): 2208–2219. https://doi.org/10.1111/ajt.14875.
66. *Gautier SV, Tsiroulnikova OM, Moysyuk YG, Akhaladze DG, Tsiroulnikova IE, Silina OV et al*. Liver transplantation in children: six-year experience analysis. *Russian Journal of Transplantology and Artificial Organs*. 2014; 16 (3): 54–62. (In Russ.). https://doi.org/10.15825/1995-1191-2014-3-54-62.
67. *Fullington NM, Cauley RP, Potanos KM et al.* Immediate extubation after pediatric liver transplantation: a single-center experience. *Liver Transpl*. 2015; 21 (1): 57–62. https://doi.org/10.1002/lt.24036.
68. *Sahinturk H, Ozdemirkan A, Yilmaz O et al.* Immediate tracheal extubation after pediatric liver transplantation. *Exp Clin Transplant*. 2021; 19 (10): 1063–1068. https://doi.org/10.6002/ect.2018.0067.
69. *Chatterjee C, Shankar V, Dhar P, Raj A*. Use of ultrasound guided subcostal TAP block along with bilateral rectus sheath block – a novel way to aid on table extubation of pediatric liver recipients. *Ann Clin Case Rep*. 2020; 5: 1857.
70. *Gautier S, Monakhov A, Tsiroulnikova O, Mironkov B, Voskanov M, Dzhanbekov T et al*. Time is of the essence: A single-center experience of hepatic arterial supply impairment management in pediatric liver transplant recipients. *Pediatr Transplant*. 2021 May; 25 (3): e13934. https://doi.org/10.1111/petr.13934.

The article was submitted to the journal on 17.12.2024

DOI: 10.15825/1995-1191-2025-3-55-65

PSYCHOLOGICAL PROFILES OF END-STAGE RENAL DISEASE PATIENTS UNDERGOING PRE-TRANSPLANT EVALUATION

E.V. Dubinina, M.S. Nesterova

Shumakov National Medical Research Center of Transplantology and Artificial Organs, Moscow, Russian Federation

Objective: to identify specific psychological characteristics of individuals with end-stage renal disease (ESRD) who are undergoing evaluation for inclusion on the kidney transplant waiting list, as well as those already on the list. **Materials and methods.** The study was based on the hypothesis that individuals with ESRD exhibit a correlation between family-related anxiety and psychological traits such as weak personal boundaries, depressive symptoms, and difficulty recognizing and expressing emotions. To test this hypothesis, the following validated instruments were employed: Karpov's Reflexivity Diagnostic Method, Beck Depression Inventory (BDI), the Sovereignty of Psychological Space Questionnaire – 2010, Toronto Alexithymia Scale (TAS-20) and Family Anxiety Analysis Questionnaire (FAA). The study sample included 60 people aged 18 to 71 years. The main group consisted of 30 respondents diagnosed with kidney failure, while the control group included 30 ESRD-free individuals. Statistical analysis was conducted using SPSS Statistics version 27.0. **Results.** The study found that patients with ESRD exhibited reduced levels of reflexivity compared to the control group ($p \leq 0.01$). However, no statistically significant differences were observed between the groups in terms of depression levels, personal boundary preservation, or the ability to identify and describe emotions ($p > 0.05$). ESRD patients reported lower levels of family-related anxiety than the healthy individuals ($p \leq 0.05$). Correlation analysis revealed a significant positive relationship between depression and the difficulty in recognizing and identifying emotions among ESRD patients ($R = 0.491$, $p \leq 0.01$), as well as between depression and levels of anxiety ($R = 0.418$, $p \leq 0.05$) and psychological tension ($R = 0.640$, $p \leq 0.01$). An inverse correlation was found between the ability to recognize internal states and make informed decisions, and the perceived sense of security within one's physical and psychological space ($R = –0.385$, $p \leq 0.05$). Additionally, a direct correlation was identified between the level of depression and the duration of hemodialysis treatment in the ESRD population. **Conclusion**. The findings underscore the importance of considering psychological factors in the pre-transplant assessment and preparation of patients with kidney failure. Incorporating psychological evaluation into the transplant protocol may enhance both surgical outcomes and long-term adaptation to post-transplant life.

Keywords: psychological characteristics, end-stage CKD.

INTRODUCTION

Approximately 13% of the global population suffers from chronic kidney disease (CKD) [1], with similar prevalence rates observed in both developed and developing countries. Moreover, the number of patients is growing by nearly 10% each year, highlighting its increasing public health burden.

A major challenge in CKD management is that the disease is often asymptomatic in its early stages and therefore tends to be diagnosed only when it has already progressed significantly. In some cases, despite intensive medical interventions, including drug therapy, renal replacement therapy (hemodialysis and peritoneal dialysis), and even kidney transplantation, patients experience clinical deterioration and, in certain instances, graft rejection. Importantly, such unfavorable outcomes cannot always be fully explained by current medical understanding.

In our view, one crucial factor that should also be kept in mind for any human disease is the patient's mental and emotional state. A substantial body of research by both Russian and international scholars highlights the influence of psychological factors on health recovery and postoperative survival in patients with terminal stages of chronic diseases. Notable contributions include the works of Gautier V.S., Klimusheva N.F., Baranskaya N.P., Shmakova T.V., Simonenko M.A., Fedotova P.A., Shevchenko A.O., Khalilulina T.A., Kukova K., and Dzhordzhanova A. [1–6].

Further investigations by Vanchakova N.P., Petrova N.N., Vasilyeva I.A., Babarykina E.V., Dobronravov V.A., Baranetskaia V.N., Guerra F., Di Giacomo D., and others have placed particular emphasis on patients receiving hemodialysis [7–12].

This article presents a study of certain traits and personality characteristics of psychosomatic patients with

Corresponding author: Ekaterina Dubinina. Address: 1, Shchukinskaya str., Moscow, 123182, Russian Federation. Phone: (985) 828-46-96. E-mail: gavr9094@mail.ru

end-stage renal disease (ESRD). The psychological profile of these patients has previously been examined, for example, using Cattell's multifactor personality questionnaire [9]. In our research, we applied alternative methods and conducted a comparative analysis of the personality traits of ESRD patients and individuals without CKD (hereafter referred to as "healthy" controls).

Aim of the study: To identify specific psychological characteristics of individuals with ESRD who are either undergoing evaluation for placement on the kidney transplant waiting list or are already on the list.

Relevance of the study: A deeper understanding of the psychological characteristics of patients with ESRD may significantly contribute to their physical, psychological, and social adaptation both before and after kidney transplantation. This, in turn, may help lower the risk of transplant rejection.

MATERIALS AND METHODS

The empirical material for this study was collected in 2024. For the purposes of the research, we focused on a set of psychological characteristics commonly observed in individuals with psychosomatic illnesses, namely:

– Reduced reflectivity – diminished capacity to analyze and evaluate events, limited self-reflection in specific life situations, and a low degree of elaboration in decision-making processes (manifested as a tendency toward impulsivity in decision-making).
– Depressiveness.
– Reduced level of sovereignty of psychological space – diminished preservation of personal boundaries.
– Increased level of alexithymia – difficulty in identifying and describing one's own feelings, limited ability to understand the emotions of others, and externally oriented thinking.
– Elevated general family anxiety – encompassing its key components: guilt, anxiety, and tension.

A working hypothesis was proposed that individuals with ESRD exhibit a correlation between indicators of family anxiety and such psychological traits as weak personal boundaries, depressive tendencies, and difficulty in recognizing and expressing their true emotions.

To test this hypothesis, the following diagnostic methods and questionnaires were employed: A.V. Karpov's Method for assessing the level of reflexivity; Beck Depression Inventory (BDI), adapted by N.V. Tarabrina; the "Sovereignty of Psychological Space – 2010" Questionnaire by S.K. Nartova-Bochaver; Toronto Alexithymia Scale (TAS-20) by G. Taylor, D. Ryan, and R. Bagby, adapted by E.G. Starostina et al.; the "Analysis of Family Anxiety" (ACT) Questionnaire by E. Eidemiller and V. Justickis.

The study sample consisted of 60 participants aged 18 to 71 years (mean age 41.8), of whom 66.7% were women and 33.3% men. The participants were divided into two groups:

Main (experimental) group: 30 individuals with ESRD, including 20 undergoing evaluation for placement on the kidney transplant waiting list and 10 already listed; Control group: 30 individuals without chronic kidney disease. All participants provided informed consent prior to their inclusion in the study.

The study was conducted among patients at Shumakov National Medical Research Center of Transplantology and Artificial Organs, as well as online through Google Forms, which was used to recruit participants for the control group. Statistical analysis was performed using SPSS Statistics, version 27.0.

In the main group, women accounted for 53.3% and men for 46.7%, while in the control group, women comprised 73.3% and men 26.7%. However, the difference in gender distribution between the two groups was not statistically significant ($p > 0.05$). The age of respondents in the main group ranged from 18 to 71 years (mean age: 41.13 years), while in the control group it ranged from 18 to 63 years (mean age: 42.46 years). Similarly, no statistically significant differences were found between the groups in terms of age ($p > 0.05$).

The absence of significant differences in gender and age composition between the groups provides a valid basis for subsequent comparison of their psychological characteristics.

Respondents in the main group were additionally examined based duration of dialysis and length of time spent on the waiting list for a donor kidney transplant. The median duration of hemodialysis was 1.9 years. For most patients with ESRD, dialysis duration ranged from 1 month to 4 years, with periods exceeding 4 years observed only in isolated cases. Approximately one-third of patients were already on the waiting list, while the remaining participants were still undergoing evaluation for inclusion. The median waiting time on the list was 1.1 years, and only in rare cases did it exceed 2 years.

At the initial stage, the test results were processed according to scoring keys, after which mean values were calculated and distributions were analyzed by the degree of severity of specific psychological characteristics. Subsequently, the data were subjected to statistical processing in accordance with the proposed hypothesis.

RESULTS

Table 1 presents the results of the analysis of respondents in the main and control groups with respect to their level of reflectivity.

According to the data, patients with ESRD in the main group were almost evenly distributed between low and medium levels of reflectivity, with no respondents demonstrating a high level. At the same time, all three levels of reflectivity were observed in the control group, with the majority (63.3%) showing a medium level.

These findings suggest that the main group is generally characterized by a lower level of reflectivity com-

pared to the control group. In practical terms, patients with ESRD display reduced attention to their inner states and greater impulsiveness in decision-making.

Next, we will examine the severity of depression among respondents in both groups.

According to the data presented in Table 2, depression among respondents in both groups was distributed across three levels: absence of symptoms, moderate, and severe. However, in the main group, the proportion of respondents without signs of depression was lower, while the share of those with moderate and severe depression was correspondingly higher compared to the control group. Overall, the severity of depression in patients with ESRD did not show a statistically significant difference from that observed in healthy individuals.

The next stage of analysis focuses on sovereignty of psychological space (SPS) in both patients and healthy respondents.

The data presented in Table 3 indicate that patients with ESRD most frequently demonstrate high levels of physical sovereignty and least frequently exhibit high levels of social sovereignty. This suggests that such patients often lack freedom in choosing friends and social circles, with their social lives being constrained by the influence of significant others, whose actions are aimed at preserving their somatic well-being. These findings are consistent with earlier research [7, 8], which highlighted the pronounced frustration of the need for social achievement in patients undergoing hemodialysis.

Table 1

Levels of reflectivity among respondents

Group	Reflectivity level					
	Low		Medium		High	
	Number of respondents	Percentage	Number	Percentage	Number of respondents	Percentage
Main	**15**	50.0%	15	50.0%	**0**	0.0%
Control	7	23.3%	19	63.3%	4	13.4%

Table 2

Severity of depression among respondents

Signs of depression symptoms	Main group		Control group	
	Number of respondents	Percentage	Number of respondents	Percentage
No symptoms of depression	17	56.7%	21	70.0%
Moderate depression	10	33.3%	7	23.3%
Severe depression	3	10.0%	2	6.7%
Total	30	100.0%	30	100.0%

Table 3

Sovereignty of psychological space among respondents

Indicator	No. / %	Main group				Control group			
		Low	Medium	High	Total	Low	Medium	High	Total
Sovereignty of the physical body	N	10	6	14	30	10	7	13	30
	%	33.3%	20.0%	**46.7%**	100%	33.3%	23.3%	43.3%	100%
Sovereignty of territory	N	12	5	13	30	13	7	10	30
	%	40%	16.70%	43.30%	100%	43.3%	23.3%	33.3%	100%
Sovereignty of the world of things	N	12	5	13	30	10	6	14	30
	%	40.0%	16.7%	43.3%	100%	33.3%	20.0%	**46.7%**	100%
Sovereignty of habits	N	10	9	11	30	10	10	10	30
	%	33.3%	30%	36.7%	100%	33.3%	33.3%	33.3%	100%
Sovereignty of social connections	N	11	12	7	30	10	5	15	30
	%	36.7%	40.0%	**23.3%**	100%	33.3%	16.7%	**50.0%**	100%
Sovereignty of values	N	12	5	13	30	11	6	13	30
	%	40%	16.7%	43.3%	100%	36.7%	20%	43.3%	100%
Sovereignty of the psychological space of the individual	N	10	8	12	30	10	8	12	30
	%	33.3%	26.7%	40%	100%	33.3%	26.7%	40.0%	100%

In contrast, respondents in the control group most commonly display high scores on the scales of sovereignty of social connections and sovereignty of the world of things, while lower scores are observed for sovereignty of territory and sovereignty of habits.

Overall, respondents with ESRD place the greatest value on respect for physical well-being and personal property, freedom of worldview, and physical safety, whereas independence in choosing their social circle is considered the least important factor. By contrast, respondents in the control group place the highest importance on independence in choosing their circle of communication, followed by respect for property, somatic well-being, and freedom of worldview.

The level of sovereignty of social connections in the control group (50.0%) differs significantly from that in the ESRD group (23.3%). A likely explanation for this difference is the "attachment" of ESRD patients to dialysis machines and the necessity of organizing their daily lives around the dialysis schedule. In addition, for these patients, maintaining health becomes the central life priority.

Table 4 presents the results regarding the severity of alexithymia, understood as the inability to recognize and describe one's own feelings.

Nearly half of the ESRD patients demonstrate moderate levels of alexithymia, while about one-third fall into the low-level category, and the remainder exhibit high levels. In the control group, by contrast, only a single case of high alexithymia was recorded, with all other respondents showing moderate or low levels. This indicates that patients with ESRD generally experience greater difficulty in identifying and expressing their emotions compared to healthy individuals.

Next, we turn to the distribution of respondents in both groups according to family anxiety analysis (FAA) indicators, including general family anxiety and its key components: guilt, anxiety, and tension.

The data presented in Table 5 show that patients with ESRD generally do not exhibit elevated levels of guilt, anxiety, tension, or overall family anxiety. Only 10% of patients reported increased family tension, meaning they do not feel completely at ease when interacting with family members.

Similarly, respondents in the control group showed levels of family guilt, anxiety, and tension that remained within normal limits.

To further explore the relationship between the identified psychological characteristics, we conducted a comparative analysis of the differences between ESRD patients and the control group. Differences in quantitative variables were assessed using the Mann–Whitney U test for two independent samples. Given the non-normal distribution of most scales and the predominance of ordinal-level variables, central tendency and variability were described using the median and interquartile range (lower and upper quartiles).

The results of this comparative analysis of reflectivity, depression, alexithymia, sovereignty of the psychological space, and family anxiety (including its components) are presented in Table 6.

According to the data presented in Table 6, significant differences between respondents in the main and control groups were observed only for reflectivity ($p \leq 0.05$) and for several indicators of the Family Anxiety Analysis (FAA) questionnaire: Guilt ($p \leq 0.01$), Tension, and overall family anxiety ($p \leq 0.05$).

Table 4

Severity of alexithymia among respondents

Severity level	Main group		Control group	
	Number of respondents	Percentage	Number of respondents	Percentage
Low	11	36.7%	13	43.4%
Medium	14	46.7%	16	53.3%
High	5	**16.7%**	1	3.3%
Total	30	100.0%	30	100.0%

Table 5

Distribution of respondents by family anxiety level indicators

Indicators	Main group				Control group			
	Normal		Elevated level		Normal		Elevated level	
	Number	%	Number	%	Number	%	Number	%
Guilt	30	100%	0	0%	30	100%	0	0%
Anxiety	30	100%	0	0%	29	96.7%	1	**3.3%**
Tension	27	90%	3	**10%**	29	96.7%	1	**3.3%**
General family anxiety	30	100%	0	0%	30	100%	0	0%

The median reflectivity in the control group was significantly higher than in the main group. The average score for guilt towards family members was also significantly lower in patients with ESRD, with more than half of them reporting zero scores, whereas respondents in the control group typically scored between 0 and 2 points (out of 5).

In addition, family tension and general family anxiety were moderately lower among patients with ESRD than in the control group. This suggests that, family-related anxiety appears to be less pronounced in ESRD patients than in healthy individuals.

Analysis of depression indicators (overall scores, as well as results on the cognitive-affective and somatization subscales) revealed no significant differences between patients with ESRD and individuals without this disease ($p > 0.05$). This finding does not align with previously reported data on the higher prevalence of mental disorders among ESRD patients undergoing hemodialysis; this issue will be addressed in more detail in the Discussion section

An analysis was also conducted to compare the main psychological indicators – reflectivity, depression, alexithymia, sovereignty of psychological space, and family anxiety – within the ESRD group, distinguishing between patients already on the kidney transplant waitlist and those undergoing examination for potential inclusion. The results showed moderate differences only in reflectivity ($p \leq 0.05$).

According to the data presented in Table 7, reflexivity in patients undergoing examination for inclusion on the kidney transplant waitlist was moderately lower than in patients already placed on the waiting list. In other words, reflexivity was lowest prior to waiting list placement, and although it increased slightly thereafter, it still remained within the low range. The overall absence of high levels of reflectivity among ESRD patients, along with significantly lower median values compared to the control group, suggests that low reflectivity may be a distinguishing psychological characteristic of ESRD patients.

Table 6

Comparative analysis of psychological characteristics of respondents

Test indicators	Main group, N = 30		Control group, N = 30		Asymptotic significance (Mann–Whitney U test)
	Me	Q25%–Q75%	Me	Q25%–Q75%	
Reflectivity	3.5	1–4	5	3.75–6	**<0.001****
Cognitive-affective subscale	3.5	1–7	3.5	1–6.5	0.789
Somatization subscale	5	2.75–7.25	3	1–6	0.078
Depression	9	5–13.25	7.5	2.75–10.25	0.208
Difficulty identifying emotions (DIE)	16	12.75–23	16.5	12–20.5	0.436
Difficulty describing emotions (DDE)	12	8.75–15	11.5	9–16	0.688
Externally oriented thinking (EOT)	18	12.75–23.25	14	12.75–9	0.072
Alexithymia	46	35.5–62.25	44.5	35.75–53.25	0.277
Sovereignty of the physical body (SPB)	4	2–6.5	4	2–8	0.958
Sovereignty of territory (ST)	6	2–8	5	1.5–8	0.471
Sovereignty of the world of things (SWT)	5	2–9.5	5	2.5–7	0.487
Sovereignty of habits (SH)	6	3.5–8	6	1.5–8.5	0.454
Social connection sovereignty (SCS)	3	1–3.5	2	–1…5	0.241
Value sovereignty (VS)	4	0–8	4	–2…8.5	0.8
Sovereignty of psychological space (SPS)	29	15–41.5	27	12.5–37.5	0.487
Guilt	0.13	0–0	0.77	0–2	**0.006****
Anxiety	0	0–1	0	0–2	0.265
Tension	1	0–2	2	1–3	**0.031***
General family anxiety level (FAA)	0.33	0–1	0.67	0.33–1.75	**0.02***

Note: *, Differences are significant at the $p \leq 0.05$ level; **, Differences are significant at the $p \leq 0.01$ level.

Table 7

Analysis of significant intragroup differences in psychological characteristics among Patients with ESRD

	ESRD – undergoing examination for inclusion in the KT waiting list		ESRD – already included in the KT waiting list		Asymptotic significance (Mann–Whitney U test)
	Me	LQ – HQ	Me	LQ – HQ	
Reflexivity	3	1–4	4	3.25–4.25	0.04*

Note: *, Differences are significant at the $p \leq 0.05$ level.

It should also be noted that increased feelings of guilt towards family members, tension, or general family anxiety were not characteristic of patients with ESRD.

Based on the results obtained for the main group, it was also suggested that the severity of depression in ESRD patients may be associated with age and duration of hemodialysis. To verify this assumption, a correlation analysis was performed using Spearman's rank correlation coefficient. The results of this analysis of the main group are presented as a correlation cluster in Fig. 1.

The central correlation identified was between duration of dialysis and depression ($R = 0.391$; $p \leq 0.05$), which was also linked to several other psychological characteristics. Specifically, as the duration of hemodialysis increased, levels of depression rose, accompanied by higher tension, family anxiety, and alexithymia (including its components: difficulty identifying emotions, difficulty describing emotions, and externally oriented thinking).

An additional inverse relationship was found between reflectivity and sovereignty of territory ($R = –0.385$; $p \leq 0.05$). In other words, patients with ESRD who showed lower levels of reflectivity reported a greater sense of safety and control over their physical space.

Overall, the findings suggest that prolonged hemodialysis contributes to depression, which in turn manifests through alexithymia, emotional detachment, and heightened family anxiety and tension. These results align with earlier studies confirming the negative psychological impact of extended dialysis treatment on patients' mental health [7, 10].

Next, we turn to the relationships observed in the control group, presented in Fig. 2.

Fig. 2 shows that in the control group, higher levels of depression are associated with increased family tension and lower levels of sovereignty over territory, possessions, habits, and overall psychological space. In this group, depression shows a more limited pattern of associations, being primarily linked to diminished sovereignty rather than to a broad range of psychological indicators. Notably, depression in the control group is not directly connected to alexithymia or its components, but only indirectly through the sovereignty of the world of things.

Unlike the control group respondents, depression in patients with ESRD is not associated with the sovereignty of territories and the sovereignty of the world of things ($p > 0.05$). Also, in contrast to the control group, additional associations with indicators of family anxiety as

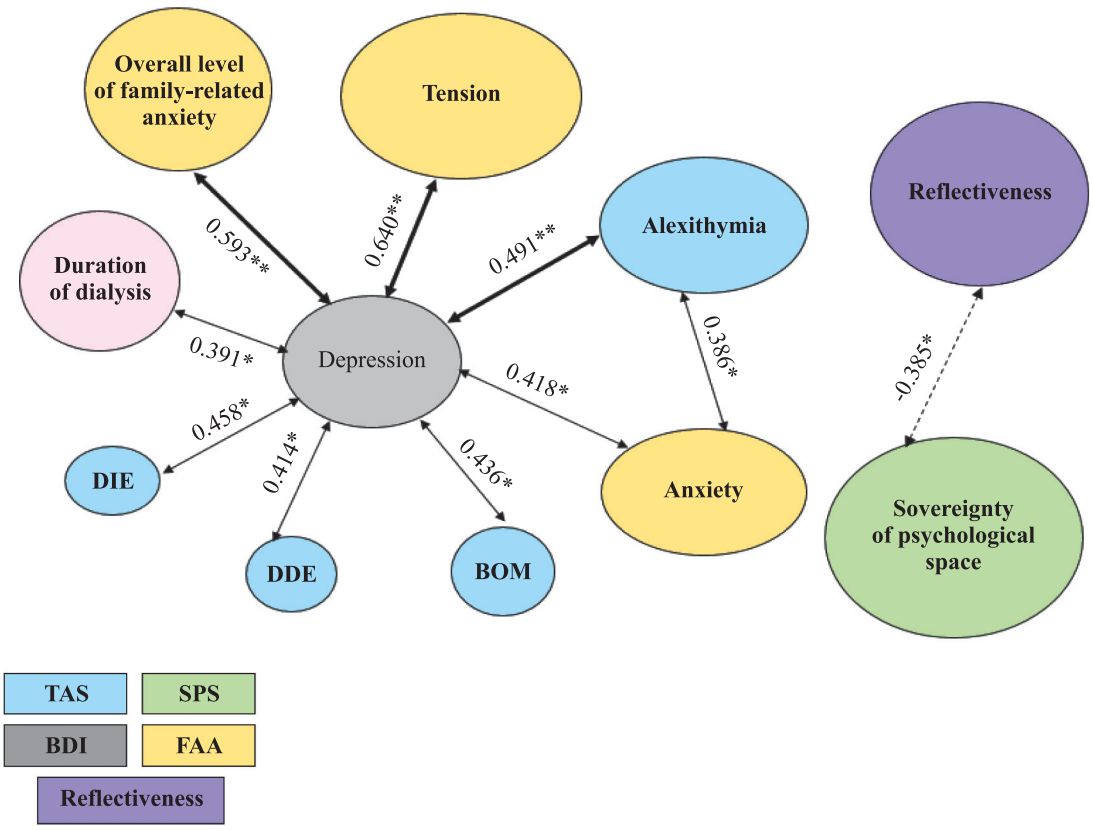

Fig. 1. Significant correlations between depression in patients with CKD, and other psychological characteristics and duration of hemodialysis. Abbreviations: DIE, difficulty in identifying emotions; DDE, difficulty in describing emotions; TAS, Toronto Alexithymia Scale; BDI, Beck Depression Inventory; SPS, sovereignty of psychological space; FAA, general family anxiety level. *, Correlation is significant at $p \leq 0.05$; **, Correlation is significant at $p \leq 0.01$. ——— – Positive strong correlation; ——— – Positive moderate correlation; ------- – Negative moderate correlation

well as with overall alexithymia score and its individual components were found in patients with ESRD.

In the control group, reflectivity is not associated with other psychological characteristics ($p > 0.05$), whereas depression shows significant connections with several indicators. This suggests that reduced reflectivity in patients with ESRD is likely an inherent trait rather than a consequence of the illness itself. One possible explanation is that such individuals develop psychological defenses through detachment from their own bodies as a means of creating a safe space around oneself. Decisions to create this kind of psychologically protective space through bodily detachment are often rooted in early life experiences, frequently as a response to psychologically traumatic events in childhood.

Next, we will examine the relationship between age and manifestations of depression, along with other psychological indicators, in both groups of respondents. Significant correlations between age of respondents in the main and control groups and the studied parameters of reflectivity, depression, alexithymia, sovereignty, and anxiety are presented in Table 8.

In the control group, age was not associated with indicators of reflectivity, depression, alexithymia, sovereignty, or family anxiety ($p > 0.05$).

Table 8

Significant correlations between respondents' age and psychological characteristics

Indicators	R/p	Age (years)	
		Main group	Control group
Somatization subscale	R	**0.384***	0.361
	p	0.036	0.05
DIE	R	**0.394***	–0.017
	p	0.033	0.976
DDE	R	**0.396***	0.102
	p	0.030	0.594
Alexithymia	R	**0.408***	0.169
	p	0.025	0.373

Note: R, Spearman's correlation coefficient; p, asymptotic significance level; *, Differences are significant at the $p \leq 0.05$ level; **, Differences are significant at the $p \leq 0.01$ level. Abbreviations: DIE, difficulty in identifying emotions; DDE, difficulty in describing emotions.

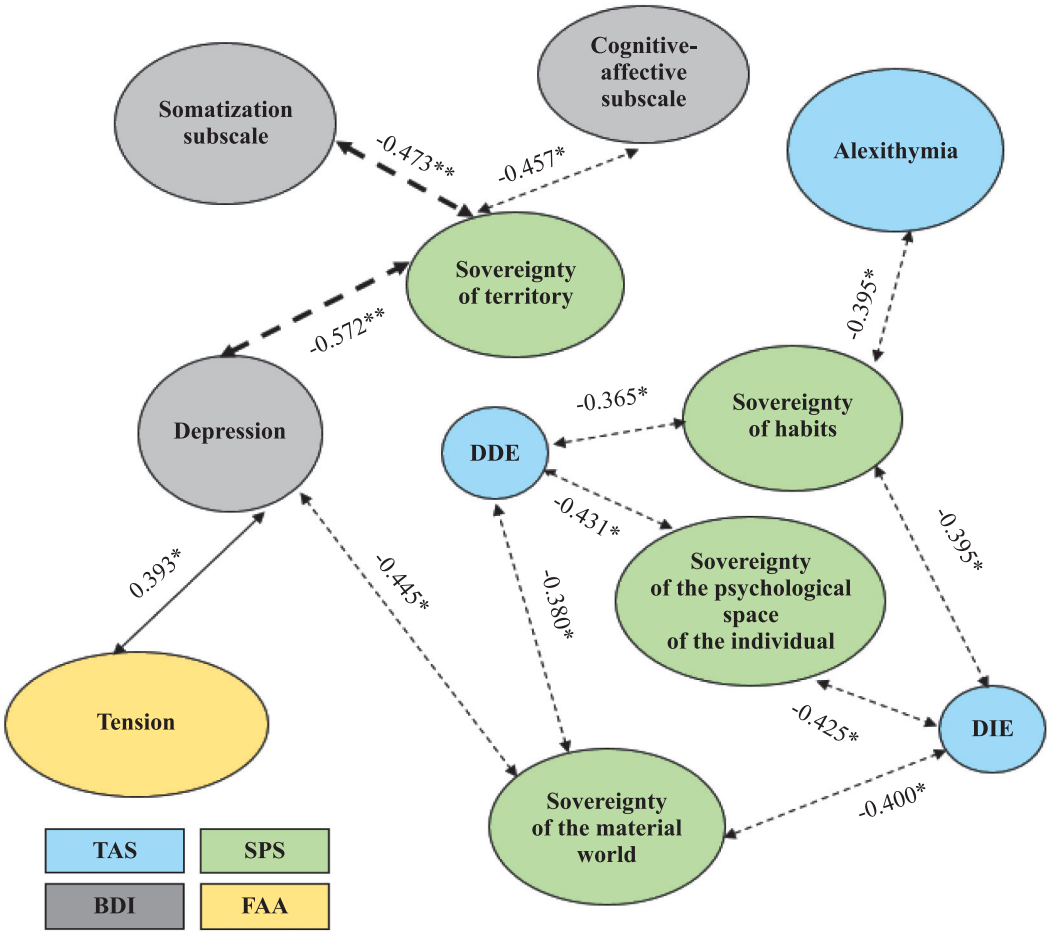

Fig. 2. Significant psychological associations among respondents in the control group. Abbreviations: DIE, difficulty in identifying emotions; DDE, difficulty in describing emotions; TAS, Toronto Alexithymia Scale; BDI, Beck Depression Inventory; SPS, sovereignty of psychological space; FAA, general family anxiety level. *, Correlation is significant at $p \leq 0.05$; **, Correlation is significant at $p \leq 0.01$; – – – – Negative close correlation; ------- – Negative moderate correlation; ——— – Positive moderate correlation

In contrast, among patients with ESRD, no associations were found between age and reflectivity, sovereignty, or family anxiety ($p > 0.05$). However, age showed a moderate positive correlation with depression (somatization subscale) and alexithymia (difficulty identifying one's own emotions, difficulty describing the feelings of others, and overall alexithymia). This suggests that older patients with ESRD are more likely to experience difficulties in recognizing and expressing emotions, along with a tendency to repress negative feelings and manifest them as physical (somatic) symptoms. This may indicate the activation of psychological defenses.

Importantly, these age-related associations with psychological characteristics were not observed in the control group.

Taken together, the findings suggest that somatization, i.e., deterioration of health, increases with age. Patients with ESRD also tend to distance themselves from their inner experiences and interpersonal relationships as they grow older.

DISCUSSION

The results obtained for depression differ from those reported by other researchers. In particular, several studies [7–9] describe pronounced depressive and anxiety disorders in patients with ESRD undergoing hemodialysis. Our study demonstrated a link primarily between duration of hemodialysis treatment and increased depression [7–10].

However, our initial assumptions regarding the severity of depression, preservation of personal boundaries, ability to identify and describe emotions, and level of family anxiety (including feelings of guilt, tension, and anxiety) in patients with ESRD were not fully confirmed. We suggest that this may be related to activation of psychological defense mechanisms (such as repression and denial), which allow patients to adapt psychologically to hemodialysis and organize their lifestyle around it. In addition, the severity of anxiety symptoms may be reduced by profound asthenia [7].

The following should be noted with regard to alexithymia indicators. Alexithymia (manifested as difficulty identifying and describing one's own emotions, along with externally oriented thinking) is understood as a deficit in cognitive processing and emotion regulation. It has been linked to a range of somatic and mental disorders, including a tendency toward somatization [13]. Alexithymia is often accompanied by anhedonia (a diminished capacity to experience pleasure) and a general tendency toward undifferentiated negative emotions. Our study established a direct link between alexithymia and anxiety.

According to N.P. Vanchakova, preservation of social activity (and thereby improvement of quality of life) in ESRD patients undergoing hemodialysis is achieved through mechanisms that simultaneously increase their level of neuroticism [7, 8]. Similarly, N.N. Petrova and I.A. Vasilyeva demonstrated that transformation of life values, heightened importance of the search for meaning in life, a need to adapt to artificially created living conditions during hemodialysis treatment, and the influence of specific psychotraumatic factors associated with hemodialysis contribute to the activation of psychological defenses [9].

In their work, Gautier et al. demonstrated that kidney transplant recipients often experience psychological difficulties integrating the donor organ into their body image. Whether patients are on dialysis or have already received a transplant, they frequently report a sense of compromised integrity. This suggests that they lack sufficient emotional resources to cope with the profound changes imposed by the disease. Addressing this issue requires comprehensive rehabilitation for patients with ESRD – spanning the entire treatment trajectory from placement on the waiting list to postoperative follow-up and eventual reintegration into everyday life. Such rehabilitation must be multidimensional – medical, social, and psychological – and widely accessible [2].

Studies conducted by international researchers have shown that restoring body image integrity and promoting emotional well-being in kidney recipients during the immediate postoperative period contribute to improved health outcomes and significantly reduce the risk of transplant rejection [2].

Studies of the affective sphere of ESRD patients after transplantation have also shown that, as life expectancy with a functioning graft increases, both the somatic and associated psycho-emotional state of patients undergo notable changes. These findings highlight the importance of developing and implementing targeted psychological correction programs aimed at enhancing psychosocial adaptation, thereby improving graft stability and long-term patient survival [11].

CONCLUSION

The present study confirmed that patients with ESRD demonstrate a reduced level of reflectivity, meaning they possess a diminished capacity for self-analysis and tend to make more impulsive decisions.

No significant differences were observed between ESRD patients and healthy individuals in terms of depression, preservation of personal boundaries, or ability to identify and describe emotions. The overall level of family anxiety (including feelings of guilt, tension, and anxiety) was found to be lower in ESRD patients compared to healthy respondents.

Analysis of interrelationships among the studied indicators revealed a direct correlation between depression and inability of ESRD patients to recognize and identify their emotions, as well as elevated anxiety and tension. In other words, increased depression, anxiety, and tension indicates that they are "out of touch" with

their feelings. This diminished emotional awareness may serve as an indicator of underlying depression.

A correlation was identified between patients' ability to recognize their internal state and make informed decisions, and the level of security they perceive within their personal boundaries and physical space.

Furthermore, a direct association was found between severity of depression in ESRD patients and duration of hemodialysis, supporting the findings of earlier studies. In other words, while hemodialysis prolongs patients' lives, it may simultaneously exacerbate deterioration in their as they struggle with emotional awareness. Somatization also increases with age.

A comparison between ESRD patients already on the kidney transplant waitlist and those undergoing preliminary evaluation revealed only moderate differences. Specifically, patients still in the examination stage demonstrated lower levels of reflectivity. This suggests that once placed on the waiting list, patients exhibit a slight increase in self-reflection and a corresponding decrease in impulsive decision-making.

The absence of confirmation of our assumptions regarding levels of depression, preservation of personal boundaries, ability to identify and describe emotions, and levels of family anxiety (including feelings of guilt, tension, and anxiety) in ESRD patients is, in our opinion, associated with the presence and activation of psychological defense mechanisms (such as repression and denial). These defenses appear to facilitate psychological adaptation to the realities of hemodialysis and the need to structure one's lifestyle around it. This interpretation aligns with the conclusions of previous studies on patients undergoing hemodialysis, although it requires further research.

The authors declare no conflict of interest.

REFERENCES

1. *Hill NR, Fatoba ST, Oke JL, Hirst JA, O'Callaghan CA, Lasserson DS et al*. Global Prevalence of Chronic Kidney Disease – A Systematic Review and Meta-Analysis. *PLoS One*. *2016*; 11 (7): e0158765. doi: 10.1371/journal.pone.0158765. PMID: 27383068.
2. *Gautier SV, Klimusheva NF. Psychological adaptation and rehabilitation of recipients of donor organs. Russian Journal of Transplantology and Artificial Organs.* 2016; 18 (2): 37–45. [In Russ, English abstract]. doi: 10.15825/1995-1191-2016-2-37-45.
3. *Klimusheva NF, Baranskaya LT, Shmakova TV*. Psihologicheskaya reabilitaciya pacientov s transplantirovannymi organami v posleoperacionnyj period. *Vestnik Yuzhno-Ural'skogo gosudarstvennogo universiteta. Seriya: Psihologiya*. 2013; 4: 99–105. [In Russ].
4. *Simonenko MA, Fedotov PA, Shirobokova PV, Sazonova YuV, BortsovaMA, Berezina AV et al.* Personality factors in heart transplant recipients. *Russian Journal of Transplantology and Artificial Organs.* 2020; 22 (3): 62–68. [In Russ, English abstruct]. doi: 10.15825/1995-1191-2020-3-62-68.
5. *Shevchenko AO, Khalilulin TA, Mironkov BL, Saitgareev RSh, Zakharevich VM, Kormer AYa et al.* Quality of life assessment in cardiac transplant recipients. *Russian Journal of Transplantology and Artificial Organs*. 2014; 16 (4): 11–16. [In Russ, English abstruct]. doi: 10.15825/1995-1191-2014-4-11-16.
6. *Kukov K, Dzhordzhanova A.* Psihologicheskie aspekty transplantologii i organnogo donorstva kak problema klinicheskoj psihologii. *Vestnik Yuzhno-Ural'skogo gosudarstvennogo universiteta. Seriya: Psihologiya.* 2014; 4: 52–58. [In Russ].
7. *Vanchakova NP.* Mental and psychosomatic disorders in patients with different degrees of renal diseases and problems of their adaptation. *Nephrology (Saint-Petersburg).* 2002; 6 (4): 25–33. [In Russ]. doi: 10.24884/1561-6274-2002-6-4-25-33.
8. *Vanchakova NP*. Experience of Balint groups with practical treatment of patients with chronic renal failure and chronic hemodialysis. *Nephrology (Saint-Petersburg)*. 2003; 7 (1): 120–125. [In Russ]. doi: 10.24884/1561-6274-2003-7-1-120-125.
9. *Petrova NN, Vasilieva IA.* Psychological portrait of patients under chronic haemodialysis. *Nephrology (Saint-Petersburg)*. 1998; 2 (3): 84–91. [In Russ]. doi: 10.24884/1561-6274-1998-2-3-84-91.
10. *Vasilieva IA, Babarykina EV, Dobronravov VA.* Age-related aspects of quality of life in patients undergoing chronic hemodialysis treatment. *Nephrology (Saint-Petersburg).* 2004; 8 (3): 32–36. [In Russ, English abstruct]. doi: 10.24884/1561-6274-2004-8-3-32-36.
11. *Baranetskaya VN*. Osobennosti affektivnoj sferyi bolnyix xronicheskoj pochechnoj nedostatochnostyu, perenesshix transplantacziyu pochki. *Vestnik Yuzhno-Uralskogo gosudarstvennogo universiteta. Seriya: Psixologiya*. 2015; 1: 63–70. [In Russ].
12. *Guerra F., Di Giacomo D., Ranieri J., Tunno M., Piscitani L., Ferri C.* Chronic Kidney Disease and Its Relationship with Mental Health: Allostatic Load Perspective for Integrated Care. *J Pers Med*. 2021; 11 (12). 1367. doi: 10.3390/jpm11121367. PMID: 34945839.
13. *Starostina EG, Tejlor GD, Kvilti LK, Bobrov AE, Moshnyaga EN, Puzyireva NV et al*. Torontskaya shkala aleksitimii (20 punktov): validizacziya russkoyazyichnoj versii na vyiborke terapevticheskix bolnyix. *Soczialnaya i klinicheskaya psixiatriya*. 2010; 4: 31–38. [In Russ].

The article was submitted to the journal on 28.04.2025

DOI: 10.15825/1995-1191-2025-3-66-77

INTRAPORTAL INDUCTION OF MESENCHYMAL STEM CELLS FOR IMMUNOSUPPRESSION INDUCTION IN LIVER TRANSPLANTATION

S.V. Korotkov[1], E.A. Primakova[1], A.A. Symanovich[1], O.A. Lebed[2], T.V. Lebedeva[1], A.E. Shcherba[1], S.I. Krivenko[1], O.O. Rummo[1]

[1] Minsk Scientific Research Center of Surgery, Transplantology and Hematology, Minsk, Republic of Belarus

[2] City Clinical Pathological Bureau, Minsk, Republic of Belarus

Background. Despite the effectiveness of modern immunosuppressive therapy protocols, acute rejection remains a significant challenge in liver transplantation (LT), occurring in up to 40% of cases. One promising strategy to improve graft tolerance and reduce rejection rates is the use of mesenchymal stem cells (MSCs). Administering MSCs directly into the regional circulation of the transplanted liver offers the potential to enhance the effects of standard immunosuppressive therapy by exerting a localized immunosuppressive effect at the graft site. **Objective:** to evaluate the clinical efficacy of intraportal administration of MSCs during the induction phase of immunosuppressive therapy in patients undergoing LT. **Materials and methods.** A randomized prospective study was conducted involving two groups of LT recipients. In the experimental group (n = 14), patients received an intraportal infusion of MSCs during transplantation at a dose of 20×10^6 cells. The control group (n = 14) underwent standard transplant reperfusion without MSC administration. The study assessed the safety of the MSC infusion procedure, graft function, incidence and severity of acute rejection, renal function, and tacrolimus levels. Additional assessments included histological and immunohistochemical analyses, as well as fluorescence *in situ* hybridization (FISH). **Results.** No complications associated with MSC administration were observed. The MSC group demonstrated faster restoration of graft function, with significantly lower levels of aspartate aminotransferase (AST) and alanine aminotransferase (ALT) by postoperative day 4 ($p < 0.05$), and normalization of AST achieved by day 10. The incidence of acute rejection was lower in the MSC group (21%) compared to the control group (28%), with only mild to moderate rejection observed in the MSC group. Additionally, expression of matrix metalloproteinase-10 (MMP10) was significantly reduced in the MSC group ($p = 0.01$). Tacrolimus levels were lower in the MSC group, yet adequate immunosuppression was maintained. This correlated with faster renal function recovery, with serum creatinine levels on day 4 significantly lower in the MSC group compared to controls (80 *vs* 101 μmol/L, $p < 0.05$). FISH analysis confirmed the presence of MSCs within the liver graft tissue on postoperative day 7. **Conclusion.** Intraportal administration of MSCs during LT is a safe approach that enhances faster graft function recovery, reduces the severity of acute rejection, and mitigates tacrolimus-associated nephrotoxicity. These findings support the potential of MSC therapy as a valuable adjunct to standard immunosuppressive regimens in LT.

Keywords: liver transplantation, mesenchymal stem cells, intraportal infusion, acute kidney injury, graft rejection.

INTRODUCTION

Liver transplantation (LT) remains one of the most effective treatment options for patients with diffuse and focal liver lesions at end stages of the disease. Current data indicate that five-year survival after LT from brain-dead donors reaches approximately 75%, while ten-year survival approaches 70% [1, 2]. A critical determinant of long-term transplant success is the use of immunosuppressive therapy (IST), which helps prevent graft rejection, ensuring long-term patient survival.

Despite advances in modern immunosuppressive protocols, the incidence of acute rejection during the early postoperative period remains quite high, with rates reported as high as 40% [3, 4]. One promising avenue is the application of cellular biotechnology, particularly the use of mesenchymal stem cells (MSCs). Owing to their potent immunomodulatory properties, MSCs are increasingly regarded as a potential adjunct or alternative to conventional IST, offering fewer complications and side effects [5–7].

Of particular interest is the use of local MSC therapy, achieved by introducing the cells directly into the

Corresponding author: Sergey Korotkov. Address: 79-115, Sergeya Yesenina str., Minsk, 220051, Republic of Belarus. Phone: +375 29 1982818. E-mail: skorotkov@tut.by

regional blood flow of the liver graft. This approach enables the creation of a high concentration of the cellular product within the target organ, thereby enhancing therapeutic effectiveness. This targeted approach can significantly enhance the effectiveness of standard immunosuppression protocols by modulating immune response mechanisms directly within the transplanted liver [8, 9].

In this regard, the present study aimed to evaluate the clinical efficacy of intraportal administration of MSCs during the induction phase of IST in liver transplantation.

MATERIALS AND METHODS

Study design

To assess the efficacy of intraportal MSC administration, we conducted an interventional, randomized, prospective, comparative study involving two groups (n = 28). The main group included 14 patients who received intraportal MSC infusion during transplantation, while the comparison group comprised 14 recipients who underwent standard donor liver reperfusion without MSCs.

Inclusion criteria included patients with liver cirrhosis listed for transplantation; age ≥18 years; liver graft from a deceased donor; and transplantation performed using the classic technique (resection of the retrohepatic segment of the portal vein). Exclusion criteria included: age <18 years; split or living-related LT; non-standard portal reconstruction (e.g., reno-portal, cava-portal, or porto-caval shunt anastomosis); retransplantation; primary graft non-function; or severe graft dysfunction requiring retransplantation.

Endpoints of the study: 1) primary endpoints – frequency of complications associated with intraportal application of MSCs; frequency of histologically confirmed graft rejection; intensity of immune-inflammatory reactions based on immunohistochemical expression of matrix metalloproteinase-10 (MMP10) and caspase-3 (Casp3); 2) secondary endpoints – dynamics of liver function recovery, dynamics of kidney function recovery, tacrolimus levels, frequency of postoperative complications, duration of treatment.

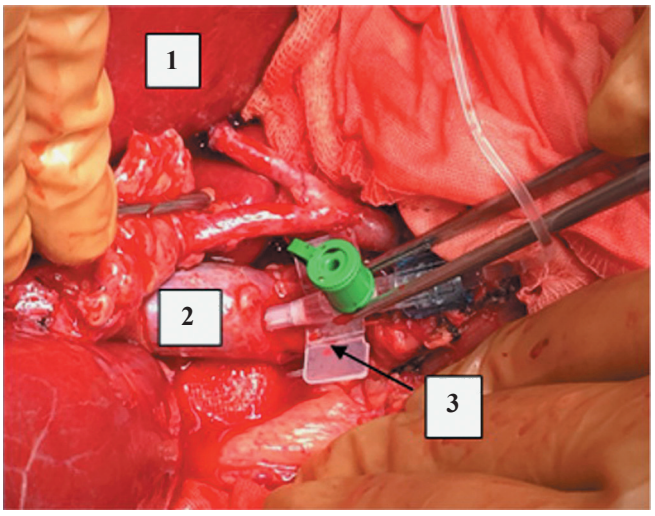

Fig. 1. Intraoperative intraportal infusion of mesenchymal stem cells. 1 – Liver graft; 2 – Portal vein; 3 – Venous catheter

Characteristics of the cell product

To meet the research objectives, biomedical cell product (BMCP) "Human Mesenchymal Cells TU BY 100660677.001" (registration certificate No. IM-7.101480, registration number Mn-7.117650-1402, dated May 29, 2014) was used. The BMCP was produced from allogeneic MSCs isolated from the adipose tissue of brain-dead donors and complied with the minimum criteria for MSCs established by the International Society for Cellular Therapy (ISCT, 2006) [10].

Intraportal administration of MSCs

The developed method for intraportal administration of MSCs involved the following steps:

1. A 16G venous catheter was introduced into the portal vein of the graft and connected to a syringe containing the cell product. The infusion volume was 20 million MSCs suspended in 20 ml of 0.9% NaCl solution.
2. MSCs were administered after portal blood flow was initiated, at an infusion rate of 2 ml/min (Fig. 1).
3. Upon completion of the infusion, the catheter was carefully removed from the portal vein, and the puncture site was sutured.

Histological and immunohistochemical examination of transplant

Puncture biopsy of the liver graft was performed on postoperative day 7 (POD 7), as well as when clinically indicated in cases of graft dysfunction. The presence or absence of rejection was assessed according to the Banff classification. The Rejection Activity Index (RAI) was applied to quantitatively determine the severity of acute cellular rejection. Humoral rejection was identified by immunohistochemistry (IHC) through detection of the complement fragment C4d, which is associated with antibody-mediated tissue injury [11–13].

To further evaluate the intensity of the alloimmune response, IHC analysis was also performed to assess tissue expression of matrix metalloproteinase-10 (MMP-10) and caspase-3 (Casp3) [14, 15].

Molecular cytogenetic studies

Molecular cytogenetic analysis was conducted using fluorescence *in situ* hybridization (FISH) to verify the presence of MSCs in the transplanted liver. This was achieved by detecting alpha satellite sequences in the Xp11.1–Xq11.1 region and satellite DNA III in the Yq12 region. To ensure accurate identification of MSCs, a pre-

requisite was adherence to the principle of gender mismatch between the donor, recipient, and administered MSCs – that is, the donor and recipient had to differ in sex from the MSC product being administered [16].

Statistical analysis

All statistical analyses were performed using Statistica 8.0 software. The Shapiro–Wilk test was applied to assess the normality of data distribution. Data with non-normal distributions were expressed as median (25th–75th percentiles). For comparisons of quantitative variables between groups, the Mann–Whitney U test (MW) was employed. Categorical variables were analyzed using Fisher's exact test (F).

RESULTS

The study and control groups were comparable in terms of clinical and demographic features (Table 1). The mean age of patients in the MSC group was 46 years (39–52), while in the control group it was 47 years (40–55) (MW, $p > 0.05$). Gender distribution was also similar: in the MSC group, there were 7 men (50%) and 7 women (50%), whereas the control group included 8 men (57%) and 6 women (43%) (F, $p > 0.05$).

In the MSC group, the indications for liver transplantation were: hepatitis B (HBV) cirrhosis – 1 patient (7%); HBV + HDV cirrhosis – 2 patients (14%); HCV cirrhosis – 2 patients (14%); HCV cirrhosis with hepatocellular carcinoma (HCC) – 3 patients (21%); cryptogenic cirrhosis – 3 patients (21%); cryptogenic cirrhosis with giant cell transformation – 1 patient (7%); PSC with cholangiocellular carcinoma – 1 patient (7%); cirrhosis secondary to autoimmune hepatitis (AIH) – 1 patient (7%).

In the control group, the indications were distributed as follows: HBV cirrhosis – 1 patient (7%); HBV + HDV cirrhosis – 1 patient (7%); HCV cirrhosis – 3 patients (21%); HCV cirrhosis with HCC – 1 patient (7%); cirrhosis due to non-alcoholic steatohepatitis – 1 patient (7%); cryptogenic cirrhosis – 2 patients (14%); cirrhosis from Wilson–Konovalov disease – 2 patients (14%); cirrhosis due to PSC – 1 patient (7%); primary biliary cirrhosis – 1 patient (7%); cirrhosis secondary to AIH – 1 patient (7%) (F, $p > 0.05$).

In the MSC group, immunosuppression induction (IS) was achieved with glucocorticosteroids (GCS) in 10 patients (71%), while 4 patients (29%) received a combination of GCS and interleukin-2 receptor antagonists (IL2RA, Basiliximab). In the control group, 9 patients (64%) received GCS, and 5 patients (36%) received GCS + IL2RA (F, $p > 0.05$) [17].

Maintenance IS consisted of standard triple therapy with calcineurin inhibitors (tacrolimus), mycophenolate mofetil (MMF), and GCS (methylprednisolone). Tacrolimus was initiated on POD 1 at 0.1 mg/kg/day, but its administration was delayed in cases of acute kidney injury until renal function normalized or showed stable improvement. In patients with stable graft function under acute kidney injury (AKI), tacrolimus trough levels were maintained at a lower threshold (<5 ng/ml) [17].

Management of rejection episodes followed established protocols: in acute cellular rejection (ACR), patients received pulse methylprednisolone therapy; in antibody-mediated rejection (AMR), plasmapheresis and intravenous immunoglobulin were administered. For cases of immunological graft dysfunction, everolimus (a macrolide immunosuppressant) was added as a fourth agent, and the MMF dosage was escalated to 2000 mg/day [17].

The study showed that intraportal administration of MSCs was safe and did not result in local complications related to catheter placement, such as thrombosis, bleeding, vascular rupture, or injury to the posterior wall of the vena cava. Likewise, no systemic complications were observed, including hypotension, cardiac arrhythmia, hyperthermia, or allergic reactions.

Importantly, MSC infusion did not cause local hemodynamic disturbances within the graft. Portal vein blood

Table 1

Clinical parameters of patients

Parameter	MSC	Control	MW, p
Recipients			
MELD score, points	18 (10; 23)	19 (14; 24)	>0.05
Na, mmol/L	137 (134; 140)	137 (136; 138)	
Bilirubin, μmol/L	67 (18; 126)	59 (25; 118)	
INR	1.45 (1.19; 1.81)	1.4 (1.19; 1.77)	
Urea, mmol/L	4.6 (3.9; 6.7)	4.9 (4.45; 9.25)	
Creatinine, μmol/L	61 (51; 95)	65 (65; 101)	
GFR, mL/min	56 (43; 75.5)	53 (28; 70)	
Donor factors			
Donor age, years	49 (40; 54)	48 (41; 60)	>0.05
Days in the ICU	4 (3; 5)	4 (3; 5)	
Hb, g/L	125 (102; 141)	130 (104; 150)	
AST, U/L	49 (38; 68)	62 (46; 76)	
ALT, U/L	33 (20; 91)	40 (24; 81)	
Na, mmol/L	148 (142; 158)	151 (147; 162)	
INR	1.27 (1.03; 1.4)	1.2 (0.94; 1.32)	
Operation:			
Blood loss, mL	1500 (900; 2000)	1300 (1000; 2000)	>0.05
Total ischemia time, min	515 (480; 570)	555 (460; 600)	
Warm ischemia time, min	45 (35; 50)	46 (40; 52)	
Anhepatic phase duration, min	50 (38; 60)	55 (46; 60)	

flow velocity after reperfusion and MSC administration in the main group was 33 (27; 41) cm/s, compared with 36 (29; 42) cm/s in the control group (MW, $p > 0.05$).

Histological examination of intraoperative liver graft biopsies in both groups, obtained after reperfusion, confirmed the absence of microcirculatory thrombosis (Fig. 2).

On the first postoperative day, patients in both groups exhibited biochemical signs of graft dysfunction, primarily attributable to preservation and ischemia–reperfusion injury (Fig. 3).

Subsequently, progressive improvement in graft function was observed in all patients; however, recovery was notably faster in those who received local therapy with MSCs (Fig. 3).

By POD 4, serum transaminase levels were significantly lower in the MSC group compared to controls. Specifically, the AST level was 125 (85; 321) U/L in the MSC group versus 190 (140; 352) U/L in the control group (MW, $p = 0.02$). Similarly, ALT levels were 279 (125; 456) U/L and 358 (211; 606) U/L, respectively (MW, $p = 0.04$) (Fig. 4).

In the main group, normalization of AST levels was achieved by POD 10, with a median value of 34 (19; 51) U/L. In contrast, patients in the control group had AST levels that remained above the normal range at POD 10, reaching 53 (29; 92) U/L (MW, $p = 0.04$) (Fig. 5).

No significant differences between the groups were observed in the recovery dynamics of bilirubin, alkaline phosphatase, gamma-glutamyl transferase, or international normalized ratio (MW, $p > 0.05$).

Histological examination of liver graft biopsies revealed acute cellular rejection (ACR) in 3 patients (21%) of the main group. Of these, 2 cases were mild (RAI score 4) and 1 was moderate (RAI score 6). In the control group, rejection was confirmed in 4 patients (28%):

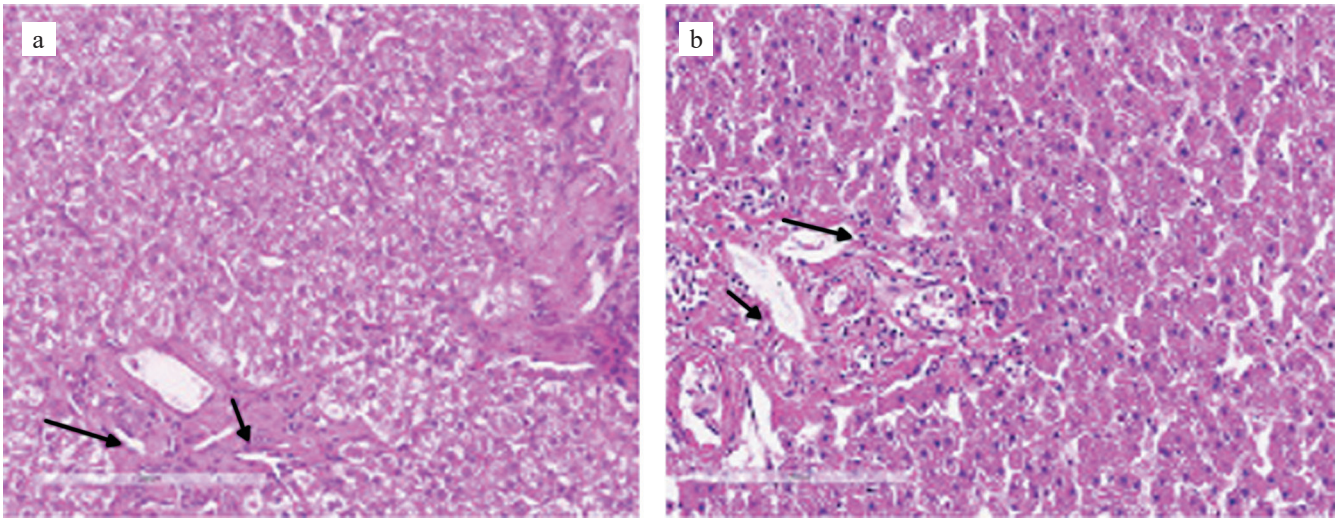

Fig. 2. Intraoperative liver transplant biopsies (hematoxylin and eosin staining, 200× magnification). Arrows indicate portal capillaries with open lumens. a – Biopsy after reperfusion and intraportal MSC administration (main group); b – Biopsy after reperfusion without MSCs (control group)

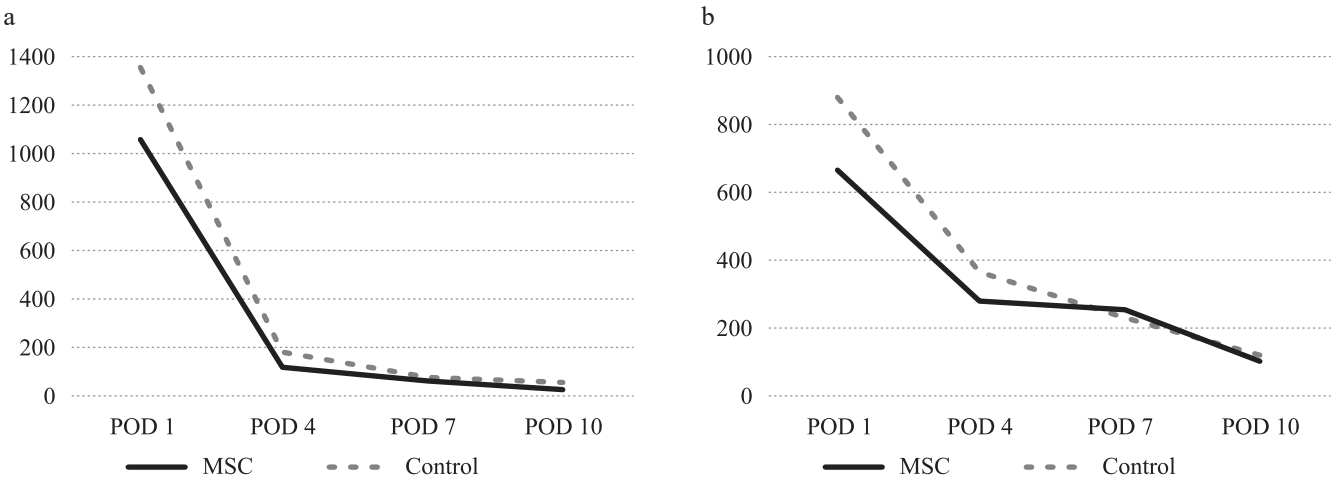

Fig. 3. Dynamics of AST and ALT levels in the study groups. a – AST levels (U/L); b – ALT levels (U/L)

3 with ACR and 1 with antibody-mediated rejection (AMR). The severity of ACR was higher in the control group, with 1 moderate case (RAI score 7) and 2 severe cases (RAI score 8) (F, $p > 0.05$) (Table 2).

Immunohistochemical analysis of liver biopsies obtained on POD 7 included assessment of MMP-10 and caspase-3 expression to quantify the severity of immunological graft injury (Table 2).

In the MSC group, MMP-10 expression in hepatocytes was significantly lower, with a median value of 5% (3; 25), compared with 20% (10; 30) in the control group (MW, $p = 0.01$) (Figs. 6, 7).

Fig. 7 demonstrates more intense MMP-10 expression in the control group (Fig. 7, b) compared with the MSC group (Fig. 7, a).

Immunohistochemical assessment of caspase-3 expression revealed no statistically significant differences between groups, with values of 70 (60; 85)% in the MSC group and 75 (70; 90)% in the control group (MW, $p > 0.05$).

Table 2

Comparative histological characteristics of liver transplant biopsies

	MSC (n = 14)	Control (n = 14)
Rejection	3 (21%)	4 (28%)
ACR	3	3
Mild (RAI 4–5) Moderate (RAI 6–7) Severe (RAI 8–9)	2 1 –	– 1 2
AMR	–	1
MMP10, %	5 (3; 25)*	20 (10; 30)
Caspase-3, %	70 (60; 85)	75 (70; 90)

Note: * indicates a statistically significant difference compared to the control group ($p < 0.05$).

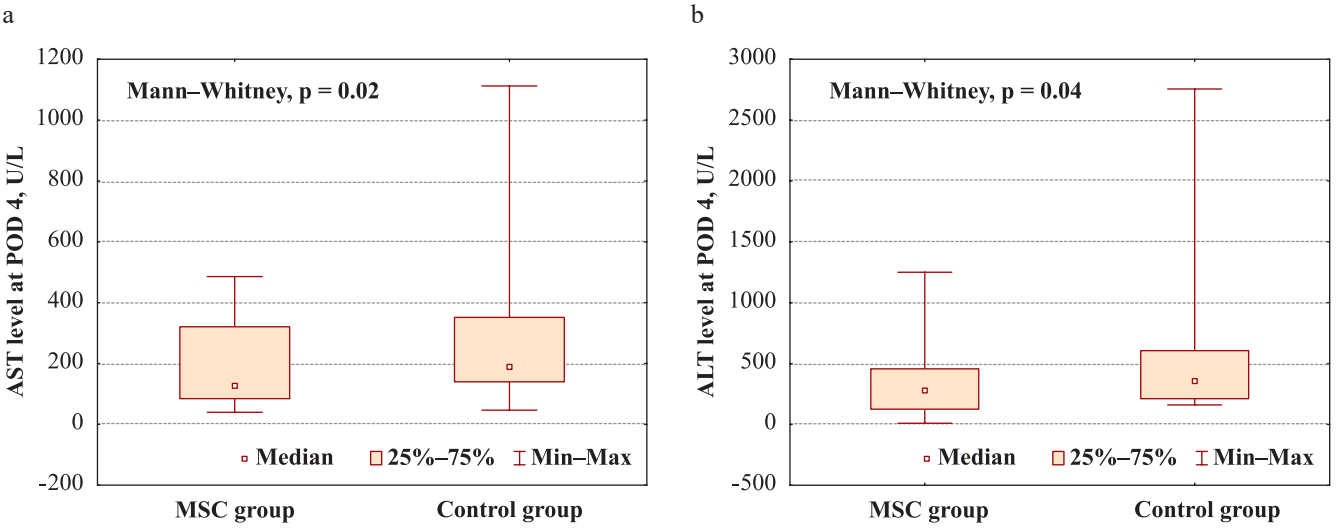

Fig. 4. Mean AST and ALT levels in the study groups on postoperative day (POD) 4. a – AST level; b – ALT level

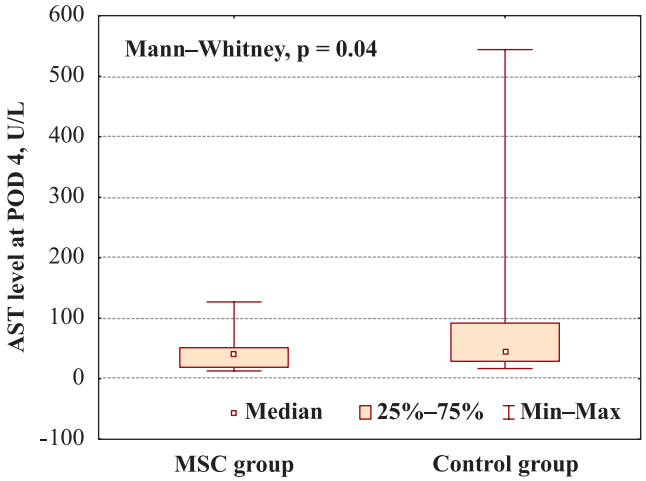

Fig. 5. Mean AST levels in the study groups on postoperative day (POD) 10

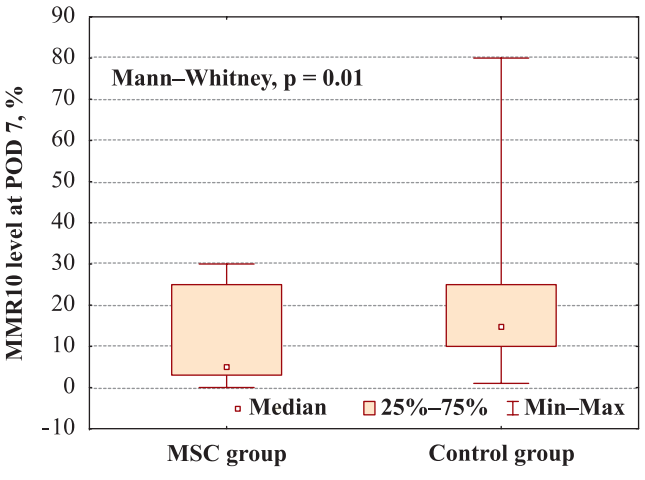

Fig. 6. Mean MMP10 expression levels in liver transplant biopsies at postoperative (POD) day 7

FISH analysis performed on POD 7 confirmed the presence of MSCs, identifiable by a karyotype distinct from that of both the donor and the recipient (Fig. 8).

Determination of tacrolimus levels showed consistently lower concentrations of the immunosuppressant in the MSC group throughout the early postoperative period (Table 3).

On POD 14, this difference reached statistical significance: tacrolimus levels were 5.2 (2.6; 6.7) ng/ml in the MSC group versus 6.7 (4.3; 9.5) ng/ml in the control group (MW, $p = 0.04$).

The dynamics of renal function are summarized in Table 4. During the first two postoperative days, patients in both groups demonstrated elevated urea and creatinine levels, along with reduced glomerular filtration rate, reflecting the development of perioperative renal injury.

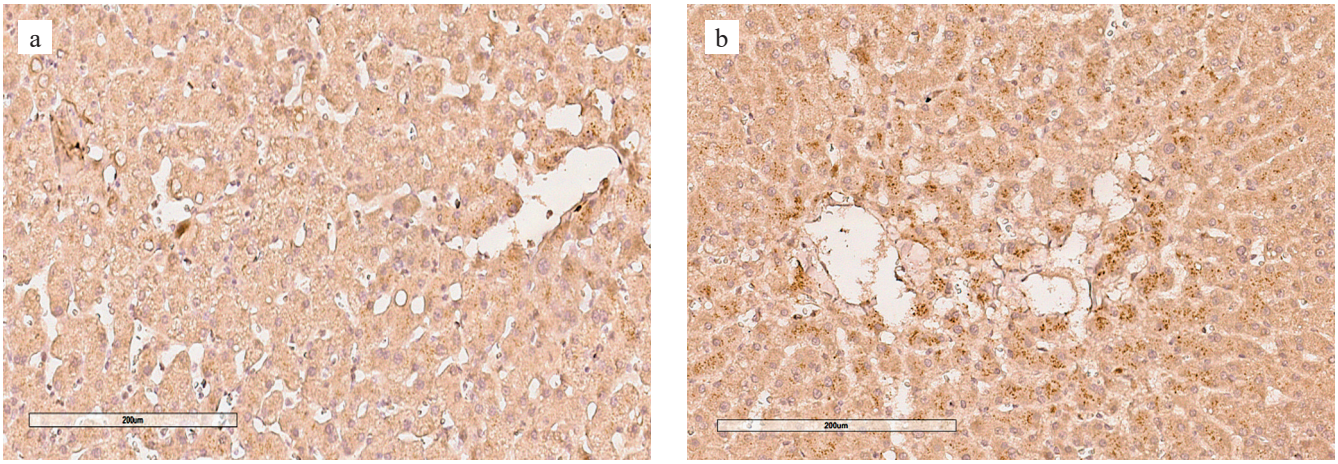

Fig. 7. Immunohistochemical (IHC) staining of MMP-10 expression in liver transplant biopsies (200× magnification): a – MSC group; b – control group

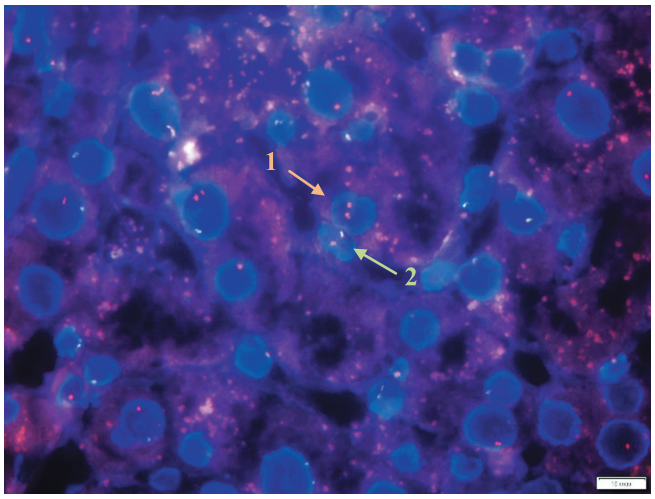

Fig. 8. FISH analysis of liver transplant biopsy: (1) – cell with two copies of alpha satellite sequences in the centromeric region of chromosome X (Xp11.1–Xq11.1); (2) – remaining cell population containing both an alpha satellite sequence in the centromeric region of chromosome X (Xp11.1–Xq11.1) and satellite DNA III in the Yq12 region of chromosome Y

According to the KDIGO (2012) international guidelines [18], AKI is defined by one of the following criteria: (1) an increase in serum creatinine by more than 1.5 times baseline, (2) an absolute increase in creatinine of 26.5 μmol/L within 48 hours, or (3) a reduction in urine output to 0.5 mL/kg/h for at least 6 hours.

Analysis of renal function showed that the ratio of POD 1 creatinine to baseline was 1.51 (1.13; 2.19) in the MSC group and 1.58 (1.32; 1.88) in the control group (MW, $p > 0.05$). On day 2, these ratios were 1.63 (1.28; 2.49) and 1.64 (1.26; 2.43), respectively (MW, $p > 0.05$). The absolute increase in creatinine from baseline to day 1 was 45 (8; 90) μmol/L in the MSC group and 41 (21; 53) μmol/L in the control group (MW, $p > 0.05$), while from baseline to day 2 the increase was 39 (13; 125) and 50 (24; 84) μmol/L, respectively (MW, $p > 0.05$). These findings indicate the presence of postoperative renal injury in both groups (Table 5).

Table 3

Comparative characteristics of tacrolimus levels between the groups

Days	Group	POD				
		2	4	7	10	14
Tac, ng/mL	MSC	0 (0; 0.6)	0.8 (0; 2)	3.2 (0.8; 4.9)	4.9 (3; 8.2)	5.2* (2.6; 6.7)
	Control	1 (0; 2.5)	2 (0.9; 3.4)	4.1 (2.1; 6.1)	5.7 (3.3; 7.1)	6.7 (4.3; 9.5)

Note: * indicates a statistically significant difference compared to the control group ($p < 0.05$).

The absence of statistically significant differences in creatinine ratios and absolute changes on POD 1 and 2 compared with baseline confirmed the homogeneity of the groups with respect to renal function and indicated that MSCs did not influence early development of AKI.

Because of AKI, initiation of tacrolimus therapy was delayed in both groups. The time to treatment initiation was comparable: 3 (2; 4) days in the MSC group and 2 (1; 4) days in the control group (MW, p = 0.15). Clinically, this finding indicates that the timing of tacrolimus administration did not affect the postoperative course or clinical outcomes in either group.

However, patients in the MSC group had lower tacrolimus levels and faster recovery of renal function. By POD 4, urea levels were 10.8 (8; 17.2) mmol/L in the MSC group versus 14 (7.4; 18) mmol/L in the control group (MW, p = 0.03), and creatinine levels were 80 (62; 123) μmol/L versus 101 (70; 132) μmol/L, respectively (MW, p = 0.04). Based on these observations, a correlation analysis was performed to assess the relationship between renal function and tacrolimus level.

On POD 4, a direct correlation was found between tacrolimus and creatinine levels: higher tacrolimus concentrations were associated with elevated creatinine levels (Sp, p = 0.008) (Fig. 9).

Table 4

Comparative characteristics of laboratory indicators of kidney function.

Days	Group	POD						
		0	1	2	4	7	10	14
Urine, mmol/L	MSC	4.6 (4.1; 6.6)	10.75 (9; 13)	16.15 (12.2; 20.4)	10.8* (8; 17.2)	8.25 (5.1; 12)	7.05 (5.5; 10.1)	7.85 (5.2; 11)
	Control	4.9 (3.4; 7.6)	8 (6.5; 13)	14.7 (9.2; 20.8)	14 (7.4; 18)	6.1 (4.4; 8.4)	7.2 (5.8; 10.2)	7.6 (5.1; 12.2)
Creatinine, μmol/L	MSC	61 (52; 91)	110 (79; 154)	128 (70; 186)	80* (62; 123)	78.4 (57; 99)	78 (61; 108)	86 (65; 94)
	Control	65 (57; 84)	112 (81; 137)	118 (84; 166)	101 (70; 132)	84 (63; 108)	78 (66; 102)	82 (65; 107)
GFR, mL/min	MSC	56 (34; 70)	37 (20; 61)	31 (19; 47)	33 (14; 44)	45.5 (25; 57)	42.5 (32; 59)	38 (28.3; 57)
	Control	53 (45; 64)	32.25 (24; 45)	25 (16.2; 38)	31 (18; 50)	33 (23; 56)	41 (29; 54)	38 (24.7; 59)

Note: * indicates a statistically significant difference compared to the control group (p < 0.05).

Table 5

Characteristics of groups according to development of AKI in the early postoperative period

Creatinine, μmol/L	MSC (n = 14)	Control (n = 14)	MW, p
POD 1 / POD 0	1.51 (1.13; 2.19)	1.58 (1.32; 1.88)	>0.05
POD 2 / POD 0	1.63 (1.28; 2.49)	1.64 (1.26; 2.43)	>0.05
Δ POD 1 – POD 0	45 (8; 90)	41 (21; 53)	>0.05
Δ POD 2 – POD 0	39 (13; 125)	50 (24; 84)	>0.05

Table 6

Early postoperative complications following liver transplantation

Complication	MSC (n = 14)		Control (n = 14)	
Vascular	1	7%	0	0%
– arterial (hepatic artery stenosis)	1	7%	0	0%
Biliary	2	14%	1	7%
– bile leakage	1	7%	0	0%
– anastomotic stricture	1	7%	1	7%
SSI (surgical site infection)	1	7%	2	14%
– superficial	0	0%	1	7%
– deep	1	7%	1	7%
Intra-abdominal hemorrhage	1	7%	1	7%

The incidence of early postoperative complications was comparable between the groups and did not differ significantly (F, p > 0.05) (Table 6).

The median length of stay in the intensive care unit was 3 (2; 4) days in the MSC group and 3 (2; 5) days in the control group (MW, p > 0.05). The total duration of inpatient treatment after transplantation was slightly shorter in the MSC group – 17 (14; 20) days compared with 19 (15; 24) days in the control group – although this difference was not statistically significant (MW, p > 0.05).

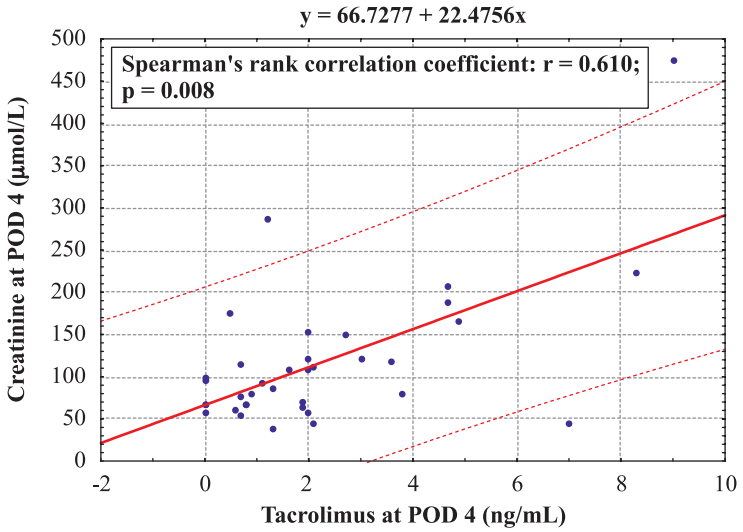

Fig. 9. Correlation between serum creatinine levels and tacrolimus concentration on postoperative day (POD) 4

DISCUSSION

The results of this study demonstrated both the safety and potential efficacy of intraportal administration of MSCs in liver transplantation. The absence of local or systemic complications related to MSC infusion, together with preserved portal hemodynamics and the lack of microthrombosis in biopsy samples, confirmed the safety of the developed technique.

Analysis of graft function revealed faster recovery of liver function in the MSC group, reflected by significantly lower transaminase levels on POD 4 and earlier normalization of AST by POD 10.

Another positive finding was a trend toward reduced frequency and severity of acute rejection in the MSC group. Although the overall incidence of immunological graft dysfunction did not differ significantly between groups (21% in the MSC group *vs* 28% in controls), only mild to moderate cellular rejection occurred in the MSC group, whereas cases of severe cellular and antibody-mediated rejection were observed in the control group. This was supported by significantly lower MMP10 expression in MSC-group biopsies, suggesting less severe immunological injury to the graft.

The beneficial effects observed following intraportal administration of MSCs may be due to several mechanisms of action. First, MSCs secrete a range of anti-inflammatory mediators, including IL-10 and TGF-β, which suppress T-lymphocyte activation and proliferation. Second, they modulate the function of antigen-presenting cells and reduce the production of proinflammatory cytokines. Third, MSCs promote the expansion of regulatory T cells, which play a central role in maintaining immunological tolerance to the graft [5–7].

The detection of administered MSCs within the graft on POD 7, as confirmed by FISH analysis, demonstrates their ability to persist in the target organ, which may underlie the observed immunomodulatory effects.

Although MSCs have a low immunogenic profile, characterized by weak HLA class I expression and absence of HLA class II antigen expression, the possibility of an immune response from the recipient cannot be ruled out, particularly in the context of repeated cell administrations or insufficient immunosuppression [19]. In our study, no clinically significant immune reactions against MSCs or cases of MSC-associated acute rejection were observed. This outcome was likely facilitated by the standard immunosuppressive regimen used after liver transplantation, the single local administration of MSCs into the graft, and the intrinsic immunosuppressive effect of MSCs themselves on the immune system.

The potential to reduce tacrolimus levels in the MSC group while maintaining adequate immunosuppression is a particularly important finding. Given the observed correlation between tacrolimus and creatinine levels, lowering calcineurin inhibitor exposure may help mitigate nephrotoxicity and accelerate renal recovery, as evidenced in the MSC group by POD 4.

The absence of differences in the frequency of other postoperative complications, together with the trend toward shorter hospitalization in the MSC group, further supports the safety and potential clinical value of the proposed technique.

Our findings are in line with previous reports on the use of cell therapy in solid organ transplantation. Sun et al. (2018) demonstrated both safety and efficacy of local MSC administration via the renal artery in kidney transplantation [8].

Popp et al. (2011) showed the safety of MSC infusion into the portal vein of a liver transplant [9]. Their study highlighted the potential of MSCs to partially replace calcineurin inhibitors and confirmed the effectiveness of combining MSC therapy with mycophenolates, thereby supporting our proposed immunosuppression strategy aimed at minimizing calcineurin inhibitor exposure.

Taken together, our findings reinforce the potential of MSCs as an adjunct to standard immunosuppressive therapy and align with existing evidence on the safety and efficacy of cell therapy in solid organ transplantation. These results underscore the promise of MSCs in preventing rejection and enhancing liver graft function.

CONCLUSION

This study led to the development and successful implementation of a safe technique for intraportal administration of mesenchymal stem cells during liver transplantation. The approach demonstrated several important clinical advantages:

1. Safety – no local or systemic complications were observed during MSC administration.
2. Efficacy in graft function recovery – faster normalization of liver function parameters was achieved in the MSC group.
3. Immunomodulatory effects – a trend toward reduced severity of rejection episodes and lower expression of immune injury markers was observed.
4. Reduction of nephrotoxicity risk – the possibility of lowering tacrolimus levels without compromising immunosuppressive efficacy was demonstrated, thereby reducing the nephrotoxic burden of calcineurin inhibitors.

Overall, these findings highlight the promise of intraportal MSC infusion as an adjunct to standard immunosuppressive therapy in liver transplantation.

The authors declare no conflict of interest.

REFERENCES

1. *Ahmad J, Friedman S, Dancygier H.* Mount Sinai expert guides. Hepatology. Wiley Blackwell; 2014.
2. *Millson C, Considine A, Cramp M, Holt A, Hubscher S, Hutchinson J et al.* Adult liver transplantation: UK clinical guideline – part 2: surgery and post-operation. *Frontline Gastroenterology*. 2020; 11 (5): 1–12. doi: 10.1136/flgastro-2019-101216.
3. *Busuttil R, Klintmalm G.* Transplantation of the liver. 3d ed. Elsiver; 2015.
4. *Taner T.* Liver Transplantation: Rejection and Tolerance. *Liver Transplantation*. 2017; 23 (S1): S85–S88. doi: 10.1002/lt.24840.
5. *Vandermeulen M, Grégoire C, Briquet A, Lechanteur C, Beguin Y, Detry O.* Rationale for the potential use of mesenchymal stromal cells in liver transplantation. *World J Gastroenterol*. 2014; 20 (44): 16418–16432. doi: 10.3748/wjg.v20.i44.16418.
6. *Wen F, Yang G, Yu S, Liu H, Liao N, Liu Z.* Mesenchymal stem cell therapy for liver transplantation: clinical progress and immunomodulatory properties. *Stem Cell Research and Therapy*. 2024; 15 (320): 1–12. doi: 10.1186/s13287-024-03943-6.
7. *Basok YuB, Ponomareva AS, Grudinin NV, Kruglov DN, Bogdanov VK, Belova AD et al*. Use of mesenchymal stem cells in solid organ transplantation: challenges and prospects. *Russian Journal of Transplantology and Artificial Organs*. 2025; XXVII (1): 114–134. [In Russ, English abstract]. doi: 10.15825/1995-1191-2025-1-114-134.
8. *Sun Q, Huang Z, Han F, Zhao M, Cao R, Zhao D et al.* Allogeneic mesenchymal stem cells as induction therapy are safe and feasible in renal allografts: pilot results of a multicenter randomized controlled trial. *J Transl Med*. 2018; 16 (52): 1–10. doi: 10.1186/s12967-018-1422-x.
9. *Popp F, Fillenberg B, Eggenhofer E, Renner P, Dillmann J, Benseler V et al.* Safety and feasibility of third-party multipotent adult progenitor cells for immunomodulation therapy after liver transplantation – a phase I study (MISOT-I). *J Transl Med*. 2011; 9 (124): 1–10. doi: 10.1186/1479-5876-9-124.
10. *Dominici M, Blanc K, Mueller I, Slaper-Cortenbach I, Marini F, Krause D et al*. Minimal criteria for defining multipotent mesenchymal stromal cells. The International Society for Cellular Therapy position statement. *Cytotherapy*. 2006; 8 (4): 315–317. doi: 10.1080/14653240600855905.
11. *Demetris A, Bellamy C, Hübscher S, O'Leary J, Randhawa P, Feng S et al*. 2016 Comprehensive Update of the Banff Working Group on Liver Allograft Pathology: Introduction of Antibody-Mediated Rejection. *Am J Transplant*. 2016; 16 (10): 2816–2835. doi: 10.1111/ajt.13909.
12. *Borbat AM, Dubova EA, Gainullina ER, Lishchuk SV*. Protokol gistologicheskogo issledovaniya disfunktsii transplantata pecheni. *Arkhiv patologii*. 2019; 81 (6): 71–73. doi: 10.17116/patol20198106171.
13. *Shkalova LV, Mozheyko NP, Ilyinskiy M, Moisyuk YaG, Tsirulnikova OM, Gautier SV.* The diagnosis of liver allograft acute rejection in liver biopsies. *Russian Journal of Transplantology and Artificial Organs*. 2011; 13 (3): 15–19.
14. *Duarte S, Baber J, Fujii T, Coito A*. Matrix metalloproteinases in liver injury, repair and fibrosis. *Matrix Biology*. 2015; 44: 147–156. doi: 10.1016/j.matbio.2015.01.004.
15. *Fedoryuk DA, Kirkovsky LV, Sadovsky DN, Petrenko KI, Lebed OA, Fedoryuk AM et al.* Influence of hypothermic oxygenated machine perfusion on the degree of ischemic damage of ecd liver grafts. *Military medicine*. 2020; 2: 68–75. [In Russ, English abstract].
16. *McGowan-Jordan J, Hastings RJ, Moore S*. ISCN (2020). An International System for Human Cytogenomic Nomenclature. S. Karger AG; 2020.
17. Minzdrav.gov.by [Internet] Klinicheskiy protokol "Transplantatsiya pecheni (vzrosloe i detskoe naselenie)" (utverzhden MZ RB 13.02.2023 № 31). https://minzdrav.gov.by.
18. Kidney-international.org [Internet]. KDIGO. Clinical Practice Guideline for Acute Kidney Injury. Kidney International Supplements. 2012; 2 (16): 1–138. https://kidney-international.org.
19. *Le Blanc K, Mougiakakos D.* Multipotent mesenchymal stromal cells and the innate immune system. *Nat Rev Immunol*. 2012; 12 (5): 383–396. doi: 10.1038/nri3209.

The article was submitted to the journal on 21.04.2025

DOI: 10.15825/1995-1191-2025-3-78-87

CLINICAL AND LABORATORY FEATURES OF INVASIVE ASPERGILLOSIS IN INTERNAL ORGAN TRANSPLANT RECIPIENTS: A CASE REPORT, REGISTRY ANALYSIS, AND LITERATURE REVIEW

S.N. Khostelidi[1, 2], O.V. Shadrivova[1], M. Ten[1], M.A. Zaitsev[1], E.V. Shagdileeva[1], E.A. Desyatik[1], T.S. Bogomolova[1], S.M. Ignatieva[1], Yu.V. Borzova[1]

[1] North-Western State Medical University, St. Petersburg, Russian Federation

[2] Leningrad Regional Clinical Hospital, St. Petersburg, Russian Federation

Internal organ transplantation is a high-tech medical intervention that significantly improves patient survival and quality of life. However, infections remain the leading cause of mortality in organ transplant recipients. Invasive aspergillosis (IA) is the second most common invasive fungal infection in this population and is associated with high mortality rates, reaching up to 90%. This article presents a clinical case of IA following heart transplantation (HT), along with an analysis of registry data and institutional experience in managing this serious complication based on registry data. Between September 2010 and October 2024, 23 adult patients with IA following an internal organ transplantation were included in the institutional registry. Most IA cases occurred after heart transplantation (65%), followed by kidney transplantation (31%), and, less commonly, lung transplantation (4%). The lungs were the primary site of IA (96% of cases). Diagnosis was confirmed through direct microscopy of clinical samples, such as bronchoalveolar lavage (BAL) fluid and tissue biopsies, in 50% of patients, while fungal cultures yielded positive results in 35% of cases. The predominant pathogen was *Aspergillus fumigatus* (73%), followed by *Aspergillus niger* (18%) and *Aspergillus flavus* (9%). A positive galactomannan test in BAL was detected in 85% of patients. All patients received targeted antifungal therapy, primarily with voriconazole (87%), while echinocandins and itraconazole were used in 17% and 4% of cases, respectively. Overall 90-day patient survival was 78%. The literature review outlines the main approaches to the diagnosis and management of invasive infections associated with *Aspergillus spp.*

Keywords: Aspergillus spp., aspergillosis, invasive aspergillosis, immunosuppressive therapy, organ transplantation, heart transplantation.

INTRODUCTION

Internal organ transplantation is a complex surgical procedure that requires long-term immunosuppressive therapy to maintain the viability and function of the transplanted organ. This therapy works by suppressing the recipient's immune system to prevent graft rejection. However, immunosuppression also reduces the body's ability to mount an adequate defense against infections [1–3].

Pathogens causing infectious complications may vary depending on the timing of transplantation. Early infections (within the first month) are typically caused by nosocomial pathogens and may also stem from donor-derived infections. Opportunistic infections usually develop within 3–12 months after transplantation, reflecting the substantial impact of immunosuppressive therapy. Late infections (after 12 months) may occur in patients requiring intensive ongoing immunosuppression or those exposed to additional environmental risk factors.

However, the nature and timing of infections are influenced by factors such as the choice of immunosuppressive agents and the duration of antimicrobial prophylaxis [1–3]. Among fungal pathogens, the most common are *Candida spp.*, *Aspergillus spp.*, *Cryptococcus neoformans*, and *Pneumocystis*.

Invasive aspergillosis (IA) is the second most common invasive fungal infection in organ transplant recipients and is associated with a high mortality rate, ranging from 30% to 90%, depending on the transplanted organ type, degree of immunosuppression, and clinical form of the disease [2, 3]. In the Russian Federation, the number of publications addressing this problem remains limited.

This article presents a clinical case of invasive pulmonary aspergillosis in a heart transplant (HT) recipient, an analysis of registry data on IA in organ transplant recipients, and a review of relevant literature.

Objective: to evaluate the risk factors, etiology, clinical features, diagnostic approaches, and treatment strategies for IA in internal organ transplant recipients.

MATERIALS AND METHODS

The diagnosis of invasive mycosis was established according to the 2020 EORTC/MSG criteria [4]. Risk factors, etiology, clinical features, diagnostic findings,

Corresponding author: Sofya Khostelidi. Address: 1/28, Santiago de Cuba str., St. Petersburg, 194291, Russian Federation. Phone: (951) 674-67-91. E-mail: sofya.khostelidi@szgmu.ru; sofianic@mail.ru

and treatment outcomes were assessed using data from the registry of IA patients [5], maintained by the Department of Clinical Mycology, Allergology, and Immunology at the North-Western State Medical University, St. Petersburg. Statistical analysis was performed using Microsoft Office Excel 2010 and Statistica 13.5 (StatSoft, Inc., USA). Survival analysis was conducted using the Kaplan–Meier method.

A literature review was conducted using PubMed (as of December 2024), ClinicalKey (as of December 2024), and the Russian e-Library (as of December 2024). The search strategy employed the following keywords: *Aspergillus spp.*, aspergillosis, invasive mycoses, invasive aspergillosis, internal organ transplantation, lung transplantation, liver transplantation, heart transplantation, and kidney transplantation.

CLINICAL CASE

Patient Z., a 53-year-old female, was admitted to the mycology clinic of North-Western State Medical University with complaints of cough producing difficult-to-expectorate sputum and intermittent fever up to 37.8 °C.

Her medical history revealed a diagnosis of Hodgkin's lymphoma in 1991, for which she underwent four courses of polychemotherapy (PCT) according to the MOPP regimen (mustargen, vincristine, procarbazine, prednisolone) and 28 courses of radiation therapy. Following treatment, she achieved sustained remission, which has persisted to this day.

In 2016, the patient was diagnosed with cancer of the left breast, stage IV (T4bN3M1). In 2017, she underwent a radical Madden mastectomy on the left side, followed by eight courses of PCT according to the FAC regimen (5-fluorouracil 500 mg/m^2, doxorubicin 50 mg/m^2, and cyclophosphamide 500 mg/m^2 intravenously, every 3 weeks, for a total of six cycles) and three courses of biological therapy with trastuzumab (2016–2017). The disease has since remained in remission.

In 2019, she developed mycotic keratouveitis caused by Fusarium spp., requiring inpatient care and systemic antifungal therapy with voriconazole (400 mg daily). She subsequently underwent penetrating keratoplasty and corneal transplantation of the right eye; however, these were complicated by total graft opacity, high myopia, and chorioretinal degeneration.

Following prior radiation therapy courses, the patient developed symptoms of chronic heart failure (CHF) and was diagnosed with radiation-induced heart disease and mixed cardiomyopathy.

The patient's condition progressively deteriorated, with increasing edema and more frequent episodes of chest pain. On subsequent examination, the following were noted: decreased ejection fraction (stage IIB), bilateral hydrothorax, mitral regurgitation grade 1–2, tricuspid regurgitation grade 1–2, pulmonary hypertension grade 2, paroxysmal unstable ventricular tachycardia, and coronary artery atherosclerosis with 70% stenosis of the right coronary artery. She remained under long-term cardiology follow-up.

Due to the lack of response to standard treatment regimens and worsening signs of CHF, heart transplantation (HT) was indicated. In October 2023, she underwent orthotopic HT using the bicaval technique.

Postoperatively, immunosuppressive therapy (IST) was initiated at standard doses for the prevention of graft-versus-host disease (GvHD), including mycophenolic acid 180 mg/day (later administered intermittently and eventually discontinued one month after initiation due to agranulocytosis), prednisolone up to 12 mg/day, and tacrolimus at ≥3 mg/day, titrated according to therapeutic blood concentration.

During a routine examination in December 2023, the patient again reported shortness of breath. Chest computed tomography (CT) revealed a solitary lesion in segment S4 of the right lung (9 mm in diameter, with indistinct margins) and bilateral hydrothorax. A course of antibiotic therapy was administered, resulting in complete regression of the S4 lesion and resolution of fluid accumulation in the right pleural cavity; the left-sided pleural effusion decreased in volume.

Evaluation at the local tuberculosis dispensary showed a positive Diaskintest, while sputum analysis revealed no acid-fast bacilli.

In May 2024, the patient developed recurrent low-grade fever, with body temperature rising to 37.8 °C. Repeat chest CT demonstrated new irregularly shaped infiltrates in segments S2 and S6 of the right lung, superimposed on interstitial changes. A 10-day course of levofloxacin was prescribed, leading to clinical improvement.

The patient was referred again to a phthisiatrician and underwent an inpatient evaluation at a tuberculosis hospital in June 2024. Microscopy of sputum and bronchial lavage fluid for mycobacteria was negative, and polymerase chain reaction (PCR) testing of both samples did not detect DNA of Mycobacterium tuberculosis complex.

Bronchoalveolar lavage (BAL) culture yielded Klebsiella pneumoniae (1×10^3 CFU/mL) and Aspergillus spp. (1×10^4 CFU/mL). A BAL galactomannan assay, performed at Kashkin Research Institute of Medical Mycology, was positive (optical density index: 1.99).

A transbronchial biopsy revealed lung tissue fragments with hemorrhages, focal deposits of brown pigment, and a small necrotic focus without accompanying cellular reaction; Ziehl–Neelsen staining did not detect acid-fast mycobacteria.

Given these findings, invasive pulmonary aspergillosis was suspected. The patient was subsequently hospitalized at the mycology clinic of North-Western State Medical University.

Upon admission to the mycology clinic, the patient's condition was satisfactory; consciousness was clear; skin showed no visible changes; focal alopecia was noted. Breathing was labored, without wheezing. Pulse was 75 beats/min, blood pressure 130/85 mm Hg. Heart sounds were rhythmic on auscultation, with no pathological murmurs.

Clinical blood test: Leukocytes – 3.3 × 10^9/L; erythrocytes – 3.68 × 10^{12}/L; hemoglobin – 118 g/L; platelets – 285 × 10^9/L; neutrophils – 0.8 × 10^9/L; lymphocytes – 2.2 × 10^9/L; ESR – 27 mm/h.

Biochemical blood test: ALT – 16 U/L; AST – 23 U/L; creatinine – 119 μmol/L; urea – 11.9 mmol/L; glucose – 6.3 mmol/L; total bilirubin – 10.9 μmol/L.

Electrocardiography: sinus rhythm with tachysystole, heart rate 90 bpm, horizontal electrical axis of the heart, left ventricular hypertrophy.

Chest CT: persistent hydrothorax (left – up to 10 mm, right – up to 5 mm). In the right lung, partial regression of infiltrative changes with residual ground-glass opacities; grouped foci present, some tending to merge with blurred contours; lower lobe shows multidirectional dynamics with regression of some foci and emergence of new ones. In the left lung, paramediastinal consolidation in the upper lobe shows moderate volume increase; regression of blurred foci in the upper lobe is also noted.

Given the patient's risk factors – IST (continuous tacrolimus use), GvHD, and prolonged glucocorticosteroid (GCS) therapy – together with the examination findings (neutropenia, positive BAL galactomannan test, Aspergillus spp. culture from BAL, and focal "ground-glass" infiltrative changes on chest CT), a diagnosis of invasive pulmonary aspergillosis was established. Antifungal therapy with voriconazole at standard doses was initiated, with blood tacrolimus levels monitored.

Concomitant therapy included: fosinopril 10 mg daily, torasemide 2.5 mg daily, amlodipine 2.5 mg daily, atorvastatin 10 mg daily, folic acid 10 mg daily, iron sulfate 80 mg daily, calcium-D_3 2 tablets daily, magnesium B_6 1 tablet three times daily, prednisolone 7.5 mg daily, and tacrolimus 3 mg daily.

Tacrolimus blood levels were assessed once every three days. When the level reached 17.1 ng/mL, the daily dose was reduced to 2 mg. After 24 hours, the concentration rose to 19.2 ng/mL, necessitating a further reduction to 1 mg/day. Three days later, the tacrolimus level decreased to 9.2 ng/mL.

On the 14th day of hospitalization, follow-up chest CT imaging revealed regression of infiltrative changes in the right lung, reduced inflammatory changes in segments S2, S4–S5, S6, and S8 on the right, and decreased pleural effusion volume in the left pleural cavity (Fig. 2).

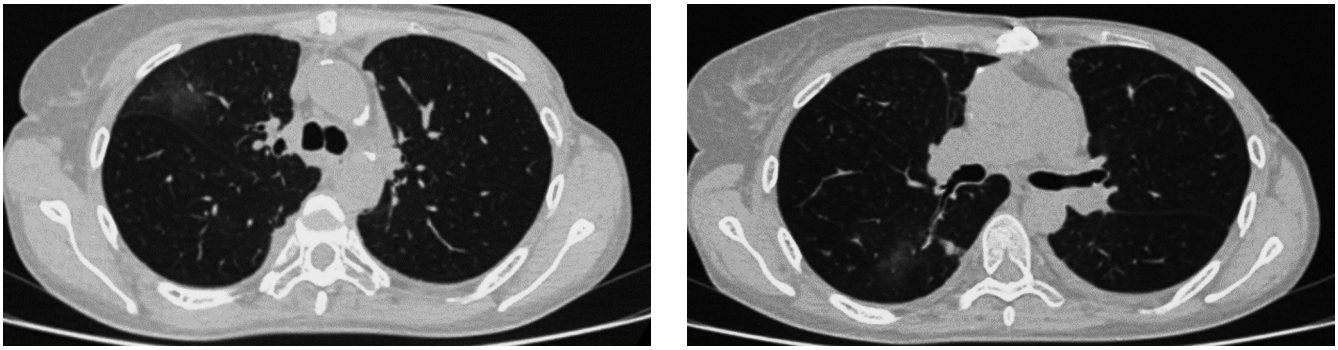

Fig. 1. Chest CT scan showing "ground-glass" opacities and confluent foci in the right lung; the left lung demonstrates a region of consolidation with moderate volume enlargement

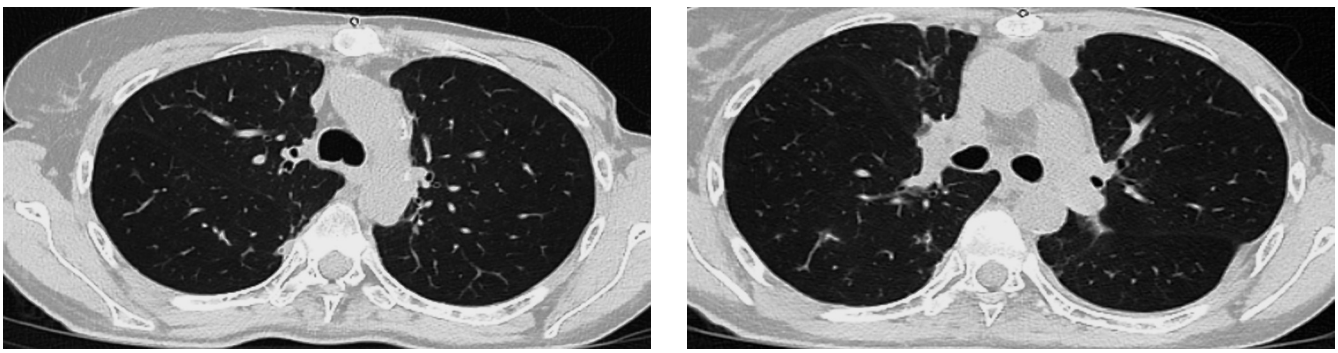

Fig. 2. Chest CT scan 14 days after initiation of therapy: regression of infiltrative changes in the right lung; decreased inflammatory involvement in segments S2, S4–5, S6, and S8 on the right; reduced pleural effusion in the left pleural cavity

The patient's condition was deemed stable, and she was discharged for outpatient follow-up. Given the persistence of risk factors, continuation of voriconazole therapy for at least two months was recommended, with regular monitoring of liver function and assessment for potential drug interactions. Outpatient follow-up at a mycology clinic was also advised.

ANALYSIS OF REGISTRY DATA

Between September 2010 and October 2024, 23 adult patients with invasive aspergillosis (IA) following internal organ transplantation were included in the registry. Of these, 48% were male, with a median age of 55.5 years (range: 19–67; Q1: 49, Q3: 61).

RESULTS

In most cases, IA developed after heart transplantation (65%), followed by kidney transplantation (31%), and less frequently after lung transplantation (4%). The predominant risk factors were the use of immunosuppressive agents – tacrolimus, sirolimus, and mycophenolate mofetil – in 96% of patients, and systemic glucocorticosteroids in 89%. Additional predisposing factors included lymphocytopenia (35%; median duration 20 days [Q1: 15; Q3: 30]) and agranulocytosis (10%; median duration 7 days [Q1: 1; Q3: 14]). Severe bacterial infections, such as pneumonia or sepsis, preceded IA in 63% of cases, while viral pneumonia was noted in 35%. At the time of IA onset, 37% of patients were in the intensive care unit (ICU).

The lungs were the primary site of IA localization (96%). Extrapulmonary involvement (13%) included lesions of the paranasal sinuses, soft tissues of the face, central nervous system aspergillosis, and abdominal organ involvement.

The clinical picture of invasive pulmonary aspergillosis (IPA) was dominated by nonspecific symptoms: fever (65%), respiratory failure (56%), and cough (41%). In isolated cases, hemoptysis was noted (4%). Radiological signs were mainly characterized by infiltrative-focal lung lesions (67%) with a predominance of bilateral processes (76%). In 46% of cases, IPA was accompanied by the appearance of hydrothorax, and in 12.5% of cases, cavities of lung tissue destruction were noted. In patients with viral co-infection or those in the period of agranulocytosis, the "ground glass" symptom was noted (31%).

The diagnosis was established on the basis of direct microscopy of biosubstrates (bronchoalveolar lavage (BAL) and biopsies) in 50% of patients, and in 35% the pathogen was isolated in culture. The main pathogen in IA was *Aspergillus fumigatus* (73%), less commonly *Aspergillus niger* (18%) and *Aspergillus flavus* (9%). A positive galactomannan test in BAL was detected in 85% of patients with IPA. Histological examination revealed characteristic thin hyaline filaments of mycelium branching at an angle of 450 in 13% of patients. A combination of IA with other invasive mycoses (cryptococcosis, pneumocystosis, and candidiasis) was observed in 17%.

Prior to the diagnosis of IA, empirical antifungal therapy with agents active against mold microfungi was administered to 30% of patients. All patients (100%) subsequently received targeted antimycotic therapy. The agents used included voriconazole (87%), echinocandins (17%), and itraconazole (4%). Combination antifungal therapy was required in one patient (4%). Median duration of IA treatment was 96 days [Q1 – 38; Q3 – 150]. Overall 90-day survival rate was 78%.

LITERATURE REVIEW

The first year after transplantation carries the highest risk for invasive fungal infections (IFI), which may result from surgical complications, donor-derived infections, or pre-existing infections in the recipient [6]. The incidence of infectious complications is higher among recipients of heart, lung, and liver transplants compared to kidney transplants. On average, the prevalence of invasive mycoses in organ transplant recipients is approximately 5%, varying by transplant type [7]. The highest rates are observed in small intestine (11.6%) and lung (8.6%) transplants, followed by liver (4.7%), heart (4%), pancreas (3.4%), and kidney (1.3%) transplants [7, 8].

Aspergillosis is the most common invasive fungal infection in this population, while mucormycosis occurs less frequently [9, 10]. In Russia, the number of IA cases has been steadily increasing. In 2024, Khostelidi et al. reported registry data on 17 patients with IA following organ transplantation [11]. By 2025, the number of recorded cases had increased by nearly 30%.

IA typically shows up 3–6 months after organ transplantation [6]. One important risk factor is fungal colonization, with cumulative airway mold colonization rates ranging from 20% to 50% [12]. *Aspergillus spp.* are the most frequent respiratory tract colonizers among potentially pathogenic microfungi. The colonization rate is notably higher in patients with cystic fibrosis. Luong M.L. et al. (2014) reported detection of *Aspergillus spp.* in 70% of cystic fibrosis patients prior to transplantation [12].

Several additional factors contribute to the risk of invasive mycosis, including prolonged ICU stay, renal replacement therapy, concurrent generalized bacterial infection, mechanical ventilation, diabetes mellitus, viral infections, and donor genetic polymorphisms [2, 6]. While all these factors play a role, the use of immunosuppressive agents to prevent transplant rejection remains the predominant risk factor.

Pathogens responsible for invasive mycoses in transplant recipients can affect virtually any organ; however, distinct clinical patterns are typically associated with specific pathogens. In the case of Aspergillus species, the predominant clinical forms are invasive pulmonary aspergillosis (74%–78%) and aspergillus tracheobron-

chitis (5%–25%) [8], with less common manifestations involving the paranasal sinuses (PNS), central nervous system (CNS), and other sites. The clinical presentation of invasive pulmonary aspergillosis is nonspecific, often including cough, dyspnea, and fever [13].

In our registry, heart transplantation was the most frequent procedure among patients with IA (65%). This contrasts with literature data indicating that mycotic lesions of the respiratory tract caused by Aspergillus species occur primarily in lung transplant recipients [8]. In such patients, bronchoscopy may reveal ulcerative or necrotic bronchial lesions, pseudomembranes that slough to form ulcerative defects, and damage often localized around the anastomotic suture line. Central airway obstruction may be the initial manifestation of fungal tracheobronchitis, with bronchoscopy demonstrating fibrinous mucosal plugs containing *Aspergillus* hyphae [8].

The necrotizing pseudomembranous form of invasive fungal tracheobronchitis represents the most severe presentation, characterized by detachment of the necrotic epithelium and submucosal layer. Importantly, invasive tracheobronchial aspergillosis (ITBA) can be asymptomatic and detected incidentally during routine bronchoscopy. Early detection through surveillance bronchoscopy facilitates diagnosis before symptom onset, allowing timely initiation of antifungal therapy. The main complications of tracheobronchial aspergillosis include bronchomalacia, bronchial stenosis, suture dehiscence, bleeding, and extension into the lung parenchyma with subsequent dissemination [8].

Thus, when clinical symptoms of lung injury appear, recipients of internal organ transplants (lungs, heart, liver, kidneys) should undergo fiberoptic bronchoscopy with BAL to test for pathogenic microorganisms, including fungi, as well as a galactomannan assay for *Aspergillus spp.* antigen (AG).

The diagnostic criteria for these patients include identifying risk factors for mycotic infection in combination with clinical findings, CT imaging features, and laboratory results [14]. On lung CT scans, early manifestations (within the first 3–5 days) most commonly present as perivascular "ground-glass" opacities (50–60%). These lesions often progress to dense foci and infiltrates, with eventual formation of areas of destruction. A surrounding "halo" of perifocal inflammation is seen in 19%–53% of cases [13, 15].

When the paranasal sinuses (PNS) are involved, CT imaging typically reveals areas of osteodestruction. In cases of central nervous system involvement, focal brain lesions are visualized [15].

The main diagnostic methods include: microscopy of material from the lesion site, which detects thin septate mycelium branching at approximately 45°; culture testing, positive in 40–50% of cases; detection of galactomannan (GM) in BAL fluid, with a sensitivity of about 60% and specificity of 95–98% [16–18]; PCR testing for *Aspergillus* DNA [17].

Microscopy is performed on both native and stained preparations, most commonly using Gram, hematoxylin–eosin, Ziehl–Neelsen, India ink, or calcofluor white stains. Given the rapid progression of the infection, direct microscopy with calcofluor white staining under a fluorescent microscope is the fastest diagnostic approach [19, 20].

The presence of characteristic fungal mycelium in normally sterile biosubstrates or BAL fluid, combined with relevant risk factors, clinical signs, and imaging findings, is a key diagnostic criterion. Notably, refrigerating the specimen or homogenizing it prior to culture may reduce the likelihood of recovering microfungi.

Cultures are identified based on macromorphological and micromorphological features, as well as molecular methods. Histological examination using specific stains – such as Grocott's methenamine silver (GMS) and the periodic acid–Schiff (PAS) reaction – enables visualization of fungal elements within tissues and assessment of the degree of invasion, including associated inflammation and necrosis [14].

The detection of GM is one of the key diagnostic tests. According to a meta-analysis by Gavaldà et al. (2014), the sensitivity of the GM test in the blood of solid organ transplant recipients is approximately 30% [21]. The specificity of the assay is reduced due to the possibility of false-positive results; therefore, GM determination in blood is not recommended for routine diagnosis or treatment monitoring.

The most diagnostically valuable application of the GM test is in BAL samples, where sensitivity reaches 60% and specificity 95–98% [22, 23].

PCR assays have been developed for the amplification of *Aspergillus* DNA, typically performed on blood and BAL specimens. It is important to recognize that a positive PCR result from a respiratory sample may indicate either airway colonization or an invasive process [24]. Current international clinical guidelines from the European Society of Clinical Microbiology and Infectious Diseases (ESCMID) and the European Organisation for Research and Treatment of Cancer/Mycoses Study Group (EORTC/MSG) do not recommend the use of PCR as a stand-alone diagnostic tool, since these systems have not yet been standardized or validated in independent studies [25].

Microfungal pathogens can be identified using matrix-assisted laser desorption/ionization time-of-flight mass spectrometry (MALDI-TOF) [24, 26]. The most common IA pathogens are *Aspergillus fumigatus* (73%), A. flavus (14%), and A. terreus (8%), although rare *Aspergillus* species are also occasionally encountered [26]. These findings are consistent with our own observations.

STRATEGIES FOR THE TREATMENT OF INVASIVE MYCOSES IN ORGAN TRANSPLANT RECIPIENTS

The main management approach in organ transplant recipients largely parallels established treatment strategies for other groups of immunocompromised patients [27].

Primary antifungal prophylaxis is indicated for all patients with extensive colonization of the respiratory and gastrointestinal tract mucosa by micromycetes in the postoperative period. Empirical antifungal therapy is recommended when clinical manifestations of localized or systemic infection are present and there is no improvement following 96 hours of standard antibacterial treatment. Etiotropic therapy should be initiated once diagnostic test results are available, with treatment tailored to the specific pathogen identified and the corresponding nosological form [28].

Senoner et al. (2023) showed that antifungal prophylaxis in liver transplantation significantly reduces the risk of proven invasive mycosis (OR 0.37; 95% CI: 0.19–0.72; p = 0.003). The use of antifungal prophylaxis in specialized departments is also associated with a marked reduction in mortality attributable to fungal infections (OR 0.32; 95% CI: 0.10–0.83; p = 0.02), although it does not significantly influence all-cause mortality (OR 0.87; 95% CI: 0.54–1.39; p = 0.55). In the absence of antifungal prophylaxis, invasive fungal infections (IFIs) develop in approximately 36% of transplant recipients [29].

Therefore, targeted prophylaxis with antifungal agents active against *Aspergillus spp.* is recommended in lung transplant recipients with documented pre-transplant colonization of the respiratory tract by *Aspergillus spp.* While the optimal duration of such prophylaxis remains undefined, it is typically administered for an average of 2–3 weeks [30].

Current clinical consensus identifies voriconazole and isavuconazole as the first-line agents for the treatment of IA (Table). Given the difficulty of conducting clinical trials specifically in organ transplant recipients, therapeutic recommendations are largely extrapolated from experience in other patient populations [14, 31, 32].

Voriconazole undergoes extensive metabolism via the cytochrome P450 enzyme system, which limits its use in transplant recipients due to the potential for significant drug–drug interactions, particularly with immunosuppressive agents. Therapeutic drug monitoring is an essential component of the management strategy in patients with multiple drug interactions [14].

Nevertheless, voriconazole has been successfully used as first-line therapy for IA in heart, lung, and liver transplant recipients [14]. Isavuconazole offers a more favorable safety profile [14, 33] and may be prescribed in cases where voriconazole is not effective.

Liposomal amphotericin B (L-AMB) represents an alternative agent for IA therapy, demonstrating *in vitro* activity against most mold species [14, 32, 34]. However, resistance has been documented in certain *Aspergillus* species, notably *Aspergillus terreus*. Echinocandins (caspofungin, micafungin, anidulafungin) are not recommended as monotherapy for IA, as they exert only fungistatic rather than fungicidal activity against *Aspergillus spp*. Their role is primarily as part of combination therapy, administered alongside voriconazole, isavuconazole, or L-AMB in selected cases [14, 32, 34].

The recommended duration of IA therapy is typically 12 weeks but may range from 6 to >50 weeks [14, 35]. Key determinants include initial therapeutic response, immune status, and activity of the underlying disease. Treatment should be maintained until all clinical manifestations and radiological abnormalities have resolved, and mycological tests yield negative results.

In organ transplant recipients, an essential component of management is to reduce the dose of immunosuppressive drugs and monitor graft function [36]. Patterson et al. (2016) and other expert groups advise a minimum treatment duration of 6–12 weeks, depending on the site

Table

Therapeutic approaches to invasive aspergillosis

Antifungal drug	Strength of recommendation and level of evidence	
Voriconazole 6 mg/kg IV twice daily on day 1, then 4 mg/kg IV twice daily; or 400 mg PO twice on day 1, then 200 mg PO twice daily (with or without food)	**A**	**I**
Isavuconazole 200 mg PO/IV three times daily for 2 days, then 200 mg once daily	**A**	**I**
Liposomal amphotericin B 3 mg/kg/day IV by infusion	B	II
Caspofungin 70 mg IV on day 1, then 50 mg/day IV	C	II
Micafungin 100 mg/day IV	C	III
Itraconazole 200 mg PO twice daily (suspension or tablets)	C	III
Lipid complex AmB 5 mg/kg/day IV	C	III
Combination: anidulafungin 200 mg IV on day 1, then 100 mg/day + voriconazole at standard dosing	C	I
Other combinations as initial therapy	C	III
Amphotericin B deoxycholate	D	I

and extent of IA, as well as the degree and persistence of immunosuppression [20].

FINDINGS

Our data indicate that IA can occur in recipients of internal organ transplants during immunosuppressive therapy. According to our registry, IA developed most frequently after heart transplantation (65%), followed by kidney transplantation (31%) and lung transplantation (4%). The predominant clinical manifestation was pulmonary involvement (96%). The most effective diagnostic method was galactomannan detection in BAL fluid, with a sensitivity of 85%. The leading causative agent was *Aspergillus fumigatus* (73%). The overall 12-week survival rate in our cohort was 78%.

CONCLUSION

The presented clinical case, combined with registry analysis and literature review, underscores that diagnosing and treating IA in organ transplant recipients remains a major challenge for clinicians and microbiologists. Advances in modern diagnostic methods facilitate early detection, which is crucial in immunocompromised patients who require lifelong immunosuppression. Timely and appropriate selection of antifungal therapy significantly improves survival and recovery outcomes in this patient population.

The authors declare no conflict of interest.

REFERENCES

1. *Khostelidi SN.* Invasive mycoses in recipients of solid organ transplants (literature review). *Problems in Medical Mycology*. 2023; 25 (4): 3–14. (In Russ). doi: 10.24412/1999-6780-2023-4-3-14. EDN YHAXVI.
2. *Pata R, Kristeva J, Kosuru B.* Pneumonia in Transplant Recipients: A Comprehensive Review of Diagnosis and Management. *Cureus.* 2024 Nov 14; 16 (11): e73669. doi: 10.7759/cureus.73669.
3. *Neofytos D, Chatzis O, Nasioudis D et al.* Epidemiology, risk factors and outcomes of invasive aspergillosis in solid organ transplant recipients in the Swiss transplant cohort study. *Transpl Infect Dis*. 2018; 20 (4): e12898. doi: 10.1111/tid.12898.
4. *Donnelly JP, Chen SC, Kauffman CA, Steinbach WJ et al.* Revision and update of the consensus definitions of invasive fungal disease from the European Organization for Research and Treatment of Cancer and the Mycoses Study Group Education and Research Consortium. *Clin Infect Dis*. 2020; 71: 1367–1376. doi: 10.1093/cid/ciz1008.
5. Certificate of state registration of the database No. 2023620879 Russian Federation. "Invasive aspergillosis in adult patients" ("Database on the results of consultations at the P.N. Kashkin Research Institute of Medical Mycology"): *O.V. Shadrivova, S.N. Hostelidi, N.N. Klimko;* applicant Federal State Budgetary Educational Institution of Higher Education "North-Western State Medical University named after I.I. Mechnikov" of the Ministry of Health of the Russian Federation. EDN VPJAHY.
6. *Dorschner P, McElroy LM, Ison MG et al.* Nosocomial infections within the first month of solid organ transplantation. *Transpl Infect Dis Off J Transplant Soc*. 2014; 16: 171–187. doi: 10.1111/tid.12203.
7. *Patel MH, Patel RD, Vanikar AV et al.* Invasive fungal infections in renal transplant patients: a single center study. Ren Fail. 2017 Nov; 39 (1): 294–298. doi: 10.1080/0886022X.2016.1268537.
8. *Samanta P, Clancy CJ, Nguyen MH et al.* Fungal infections in lung transplantation. *J Thorac* Dis. 2021 Nov; 13 (11): 6695–6707. doi: 10.21037/jtd-2021-26.
9. *Khostelidi SN, Shadrivova OV, Shagdileeva EV et al.* Invasive mycoses caused by filamentous fungi in patients after internal organ transplantation. *Russian Journal of Transplantology and Artificial Organs.* 2024; 26 (S): 219–220. doi: 10.15825/1995-1191-2024-S-219-220.
10. *Khostelidi SN, Kozlova OP, Shagdileeva EV et al.* Invasive mycoses caused by filamentous fungi in patients after internal organ transplantation. *Russian Journal of Transplantology and Artificial Organs.* 2024; 26 (3): 56–65. doi: 10.15825/1995-1191-2024-3-56-65. EDN HNPVRD.
11. *Khostelidi SN, Kozlova OP, Shadrivova OV et al.* Invasive fungal infections after solid organ transplantation (St. Petersburg, Russia). *ABSTRACT BOOK: 3rd Balkan Conference on Medical Mycology and Mycotoxicology, Belgrade, Serbia, October 10–12, 2024. Belgrade: Serbian Society of Medical Mycology*, 2024: 89. EDN HZYZTU.
12. *Luong ML, Chaparro C, Stephenson A, Rotstein C et al.* Pretransplant Aspergillus colonization of cystic fibrosis patients and the incidence of post-lung transplant invasive aspergillosis. *Transplantation.* 2014 Feb 15; 97 (3): 351–357. doi: 10.1097/01.TP.0000437434.42851.d4.
13. *Khostelidi SN.* Clinical and laboratory features of nosocomial invasive aspergillosis: Abstract of the dissertation for the degree of candidate of medical sciences. St. Petersburg, 2010; 22. EDN QHFIBR.
14. *Ullmann AJ, Aguado JM, Arikan-Akdagli S, Denning DW, Groll AH et al.* Diagnosis and management of Aspergillus diseases: executive summary of the 2017 ESCMID-ECMM-ERS guideline. *Clin Microbiol Infect.* 2018 May; 24 Suppl 1: e1–e38. doi: 10.1016/j.cmi.2018.01.002.
15. *Varotto A, Orsatti G, Crimì F et al.* Radiological Assessment of Paediatric Fungal Infections: A Pictorial Review with Focus on PET/MRI. *In vivo*. 2019; 33 (6): 1727–1735. doi: 10.21873/invivo.11663.
16. *Husain S, Sole A, Alexander BD et al.* The 2015 International Society for Heart and Lung Transplantation guidelines for the management of fungal infections in mechanical circulatory support and cardiothoracic organ transplant recipients: executive summary. *J Heart Lung Transplant*. 2016; 35 (3): 261–282. doi: 10.1016/j.healun.2016.01.007.
17. *Imbert S, Meyer I, Palous M, Brossas JY et al.* Aspergillus PCR in bronchoalveolar lavage fluid for the diagnosis

and prognosis of aspergillosis in patients with hematological and non-hematological conditions. *Front Microbiol*. 2018; 9: 1877. doi: 10.3389/fmicb.2018.01877.
18. *Ignatieva SM, Shadrivova OV, Shurpitskaya OA et al.* Determination of galactomannan from *Aspergillus spp.* In patients with COVID-associated invasive aspergillosis. *Problems of medical mycology*. 2023; 25 (2): 115. EDN UKTCPI.
19. *Terrero-Salcedo D.* Updates in Laboratory Diagnostics for Invasive Fungal Infections. *J Clin Microbiol*. 2020; 58 (6): e01487-19. doi: 10.1128/JCM.01487-19.
20. *Patterson TF, Thompson GR, Denning DW, Fishman JA et al.* Practice guidelines for the diagnosis and management of aspergillosis: 2016 update by the Infectious Diseases Society of America. *Clin Infect Dis*. 2016; 63 (4): e1–e60. doi: 10.1093/cid/ciw326.
21. *Gavaldà J, Meije Y, Fortún J, Roilides E et al.* ESCMID Study Group for Infections in Compromised Hosts. Invasive fungal infections in solid organ transplant recipients. *Clin Microbiol Infect.* 2014 Sep; 20 Suppl 7: 27–48. doi: 10.1111/1469-0691.12660.
22. *Boch T, Buchheidt D, Spiess B, Miethke T, Hofmann WK, Reinwald M.* Direct comparison of galactomannan performance in concurrent serum and bronchoalveolar lavage samples in immunocompromised patients at risk for invasive pulmonary aspergillosis. *Mycoses*. 2016; 59 (2): 80–85. doi: 10.1111/myc.12434.
23. *Singh N, Winston DJ, Limaye AP, Pelletier S, Safdar N, Morris MI et al.* Performance characteristics of Galactomannan and beta-d-Glucan in high-risk liver transplant recipients. *Transplantation*. 2015; 99 (12): 2543–2550. doi*:* 10.1097/TP.0000000000000763.
24. *Haidar G, Falcione BA, Nguyen MH.* Diagnostic modalities for in- vasive mould infections among hematopoietic stem cell transplant and solid organ recipients: performance characteristics and prac- tical roles in the clinic. *Journal of Fungi.* 2015; 1 (2): 252–276. doi: 10.3390/jof1020252.
25. *Imbert S, Gauthier L, Joly I, Brossas JY et al.* Aspergillus PCR in serum for the diagnosis, follow-up and prognosis of invasive aspergillosis in neutropenic and nonneutropenic patients. *Clin Microbiol Infect*. 2016; 22 (6): 562e1–562e8. doi: 10.1016/j.cmi.2016.01.027.
26. *Neofytos D, Garcia-Vidal C, Lamoth F, Lichtenstern C, Perrella A, Vehreschild JJ.* Invasive aspergillosis in solid organ transplant patients: diagnosis, prophylaxis, treatment, and assessment of response. *BMC Infect Dis.* 2021 Mar 24; 21 (1): 296. doi: 10.1186/s12879-021-05958-3.
27. *Andreev SS, Bronin GO, Epifanova NYu et al.* Advantages of early administration of antimycotic therapy in hematological patients. *Oncohematology.* 2024; 19 (1): 99–112. doi: 10.17650/1818-8346-2024-19-1-99-112. EDN NOYKAI.
28. *Bitterman R, Marinelli T, Husain S.* Strategies for the Prevention of Invasive Fungal Infections after Lung Transplant. *J Fungi.* 2021; 7: 122. doi: 10.3390/jof7020122.
29. *Senoner T, Breitkopf R, Treml B, Rajsic S.* Invasive Fungal Infections after Liver Transplantation. *J Clin Med.* 2023; 12: 3238. doi: 10.3390/jcm12093238.
30. *Husain S, Camargo JF.* Invasive Aspergillosis in solid-organ transplant recipients: Guidelines from the American Society of Transplantation Infectious Diseases Community of Practice. *Clin Transplant.* 2019; 33: e13544. doi: 10.1111/ctr.13544.
31. *Klimko NN, Khostelidi SN, Borzova YuV et al.* Nosocomial invasive aspergillosis in hematological oncology patients. *Clinical oncohematology*. Basic research and clinical practice. 2011; 4 (3): 228–234. EDN QALBGP.
32. *Klyasova GA.* New possibilities for the treatment of invasive aspergillosis. *Oncohematology.* 2021; 16 (4): 31–39. doi: 10.17650/1818-8346-2021-16-4-31-39. EDN LIRRGQ.
33. *Veselov AV.* Isavuconazole is a new antifungal drug of the triazole class. *Problems of medical mycology.* 2015; 17 (4): 18–24. EDN VEDMSV.
34. *Shadrivova OV.* Clinical and immunological features of invasive aspergillosis: Dissertation for the degree of Candidate of Medical Sciences. 2015; 126. EDN TYJMMI.
35. *Richardson M, Bowyer P, Sabino R.* The human lung and Aspergillus: You are what you breathe in? *Medical Mycology.* 2019; 57 (Suppl. 2): S145–S154. doi: 10.1093/mmy/myy149.
36. *Singh NM, Husain S,* The AST Infectious Diseases Community of Practice. Aspergillosis in solid organ transplantation. *American Journal of Transplantation*. 2013; 13: 228–241. doi: 10.1111/ajt.12115.

The article was submitted to the journal on 4.02.2025

DOI: 10.15825/1995-1191-2025-3-88-96

CORRELATION ANALYSIS OF RENAL SCAN AND VOLUMETRIC PERFUSION CT IN THE ASSESSMENT OF LIVING KIDNEY DONORS

N.M. Djuraeva, A.A. Davidkhodjaeva

Republican Specialized Scientific and Practical Medical Center of Surgery, Tashkent, Republic of Uzbekistan

Objective: to evaluate the correlation between renal scan (RSc) and volumetric multislice computed tomography (perfusion CT) in living kidney donors, with the goal of identifying interchangeable functional parameters and optimizing the preoperative assessment of split renal function. **Materials and methods.** The study included 54 living kidney donors (totaling 108 kidneys). Split renal function was assessed using RSc with 99mTc-mercaptoacetyltriglycine (MAG3) and contrast-enhanced volumetric MSCT. Key parameters from nephroscintigraphy included renal plasma flow (RPF), time to maximum tracer accumulation (Tmax), and excretion half-life (T½). Single-photon emission computed tomography (SPECT) analysis included arterial flow (AF), blood volume (BV), extraction fraction (FE), and indexed extraction fraction (IFE). Correlation between modalities was analyzed using Pearson's correlation coefficient and Bland–Altman plots. **Results.** Significant correlations were observed between RSc and volumetric MCT parameters. A strong negative correlation was found between Tmax and AF ($r = –0.75$, $p < 0.001$), indicating an inverse relationship between blood flow velocity and renal filtration capacity. Similarly, T½ showed a negative correlation with FE ($r = –0.75$, $p < 0.01$), suggesting that a shorter tracer half-life corresponds to more efficient renal extraction. A strong positive correlation between RPF and IFE ($r = 0.79$, $p < 0.001$) supports the feasibility of using indexed CT perfusion as a surrogate for assessing RPF. Bland-Altman analysis showed that differences between the two diagnostic methods remained within clinically acceptable limits, confirming their potential interchangeability in preoperative donor assessment. **Conclusion.** The study demonstrates the potential for partial interchangeability between RSc and volumetric CT perfusion in the preoperative assessment of kidney donors. While CT perfusion offers superior accuracy in assessing renal blood flow, nephroscintigraphy remains the method of choice for evaluating excretory function. The combined use of both modalities improves diagnostic accuracy and kidney donor selection, thereby improving the safety of kidney transplant programs.

Keywords: split renal function, nephroscintigraphy, volumetric CT perfusion, kidney donation, renal perfusion, functional diagnostics.

INTRODUCTION

Related kidney transplantation is one of the key treatment options for patients with end-stage chronic kidney disease (CKD). A critical step in this process is the selection of the most suitable donor kidney, which requires a detailed assessment of its separate function.

Split renal function refers to the relative contribution of each individual kidney to the overall renal function, often expressed as a fraction of the total activity of both kidneys. This assessment provides important information on the presence or absence of functional symmetry and serves as a decisive parameter in donor selection [1, 2].

According to current clinical guidelines, if the difference in functional contribution between the two kidneys is less than 10%, the donor retains the kidney with the higher function. However, if the difference exceeds 10%, the individual is not recommended as a donor, since significant asymmetry in kidney function may adversely affect long-term health after nephrectomy [3, 4].

At present, several methods are used in clinical practice to assess split kidney function, with renal scan (renal scintigraphy) and volumetric multislice computed tomography (CT perfusion) being the most widely used [5, 6]. According to Grenier et al. (2015) and Zhang et al. (2017), perfusion CT enables highly accurate evaluation of renal blood flow [7, 8]. In contrast, O'Connor et al. (2014) reported that renal scan provides a more precise assessment of renal excretory function, particularly in patients with nephropathy [9, 10].

A renal scan is based on the use of radiopharmaceuticals and allows for assessment of the kinetics of tracer passage through the kidneys. Key parameters include renal plasma flow (RPF), time to maximum tracer accumulation (Tmax), and excretion half-life (T½) [11, 12]. By comparison, CT perfusion provides detailed in-

Corresponding author: Asalkhon Davidkhodjaeva. Address: 8, Parkentskaya str., Mirzo-Ulugbek district, Tashkent, 100007, Republic of Uzbekistan.
Phone: +998 (90) 189-14-45. E-mail: davidxodjayevaa@gmail.com

sight into renal hemodynamics, including arterial flow (AF), blood volume (BV), extraction fraction (FE), and indexed extraction fraction (IFE), the latter being especially valuable in accounting for individual anatomical variability [13, 14].

Despite the widespread use of these techniques, the degree of correlation between their parameters and the possibility of interchangeability remain unresolved. Some studies suggest that CT angiography may, in certain cases, substitute for radionuclide techniques in evaluating renal blood flow [15, 16]. Conversely, other authors emphasize that renal scintigraphy provides a more accurate measure of excretory function in patients with concomitant renal pathology [17, 18].

The present study was designed to analyze correlations between the principal parameters of renal scan and CT perfusion in living kidney donors. The objective was to identify interchangeable indicators and to evaluate their clinical significance for optimizing the preoperative assessment of split kidney function.

MATERIALS AND METHODS

The study included 54 living kidney donors, providing a total dataset of 108 kidneys. All participants underwent a standardized diagnostic work-up that incorporated both renal scintigraphy and perfusion CT analysis.

Renal scan was performed using a Siemens Symbia T16 gamma camera with ^99mTc-mercaptoacetyltriglycine (MAG3) as the radiopharmaceutical. MAG3 was selected due to its high excretory capacity and widespread use in the assessment of RPF and excretory function.

The following key indicators of renal function were evaluated renal scan: Tmax (time from the injection of MAG3 to when the highest amount of activity is detected in the kidneys, reflecting how quickly the tracer is filtered by the kidneys and distributed within the renal cortex); T½ (the time required for renal clearance of MAG3 from peak activity, characterizing the efficiency of excretory function); RPF (the volume of plasma passing through the kidney per unit time, expressed in mL/min/m^2 of body surface area).

In addition, relative kidney function was assessed by normalizing renal scintigraphy parameters to the total functional contribution of both kidneys. This calculation was based on RPF, as MAG3 is predominantly excreted via tubular secretion, making it more sensitive to renal blood flow changes compared with other radiopharmaceuticals.

The use of MAG3 allowed for a more accurate assessment of renal excretory function, particularly in patients with potential dysfunction, as its clearance correlates closely with effective RPF and tubular secretion. This makes it an indispensable tool for detecting even subtle abnormalities in renal function among potential donors.

To determine the relative functional contribution of the right and left kidneys, renal scan data were normalized to the total functional activity of both kidneys. The relative contribution of each individual kidney was calculated using the following standard formula:

$$\text{Relative kidney contribution (\%)} = \frac{\text{Function of individual kidney}}{\text{Function of both kidneys}} \times 100.$$

Initially, individual renal scintigraphy parameters were measured, including drug accumulation level, filtration rate, and RPF. The total functional contribution of both kidneys was then determined by summing the corresponding values for the right and left kidneys. Finally, the relative contribution of each kidney was calculated as a percentage, using the ratio of the functional activity of a single kidney to the total activity of both kidneys, multiplied by 100.

For example, if the RPF of the right kidney is 225 mL/min and that of the left kidney is 275 mL/min, the total RPF is 500 mL/min. Accordingly, the relative contribution of the right kidney is: (225/500) × 100 = 45%, and the relative contribution of the left kidney is: (275/500) × 100 = 55%.

Various indicators can be used to calculate the relative functional contribution of each kidney. Among them, RPF is most frequently applied, as it directly reflects the volume of blood passing through each kidney. Additional parameters, such as the level of radioisotope accumulation and its excretion rate, are also informative, as they characterize filtration and excretory processes. Assessing relative contribution is particularly important in donor selection, as it helps determine functional symmetry and identify significant asymmetry, which may indicate underlying pathology.

Perfusion measurements were performed using a 320-slice Aquilion ONE spiral CT scanner (Canon Medical Systems, Japan). Scans were obtained with a slice thickness of 0.5 mm in soft tissue reconstruction mode. The protocol was optimized to minimize radiation exposure, using a tube voltage of 100 kV and an exposure of 60 mAs, which was sufficient for dynamic studies with a maximum coverage width of 160 mm along the Z-axis. Additional parameters included collimator dimensions of 0.5×320 mm, a matrix of 512×512, a field of view (FOV) of 320–350 mm, and a tube rotation time of 0.275 s.

This technique enabled quantitative assessment of renal hemodynamics through contrast-enhanced dynamic scanning, which recorded temporal changes in renal tissue density.

Prior to the examination, all patients underwent standard preparation, which included preliminary hydration when necessary to minimize the risk of contrast-induced nephropathy. A clinical evaluation was also performed

to rule out potential contraindications, such as allergy to iodine-containing contrast agents.

An iodine-containing contrast agent (iodhexol, iodine concentration 350 mg/mL) was used for perfusion studies. The contrast medium was administered via a peripheral venous catheter using an automatic injector at a rate of 5 mL/s. The total volume of contrast was calculated individually according to body weight, with a minimum dose of 0.5 mL/kg.

Following contrast administration, a dynamic series of scans was performed to capture temporal changes in renal tissue density. Scans were acquired at intervals of 30–90 seconds, with a slice thickness of 3–5 mm, yielding a total of 20–30 series per study. Density values of the cortical and medullary layers of the kidneys were expressed in Hounsfield units (HU) and used to construct time–density curves.

Post-processing of imaging data was performed using VITREA software (Canon Medical Systems, Japan), which enabled the calculation of renal perfusion parameters. The Patlak model was applied to analyze the linear portion of the contrast accumulation curve, providing accurate estimates of extraction fraction (FE) and blood volume (BV). Arterial flow (AF) was calculated using a standard dynamic perfusion model based on the initial rate of density increase.

AF was defined as the volume of blood passing through 100 g of kidney tissue per minute and was calculated from the slope of the initial section of the contrast enhancement curve. BV represented the total volume of circulating blood in 100 ml of kidney tissue, providing an estimate of vascular filling of the parenchyma. FE and IFE were derived from analysis of contrast accumulation and clearance, reflecting the efficiency of renal filtration.

The IFE was additionally calculated to account for individual anatomical variability. For this purpose, the volume of the renal cortex – the primary site of filtration and excretion – was measured, and the FE was normalized to cortical volume. This adjustment provided a more precise and comparable index of renal functional activity across different patients.

IFE provided an additional level of normalization of renal filtration parameters, eliminating the influence of kidney size differences, particularly when comparing the right and left kidneys. This was especially important in donor selection, as IFE allowed for an objective evaluation of excretory function independent of anatomical variations. The obtained data allowed not only assessment of the functional state of the kidneys, but also analysis of their relative contribution – an essential factor in choosing the donor organ. The correlations identified between renal scan indicators and CT perfusion parameters confirmed the feasibility of applying these methods in the comprehensive evaluation of renal function.

STATISTICAL ANALYSIS

Correlation analysis was performed using Pearson's correlation coefficient to examine the relationships between renal scan indicators (Tmax, T½, RPF) and CT perfusion parameters (AF, BV, FE, IFE). The analysis was aimed at identifying linear associations between parameters reflecting renal perfusion and functional characteristics. Statistical significance was set at $p < 0.05$.

Additionally, a Bland–Altman analysis was conducted to assess the degree of agreement between renal scan and CT perfusion measurements. This method was applied to compare differences in measurements of Tmax, T½, and RPF (renal scan data) with AF, FE, and BV (CT perfusion data), in order to identify systematic biases and establish limits of agreement between the two diagnostic approaches. The analysis enabled evaluation of the reproducibility and potential interchangeability of results obtained by these different research methods.

RESULTS AND DISCUSSION

The analysis of the relationship between functional parameters derived from renal scintigraphy and perfusion CT revealed statistically significant correlations, supporting the physiological link between renal perfusion and filtration.

A negative correlation was observed between the time to maximum tracer accumulation (Tmax) and arterial flow (AF) ($r = –0.75$, $p < 0.001$). This finding indicates that higher arterial blood flow is associated with a shorter time to peak drug concentration, reflecting the dependence of isotope uptake rate on renal tissue perfusion.

Similarly, a negative correlation was found between drug half-life (T½) and extraction fraction (FE) ($r = –0.75$, $p < 0.01$). This result confirms that higher extraction capacity facilitates faster clearance of the tracer, while lower extraction efficiency prolongs drug elimination.

The relationship between RPF and IFE showed a strong positive correlation ($r = 0.79$, $p < 0.001$). The recalculation of FE values for the cortical volume significantly improved reproducibility and provided a more objective evaluation of renal filtration capacity, minimizing the influence of anatomical variability (Table 1).

Table 1

Correlation between renal scintigraphy and perfusion CT

Renal scan index	CT perfusion index	Correlation coefficient (r)	p-value
Tmax	AF	–0.75	$p < 0.001$
T½	FE	–0.75	$p < 0.01$
RPF	IFE	0.81	$p < 0.01$

A Bland–Altman analysis was performed to further assess the agreement between renal scintigraphy and perfusion CT. Comparison of Tmax and AF showed limits of agreement ranging from –15% to +18%, with a mean difference not exceeding 3%, supporting their interchangeability for the assessment of renal blood flow in the absence of significant vascular pathology. The comparison of T½ and FE revealed a narrower range of discrepancies (–10% to +12%), indicating strong consistency between these parameters. Similarly, the average difference between RPF and IFE was only 1.5%, with limits of agreement between –8% and +9%, confirming their functional equivalence.

Assessment of the relative functional contribution of each kidney demonstrated that CT perfusion provided higher accuracy. The mean contributions of the right and left kidneys, as determined by FE and IFE, were 49.8% (±3.2%) and 50.2% (±3.4%), respectively, confirming functional symmetry in the donor cohort. In contrast, renal scintigraphy exhibited greater interindividual variability, which may limit its precision in determining relative functional contribution (Table 2).

The findings of this study indicate that renal scan and CT perfusion parameters are partially interchangeable. AF can be reliably used in place of Tmax for assessing renal blood flow. Similarly, FE is equivalent to T½ in evaluating clearance. IFE, adjusted for renal parenchyma volume, accurately reflects RPF and can serve as its substitute in functional calculations.

The identified correlations enal scan and CT perfusion confirm the feasibility of using both techniques in comprehensive assessment of renal function. While methodological differences arise from their distinct physical principles, Bland–Altman analysis showed that measurements were consistent within clinically acceptable limits. Importantly, CT perfusion yielded a more precise determination of the relative functional contribution of each kidney compared with renal scintigraphy, which makes this method preferable for preoperative evaluation of living kidney donors.

Perfusion CT provides a highly accurate quantitative assessment of renal hemodynamics. Its key advantage lies in the ability to separately evaluate the functional state of the cortical and medullary layers and to determine the relative contribution of each kidney with high precision. The combination of anatomical detail with microcirculatory parameters makes this technique particularly valuable in the selection of living kidney donors.

The primary limitations of CT perfusion are radiation exposure and the need for intravenous contrast material, which necessitates caution in patients at risk of contrast-induced nephropathy. Nevertheless, adherence to optimized preparation protocols and appropriate patient selection substantially reduces these risks.

Taken together, CT perfusion emerges as a promising tool for comprehensive evaluation of kidney donors. Its strong correlation with renal scan parameters supports its use as a reliable alternative for assessing renal blood flow and plasma flow.

Table 2

Average relative contribution of kidneys by method

Method	Right kidney (%)	Left kidney (%)	Standard deviation (SD)
CT perfusion	49.8	50.2	±3.4%
Renal scan	48.6	51.4	±5.3%

FINDINGS

The results of the study demonstrated that renal scintigraphy and CT perfusion analysis show a high degree of correlation across several key parameters, indicating their potential partial interchangeability in clinical practice.

The time to maximum tracer accumulation (Tmax), obtained from scintigraphy, showed a strong negative correlation with arterial flow (AF) derived from CT perfusion. This relationship confirms the applicability of both parameters for evaluating renal blood flow velocity and filtration capacity (Fig. 1).

Similarly, the excretion half-life of the radiopharmaceutical (T½) measured by scintigraphy demonstrated a negative correlation with extraction fraction (FE) obtained from CT perfusion. This finding supports the conclusion that both parameters reliably reflect renal filtration and excretory activity (Fig. 2).

RPF, obtained from renal scintigraphy, revealed a strong positive correlation with BV measured by CT perfusion, indicating that these parameters can be considered equivalent for assessing renal hemodynamics (Fig. 3).

The differences between renal scan and CT perfusion values remained within clinically acceptable limits of agreement, further supporting the feasibility of using both methods to evaluate renal function. The diagrams confirm the potential of CT perfusion as an alternative to renal scan, particularly in settings where the latter is not available.

Overall, both methods provide valuable information on renal physiology, though with distinct strengths. Renal scan offers more detailed insights into filtration and excretion processes, whereas perfusion CT provides a more precise assessment of blood flow and microcirculation in the kidneys.

The following indicators have been found to be interchangeable:

– Tmax ↔ AF – for assessing renal blood flow and filtration rate;

– T½ ↔ FE – for evaluating filtration and excretion functions;
– RPF ↔ IFE – for assessing renal plasma flow and indexed extraction fraction.

When one of the methods is unavailable or contraindicated, the other can provide comparable functional data. For example, in patients with contraindications to iodine-containing contrast agents used in CT perfusion, renal scan (renal scintigraphy) remains the preferred option. Conversely, in donor evaluation, where a more detailed assessment of renal hemodynamics is required, CT perfusion is preferred.

Despite the high correlation, the two methods are not completely identical. The choice of an appropriate diagnostic technique should therefore be determined by the clinical objective and the patient's condition. Renal scintigraphy has lower spatial resolution for evaluating segmental blood flow, while CT perfusion provides more detailed information on local microcirculation.

The results of this study confirm the presence of interchangeable indicators between the two modalities. A comparison of our findings with the studies of Rigatelli et al. (2020) and Lim et al. (2024) further highlights the capacity of CT perfusion to provide a quantitative

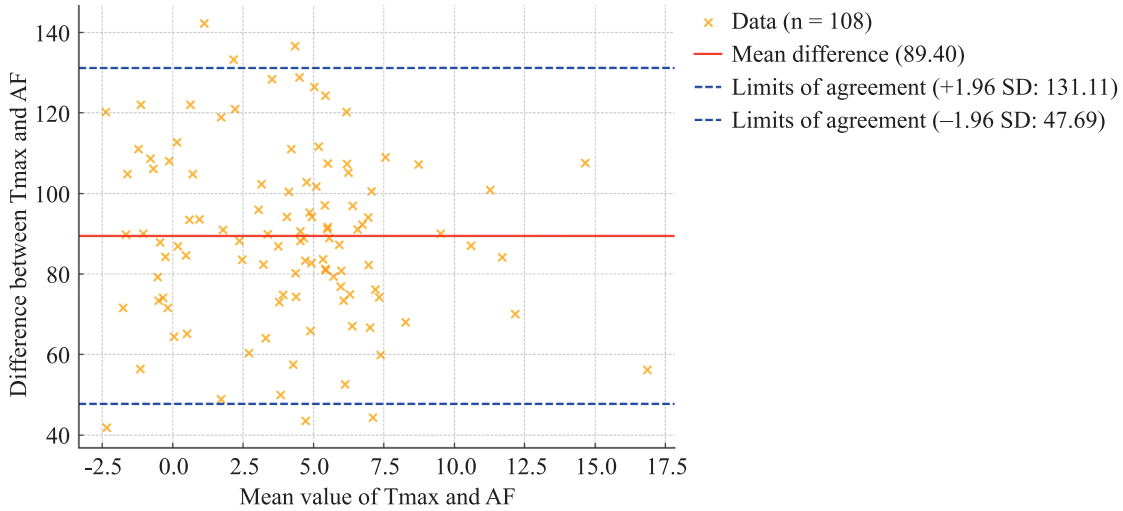

Fig. 1. Bland–Altman plot: Tmax *vs* AF (n = 108). The X-axis represents the mean of Tmax (time to maximum radiotracer accumulation from renal scan data) and AF (arterial flow from MSCT renal perfusion data). The Y-axis shows the difference between these two measurements (Tmax – AF). The red line indicates the mean difference between methods; blue lines denote the limits of agreement (±1.96 SD). The graph shows that the difference between Tmax and AF varies within the limits of agreement, confirming good reproducibility of the results. However, there is a tendency for the difference to increase with increasing AF, which may indicate individual variations in renal hemodynamics

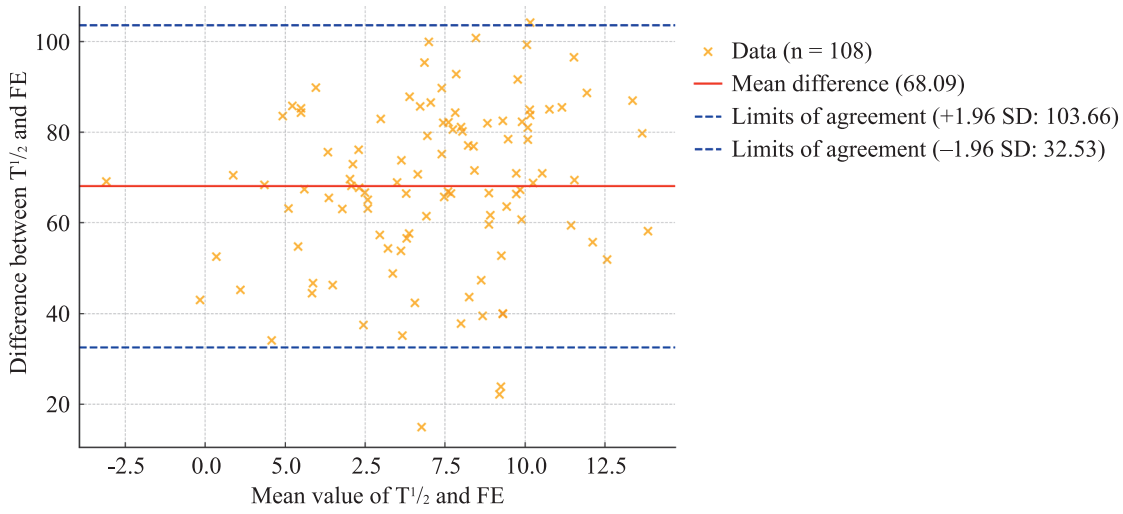

Fig. 2. Bland–Altman plot: T½ *vs* FE (n = 108). The X-axis represents the mean of T½ (radiotracer half-life from renal scan data) and FE (extraction fraction from MSCT perfusion data). The Y-axis shows the difference between T½ and FE measurements (T½ – FE). The red line indicates the mean difference; blue lines represent the limits of agreement (±1.96 SD). The plot demonstrates a high degree of agreement between T½ and FE, with most data points falling within the limits of agreement. The mean difference is close to zero, supporting the use of FE as a surrogate indicator of renal clearance dynamics

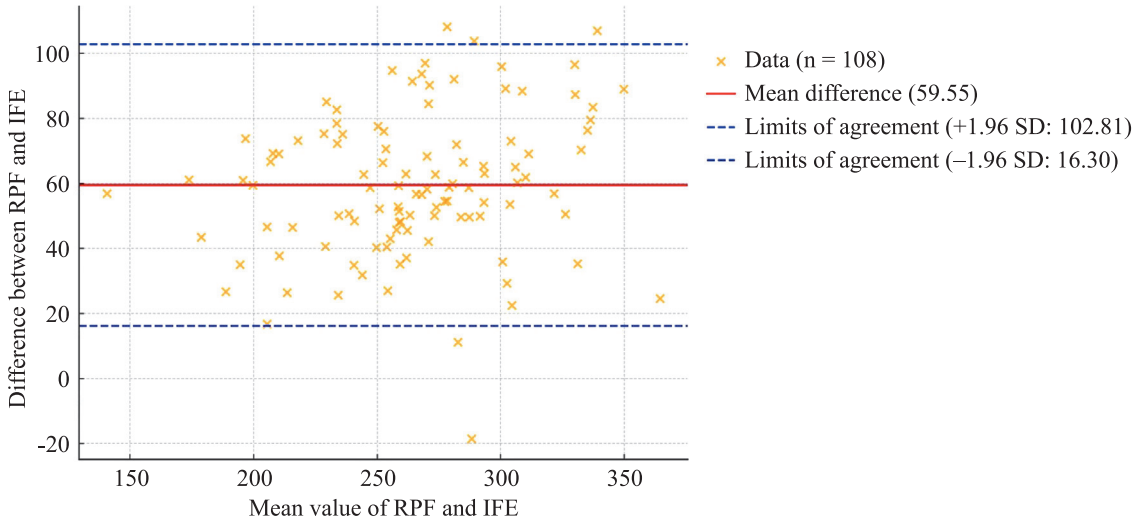

Fig. 3. Bland–Altman plot: RPF *vs* IFE (n = 108). The X-axis shows the mean values of RPF (renal plasma flow from renal scan data) and IFE (indexed extraction fraction from MSCT perfusion data). The Y-axis represents the difference between RPF and IFE measurements (RPF – IFE). The red line indicates the mean difference between methods, while the blue lines represent the limits of agreement (±1.96 standard deviations). This plot demonstrates the highest level of agreement between renal plasma flow and blood volume. The average difference is minimal, and most data points fall within the limits of agreement, supporting the strong equivalence between RPF and IFE

assessment of renal microcirculation, strengthening its role as a promising tool for preoperative evaluation and selection of donor kidneys [19, 20].

CONCLUSION

Renal scan and CT perfusion should be regarded as complementary techniques for assessing renal function. The demonstrated correlations between their key parameters support their interchangeable use depending on clinical scenario: CT perfusion provides a more precise evaluation of renal blood supply, while renal scan offers integrated indicators of filtration and excretory capacity. The choice of the appropriate method must therefore be individualized, taking into account diagnostic objectives, institutional resources, and patient condition.

Importantly, the assessment of split kidney function and use of indexed parameters such as IFE not only enhance the accuracy of donor evaluation but also contribute to improving the overall safety of kidney transplant programs.

The authors declare no conflict of interest.

REFERENCES

1. *Grenier N, Basseau F.* Functional renal imaging: magnetic resonance imaging (MRI) and computed tomography (CT). *Nephrology*. 2015; 11 (3): 179–186. doi: 10.1016/j.nephro.2015.05.002.
2. *Zhang J, Liu J, Jin Q, Wu W, Li H, Wang J.* CT perfusion in renal function assessment: advances and challenges. *Journal of Nephrology*. 2017; 30 (2): 163–170. doi: 10.1007/s40620-016-0357-6.
3. *O'Connor JPB, Port RE, Jayson GC, Waterton JC, Taylor NJ, Robinson SP et al.* Imaging biomarkers in kidney disease. *Nature Reviews Nephrology*. 2014; 10 (7): 442–452. doi: 10.1038/nrneph.2014.86.
4. *Sharfuddin A.* Imaging evaluation of kidney transplant recipients. *Seminars in Nephrology*. 2011; 31 (3): 283–292. doi: 10.1016/j.semnephrol.2011.06.008.
5. *Namazova-Baranova LS, Baranov AA, Smirnov IE.* Diagnostic Imaging in European Eastern Countries: A Russian Experience. Springer. 2016. doi: 10.1007/978-3-319-21371-2.18.
6. *Rigatelli G, Annie F, Nguyen TAN.* Renal Artery Interventions. Practical Handbook of Interventional Cardiology. 2020. doi: 10.1002/9781119383031.
7. *Sedankin MK, Leushin VY, Gudkov AG.* Modeling of Thermal Radiation by the Kidney in the Microwave Range. *Biomedical Engineering*. 2019; 52 (3): 247–254. doi: 10.1007/s10527-019-09908.
8. *Lammer J.* Occlusive Vascular Diseases of the Abdomen. Springer. 1999. doi: 10.1007/978-88-470-2141-9.45.
9. *Lim R, Kwatra N, Valencia VF.* Review of the clinical and technical aspects of 99mTc-dimercaptosuccinic acid renal imaging: the comeback "kit". *Journal of Nuclear Medicine Technology*. 2024; 52 (3): 199–208. doi: 10.2967/jnmt.122.263043.
10. *Tarkhanov A, Bartal G, Druzhin S, Shakhbazyan R.* Bladder wall and surrounding tissue necrosis following bilateral superselective embolization of internal iliac artery branches due to uncontrollable haematuria. CardioVascular and Interventional Radiology (CVIR). 2018. doi: 10.1186/s42155-018-0043.
11. *Abdullaev AYY.* Organization of Healthcare. *VSKM Journal*. 2015.

12. Dovbysh MA, Mishchenko OM. Topical issues of modern urology: educational manual. ZSMU Repository. 2023.
13. *Kogan MI, Sizov VV, Babich II, Shidaev A*. Xanthogranulomatous Pyelonephritis in a 7-Year-Old Girl. Vestnik, 2020.
14. *Stus VP, Moiseyenko MM, Polion MY*. Urology (Methodical elaborations of practical classes for students). DMA Repository. 2020.
15. *Xihong H.* MRI with SENSE evaluation of conotruncal defects in children. *Pediatric Radiology*. 2008; 38 (5): 550–556. doi: 10.1007/s00247-008-0840.
16. *Sharfuddin A*. Imaging evaluation of kidney transplant recipients. *Seminars in Nephrology*. 2011; 31 (3): 283–292. doi: 10.1016/j.semnephrol.2011.06.008.
17. *Gubar AO.* Urology: A Manual for Teachers Preparing for Practical Classes. ZSMU Repository. 2021: 1–156.
18. *Gorbatko OA, Borsukov AV*. The role of contrast-enhanced ultrasound in the early diagnosis of clinically significant angionephrosclerosis: Advances and clinical applications. *Medical Visualization Journal*. 2024. doi: 10.1007/978-3-319-21371-2.
19. *Rigatelli G, Annie F, Nguyen TAN*. CT and MRI magnetic resonance angiography in renal artery interventions. *Practical Handbook of Interventional Cardiology*. 2020. doi: 10.1002/9781119383031.ch21.
20. *Leushin VY, Gudkov AG, Sedankin MK*. Thermal radiation modeling of kidneys: assessment and applications in biomedical engineering. *Biomedical Engineering*. 2019; 52 (3): 247–254. doi: 10.1007/s10527-019-09908-x.

The article was submitted to the journal on 19.02.2025

DOI: 10.15825/1995-1191-2025-3-97-109

THE POTENTIAL OF MULTISLICE COMPUTED TOMOGRAPHY IN DIAGNOSING CORONARY ARTERY DISEASE IN HEART TRANSPLANT RECIPIENTS: A LITERATURE REVIEW

Yu.V. Sapronova, T.A. Khalilulin, N.A. Rucheva, N.N. Koloskova, S.A. Sakhovsky, A.S. Tokar, B.L. Mironkov

Shumakov National Medical Research Center of Transplantology and Artificial Organs, Moscow, Russian Federation

Coronary artery disease remains a leading cause of graft failure after heart transplantation (HT). Because the transplanted heart is denervated, graft ischemia is typically asymptomatic, necessitating annual screening to detect cardiac allograft vasculopathy (CAV), monitor established coronary lesions, and evaluate in-stent restenosis. The need for annual invasive coronary angiography, along with its associated risks, including potentially life-threatening complications, underscores the need for safer, yet equally effective, noninvasive diagnostic alternatives for evaluating coronary pathology in heart transplant recipients. Multislice computed tomography coronary angiography (MSCT–CAG) has been successfully employed in the diagnosis of ischemic heart disease (IHD) for many years and is well-established as a noninvasive alternative to conventional coronary angiography. This makes it particularly relevant to investigate its applicability and effectiveness in the post-transplant setting.

Keywords: cardiac allograft vasculopathy, MSCT coronary angiography, heart transplantation.

About 6,000 orthotopic heart transplants (OHTs) are performed worldwide each year. In 2024, a total of 450 OHTs were performed in Russia, 294 of which took place at Shumakov National Medical Research Center of Transplantology and Artificial Organs, Moscow [1]. One of the leading causes of graft loss is cardiac allograft vasculopathy (CAV), a form of coronary artery disease specific to the transplanted heart. According to the International Society for Heart and Lung Transplantation (ISHLT) registry, CAV prevalence steadily increases with time after transplantation, reaching 10% at 1 year, 22% by 4 years, 35% by 7 years, 44% by 10 years, 56% by 15 years, and 59% by 20 years post-transplantation. One in eight transplant recipients develops moderate to severe CAV (grades 2–3) within ten years of surgery (Table 1), and one in four develops it within twenty years [3].

The pathogenesis of CAV is driven by a combination of immune and non-immune factors, resulting in inflammation of the vascular wall followed by proliferative changes, fibrosis, and remodeling of the vessel [4, 5]. The disease process generally evolves in two phases. The initial phase involves endothelial injury, leading to intimal thickening with expansion of the adventitia, while the coronary lumen may initially remain relatively preserved. As the disease progresses, fibroproliferative cellular responses occur, resulting in constrictive remodeling and stenotic narrowing of the coronary artery lumen [6, 7].

Unlike the focal and eccentric atherosclerotic plaques typically seen in ischemic heart disease, CAV is characterized by a diffuse and concentric pattern of involve-

Table 1

Classification system for angiographic signs of heart transplant vasculopathy [2]

Grade	Criteria
ISHLT CAV 0 (minor)	No angiographic lesions
ISHLT CAV 1 (mild)	Left main (LM) stenosis <50%, primary vessel stenosis <70%, branch stenosis <70% (including diffuse lesions); no graft dysfunction
ISHLT CAV 2 (moderate)	LM stenosis >50%, primary vessel stenosis >70%, or stenosis >70% in any second-order branch; no graft dysfunction
ISHLT CAV 3 (severe)	Stenosis of the LM >50%, or stenosis >70% in two or more primary branches or any second-order branch in all three major territories and/or ISHLT CAV1 or CAV2 with graft dysfunction (LVEF <45%, regional wall motion abnormalities, or restrictive diastolic dysfunction)

Corresponding author: Yulia Sapronova. Address: 1, Shchukinskaya str., Moscow, 123182, Russian Federation. Phone: (499) 190-29-71. E-mail: ys1984@yandex.ru

ment. Both epicardial and intramural coronary arteries are primarily affected [8, 9].

Risk factors for the development of CAV include: donor age over 45 years, male sex of both donor and recipient, and lipid metabolism disorders in the recipient before and after transplantation (LDL >2.5 mmol/L). Additional risk factors include episodes of acute cellular rejection, presence of donor-specific HLA antibodies, smoking, hypertension, diabetes mellitus, and obesity. Cytomegalovirus (CMV) infection also plays a major role in the pathogenesis of CAV [2, 10, 11].

The main contributing factors leading to CAV are summarized in Table 2.

Due to denervation of the transplanted heart, ischemia often remains clinically silent, and CAV may remain asymptomatic for a prolonged period. When symptoms do appear, they are often nonspecific, such as fatigue, nausea, abdominal discomfort, or heart rhythm disturbances (tachyarrhythmias, bradyarrhythmias, frequent supraventricular or ventricular extrasystoles). By this stage, patients may already exhibit a reduction in left ventricular ejection fraction and symptoms of heart failure, which are associated with a poor prognosis. There-

Table 2

Comparative role of various factors in the pathogenesis of CAV *vs* native atherosclerosis [11]

CAV		Atherosclerosis
	Endothelial cell	
+++	Hyperpermeability	++
+++	Dysfunction	++
	Smooth muscle cell	
++	Proliferation	+++
+++	Apoptosis	++
	Abnormal accumulation and functioning of the extracellular matrix	
+++	Proteoglycan deposition	+
++	Collagen overexpression (fibrosis)	+++
++	Altered myogenic vascular tone (resistance vessels)	+
+++	**Expression of adhesion molecules**	+++
	Inflammatory cells	
+	Platelets	+++
++	Monocytes/macrophages	+++
+++	Lymphocytes	++
	Immune response	
+++	Innate/acquired immunity	++
+++	**Lipid retention**	++
	Risk factors	
++	High blood cholesterol levels	+++
+++	High blood triglyceride levels	+
+	Low blood HDL levels	+++
++	Hyperhomocysteinemia	+
–/+	Infection	–/+
–/+	Age	+++
–/+	Gender	++
–/+	Ethnic predisposition	+
–/+	Previously diagnosed vascular diseases	+++
++	Smoking	+++
++	Diabetes mellitus	+++
++	Arterial hypertension	++
++	Obesity	++
–/+	Physical inactivity	++
++	Special medications	+
–/+	Social class	+
–/+	Psychosocial environment	++
–/+	Type A personalities	–/+
+	Donor-associated diseases	–
–	Family history	++

fore, meticulous monitoring of the cardiac graft for early signs of CAV is necessary.

According to the ISHLT 2023 guidelines, coronary angiography remains the gold standard for diagnosing CAV (Class I, Level of Evidence: C) and is recommended every 1–2 years throughout follow-up. More frequent evaluation may be warranted in patients with previously documented coronary pathology to monitor progression or restenosis after stent implantation [2]. However, invasive coronary angiography (iCAG) carries risks, including life-threatening arrhythmias (bradycardia, tachyarrhythmias, ventricular fibrillation), contrast-induced acute kidney injury, cerebrovascular accidents, coronary artery dissection, and bleeding at the vascular access site. The overall complication rate is approximately 1.8%, with 0.1% mortality [12].

In this regard, the search for non-invasive, reliable diagnostic alternatives for CAV has become increasingly relevant. Earlier non-invasive methods such as dobutamine stress echocardiography and myocardial scintigraphy have demonstrated very low sensitivity (approximately 7%) [13] and are not recommended as screening tools for CAV (Class IIb evidence) [2]. Single-photon emission computed tomography (SPECT) has shown some prognostic utility in diagnosing CAV, with sensitivity up to 84% and specificity 78% for detecting ≥50% stenosis compared to angiography but remains Class IIb evidence [2]. Positron emission tomography (PET) has not gained wide application in routine diagnosis of CAV and falls under Class IIb evidence [2, 14, 15].

Currently, the only non-invasive modality for coronary artery imaging that is widely available in routine clinical practice is multislice computed tomography coronary angiography (MSCT-CAG). This technique is widely used in the diagnosis of IHD, demonstrating a sensitivity ranging from 71% to 100% and a negative predictive value (NPV) of 93–100% when compared with iCAG.

In 2011, Paech et al. analyzed 28 studies involving 3,674 patients, evaluating the performance of 64-slice or higher CT coronary angiography as an alternative to iCAG. The meta-analysis showed a sensitivity of 98.2% and a specificity of 81.6%. The median positive predictive value (PPV), defined as the number of true stenotic segments detected divided by the total number of stenotic segments, was 90.5% (range: 76–100%), while the NPV, defined as the proportion of non-stenosed segments correctly identified, was 99.0% (range: 83–100%).

When evaluating entire coronary vessels, pooled sensitivity was 94.9%, specificity 89.5%, with a median PPV of 75.0% (range: 53–95%) and an NPV of 99.0% (range: 93–100%) [16].

Based on numerous studies [17–28], MSCT-CAG has been incorporated into European guidelines as an alternative to iCAG, with a validated class of evidence [24]. According to data from the CONFIRM registry, introduction of MSCT-CAG has resulted in approximately a 45% reduction in the use of iCAG procedures [20].

Most of the early studies evaluating MSCT-CAG as a non-invasive alternative for the diagnosis of CAV typically included relatively small patient samples (ranging from 10 to 60 individuals) and were performed using 16-slice MSCT scanners, with findings compared directly to iCAG. The results of these studies are presented in Table 3.

One of the earliest attempts to apply MSCT-CAG in the diagnosis of CAV was conducted by Romeo et al. in 2005, using a 16-slice MSCT scanner. In this study, the authors evaluated 53 patients and analyzed 450 coronary artery segments, based on a 10-segment coronary model. Three patients were excluded due to inability to hold their breath during scanning.

Average time after OHT was 7.6 ± 3.8 years (range: 1–14.5 years), the age range was from 7.6 to 75 years (mean age 48 ± 19 years), there were 40 men and 13 women. Baseline heart rate was 83 ± 13 bpm. Heart rate after 100 mg metoprolol (administered 1 hour before

Table 3

Initial studies on the implementation of MSCT-CAG in heart recipients

Studies evaluating 16-slice MSCT for coronary artery stenosis (*vs* invasive CAG)	G. Romeo et al., 2005
	S. Nunoda et al., 2010
	P. Carrascosa et al., 2009
	E. Usta et al., 2006
	P. Pichler et al., 2008
Studies comparing 16-slice MSCT with intravascular ultrasound (IVUS)	G. Sigurdson et al., 2006
Use of 64-slice MSCT in diagnosing CAV (*vs* invasive CAG)	S. Iyengar et al., 2006
	F. von Ziegler et al., 2009
	C. Kepka et al., 2012
	F. von Ziegler et al., 2012
	T.K. Mittal et al., 2013
Use of 64-slice MSCT in diagnosing CAV (*vs* invasive CAG and IVUS)	T. Schepis et al., 2009
	S.A. Gregory et al., 2006

MSCT-CAG) was 69.5 ± 11 bpm (range: 43–95 bpm). Contrast volume used was 70–90 mL. A complete segmental analysis was achieved in 50 out of 53 patients (88%), with diagnostic image quality in 432 of 450 segments (96%). Coronary calcifications were detected in 15 (30%) of 50 patients. Two cases had severe calcification, significantly limiting analysis; 13 patients had minor calcified plaques. Among 9 coronary stents in 7 patients, only 3 stents were adequately assessed, and 2 cases of restenosis were missed. In 44 (88%) of 50 patients, a complete assessment of the coronary tree was possible. In 22 patients without stenosis confirmed by iCAG, MSCT-CAG correctly showed no stenosis. For detection of significant stenosis (≥50%), MSCT-CAG showed a sensitivity of 83%, specificity of 95%, PPV of 71%, NPV of 95%, and accuracy of 93%. This early 16-slice MSCT study demonstrated good diagnostic accuracy in identifying both significant stenoses and normal coronary arteries, which is effective in screening for CAG [29].

As CT technology advanced, newer studies using higher-slice scanners reported improved sensitivity, specificity, diagnostic accuracy, NPV, PPV, and lower radiation exposure.

The study included 28 male patients (mean age: 53 ± 13 years) who underwent both iCAG and MSCT-CAG within a one-day interval during routine examination. The mean time after OHT was 7.7 ± 4.1 years (range: 4 months to 14 years). One hour before MSCT-CAG, patients received 50–100 mg of metoprolol orally to reduce and stabilize their HR. At the time of scanning, the average HR was 86 ± 13 beats per minute (range: 65–116 bpm). The average contrast volume used was 90 mL.

The coronary artery bed was evaluated according to the 15-segment AHA model. Out of 371 coronary segments analyzed, 302 (81.4%) were of diagnostic quality. Calcified plaques were identified in 6 out of 26 patients (23.1%) but did not affect image interpretation. Segment-level analysis demonstrated a sensitivity of 87.5%, specificity of 97.3%, overall accuracy of 97%, NPV of 99.7%, and PPV of 46.7% for detecting significant stenosis or vessel occlusion.

At the patient level, the sensitivity was 100%, specificity 81%, diagnostic accuracy 84.6%, NPV 100%, and PPV 55.6%. The high NPV at both segment and patient levels suggests that MSCT-CAG is a reliable non-invasive method for ruling out significant coronary stenosis in heart transplant (HT) recipients, comparable to its predictive value in patients with IHD [30].

In 2012, Franz von Ziegler et al. employed advanced dual-source CT scanners to evaluate significant coronary stenosis in HT recipients. The study included 51 patients (43 men; mean age 52.3 ± 13.6 years) who underwent both MSCT-CAG and iCAG within a 1–2 day interval during routine follow-up. The mean time after OHT was 6.9 ± 4.1 years (range: 2 weeks to 15 years). Serum creatinine was monitored 38.1 ± 2.4 hours after MSCT-CAG.

One hour before scanning, patients received 50–100 mg of oral metoprolol. The average HR prior to beta-blocker administration was 94 ± 14 bpm (range: 63–120 bpm), which decreased to 88 ± 14 bpm (range: 61–116 bpm) following medication. Of the 717 coronary segments analyzed, 714 (99.6%) were of optimal diagnostic quality. Calcified plaques were observed in 11 of 48 patients (22.9%) but did not compromise image interpretation.

On a segmental level, MSCT-CAG demonstrated a sensitivity of 100%, specificity of 98.9%, diagnostic accuracy of 98.9%, PPV of 50%, and NPV of 98.9%. At the patient level, sensitivity was 100%, specificity 86.0%, diagnostic accuracy 93.0%, PPV 33.3%, and NPV 100%. Transplant vasculopathy was diagnosed in 6.5% of recipients. No cases of contrast-induced nephropathy were reported.

The authors concluded that the high NPV (100%), as in the previous study, confirmed the reliability of MSCT-CAG for ruling out significant coronary stenoses in transplant recipients. The reduced rate of segment exclusion (0.4% in 2012 *vs* 18.6% in 2009) highlighted some improvements in imaging quality when using the latest scanners. Consequently, the study suggested that in the absence of significant stenosis on MSCT-CAG, annual CAG may not be necessary [31].

In 2013, Mittal et al. conducted the largest study to date, analyzing 138 HT recipients (2040 coronary segments). The cohort included men aged 22–78 years (53 ± 15 years) and women aged 20–80 years (47 ± 17 years), with a mean post-OHT follow-up of 12 ± 6.2 years (range: 1–25 years). In 109 patients, MSCT-CAG and CAG were performed within 24 hours, while in the remainder, MSCT-CAG was performed within a month. Patients with prior coronary stents and those with GFR <30 ml/min/1.73 m^2 were excluded. Before MSCT-CAG, sublingual nitrates were administered, but beta blockers were not used. mean HT was 82.7 ± 4 bpm. Two patients were excluded due to contrast extravasation.

The contrast volume was 70–90 ml for MSCT-CAG and 40–60 ml for iCAG. Creatinine levels were monitored 2–3 days post-procedure, with no cases of contrast-induced nephropathy reported. Average radiation dose for MSCT-CAG was 17.5 ± 6.9 mSv (range: 10–20 mSv), compared to 5–6 mSv for CAG. Coronary anatomy was assessed using the 15-segment ANA model, with ≥50% stenosis considered as significant.

Calcified plaques were detected in 82 patients; however, only 5 patients (6%) had significant stenosis. Despite relatively high heart rates, diagnostic image quality was obtained in 130 of 136 patients (96%) and in 1900 of 1948 segments (98%), although quality declined in distal segments.

For the detection of stenosis of any degree, MSCT-CAG showed a sensitivity of 98%, specificity of 78%, PPV of 77%, and NPV of 98%. For significant stenoses, sensitivity was 96%, specificity 93%, PPV 72%, and NPV 99%.

The authors confirmed that MSCT-CAG with 64-slice scanners is highly effective for diagnosing CAV, even without reducing HR. The technique demonstrated particularly high reliability in excluding stenosis, with strong concordance between MSCT-CAG and iCAG findings in patients without significant lesions [32]. They emphasized that reliance on the coronary calcium score alone is unreliable in this patient population.

Advances in new-generation CT scanners now enable not only the evaluation of the extent of lesion (severity and length of stenosis) but also characterization of atherosclerotic plaque morphology, including identification of "unstable" lesions, provided that image quality is adequate [33].

Thus, in 2018, Károlyi et al. (Hungary) examined 35 patients, 23 of whom were male (66%), aged 50–61 years (mean age 58). All patients underwent MSCT-CAG (256-slice; slice thickness 0.8 mm; increment 0.4 mm) at 1 and 2 years after OHT. Prior to imaging, they received nitroglycerin and ivabradine (7.5–15 mg) to reduce HR. In addition to standard analysis, quantitative assessment of coronary segments was performed, including lumen volume, total lesion volume, and total lesion burden (calculated as total vessel volume minus lumen volume, divided by total vessel volume). For detected plaques, the following components were evaluated: calcified lesion volume (≥350 HU), non-calcified high-attenuation volume (131–350 HU), non-calcified intermediate-attenuation volume (75–130 HU), and low-attenuation volume (≤75 HU).

CAV progression was defined as the development of any new coronary lesion (≥10% increase in lesion volume) or enlargement of a previously identified lesion. The findings demonstrated that within 2 years after OHT, CAV progression is characterized primarily by the development of non-calcified plaques, while calcified lesions remain unchanged. Moreover, quantitative MSCT-CAG detected a greater proportion of patients with CAV (≥10%) compared to standard qualitative analysis, which can be critical for identifying disease at an early stage. Segment analysis was feasible for vessels ≥2 mm in diameter; although early CAV may involve smaller branches, these are not typically candidates for revascularization.

Thus, quantitative analysis of MSCT images identifies more patients with progressive vasculopathy than qualitative assessment. Coronary wall thickening during the first 2 years after OHT is predominantly related to non-calcified plaque components and may represent early manifestation of CAV [34].

In 2020, Foldyna et al. conducted another study using quantitative analysis of coronary segments with a second-generation 128-slice MSCT scanner. A total of 50 patients (84% male; mean age 53.6 ± 11.9 years) were included, with and without previously verified vasculopathy, and a mean follow-up of 6.7 ± 4.7 years after OHT. The interval between CAG and MSCT-CAG was one day. The study focused on quantifying lumen volume, wall volume, and segment length. The following indices were calculated: volume-length ratio VLR (ratio of lumen volume to segment length; mm^3/mm), wall burden WB (wall volume ÷ (wall volume + lumen volume); %), and plaque composition (proportions of calcified, fibrous, fibrous-fatty, and soft plaques). Results showed that WB, VLR, and the proportion of fibrous tissue are reliable markers of vasculopathy and may assist in diagnosing CAV at an early stage, when lumen size is still preserved, which is an advantage over CAG.

An 18-segment coronary model (Society of Cardiovascular Computed Tomography, SCCT) was used for analysis, evaluating a total of 632 coronary segments. Image quality was scored according to SCCT recommendations (1 = excellent, 2 = good, 3 = fair, 4 = poor), and segments rated as poor were excluded. Coronary lesions were classified visually by degree and type of stenosis, following the guidelines of the American College of Cardiology/American Heart Association (ACC/AHA) Task Force.

By degree of stenosis:
- 0 degree: 0–24%
- 1 degree: 25–49%
- 2 degree: 50–74%
- 3 degree: 75–90% and above
- 4 degree: 100%.

By type of lesion:
- Type A: stenosis <10 mm in length; concentric lesion
- Type B: stenosis 10–20 mm in length; eccentric lesion
- Type C: stenosis >20 mm in length.

By CAV classification:
- No CAV: no stenosis or stenosis 1–24%
- Mild CAV: stenosis 25–49%, type A or B
- Moderate CAV: Stenosis ≥50%, type A–C.

Average radiation dose was 5.8 mSv. The study cohort consisted of 42 men (84%) and 8 women (16%), with a CAV prevalence of 38% (19 out of 50). Mean heart rate was 74.1 ± 8.5 beats per minute. MSCT-CAG provided diagnostic-quality images for 692 coronary segments, of which 632 (91.4%) were suitable for comparison with CAG data; 56 segments were excluded due to poor image quality. Among the 632 evaluable segments, 190 (30.1%) were proximal and 442 (69.9%) were distal.

Coronary wall analysis revealed that fibrous tissue accounted for 44.7%, fibro-fatty tissue for 18.6%, soft plaques for 8.5%, and calcified plaques for 1.0%. Distal segments were more frequently affected than proximal segments. The volume indexed by segment length (VLR)

was significantly higher in segments with CAV than in those without. Similarly, wall burden (WB; lumen/(wall + lumen) volume) was greater in segments with CAV compared to unaffected segments. The vascular wall in CAV was predominantly composed of fibrous and calcified tissue, whereas the proportions of fibro-fatty and soft plaques did not differ between CAV and non-CAV segments.

This study demonstrated that MSCT-CAG is highly effective in detecting severe stenoses ≥50%, with results correlating well with iCAG in HT recipients (NPV 98–100%, sensitivity 78%, specificity 75%). Moreover, MSCT-CAG can detect CAV at early stages through quantitative assessment of coronary wall plaque volume and composition, providing opportunities for timely adjustment of drug therapy [35].

In 2022, Ojha et al. assessed the diagnostic accuracy of dual-source MSCT (192-detector, 384-slice) for detecting CAV in comparison with iCAG. Thirty-eight patients (27 men) were included in the study, with a mean age of 33.66 ± 11.45 years and a mean post-OHT interval ranging from 10 to 226 months (median 23.5 months). One to two hours before MSCT-CAG, patients received 25–50 mg of oral metoprolol, followed by nitroglycerin immediately before scanning. The mean HR during imaging was 91 ± 13.86 beats per minute (range 74–146). Calcium score was measured at baseline.

The prevalence of CAV (grades 1–5 stenosis) was 44.7% (n = 17) according to MSCT-CAG and 39.5% (n = 15) by iCAG. Significant CAV lesions (grades 3–5) were detected in 21.1% (n = 8) by MSCT-CAG and in 15.8% (n = 6) by iCAG. Image quality was considered satisfactory in 557 out of 576 segments (96.7%). The mean radiation dose was 4.24 ± 2.15 mSv for MSCT-CAG and 4.8 ± 1.8 mSv for CAG, with an average contrast volume of 42 ml.

At the patient level, the detection of signs of vasculopathy of any degree had a sensitivity of 100%, specificity of 91.3%, PPV of 88.2%, NPV of 100%, and overall accuracy of 94.7%. For significant stenoses, sensitivity was 100%, specificity 94%, PPV 75%, NPV 100%, and accuracy 95%. Comparable results were obtained in segmental analysis (sensitivity 96%, specificity 97.6%, PPV 80%, NPV 99.6%).

This study demonstrated that dual-source MSCT, even at a relatively low radiation dose (4.24 ± 2.16 mSv), provides high diagnostic accuracy with excellent sensitivity, specificity, and NPV for detecting both early CAV and significant coronary stenoses when compared with iCAG [36].

In 2021, Nous et al. reported their experience implementing MSCT-CAG as a screening tool for CAV at the University Medical Center Rotterdam (the Netherlands). Between February 2018 and May 2019, 129 patients aged 43–64 years (mean 55), 8–17 years post-OHT (mean 11 years), were included. Men accounted for 65% of the cohort, and 13% had a history of percutaneous coronary intervention (PCI). At this center, elective CAG was routinely performed in the first and fourth years after OHT or when ischemia was suspected, while annual cardiac MRI and SPECT were used in the remaining years.

Before MSCT-CAG, all patients received nitroglycerin; in cases with an HR ≥70 bpm, intravenous metoprolol (5.0–7.5 mg) was administered. On average, HR decreased by 15% to 75 ± 11 bpm, with no conduction disturbances or hypotension observed. MSCT scanners with dual sources of the 2nd generation (29%, n = 37) and 3rd generation (71%, n = 92) were used, applying a prospective ECG-triggered mode. Images were reconstructed with a slice thickness of 0.6 mm and an increment of 0.3 mm. Calcium score was obtained prior to contrast injection.

In most coronary segments with significant CAV, non-calcified plaques predominated (64%). Diagnostic image quality was achieved in 118 of 129 patients (92%), with a mean radiation dose of 2.1 mSv (range 1.6–2.8). Significant stenoses were identified in 19 patients (15%), of whom 15 were newly diagnosed and 4 had been previously recognized. Three patients were not referred for PCI due to chronic total occlusions or stenotic lesions in small-caliber branches (<2 mm).

At 90-day follow-up, 9 of 19 patients with significant stenoses (47%) underwent further evaluation with SPECT, MRI, and CAG. Additional investigations were not performed in 10 patients (53%) because lesions had already been deemed unpromising on prior iCAG. In 8 of 9 patients (89%), hemodynamically significant stenoses were confirmed: 4 underwent stenting, 2 underwent stenting combined with modification of drug therapy, and 1 received drug therapy adjustment only (e.g., statin dose increase or switch from mycophenolate mofetil to mTOR inhibitors).

Four patients with hemodynamically insignificant stenoses on MSCT-CAG underwent iCAG, after which two underwent PCI and seven required therapy adjustments. Within 90 days to 1 year, one patient with ventricular tachycardia underwent CAG and PCI despite no significant stenosis being detected by MSCT-CAG. Beyond 1 year, three patients developed major adverse cardiovascular events (MACE). These findings demonstrate that MSCT can be effectively integrated into clinical practice, providing high-quality imaging at a low radiation dose, reducing the need for invasive procedures, and enabling early detection of vasculopathy to guide timely therapy adjustments [37].

In a study by Szymon Pawlak et al., it was acknowledged that 64-slice MSCT may underestimate the progression of CAV or previously stented segments. Therefore, iCAG was performed in all 209 patients with known vasculopathy. For MSCT-CAG evaluation, 107 patients without graft dysfunction and without hemodynamically significant stenoses on CAG performed 2 years earlier

were selected (26 women, mean age 50 ± 17 years, mean time after OHT 7 years, range 4–11.5 years). All patients received sublingual nitrates, and those with an HR >90 bpm prior to MSCT-CAG additionally received 5 mg ivabradine. Control CAG was performed only when MSCT-CAG suggested significant stenosis. As a result, CAG was not performed in 98 patients without evidence of stenotic lesions. In 8 of 9 patients, stenoses detected by MSCT-CAG were confirmed by CAG, and PCI was performed in 6 of them. As in previous studies, calcium index values were not informative for diagnosing CAV. No cases of contrast-induced nephropathy were observed [38].

A recent meta-analysis of 13 prospective studies on MSCT-CAG after OHT provided robust evidence supporting its implementation in cardiac transplant recipients. The analysis demonstrated a weighted mean sensitivity of 94%, specificity of 92%, negative predictive value of 99%, and positive predictive value of 67% for detecting stenoses >50% compared with invasive angiography. The incorporation of quantitative plaque analysis was shown to further enhance sensitivity for detecting cardiac transplant vasculopathy. In total, CT angiogram data from 615 patients were prospectively evaluated [39]. In most studies, the coronary tree was segmented according to the 16-segment American Heart Association classification (see Figure).

A total of 9,481 coronary segments were analyzed across the studies, with the time after OHT ranging from 3 to 8 years. Average patient age ranged from 40 to 58 years, and the study populations were predominantly male (75–100%). Most investigations employed first-generation MSCT scanners with single- or dual-source technology (16- or 64-slice).

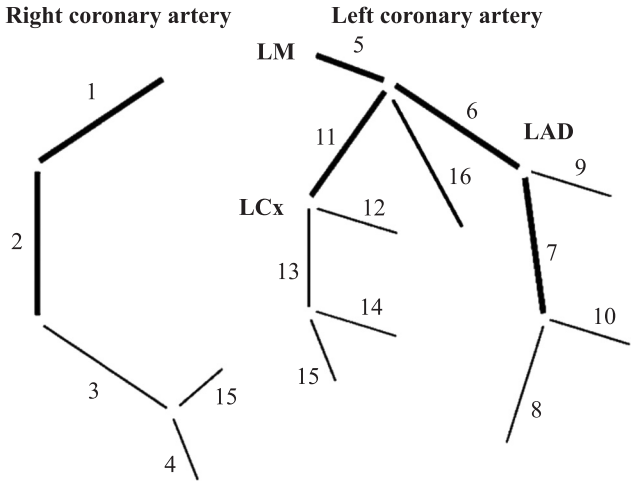

Fig. Schematic representation of the 16-segment coronary artery classification based on the American Heart Association (AHA) guidelines. Right coronary artery (RCA): segment 1 – proximal RCA; 2 – mid RCA; 3 – distal RCA; 4 – posterior descending branch. Left coronary artery (LCA): 5 – left main (LM); 6 – proximal left anterior descending (LAD); 7 – mid LAD; 8 – distal LAD; 9 – first diagonal; 10 – second diagonal; 11 – proximal left circumflex (LCx); 12 – first obtuse marginal; 13 – distal LCx; 14 – posterolateral artery; 15 – posterior descending artery; 16 – ramus intermedius [35]

Contraindications for MSCT after OHT were:
- allergy to iodine [49];
- significant decrease in glomerular filtration rate (GFR <30 ml/min/1.73 m^2 or serum creatinine >1.4 mg/dl) [49];
- pregnancy;
- claustrophobia or inability to hold your breath.

Limitations of MSCT after OHT were:
- severe general condition of the patient;
- high body mass index;
- arrhythmias or persistent tachycardia;
- pronounced coronary artery calcification or presence of stents in the coronary arteries [39, 49].

In several studies, authors reported a decline in coronary artery image quality due to the high HR characteristic of the denervated heart, which led to exclusion of a substantial number of coronary segments from analysis – particularly when older-generation MSCT scanners were used. To address this issue, beta-blockers were administered in some studies [29, 30, 31, 40, 41, 42], either as metoprolol 50–100 mg orally or 10–12 mg intravenously. Although the target HR was not always achieved, a reduction of 10–15 bpm was obtained, with mean pre-scan HR ranging from 69 to 90 bpm (average 84 bpm). An HR >85 bpm was associated with a significant decrease in image quality.

Sigurdsson and Schepis did not use β-blockers; nevertheless, despite high HR, they reported good to excellent image quality [42, 43].

Data from Nous F.M. et al. showed that beta-blockers reduce HR by an average of 15% [37]. Studies have also evaluated ivabradine, which has shown a safe and effective reduction in HR in OHT recipients with sinus rhythm [34, 45]. An equally important consideration in this patient population is monitoring renal function, as the risk of contrast-induced nephropathy (CIN) is increased due to pre-existing renal impairment, most often related to long-term use of calcineurin inhibitors. For this reason, many studies excluded patients with serum creatinine levels above 1.4 mg/dl. CIN was defined as a ≥25% increase in creatinine or an absolute rise of 44 μmol/L. Post-contrast creatinine testing was generally performed one day after MSCT. Although the mean contrast volume used in MSCT (60–115 ml) was slightly higher than that in CAG, none of the studies reported cases of CIN. However, this observation period may have been insufficient, since serum creatinine typically peaks 72 hours after contrast administration.

Several studies have focused on radiation exposure during MSCT-CAG and the development of protocols to minimize it. Reported radiation doses ranged from 3 to 18 mSv, approximately twice the average dose of iCAG [29, 40, 43]. With 16-slice MSCT, the mean radiation

dose was 14.7 ± 2.2 mSv, whereas the introduction of dual-source MSCT reduced the dose to 4.5 ± 1.2 mSv [31], which is comparable to iCAG (5.6 ± 3.6 mSv). In most studies, retrospective ECG-gated image reconstruction was used due to higher heart rates, but this method resulted in higher doses (10.2–17.5 mSv).

Given the serious concerns about cumulative radiation exposure, significant efforts have been directed toward dose reduction. Heart transplant recipients are exposed to approximately 3.5 times more radiation than the general population, with an average cumulative dose of 84 mSv over a 10-year follow-up period [46, 47]. This substantially increases cancer risk, particularly in women and younger patients. Bastarrika G. et al. later achieved a reduction in dose to 4.5 mSv while preserving diagnostic image quality by using prospective ECG-triggered MSCT with systolic phase acquisition [48].

Protocols for radiation dose reduction and optimized image reconstruction have also been developed. The use of ECG-controlled tube current modulation – where full tube current is delivered between 30% and 80% of the cardiac cycle – can lower the effective dose by approximately 40% and reduce the lifetime risk of cancer compared with standard retrospective scanning, particularly in women and younger patients, while preserving diagnostic image quality.

In 2014, Beitzke D. et al. demonstrated that with 128-row dual-source MSCT, radiation dose can be significantly reduced through the use of prospective scanning combined with automatic tube voltage selection, without compromising diagnostic quality (slice thickness 0.6 mm). Even in patients with elevated heart rates, this approach achieved a dose reduction of up to 50% [46].

Three scanning protocols were compared:

1) Retrospective scanning mode – tube voltage set at 120 kVp on both tubes, tube current at 320 mA. Adaptive tube current modulation was applied, with the scanner selecting the optimal ripple window depending on HR. This approach was associated with the highest radiation doses.
2) Prospective sequential scanning with ECG triggering – tube voltage set at 120 kVp on both tubes, tube current at 320 mA. The main acquisition window was set at 30–70% of the RR interval. This technique showed no significant advantage over retrospective scanning.
3) Prospective sequential scanning with a narrow systolic window – main acquisition window set at 35–45% of the RR interval, with automatic tube voltage adjustment enabled.

In 2017, Bartykowszki A. et al., using a 256-slice MSCT (tube voltage 100–129 kV, tube current 100 mA, gantry rotation time 270 ms) with prospective ECG triggering, achieved an average effective radiation dose as low as 3.7 mSv [48].

The latest third-generation 384-slice scanners with dual sources and 192 detectors, when combined with advanced radiation reduction and image reconstruction protocols, provide faster scanning and broader coverage at lower radiation doses, while offering improved spatial and temporal resolution that more closely aligns with CAG. Moreover, despite relatively high heart rates, the proportion of uninterpretable segments remained low (3.3%), in contrast to earlier studies [35, 41, 43].

Thus, adoption of these advanced radiation reduction and image reconstruction protocols can reduce radiation exposure while maintaining diagnostic image quality in heart transplant recipients.

CONCLUSION

Although iCAG remains the gold standard for diagnosing CAV, it requires hospitalization, carries procedural risks, and may cause patient discomfort. MSCT-CAG offers a non-invasive, safer alternative with high sensitivity (86–89%) and specificity (89–99%) for evaluating the coronary arteries after heart transplantation. With the growing number of transplant recipients, annual non-invasive outpatient screening using MSCT-CAG could facilitate early detection and monitoring of CAV progression, help stratify patients for hospitalization, and reduce both healthcare costs and hospital burden.

Heart recipients with previously verified stenoses or coronary stents are not suitable for 64-slice MSCT, and when MSCT-CAG data are inconclusive, iCAG is still recommended. Conversely, if MSCT shows no evidence of stenosis, iCAG may not be required. Special attention should be given to minimizing contrast-induced nephropathy in patients after OHT and applying optimized radiation reduction protocols in combination with a reduction in the frequency of these procedures.

While MSCT-CAG heart recipients shows high sensitivity, its lower specificity means that CAV may occasionally be underestimated. Therefore, further research is needed to refine its diagnostic accuracy.

The authors declare no conflict of interest.

REFERENCES

1. *Gautier SV*. Press-konferentsiya direktora Tsentra Shumakova Sergeya Gautier / Gautier S.V. [Elektronnyy resurs] // NMITs transplantologii i iskusstvennykh organov im. ak. V.I. Shumakova (transpl.ru). URL: https://transpl.ru/about/press-center/press-konferentsiya-direktora-tsentra-shumakova-sergeya-gote/ (date of access: 21.02.2025).
2. *Velleca A, Shullo MA, Dhital K, Azeka E, Colvin M, DePasquale E et al.* The International Society for Heart and Lung Transplantation (ISHLT) guidelines for the care of heart transplant recipients. *J Heart Lung Transplant*. 2023 May; 42 (5): e1–e141. doi: 10.1016/j.healun.2022.10.015. Epub 2022 Dec 20. PMID: 37080658.

3. *Van Keer JM, Van Aelst LNL, Rega F, Droogne W, Voros G, Meyns B et al*. Long-term outcome of cardiac allograft vasculopathy: Importance of the International Society for Heart and Lung Transplantation angiographic grading scale. *J Heart Lung Transplant*. 2019 Nov; 38 (11): 1189–1196. doi: 10.1016/j.healun.2019.08.005. Epub 2019 Aug 10. PMID: 31543298.
4. *Lee MS, Tadwalkar RV, Fearon WF, Kirtane AJ, Patel AJ, Patel CB et al*. Cardiac allograft vasculopathy: A review. *Catheter Cardiovasc Interv*. 2018 Dec 1; 92 (7): E527–E536. doi: 10.1002/ccd.27893. Epub 2018 Sep 28. PMID: 30265435.
5. *Chih S, Chong AY, Mielniczuk LM, Bhatt DL, Beanlands RS*. Allograft Vasculopathy: The Achilles' Heel of Heart Transplantation. *J Am Coll Cardiol*. 2016 Jul 5; 68 (1): 80–91. doi: 10.1016/j.jacc.2016.04.033. PMID: 27364054.
6. *Tsutsui H, Ziada KM, Schoenhagen P, Iyisoy A, Magyar WA, Crowe TD et al*. Lumen loss in transplant coronary artery disease is a biphasic process involving early intimal thickening and late constrictive remodeling: results from a 5-year serial intravascular ultrasound study. *Circulation*. 2001 Aug 7; 104 (6): 653–657. doi: 10.1161/hc3101.093867. PMID: 11489770.
7. *Khush KK, Cherikh WS, Chambers DC, Goldfarb S, Hayes D Jr, Kucheryavaya AY et al.* International Society for Heart and Lung Transplantation. The International Thoracic Organ Transplant Registry of the International Society for Heart and Lung Transplantation: Thirty-fifth Adult Heart Transplantation Report – 2018; Focus Theme: Multiorgan Transplantation. *J Heart Lung Transplant*. 2018 Oct; 37 (10): 1155–1168. doi: 10.1016/j.healun.2018.07.022. Epub 2018 Aug 10. PMID: 30293612.
8. *Pober JS, Chih S, Kobashigawa J, Madsen JC, Tellides G*. Cardiac allograft vasculopathy: current review and future research directions. *Cardiovasc Res*. 2021 Nov 22; 117 (13): 2624–2638. doi: 10.1093/cvr/cvab259. PMID: 34343276; PMCID: PMC8783389.
9. *Olymbios M, Kwiecinski J, Berman DS, Kobashigawa JA*. Imaging in Heart Transplant Patients. *JACC Cardiovasc Imaging*. 2018 Oct; 11 (10): 1514–1530. doi: 10.1016/j.jcmg.2018.06.019. PMID: 30286911.
10. *Shetty M, Chowdhury YS.* Heart Transplantation Allograft Vasculopathy. 2023 May 22. In: StatPearls [Internet]. Treasure Island (FL): StatPearls Publishing; 2025 Jan. PMID: 32310459.
11. *Rahmani M et al.* Allograft vasculopathy versus atherosclerosis. *Circ Res*. 2006; 99 (8): 801–815.
12. *Bashore TM, Bates ER, Berger PB, Clark DA, Cusma JT, Dehmer GJ et al*. American College of Cardiology. Task Force on Clinical Expert Consensus Documents. American College of Cardiology/Society for Cardiac Angiography and Interventions Clinical Expert Consensus Document on cardiac catheterization laboratory standards. A report of the American College of Cardiology Task Force on Clinical Expert Consensus Documents. *J Am Coll Cardiol*. 2001 Jun 15; 37 (8): 2170–2214. doi: 10.1016/s0735-1097(01)01346-8. PMID: 11419904.
13. *Chirakarnjanakorn S, Starling RC, Popović ZB, Griffin BP, Desai MY*. Dobutamine stress echocardiography during follow-up surveillance in heart transplant patients: Diagnostic accuracy and predictors of outcomes. *J Heart Lung Transplant*. 2015 May; 34 (5): 710–717. doi: 10.1016/j.healun.2014.11.019. Epub 2014 Nov 17. PMID: 25682552.
14. *Madamanchi C, Konerman MC, Murthy VL*. Imaging Coronary Allograft Vasculopathy with Cardiac PET and Cardiac MRI. *Curr Cardiol Rep*. 2021 Oct 16; 23 (12): 175. doi: 10.1007/s11886-021-01606-z. PMID: 34657220.
15. *Feher A, Miller EJ*. PET Myocardial Blood Flow for Post-transplant Surveillance and Cardiac Allograft Vasculopathy in Heart Transplant Recipients. *Curr Cardiol Rep*. 2022 Dec; 24 (12): 1865–1871. doi: 10.1007/s11886-022-01804-3. Epub 2022 Oct 24. PMID: 36279035.
16. *Paech DC, Weston AR*. A systematic review of the clinical effectiveness of 64-slice or higher computed tomography angiography as an alternative to invasive coronary angiography in the investigation of suspected coronary artery disease. *BMC Cardiovasc Disord*. 2011 Jun 16; 11: 32. doi: 10.1186/1471-2261-11-32. PMID: 21679468; PMCID: PMC3141758.
17. *Bittencourt MS, Hulten E, Ghoshhajra B, O'Leary D, Christman MP, Montana P et al.* Prognostic value of nonobstructive and obstructive coronary artery disease detected by coronary computed tomography angiography to identify cardiovascular events. *Circ Cardiovasc Imaging*. 2014 Mar; 7 (2): 282–291. doi: 10.1161/CIRCIMAGING.113.001047. Epub 2014 Feb 18. PMID: 24550435.
18. *Ferencik M, Mayrhofer T, Puchner SB, Lu MT, Maurovich-Horvat P, Liu T et al.* Computed tomography-based high-risk coronary plaque score to predict acute coronary syndrome among patients with acute chest pain – Results from the ROMICAT II trial. *J Cardiovasc Comput Tomogr*. 2015 Nov-Dec; 9 (6): 538–545. doi: 10.1016/j.jcct.2015.07.003. Epub 2015 Jul 10. PMID: 26229036; PMCID: PMC4684738.
19. *Min JK, Dunning A, Lin FY, Achenbach S, Al-Mallah M, Budoff MJ et al.* CONFIRM Investigators. Age- and sex-related differences in all-cause mortality risk based on coronary computed tomography angiography findings results from the International Multicenter CONFIRM (Coronary CT Angiography Evaluation for Clinical Outcomes: An International Multicenter Registry) of 23,854 patients without known coronary artery disease. *J Am Coll Cardiol*. 2011 Aug 16; 58 (8): 849–860. doi: 10.1016/j.jacc.2011.02.074. PMID: 21835321.
20. *Leslee J.* Shaw PhD Coronary Computed Tomographic Angiography as a Gatekeeper to Invasive Diagnostic and Surgical Procedures: Results From the Multicenter CONFIRM (Coronary CT Angiography Evaluation for Clinical Outcomes: An International Multicenter) Registry 13 November 2012, Pages 2103–2114. https://doi.org/10.1016/j.jacc.2012.05.062.

21. SCOT-HEART investigators. CT coronary angiography in patients with suspected angina due to coronary heart disease (SCOT-HEART): an open-label, parallel-group, multicentre trial. *Lancet*. 2015 Jun 13; 385 (9985): 2383–2391. doi: 10.1016/S0140-6736(15)60291-4. Epub 2015 Mar 15. Erratum in: Lancet. 2015 Jun 13; 385 (9985): 2354. doi: 10.1016/S0140-6736(15)61103-5. PMID: 25788230.
22. *Hoffmann U, Bamberg F, Chae CU, Nichols JH, Rogers IS, Seneviratne SK et al*. Coronary computed tomography angiography for early triage of patients with acute chest pain: the ROMICAT (Rule Out Myocardial Infarction using Computer Assisted Tomography) trial. *J Am Coll Cardiol*. 2009 May 5; 53 (18): 1642–1650. doi: 10.1016/j.jacc.2009.01.052. PMID: 19406338; PMCID: PMC2747766.
23. *Budoff MJ, Dowe D, Jollis JG, Gitter M, Sutherland J, Halamert E et al*. Diagnostic performance of 64-multidetector row coronary computed tomographic angiography for evaluation of coronary artery stenosis in individuals without known coronary artery disease: results from the prospective multicenter ACCURACY (Assessment by Coronary Computed Tomographic Angiography of Individuals Undergoing Invasive Coronary Angiography) trial. *J Am Coll Cardiol*. 2008 Nov 18; 52 (21): 1724–1732. doi: 10.1016/j.jacc.2008.07.031. PMID: 19007693.
24. *Knuuti J, Wijns W, Saraste A, Capodanno D, Barbato E, Funck-Brentano C et al.* ESC Scientific Document Group. 2019 ESC Guidelines for the diagnosis and management of chronic coronary syndromes. *Eur Heart J*. 2020 Jan 14; 41 (3): 407–477. doi: 10.1093/eurheartj/ehz425. Erratum in: *Eur Heart J*. 2020 Nov 21; 41 (44): 4242. doi: 10.1093/eurheartj/ehz825. PMID: 31504439.
25. *Goldstein JA, Chinnaiyan KM, Abidov A, Achenbach S, Berman DS, Hayes SW et al.* CT-STAT Investigators. The CT-STAT (Coronary Computed Tomographic Angiography for Systematic Triage of Acute Chest Pain Patients to Treatment) trial. *J Am Coll Cardiol*. 2011 Sep 27; 58 (14): 1414–1422. doi: 10.1016/j.jacc.2011.03.068. PMID: 21939822.
26. *Litt HI, Gatsonis C, Snyder B, Singh H, Miller CD, Entrikin DW et al*. CT angiography for safe discharge of patients with possible acute coronary syndromes. *N Engl J Med*. 2012 Apr 12; 366 (15): 1393–1403. doi: 10.1056/NEJMoa1201163. Epub 2012 Mar 26. PMID: 22449295.
27. *Barbosa MF, Canan A, Xi Y, Litt H, Diercks DB, Abbara S, Kay FU.* Comparative Effectiveness of Coronary CT Angiography and Standard of Care for Evaluating Acute Chest Pain: A Living Systematic Review and Meta-Analysis. *Radiol Cardiothorac Imaging*. 2023 Aug 24; 5 (4): e230022. doi: 10.1148/ryct.230022. PMID: 37693194; PMCID: PMC10483255.
28. *Raff GL, Gallagher MJ, O'Neill WW, Goldstein JA*. Diagnostic accuracy of noninvasive coronary angiography using 64-slice spiral computed tomography. *J Am Coll Cardiol*. 2005 Aug 2; 46 (3): 552–557. doi: 10.1016/j.jacc.2005.05.056. PMID: 16053973.
29. *Romeo G, Houyel L, Angel CY, Brenot P, Riou JY, Paul JF*. Coronary stenosis detection by 16-slice computed tomography in heart transplant patients: comparison with conventional angiography and impact on clinical management. *J Am Coll Cardiol*. 2005 Jun 7; 45 (11): 1826–1831. doi: 10.1016/j.jacc.2005.02.069. PMID: 15936614.
30. *Ziegler F, Leber AW, Becker A, Kaczmarek I, Schönermarck U, Raps C et al*. Detection of significant coronary artery stenosis with 64-slice computed tomography in heart transplant recipients: a comparative study with conventional coronary angiography. *Int J Cardiovasc Imaging*. 2009 Jan; 25 (1): 91–100. doi: 10.1007/s10554-008-9343-z. Epub 2008 Jul 19. PMID: 18642098. *Ziegler F, Rümmler J, Kaczmarek I, Greif M, Schenzle J, Helbig S et al*. Detection of significant coronary artery stenosis with cardiac dual-source computed tomography angiography in heart transplant recipients. *Transpl Int*. 2012 Oct; 25 (10): 1065–1071. doi: 10.1111/j.1432-2277.2012.01536.x. Epub 2012 Jul 21. PMID: 22816613.
31. *Mittal TK, Panicker MG, Mitchell AG, Banner NR.* Cardiac allograft vasculopathy after heart transplantation: electrocardiographically gated cardiac CT angiography for assessment. *Radiology*. 2013 Aug; 268 (2): 374–381. doi: 10.1148/radiol.13121440. Epub 2013 May 8. PMID: 23657888.
32. *Graaf MA, Broersen A, Kitslaar PH, Roos CJ, Dijkstra J, Lelieveldt BP et al*. Automatic quantification and characterization of coronary atherosclerosis with computed tomography coronary angiography: cross-correlation with intravascular ultrasound virtual histology. *Int J Cardiovasc Imaging*. 2013 Jun; 29 (5): 1177–1190. doi: 10.1007/s10554-013-0194-x. Epub 2013 Feb 16. PMID: 23417447.
33. *Károlyi M, Kolossváry M, Bartykowszki A, Kocsmár I, Szilveszter B, Karády J et al*. Quantitative CT assessment identifies more heart transplanted patients with progressive coronary wall thickening than standard clinical read. *J Cardiovasc Comput Tomogr*. 2019 Mar-Apr; 13 (2): 128–133. doi: 10.1016/j.jcct.2018.11.006. Epub 2018 Nov 19. PMID: 30528167.
34. *Foldyna B, Sandri M, Luecke C, Garbade J, Gohmann R, Hahn J et al*. Quantitative coronary computed tomography angiography for the detection of cardiac allograft vasculopathy. *Eur Radiol*. 2020 Aug; 30 (8): 4317–4326. doi: 10.1007/s00330-019-06653-3. Epub 2020 Mar 16. PMID: 32179995; PMCID: PMC7338811.
35. *Ojha V, Ganga KP, Mani A, Jagia P, Gulati G, Seth S et al*. Detection of cardiac allograft vasculopathy on dual source computed tomography in heart transplant recipients: comparison with invasive coronary angiography. *Br J Radiol*. 2022 Jun 1; 95 (1134): 20211237. doi: 10.1259/bjr.20211237. Epub 2022 Mar 8. PMID: 35230144; PMCID: PMC10996423.
36. *Nous FMA, Roest S, van Dijkman ED, Attrach M, Caliskan K, Brugts JJ et al*. Clinical implementation of coronary computed tomography angiography for routine detection of cardiac allograft vasculopathy in heart transplant patients. *Transpl Int*. 2021 Oct; 34 (10): 1886–1894. doi: 10.1111/tri.13973. Epub 2021 Sep 19. PMID: 34268796; PMCID: PMC8519137.

37. *Kuczaj A, Pawlak S, Głowacki J, Antończyk R, Śliwka J, Przybyłowski P, Hrapkowicz T*. Utility of 64-Slice Coronary Computed Tomography Angiography in Heart Transplant Recipients. *Transplant Proc*. 2024 May; 56 (4): 836–840. doi: 10.1016/j.transproceed.2024.03.035. Epub 2024 May 10. PMID: 38729834.
38. *Wever-Pinzon O, Romero J, Kelesidis I, Wever-Pinzon J, Manrique C, Budge D et al*. Coronary computed tomography angiography for the detection of cardiac allograft vasculopathy: a meta-analysis of prospective trials. *J Am Coll Cardiol*. 2014 May 20; 63 (19): 1992–2004. doi: 10.1016/j.jacc.2014.01.071. Epub 2014 Mar 26. PMID: 24681148.
39. *Usta E, Burgstahler C, Aebert H, Schroeder S, Helber U, Kopp AF, Ziemer G*. The challenge to detect heart transplant rejection and transplant vasculopathy non-invasively – a pilot study. *J Cardiothorac Surg*. 2009 Aug 16; 4: 43. doi: 10.1186/1749-8090-4-43. PMID: 19682394; PMCID: PMC2735733.
40. *Kępka C, Sobieszczańsk-Małek M, Pręgowski J, Kruk M, Bekta P, Opolski M et al*. Usefulness of dual-source computed tomography for the evaluation of coronary arteries in heart transplant recipients. *Kardiol Pol*. 2012; 70 (11): 1111–1119. PMID: 23180518.
41. *Gregory SA, Ferencik M, Achenbach S, Yeh RW, Hoffmann U, Inglessis I et al*. Comparison of sixty-four-slice multidetector computed tomographic coronary angiography to coronary angiography with intravascular ultrasound for the detection of transplant vasculopathy. *Am J Cardiol*. 2006 Oct 1; 98 (7): 877–884. doi: 10.1016/j.amjcard.2006.04.027. Epub 2006 Aug 4. PMID: 16996866.
42. *Schepis T, Achenbach S, Weyand M, Raum P, Marwan M, Pflederer T et al*. Comparison of dual source computed tomography versus intravascular ultrasound for evaluation of coronary arteries at least one year after cardiac transplantation. *Am J Cardiol*. 2009 Nov 15; 104 (10): 1351–1356. doi: 10.1016/j.amjcard.2009.06.060. PMID: 19892049.
43. *Sigurdsson G, Carrascosa P, Yamani MH, Greenberg NL, Perrone S, Lev G et al*. Detection of transplant coronary artery disease using multidetector computed tomography with adaptative multisegment reconstruction. *J Am Coll Cardiol*. 2006 Aug 15; 48 (4): 772–778. doi: 10.1016/j.jacc.2006.04.082. Epub 2006 Jul 25. PMID: 16904548.
44. *Doesch AO, Celik S, Ehlermann P, Frankenstein L, Zehelein J, Koch A et al*. Heart rate reduction after heart transplantation with beta-blocker versus the selective If channel antagonist ivabradine. *Transplantation*. 2007 Oct 27; 84 (8): 988–996. doi: 10.1097/01.tp.0000285265.86954.80. PMID: 17989604.
45. *Beitzke D, Berger-Kulemann V, Schöpf V, Unterhumer S, Spitzer E, Feuchtner GM et al*. Dual-source cardiac computed tomography angiography (CCTA) in the follow-up of cardiac transplant: comparison of image quality and radiation dose using three different imaging protocols. *Eur Radiol*. 2015 Aug; 25 (8): 2310–2317. doi: 10.1007/s00330-015-3650-2. Epub 2015 Apr 26. PMID: 25913571.
46. *Noor M, Shekhdar J, Banner NR*. Radiation exposure after heart transplantation: trends and significance. *J Heart Lung Transplant*. 2011 Mar; 30 (3): 309–314. doi: 10.1016/j.healun.2010.09.010. Epub 2010 Nov 20. PMID: 21095137.
47. *Bastarrika G, Calvo M, Ezponda A, García-Baizán A, Caballeros M, Rábago G.* Systolic High-Pitch Coronary CT Angiography for Evaluation of the Coronary Arteries in Heart Transplant Recipients. *AJR Am J Roentgenol*. 2020 Oct; 215 (4): 828–833. doi: 10.2214/AJR.19.22639. Epub 2020 Aug 12. PMID: 32783558.
48. *Bartykowszki A, Kolossváry M, Jermendy ÁL, Karády J, Szilveszter B, Károlyi M et al*. Image Quality of Prospectively ECG-Triggered Coronary CT Angiography in Heart Transplant Recipients. *AJR Am J Roentgenol*. 2018 Feb; 210 (2): 314–319. doi: 10.2214/AJR.17.18546. Epub 2017 Nov 1. PMID: 29091000.
49. *Rozhkov AN, Schekochikhin DYu, Tebenkova ES et al.* Possibilities of using coronary artery MSCT to determine the risk of cardiovascular catastrophes in asymptomatic patients. *Russian Journal of Preventive Medicine*. 2020; 23(4): 108–114. (In Russ.). https://doi.org/10.17116/profmed202023041108.

The article was submitted to the journal on 17.03.2025

DOI: 10.15825/1995-1191-2025-3-110-116

EXPERIENCE IN MANAGING PRIMARY GRAFT DYSFUNCTION AFTER HEART TRANSPLANTATION

F.A. Gladkikh, A.V. Tsarkov, M.D. Nuzhdin, Yu.V. Malinovskiy, Yu.M. Marchenko
Chelyabinsk Regional Clinical Hospital, Chelyabinsk, Russian Federation

Heart transplantation (HT) is a cardiac surgical procedure involving the replacement of a recipient's pathologically impaired heart with a functionally adequate donor organ. As with any major surgical intervention, HT comes with possible complications, one of which is primary graft dysfunction (PGD). This report presents our initial experience in the diagnosis and management of a patient who developed PGD, necessitating the use of mechanical circulatory support.

Keywords: heart transplantation, primary graft dysfunction, mechanical circulatory support, ECMO, acute kidney injury, renal replacement therapy.

INTRODUCTION

Heart transplantation (HT) is a surgical procedure in which a pathologically altered heart is replaced with a viable donor heart. It is primarily indicated for patients with end-stage heart failure – classified as stage IIB–III according to the Vasilenko–Strazhesko system – and who experience significant limitations in physical activity (NYHA functional class III–IV). Candidates typically exhibit poor response to pharmacological therapy or mechanical circulatory support (MCS), and are not suitable for other surgical interventions, yet possess the potential for clinical remission following transplantation [1]. HT remains the gold standard in the management of end-stage chronic heart failure (HF).

Like any major surgical procedure, HT is associated with the risk of complications, among which primary graft dysfunction (PGD) is one of the most serious. According to various studies, PGD incidence ranges from 2.3% to 32.4% [2–6]. PGD is defined as mono- or biventricular dysfunction of the allograft occurring within the first 24 hours post-transplantation. This condition results in hypotension due to inadequate cardiac output that fails to meet the recipient's circulatory needs [7].

Despite advances in perioperative management, particularly regarding immunosuppressive therapy, the risk of early graft dysfunction remains significant, with a reported 30-day mortality rate of 5–10% [8]. Between 2017 and 2023, a total of 13 heart transplants were performed at Chelyabinsk Regional Clinical Hospital. PGD occurred in only one case. This report presents our first clinical experience with the diagnosis and management of PGD requiring MCS.

CLINICAL CASE

Patient B., a 53-year-old male, was placed on the heart transplant waiting list in April 2023 with a diagnosis of coronary artery disease and ischemic cardiomyopathy, classified as HF stage IIa, functional class III.

In June 2023, the patient was admitted to the cardiac surgery department of Chelyabinsk Regional Clinical Hospital for a heart transplant.

During the preoperative period, he underwent a standard pre-transplant evaluation. On the day of surgery, he was transported to the operating room. Upon arrival and transfer to the operating table, the patient remained stable. An initial anesthesiology assessment revealed a sinus rhythm with a heart rate of 70 beats per minute. Oxygen saturation was 97% on room air (FiO_2 21%). Preoxygenation was initiated via face mask.

The left radial artery was catheterized to enable invasive blood pressure monitoring and facilitate blood sampling for laboratory analysis. Standard induction of anesthesia was carried out, and the patient was transitioned to mechanical ventilation using lung-protective parameters.

Initial central hemodynamic assessment was performed using a Swan–Ganz catheter. At the time of measurement, the patient was receiving inotropic support with dobutamine at 5 μg/kg/min and vasopressor support with norepinephrine at 0.03 μg/kg/min. The following hemodynamic parameters were recorded: central venous pressure (CVP) = 14/9 mmHg; right ventricular systolic/diastolic pressure ($RVP_{sys/dia}$) = 25/10 (mean 17) mmHg; pulmonary artery systolic/diastolic pressure ($PAP_{sys/dia}$) = 27/18 (mean 19) mmHg; pulmonary capillary wedge pressure ($PCWP_{sys/dia}$) = 16/14 (mean 12) mmHg; cardiac output (CO) = 2.9 L/min; cardiac index (CI) = 1.5 L/min/m^2.

Intraoperatively, immunosuppression was initiated in accordance with the protocol developed at Shumakov National Medical Research Center of Transplantology

Corresponding author: Filipp Gladkikh. Address: 70, Vorovskogo str., Chelyabinsk, 454076, Russian Federation.
Phone: (905) 836-04-02. E-mail: filipphome@mail.ru

and Artificial Organs, Moscow, Russian Federation. The protocol included:

1. *Administration of basiliximab 2 hours prior to HT.*
2. *Administration of methylprednisolone 1000 mg before aortic unclamping.*

Hemodynamic parameters remained stable throughout the pre-perfusion period. Infusion therapy followed a restrictive strategy, with a total infusion volume of 300 mL administered prior to initiation of cardiopulmonary bypass (CPB).

After administration of heparin and achievement of the target activated clotting time (ACT), CPB was initiated as planned. The procedure was performed under mild hypothermia (33–34 °C), with a perfusion rate ranging from 4.6 to 6.3 L/min (100–120% of the target flow). Mean arterial perfusion pressure was maintained at 50–70 mmHg.

At the time of aortic unclamping, the patient had been rewarmed to 36.0 °C. Methylprednisolone was administered at a dose of 1 g. After heart deaeration procedure, the aortic cross-clamp was removed. Total cold ischemia time of the donor heart was 2 hours and 37 minutes.

During reperfusion of the transplant, spontaneous cardiac activity resumed; however, it was accompanied by signs of atrioventricular block, with a heart rate of 25–30 beats per minute prior to the initiation of inotropic support with dobutamine at 10 μg/kg/min. Due to the inadequate heart rate and rhythm, dual-chamber epicardial pacing was initiated at a rate of 90–100 beats per minute using epicardial electrodes.

Following 30 minutes of reperfusion – during which the patient's blood pressure was maintained at 90/60 mmHg and CVP at 16/10 mmHg – CPB was discontinued. At that point, cardiotonic support included epinephrine at 0.03 μg/kg/min, norepinephrine at 0.1 μg/kg/min, and dobutamine at 5 μg/kg/min, yielding a vasoactive-inotropic score (VIS) of 18. Fractional administration of protamine sulfate was initiated.

Subsequently, a gradual decrease in arterial pressure to 80/50 mmHg was observed, despite an escalation in inotropic and vasopressor support: epinephrine increased to 0.05 μg/kg/min, norepinephrine to 0.3 μg/kg/min, and dobutamine to 20 μg/kg/min (VIS = 55). At the same time, 100 mg of protamine sulfate was administered over 10 minutes. To rule out peripheral vasospasm as a contributing factor, the left femoral artery was punctured and catheterized. No significant difference in invasive blood pressure was observed when measured in the supine position. At this stage, graft dysfunction was suspected.

Due to persistent hemodynamic instability, an increase in VIS to 55, and worsening signs of hypoperfusion, evidenced by progressive hyperlactatemia (increasing from 5.2 to 7.9 mmol/L), veno-arterial extracorporeal membrane oxygenation (VA-ECMO) was initiated. Prior to ECMO initiation, central hemodynamic parameters were reassessed, which further confirmed the diagnosis of graft dysfunction: $CVP_{sys/dia}$ = 16/14 (mean 12) mmHg; $RVP_{sys/dia}$ = 42/24 (mean 28) mmHg; $PAP_{sys/dia}$ = 45/40 (mean 30) mmHg; $PCWP_{sys/dia}$ = 30/28 (mean 20) mmHg; transpulmonary gradient (TPG) = 10 mmHg, CO = 3.8 L/min; CI = 2.1 L/min/m^2.

After achieving an ACT of 160 seconds, VA-ECMO was initiated via central cannulation. The targeted volumetric perfusion rate was 2.4 L/min/m^2 (approximately 5 L/min total flow). ECMO support was provided using a Maquet system equipped with a Maquet PLS ECMO circuit (Maquet AG, Germany).

To minimize postoperative blood loss and reduce the risk of infectious complications, the surgical wound was closed using polypastic sutures to secure the sternal fragments.

In the intensive care unit (ICU), the patient continued VA-ECMO at a flow rate of 2.4–2.6 L/min/m^2. On postoperative day 1, levosimendan was administered at a dose of 2 μg/kg/min. After initiation of ECMO, there was a marked reduction in cardiotonic support requirements, with the Levosimendan Vasoactive-Inotropic Score (LVIS) decreasing to 24–23 points. Perfusion pressure was maintained at 90/70 mmHg, despite minimal native cardiac output. Sinus rhythm was restored within the first 24 hours. Mechanical ventilation was provided using a lung-protective volume-controlled mode.

On postoperative day 2, transthoracic echocardiography was performed. The findings showed no significant changes compared to the initial assessment of the donor heart. Comparative echocardiographic parameters are summarized in Table.

By day 3, a progressive decline in urine output was observed, despite pharmacological stimulation.

By the beginning of postoperative day 4, cardiotonic support had been significantly tapered, consisting only of a dobutamine infusion at 3 μg/kg/min. MCS was also reduced to 1.0 L/min/m^2. Despite these improvements, the trend of reduced urine output persisted.

Given the stabilization of hemodynamic parameters and the absence of arrhythmias, a decision was made to initiate weaning from ECMO on day 4 of ECMO therapy. After volume loading and an increase in inotropic therapy to achieve a VIS of 25, ECMO was successfully discontinued. Additional volume loading allowed for a subsequent reduction in inotropic support, lowering the VIS to 10.

Following ECMO weaning, transesophageal echocardiography was performed. Findings included thickening of the left ventricular walls and interventricular septum, with a reduction in left ventricular volume: left ventricular end-diastolic volume (LVEDV) = 50.0 mL; left ventricular end-systolic volume (LVESV) = 32.0 mL; interventricular septal thickness: 1.6 cm; posterior wall thickness: 1.5 cm; ejection fraction (EF) = 51% (Simpson's method); tricuspid annular plane systolic excursion (TAPSE): 1.6–1.8 cm. Blood pressure was

maintained at ≥95/65 mmHg with moderately increased catecholamine support compared to intraoperative levels (VIS = 14).

By postoperative day 5, the patient developed acute kidney injury. Glomerular filtration rate (GFR) declined to 18 mL/min/1.73 m^2, accompanied by a reduction in urine output to 0.5–0.7 mL/kg/hour, despite increased diuretic stimulation with furosemide at 20 mg/hour. Pulmonary oxygenation deteriorated significantly, with a drop in the P/F ratio to 127. In response, a session of prolonged veno-venous hemofiltration was initiated using the PrismaFlex system (Gambro Lundia AB, Sweden).

A telemedicine consultation was held with Professor V.N. Poptsov, MD, from Shumakov National Medical Research Center of Transplantology and Artificial Organs, Moscow, Russian Federation, Moscow, during which indications for the resumption of MCS were established.

However, given the lack of a rising trend in inotropic requirements, the predominance of respiratory distress and renal failure in the clinical picture, and the extremely high risk of infectious complications, it was decided to discontinue MCS and to continue with prolonged veno-venous hemodiafiltration.

On postoperative day 6, central hemodynamic monitoring revealed an increase in both cardiac output and cardiac index, achieved with relatively low levels of inotropic support (VIS = 15).

By day 7, the session of high volume venovenous hemodiafiltration (HV-CVVHDF) was discontinued. It lasted for 52 hours, during which hemofiltration rate was maintained at 30 mL/kg/h. A gradual return of spontaneous diuresis was observed, along with a continued decrease in inotropic requirements (VIS = 11). However, respiratory failure persisted, with a P/F ratio of 170.

On day 8, a tracheostomy was performed. By that time, inotropic support had been reduced to a minimal level (VIS = 2), and oxygenation had significantly improved, with the P/F ratio rising to 300.

Three days later, a downward trend in serum creatinine and urea levels was observed, eliminating the need for further renal replacement therapy.

Over the next eight days, efforts were focused on weaning the patient from mechanical ventilation using high-flow oxygen therapy. On postoperative day 15, the tracheostomy tube was successfully removed. Cardiovascular support was fully withdrawn by postoperative day 10.

On postoperative day 18, the patient was transferred to the cardiac surgery department. A follow-up transthoracic echocardiography was performed on day 28, with findings summarized in Table. Endomyocardial biopsies were conducted on postoperative days 14 and 29. Both specimens showed no evidence of acute cellular rejection – graded as 0 according to the ISHLT classification – with no perivascular or interstitial infiltrates identified.

On postoperative day 33 (August 1, 2023), following comprehensive follow-up assessments, the patient was discharged from the hospital in stable condition.

DISCUSSION

Early graft dysfunction is a serious post-HT complication. According to the literature [9], three major categories of risk factors contribute to the development of primary dysfunction: donor-related factors, recipient-related factors, and perioperative/surgical factors.

In the present case, risk factors from all three categories were present. The recipient had a significant comorbidity – type 2 diabetes mellitus. From the donor side, moderate hypernatremia (serum sodium of 149 mmol/L) was documented. In addition, there was a gender mismatch between donor and recipient.

The combination of these risk factors likely triggered the development of biventricular graft dysfunction (BGD) in this patient.

The diagnosis of biventricular graft dysfunction in this case is supported by several clinical findings consistent with the consensus definition provided by the

Table

Comparative echocardiographic parameters of the transplanted heart

Parameters	Pre-transplant value	Post-transplant value	At discharge
LVEDV	4.9 cm	4.1 cm	5.4 cm
LVESV	3.3 cm	2.6 cm	3.6 cm
EF	63%	66%	56%
CF	34%	36%	33%
IVS thickness	1.1 cm, with basal segment thickening up to 1.3 cm	1.2 cm, with basal segment thickening up to 1.3 cm	1.3 cm
LVPWT	1.2 cm	1.1 cm	1.25 cm
Right ventricular systolic pressure	30–35 mmHg	35 mmHg	34 mmHg

Abbreviations: LVEDV, left ventricular end-diastolic diameter; LVESV, left ventricular end-systolic diameter; EF, ejection fraction; CF, contractility fraction; IVS, interventricular septal; LVPWT, left ventricular posterior wall thickness; RVSP, right ventricular systolic pressure.

International Society for Heart and Lung Transplantation (ISHLT) [10]:
- High levels of cardiotonic and vasopressor support, reflected by a VIS of 55 points.
- Persistent hemodynamic instability, evidenced by sustained hypotension; despite maximal inotropic therapy, arterial blood pressure remained no higher than 80/50 mmHg.
- Central hemodynamic parameters indicating biventricular dysfunction: right heart overload, demonstrated by elevated right ventricular and pulmonary artery pressures; and left ventricular dysfunction, reflected by PCWP at the upper limit of normal, coupled with low cardiac output and cardiac index.

Thus, the development of severe biventricular graft dysfunction influenced the clinical course of this case. The severe form of this condition is associated with high perioperative mortality. According to various studies [10, 11], the risk of death or the need for retransplantation varies with the severity of the dysfunction. In severe cases, the probability of death or retransplantation – often necessitating MCS in the early post-transplant period – ranges from 40% to 50%.

Regardless of the underlying cause or specific type of early graft dysfunction, the first-line treatment is pharmacological hemodynamic support. This involves the administration of inotropic and vasopressor agents to maintain adequate metabolic homeostasis, thereby providing a critical window for further diagnostic evaluation and intervention.

The VIS is a useful tool for objectively assessing the level of pharmacological circulatory support. The concept was originally introduced by Wernovsky et al. in 1995 [12], who developed an inotropic index based solely on inotropic agents. In 2010, Gaies et al. updated this scoring system by incorporating vasopressors, resulting in the modern VIS formula now widely used to evaluate the severity of graft dysfunction [13]. A more recent adaptation of the VIS, known as the Levosimendan VIS (LVIS), includes levosimendan as an additional parameter [14]. The formula is as follows:

LVIS = Dopamine (μg/kg/min) + Dobutamine (μg/kg/min) + 100 × Epinephrine (μg/kg/min) + 10 × Milrinone (μg/kg/min) + 10,000 × Vasopressin (units/kg/min) + 100 × Norepinephrine (μg/kg/min) + 50 × Levosimendan (μg/kg/min).

Failure to achieve hemodynamic stability with drug treatment suggests severe graft dysfunction, which is clinically equivalent to severe cardiogenic shock and may necessitate the initiation of MCS. A rising VIS can indicate worsening clinical status and treatment ineffectiveness. Although VIS alone should not serve as the sole criterion for initiating MCS [15], a score ≥32 points has been associated with delayed initiation of MCS and increased mortality risk [16].

MCS serves several critical functions in the management of severe graft dysfunction:
- Enhancing systemic perfusion;
- Improving coronary perfusion;
- Reducing left ventricular filling pressure (decreasing wall tension and myocardial oxygen demand).

Several retrospective studies have demonstrated the advantages of ECMO over other circulatory support modalities in such clinical scenarios [17, 18].

Acute kidney injury (AKI) is another serious complication that we encountered in this case. Among the established risk factors for AKI [19], the most relevant in this patient were prolonged CPB time, pre-existing diabetes mellitus, and the use of ECMO.

The potential for ECMO-related AKI was a key consideration in the decision to wean the patient early from MCS. On one hand, discontinuing ECMO helped eliminate the extracorporeal circuit as a contributing factor to kidney injury. On the other hand, MCS plays a vital role in improving renal perfusion by supporting cardiac output and ensuring adequate oxygenation, which together contribute to improved tissue oxygen delivery to the tissues.

AKI is a relatively common complication in heart transplant recipients, with an incidence reported as high as 47.1% [20]. When AKI develops and necessitates treatment, the choice of an appropriate therapeutic approach becomes critical. According to the 2012 KDIGO guidelines for AKI in critically ill patients [21], prolonged renal replacement therapy (RRT) modalities are preferred in cases of hemodynamic instability. In this patient, prolonged veno-venous hemodiafiltration was implemented in accordance with these guidelines. This preference is based on the slower rate of fluid removal and the absence of fluid migration, which occurs with the rapid removal of dissolved substances.

The simultaneous use of MCS and prolonged RRT has been previously discussed by Ostermann et al. [22], who noted that current evidence does not conclusively demonstrate a reduction in mortality with this combination.

However, in contrast to these findings, we observed an improvement in hemodynamic stability after the use of RRT in our patient. This was evidenced by a marked reduction in the need for cardiotonic support.

The timing of RRT initiation remains a subject of ongoing debate. However, Poz et al. [23] argue that early initiation may offer the greatest benefit, particularly by maximizing the therapeutic potential of the method.

In the present case, cardiorenal syndrome played a pivotal role in the clinical trajectory [24]. This syndrome arises from the bidirectional relationship between cardiac and renal dysfunction, whereby acute or chronic failure of one organ precipitates or exacerbates dysfunction in the other. In this patient, severe graft dysfunction of the transplanted heart precipitated renal failure. Given this

dynamic, a multimodal treatment approach, incorporating both MCS and prolonged RRT, was likely instrumental in achieving the favorable clinical outcome observed in this case.

CONCLUSIONS

The combined use of MCS – which ensures adequate oxygen delivery to tissues – and prolonged RRT – which facilitates the removal of metabolic waste, inflammatory mediators, and hemolytic byproducts – may contribute to improved clinical outcomes and supports the recovery of vital organ function.

This simultaneous application of MCS and RRT may improve clinical outcomes, which requires further research.

Early initiation of RRT in patients with transplant cardiac dysfunction requiring MCS shows promise and warrants further investigation.

Based on the findings from the presented clinical case, it is essential to adopt an individualized and multidisciplinary approach to the intensive care management of acute heart failure secondary to heart transplant dysfunction.

The authors declare no conflict of interest.

REFERENCES

1. Klinicheskie rekomendatsii. Transplantatsiya serdtsa, nalichie transplantirovannogo serdtsa, otmiranie i ottorzhenie transplantata serdtsa. Ministerstvo zdravookhraneniya RF. 2023.
2. *Russo MJ, Iribarne A, Hong KN, Ramlawi B, Chen JM, Takayama H et al*. Factors associated with primary graft failure after heart transplantation. *Transplantation*. 2010; 90 (4): 444–450. https://doi.org/10.1097/TP.0b013e3181e6f1eb.
3. *Dronavalli VB, Rogers CA, Banner NR*. Primary Cardiac Allograft Dysfunction-Validation of a Clinical Definition. *Transplantation.* 2015; 99 (9): 1919–1925. https://doi.org/10.1097/TP.0000000000000620.
4. *D'Alessandro C, Aubert S, Golmard JL, Praschker BL, Luyt CE, Pavie A et al*. Extra-corporeal membrane oxygenation temporary support for early graft failure after cardiac transplantation. European journal of cardio-thoracic surgery: official journal of the European Association for Cardio-thoracic *Surgery*. 2010; 37 (2): 343–349. https://doi.org/10.1016/j.ejcts.2009.05.034.
5. *Oto T, Excell L, Griffiths AP, Levvey BJ, Bailey M, Marasco S et al*. Association between primary graft dysfunction among lung, kidney and heart recipients from the same multiorgan donor. *American journal of transplantation: official journal of the American Society of Transplantation and the American Society of Transplant Surgeons*. 2008; 8 (10); 2132–2139. https://doi.org/10.1111/j.1600-6143.2008.02357.x.
6. *Ibrahim M, Hendry P, Masters R, Rubens F, Lam BK, Ruel M et al*. Management of acute severe perioperative failure of cardiac allografts: a single-centre experience with a review of the literature. *The Canadian journal of cardiology*. 2007; 23 (5): 363–367. https://doi.org/10.1016/s0828-282x(07)70769-9.
7. *Kobashigawa J, Zuckermann A, Macdonald P, Leprince P, Esmailian F, Luu M et al*. Consensus Conference participants. Report from a consensus conference on primary graft dysfunction after cardiac transplantation. *The Journal of heart and lung transplantation: the official publication of the International Society for Heart Transplantation*. 2014; 33 (4): 327–340. https://doi.org/10.1016/j.healun.2014.02.027.
8. *Subramani S, Aldrich A, Dwarakanath S, Sugawara A, Hanada S.* Early Graft Dysfunction Following Heart Transplant: Prevention and Management. *Seminars in Cardiothoracic and Vascular Anesthesia*. 2020; 24 (1): 24–33. doi: 10.1177/1089253219867694.
9. *Hull TD, Crowley JC, Villavicencio MA, D'Alessandro DA.* Primary graft dysfunction in heart transplantation: How to recognize it, when to institute extracorporeal membrane oxygenation, and outcomes. *JTCVS Open*. 2021 May 27; 8: 128–133. doi: 10.1016/j.xjon.2021.05.010. PMID: 36004187; PMCID: PMC9390270.
10. *Sabatino M, Vitale G, Manfredini V, Masetti M, Borgese L, Maria Raffa G et al*. Clinical relevance of the International Society for Heart and Lung Transplantation consensus classification of primary graft dysfunction after heart transplantation: Epidemiology, risk factors, and outcomes. *The Journal of heart and lung transplantation: the official publication of the International Society for Heart Transplantation*. 2017; 36 (11): 1217–1225. https://doi.org/10.1016/j.healun.2017.02.014.
11. *Jacob S, Lima B, Gonzalez-Stawinski GV, El-Sayed Ahmed MM, Patel PC, Belli EV et al*. Extracorporeal membrane oxygenation as a salvage therapy for patients with severe primary graft dysfunction after heart transplant. *Clinical transplantation*. 2019; 33 (5): e13538. https://doi.org/10.1111/ctr.13538.
12. *Wernovsky G, Wypij D, Jonas RA, Mayer JE Jr, Hanley FL, Hickey PR et al*. Postoperative course and hemodynamic profile after the arterial switch operation in neonates and infants. A comparison of low-flow cardiopulmonary bypass and circulatory arrest. *Circulation*. 1995; 92 (8): 2226–2235. https://doi.org/10.1161/01.cir.92.8.2226.
13. *Gaies MG, Gurney JG, Yen AH, Napoli ML, Gajarski RJ, Ohye RG et al*. Vasoactive-inotropic score as a predictor of morbidity and mortality in infants after cardiopulmonary bypass. *Pediatric critical care medicine: a journal of the Society of Critical Care Medicine and the World Federation of Pediatric Intensive and Critical Care Societies*. 2010; 11 (2): 234–238. https://doi.org/10.1097/PCC.0b013e3181b806fc.
14. *Favia I, Vitale V, Ricci Z*. The vasoactive-inotropic score and levosimendan: Time for LVIS? *J Cardiothorac Vasc Anesth*. 2013; 27: e15–e16. doi: 10.1053/j.jvca.2012.11.009.
15. *Caruso V, Berthoud V, Bouchot O, Nguyen M, Bouhemad B, Guinot PG*. ECMOVIS Study Group. Should the Vasoactive Inotropic Score be a Determinant for Early

Initiation of VA ECMO in Postcardiotomy Cardiogenic Shock? *J Cardiothorac Vasc Anesth*. 2024 Mar; 38 (3): 724–730. doi: 10.1053/j.jvca.2023.11.040. Epub 2023 Dec 1. PMID: 38182434.

16. *Hyun J, Kim AR, Lee SE, Hong JA, Kang PJ, Jung SH, Kim MS.* Vasoactive-Inotropic Score as a Determinant of Timely Initiation of Venoarterial Extracorporeal Membrane Oxygenation in Patients With Cardiogenic Shock. *Circ J*. 2022 Mar 25; 86 (4): 687–694. doi: 10.1253/circj.CJ-21-0614. Epub 2021 Nov 9. PMID: 34759121.
17. *Leprince P, Aubert S, Bonnet N, Rama A, Léger P, Bors V et al*. Peripheral extracorporeal membrane oxygenation (ECMO) in patients with posttransplant cardiac graft failure. *Transplantation proceedings.* 2005; 37 (6): 2879–2880. https://doi.org/10.1016/j.transproceed.2005.05.018.
18. *Taghavi S, Zuckermann A, Ankersmit J, Wieselthaler G, Rajek A, Laufer G et al*. Extracorporeal membrane oxygenation is superior to right ventricular assist device for acute right ventricular failure after heart transplantation. *The Annals of thoracic surgery*. 2004; 78 (5): 1644–1649. https://doi.org/10.1016/j.athoracsur.2004.04.059.
19. *Thongprayoon C, Lertjitbanjong P, Hansrivijit P, Crisafio A, Mao MA, Watthanasuntorn K et al*. Acute Kidney Injury in Patients Undergoing Cardiac Transplantation: A Meta-Analysis. *Medicines (Basel)*. 2019 Nov 1; 6 (4): 108. doi: 10.3390/medicines6040108. PMID: 31683875; PMCID: PMC6963309.
20. *Poz IL, Strokov AG, Poptsov VN, Shevchenko AO, Gautier SV*. Pathogenetic mechanisms, epidemiology and classification of acute kidney injury in heart transplant recipients. *Russian Journal of Transplantology and Artificial Organs*. 2021; 23 (2): 147–157. https://doi.org/10.15825/1995-1191-2021-2-147-157.
21. Kidney disease: Improving Global Outcomes (KDIGO) Acute Kidney Injury Work Group: KDIGO Clinical Practice Guideline for Acute Kidney Injury. *Kidney Inter Suppl*. 2012; 2: 1–138. doi: 10.1038/kisup.2012.1.
22. *Ostermann M, Connor M Jr, Kashani K*. Continuous renal replacement therapy during extracorporeal membrane oxygenation: why, when and how? *Current opinion in critical care*. 2018; 24 (6): 493–503. https://doi.org/10.1097/MCC.0000000000000559.
23. *Poz IL, Strokov AG, Kopylova YuV, Poptsov VN, Gautier SV*. Renal replacement therapy in heart transplant recipients. *Russian Journal of Transplantology and Artificial Organs*. 2021;23 (4): 62–72. https://doi.org/10.15825/1995-1191-2021-4-62-72.
24. *Ajibowo AO, Okobi OE, Emore E, Soladoye E, Sike CG, Odoma VA et al*. Cardiorenal Syndrome: A Literature Review. *Cureus*. 2023 Jul 1; 15 (7): e41252. doi: 10.7759/cureus.41252. PMID: 37529809; PMCID: PMC10389294.

The article was submitted to the journal on 20.03.2025

DOI: 10.15825/1995-1191-2025-3-117-124

ASSESSMENT OF BLOOD HEMOLYSIS DURING OPTIMIZATION OF THE ROTAFLOW CENTRIFUGAL PUMP IMPELLER

A.P. Kuleshov, N.V. Grudinin, A.S. Buchnev, V.A. Elenkin, D.N. Shilkin, V.K. Bogdanov

Shumakov National Medical Research Center of Transplantology and Artificial Organs, Moscow, Russian Federation

This study focuses on the evaluation of a modernized impeller for the RotaFlow centrifugal pump (Maquet, Germany), carried out as part of efforts to design a domestic counterpart. The proposed impeller features a combination of primary elongated blades, responsible for generating the majority of pressure, and secondary shortened blades. The investigation examined pump performance under extracorporeal membrane oxygenation (ECMO) therapy conditions at a pressure of 350 mmHg and flow rate of 5 L/min. Computational analyses were conducted to evaluate fluid flow parameters associated with hemolysis risk. The optimized impeller demonstrated a significant increase in low tangential stress zones (<10 Pa), reduced exposure time, and a lower hemolysis index. Comparative mathematical modeling and bench testing with donor blood confirmed the improved hemodynamic performance of the redesigned impeller over the original configuration.

Keywords: hemolysis index, centrifugal pump, tangential stresses, impeller.

INTRODUCTION

In vitro evaluation of centrifugal heads for extracorporeal membrane oxygenation (ECMO) systems is often conducted under left ventricular bypass (LVB) conditions. In such studies, standard hemolysis testing is carried out using a validated method designed for LVB applications, typically at a pressure of 100 ± 5 mm Hg and a flow rate of 5 L/min on a dedicated test bench [1, 2].

In clinical practice, however, LV bypass pumps are frequently adapted for ECMO therapy. While these pumps are engineered to function within a specific flow and pressure range, they are often operated across a much broader spectrum of hemodynamic conditions, which results in a loss of efficiency.

A more effective strategy in this case is to develop centrifugal pump (CP) product lines, such as the Jarvik [3] or Excor [4] axial pump families. These lines incorporate pumps optimized for different flow and pressure ranges, enabling adaptation to various ECMO modes and oxygenators with different resistances.

However, it should be noted that implementing this strategy is very costly, and currently, CPs continue to serve as universal components for different ECMO operating modes. Under conditions requiring pressures of 300–400 mmHg to overcome oxygenator resistance and maintain flow rates of up to 5 L/min, pumps are often forced to operate outside their optimal range, which negatively impacts performance. This mismatch leads to a reduction in hydraulic efficiency, promoting the development of recirculation and turbulence zones, particularly at lower flow rates. To compensate, the rotor speed must increase, which in turn exerts a harmful effect on blood elements. Moreover, it is well established that the thrombogenic potential of ECMO systems is linked to mechanical stress, which triggers activation of biochemical cascades [5]. This is mainly associated with blood–surface interactions in the wall layer and the mechanical impact of the impeller blades.

Hastings et al. [6] demonstrated that the CP, along with tubing and connectors, plays a key role in thrombus formation within the ECMO circuit. For this reason, CPs used in ECMO are routinely tested under elevated pressure conditions *in vitro*. For example, Li et al. [7] tested their device at 290 mmHg and 5 L/min, while patent studies of a Chinese CP model conducted at 350 mmHg and 5 L/min showed lower hemolysis rates compared to pumps tested under LVB test benches [8].

Methods of preliminary computer assessment of parameters [9, 10] are widely used for early evaluation of CPs. These approaches are particularly effective for assessing the risk of hemolysis, and are especially relevant when pumps must be tested under high-pressure operating conditions.

When analyzing mechanical effects, such parameters include shear stress (SN), denoted as τ, which, at a steady fluid velocity υ, changes linearly with distance (y) from the wall, regardless of the nature of movement [11] (1):

$$\tau = \mu \frac{d\upsilon}{dy}. \quad (1)$$

The effect of shear stress (τ) is most pronounced near surfaces in direct contact with blood. On these surfaces,

Corresponding author: Arkady Kuleshov. Address: 1, Shchukinskaya str., Moscow, 123182, Russian Federation. Phone: (915) 292-47-98. E-mail: ilovemylene@yandex.ru

regions with different shear stress levels develop, directly influencing the formed elements of blood. Importantly, shear stress is closely linked to exposure time of blood to the mechanical components of the system: the longer the duration of contact, the higher the probability of hemolysis.

Erythrocytes can often withstand very high transient loads if the time spent passing through the pump is minimal. However, under relatively low shear stress conditions, prolonged stagnation within the pump can lead to hemoglobin release. This phenomenon is particularly relevant when pumps are operated outside their intended design range, especially at low flow rates.

A recent study by Gross-Hardt et al. [12] highlighted this problem. The authors examined ECMO pumps operating at flow rates of 0.5–1.5 L/min. Pumps originally designed for adults and children weighing >6 kg (with a flow capacity of 0.5–8.0 L/min) were applied in newborns weighing 3–6 kg, at flow rates as low as 0.3–0.5 L/min. The results demonstrated increased internal recirculation, elevated shear stress, and consequently higher levels of hemolysis.

As rotational speed increases, interactions between blood cells intensify, a phenomenon that, under turbulent flow conditions, is described by Reynolds stress [11] (2):

$$\tau = \varrho l^2 \left(\frac{d\upsilon}{dy}\right)^2. \quad (2)$$

This effect further contributes to hemolysis, underscoring the need to limit pump rotation speed in ECMO applications.

A reduction in the index of hemolysis (IH) under ECMO conditions has been reported by studies of the RotaFlow pump (Maquet, Germany) [11], which served as the basis for the present research and modernization. The proposed optimization method focuses on redesigning the impeller to enhance pump efficiency while lowering rotational speed. Such an approach is especially relevant when adapting pumps for ECMO. This can reduce hemolysis and improve pump performance under high loads.

The optimized design aims to reduce both specific energy consumption and exposure time, leading to a measurable improvement in the calculated IH. Validation of the concept was carried out under ECMO conditions using both computational modeling and *in vitro* bench testing.

MATERIALS AND METHODS

A computer model of the RotaFlow centrifugal pump (Maquet, Germany) was developed. At the initial stage, the pump components were scanned using a 3DMakerpro Seal 3D scanner (China), which enabled the creation of accurate sketches and three-dimensional (3D) models of all parts with a precision of 0.1 mm. The final assembly was rendered in the SolidWorks PhotoView 360 graphics module, where the appropriate materials and textures were applied. The resulting model, shown in Fig. 1, replicates the mass and dimensional characteristics of the original pump.

The mass of the parts generated from SolidWorks materials corresponded closely to those of the original RotaFlow pump, with a total deviation of 0.5 ± 0.1 g. The redesigned impeller blade, compared with the original, is shown in Fig. 2. It consists of a rotor equipped with a primary elongated blade and a secondary shortened blade. The blade profile was defined with specific geometric parameters to reduce flow restriction while simultaneously increasing pressure generation during rotation. The shortened blade shares the same profile as the primary blade but has a length equal to one-third of the main blade.

The model was developed for numerical analysis of fluid flow. A 3D design was created for both the original impeller and the modified variant. The reference rotor, shown in Fig. 2, a, served as the base model, while the new impeller design, shown in Fig. 2, b, was evaluated relative to it. Among several design iterations, the selected impeller proved to be the most effective and optimal for the intended application.

Fig. 1. Reconstructed 3D model of the RotaFlow pump (Maquet, Germany)

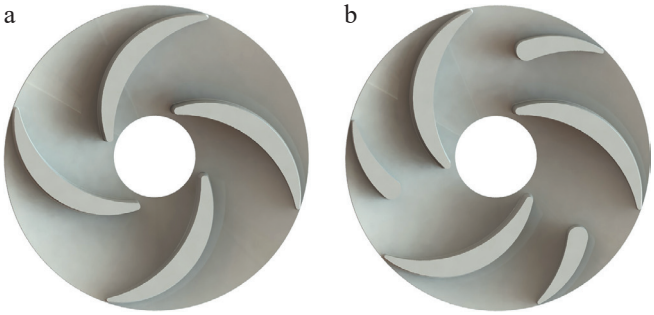

Fig. 2. Impeller blade profiles of the original (a) and modified (b) RotaFlow pump designs

Computational fluid dynamics (CFD) analysis

Numerical simulation of flow through the two pumps was performed using ANSYS Fluent 14.2. The flow distribution was obtained by solving the Navier–Stokes equations on an unstructured finite-volume grid. Boundary conditions were defined with zero pressure at the inlet and a fixed outlet pressure of 350 mm Hg. A flow rate of 5 L/min was achieved by adjusting the rotor speed.

Pump walls were assumed to be rigid with a surface roughness of 5 μm, consistent with die-casting quality. Blood was modeled as an incompressible Newtonian fluid with a density of 1060 kg/m^3 and a viscosity of 0.003763 Pa·s [13]. To solve the governing equations, the s-w turbulence model was applied, as it provides high efficiency and accuracy for near-wall flow conditions. A convergence criterion of 10^{-5} was used.

The computational mesh employed a minimum element size of 50 μm (tetrahedrons), which allowed calculations to be performed with minimal time and software costs.

Hemolysis index assessment

An important aspect of flow-induced blood damage is hemolysis, defined as the release of hemoglobin into plasma resulting from erythrocyte membrane damage. The two primary factors contributing to hemolysis are the shear stress generated by the pump and the duration of exposure of blood cells within the flow.

For engineering applications, the power-law equation proposed by Giersiepen et al. remains a widely used tool for estimating the amount of released hemoglobin (ΔHb, expressed as a concentration relative to baseline hemoglobin, Hb). This model incorporates both exposure time and shear stress acting on red blood cells (3) [14]. Although it is well established that this equation tends to overestimate hemolysis and does not fully reproduce *in vivo* conditions, it continues to be applied successfully.

$$\frac{\Delta Hb}{Hb} = A \times t^{\alpha}\tau^{\beta}, \quad (3)$$

where τ is the shear stress acting on the blood, expressed in Pa, and t is the time of interaction of the blood within the shear field, expressed in seconds, and the relative increase in plasma hemoglobin is normalized in the range of 0–1. Different researchers have obtained empirical constants (A, α, β) by regression analysis of experimental hemolysis data. Two formulas obtained from different sources were used to solve the problems.

The first model applied was the well-known formulation by Thamsen and Affeld [15], which uses an Euler-based numerical approach to hemolysis prediction. The corresponding empirical coefficients are: $A = 3.62 \cdot 10^{-7}$, $\alpha = 0.785$, and $\beta = 2.416$. The second model was that of Heuser and Opitz [16], which defines a different set of coefficients: $A = 1.8 \cdot 10^{-6}$, $\alpha = 0.785$, $\beta = 1.991$. Both models were used to calculate the index of hemolysis (IH).

Following Thamsen et al. [15], the HI is defined as the integral of hemolysis productivity over the entire computational domain, normalized to the mass flow rate of intact blood entering the pump. Thus, we obtain a productivity term for hemolysis that includes shear stress and the cumulative damage carried over from the previous time step [15].

$$\frac{\Delta Hb}{Hb} = A \times t^{\alpha}\tau^{\beta}, \quad (4)$$

This equation reflects the nonlinear dependence of blood damage on exposure time (t) and served as the basis for determining the probable HI.

To evaluate the potential traumatic effect on blood flowing inside the pumps, shear stress was calculated on all surfaces in contact with blood. In addition, the exposure time of blood elements – defined as the residence time of blood within the pump from entry at the inlet to exit – was assessed. Different criteria have been proposed in the literature for the maximum permissible shear stress value for red blood cells.

Two key parameters influence blood trauma: shear stress and exposure time. An empirical curve developed by Leverett and Hellums [17] describes the relationship between these parameters. This curve is widely used to distinguish between two regimes of blood damage: one dominated by surface-induced hemolysis due to direct contact with pump walls, and the other by shear-induced hemolysis in the bulk flow.

Leverett and colleagues conducted experiments with concentric cylinder viscometers to investigate the combined effects of surface interaction, centrifugal forces, mixing, cell collisions, and viscous heating. The study confirmed that contact between red blood cells and solid surfaces significantly exacerbates blood trauma. Furthermore, they established a critical shear stress threshold of 150 Pa for concentric cylinder systems.

According to [16], the critical shear stress value is also 150 Pa, while other studies report higher thresholds of up to 250 Pa [18]. Importantly, zones of elevated shear stress may occupy only a small portion of the surface and be associated with very short erythrocyte exposure times. Therefore, to numerically determine the HI, the calculated average shear stress was used, determined along an average erythrocyte trajectory. By combining shear stress and exposure time, the models yielded an estimate of the expected average HI, expressed as the percentage increase in plasma free hemoglobin relative to the total hemoglobin content.

Creation of a bench sample

Based on preliminary computer simulations, 3D models of two centrifugal pump (CP) samples were created and exported to STL format. Using these files, physical parts of the mock-up were fabricated on a Formlabs 3B+ medical 3D printer (USA) by stereolithography (SLA).

This process employed a biocompatible, sterilizable surgical photopolymer, achieving a dimensional accuracy of 25 μm.

The fittings and blades were printed on a Stereotech Fiber 5D printer using the 5D Spiral Full method with PLA plastic. These elements were subsequently polished to achieve a smooth surface finish.

A 4-pole magnet, a 10 steel closing ring, and a custom-made support ball made of durable Al_2O_3 aluminum oxide (corundum, alundum) were integrated into the assembly unit. Prototype pumps with both the original and modified rotors, prepared for bench testing, are shown in Fig. 3. The CP housing is equipped with an outlet fitting with an internal diameter of $^3/_8$ inch. The impeller is driven by an external motor via a magnetic coupling.

Experimental tests were conducted on the developed CP, which was fitted with a single ball-bearing hybrid impeller and operated using a magnetic coupling. The drive system employed an Ex-Stream system motor (Biosoft-M, Russia), manufactured in accordance with the specifications described in this invention.

The Rotaflow pump prototypes weighed 61.3 ± 1.0 g with a priming volume of 32 ± 1 ml and were capable of delivering blood flow rates exceeding 10 L/min at normal rotation speeds between 1000 and 5000 rpm.

In vitro hemolysis testing

In vitro hemolysis was evaluated using a donor blood circulation circuit in accordance with the protocol recommended by the American Society for Testing and Materials (ASTM F1841-19). Each test was carried out on a bench setup containing 450 ml of donor blood (hematocrit: 38%, hemoglobin: 127 g/L). To assess the hemolytic performance of the two pumps, four hemolysis tests were conducted at a flow rate of 5.0 ± 0.2 L/min under two pressure conditions: 350 ± 5 mmHg and 100 ± 5 mmHg. The blood reservoir was immersed in a water bath at 37 °C to maintain a constant blood temperature.

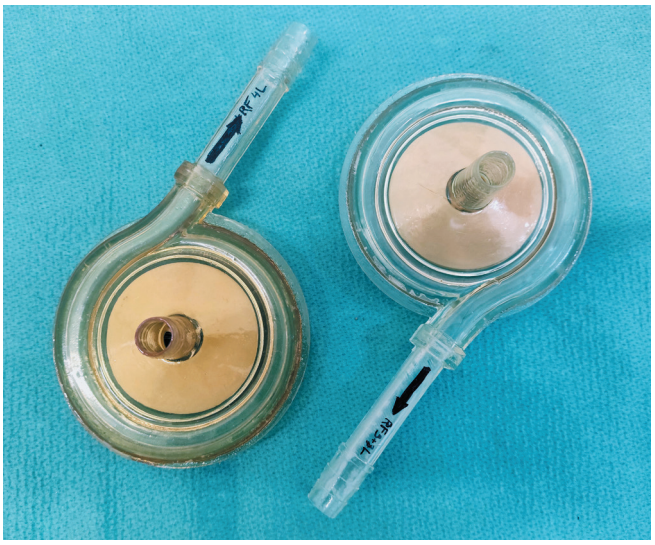

Fig. 3. Experimental photopolymer pump models with the original and modified rotor designs

Volumetric flow rate was measured using a Transonic T410 ultrasonic flowmeter. Inlet and outlet pressures were monitored with BBraun sensors. Citrated blood had a hematocrit level of 40 ± 2%.

The measurement procedure for free hemoglobin concentration followed the method described in [1]. Both the normalized index of hemolysis (NIH) and the modified index of hemolysis (MIH) were calculated as outlined in the same reference.

RESULTS

Distribution of shear stress on pump walls

To evaluate the distribution of shear stress, it was divided into three levels depending on the expected impact on blood cells: 1) shear stress <10 Pa – corresponds to physiological shear stress; 2) shear stress 10–100 Pa – may induce formation of high-molecular-weight compounds, degradation of von Willebrand factor (VWF), and platelet activation; 3) shear stress >100 Pa – represents non-physiological shear stress, associated with damage to blood components. An example of shear stress distribution within the pumps are illustrated in Figs. 4 and 5.

High shear stress was primarily observed at the trailing edges of the impeller blades and within the casing surface gaps. In the modified model, blood flow was more uniform, resulting in lower shear stress at the inlet. However, shear stress remained elevated along the blade edges. A significant difference was noted in the upper and lower gaps: the original model showed more extensive high-shear stress (red) zones at the gap inlet. These differences were evident under both standard LVB conditions (100 mmHg, 5 L/min) and ECMO conditions (350 mmHg, 5 L/min).

In LVB mode, most of the blood in both pumps was exposed to shear stress levels below 10 Pa. The main differences emerged in the distribution of zones up to 100 Pa and above. The modified impeller reduced loading in the gap regions and operated at a lower rotational speed, thereby reducing the pressure level above 100 Pa (Fig. 6, a). As expected, under ECMO conditions the percentage distribution shifted for both models compared to LVB mode. The overall area of high-shear stress zones increased significantly, although the relative difference between the models remained consistent (Fig. 6, b).

Average exposure time of blood in the modified and original designs was 0.22 s and 0.26 s, respectively, under operating conditions (350 mmHg, 5 L/min). At lower loading conditions (100 mmHg, 5 L/min), the exposure times were 0.24 s for the modified design and 0.31 s for the original design.

Under ECMO pressure conditions, the number of recirculation trajectories was lower than under LVB

conditions, resulting in a slight reduction of the average trajectory time despite identical flow rates. Since both pumps had nearly comparable priming volume, the modified model provided more effective flushing.

Analysis of mathematical and experimental hemolysis

The modified impeller design demonstrated a consistently lower potential IH compared to the original

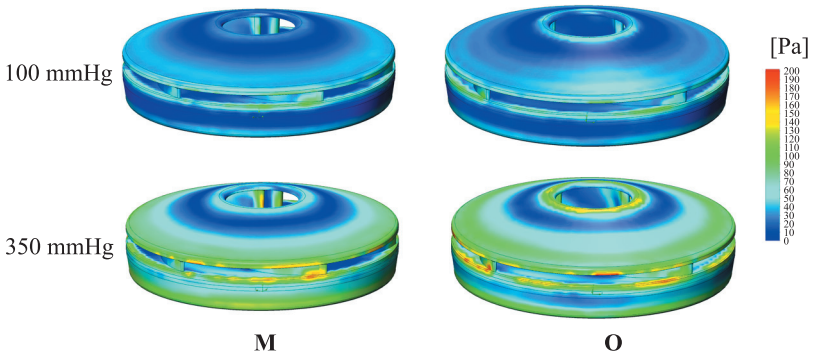

Fig. 4. Variation of tangential stress (TS) on the rotor surface for the modified (M) and original (O) impeller designs

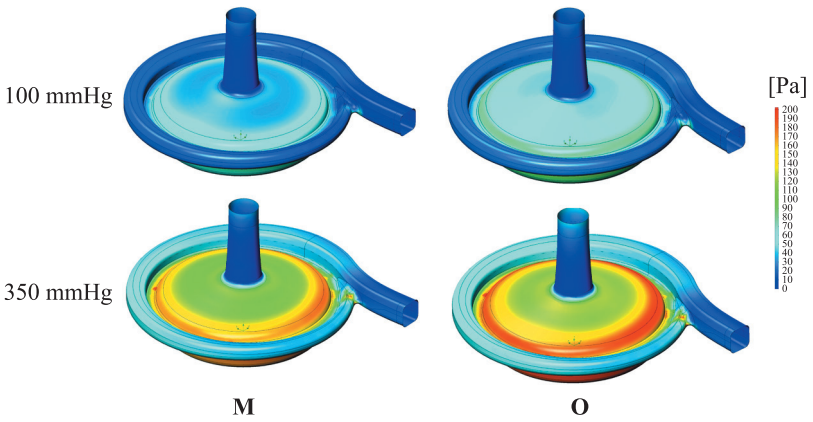

Fig. 5. Variation of tangential stress (TS) on the surface of the hull for the modified (M) and original (O) impeller designs

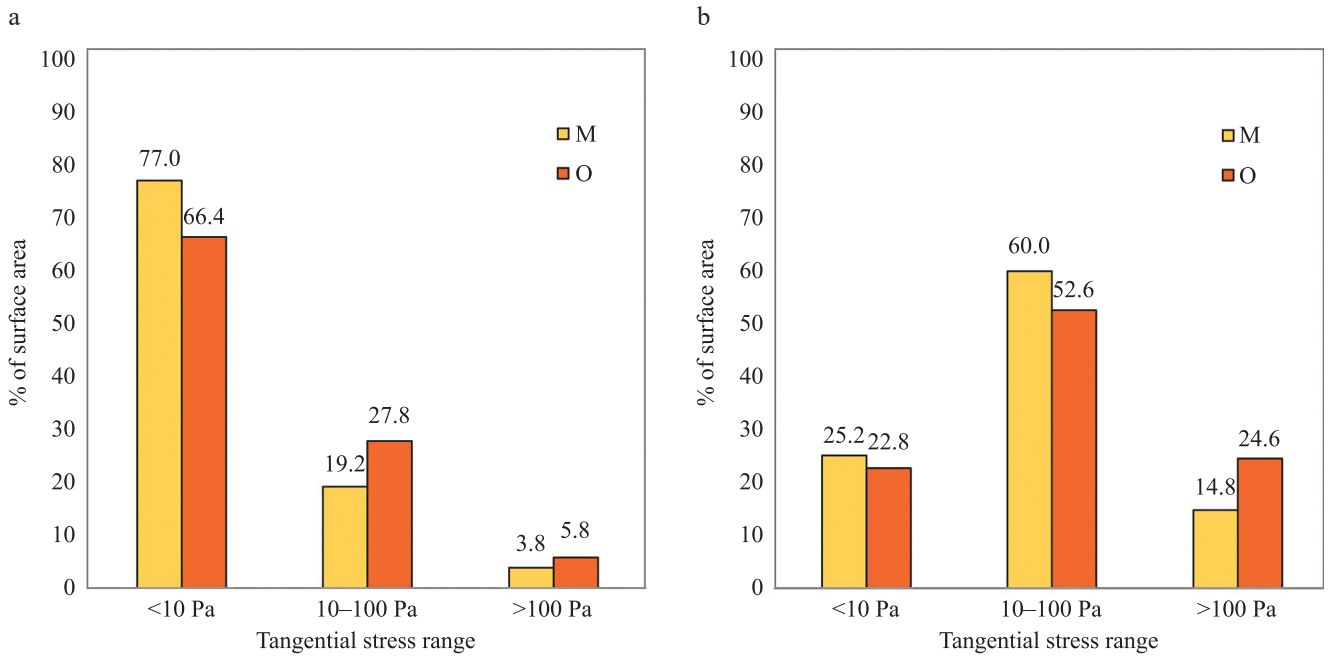

Fig. 6. Percentage distribution of tangential stress (TS) zones across three ranges in LVB mode (a) and ECMO mode (b)

Table

Hemolysis parameters of models with original (O) and modified (M) rotors

Operating conditions	Pressure 100 mmHg, flow rate 5 L/min		Pressure 350 mmHg, flow rate 5 L/min	
	O	M	O	M
Impeller rotation speed, rpm	2155	2080	3560	3475
Maximum tangential stress (TS), Pa	250	238	504	462
Average TS, Pa	38	31	78	66
Average exposure time, s	0.31	0.24	0.26	0.22
Index of hemolysis (IH) growth model [15], $\times 10^{-4}$	9.46	4.47	46.84	27.45
IH growth model [16], $\times 10^{-4}$	10.00	5.47	36.53	23.00
IH model [18], based on coefficient from [15], $\times 10^{-3}$	3.41	2.20	20.15	14.02
IH model [18], based on coefficient from [16], $\times 10^{-3}$	3.48	2.45	15.05	11.10
NIH, g/100 L	0.00093	0.00084	0.00276	0.00254
MIH	0.1845	0.1677	0.5535	0.532

Rotaflow RC. At a hydraulic point of 100 mmHg and 5 L/min, the predicted IH was 1.21×10^{-4} for the modified model versus 1.77×10^{-4} for the original. Under ECMO conditions (350 mmHg, 5 L/min), the IH was 7.93×10^{-4} and 8.35×10^{-4}, respectively.

These predictions aligned with the experimentally measured NIH and MIH. At 100 mmHg and 5 L/min, the NIH was 0.00084 g/100 L for the modified model versus 0.00093 g/100 L for the original. Under ECMO loading conditions (350 mmHg, 5 L/min), the NIH values were 0.00254 g/100 L and 0.00276 g/100 L, respectively. The comparative parameters of both models are summarized in Table.

DISCUSSION

The dynamics of the IH generated by the centrifugal pump with the new rotor demonstrate excellent performance under clinically relevant ECMO support conditions. Both wall shear stresses and hemolysis characteristics were evaluated. Computational analyses showed that the average shear stress of the modified model was consistently lower than those of the original Rotaflow pump under identical operating conditions. This reduction is attributed to the unique impeller design, which achieves the required performance at a lower rotational speed.

Shear stress analysis further confirmed that the IH level of the modified model was lower compared to the Rotaflow pump. Since the numerically calculated IH depends on both exposure time and shear stress, and given that both pumps have nearly identical priming volumes, the shorter exposure time of the modified model indicates improved washability under the same operating conditions.

Therefore, the design of Model M, characterized by reduced shear stress, is expected to lower hemolysis. This assumption, based on IH assessment methods [18, 19], was validated by the experimentally measured NIH and MIH values for both pumps.

Calculations and tests on two CP prototypes demonstrated that hydrodynamic performance can be modestly improved without a complete redesign of the CP. This means that with this modification, the rotor speed can be reduced by 70–100 rpm, resulting in a 3–5% increase in hydraulic efficiency. This improvement is attributed to the enhanced flushing effect of the six blades, which more effectively flushes the flow from the central axial zone and thereby reduce exposure time. Shorter exposure time limits the duration of stress imposed on blood cells as they traverse the pump cavity.

The data obtained allow preliminary conclusions to be drawn regarding the quality of the modified design. It was observed that as impeller speed increases, the area of red blood cell exposure above 150 Pa also expands. Under ECMO conditions, these high-shear regions occupy up to 50% of the total flow area, inevitably increasing hemolysis. Nevertheless, shear stress distribution in the modified model proved more optimal compared to the original design.

The largest high-shear regions were located at the entrances to the gaps between the impeller and the casing (Fig. 5). In these zones, red blood cells reached maximum velocity and flow density and experienced strong turbulence from intense interactions with pump walls. The highest shear stress recorded in ECMO mode reached 504 Pa and 462 Pa, respectively.

The hemolysis values obtained in the experiments can be considered overestimated, as the tests were carried out on photopolymer prototypes whose relatively high surface roughness significantly influenced the results. However, the observed dynamics of hemolysis remain informative, and at this preliminary stage they support the relevance of the proposed modifications. The modified CP demonstrated good and predictable performance, and the results of laboratory experiments correlated well with the calculated data.

CONCLUSION

Computational fluid dynamics (CFD) analysis in computer-aided design systems is becoming a key tool for evaluating medical device designs. However, this tool has inherent limitations. Shear stress distributions calculated in centrifugal pumps are useful for preliminary assessment and serve as important indicators of potential hemolysis. However, conclusions drawn from CFD analysis must also incorporate the exposure time of blood cells at the given shear stress level.

When designing ECMO pumps, two critical factors must be considered: minimizing blood trauma and maintaining a low priming volume, which is especially important in pediatric applications. The flow path must therefore include smooth transitions and a highly efficient impeller capable of operating at minimal rotational speeds and relatively low flow rates, as required for centrifugal systems. Achieving high efficiency under these conditions is challenging, and operating pumps across their entire pressure–flow range is not rational. Significant deviations from the optimal operating point inevitably reduce hydraulic efficiency and alter flow dynamics.

The proposed invention represents a new technical solution within the class of implantable blood pumps. It is industrially applicable, as the pump components have been specifically designed for manufacturability, including molding processes and simplified assembly and bonding methods.

It can be concluded that the transition to a rotor with three long and three short blades offers clear advantages. Nevertheless, the development of a full product line of pumps, capable of covering the necessary range of flows and pressures for different patients remains a priority.

The authors declare no conflict of interest.

REFERENCES

1. *Itkin GP, Bychnev AS, Kuleshov AP et al.* Haemodynamic evaluation of the new pulsatile-flow generation method *in vitro*. *The Inter-national Journal of Artificial Organs*. 2020; 43 (6): 157–164.
2. *Roberts N, Chandrasekaran U, Das S et al.* Hemolysis associated with Impella heart pump positioning: *In vitro* hemolysis testing and computational fluid dynamics modeling. *Int J Artif Organs*. 2020. Mar 4: 391398820909843. doi: 10.1177/0391398820909843.
3. *Kilic A, Nolan TD, Li T et al.* Early *in vivo* experience with the pediatric Jarvik 2000 heart. *ASAIO J.* 2007; 53 (3): 374–378. doi: 10.1097/MAT.0b013e318038fc1f.
4. *Schmid C, Tjan T, Etz C et al.* The excor device – revival of an old system with excellent results. *Thorac Cardiovasc Surg*. 2006; 54 (6): 393–399. doi: 10.1055/s-2006-924268.
5. *Liu GM, Jin DH, Jiang XH et al.* Numerical and *In Vitro* Experimental Investigation of the Hemolytic Performance at the Off-Design Point of an Axial Ventricular Assist Pump. *ASAIO J*. 2016; 62 (6): 657–665. doi: 10.1097/MAT.0000000000000429.
6. *Hastings SM, Ku DN, Wagoner S et al.* Sources of circuit thrombosis in pediatric extracorporeal membrane oxygenation. *ASAIO J*. 2017; 63: 86–92.
7. *Li P, Mei X, Ge W et al.* A comprehensive comparison of the *in vitro* hemocompatibility of extracorporeal centrifugal blood pumps. *Front Physiol*. 2023. May 9; 14: 1136545. doi: 10.3389/fphys.2023.1136545.
8. *Zhongjun WU*. US20240198080A1/ Improved centrifugal blood pump. 2024.
9. *Kuleshov AP, Itkin GP, Buchnev AS, Drobyshev AA*. Mathematical evaluation of hemolysis in a channel centrifugal blood pump. Russian Journal of Transplantology and Artificial Organs. 2020; 22 (3): 79–85. https://doi.org/10.15825/1995-1191-2020-3-79-85.
10. *Sarfare S, Ali MS, Palazzolo A, Rodefeld M, Conover T, Figliola R et al*. Computational Fluid Dynamics Turbulence Model and Experimental Study for a Fontan Cavopulmonary Assist Device. *J Biomech Eng*. 2023 Nov 1; 145 (11): 111008. doi: 10.1115/1.4063088.
11. *Lomakin AA.* Tsentrobezhnye i osevye nasosy. 2-e izd. pererab. i dop. M.–L.: Mashinostroenie, 1966; 364.
12. *Gross-Hardt S, Hesselmann F, Arens J et al*. Low-flow assessment of current ECMO/ECCO2R rotary blood pumps and the potential effect on hemocompatibility. *CritCare*. 2019; 23: 348.
13. *Fiusco F, Broman LM, Prahl Wittberg L.* Blood Pumps for Extracorporeal Membrane Oxygenation: Platelet Activation During Different Operating Conditions. *ASAIO J*. 2022; 68 (1): 79–86. doi: 10.1097/MAT.0000000000001493.
14. *Giersiepen M, Wurzinger LJ, Opitz R, Reul H*. Estimation of shear-related blood damage in heart valve prostheses – *in vitro* comparison of 25 aortic valves. *Int J Artif Organs.* 1990; 13: 300–306.
15. *Thamsen B, Blümel B, Schaller J et al*. Numerical analysis of blood damage potential of the HeartMate II and HeartWare HVAD rotary blood pumps. *Artificial Organs*. 2015; 39 (8): 651–659.
16. *Heuser G, Opitz R.* A Couette viscometer for short time shearingof blood. *Biorheology.* 1980; 17: 17–24.
17. *Leverett L et al.* Red Blood Cell Damage by Shear Stress. *Biophysical Journal*. 1972; 3 (12): 257–273.
18. *Fang P, Du J, Yu S.* Effect of the Center Post Establishment and Its Design Variations on the Performance of a Centrifugal Rotary Blood Pump. *Cardiovasc Eng Technol*. 2020; 11 (4): 337–349. doi: 10.1007/s13239-020-00464-0.

The article was submitted to the journal on 23.06.2025

DOI: 10.15825/1995-1191-2025-3-125-133

OPTIMIZATION OF IMPELLER DESIGN IN THE ROTAFLOW CENTRIFUGAL PUMP

A.P. Kuleshov, N.V. Grudinin, A.S. Buchnev

Shumakov National Medical Research Center of Transplantology and Artificial Organs, Moscow, Russian Federation

As part of the development of a domestic counterpart, the impeller of the RotaFlow centrifugal pump (Maquet, Germany) was modernized within the framework of research into the operating conditions of centrifugal pumps used in extracorporeal membrane oxygenation (ECMO) therapy. A novel rotor impeller design was proposed, featuring two types of blades: the primary elongated blades responsible for generating most of the pressure, and secondary shortened auxiliary blades. A three-dimensional computational model of the RotaFlow pump was created incorporating the redesigned impeller. To evaluate the effectiveness of the modernization, the new design was compared to the original Maquet impeller. Computational simulations were conducted to analyze key fluid dynamics parameters, such as turbulence intensity and flow velocity, within the typical operating range of the pump (flow rates from 1 to 5 L/min at a pressure drop of 350 mmHg). Mathematical modeling demonstrated that the new blade configuration yields improved flow characteristics compared to the original design.

Keywords: 3-dimensional computer model, centrifugal pump, turbulence, impeller.

INTRODUCTION

Although ECMO pumps are designed for specific flow rates and pressures, in practice they are frequently used across a wide range of hemodynamic conditions. In certain clinical scenarios, these pumps must generate high pressures of 300–400 mmHg to overcome the resistance of the oxygenator membrane and deliver flow rates of up to 5 L/min to meet the patient's needs [1].

Centrifugal pumps commonly used in ECMO are compact, with impeller diameters not exceeding 50 mm, such as the RotaFlow (Maquet, Germany) [2], CentriMag (USA) [3], and Deltastream Medos (Germany) [4]. However, reducing impeller size inevitably requires higher rotational speeds and results in larger incremental changes when adjusting hemodynamic parameters. Empirical data indicate that halving the impeller diameter reduces efficiency by 5–10 percentage points [5], largely due to altered surface area–to–volume ratios and increased hydraulic losses.

Small pumps are often operated in ECMO at minimal flow rates, even though they are designed for higher operating points. This mismatch reduces efficiency and increases turbulence and stagnant flow zones, as blood spends more time within the pump. Operating outside the intended range of application further decreases efficiency and, at higher speeds, prolongs blood exposure to shear stress, thereby exacerbating hemolysis [6].

Shear stress and increased blood exposure time dramatically elevate hemolysis, while the thrombogenic potential of ECMO circuits is also attributed to mechanical factors that trigger biochemical cascades. Hastings et al. [7] investigated thrombus formation *in vivo*, showing that the centrifugal pump, tubing, and connectors are the main contributors to thrombogenesis within ECMO systems.

Today, evaluation methods allow for pump performance testing not only under validated conditions for left ventricular bypass (LVB) [8–10], but also under ECMO-specific conditions [11]. Importantly, pumps optimized for favorable flow characteristics in LVB may not demonstrate comparable performance in ECMO, underscoring the limitations of their universal application.

The most appropriate solution would be the development of a range of pumps tailored to specific applications, with effective flow and pressure ranges designed for different clinical modes and compatible with oxygenators of varying resistance. An example of this approach is the Jarvik family of implantable systems [12]. However, such specialization is prohibitively expensive, and in practice, pumps continue to be used as universal components across all ECMO operating modes.

A more feasible alternative is to optimize or redesign the pump impeller. The goal of such improvements is either to reduce rotational speed while maintaining the required pressure and flow, or to enhance fluid dynamics within the pump, thereby shortening blood exposure time. In this study, we propose a method for optimizing the RotaFlow pump impeller. The modification reduces hemolysis by lowering the impeller's rotational speed and improves overall pump performance under high-load conditions.

Corresponding author: Arkady Kuleshov. Address: 1, Shchukinskaya str., Moscow, 123182, Russian Federation. Phone: (915) 292-47-98. E-mail: ilovemylene@yandex.ru

MATERIALS AND METHODS

The following section provides an overview of the process used to upgrade the rotor of a RotaFlow pump. The initial stage involved scanning the pump components to reconstruct a detailed 3D model. Scanning was performed using a 3DMakerpro Seal 3D scanner (China), achieving an accuracy of 0.01 mm. Based on the scanned images, sketches and 3D designs of each component were created individually. The final pump assembly was rendered in the SolidWorks PhotoView 360 graphics module, where materials and textures were applied. The resulting model of the pump is shown in Fig. 1.

The pump rotor is divided into two elements: cap and impeller. The impeller, in turn, consists of blades specifically designed to generate pressure while minimizing shear stress on the blood flowing through the pump. This model consists of a combination of two types of blades: a primary elongated blade and an secondary shortened blade. This configuration aims to reduce hemolysis by improving flow distribution and lowering localized shear stresses. An example of the conversion from the original impeller design to the optimized configuration is shown in Fig. 2.

The blade combination incorporates an equal number of each blade type – three primary elongated blades and three secondary shortened blades – arranged alternately on the cap to ensure sectoral symmetry. Each primary blade is positioned 50° behind the subsequent secondary blade in a clockwise direction. The secondary blade is a truncated version of the primary blade, with its length reduced to one-third of the primary blade.

Both blade types feature a streamlined profile, constructed using a simplified geometric method in which the blades are defined along a circular arc. This profile was further optimized through computational hydrodynamic modeling to minimize shear stress on the blood as it passes through the device.

The process of creating the impeller is illustrated in Fig. 3, which presents a schematic drawing of the blade construction and the profile of the central arc.

The blade construction proceeds as follows. Circles 1 and 2 are drawn at the beginning and end of the blade, with diameters D_1 and D_2, respectively. On the end circle (2), point A is selected and connected to the circle center O. From radius OA, an angle equal to the sum of the inlet (β_1) and outlet (β_2) blade angles is measured. At this angle, draw radius OB on the starting circle (1). The intersection of segment OB with circle (1) defines point C. A ray is then drawn through points A and C until it intersects the wheel inlet circle at point D. Point D represents the starting point of the blade, while point A is its endpoint. From A, a ray is drawn at an angle β_2 relative to AO, measured counterclockwise. From the midpoint E of segment AD, a perpendicular is dropped, intersecting the ray from A at point O_1. Point O_1 becomes the arc center, with segments AO_1 and EO_1 equal to the blade arc radius R_L. With O_1 as the center, arc AD is drawn, forming the centerline of the blade profile. Conventionally, arc AD is taken as the blade length. Under

Fig. 1. Reconstructed 3D model of the RotaFlow pump (Maquet, Germany)

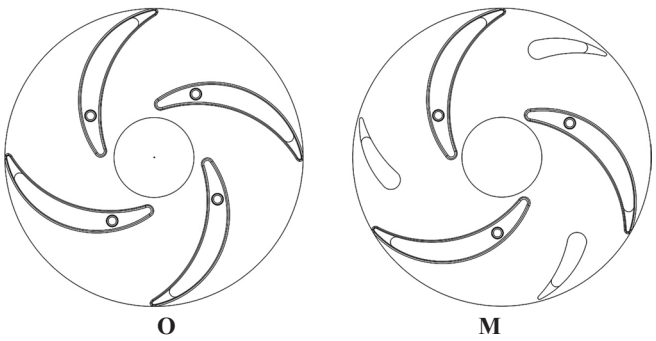

Fig. 2. Impeller blade profiles of the original (O) and modified (M) RotaFlow pump designs

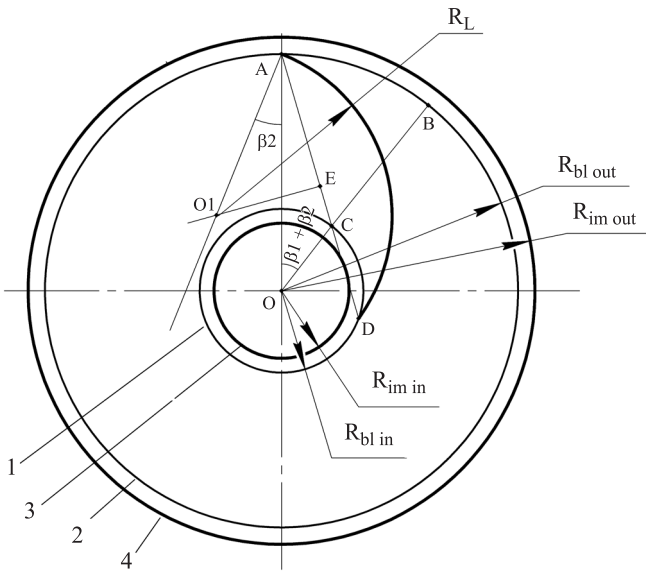

Fig. 3. Structural design of the main blade in the modified RotaFlow pump impeller. Abbreviations: $R_{bl\ in}$, inlet blade radius; $R_{im\ in}$, inlet impeller radius; $R_{bl\ out}$, outlet blade radius; $R_{im\ out}$, outlet impeller radius

boundary conditions, the blade tip circle and blade root circle coincide with the rotor inlet diameter (3) and the rotor diameter (4). In this case, the radius of the wheel blades is determined by formula (1):

$$R_L = \frac{\left(\frac{D_2}{2}\right)^2 - \left(\frac{D_1}{2}\right)^2}{D_2 \cdot \cos\beta_2 - D_1 \cdot \cos\beta_2}. \quad (1)$$

The profiles of the inner and outer walls of the main blade were constructed using the same geometric method, with parameter adjustments applied to define the blade thickness (Fig. 3, b). In the example shown, the middle arc of the blade was designed with an inlet angle (β_1) of 33° and an outlet angle (β_2) of 22° for the modified model. In practice, the inlet and outlet angles can vary between 10° and 60°, depending on hydrodynamic calculations tailored to the specific operating conditions of the device.

The additional blade was constructed using the same method as the main blade, but with the arc length reduced to one-third of the main blade's arc. Among several design variations tested, the ⅓ length ratio provided the optimal performance, outperforming both shorter (¼) and longer (½) blade ratios.

Each blade includes a localized thickening at the midpoint of the curvature, with a maximum thickness of no more than 4 mm. This corresponds to approximately 1.5–2 times the thickness at the trailing edge.

Computational fluid dynamics (CFD) analysis

The geometries of the two pumps, reconstructed from measurements of actual device components, were converted into CAD format for export to computer-aided design systems. Numerical simulations of flow inside the three pump configurations were performed using a commercial computational fluid dynamics (CFD) package FLUENT 14.2 (ANSYS Inc., Canonsburg, Pennsylvania). Both structured and unstructured meshes were employed to compute flow fields, with details of the meshing procedure available in [13].

Flow distribution was obtained by numerically solving the governing fluid dynamics equations using an unstructured finite-volume mesh in FLUENT 14.2. Zero-pressure and high-pressure boundary conditions were applied at the pump inlet and outlet, respectively, corresponding to the pressure head the pump is expected to overcome at a given rotational speed. Pump walls were assumed rigid, with a specified roughness of 5 μm, representative of die-cast surface quality.

Blood was modeled as an incompressible Newtonian fluid, with a density of 1060 kg/m^3 and a viscosity of 0.003763 Pa·s [14]. The standard k-ε turbulence model was applied to solve the flow equations. Simulations were performed at pump rotation speeds of 2000, 2500, 3000, and 3500 rpm. Solution convergence was defined at 10^{-4}.

For both the computational model and the physical mock-up, the rotor speed range was set between 1100 and 3500 rpm. In the numerical model, a minimum mesh element size of 50 μm (tetrahedral elements) was applied. This resolution provided a balance between accuracy and computational efficiency, allowing simulations to be performed with less time and software resources.

Modeling of flow and head-capacity curve (HCC) characteristics

The head-capacity curve of two impeller designs – the original and the modified – were evaluated using the frozen rotor method. At the pump inlet, the pressure was set to 1 mmHg, while the outlet pressure was adjusted to achieve flow rates ranging from 1 to 5 L/min. Minimum turbulence conditions were imposed at the inlet, with an intensity of 1% and a turbulence scale of 0.1 mm.

Simulation and analysis of flow in ECMO operating mode were carried out under slightly modified boundary conditions. In this case, pressure–flow characteristics were assessed for both pumps at an outlet pressure of 350 mmHg, with flow rates of 1, 3, and 5 L/min. To account for increased turbulence under these operating conditions, the inlet turbulence parameters were doubled, which now had the following values.

Under these conditions, the flow distribution and turbulence parameters (turbulence intensity and turbulence scale) were evaluated across different areas of the pump, including the horizontal section of the rotor. Analytical comparisons of turbulence patterns between the two impeller designs were then performed.

A numerical assessment of turbulence was conducted using the Reynolds number (Re). The highest flow velocities were observed at the outlet of the rotor channels, while lower velocities were detected at the pump inlet and outlet regions. The Reynolds number was calculated for the flow domain based on simulation data and using formula (2):

$$Re_{imp} = \frac{2r^2\omega}{\upsilon},$$
$$\upsilon = \eta/\rho, \quad (2)$$

where dynamic viscosity $\eta = 0.0035$ kg·m^{-1}·s^{-1}; blood density $\rho = 1050$ kg·m^{-3}; ω – permissible maximum rotor angular velocity; r – rotor radius.

RESULTS

Hydrodynamic characteristics

The CFD models were evaluated by comparing the numerically predicted head of the original rotor design with that of the optimized design. The pressure–flow relationships are presented in Fig. 4.

In the graphs, solid lines correspond to the four-bladed rotor prior to modification, while dashed lines represent simulation data for the redesigned rotor with

three long and three short blades. The line colors indicate the specified pump rotational speed. An increase in head is observed when the rotor is optimized.

Turbulence and flow distribution

Fig. 5 illustrates fluid motion in the transverse axial section of the volute at the rotor outlet. The flow struc-

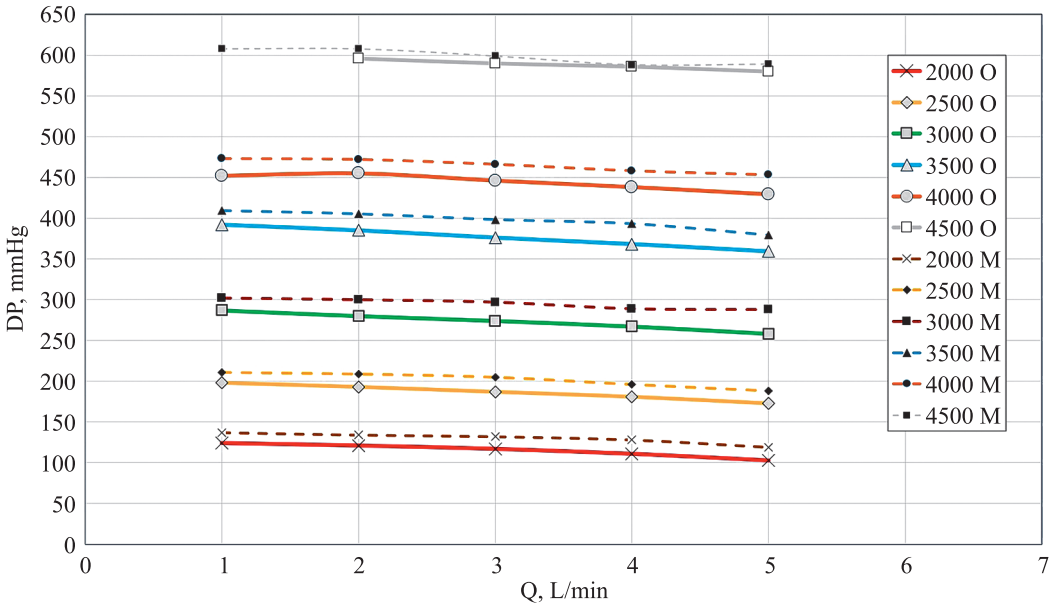

Fig. 4. Measurement of the Rotaflow pump's head-capacity curve (HCC). Solid lines represent the original rotor, dashed lines correspond to the modified rotor

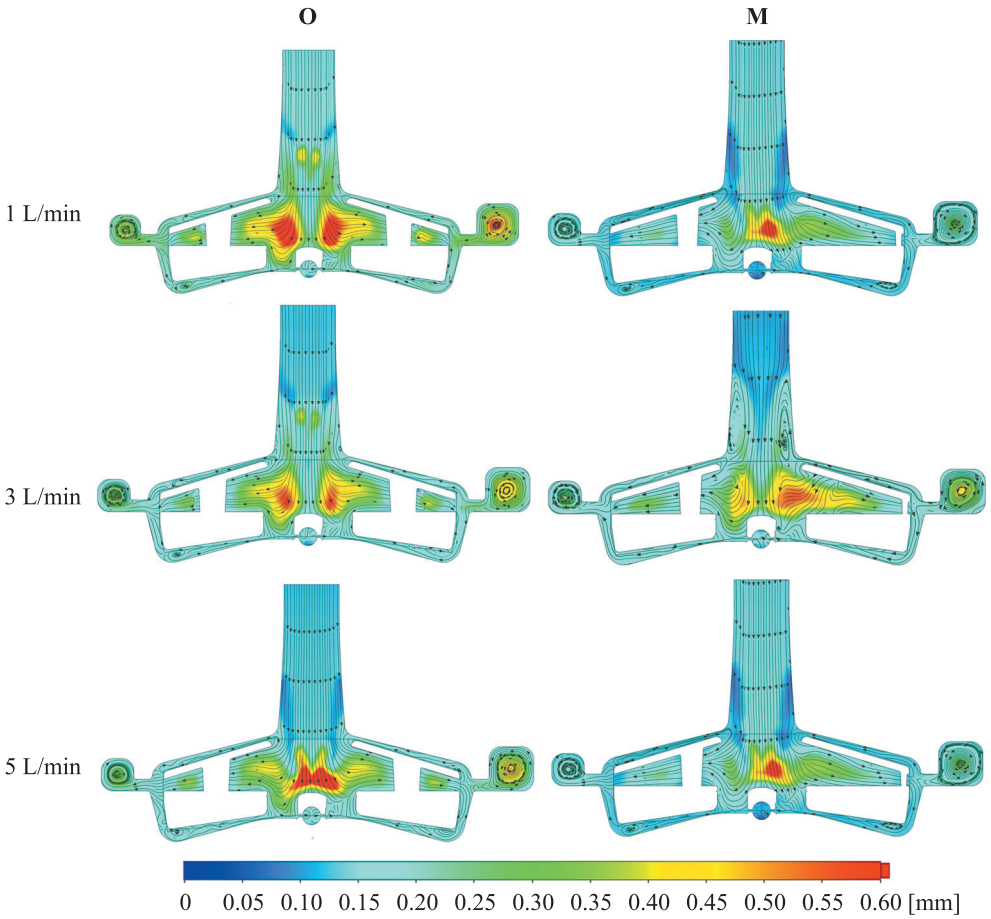

Fig. 5. Distribution of turbulence intensity in a cross-sectional view of the pump, comparing the original (O) and modified (M) impeller designs

ture in the section perpendicular to the radial stream exhibits a symmetrical vortex that fills the entire outlet area. The color scale indicates turbulence levels (scale and intensity) at flow rates of 1, 3, and 5 L/min. Velocity distributions in the longitudinal section are shown in Fig. 6.

Table 1 presents the numerical changes in flow structure, highlighting the dynamics of blood flow improvement achieved with the optimized impeller design. Key turbulent flow parameters – scale, intensity, and exposure time – were analyzed.

A numerical assessment of turbulence was also performed using the Reynolds number (Re). The highest flow velocities were observed at the outlet of the rotor channels, while significantly lower velocities were recorded at both the pump inlet and outlet regions.

DISCUSSION

The calculations and experimental tests of the two centrifugal pump samples demonstrated that hydrodynamic performance can be moderately improved without the need for a complete redesign of the pump. The head-capacity curve of the optimized rotor maintained flat flow characteristics up to 5 L/min, consistent with typical centrifugal pump behavior, while the average pressure at a fixed rotational speed increased by 80–90 mmHg.

This improvement allows the rotor speed to be reduced by 70–100 rpm, resulting in an increase in hydraulic efficiency of approximately 3–5%. In addition, the six-blade configuration enhanced flushing of the central axial zone, thereby reducing exposure time. The maximum particle passage time decreased by 0.10–0.15 seconds.

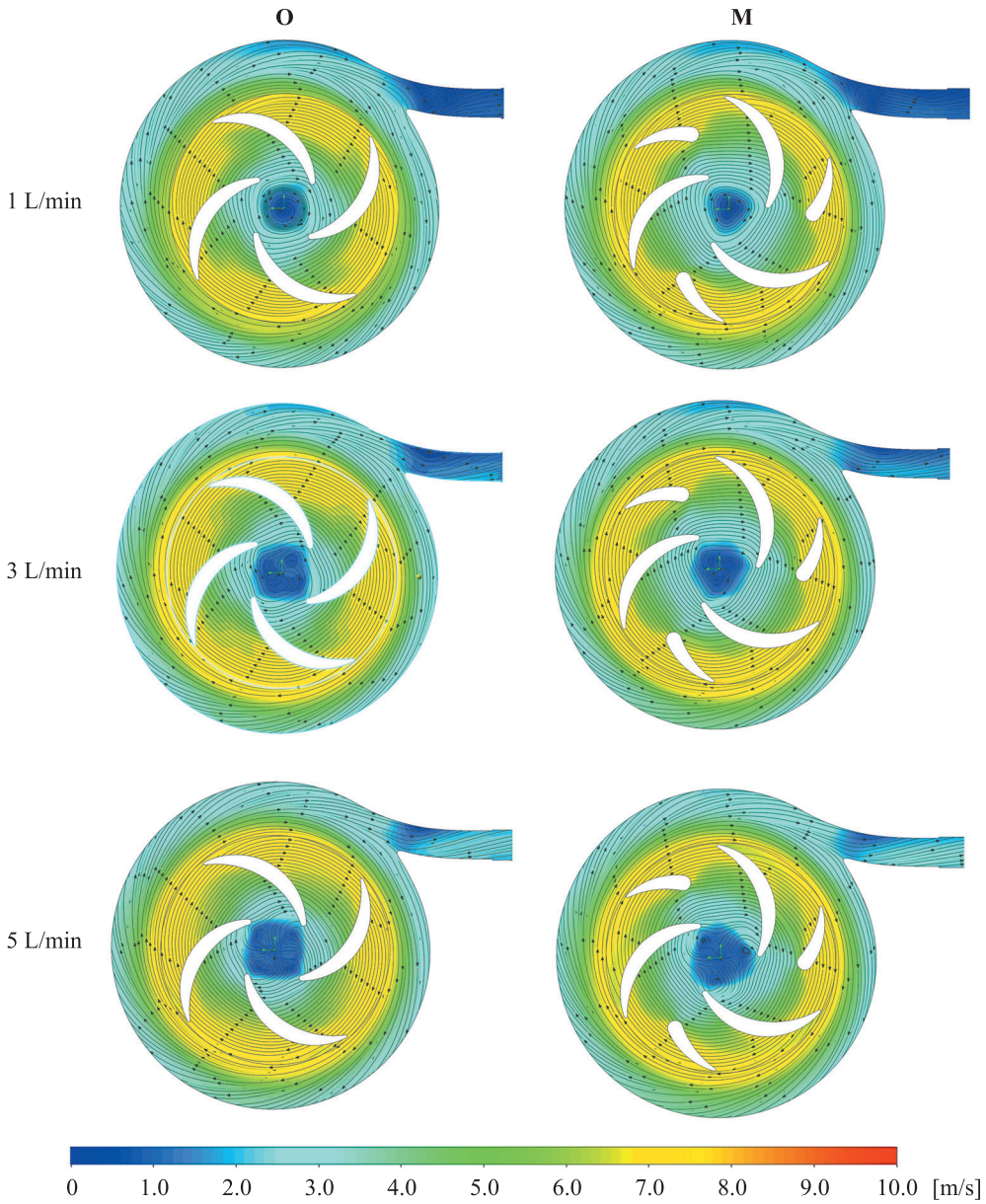

Fig. 6. Distribution of flow velocities in the longitudinal section of the pump with the original (O) and modified (M) impeller designs. Zones of active turbulence and flow stagnation are highlighted

Flow visualization showed a reduction in turbulence scale, with vortex size decreasing in the optimized model. At the same time, the average flow velocity and the number of visible vortices were moderately reduced. Collectively, these changes may contribute to a slight reduction in the overall mechanical load on blood cells.

A critical factor in optimizing centrifugal pump performance is maintaining smooth velocity transitions between surfaces in the flow region to minimize turbulence. This effect is evident in Figs. 5 and 6. While high Reynolds numbers were observed in both rotor models, the values were approximately 500 points lower in the modified design.

The distribution patterns of flow velocity vectors and turbulence parameters indicated turbulence at the rotor outlet and at the junction where channel flows entered the spiral volute. However, cross-sectional velocity vector plots showed a more balanced and uniform flow in the optimized rotor, contributing to reduced energy loss and lower shear stress.

Clear differences also emerged in the recirculation patterns at different flow rates. In both rotor models, decreasing flow rate led to the formation of recirculation zones at the junction of the spiral volute and the outlet tract, associated with a sharp edge commonly referred to as the “tongue”. Notably, this recirculation zone was significantly larger in the original model, resulting in increased exposure time.

At higher rotational speeds and reduced flow rates, mutually oriented vortices, identified as Taylor–Couette vortices, were observed in both designs within the upper and lower gaps between the rotor and the housing (Fig. 7).

Analysis revealed that vortices at the blade tips were more pronounced in the original rotor compared to the modified design. This effect is attributed to the lower flow velocity and higher impeller rotation speed.

At low flow rates, the maximum number of particle trajectories with prolonged exposure times was observed. Under these conditions, particles tended to remain longer in the pump volute, with up to 30% of total trajectories

Table 1

Flow parameters of the pump with the original and modified impeller designs

Flow parameters	(Pressure 350 mm Hg, flow rate 1 L/min)		(Pressure 350 mm Hg, flow rate 3 L/min)		(Pressure 350 mm Hg, flow rate 5 L/min)	
Model	Original	Modified	Original	Modified	Original	Modified
Impeller rotation speed, rpm	3470	3375	3535	3445	3595	3505
Turbulence scale, mm (avg./max.)	0.37 / 0.70	0.44 / 0.68	0.33 / 0.62	0.26 / 1.03	0.71 / 1.02	0.71 / 1.2
Turbulence intensity, %	40 / 211	20 / 118	18 / 247	30 / 223	13 / 474	15 / 823
Exposure time, sec (avg./max.)	0.53 / 0.87	0.32 / 0.51	0.28 / 0.438	0.3 / 0.45	0.27 / 0.34	0.31 / 0.41
Maximum speed, m/s	3.5 / 9.0	3.4 / 8.9	3.6 / 9.3	3.6 / 9.0	3.4 / 9.2	3.5 / 9.1
Reynolds number	25505	25034	26026	25322	26243	25531

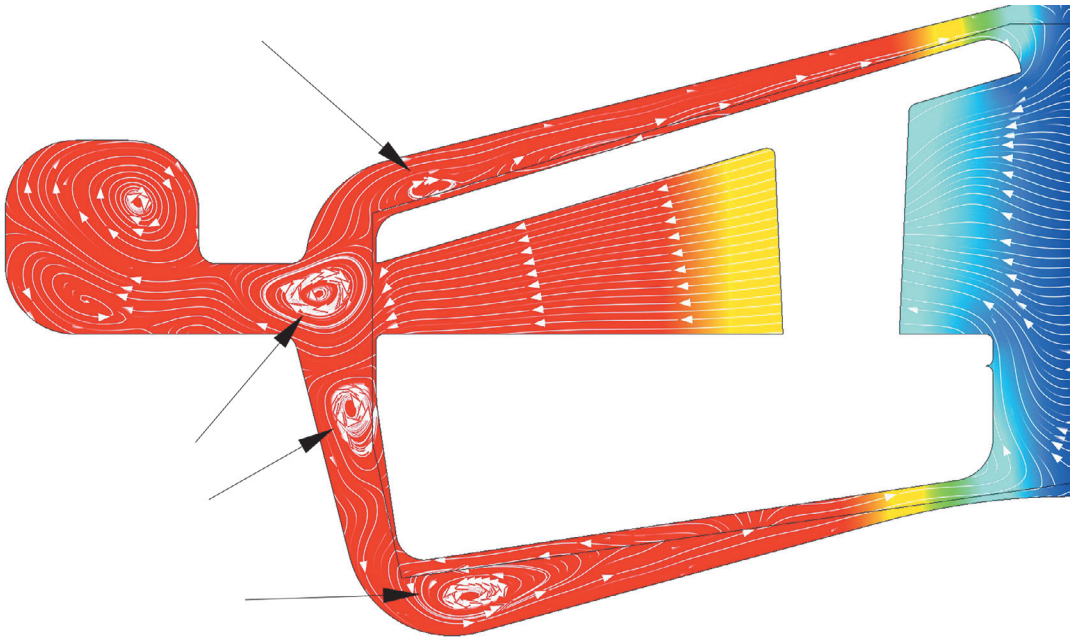

Fig. 7. Formation of Taylor–Couette vortices in the flow path of the pump at a flow rate of 1 L/min

entering recirculation zones. The presence of Taylor–Couette vortices substantially increased the residence time of particles, as these vortical structures promoted reverse flow and swirling motion. This reverse swirling was especially evident in the inlet pipe near the wall (Fig. 7).

To validate these findings, additional simulations were performed using both water and Newtonian blood models. The reverse flow phenomenon was consistently observed at 1 L/min and persisted at 3 L/min. However, at 5 L/min, the phenomenon was absent.

Pump efficiency is a key economic and technological parameter. Modern standards require that centrifugal pumps achieve a minimum efficiency of at least 65% at nominal load to ensure energy-efficient operation. In ECMO systems, however, this indicator decreases sharply due to the necessity of miniaturization.

According to an empirical rule, pump efficiency is strongly dependent on impeller size. For geometrically similar pumps, doubling the impeller diameter increases efficiency by 5–8 percentage points [5]. This is due to changes in the surface-area-to-volume ratio and the resulting reduction in relative hydraulic losses, and is explained by efficiency gain formula (3):

$$\Delta\eta \approx 6\% \cdot \log(D_1/D_2), \quad (3)$$

where D_1 and D_2 are rotor diameters before and after modification. Similarly, an increase in pump flow rate contributes positively to efficiency, as shown by ratio (4):

$$\eta_{max} \approx 0.8 + 0.0323 \cdot \log(Q), \quad (4)$$

where Q is volumetric flow rate [m^3/h]. An empirical rule for the practical application of affinity laws states that a 10% increase in speed results in an approx. 10% increase in flow and a 21% increase in pressure; a 10% decrease in speed reduces the flow by 10% and the pressure by 19% [5]. The modified rotor design leveraged these principles. Although the rotor speed was reduced, the improved impeller geometry preserved both flow rate and pressure head. Consequently, the rotor modifications resulted in a slight increase in overall system efficiency, as summarized in Table 2.

Table 2

Comparison of pump efficiency using the original and modified rotor designs

	Efficiency, %	
Rotor	Original	Modified
Flow rate 1 L/min	47.7	48.3
Flow rate 3 L/min	39.7	40.2
Flow rate 5 L/min	14.0	15.2

CONCLUSION

The laws of affinity for centrifugal pumps are valid within approximately ±30% of the nominal rotational speed, with an accuracy of about 5%. However, when designing pumps for ECMO applications, other factors become equally critical, particularly blood trauma and low priming volume, which are especially important in pediatric use.

To address these requirements, the flow path must incorporate smooth geometric transitions and a highly efficient impeller that operates effectively at minimum speeds and relatively low flow rates. These conditions, however, make it inherently difficult to achieve the high efficiencies typically expected of centrifugal systems. Furthermore, it is not practical to operate pumps across their entire HCC range, since large deviations from the design operating point inevitably result in loss of hydraulic efficiency and unstable flow regimes.

The results of this study demonstrate that transitioning to a rotor design with three long and three short blades offers clear advantages, including improved hydrodynamics and reduced shear stress. Nonetheless, the development of a line of pumps that can cover the flow and pressure range for different patient populations remains essential.

The authors declare no conflict of interest.

REFERENCES

1. *Gautier SV, Poptsov VN, Spirina EA*. Ekstrakorporal'naya membrannaya oksigenatsii kardiokhirurgii i transplantologii. M.: Triada, 2013; 272.
2. *Orime Y, Shiono M, Yagi S.* Jostra Rota Flow RF-30 Pump System: A New Centrifugal Blood Pump for Cardiopulmonary BypassCEntrimag. *Artificial Organs*. 2000; 24 (6): 437–441.
3. *Nagaoka E et al.* MedTech Mag-Lev, single-use, extracorporeal magnetically levitated centrifugal blood pump for mid-term circulatory support. *ASAIO J*. 2013. 59: 246–252.
4. *Fleck T, Benk C, Klemm R et al.* First serial *in vivo* results of mechanical circulatory support in children with a new diagonal pump. *Eur J Cardiothorac Surg*. 2013; 44 (5): 828–835. doi: 10.1093/ejcts/ezt427.
5. *Karelin VYa, Minaev AV.* Nasosy i nasosnye stantsii. M.: Stroyizdat, 2016; 320.
6. *Liu GM, Jin DH, Jiang XH et al.* Numerical and *In Vitro* Experimental Investigation of the Hemolytic Performance at the Off-Design Point of an Axial Ventricular Assist Pump. *ASAIO J*. 2016; 62 (6): 657–665. doi: 10.1097/MAT.0000000000000429.
7. *Hastings SM, Ku DN, Wagoner S et al.* Sources of circuit thrombosis in pediatric extracorporeal membrane oxygenation. *ASAIO J*. 2017. 63: 86–92.
8. *Buchnev AS, Kuleshov AP, Esipova OYu, Drobyshev AA, Grudinin NV*. Hemodynamic evaluation of pulsatile-flow generating device in left ventricular assist devices. *Russian Journal of Transplantology and Artificial Organs*. 2023; 25 (1): 106–112. https://doi.org/10.15825/1995-1191-2023-1-106-112.

9. *Itkin GP, Bychnev AS, Kuleshov AP et al.* Haemodynamic evaluation of the new pulsatile-flow generation method *in vitro*. *The International Journal of Artificial Organs*. 2020; 43 (6): 157–164.
10. *Roberts N, Chandrasekaran U, Das S et al.* Hemolysis associated with Impella heart pump positioning: *In vitro* hemolysis testing and computational fluid dynamics modeling. *Int J Artif Organs*. 2020. Mar 4: 391398820909843. doi: 10.1177/0391398820909843.
11. *Li P, Mei X, Ge W et al.* A comprehensive comparison of the *in vitro* hemocompatibility of extracorporeal centrifugal blood pumps. *Front Physiol*. 2023. May 9; 14: 1136545. doi: 10.3389/fphys.2023.1136545.
12. *Kilic A, Nolan TD, Li T et al.* Early *in vivo* experience with the pediatric Jarvik 2000 heart. *ASAIO J*. 2007; 53 (3): 374–378. doi: 10.1097/MAT.0b013e318038fc1f.
13. *Tanikawa C, Kamatani Y, Terao C et al.* Risk Loci Identified in a Genome-Wide Association Study of Urolithiasis in a Japanese Population. *J Am Soc Nephrol*. 2019; 30 (5): 855–864. doi: 10.1681/ASN.2018090942.
14. *Fiusco F, Broman LM, Prahl Wittberg L.* Blood Pumps for Extracorporeal Membrane Oxygenation: Platelet Activation During Different Operating Conditions. *ASAIO J*. 2022; 68 (1): 79–86. doi: 10.1097/MAT.0000000000001493.

The article was submitted to the journal on 5.06.2025

DOI: 10.15825/1995-1191-2025-3-134-145

BIBLIOMETRIC ANALYSIS OF RESEARCH ON THE USE OF MESENCHYMAL STEM CELLS IN ACUTE AND CHRONIC LIVER DISEASES

M.Yu. Shagidulin[1, 2], N.A. Onishchenko[1], A.I. Kostysheva[2], I.A. Lychagin[2], A.O. Nikolskaya[1], S.V. Gautier[1, 2]

[1] Shumakov National Medical Research Center of Transplantology and Artificial Organs, Moscow, Russian Federation

[2] Sechenov University, Moscow, Russian Federation

Objective: to conduct a comprehensive bibliometric analysis of publications from 2008 to 2024 on the problem of cell therapy for liver diseases using mesenchymal stem cells (MSCs) with stem-like properties, with the goal of identifying new ways to tackle this problem. **Materials and methods.** A bibliometric analysis was carried out using the Scopus electronic database. The search included article titles, abstracts, and keywords. The dataset was exported in BibTeX and CSV formats for compatibility with VOSviewer and R software. Data were analyzed using R (version 4.4.2) and visualized through the Bibliometrix online analytical platform and VOSviewer (version 1.6.20). **Results.** The analysis identified four distinct periods of publication activity reflecting the evolution of research into the use of MSCs for liver regeneration in cases of liver injury. Period 1 (2008–2012) – This phase was marked by exploratory studies investigating the therapeutic potential of MSCs derived from various sources, including bone marrow, adipose tissue, and umbilical cord cells. Early findings highlighted the promise of MSC-based therapy and underscored the need for more rigorous and targeted research. Period 2 (2013–2016) – During this period, research focused on elucidating the mechanisms underlying the regulatory and regenerative effects of MSCs on damaged organs. Significant progress was made in the field of tissue engineering, aimed at enhancing the survival and functional integration of apoptotic MSCs post-transplantation. Period 3 (2017–2020), and more notably period 4 (2021–2024), were marked by the expansion, deepening, and intensification of research into the properties of apoptotic MSCs. Particular emphasis was placed on the regulatory functions and therapeutic potential of their secreted paracrine and trophic factors – specifically exosomes, extracellular vesicles, and apoptotic bodies. **Conclusion.** This bibliometric analysis has outlined key directions for further research in the development and application of cell technologies, particularly the use of MSCs in regenerative medicine. Future studies will likely focus on identifying the most active paracrine and trophic factors, elucidating their chemical structures and biological functions, and subsequently manufacturing chemical and pharmaceutical agents with bioactive regenerative properties. Such advancements would help standardize the production of MSC-based therapeutics and increase their availability for clinical use. Moreover, the bibliometric approach applied in this study can serve as a valuable tool for tracking and forecasting trends in related biomedical research fields.

Keywords: mesenchymal stromal cells, transplantation, stem cells, chronic liver disease, liver failure, fibrosis, cirrhosis, regenerative medicine, bibliometric analysis.

INTRODUCTION

The problem of treating chronic liver failure remains unresolved worldwide. Mortality reaches approximately 2 million people annually (about 4% of all deaths), with severe liver failure due to fibrosis or cirrhosis accounting for nearly 50% of these cases [1]. Liver cirrhosis is currently the 11th leading cause of death globally, while liver cancer ranks 16th; together, they represent 3.5% of all deaths worldwide. Cirrhosis also ranks among the top 20 causes of disability and accounts for 2.1% of disability worldwide [2].

At the current stage of medical therapeutic options, this problem can be definitively addressed only by donor liver transplantation [2–5]. Meanwhile, the persistent shortage of donor organs and the steadily increasing number of patients requiring liver transplantation severely limit access to this method. Given the limited efficacy of available medications and antifibrotic therapies, there is ongoing interest in developing more accessible, physiological, and effective approaches – particularly those that can stimulate the patient's own regenerative capacity of the liver.

Corresponding author: Murat Shagidulin. Address: 1, Shchukinskaya str., Moscow, 123182, Russian Federation. Phone: (499) 196-87-90. E-mail: dr.shagidulin@mail.ru

The use of mesenchymal stromal cells (MSCs) with stem cell properties isolated from autologous or allogeneic human tissues has become a promising new therapeutic strategy that has been developed worldwide since the last third of the 20th century.

Research into the therapeutic potential of MSCs in liver diseases is still ongoing. However, we were unable to find any studies that highlight and evaluate the trends and patterns of further development of biomedical research in this field in the 21st century, which could bring us closer to solving the problem of cell therapy and make MSCs and MSC-derived products widely available in clinical practice.

The objective of this work is to conduct an comprehensive bibliometric analysis of published studies conducted over the past 16 years (2008–2024) on the problem of cell therapy for liver diseases using MSCs in order to identify possible new ways to tackle this problem.

MATERIALS AND METHODS

In this study, a bibliometric (quantitative) analysis was performed using a comprehensive set of methods aimed at describing the current state, identifying research trends, and projecting future directions in global scientific work on the use of MSCs in the treatment of liver diseases over the past 16 years (2008–2024). The analysis was conducted using the Scopus electronic database, which offers extensive metadata (authors, keywords, countries, citations, etc.) and enables dynamic and detailed bibliometric evaluation over time (years).

The search was performed by abstract, article title, and keywords using the following query: (“hepatic*” OR “liver*”) AND (“mesenchymal stem cell*” OR “mesenchymal stromal cell*”). To assess the proportion of clinical studies within the initial dataset, an additional query was applied using the terms: treatment or case report or treat or clinical trial.

The search was carried out on December 24, 2024, and all files were downloaded on the same day to avoid discrepancies related to daily database updates. Complete publication records and cited references were exported in both BibTeX and CSV formats (the Scopus interface allows export in several formats: text, CSV, and BibTeX). The BibTeX file was imported into R software (version 4.4.2) and then into the online analytical platform Bibliometrix (https://www.bibliometrix.org), as described in [6]. To visually construct tag clouds (keywords), the CSV file was imported into VOSviewer (version 1.6.20, https://www.vosviewer.com) [7].

The dataset was filtered using the following criteria: document type (article), publication period (2008–2024), with no restrictions on language or country of publication.

While working on the Bibliometrix platform, a bibliometric analysis was carried out, beginning with general descriptive statistics. The analysis initially focused on the core bibliometric indicators reported by the original authors and then expanded to include country-specific metrics. Each of the major categories was examined in detail, including: annual scientific output; publication sources; number of articles per author; frequency distributions of scientific contributions; author keywords; thematic dendrograms; article citation metrics; national publication activity; national citation impact; and national collaboration networks.

For keyword analysis, the most frequently occurring author keywords were used. A list of synonyms was compiled and grouped under a single keyword or phrase. In each case, the first word in the list was selected as the representative keyword.

1. Mesenchymal stem cell, mesenchymal stem cells, mesenchymal stromal cell, mesenchymal stromal cells, stem cells, stem cell, mscs, mesenchymal stem cells (mscs), msc, mesenchymal stromal cell.
2. Stem cell transplantation, mesenchymal stem cell transplantation, stem cell therapy, stem cell transplantation, cell transplantation, cellular therapy.
3. Rat, rats, rats sprague-dawley.
4. Animals, animal, animal experiment, animal model, disease models.
5. Mouse, mice, mice inbred C57BL, C57BL mouse.
6. Exosome, exosomes.
7. Cell culture, cells cultured.
8. Bone marrow cell, bone marrow, bone marrow cells, bone marrow mesenchymal stem cell, bone marrow-derived mesenchymal stem cells, bone marrow mesenchymal stem cells, bmscs.
9. Human, humans.
10. Umbilical cord, human umbilical.
11. Liver fibrosis, fibrosis, hepatic fibrosis.
12. Regenerative medicine, regeneration.
13. Liver cirrhosis, cirrhosis.
14. Differentiation, cell differentiation.
15. Hepatocyte, hepatocytes.
16. Acute liver failure, acute liver injury.
17. Chronic liver failure, Chronic liver injury.
18. Immunotherapy, immunomodulation, immunosuppression.

A number of stop words were identified and excluded from the analysis:

1. Article.
2. Priority Journal.
3. Review.

Excel (version 2411) was used to create tables and graphs.

RESULTS

A total of 6,527 articles were initially identified, after which a selection algorithm was applied to isolate topic-relevant publications. The overall dataset consisted of: original articles (4,181), reviews (1,844), editorials

(123), book chapters (113), conference papers (75), notes (57), short surveys (47), letters (41), errata (33), retracted publications (8), conference reviews (2), books (2), and data papers (1). Only original articles (4,181) were retained for further analysis; therefore, 2,346 publications were excluded.

Next, filtering based on the publication timeframe (2008–2024) was applied without restrictions on language or country of origin. This resulted in 244 additional exclusions, and a refined total of 3,937 articles. However, only 3,892 articles were successfully imported and analyzed using the Bibliometrix platform (https://bibliometric.com/), as 45 articles were unavailable or incompatible with the analytics software.

The initial set of 6,527 publications was composed of articles written in multiple languages, including English (5,925), Chinese (486), Russian (63), Japanese (9), French (9), German (7), Ukrainian (5), Polish (4), Persian (4), Korean (4), Hungarian (4), Portuguese (3), Spanish (2), Czech (1), and Arabic (1).

An additional search query targeting clinical research terms revealed that a big chunk of the analyzed publications were clinical studies – 2,304 articles, representing 58.6% of the 3,892 publications analyzed during the study period.

We analyzed the dynamics of publication activity over the entire study period (2008–2024) using the previously defined search query (by abstract, title, and keywords). The results showed that 655 articles were published during 2008–2012, 914 articles during 2013–2016, 1,027 articles during 2017–2020, and 1,296 articles during 2021–2024. Thus, a consistent and steady increase in thematic publications was observed across the four time intervals.

Similarly, year-by-year analysis indicated an increase from 89 publications in 2008 to 353 publications in 2021. In particular, two notable peaks of heightened publication activity were observed in 2015 and 2021 (Fig. 1).

The number of articles reporting the results of clinical studies has also shown a steady upward trend. In 2008, clinical studies accounted for 33.7% of total publications (30 out of 89 articles); in 2016, this figure rose to 54.9% (134 out of 244); and by 2024, it had reached 71.25% (228 out of 320 articles). These data indicate growing interest among clinicians in the potential of cell therapy, with most publications representing pilot studies or early-phase clinical trials.

In the next phase of our study, we proceeded to consolidate and summarize the bibliometric data for the selected articles based on key parameters for the period 2008–2024.

The analysis revealed that the total number of sources (journals and books) amounted to 1,148, and the total number of articles analyzed was 3,892. The annual growth rate in publications was calculated at 8.33%. The average age of the documents reviewed was 6.46 years, and the average number of citations per article was 29.65. A total of 6,481 author keywords (DE) were identified across the dataset. The articles were authored by 16,245 persons, with an average of 7.9 co-authors per publication, and the proportion of international co-authorship was 17.78%.

Thus, bibliometric evaluation according to our selected parameters confirmed a steady annual increase in publication output (8.33%) and demonstrated that the published work in this field is characterized by extensive multi-authorship and a relatively high level of international collaboration (17.78%).

Fig. 2 presents the dynamics of publication activity in the 10 most prolific journals on this topic and lists the titles of the journals that most frequently published relevant articles during the study period (2008–2024).

Analysis of the data shown in Fig. 2 confirms that the number of publications appearing in the leading thematic journals on this topic has been steadily increasing from year to year.

Next, our study focused on identifying the most influential and highly cited articles in the field, as well as the most active authors contributing to the subject area. Table 1 provides a list of the 25 most cited publications,

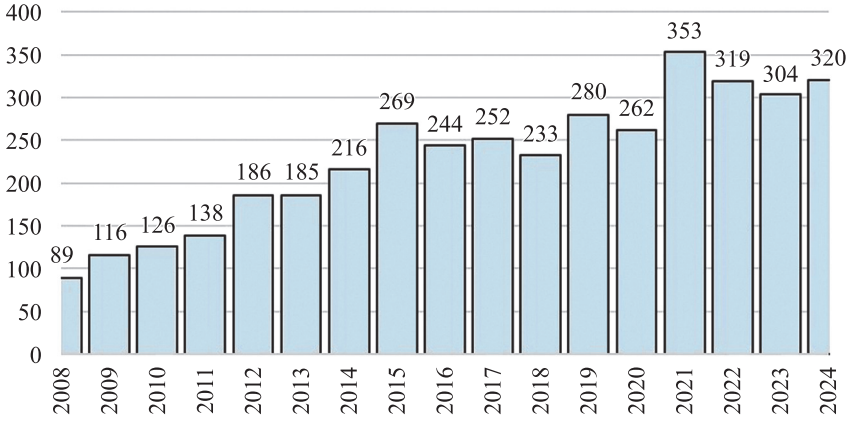

Fig. 1. Trends in the annual number of global publications on the use of mesenchymal stem cells in liver diseases, 2008–2024

including their title, first author, journal, year of publication, and DOI.

A comparative analysis of the publication activity of the 25 most productive authors showed that they maintained a consistently high publication output across all periods beginning in 2008. However, these highly active authors rarely appeared among the first authors of the 25 most cited articles (Table 1). This finding suggests that the most frequently publishing authors likely lead large research teams, and the most highly cited works may reflect the collective output of these groups.

The next stage of our study involved analysis of overall scientific activity across different countries with respect to the topic under investigation. The evaluation was conducted according to five key criteria: Articles (total number of theme-specific publications from a country), Articles % (percentage of thematic articles relative to the country's total scientific output), SCP (single country publications, number of articles authored solely by researchers from one country), MCP (multiple country publications, number of articles co-authored by researchers from different countries), MCP % (proportion of internationally co-authored articles relative to the country's total thematic publications). The results of this country-level analysis are presented in Fig. 3.

Analysis of the results presented in Fig. 3 shows that the most active countries in this field are China, the United States, South Korea, Japan, Iran, Egypt, and Germany. Among them, China exhibits the highest absolute number of publications on this topic, with most of its articles authored exclusively by Chinese researchers. By contrast, countries with lower absolute publication output demonstrate a markedly higher proportion of international collaboration.

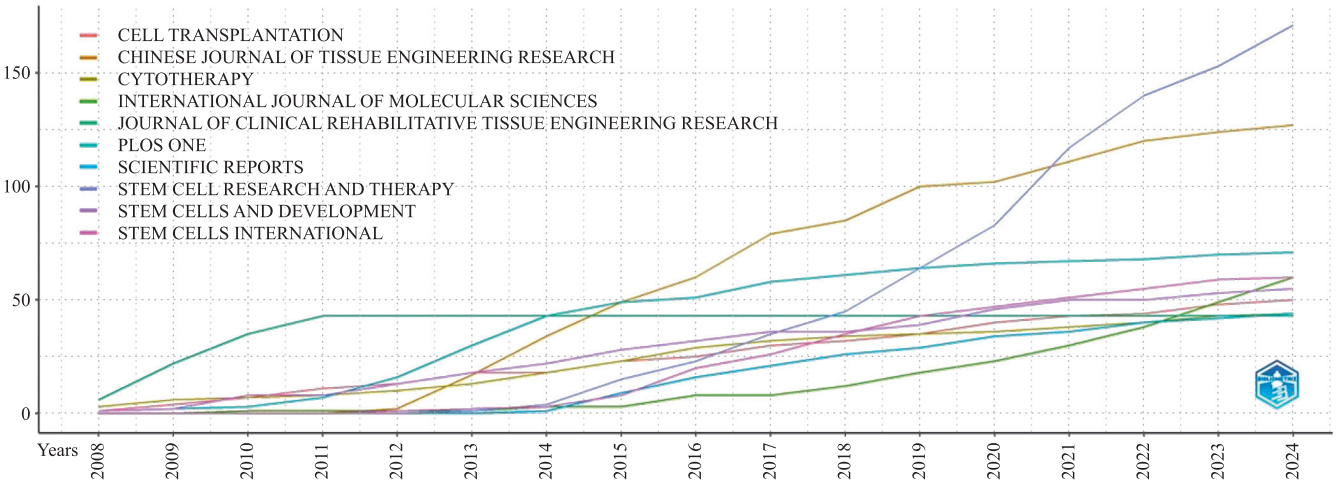

Fig. 2. Trends in the number of publications from 2008 to 2024 in the 10 most prominent thematic journals in the world (journal names indicated in the figure)

Table 1

Most cited articles on the use of MSCs in liver disease: a bibliometric overview

Article	DOI	Citation count
A randomized, double-blind, placebo-controlled, dose-escalation study of intravenous adult human mesenchymal stem cells (prochymal) after acute myocardial infarction. HARE JM, 2009, J AM COLL CARDIOL	10.1016/j.jacc.2009.06.055	1161
Extracellular vesicle *in vivo* biodistribution is determined by cell source, route of administration and targeting. WIKLANDER OPB, 2015, J EXTRACELL VESICLES	10.3402/jev.v4.26316	1103
Multivascular networks and functional intravascular topologies within biocompatible hydrogels. GRIGORYAN B, 2019, SCI	10.1126/science.aav9750	1007
Pulmonary passage is a major obstacle for intravenous stem cell delivery: the pulmonary first-pass effect. FISCHER UM, 2009, STEM CELLS DEV	10.1089/scd.2008.0253	993
Adipose tissue dysfunction as determinant of obesity-associated metabolic complications. LONGO M, 2019, INT J MOL SCI	10.3390/ijms20092358	975
Coronavirus disease 2019 (COVID-19): current status and future perspectives. LI H, 2020, INT J ANTIMICROB AGENTS	10.1016/j.ijantimicag.2020.105951	822

End of Table 1

Article	DOI	Citation count
Aggregation of human mesenchymal stromal cells (MSCs) into 3D spheroids enhances their antiinflammatory properties. BARTOSH TJ, 2010, PROC NATL ACAD SCI USA	10.1073/pnas.1008117107	783
Exosomes derived from human umbilical cord mesenchymal stem cells alleviate liver fibrosis. LI T, 2013, STEM CELLS DEV	10.1089/scd.2012.0395	733
Perivascular Gli1+ progenitors are key contributors to injury-induced organ fibrosis. KRAMANN R, 2015, CELL STEM CELL	10.1016/j.stem.2014.11.004	725
Mesenchymal stem cells: mechanisms of inflammation. SINGER NG, 2011, ANNU REV PATHOL MECH DIS	10.1146/annurev-pathol-011110-130230	713
Allogeneic human mesenchymal stem cells for treatment of *E. coli* endotoxin-induced acute lung injury in the *ex vivo* perfused human lung. LEE JW, 2009, PROC NATL ACAD SCI USA	10.1073/pnas.0907996106	621
Mesenchymal stem cells are short-lived and do not migrate beyond the lungs after intravenous infusion. EGGENHOFER E, 2012, FRONT IMMUNOL	10.3389/fimmu.2012.00297	614
Direct evidence of mesenchymal stem cell tropism for tumor and wounding microenvironments using *in vivo* bioluminescent imaging. KIDD S, 2009, STEM CELLS	10.1002/stem.187	594
Exosomes derived from miR-122-modified adipose tissue-derived MSCs increase chemosensitivity of hepatocellular carcinoma. LOU G, 2015, J HEMATOL ONCOL	10.1186/s13045-015-0220-7	587
Immunosuppressive properties of mesenchymal stem cells: advances and applications. DE MIGUEL MP, 2012, CURR MOL MED	10.2174/156652412800619950	568
Multipotent mesenchymal stromal cells obtained from diverse human tissues share functional properties and gene-expression profile with CD146+ perivascular cells and fibroblasts. COVAS DT, 2008, EXP HEMATOL	10.1016/j.exphem.2007.12.015	523
Microvesicles derived from adult human bone marrow and tissue specific mesenchymal stem cells shuttle selected pattern of miRNAs. COLLINO F, 2010, PLOS ONE	10.1371/journal.pone.0011803	521
Mesenchymal stem cell–derived molecules directly modulate hepatocellular death and regeneration *in vitro* and *in vivo*. VAN POLL D, 2008, HEPATOLOGY	10.1002/hep.22236	473
Mesenchymal stem cell-derived exosomes promote hepatic regeneration in drug-induced liver injury models. TAN CY, 2014, STEM CELL RES THER	10.1186/scrt465	459
Stem cell therapy for liver disease: parameters governing the success of using bone marrow mesenchymal stem cells. KUO TK, 2008, GASTROENTEROLOGY	10.1053/j.gastro.2008.03.015	428
Unique multipotent cells in adult human mesenchymal cell populations. KURODA Y, 2010, PROC NATL ACAD SCI USA	10.1073/pnas.0911647107	416
Airway delivery of mesenchymal stem cells prevents arrested alveolar growth in neonatal lung injury in rats. VAN HAAFTEN T, 2009, AM J RESPIR CRIT CARE MED	10.1164/rccm.200902-0179OC	395
Improvement of liver function in liver cirrhosis patients after autologous mesenchymal stem cell injection: a phase I–II clinical trial. KHARAZIHA P, 2009, EUR J GASTROENTEROL HEPATOL	10.1097/MEG.0b013e32832a1f6c	395
Immunomodulation by therapeutic mesenchymal stromal cells (MSC) is triggered through phagocytosis of MSC by monocytic cells. DE WITTE SFH, 2018, STEM CELLS	10.1002/stem.2779	391
Bone marrow stromal/stem cell-derived extracellular vesicles regulate osteoblast activity and differentiation *in vitro* and promote bone regeneration *in vivo*. QIN Y, 2016, SCI REP	10.1038/srep21961	380

For example, Switzerland shows 71.4% of its publications as collaborative (MCP), while Saudi Arabia and Sweden show 61.5% and 58.5%, respectively.

To identify further trends in the development of MSC-based therapies for acute and chronic liver diseases, and to reveal potential new research directions, we next analyzed the changing frequency of major author keywords across different time intervals.

After reviewing 3,892 articles published between 2008 and 2024 (655 articles in 2008–2012; 914 in 2013–2016; 1,027 in 2017–2020; and 1,296 in 2021–2024), we identified a total of 52 recurring author keywords, from which we selected what we consider to be the 32 most thematically significant keywords used in articles related to MSC-based treatment of liver diseases.

Based on the annual frequency of use of these keywords within each time period, trend trajectories were constructed for each of the selected keywords. The results are summarized in Table 2, where each keyword appears with the identifier assigned to it by the analytical software used in the study.

To obtain the absolute number of keyword occurrences across the study periods, the frequency indicated for the period 2008–2012 should be multiplied by 5 (representing 5 years), and those for subsequent periods (2013–2016, 2017–2020, 2021–2024) should each be multiplied by 4 years. The combined total across all periods gives the absolute frequency of a given keyword. For example, for the term mesenchymal stem cell: $50.2 \times 5 + 88 \times 4 + 93.75 \times 4 + 116.75 \times 4 = 1445$ total occurrences.

Analysis of the keyword usage trends presented in Table 2 shows that the problem of treating acute and chronic liver failure using cellular technologies remains highly relevant and unresolved. This is evidenced by the steadily increasing total number of publications and the rising proportion of clinical studies – most of which are still pilot trials.

A growing number of studies now focus on the effects of MSCs in promoting regeneration of hepatocytes and hepatic stellate cells, as well as their role in modulating immune-mediated inflammation in the liver and restoring systemic immune homeostasis – conditions necessary for effective regenerative repair. While bone marrow-derived MSCs remain a major source, interest in adipose-derived MSCs is increasing, likely due to their easier accessibility.

There is also a notable rise in studies exploring the involvement of apoptosis and oxidative stress mechanisms in MSC activity. Importantly, a surge of new keywords appeared in Period 3 (2017–2020) and especially in Period 4 (2021–2024), such as exosomes and extracellular

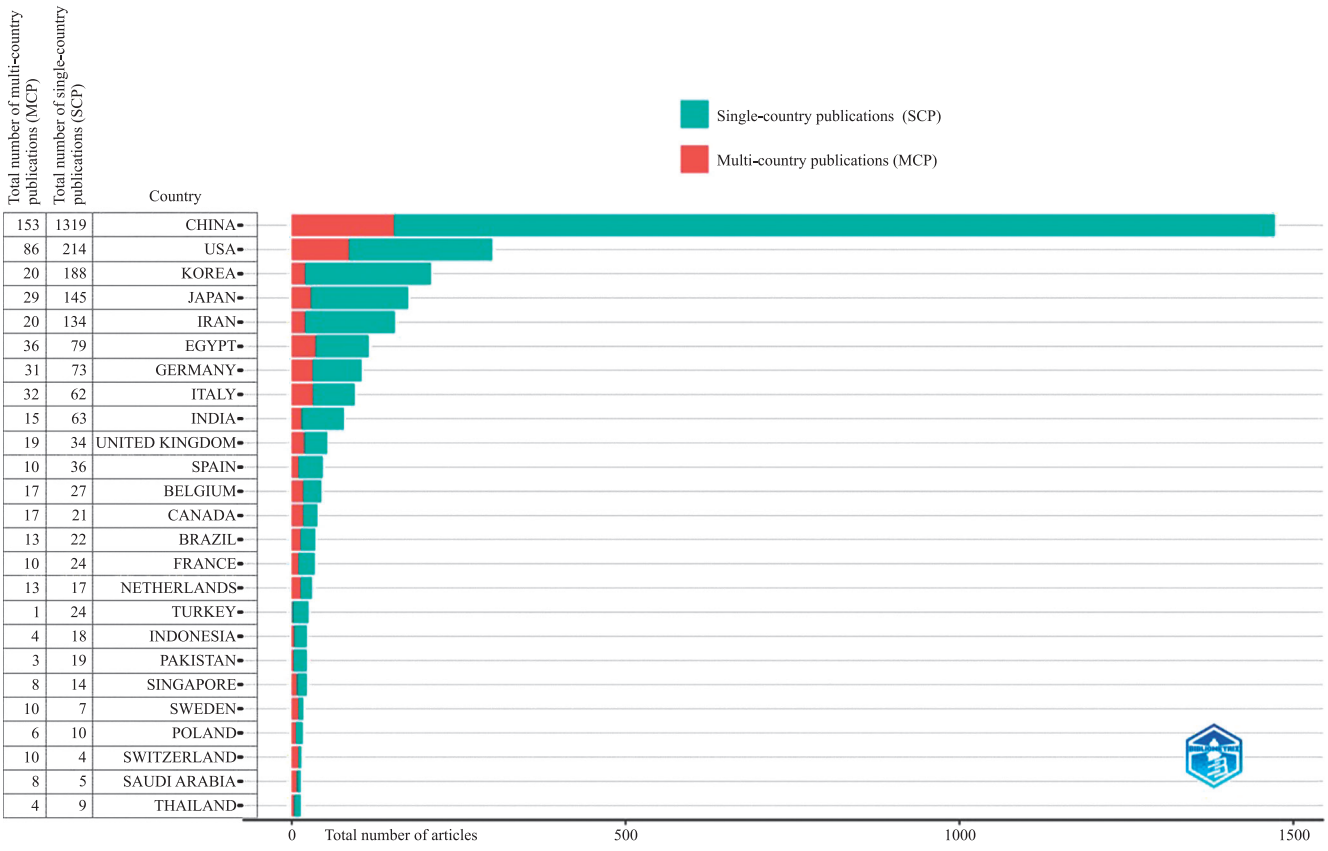

Fig. 3. Total number of thematic publications on MSCs in liver disease, categorized by country. The bars represent the number of publications produced solely by authors from the same country (SCP, single-country publications) and those resulting from international collaborations (MCP, multiple country publications)

vesicles, indicating a shift toward cell-free MSC-based therapies, focusing on paracrine and trophic mechanisms.

To visualize the dynamics of research focus across the observation periods, we constructed a Sankey diagram presented in Fig. 4. This diagram illustrates the evolving interaction between the most prominent keywords in different periods.

In the first stage (2008–2012), several keywords were only loosely connected to the topic of MSCs; however, many of these terms later converged into a clearly defined mesenchymal cell cluster in the second stage. During the second period (2013–2016), a separate set of keywords emerged that had not appeared in the earlier stage. In the third stage (2017–2020) these terms merged into thematic clusters such as liver regeneration and hepatocyte, reflecting a growing focus on the cellular sources and specific liver pathologies being addressed.

In the third stage, new branches also appeared from the earlier mesenchymal cell cluster of the second stage and are involved in the implementation of the mechanisms of their therapeutic potential in the models used. The fourth stage (2021–2024) is characterized by a more detailed exploration of the role of MSCs in associated conditions and complications of liver disease, as well as their influence on specific mechanisms that determine therapeutic efficacy.

Thus, Fig. 4 clearly visualizes both the direction and intensity of evolution in research priorities across different time intervals, based on the dynamics and clustering of the most commonly used keywords.

Table 2

Trends in keyword usage over time: annual frequency of key terms in publications across distinct time periods

S/N	Keywords	Research periods					
		2008–2024	2008–2012	2013–2016	2017–2020	2021–2024	2008–2024 trend
		Total	Per year	Per year	Per year	Per year	
1	Mesenchymal stem cell	1445	50,2	88	93,75	116,75	
2	Bone marrow cell	275	10,6	21	17,25	17,25	
3	Liver fibrosis	254	3,8	8,75	17	47	
4	Stem cell transplantation	172	5,6	14	14	8	
5	Cell therapy	164	4,4	5	15,5	15	
6	Hepatocyte	155	8	12,25	9	7,5	
7	Liver cirrhosis	149	3	11,25	10,75	11,5	
8	Liver	139	5,4	5	10,75	12,25	
9	Differentiation	132	10	9,75	5	5,75	
10	Exosomes	110	0,2	2	12,25	28,75	
12	Acute liver failure	97	2	8,25	6	7,5	
13	Transplantation	96	4,8	10	5	3	
14	Extracellular vesicles	95	0	1	6,25	16,5	
15	Tissue engineering	91	0,8	6,75	11,25	3,75	
16	Inflammation	90	1	2,5	6,75	12	
18	Liver regeneration	86	2	6,5	5,5	7	
19	Apoptosis	84	2,2	6,75	5,25	6,25	
20	Hepatic differentiation	65	3,6	4	5,5	2,25	
21	Immunotherapy	58	1,4	1	5,5	6,25	
22	Liver injury	58	1,4	2,25	5	5,5	
23	Adipose tissue	54	2,4	2,75	3,25	4,5	
24	Oxidative stress	54	0,2	1,25	3,5	8,5	
25	Liver transplantation	53	1,2	3	3,5	5,25	
26	Hepatic stellate cells	51	1,4	2,75	3	5,25	
27	Hepatocyte-like cells	47	2,2	4,25	4	0,75	
28	Cirrhosis	44	1	3,5	3	3,25	
30	Liver failure	43	0,8	2,25	4,5	3	
31	Hepatocyte growth factor	41	2	3	2,5	2,25	
32	Regeneration	40	0,4	2	3,75	3,75	
36	Autophagy	33	0	0,75	3	4,5	
44	Acute liver injury	26	0,6	1,5	2,25	2	
50	Liver disease	24	1	1,5	1,5	1,75	

Fig. 4 demonstrates that the evolution of priority research areas follows a wave-like dynamic, with scientific interests converging, diverging, and influencing one another across time, ultimately shaping both current and future investigative directions.

DISCUSSION

Analysis of the results shows that during the first (early) period, 2008–2012, research worldwide was predominantly exploratory, focusing on the therapeutic potential of MSCs. MSCs from various sources, mainly bone marrow (BM), adipose tissue, and umbilical cord, were applied in models of liver injury (acute and chronic liver failure, fibrosis, cirrhosis, hepatocellular carcinoma) in an effort to restore regenerative processes in hepatocytes and hepatic stellate cells.

During this period, research began to investigate proposed mechanisms of MSC action, such as their ability to differentiate into hepatocyte-like cells or to exert effects via homing and secretion of hepatocyte growth factor. However, in subsequent years, the importance of these mechanisms was disputed or not fully confirmed, and publication activity in these specific mechanistic directions gradually declined [8–13].

Notably, in this first period, there was almost a complete absence of keywords such as exosomes, extracellular vesicles, tissue engineering, oxidative stress, immunomodulation, and immunosuppression – terms whose usage increased beginning in the second period, and especially in the third and fourth periods of analysis.

These findings suggest that as early as the second period, a new conceptual framework was emerging regarding the regulatory and regenerative mechanisms of MSCs in damaged organs. The pivotal shift occurred with the landmark hypothesis proposed by Thum et al. in 2005 [12], later confirmed scientifically, which suggested that the therapeutic effect of MSCs and other stem cells is largely mediated through apoptosis of the transplanted cells, developing after isolation, followed by release of paracrine and trophic factors (including exosomes, extracellular vesicles, apoptotic bodies, growth factors, various RNAs, lipids, amino acids, cytokines, chemokines, etc.). These released components act as biologically adequate adaptogenic regulators on cells in the damaged tissue [14, 15].

In the second period, research on tissue engineering intensified, with a focus on developing strategies to maintain MSC viability after transplantation and to prolong their functional presence in the body [16–19]. The positive and encouraging results obtained during the third and fourth periods contributed substantially to the expansion and consolidation of a new research direction centered not only on MSCs themselves, but increasingly on the paracrine factors they secrete.

It became evident that paracrine factors, such as exosomes, extracellular vesicles, and apoptotic bodies, along with trophic factors like hepatocyte growth factor, have a powerful ability to restore structural and functional integrity in the liver and other organs, as well as to modulate systemic immune homeostasis. These factors create a favorable microenvironment for regenerative recovery of damaged tissues [20–26]. This shift is reflected in the sharp rise in the frequency of keywords such as exosomes, extracellular vesicles, conditioned medium, inflammation, immunomodulation, and immunosuppression during the third and especially the fourth periods.

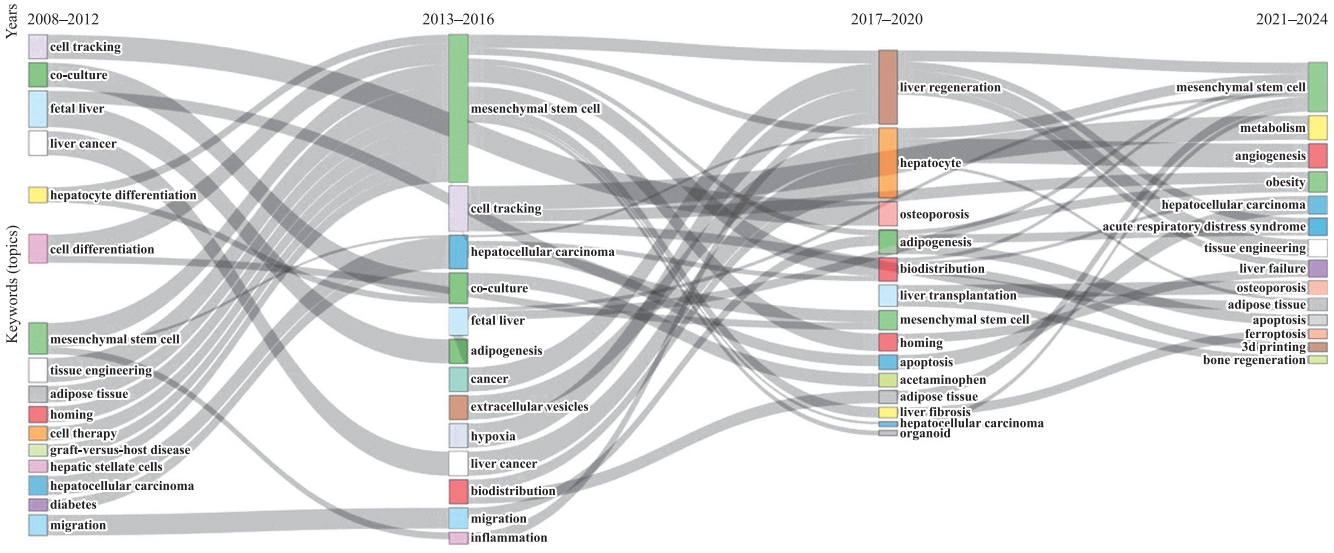

Fig. 4. Wave dynamics illustrating the evolution of keyword frequency and thematic interrelationships in publications from 2008 to 2024 (Sankey diagram). Nodes represent key thematic terms – points where flows begin, end, or intersect. The size of each node reflects the relative frequency and prominence of the keyword in a given period. Flows (connecting lines) indicate the continuity and transition of research themes across time. The width of each flow is proportional to the number of articles in which the linked terms co-occurred, demonstrating how research focus has shifted or evolved over the years

The advantage of using paracrine factors over MSCs is that they have immunosuppressive properties without posing the same oncogenic risk.

Based on the results of the bibliometric analysis, it can be assumed that future research in the field of cell technologies, particularly MSCs for regenerative medicine, will focus on identifying the most bioactive paracrine and trophic factors, determining their chemical structure and functional properties, and subsequently developing pharmaceutical preparations with regenerative bioactivity.

CONCLUSION

For the first time in Russian scientific literature, a bibliometric approach has been applied to quantitatively analyze global patterns and trends in MSC-based research for the treatment of liver diseases.

The findings show that during the period from 2008 to 2024, there was a consistent annual increase in research activity (including clinical studies), with two peaks in publication output observed in 2015 and 2021.

It was also established that research articles on MSCs in the context of liver disease treatment are primarily published in highly rated, specialized journals, and authored by researchers working in countries with strong scientific capacity, mainly China, the United States, South Korea, Japan, Iran, Germany, and others, where a high level of international collaboration is consistently observed.

The analysis of keyword frequency across different time intervals made it possible to identify both scientific patterns and emerging practical trends in the development of MSC isolation and application technologies.

During the early period (2008–2012), studies were largely exploratory and focused on the biological potential and therapeutic benefits of MSCs in treating liver fibrosis and cirrhosis as a form of cell therapy. The rare use of terms such as apoptosis, regenerative medicine, inflammation, and gene therapy – as well as the complete absence of keywords like exosomes, extracellular vesicles, oxidative stress, conditioned medium, immunomodulation, and tissue engineering – reflect a lack of understanding at that time regarding both the paracrine mechanisms of MSC action and the methods required to prolong their viability *in vivo* through tissue engineering strategies.

The 2013–2016 period (second period) is characterized by the rapid development of tissue engineering methods and active research into the mechanisms of MSC therapeutic action. During this time, attention shifted toward MSCs from different sources (bone marrow, adipose tissue, umbilical cord blood, etc.) and their role in apoptosis, with the release of paracrine and trophic factors that exert therapeutic effects.

The 2017–2020 (third period) and 2021–2024 (fourth period) periods are marked by further intensification in the study of MSC mechanisms, particularly the influence of their paracrine and trophic factors – exosomes, extracellular vesicles, growth factors, various RNAs, etc. – on restoring immune homeostasis (inflammation control, immunomodulation, immunosuppression) and structural-functional homeostasis in the liver (regeneration of hepatocytes and hepatic stellate cells, and activation of antifibrotic processes).

The next phase of research will apparently be directed at identifying the most bioactive paracrine and trophic factors, determining their chemical structure and biological properties, and manufacturing chemotherapeutic drugs with bioactive properties.

The bibliometric approach presented in this study can serve as a universal analytical tool for identifying developmental trends in emerging areas of biomedical research and may be effectively used in writing dissertation research.

The authors declare no conflict of interest.

REFERENCES

1. *Yang X, Li Q, Liu W, Zong C, Wei L, Shi Y, Han Z*. Mesenchymal stromal cells in hepatic fibrosis/cirrhosis: from pathogenesis to treatment. *Cell Mol Immunol*. 2023; 20 (6): 583–599. doi: 10.1038/s41423-023-00983-5. Epub 2023 Feb 24.
2. *Halliday N, Wesrtbrook RH*. Liver transplantation: need, indications, patient selection and pre-transplant care. *Br J Hosp Med (Lond)*. 2017; 78 (5): 252–259. doi: 10.12968/hmed.2017.78.5.252.
3. *Olivo R, Guarrera JV, Pyrsopoulos NT*. Liver Transplantation for Acute Liver Failure. *Clin Liver Dis*. 2018; 22 (2): 409–417. doi: 10.1016/j.cld.2018.01.014.
4. Transplantologija i iskusstvennye organy: uchebnik / Pod red. akad. RAN S.V. Gautier. M.: Laboratorija znanij, 2018; 319.
5. *Gautier SV, Konstantinov BA, Cirul'nikova OM*. Transplantacija pecheni. M.: MIA, 2008; 246.
6. https://bibliometric.com/.
7. https://www.vosviewer.com/.
8. *Schwartz RE, Reyes M, Koodie L, Jiang Y, Blackstad M, Lund T et al.* Multipotent adult progenitor cells from bone marrow differentiate into functional hepatocyte-like cells. *J Clin Invest*. 2002; 109 (10): 1291–1302. doi: 10.1172/JCI15182.
9. *Chivu M, Dima SO, Stancu CI, Dobrea C, Uscatescu V, Necula LG et al*. *In vitro* hepatic differentiation of human bone marrow mesenchymal stem cells under differential exposure to liver-specific factors. *Transl Res*. 2009; 154 (3): 122–132. doi: 10.1016/j.trsl.2009.05.007. Epub 2009 Jun 24.
10. *Lange C, Bassler P, Lioznov MV, Bruns H, Kluth D, Zander AR, Fiegel HC*. Liver-specific gene expression in mesenchymal stem cells is induced by liver cells. *World J Gastroenterol*. 2005; 11 (29): 4497–4504. doi: 10.3748/wjg.v11.i29.4497.Chivu.

11. *Ullah M, Liu DD, Thakor AS*. Mesenchymal Stromal Cell Homing: Mechanisms and Strategies for Improvement. *iScience*. 2019; 15: 421–438. doi: 10.1016/j.isci.2019.05.004. Epub 2019 May 9.Liesveld.
12. *Thum T, Bauersachs J, Poole-Wilson PA, Volk HD, Anker SD*. The dying stem cell hypothesis: immune modulation as a novel mechanism for progenitor cell therapy in cardiac muscle. *J Am Coll Cardiol*. 2005; 46 (10): 1799–1802. doi: 10.1016/j.jacc.2005.07.053. Epub 2005 Oct 17.
13. *Liesveld JL, Sharma N, Aljitawi OS*. Stem cell homing: From physiology to therapeutics. *Stem Cells*. 2020; 38 (10): 1241–1253. doi: 10.1002/stem.3242. Epub 2020 Jul 21.
14. *Onishchenko NA, Nikolskaya AO, Gonikova ZZ, Kirsanova LA, Shagidulin MYu, Sevastianov VI*. Apoptotic bone marrow-derived mononuclear cells Accelerate liver regeneration after extended resection. *Russian Journal Of Transplantology And Artificial Organs*. 2022; 24 (4): 85–93. https://doi.org/10.15825/1995-1191-2022-4-85-93.
15. *Kholodenko IV, Kholodenko RV, Majouga AG, Yarygin KN*. Apoptotic MSCs and MSC-Derived Apoptotic Bodies as New Therapeutic Tools. *Curr Issues Mol Biol*. 2022; 44 (11): 5153–5172. doi: 10.3390/cimb44110351.
16. *Gautier SV, Shagidulin MY, Onishchenko NA, Krasheninnikov ME, Il'inskii IM, Mozheiko NP et al*. Correction of cronic liver failure by transplantation of liver cells suspension and cell-engineering designs (experimental investigation). *Annals of the Russian academy of medical sciences*. 2013; 4: 44–51.
17. *Shagidulin MJu, Onishhenko NA, Krasheninnikov ME, Il'inskij IM, Ljundup AV, Mozhejko NP et al*. Transplantacija kletochno-inzhenernyh konstrukcij v pechen' obespechivaet dlitel'nuju podderzhku processov vosstanovitel'noj regeneracii v povrezhdennoj pecheni. *Russian Journal Of Transplantology And Artificial Organs*. 2013; 15 (2): 64–74.
18. *Franquesa M, Hoogduijn MJ, Eggenhofer E, Pinxteren J, Christ B, Shagidulin M et al*. The MiSOT Study Group. Mesenchymal Stem Cells in Solid Organ Transplantation (MiSOT) Fourth Meeting: Lessons Learned from First Clinical Trials. *Transplantation*. 2013; 96 (3): 234–238.
19. *Shagidulin MJu, Onishhenko NA*. Bone marrow stem cells transplantation as a new method of treatment of hepatic failure. The current state of the problem. *Farmateka*. 2013; 18: 130–135.
20. *Zhao T, Sun F, Liu J, Ding T, She J, Mao F et al*. Emerging Role of Mesenchymal Stem Cell-derived Exosomes in Regenerative Medicine. *Curr Stem Cell Res Ther*. 2019; 14 (6): 482–494. doi: 10.2174/1574888X14666190228103230.
21. *Fu Q, Ohnishi S, Sakamoto N*. Conditioned Medium from Human Amnion-Derived Mesenchymal Stem Cells Regulates Activation of Primary Hepatic Stellate Cells. *Stem Cells Int*. 2018; 8: 4898152. doi: 10.1155/2018/4898152. eCollection 2018.
22. *Parekkadan B, van Poll D, Suganuma K, Carter EA, Berthiaume F, Tilles AW, Yarmush ML*. Mesenchymal stem cell-derived molecules reverse fulminant hepatic failure. *PLoS One*. 2007; 2 (9): e941. doi: 10.1371/journal.pone.0000941.
23. *Ohara M, Ohnishi S, Hosono H, Yamamoto K, Yuyama K, Nakamura H et al*. Extracellular Vesicles from Amnion-Derived Mesenchymal Stem Cells Ameliorate Hepatic Inflammation and Fibrosis in Rats. *Stem Cells Int*. 2018; 2018: 3212643. doi: 10.1155/2018/3212643. eCollection 2018.
24. *Nooshabadi VT, Mardpour S, Yousefi-Ahmadipour A, Allahverdi A, Izadpanah M, Daneshimehr F et al*. The extracellular vesicles-derived from mesenchymal stromal cells: A new therapeutic option in regenerative medicine. *J Cell Biochem*. 2018; 119 (10): 8048–8073. doi: 10.1002/jcb.26726. Epub 2018 Jun 22.
25. *Mardpour S, Hassani SN, Mardpour S, Sayahpour F, Vosough M, Ai J et al*. Extracellular vesicles derived from human embryonic stem cell-MSCs ameliorate cirrhosis in thioacetamide-induced chronic liver injury. *J Cell Physiol*. 2018; 233 (12): 9330–9344. doi: 10.1002/jcp.26413. Epub 2018 Jun 19.
26. *Lei Qin, Nian Liu, Chao-le-Meng Bao, Da-Zhi Yang, Gui-Xing Ma, Wei-Hong Yi et al*. Mesenchymal stem cells in fibrotic diseases – the two sides of the same coin. *Acta Pharmacol Sinica*. 2023; 44 (2): 268–287. doi: 10.1038/s41401-022-00952-0.

The article was submitted to the journal on 9.02.2025

DOI: 10.15825/1995-1191-2025-3-146-159

EXTRACELLULAR MATRIX BIOMIMETICS FOR PANCREATIC TISSUE ENGINEERING

A.S. Ponomareva[1], N.V. Baranova[1], Yu.B. Basok[1], V.I. Sevastianov[1, 2]

[1] Shumakov National Medical Research Center of Transplantology and Artificial Organs, Moscow, Russian Federation

[2] Institute of Biomedical Research and Technology, Moscow, Russian Federation

Isolated islet transplantation offers a safer and less invasive alternative to whole pancreas transplantation for patients with complicated type 1 diabetes mellitus. However, the procedure faces significant challenges, including the loss of vascularization, innervation, and extracellular matrix (ECM) support. Additionally, factors such as hypoxia, oxidative stress, inflammatory responses, and the cytotoxic effects of immunosuppressive therapy compromise islet viability significantly and limit long-term graft function. Tissue engineering and regenerative medicine strategies aim to address these challenges. A central objective is the development of biocompatible, biomimetic ECM scaffolds (frameworks, carriers, or matrices) that can provide both mechanical support and a suitable microenvironment for islet cells *in vitro* and *in vivo*. This review aims to systematize current data on the use of biomimetic ECMs in the creation of stable, tissue-engineered pancreatic constructs.

Keywords: diabetes mellitus, pancreas, islets of Langerhans, extracellular matrix, biomimetics, scaffold, biomaterials.

INTRODUCTION

Type I diabetes mellitus (T1D) is characterized by autoimmune destruction of insulin-producing pancreatic beta cells, resulting in absolute insulin deficiency and development of diabetic complications such as angiopathy, retinopathy, nephropathy, and neuropathy [1, 2]. In patients with high susceptibility to severe hypoglycemia and poor glycemic control, transplantation of functionally active pancreatic islets using the Edmonton protocol has emerged as a modern therapeutic option. This approach typically requires a substantial islet mass, often obtained from multiple donors [3]. Pancreatic islet transplantation represents a safer and less invasive alternative to whole-organ transplantation [4, 5], enabling the achievement of stable euglycemia, lowering the risk of secondary diabetic complications, and improving quality of life compared with conventional insulin therapy [6–8].

Despite advances in clinical islet transplantation, its widespread application remains limited by the shortage of donor organs and decline in islet viability at all stages of graft isolation, preparation, and engraftment. The reduction in functional activity is primarily associated with impaired blood supply, loss of innervation and contact with the extracellular matrix (ECM), oxidative stress, hypoxia, inflammatory responses, and the toxic effects of immunosuppressants [9]. At the same time, there is currently no alternative source of insulin-producing cells suitable for clinical use other than islets. Although induced pluripotent stem cells are under intensive research, their clinical translation is hindered by risks such as teratoma formation and other unpredictable consequences related mainly to genetic modifications. Another major challenge is preserving the feedback mechanisms that regulate glucose homeostasis, which are mediated by the coordinated activity of islet cell types: alpha cells (secreting glucagon), beta cells (secreting insulin), delta cells (secreting somatostatin), and minor populations producing pancreatic polypeptide and ghrelin [10, 11]. The main advantage of islet transplantation over insulin-producing cells of other origins is the retention of intra-islet paracrine interactions between beta cells and other endocrine cell types [12].

Recent studies provide encouraging evidence for the potential of tissue engineering and regenerative medicine technologies to ensure long-term preservation of the viability and functional activity of human pancreatic islets after transplantation [13]. Of particular interest is the development of tissue-engineered pancreatic constructs (TEPCs), which are based on insulin-producing cells immobilized within a biocompatible scaffold. Such scaffolds not only provide mechanical support but also prolongs cell viability and function. The creation and application of these constructs may offer an alternative therapeutic strategy for diabetes mellitus and serve as a valuable platform for the development and preclinical testing of new drugs.

Biocompatible scaffolds are also used for encapsulation of islet cells, an effective strategy to protect transplants from immune rejection [14]. This encapsulation technology involves placing insulin-producing cells

Corresponding author: Anna Ponomareva. Address: 1, Shchukinskaya str., Moscow, 123182, Russian Federation. Phone: (499) 196-26-61; (926) 585-23-73. E-mail: a.s.ponomareva@gmail.com

within semi-permeable biomaterials, where the defined pore size of the capsule membrane allows diffusion of nutrients and secreted insulin while blocking immune cells and large molecules such as immunoglobulins. Successful encapsulation is expected to eliminate the need for lifelong immunosuppression. The use of biocompatible materials for encapsulation has resulted in increased survival and functional activity of islet grafts [15, 16].

To further improve the secretory function of transplanted islets, co-encapsulation approaches have been explored, incorporating ECM molecules or supportive cells such as mesenchymal stromal cells. These cells exert beneficial paracrine and immunoregulatory effects [12, 17]. Some of the developed immunosuppressive devices, such as PEC-Encap (ViaCyte, Inc., USA), βAir (BetaO2 Technologies Ltd., Israel), and the Cell Housing Device (Vertex Pharmaceuticals, USA), have already undergone clinical trials [14].

Despite these advances, translation of encapsulation technology into routine clinical practice faces several critical challenges. Among them are insufficient biocompatibility of capsules that may trigger inflammatory responses and foreign-body reactions; fibrotic overgrowth around implanted capsules; and incomplete vascularization of surrounding tissues, leading to cell hypoxia [16].

The key tasks in the development of TEPCs are to establish optimal conditions for obtaining and culturing enough insulin-producing cells and to identify suitable scaffolds (frames, matrices, carriers) capable of mimicking the structure and composition of the native ECM. Such scaffolds should provide the most favorable microenvironment for sustaining the functional activity of the transplanted cells [18].

DEVELOPMENT OF SCAFFOLDS FOR TISSUE-ENGINEERED CONSTRUCTS

Scaffolds used in tissue engineering must have physical, mechanical, and biological properties that support the survival and functionality of specific cell types both *in vitro* and *in vivo*. Investigations into the composition and organization of native tissue ECM are critical, as they reveal the specific structural and biochemical characteristics that should guide the selection of scaffold materials.

ECM is a complex and dynamic network of macromolecules synthesized by cells, essential for maintaining tissue integrity and providing rigidity, elasticity, and resilience [15]. The ECM supports tissue-specific cell homeostasis, phenotype, and function. Its components interact with growth factors and cell surface receptors to regulate key cellular processes, including proliferation, differentiation, morphology, gene expression, intracellular signaling, adhesion, migration, secretory activity, and survival [19].

Recent studies in mice and pigs have identified 12 distinct ECM proteins in the pancreas, including collagens I, III, IV, V, and VI, laminin, elastin, fibronectin, fibrillin, glycosaminoglycans (GAGs), among others [18, 20–23]. The three-dimensional (3D) architecture of the pancreatic ECM determines the topographical location of endocrine cells, which influences the viability and secretory function of the islets [12].

When selecting a scaffold, it is essential to account for the multicomponent, biochemically complex composition of the ECM, its structural specificity, and tissue-specific functions. For the creation of TEPCs, bioresorbable scaffolds designed to mimic the properties of native ECM, the so-called ECM mimetics, are used. These scaffolds are developed from natural and synthetic materials, as well as their composites [12, 15, 18]. Critically, scaffold materials must provide controlled 3D structural parameters, including porosity, pore size, and surface roughness, in order to mimic the native cellular niche [15, 24–26].

Examples of biomaterials applied in liver tissue engineering are presented in Table 1.

Various types of scaffolds are used in tissue engineering, including films, membranes, sponges, gels, cryogels, fibrous materials produced by electrospinning, as well as decellularized tissues and organs [26].

Simpler two-dimensional scaffolds can reproduce certain aspects of cell–matrix interactions and help modulate cell behavior and signaling. However, they may also alter the normal cell phenotype compared to more complex 3D structures. In contrast, porous 3D scaffolds more closely simulate the native tissue microenvironment, enabling higher cell density, improved nutrient and oxygen diffusion, thereby prolonging cell survival and enhancing secretory capacity [18, 25, 83].

In a study by Buitinga et al., three methods for fabricating scaffolds with microcavities and pore diameters not exceeding 40 μm were compared: leaching, casting, and laser drilling. The evaluation focused on pore size and geometry, reproducibility of the method, and the shape and stability of the resulting scaffold. In a T1D

Table 1

Biomaterials used for pancreatic tissue engineering

Natural	
Alginate	[27–32]
Collagen	[33–42]
Chitosan	[35, 38, 43]
Fibrin	[44–48]
Gelatin	[43, 49, 50]
Silk	[51–53]
Decellularized tissues	[13, 54–64]
Synthetic	
Polyethylene glycol	[65–73]
Polycaprolactone	[74–76]
Polyglycolic acid	[77–79]
Poly(lactic-co-glycolic acid)	[51, 80–82]

mouse model, scaffolds produced by laser drilling proved most effective, ensuring the retention and engraftment of islets when implanted into the white adipose tissue of the epididymis. Transplantation of 300 islets using the scaffold restored normoglycemia in 75% of diabetic mice, whereas transplantation of the same number of islets without a scaffold achieved stable glucose control in only 28.5% of animals [84].

A promising strategy for creating macroporous scaffolds with interconnected pore networks – meeting the structural requirements for cell-based technologies and tissue engineering – is cryogenic structuring of polymer systems [85–87]. For example, cryogenically structured biopolymer substrates based on spongy agarose cryogels modified with gelatin have shown high biocompatibility and supported the long-term viability and insulin-secreting activity of mouse islet cell lines *in vitro* [88, 89].

It is worth noting that scaffold modification with ECM components not only provides structural and mechanical support for islets, thereby preserving their viability and insulin-secreting function, but also serves as a reservoir of growth factors, cytokines, and antioxidants [19]. Furthermore, incorporating biochemical cues that promote rapid vascularization, such as vascular endothelial growth factor (VEGF), into the scaffold prolongs the functional lifespan of the islet transplant [90].

SCAFFOLDS MADE OF SYNTHETIC MATERIALS

Synthetic materials such as polyethylene glycol, polycaprolactone, polylactic acid, polyglycolic acid, and their copolymers are widely applied in tissue engineering owing to their adjustable physicochemical properties. These materials allow precise control and reproducibility of scaffold characteristics, including elasticity, stiffness, porosity, biodegradability, and ease of chemical modification [14, 15, 91]. Both single-polymer systems and multi-component composites can be processed into scaffolds with predetermined architectures, for example, using 3D printing and electrospinning.

In an experimental study, Chun et al. demonstrated that islets immobilized on a fibrous scaffold made of polyglycolic acid exhibited a four-fold increase in insulin secretion index and a two-fold increase in cell survival compared with islets cultured without a scaffold over 15 days [77].

In a comparative study, Daoud et al. cultured equal numbers of human islets for 10 days under different conditions: on microscaffolds composed of a polylactic–polyglycolic acid copolymer modified with ECM proteins (type I collagen, type IV collagen, and fibronectin); in a gel containing the same ECM proteins; in a gel containing only type I collagen; and in suspension culture without additives as a control. The highest glucose stimulation index, comparable to that of freshly isolated islets, was observed when islets were immobilized on microscaffolds. This effect was attributed to the combined influence of mechanical support, presence of ECM components, and enhanced diffusion and cell–cell interactions afforded by the interconnected pore system of the scaffold [81].

Knobeloch et al. further explored the potential of a polyethylene glycol–based injectable hydrogel as an encapsulation material. Human islets cultured in this hydrogel for 6 days maintained their shape and structural integrity, both of which are crucial for functional performance. Importantly, basal and glucose-stimulated insulin secretion were significantly higher in hydrogel-encapsulated islets compared to those cultured in suspension [73].

Despite examples of successful use of synthetic scaffolds in tissue engineering, their inherent limitations, such as hydrophobicity, absence of cell adhesion sites, and lack of cell recognition signals, often necessitate pre-modification with angiogenic factors or ECM components.

SCAFFOLDS FROM NATURAL MATERIALS

Natural materials such as polysaccharides (chitosan, alginate, hyaluronic acid) and proteins (collagen, fibrin, silk), are also widely employed in the creation of TEPCs. These materials offer several advantages, such as low toxicity, biocompatibility, and biodegradability. Moreover, scaffolds derived from natural sources contain bioactive components that facilitate stronger interactions with insulin-producing cells, thereby enhancing the functionality of the formed TEPC. However, their use is not without limitations, which include temperature sensitivity, potential immunogenicity, and heterogeneity that may vary depending on the source material.

Alginate, a natural and biocompatible polysaccharide with mild gel-forming properties, is widely used as a functional biomaterial for the production of injectable hydrogels designed for encapsulating islets [32].

Collagen, the most abundant protein in mammals, plays a central role in providing structural support to tissues, mediating intercellular contacts, and regulating cell behavior, including the function of islet cells [15, 19]. Studies have shown that isolated islets incubated with collagen-containing scaffolds retain their integrity, viability, and secretory function for longer periods compared to islets cultured in suspension.

In particular, Pinkse et al. reported that rat pancreatic islets cultured in standard Petri dishes rapidly underwent structural degradation, with fewer than 10% remaining viable after 48 hours of incubation. Coating the culture surface with type I collagen improved islet viability to 60%, while modification with type IV collagen – the principal protein of the basement membrane – further enhanced survival to 89% [92].

Llacua et al. demonstrated that the addition of type VI collagen to alginate capsules positively influences

both the viability and functional activity of encapsulated human pancreatic islets *in vitro* [23].

Among biomimetic materials that replicate the composition of native ECM, particular attention has been given to collagen-containing hydrogels such as Sphero®GEL (AO BIOMIR, Russia), derived from natural compounds. This material has been successfully applied to the development of liver and cartilage tissue-engineered constructs [13, 93]. In a related study, Baranova et al. reported that rat islets cultured within a collagen-containing hydrogel remained structurally intact and free from degradation for 10 days compared to islets cultured in suspension [42].

Taken together, these findings confirm that collagen-containing scaffolds play a critical role in preserving the native architecture and functional integrity of islets, both *in vitro* and *in vivo* [13, 18, 23].

Gelatin, a water-soluble substrate derived from collagen hydrolysis, retains peptide sequences that promote cell adhesion and migration. Muthyala et al. demonstrated that incorporating gelatin into polymer scaffolds preserved the structural integrity and viability of mouse islets of Langerhans *in vitro* for up to 30 days, compared to scaffolds without gelatin [49].

Laminin, a structural non-collagenous glycoprotein of the basement membrane, interacts with all ECM components and plays a crucial role in modulating cell behavior. It influences cell morphology, proliferation, motility, and differentiation, thereby enhancing the survival and insulin-producing function of islet cells *in vitro* [19]. Sojoodi et al. reported upregulation of specific genes and increased insulin secretion in rat islets of Langerhans cultured for 7 days on laminin-coated scaffolds [20]. Similarly, Sigmundsson et al. reported sustained functional activity of both mouse and human islets incubated on α5-laminin–coated membranes for 1–2 weeks. Notably, implantation of 110–150 islets on laminin-coated membranes under the renal capsule of T1D mice restored normoglycemia in 27% of animals within 3 days, in 68% by 7 days, and in 100% by 14 days [21].

Fibronectin is a non-collagenous ECM glycoprotein predominantly expressed in blood vessels, ductal cells of the developing mammary gland, and in the basement membrane. It plays a central role in cell adhesion, migration, proliferation, differentiation, and apoptosis by directly mediating cell interactions. In tissue engineering, fibronectin is used as a component of the culture medium or as a substrate in cell culture, including islet cells, in order to preserve their viability and functionality. Incubation of human and rat islets with soluble fibronectin has been shown to enhance insulin secretion in response to glucose stimulation and to increase the expression of the t-SNARE proteins syntaxin 1 and SNAP-25 *in vitro* [22]. Similarly, Hamamoto et al. reported improved secretory function of islets after 48 hours of culture with fibronectin compared to standard culture conditions. Notably, transplantation of islets preconditioned with fibronectin into rats resulted in decreased blood glucose levels and elevated plasma insulin concentrations within 2 weeks [94].

Thus, the use of fibronectin in pancreatic tissue engineering improves the preservation and function of islets *in vitro* and extends the viability of islet transplants *in vivo*.

Elastin is the principal fibrillar protein of elastic fibers in native tissue, providing mechanical strength, elasticity, resilience, and extensibility. Scaffolds composed of elastin and collagen have been shown to stimulate vascularization at extrahepatic transplantation sites in mice, thereby enhancing islet engraftment, survival, and function sufficient to restore euglycemia in diabetic recipients [90]. Modern strategies in pancreatic tissue engineering increasingly employ decellularized tissues enriched with elastin, elastin-containing synthetic biomaterials, and methods that stimulate *de novo* elastin synthesis [95].

In summary, scaffolds derived from natural materials, owing to their intrinsic bioactive components, are promising for use in pancreatic tissue engineering.

TISSUE-SPECIFIC SCAFFOLDS

Current research in tissue engineering is increasingly directed toward the development of scaffolds derived from decellularized tissues and organs [13, 19]. Decellularization is a multi-step process in which the cellular components of native tissue are removed while preserving the ECM architecture and composition [96]. This strategy enables the production of biomimetic ECM scaffolds with high biocompatibility, reduced immunogenicity, and structural and biochemical characteristics resembling native tissue, thereby providing a microenvironment close to the native one for recellularized cells.

Effective decellularization typically requires the use of combined approaches – integrating physical, chemical, and enzymatic methods of tissue processing (Table 2).

Among the physical methods of decellularization, the most widely used are freezing–thawing, perfusion, mechanical agitation, grinding, and ultrasonic exposure [13]. Freezing causes the formation of ice crystals within cells, leading to membrane rupture and subsequent cell lysis. However, this process can also damage ECM proteins; therefore, careful control of the cooling and thawing rates is required to regulate crystal size [97].

Cell lysis can also be achieved by applying direct pressure to the tissue, though this approach is effective primarily for organs with a less dense ECM organization, such as the liver or lungs. In addition, mechanical mixing methods – including rotation, rocking, or shaking – help to dislodge and remove cellular debris [62].

Physical methods alone are insufficient to ensure complete removal of cellular components from the tissue. Combining them with chemical and enzymatic techniques significantly improves decellularization ef-

Table 2

Tissue decellularization methods

Physical methods
Freezing/thawing Mechanical grinding Micronization Mixing, rotation, shaking Perfusion Mechanical pressure Ultrasonic exposure
Chemical methods
Ionic surfactants (SDS) Nonionic surfactants (Triton X-100) Zwitterionic (amphoteric) surfactants (CHAPS) Acids (EDTA) Alkalis (NaOH) Hypotonic/hypertonic solutions
Enzymatic methods
Proteases (trypsin, pepsin) Nucleases (DNase, RNase)

ficiency. For example, surfactants are commonly applied to dissociate and dissolve cell membranes and residual debris.

Among the chemical methods of decellularization, the most commonly used surfactants are Triton X-100 (nonionic) and sodium dodecyl sulfate (SDS) (ionic). Triton X-100 disrupts lipid–protein and lipid–lipid interactions while largely preserving protein–protein bonds, leading to cell separation and membrane lysis. Because of its relatively mild effect, it is often applied to tissues with high protein content, though caution is required when decellularizing tissues rich in glycosaminoglycans (GAGs) [64].

SDS dissolves both cytoplasmic and nuclear cell membranes well and can denature proteins by disrupting protein-protein interactions. However, prolonged SDS exposure may damage the overall structure of ECM [13]. Another chemical approach is osmotic shock, achieved by sequential exposure of tissue to hypotonic and hypertonic solutions. While this effectively induces cell lysis, it does not fully remove cellular debris [98].

The zwitterionic surfactant CHAPS (a bile acid derivative) acts by disrupting lipid–lipid and lipid–protein interactions, thereby lysing cell membranes. Due to its limited penetration capacity, CHAPS is primarily used for thin-layer tissues [96].

Because residual nuclear material can strongly bind to ECM proteins, enzymatic processing is often combined with chemical methods. DNases are widely used to degrade and remove nuclear remnants [62, 96]. Proteolytic enzymes are also employed, including trypsin (hydrolyzes proteins), elastase (degrades elastin), and dispase (cleaves type I/IV collagen and fibronectin). However, excessive enzymatic exposure may result in loss of ECM components such as collagen, elastin, fibronectin, and laminin [96].

Trypsin is frequently used in combination with ethylenediaminetetraacetic acid (EDTA) to detach cells from the ECM. Yet, prolonged trypsin–EDTA treatment can significantly alter ECM integrity by degrading laminin, removing GAGs, and ultimately reducing the mechanical strength of the tissue [13].

When developing decellularization protocols, it is essential to account for all processing conditions, since physical methods may disrupt ECM ultrastructure, while chemical and enzymatic treatments can degrade ECM components or trigger reactions that alter its biochemical composition [96]. To obtain an optimal scaffold, it is also important to consider the structural characteristics of the native tissue, such as thickness, density, and the presence of fibrosis or lipomatosis, which depend on the individual characteristics of the donor [99]. Therefore, for each individual case of obtaining a tissue-specific scaffold, it is necessary to determine a special original protocol for effective decellularization.

Several studies have reported the generation of scaffolds through whole-pancreas decellularization (Table 3). However, major challenges remain, particularly in achieving uniform recellularization and restoring functional vascularization within these large scaffolds. As an alternative, researchers have proposed the development of injectable TEPCs derived from finely dispersed pancreatic ECM fragments that are recellularized with insulin-producing cells [63, 64, 99]. The availability of TEPCs with specific functional properties and the minimally invasive administration of such a construct make this approach promising for tissue engineering technologies [19, 100]. Moreover, by preserving the natural ECM composition, such scaffolds provide a biomimetic microenvironment for the recellularized islet cells, while complete removal of cellular material from the scaffold ensures low immunogenicity [15, 62, 96, 97].

The liver and pancreas share similar embryonic origins and possess comparable ECM components, including collagens (types I, III, and IV), elastin, laminin, fibronectin, and GAGs [105, 106]. Consequently, decellularized liver scaffolds have emerged as promising alternatives for developing TEPCs, providing a favorable microenvironment for insulin-producing cells. For example, Xu et al. demonstrated that scaffolds derived from decellularized whole mouse liver lobes supported long-term survival and functional maintenance of isolated mouse islets *in vitro* [54]. Similarly, Goh et al. reported successful colonization of decellularized mouse liver scaffolds with insulin-producing cell aggregates differentiated from human pluripotent stem cells [104].

The potential of scaffolds derived from other decellularized organs to prolong the function of insulin-producing cells has also been reported. Khorsandi et al. showed that a rat spleen-derived scaffold increased insulin secretion of MIN6 cells compared with conventional monolayer culture, identifying it as a suitable carrier for

Table 3

Examples of protocols for decellularization of pancreatic tissue

Human	Whole organ	Cold perfusion was performed sequentially using the following solutions: phosphate-buffered saline (PBS) with heparin; Triton X-100 combined with ammonium hydroxide; DNase IV with magnesium chloride; PBS (for removal of remaining surfactants) [101]
	Fragments	Homogenization of pancreatic tissue, followed by centrifugation to remove insoluble fat. The tissue was then incubated in PBS and sodium deoxycholate, followed by treatment with PBS and an antibiotic/antimycotic solution to remove residual surfactants. The material was subsequently lyophilized and subjected to gelation [62]
		Mechanical grinding of pancreatic tissue with sequential treatment using hypotonic and hypertonic solutions containing SDS. This was followed by SDS treatment in the presence of PBS, and surfactant removal with PBS and an antibiotic/antimycotic solution [102]
		For pancreases with lipomatosis: Three cycles of freezing at –80 °C and thawing at +37 °C were performed. The tissue was then ground and treated with surfactant solutions (SDS and Triton X-100). Final rinsing was done using PBS and an antibiotic/antimycotic solution to remove residual surfactants [98, 99]
		For pancreases with fibrosis: The tissue was mechanically ground and subjected to sequential treatment with hypertonic and hypotonic solutions containing SDS. This was followed by treatment with SDS in PBS, and final surfactant removal using PBS with antibiotic/antimycotic agents [98]
Pig	Whole organ	Perfusion with sequential solutions: distilled H_2O, EDTA, and sodium azide; sodium deoxycholate, Triton X-100, and DNase. Cold perfusion using sodium deoxycholate, Triton X-100, and phenylmethylsulfonyl fluoride; distilled H_2O; DNase I in Dulbecco's PBS supplemented with calcium and magnesium chloride. Final surfactant removal was achieved using distilled H_2O containing sodium azide [103]
	Fragments	A total of 8 decellularization protocols were tested, varying by temperature (+4 °C *vs* +24 °C), washing agent (PBS *vs* $NH_3 \cdot H_2O$), and native tissue disintegration method (grinding *vs* cutting). Sequential treatment involving Triton X-100, $NH_3 \cdot H_2O$, and PBS; followed by $NH_3 \cdot H_2O$ washing; DNase incubation in PBS with calcium and magnesium ions; and repeated PBS washes [64]
		Tissue grinding; sequential treatment with hypotonic and hypertonic solutions containing SDS; subsequent treatment with SDS in PBS; and surfactant removal using PBS with antibiotic/antimycotic agents [13]
Rat	Whole organ	Perfusion via the pancreatic duct, gastric artery, portal vein, or splenic vein using the following sequence of solutions: Triton X-100 → SDS → Triton X-100 → DNase → PBS with antibiotic/antimycotic (for surfactant removal) [63]
		Sequential perfusion using: Triton X-100 → SDS → Triton X-100 → PBS (for surfactant removal) [61]
	Fragments	Grinding of fresh pancreatic tissue; sequential treatment with hypotonic and hypertonic solutions containing SDS; SDS treatment in FSB; surfactant removal with PBS containing antibiotic/antimycotic agents [42]
Mouse	Whole organ	Sequential perfusion using: SDS in deionized water; deionized water rinse; Triton X-100 in deionized water; benzonase solution; final wash with PBS containing 10% fetal bovine serum (FBS) and antibiotic/antimycotic agents for surfactant removal [104]
		Perfusion with double-distilled water, followed by freezing of the lipid bilayer at –80 °C and thawing at room temperature. Subsequent perfusion was performed using PBS, Triton X-100, and ammonium hydroxide, with final washing in PBS to remove residual surfactants [55]

beta-cell transplantation [107]. A bioartificial pancreas generated from decellularized pig lung tissue seeded with human islets exhibited prolonged viability and insulin secretion *in vitro*, comparable to freshly isolated islets. This construct was recommended as a reliable platform for real-time drug screening [108].

The introduction of a hydrogel phase into the composition of TEPC can prevent sticking and rapid sedimentation of scaffold microparticles derived from decellularized pancreatic tissue [15, 62]. Recent approaches have focused on the development of hydrogels based on decellularized pancreatic tissue that are capable of polymerizing *in situ* under physiological conditions [109]. Hydrogels not only facilitate the delivery of ECM components and growth factors to insulin-producing cells within TEPC, but can also be applied for encapsulating islet cells or serve as bio-inks for bioprinting.

In addition, methods have been established for fabricating 3D macroporous spongy scaffolds from hydrolysates of decellularized tissues, with cryogenic structuring emerging as a particularly promising technique. In this process, the macroporous architecture is generated at subzero temperatures, where frozen solvent crystals function as porogens [110]. For example, Kim et al. produced a macroporous sponge material from decellularized pig kidney tissue by creating a chemically cross-linked cryogel followed by lyophilization [111]. This material was successfully applied both as a hemostatic sponge and as a cell carrier in tissue-engineered constructs using fibroblasts isolated from rat kidneys. Borg et al. showed that the interconnected macroporous structure of cryogels of varying sizes enabled uniform colonization by mesenchymal stem cells and immobilization of islets. The survival and functional activity of

islets seeded into cryogels were confirmed *in vitro* and *in vivo* following implantation in mice [112].

As shown by the data reviewed, the development of biocompatible and functional scaffolds based on natural ECM, possessing properties characteristic of the native pancreatic microenvironment, remains a pressing challenge.

CONCLUSION

The design of ECM biomimetic scaffolds that closely mimic the native microenvironment of insulin-producing cells holds great potential for improving the clinical outcomes of islet transplantation by prolonging cell viability and maintaining insulin secretory function both *in vitro* and *in vivo*. Various scaffold materials, derived from different sources, offer distinct advantages and limitations, underscoring the need for ongoing research to determine the optimal composition and architecture of scaffolds for TEPC formation and clinical translation.

Among the most promising approaches in regenerative medicine is the use of scaffolds generated from decellularized tissues, whose multicomponent composition closely resembles that of native ECM. Particularly noteworthy is the emerging technology of cryogenic structuring of decellularized tissue hydrolysates, which enables fabrication of highly biocompatible scaffolds with predefined shapes, optimal mechanical properties, and interconnected porous networks.

At the same time, the search for renewable and functionally active insulin-producing cells, capable of responding to fluctuations in the recipient's blood glucose levels, remains a priority. The synergistic integration of innovations in materials science and cell technologies will advance the effectiveness and accessibility of cell replacement therapies for type 1 diabetes, making them available to a broader patient population.

This research was supported by the Russian Science Foundation, Grant No. 25-25-00425 (https://rscf.ru/project/25-25-00425/).

The authors declare no conflict of interest.

REFERENCES

1. *Dedov II, Shestakova MV, Mayorov AY, Shamkhalova MS, Nikonova TV, Sukhareva OY et al.* Diabetes mellitus type 1 in adults. *Diabetes mellitus*. 2020; 23 (1S): 42–114. (In Russ.). doi: 10.14341/DM12505.
2. *Norris JM, Johnson RK, Stene LC*. Type 1 diabetes-early life origins and changing epidemiology. *Lancet Diabetes Endocrinol*. 2020; 8 (3): 226–238. doi: 10.1016/S2213-8587(19)30412-7.
3. *Shapiro AM, Lakey JR, Ryan EA, Korbutt GS, Toth E, Warnock GL et al.* Islet transplantation in seven patients with type 1 diabetes mellitus using a glucocorticoid-free immunosuppressive regimen. *N Engl J Med.* 2000; 343 (4): 230–238. doi: 10.1056/NEJM200007273430401.
4. *Piemonti L. In: Feingold KR, Anawalt B, Blackman MR, Boyce A, Chrousos G, Corpas E et al editors.* Islet Transplantation. *Endotext [Internet]. South Dartmouth (MA): MDText.com, Inc.* 2022; 2000. PMID: 25905200.
5. *Gruessner AC, Gruessner RWG*. The 2022 International Pancreas Transplant Registry Report – A Review. *Transplant Proc.* 2022; 54 (7): 1918–1943. doi: 10.1016/j.transproceed.2022.03.059.
6. *Lablanche S, Borot S, Wojtusciszyn A, Skaare K, Penfornis A, Malvezzi P et al.* Ten-year outcomes of islet transplantation in patients with type 1 diabetes: Data from the Swiss-French GRAGIL network. *Am J Transplant*. 2021; 21 (11): 3725–3733. doi: 10.1111/ajt.16637.
7. *Hering BJ, Ballou CM, Bellin MD, Payne EH, Kandeel F, Witkowski P et al.* Factors associated with favourable 5 year outcomes in islet transplant alone recipients with type 1 diabetes complicated by severe hypoglycaemia in the Collaborative Islet Transplant Registry. *Diabetologia.* 2023; 66: 163–173. doi: 10.1007/s00125-022-05804-4.
8. *Reid L, Baxter F, Forbes S*. Effects of islet transplantation on microvascular and macrovascular complications in type 1 diabetes. *Diabet Med.* 2021; 38 (7): e14570. doi: 10.1111/dme.14570.
9. *Langlois A, Pinget M, Kessler L, Bouzakri K.* Islet Transplantation: Current Limitations and Challenges for Successful Outcomes. *Cells.* 2024; 13 (21): 1783. doi: 10.3390/cells13211783.
10. *Olaniru OE, Persaud SJ*. Identifying novel therapeutic targets for diabetes through improved understanding of islet adhesion receptors. *Curr Opin Pharmacol.* 2018; 43: 27–33. doi: 10.1016/j.coph.2018.07.009.
11. *Kahraman S, Okawa ER, Kulkarni RN.* Is Transforming Stem Cells to Pancreatic Beta Cells Still the Holy Grail for Type 2 Diabetes? *Curr Diab Rep.* 2016; 16 (8): 70. doi: 10.1007/s11892-016-0764-0.
12. *Abadpour S, Wang C, Niemi EM, Scholz H.* Tissue Engineering Strategies for Improving Beta Cell Transplantation Outcome. *Curr Transpl Rep*. 2021; 8: 205–219. doi: 10.1007/s40472-021-00333-2.
13. *Sevastianov VI, Basok YuB et al.* Biomimetics of Extracellular Matrices for Cell and Tissue Engineered Medical Products. *Eds. Victor I. Sevastianov and Yulia B. Basok*. Newcastle upon Tyne, UK: Cambridge Scholars Publishing; 2023: 339.
14. *Zhang Q, Gonelle-Gispert C, Li Y, Geng Z, Gerber-Lemaire S, Wang Y et al.* Islet Encapsulation: New Developments for the Treatment of Type 1 Diabetes. *Front Immunol.* 2022; 13: 869984. doi: 10.3389/fimmu.2022.869984.
15. *Salg GA, Giese NA, Schenk M, Hüttner FJ, Felix K, Probst P et al.* The emerging field of pancreatic tissue engineering: A systematic review and evidence map of scaffold materials and scaffolding techniques for insulin-secreting cells. *J Tissue Eng.* 2019; 10: 2041731419884708. doi: 10.1177/2041731419884708.
16. *Ho BX, Teo AKK, Ng NHJ*. Innovations in bio-engineering and cell-based approaches to address immunological challenges in islet transplantation. *Front Immunol.* 2024; 15: 1375177. doi: 10.3389/fimmu.2024.1375177.

17. *Basok YuB., Ponomareva AS, Grudinin NV, Kruglov DN, Bogdanov VK, Belova AD, Sevastyanov VI.* Application of mesenchymal stromal cells in solid organ transplantation: challenges and prospects (systematic review). *Russian Journal of Transplantology and Artificial Organs.* 2025; 27 (1): 114–134.
18. *Amer LD, Mahoney MJ, Bryant SJ.* Tissue engineering approaches to cell-based type 1 diabetes therapy. *Tissue Eng Part B Rev*. 2014; 20 (5): 455–467. doi: 10.1089/ten.TEB.2013.0462.
19. *Santos da Silva T, Silva-Júnior LND, Horvath-Pereira BO, Valbão MCM, Garcia MHH, Lopes JB et al.* The Role of the Pancreatic Extracellular Matrix as a Tissue Engineering Support for the Bioartificial Pancreas. *Biomimetics (Basel)*. 2024; 9 (10): 598. doi: 10.3390/biomimetics9100598.
20. *Sojoodi M, Farrokhi A, Moradmand A, Baharvand H.* Enhanced maintenance of rat islets of Langerhans on laminin-coated electrospun nanofibrillar matrix *in vitro*. *Cell Biol Int*. 2013; 37 (4): 370–379. doi: 10.1002/cbin.10045.
21. *Sigmundsson K, Ojala JRM, Öhman MK, Österholm AM, Moreno-Moral A, Domogatskaya A et al*. Culturing functional pancreatic islets on α5-laminins and curative transplantation to diabetic mice. *Matrix Biol.* 2018; 70: 5–19. doi: 10.1016/j.matbio.2018.03.018.
22. *Fernández-Montes RD, Blasi J, Busquets J, Montanya E, Nacher M.* Fibronectin enhances soluble N-ethylmaleimide-sensitive factor attachment protein receptor protein expression in cultured human islets. *Pancreas*. 2011; 40 (7): 1153–1155. doi: 10.1097/MPA.0b013e318222bcaf.
23. *Llacua LA, Hoek A, de Haan BJ, de Vos P.* Collagen type VI interaction improves human islet survival in immunoisolating microcapsules for treatment of diabetes. *Islets.* 2018; 10 (2): 60–68. doi: 10.1080/19382014.2017.1420449.
24. *Surguchenko VA, Ponomareva AS, Efimov AE, Nemets EA, Agapov II, Sevastianov VI.* Characteristics of adhesion and proliferation of mouse nih/3t3 fibroblasts on the poly(3-hydroxybutyrate-co-3-hydroxyvalerate) films with different surface roughness values. *Russian Journal of Transplantology and Artificial Organs*. 2012; 14 (1): 72–77. (In Russ.). doi: 10.15825/1995-1191-2012-1-72-77.
25. *Mehdi Ebrahimi*. Porosity parameters in biomaterial science: Definition, impact, and challenges in tissue engineering. *Front Mater Sci.* 2021; 15 (3): 352–373. doi: 10.1007/s11706-021-0558-4.
26. *Sevastyanov VI, Kirpichnikov MP.* Biosovmestimye materialy. M.: MIA, 2011; 544.
27. *Johnson AS, O'Sullivan E, D'Aoust LN, Omer A, Bonner-Weir S, Fisher RJ et al*. Quantitative assessment of islets of Langerhans encapsulated in alginate. *Tissue Eng Part C Methods*. 2011; 17 (4): 435–449. doi: 10.1089/ten.TEC.2009.0510.
28. *Formo K, Cho CH, Vallier L, Strand BL.* Culture of hESC-derived pancreatic progenitors in alginate-based scaffolds. *J Biomed Mater Res A*. 2015; 103 (12): 3717–3726. doi: 0.1002/jbm.a.35507.
29. *Köllmer M, Appel AA, Somo SI, Brey EM.* Long-term function of alginate-encapsulated islets. *Tissue Eng Part B Rev.* 2015; 22: 34–46. doi: 10.1089/ten.TEB.2015.0140.
30. *Li N, Sun G, Wang S, Wang Y, Xiu Z, Sun D et al.* Engineering islet for improved performance by optimized reaggregation in alginate gel beads. *Biotechnol Appl Biochem.* 2017; 64 (3): 400–405. doi: 10.1002/bab.1489.
31. *Noverraz F, Montanari E, Pimenta J, Szabó L, Ortiz D, Gonelle-Gispert C et al.* Antifibrotic effect of ketoprofen-grafted alginate microcapsules in the transplantation of insulin producing cells. *Bioconjug Chem.* 2018; 29 (6): 1932–1941. doi: 10.1021/acs.bioconjchem.8b00190.
32. *Espona-Noguera A, Ciriza J, Cañibano-Hernández A, Fernandez L, Ochoa I, Saenz Del Burgo L et al.* Tunable injectable alginate-based hydrogel for cell therapy in Type 1 Diabetes Mellitus. *Int J Biol Macromol*. 2018; 107 (Pt A): 1261–1269. doi: 10.1016/j.ijbiomac.2017.09.103.
33. *Kawazoe N, Lin XT, Tateishi T, Chen G.* Three-dimensional cultures of rat pancreatic RIN-5F cells in porous PLGA-collagen hybrid scaffolds. *J Bioact Compat Pol*. 2009; 24: 25–42. doi: 10.1177/0883911508099439.
34. *Jalili RB, Moeen Rezakhanlou A, Hosseini-Tabatabaei A, Ao Z, Warnock GL, Ghahary A*. Fibroblast populated collagen matrix promotes islet survival and reduces the number of islets required for diabetes reversal. *J Cell Physiol*. 2011; 226 (7): 1813–1819. doi: 10.1002/jcp.22515.
35. *Deng C, Vulesevic B, Ellis C, Korbutt GS, Suuronen EJ*. Vascularization of collagen-chitosan scaffolds with circulating progenitor cells as potential site for islet transplantation. *J Control Release*. 2011; 152 (Suppl 1): e196–e198. doi: 10.1016/j.jconrel.2011.09.005.
36. *Yap WT, Salvay DM, Silliman MA, Zhang X, Bannon ZG, Kaufman DB et al.* Collagen IV-modified scaffolds improve islet survival and function and reduce time to euglycemia. *Tissue Eng Part A*. 2013; 19 (21–22): 2361–2372. doi: 10.1089/ten.TEA.2013.0033.
37. *Riopel M, Wang K.* Collagen matrix support of pancreatic islet survival and function. *Front Biosci (Landmark Ed)*. 2014; 19 (1): 77–90. doi: 10.2741/4196.
38. *McEwan K, Padavan DT, Ellis C, McBane JE, Vulesevic B, Korbutt GS et al.* Collagen-chitosan-laminin hydrogels for the delivery of insulin-producing tissue. *J Tissue Eng Regen Med*. 2016; 10 (10): E397–E408. doi: 10.1002/term.1829.
39. *Szebeni GJ, Tancos Z, Feher LZ, Alfoldi R, Kobolak J, Dinnyes A et al*. Real architecture for 3D Tissue (RAFT) culture system improves viability and maintains insulin and glucagon production of mouse pancreatic islet cells. *Cytotechnology.* 2017; 69 (2): 359–369. doi: 10.1007/s10616-017-0067-6.
40. *Vlahos AE, Cober N, Sefton MV*. Modular tissue engineering for the vascularization of subcutaneously transplanted pancreatic islets. *Proc Natl Acad Sci USA*. 2017; 114 (35): 9337–9342. doi: 10.1073/pnas.1619216114.
41. *Montalbano G, Toumpaniari S, Popov A, Duan P, Chen J, Dalgarno K et al.* Synthesis of bioinspired collagen/alginate/fibrin based hydrogels for soft tissue en-

gineering. *Mater Sci Eng C Mater Biol Appl*. 2018; 91: 236–246. doi: 10.1016/j.msec.2018.04.101.
42. *Baranova NV, Kirsanova LA, Ponomareva AS, Nemets EA, Basok YB, Bubentsova GN et al.* Comparative analysis of the secretory capacity of islets of langerhans cultured with biopolymer-based collagen-containing hydrogel and tissue-specific matrix. *Russian Journal of Transplantology and Artificial Organs*. 2019; 21 (4): 45–53. doi: 10.15825/1995-1191-2019-4-45-53.
43. *Yang KC, Wu CC, Lin FH, Qi Z, Kuo TF, Cheng YH et al*. Chitosan/gelatin hydrogel as immunoisolative matrix for injectable bioartificial pancreas. *Xenotransplantation.* 2008; 15 (6): 407–416. doi: 10.1111/j.1399-3089.2008.00503.x.
44. *Kuehn C, Fülöp T, Lakey JR, Vermette P*. Young porcine endocrine pancreatic islets cultured in fibrin and alginate gels show improved resistance towards human monocytes. *Pathol Biol*. 2014; 62 (6): 354–364. doi: 10.1016/j.patbio.2014.07.010.
45. *Bhang SH, Jung MJ, Shin JY, La WG, Hwang YH, Kim MJ et al.* Mutual effect of subcutaneously transplanted human adipose-derived stem cells and pancreatic islets within fibrin gel. *Biomaterials.* 2013; 34 (30): 7247–7256. doi: 10.1016/j.biomaterials.2013.06.018.
46. *Kuehn C, Lakey JR, Lamb MW, Vermette P*. Young porcine endocrine pancreatic islets cultured in fibrin show improved resistance toward hydrogen peroxide. *Islets.* 2013; 5 (5): 207–215. doi: 10.4161/isl.26989.
47. *Niknamasl A, Ostad SN, Soleimani M, Azami M, Salmani MK, Lotfibakhshaiesh N et al.* A new approach for pancreatic tissue engineering: human endometrial stem cells encapsulated in fibrin gel can differentiate to pancreatic islet beta-cell. *Cell Biol Int.* 2014; 38 (10): 1174–1182. doi: 10.1002/cbin.10314.
48. *Seyedi F, Farsinejad A, Nematollahi-Mahani SN*. Fibrin scaffold enhances function of insulin producing cells differentiated from human umbilical cord matrix-derived stem cells. *Tissue Cell*. 2017; 49 (2 Pt B): 227–232. doi: 10.1016/j.tice.2017.03.001.
49. *Muthyala S, Bhonde RR, Nair PD.* Cytocompatibility studies of mouse pancreatic islets on gelatin – PVP semi IPN scaffolds *in vitro*: potential implication towards pancreatic tissue engineering. *Islets.* 2010; 2 (6): 357–366. doi: 10.4161/isl.2.6.13765.
50. *Kuo YC, Liu YC, Rajesh R.* Pancreatic differentiation of induced pluripotent stem cells in activin A-grafted gelatin-poly(lactide-co-glycolide) nanoparticle scaffolds with induction of LY294002 and retinoic acid. *Mater Sci Eng C Mater Biol Appl*. 2017; 77: 384–393. doi: 10.1016/j.msec.2017.03.265.
51. *Davis NE, Beenken-Rothkopf LN, Mirsoian A, Kojic N, Kaplan DL, Barron AE et al.* Enhanced function of pancreatic islets co-encapsulated with ECM proteins and mesenchymal stromal cells in a silk hydrogel. *Biomaterials.* 2012; 33 (28): 6691–6697. doi: 10.1016/j.biomaterials.2012.06.015.
52. *Shalaly ND, Ria M, Johansson U, Åvall K, Berggren PO, Hedhammar M*. Silk matrices promote formation of insulin-secreting islet-like clusters. *Biomaterials*. 2016; 90: 50–61. doi: 10.1016/j.biomaterials.2016.03.006.
53. *Kumar M, Nandi SK, Kaplan DL, Mandal BB.* Localized immunomodulatory silk macrocapsules for islet-like spheroid formation and sustained insulin production. *ACS Biomater Sci Eng.* 2017; 3: 2443–2456. doi: 10.1021/acsbiomaterials.7b00218.
54. *Xu T, Zhu M, Guo Y, Wu D, Huang Y, Fan X et al*. Three-dimensional culture of mouse pancreatic islet on a liver-derived perfusion-decellularized bioscaffold for potential clinical application. *J Biomater Appl*. 2015; 30 (4): 379–387. doi: 10.1177/0885328215587610.
55. *Wu D, Wan J, Huang Y, Guo Y, Xu T, Zhu M et al.* 3D culture of MIN-6 cells on decellularized pancreatic scaffold: *in vitro* and *in vivo* study. *Biomed Res Int*. 2015: 432645. doi: 10.1155/2015/432645.
56. *Abualhassan N, Sapozhnikov L, Pawlick RL, Kahana M, Pepper AR, Bruni A et al.* Lung-derived microscaffolds facilitate diabetes reversal after mouse and human intraperitoneal islet transplantation. *PLoS ONE*. 2016; 11 (5): e0156053. doi: 10.1371/journal.pone.0156053.
57. *Katsuki Y, Yagi H, Okitsu T, Kitago M, Tajima K, Kadota Y et al.* Endocrine pancreas engineered using porcine islets and partial pancreatic scaffolds. *Pancreatology.* 2016; 16 (5): 922–930. doi: 10.1016/j.pan.2016.06.007.
58. *Zhou P, Guo Y, Huang Y, Zhu M, Fan X, Wang L et al.* The dynamic three-dimensional culture of islet-like clusters in decellularized liver scaffolds. *Cell Tissue Res.* 2016; 365 (1): 157–171. doi: 10.1007/s00441-015-2356-8.
59. *Wang X, Wang K, Zhang W, Qiang M, Luo Y*. A bilaminated decellularized scaffold for islet transplantation: structure, properties and functions in diabetic mice. *Biomaterials*. 2017; 138: 80–90. doi: 10.1016/j.biomaterials.2017.05.033.
60. *Wan J, Huang Y, Zhou P, Guo Y, Wu C, Zhu S et al*. Culture of iPSCs derived pancreatic beta-like cells *in vitro* using decellularized pancreatic scaffolds: a preliminary trial. *Biomed Res Int*. 2017; 2017: 4276928. doi: 10.1155/2017/4276928.
61. *Napierala H, Hillebrandt KH, Haep, N, Tang P, Tintemann M, Gassner J et al.* Engineering an endocrine Neo-Pancreas by repopulation of a decellularized rat pancreas with islets of Langerhans. *Sci Rep.* 2017; 7: 41777. doi: 10.1038/srep41777.
62. *Sackett SD, Tremmel DM, Ma F, Feeney AK, Maguire RM, Brown ME et al.* Extracellular matrix scaffold and hydrogel derived from decellularized and delipidized human pancreas. *Sci Rep.* 2018; 8 (1): 10452. doi: 10.1038/s41598-018-28857-1.
63. *Berkova Z, Zacharovova K, Patikova A, Leontovyc I, Hladikova Z, Cerveny D et al.* Decellularized pancreatic tail as matrix for pancreatic islet transplantation into the greater omentum in rats. *J Funct Biomater.* 2022; 13 (4): 171. doi: 10.3390/jfb13040171.
64. *Klak M, Łojszczyk I, Berman A, Tymicki G, Adamiok-Ostrowska A, Sierakowski M et al.* Impact of porcine pancreas decellularization conditions on the quality of obtained dECM. *Int J Mol Sci*. 2021; 22 (13): 7005. doi: 10.3390/ijms22137005.
65. *Kizilel S, Scavone A, Liu X, Nothias JM, Ostrega D, Witkowski P et al*. Encapsulation of pancreatic islets within

nano-thin functional polyethylene glycol coatings for enhanced insulin secretion. *Tissue Eng Part A*. 2010; 16 (7): 2217–2228. doi: 10.1089/ten.TEA.2009.0640.

66. *Mason MN, Mahoney MJ.* A novel composite construct increases the vascularization potential of PEG hydrogels through the incorporation of large fibrin ribbons. *J Biomed Mater Res A.* 2010; 95 (1): 283–293. doi: 10.1002/jbm.a.32825.
67. *Lin CC, Anseth KS*. Cell-cell communication mimicry with poly(ethylene glycol) hydrogels for enhancing beta-cell function. *Proc Natl Acad Sci USA.* 2011; 108 (16): 6380–6385. doi: 10.1073/pnas.1014026108.
68. *Hall KK, Gattas-Asfura KM, Stabler CL.* Microencapsulation of islets within alginate/poly(ethylene glycol) gels cross-linked via Staudinger ligation. *Acta Biomater.* 2011; 7 (2): 614–624. doi: 10.1016/j.actbio.2010.07.016.
69. *Hume PS, Anseth KS*. Polymerizable superoxide dismutase mimetic protects cells encapsulated in poly(ethylene glycol) hydrogels from reactive oxygen species-mediated damage. *J Biomed Mater Res A.* 2011; 99 (1): 29–37. doi: 10.1002/jbm.a.33160.
70. *Raza A, Lin CC*. The influence of matrix degrada tion and functionality on cell survival and morphogenesis in PEG-based hydrogels. *Macromol Biosci.* 2013; 13 (8): 1048–1058. doi: 10.1002/mabi.201300044.
71. *Marchioli G, Luca AD, de Koning E, Engelse M, Van Blitterswijk CA, Karperien M et al.* Hybrid polycaprolactone/alginate scaffolds functionalized with VEGF to promote *de novo* vessel formation for the transplantation of islets of Langerhans. *Adv Healthc Mater.* 2016; 5 (13): 1606–1616. doi: 10.1002/adhm.201600058.
72. *Bal T, Nazli C, Okcu A, Duruksu G, Karaöz E, Kizilel S*. Mesenchymal stem cells and ligand incorporation in biomimetic poly(ethylene glycol) hydrogels significantly improve insulin secretion from pancreatic islets. *J Tissue Eng Regen Med*. 2017; 11 (3): 694–703. doi: 10.1002/term.1965.
73. *Knobeloch T, Abadi SEM, Bruns J, Petrova Zustiak S, Kwon G.* Injectable polyethylene glycol hydrogel for islet encapsulation: an *in vitro* and *in vivo* Characterization. *Biomed Phys Eng Express*. 2017; 3: 035022. doi: 10.1088/2057-1976/aa742b.
74. *Smink AM, Li S, Hertsig DT, de Haan BJ, Schwab L, van Apeldoorn AA et al.* The efficacy of a prevascularized, retrievable poly(D,L,-lactide-co-ε-caprolactone) subcutaneous scaffold as transplantation site for pancreatic islets. *Transplantation*. 2017; 101 (4): e112–e119. doi: 10.1097/TP.0000000000001663.
75. *Marchioli G, Zellner L, Oliveira C, Engelse M, Koning E, Mano J et al.* Layered PEGDA hydrogel for islet of Langerhans encapsulation and improvement of vascularization. *J Mater Sci Mater Med.* 2017; 28 (12): 195. doi: 10.1007/s10856-017-6004-6.
76. *Abazari MF, Soleimanifar F, Nouri Aleagha M, Torabinejad S, Nasiri N, Khamisipour G et al.* PCL/PVA nanofibrous scaffold improve insulin-producing cells generation from human induced pluripotent stem cells. *Gene.* 2018; 671: 50–57. doi: 10.1016/j.gene.2018.05.115.
77. *Chun S, Huang Y, Xie WJ, Hou Y, Huang RP, Song YM et al.* Adhesive growth of pancreatic islet cells on a polyglycolic acid fibrous scaffold. *Transplant Proc*. 2008; 40 (5): 1658 doi: 10.1016/j.transproceed.2008.02.088.
78. *Mao GH, Chen GA, Bai HY, Song TR, Wang YX*. The reversal of hyperglycaemia in diabetic mice using PLGA scaffolds seeded with islet-like cells derived from human embryonic stem cells. *Biomaterials.* 2009; 30 (9): 1706–1714. doi: 10.1016/j.biomaterials.2008.12.030.
79. *Li Y, Fan P, Ding XM, Tian XH, Feng XS, Yan H et al*. Polyglycolic acid fibrous scaffold improving endothelial cell coating and vascularization of islet. *Chin Med J.* 2017; 130 (7): 832–839. doi: 10.4103/0366-6999.202730.
80. *Kheradmand T, Wang S, Gibly RF, Zhang X, Holland S, Tasch J et al.* Permanent protection of PLG scaffold transplanted allogeneic islet grafts in diabetic mice treated with ECDI-fixed donor splenocyte infusions. *Biomaterials.* 2011; 32 (20): 4517–4524. doi: 10.1016/j.biomaterials.2011.03.009.
81. *Daoud JT, Petropavlovskaia MS, Patapas JM, Degrandpré CE, Diraddo RW, Rosenberg L et al.* Long-term *in vitro* human pancreatic islet culture using three dimensional microfabricated scaffolds. *Biomaterials.* 2011; 32 (6): 1536–1542. doi: 10.1016/j.biomaterials.2010.10.036.
82. *Liu L, Tan J, Li B, Xie Q, Sun J, Pu H et al.* Construction of functional pancreatic artificial islet tissue composed of fibroblast-modified polylactic-co-glycolic acid membrane and pancreatic stem cells. *J Biomater Appl*. 2017; 32 (3): 362–372. doi: 10.1177/0885328217722041.
83. *Sevastianov VI.* Cell-engineered constructs in tissue engineering and regenerative medicine. *Russian Journal of Transplantology and Artificial Organs*. 2015; 17 (2): 127–130. (In Russ.). doi: 10.15825/1995-1191-2015-2-127-130.
84. *Buitinga M, Assen F, Hanegraaf M, Wieringa P, Hilderink J, Moroni L et al.* Micro-fabricated scaffolds lead to efficient remission of diabetes in mice. *Biomaterials.* 2017; 135: 10–22. doi: 10.1016/j.biomaterials.2017.03.031.
85. *Kumar A.* Supermacroporous Cryogels: Biomedical and Biotechnological Applications. 1st Edition. USA: CRC Press. 2016; 480. doi: 10.1201/b19676.
86. *Lozinsky VI*. A breif history of polymeric cryogels. *Adv Polym Sci*. 2014; 263: 1–48. doi: 10.1007/978-3-319-05846-7_1.
87. *Lozinsky VI, Kulakova VK, Grigoriev AM, Podorozhko EA, Kirsanova LA, Kirillova AD et al*. Cryostructuring of Polymeric Systems: 63. Synthesis of Two Chemically Tanned Gelatin-Based Cryostructurates and Evaluation of Their Potential as Scaffolds for Culturing of Mammalian Cells. *Gels.* 2022; 8 (11): 695. doi: 10.3390/gels8110695.
88. *Bloch K, Lozinsky VI, Galaev IY, Yavriyanz K, Vorobeychik M, Azarov D et al.* Functional activity of insulinoma cells (INS-1E) and pancreatic islets cultured in agarose cryogel sponges. *J Biomed Mater Res A*. 2005; 75: 802–809. doi: 10.1002/jbm.a.30466.
89. *Lozinsky VI, Damshkaln LG, Bloch RO, Vardi P, Grinberg NV, Burova TV et al.* Cryostructuring of polymer systems. Preparation and characterization of superma-

croporous (spongy) agarose-based cryogels used as three-dimensional scaffolds for culturing insulin-producing cell aggregates. *J Appl Polym Sci.* 2008; 108: 3046–3062. doi: 10.1002/app.27908.

90. *Minardi S, Guo M, Zhang X, Luo X*. An elastin-based vasculogenic scaffold promotes marginal islet mass engraftment and function at an extrahepatic site. *J Immunol Regen Med.* 2019; 3: 1–12. doi: 10.1016/j.regen.2018.12.001.
91. *Sevastianov VI, Grigoriev AM, Basok YuB, Kirsanova LA, Vasilets VN, Malkova AP et al*. Biocompatible and matrix properties of polylactide scaffolds. *Russian Journal of Transplantology and Artificial Organs*. 2018; 20 (2): 82–90. (In Russ.). doi: 10.15825/1995-1191-2018-2-82-90.
92. *Pinkse GG, Bouwman WP, Jiawan-Lalai R, Terpstra OT, Bruijn JA, de Heer E.* Integrin signaling via RGD peptides and anti-beta1 antibodies confers resistance to apoptosis in islets of Langerhans. *Diabetes.* 2006; 55 (2): 312–317. doi: 10.2337/diabetes.55.02.06.db04-0195.
93. *Sevastianov VI, Basok YB, Kirsanova LA, Grigoriev AM, Kirillova AD, Nemets EA et al.* A Comparison of the Capacity of Mesenchymal Stromal Cells for Cartilage Regeneration Depending on Collagen-Based Injectable Biomimetic Scaffold Type. *Life (Basel).* 2021; 11 (8): 756. doi: 10.3390/life11080756.
94. *Hamamoto Y, Fujimoto S, Inada A, Takehiro M, Nabe K, Shimono D et al.* Beneficial effect of pretreatment of islets with fibronectin on glucose tolerance after islet transplantation. *Horm Metab Res.* 2003; 35 (8): 460–465. doi: 10.1055/s-2003-41802.
95. *Yeo GC, Mithieux SM, Weiss AS.* The elastin matrix in tissue engineering and regeneration. *Current Opinion in Biomedical Engineering.* 2018; 6: 27–32. doi: 10.1016/j.cobme.2018.02.007.
96. *Mendibil U, Ruiz-Hernandez R, Retegi-Carrion S, Garcia-Urquia N, Olalde-Graells B, Abarrategi A.* Tissue-Specific Decellularization Methods: Rationale and Strategies to Achieve Regenerative Compounds. *Int J Mol Sci*. 2020; 21: 5447. doi: 10.3390/ijms21155447.
97. *Rabbani M, Zakian N, Alimoradi N.* Contribution of Physical Methods in Decellularization of Animal Tissues. *Journal of Medical Signals & Sensors*. 2021; 11 (1): 1. doi: 10.4103/jmss.JMSS_2_20.
98. *Ponomareva AS, Baranova NV, Kirsanova LA, Bubentsova GN, Nemets EA, Miloserdov IA, Sevastianov VI.* Determining the optimal pancreatic decellularization protocol, taking into account tissue morphological features. *Russian Journal of Transplantology and Artificial Organs*. 2022; 24 (1): 64–71. doi: 10.15825/1995-1191-2022-1-64-71.
99. *Sevastianov VI, Ponomareva AS, Baranova NV, Kirsanova LA, Basok YuB, Nemets EA et al.* Decellularization of Human Pancreatic Fragments with Pronounced Signs of Structural Changes. *Int J Mol Sci*. 2023; 24: 119. doi: 10.3390/ijms24010119.28.
100. *Sevastianov VI, Ponomareva AS, Baranova NV, Belova AD, Kirsanova LA, Nikolskaya AO et al.* A Tissue-Engineered Construct Based on a Decellularized Scaffold and the Islets of Langerhans: A Streptozotocin-Induced Diabetic Model. *Life (Basel).* 2024; 14 (11): 1505. doi: 10.3390/life14111505.
101. *Peloso A, Urbani L, Cravedi P, Katari R, Maghsoudlou P, Fallas MEA et al.* The human pancreas as a source of pro-tolerogenic extracellular matrix scaffold for a new generation bio-artificial endocrine pancreas. *Ann Surg*. 2016; 264 (1): 169–179. doi: 10.1097/SLA.0000000000001364.
102. *Ponomareva AS, Kirsanova LA, Baranova NV, Surguchenko VA, Bubentsova GN, Basok YuB et al*. Decellularization of donor pancreatic fragment to obtain a tissue-specific matrix scaffold. *Russian Journal of Transplantology and Artificial Organs*. 2020; 22 (1): 123–133. doi: 10.15825/1995-1191-2020-1-123-133.
103. *Elebring E, Kuna VK, Kvarnstrom N, Sumitran-Holgersson S.* Cold-perfusion decellularization of whole-organ porcine pancreas supports human fetal pancreatic cell attachment and expression of endocrine and exocrine markers. *J Tissue Eng.* 2017; 8: 2041731417738145. doi: 10.1177/2041731417738145.
104. *Goh SK, Bertera S, Richardson T, Banerjee I.* Repopulation of decellularized organ scaffolds with human pluripotent stem cell-derived pancreatic progenitor cells. *Biomed Mater*. 2023; 18 (2). doi: 10.1088/1748-605X/acb7bf.
105. *Song JJ, Ott HC*. Organ engineering based on decellularized matrix scaffolds. *Trends Mol Med*. 2011; 17 (8): 424–432. doi: 10.1016/j.molmed.2011.03.005.
106. *Damodaran GR, Vermette P.* Decellularized pancreas as a native extracellular matrix scaffold for pancreatic islet seeding and culture. *J Tissue Eng Regen Med*. 2018; 12 (5): 1230–1237. doi: 10.1002/term.2655.
107. *Khorsandi L, Orazizadeh M, Bijan Nejad D, Heidari Moghadam A, Nejaddehbashi F, Asadi Fard Y.* Spleen extracellular matrix provides a supportive microenvironment for β-cell function. *Iran J Basic Med Sci.* 2022; 25 (9): 1159–1165. doi: 10.22038/IJBMS.2022.65233.14360.
108. *Goldman O, Puchinsky D, Durlacher K, Sancho R, Ludwig B, Kugelmeier P et al.* Lung Based Engineered Micro-Pancreas Sustains Human Beta Cell Survival and Functionality. *Horm Metab Res*. 2019; 51 (12): 805–811. doi: 10.1055/a-1041-3305.
109. *Saldin LT, Cramer MC, Velankar SS, White LJ, Badylak SF*. Extracellular matrix hydrogels from decellularized tissues: Structure and function. *Acta Biomater*. 2017; 49: 1–15. doi: 10.1016/j.actbio.2016.11.068.
110. *Lozinsky VI.* Cryostructuring of Polymeric Systems. 50.† Cryogels and Cryotropic Gel-Formation: Terms and Definitions. *Gels.* 2018; 4: 77. doi: 10.3390/gels4030077.
111. *Kim JY, Sen T, Lee JY, Cho D-W.* Degradation-controlled tissue extracellular sponge for rapid hemostasis and wound repair after kidney injury. *Biomaterials.* 2024; 307: 122524. doi: 10.1016/j.biomaterials.2024.122524.
112. *Borg DJ, Welzel PB, Grimmer M, Friedrichs J, Weigelt M, Wilhelm C et al.* Macroporous biohybrid cryogels for co-housing pancreatic islets with mesenchymal stromal cells. *Acta Biomater*. 2016; 44: 178–187. doi: 10.1016/j.actbio.2016.08.007.

The article was submitted to the journal on 14.04.2025

DOI: 10.15825/1995-1191-2025-3-160-172

CARDIOVASCULAR RISK FACTORS IN CHRONIC KIDNEY DISEASE PATIENTS ON RENAL REPLACEMENT THERAPY

Yu.V. Semenova, B.L. Mironkov, Ya.L. Poz, A.G. Strokov

Shumakov National Medical Research Center of Transplantology and Artificial Organs, Moscow, Russian Federation

Cardiovascular disease (CVD) remains the leading cause of mortality in patients with end-stage renal disease (ESRD). The risk factors for CVD in this population can be categorized into three main groups: traditional (non-modifiable factors such as male gender, age over 65 years in men and over 75 years in women, and a family history of cardiovascular disease; modifiable factors encompass hypertension, diabetes mellitus, dyslipidemia, smoking, obesity, and physical inactivity), renal-specific (anemia, chronic fluid overload, mineral and bone disorders, chronic inflammation, electrolyte imbalances, and oxidative stress), and transplant-specific (immunosuppressive therapy and graft dysfunction). Risk factors related to renal pathology and immunosuppressive therapy following kidney transplantation play a role comparable in significance to traditional CVD risk factors. Early detection and management of these factors are critical for reducing CVD incidence in this patient population.

Keywords: cardiovascular disease, cardiovascular risk factors, chronic kidney disease, end-stage renal disease, dialysis.

INTRODUCTION

Chronic kidney disease (CKD) has emerged as a major global health problem, reaching pandemic proportions in recent decades. It is estimated that more than 850 million people, approximately 10% of the world's population, are affected by CKD, a figure that is twice the global prevalence of diabetes [1].

The number of patients progressing to end-stage renal disease (ESRD) and requiring renal replacement therapy (RRT) is also steadily rising, with estimates ranging from 4.9 to 7.1 million worldwide [2]. A similar trend is observed in Russia. According to the Russian RRT Registry, 24,195 patients (170.5 per million population) were receiving RRT in 2009 [3]; by 2024, this number had increased more than threefold to 74,238 (499 per million population) [4].

Although kidney transplantation (KT) offers better survival rates and quality of life compared to dialysis, approximately 80% of patients with ESRD remain on dialysis due to the persistent shortage of donor organs. In 2023, a total of 111,135 kidney transplants were performed worldwide [5], including 1,817 in the Russian Federation [6]. By early 2025, 15,240 patients in Russia were living with functioning kidney transplants [4].

Cardiovascular disease (CVD) remains the leading cause of death among patients with CKD, particularly those with kidney failure [7]. Cardiovascular risk factors in this population can be grouped into three categories: traditional [8], renal-specific, and transplant-specific factors (Table 1).

Table 1

CVD risk factors in ESRD patients

Traditional CVD risk factors [8]	**Non-modifiable:** – Male gender – Age: high 10-year cardiovascular risk in men over 65 years and women over 75 years – Family history **Modifiable:** – Hypertension (HT) – Diabetes mellitus (DM) – Dyslipidemia – Smoking – Obesity – Sedentary lifestyle
"Renal" CVD risk factors	– Anemia – Chronic hyperhydration – Mineral and bone disorders – Chronic inflammation – Electrolyte disturbances – Oxidative stress
Post-kidney transplant CVD risk factors	– Immunosuppressive therapy – Transplanted kidney dysfunction

CVD RISK FACTORS IN ESRD

Given that traditional CVD risk factors in patients with kidney failure are similar to those observed in the general population and are widely discussed in the literature [8], this paper focuses on "renal" factors and factors specific to patients following KT.

Corresponding author: Yulia Semenova. Address: 1, Shchukinskaya str., Moscow, 123182, Russian Federation. Phone: (985) 250-72-82. E-mail: julie11.89@mail.ru

Anemia

Anemia is one of the most common complications of CKD, resulting from decreased erythropoietin production, shortened red blood cell lifespan, and other factors. As a recognized risk factor for CVD, anemia contributes to morphological and functional cardiac changes, including left ventricular (LV) hypertrophy and dilatation, diastolic dysfunction, arrhythmias, and heart failure (HF) [9].

The international DOPPS study reported that approximately 47% of dialysis patients had hemoglobin (Hb) levels below 110 g/L, while 84% were receiving erythropoietin (EPO) therapy. Importantly, Hb concentrations in the range of 110–120 g/L were associated with lower mortality and hospitalization rates [10].

At the same time, it has been shown that increasing Hb levels to higher values (≥135 g/L) is associated with a greater risk of composite cardiovascular complications [11]. Specifically, the use of EPO preparations to achieve Hb concentrations of ~130 g/L was linked to an increased incidence of stroke, more aggressive hypertension, and vascular access thrombosis compared with achieving levels of ~101 g/L [12].

According to the KDOQI and KDIGO clinical practice guidelines, EPO therapy may be initiated when Hb levels fall within 90–100 g/L, to prevent further decline below 90 g/L. However, it is not recommended to use EPO to maintain Hb levels above 115 g/L or to deliberately raise them above 130 g/L [13, 14]. Importantly, target Hb levels should be individualized and guided by the patient's clinical status and comorbid conditions. The Russian Ministry of Health has adopted a similar approach in its recommendations for the management of anemia in CKD [15]. The main goal of using EPO preparations is to reduce the need for blood transfusions [9].

After KT, anemia is observed in 20–60% of patients, most is in the early post-transplant period (within the first 2 months after surgery) [16]. The main causes of post-transplant anemia are summarized in Table 2 [17].

Table 2

Main causes of anemia in patients after kidney transplantation [17]

In the early post-transplant period
– Perioperative blood loss
– Discontinuation of erythropoietin (EPO) therapy
– Iron deficiency
– Bone marrow suppression associated with induction immunosuppressive therapy
– EPO resistance, triggered by ongoing infections, inflammatory processes, or the use of certain medications (e.g., mycophenolate mofetil)
In the late post-transplant period
– Decreased endogenous erythropoietin production due to allograft dysfunction
– EPO resistance associated with secondary hyperparathyroidism
– Chronic inflammatory conditions

Post-transplant anemia, defined as Hb levels below 110 g/L at 3 months after KT, is associated with adverse outcomes, including congestive heart failure, poorer graft and patient survival, and a higher incidence of acute rejection [18].

In kidney transplant recipients, treatment should be initiated with EPO when Hb falls below 110 g/L, with the therapeutic goal of maintaining Hb in the range of 110–120 g/L [16].

Chronic overhydration

Overhydration represents a major pathogenetic factor contributing to CKD progression and unfavorable outcomes. Multiple observational studies have shown that chronic fluid overload in dialysis patients significantly increases the risk of both all-cause mortality and CVD [19, 20].

A major challenge in both clinical practice and research is the quantitative assessment of hyperhydration in individual patients. This challenge has been partly addressed by the widespread adoption of Bioelectrical impedance analysis (BIA), which enables the assessment of total body fluid volume as well as the distribution of intracellular and extracellular fluid [21, 22]. Today, BIA techniques are routinely used in most modern studies on hydration.

Hyperhydration has been shown to be strongly associated with left ventricular hypertrophy (LVH) [23] and increased mortality, [24] even in the pre-dialysis stages of CKD, regardless of disease severity. Among patients with stage 4–5 CKD, overhydration is linked not only to higher mortality but also to a greater incidence of CVD [25].

Evidence from several meta-analyses confirms that hyperhydration in ESRD patients receiving RRT is an independent predictor of all-cause mortality, as well as a risk factor for cardiovascular complications and mortality [26–28]. Numerous studies further demonstrate associations between hyperhydration and LVH, diastolic dysfunction, reduced cardiac output, endothelial dysfunction, increased arterial stiffness [29, 30], and chronic systemic inflammation [31]. Even after adjusting for confounding variables and in the absence of overt cardiovascular pathology, hyperhydration remains an independent risk factor that worsens prognosis in patients with ESRD.

This dependence is observed in patients undergoing peritoneal dialysis (PD) [32], as well as in those on hemodialysis (HD) [33].

In PD patients, hyperhydration is predominantly persistent, often resulting from inaccurate assessment of "dry weight" or inadequate ultrafiltration volume. Patients receiving maintenance HD may experience a combination of both persistent and intermittent hyperhy-

dration. Persistent hyperhydration is generally absent if fluid status is correctly assessed in these patients. However, because most HD patients have almost complete loss of renal function, including the ability to excrete water, fluid intake accumulates between sessions. The most pronounced cardiovascular system (CVS) changes are typically observed at the end of the three-day interdialysis interval, when intermittent hyperhydration reaches its peak [34, 35].

Studies indicate that exceeding a threshold of interdialytic weight gain – typically estimated at 15% of extracellular fluid volume – is strongly associated with increased mortality [36]. With fixed dialysis session durations, excessive weight gain necessitates higher ultrafiltration rates, which further elevate mortality risk [37]. Rapid volumetric ultrafiltration, even in the absence of overt complications such as intradialytic hypotension, can induce myocardial "stunning", characterized by regional hypokinesia, and, with prolonged exposure, may progress to systolic dysfunction, heart failure, and increased mortality [38, 39].

Minimizing intermittent hyperhydration is therefore closely linked to optimizing sodium balance in patients on maintenance HD. This is achieved through a combination of dietary sodium restriction and individualized adjustment of dialysate composition [40].

Over the past decade, lung ultrasound has been increasingly studied as a tool for assessing hydration status in dialysis patients. An increase in pulmonary interstitial water content produces characteristic artifacts known as "comets" or B-lines [41]. Several studies have reported a correlation between the number of B-lines and clinical outcomes in HD patients [42]. However, lung ultrasound findings often do not align with BIA results. This discrepancy may be explained by the fact that BIA measures total extracellular fluid without distinguishing between interstitial and intravascular compartments, whereas B-lines may also be influenced by left ventricular dysfunction and pulmonary congestion [43, 44]. In other words, BIA provides a broader estimate of hydration status, while lung ultrasound is more closely associated with intravascular volume. Given its accessibility and non-invasive nature, lung ultrasound merits further investigation and may ultimately become a standard tool in routine clinical practice.

Hyperhydration is one of the most critical factors contributing to cardiovascular pathology and reduced survival in patients with kidney failure. Addressing both persistent and intermittent hyperhydration remains a major challenge, as it requires reliable methods for assessing hydration status, minimizing interdialytic weight gain in patients on long-term HD, and ensuring safe ultrafiltration – all of which demand further research and the development of effective therapeutic strategies.

Mineral and bone disorders

The kidneys play a central role in mineral and bone metabolism (Fig. 1). Current evidence suggests that a reduction in the functional nephron mass and progression of CKD initially disrupt vitamin D metabolism, resulting in hypocalcemia and hyperphosphatemia [45]. In addition, reduced expression of the α-klotho gene

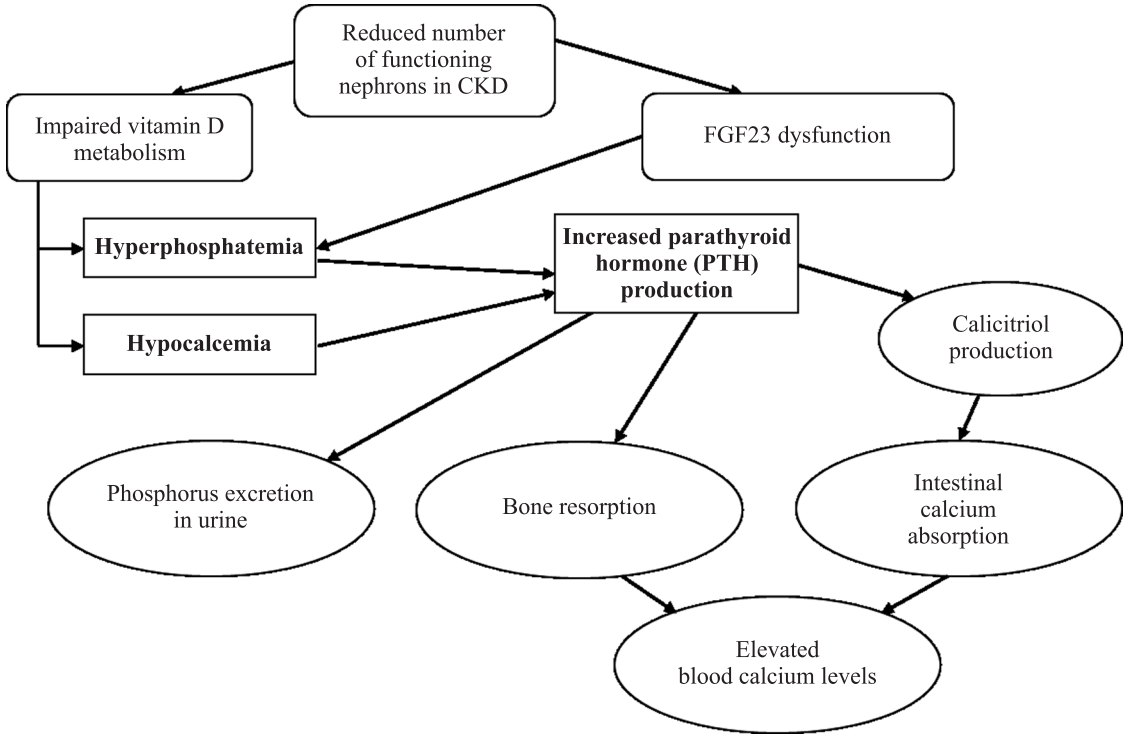

Fig. 1. Mineral and bone disorders in CKD

in distal renal tubules impairs the activity of fibroblast growth factor 23 (FGF23) as a phosphaturic hormone, ultimately leading to the retention of inorganic phosphate in the body [46].

As a compensatory response, FGF23 production increases in bone tissue, followed by suppression of 25-hydroxyvitamin D hydroxylase activity, thereby reducing calcitriol synthesis and stimulating parathyroid hormone (PTH) secretion [47].

The combined effects of FGF23 and PTH inhibit phosphate reabsorption in the proximal tubules, enhancing urinary phosphate excretion. In addition, PTH promotes bone resorption and sustains calcitriol production, which facilitates intestinal calcium absorption and contributes to the maintenance of normal serum calcium levels [48].

With progressive loss of kidney tissue, these compensatory mechanisms become ineffective, resulting in mineral and bone disorders characteristic of ESRD, which exert profound pathological effects on CVS. Numerous studies have reported that hyperphosphatemia is strongly associated with an increased risk of adverse cardiovascular outcomes, including myocardial infarction, stroke, heart failure, sudden cardiac death, and peripheral arterial disease [49, 50]. Hyperphosphatemia contributes to endothelial dysfunction and promotes vascular and valvular calcification [51]. It also stimulates elevated PTH levels, which are linked to increased cardiovascular mortality [52]. Similarly, elevated FGF23 levels are associated with higher cardiovascular morbidity and mortality in CKD patients. Both PTH and FGF23 are believed to exert direct effects on cardiomyocytes, triggering LVH [53].

Hypocalcemia, a hallmark of mineral and bone metabolism disorders in CKD, is linked to arterial hypotension, congestive heart failure, and cardiac arrhythmias. It is also associated with QT interval prolongation, which increases the risk of ventricular tachycardia and ventricular fibrillation [54, 55]. At the same time, CKD patients may develop excessive calcium overload, particularly when treated with calcium-containing phosphate binders and active vitamin D analogues. This condition accelerates the formation and maturation of calciprotein particles, thereby promoting vascular and valvular calcification and advancing atherosclerosis. Ectopic calcification within the cardiac conduction system further elevates the risk of fatal bradyarrhythmias [56].

In severe renal failure, expression of the α-klotho gene and synthesis of calcitriol, both of which exert cardioprotective effects, are reduced [57, 58]. Moreover, CKD is often associated with magnesium deficiency, despite evidence suggesting that adequate magnesium levels may slow or even halt CVS calcification processes [59].

Extracartilaginous calcification affecting the CVS is the main manifestation of mineral and bone disorders in CKD and is a major determinant of the elevated mortality risk in CKD [60]. Calcification primarily affects the medial layer of arterial walls and the cardiac valves. The underlying mechanism is thought to involve the formation of calcium–phosphorus particles containing fetuin-1 and other proteins, which induce vascular smooth muscle cells to undergo phenotypic transformation into osteoblast-like cells capable of producing bone matrix within the vessel wall [61]. These particles also stimulate the release of pro-inflammatory cytokines, further amplifying the calcification process [51].

Current therapeutic approaches to mineral and bone disorders in CKD focus on achieving recommended target levels of key modulators of mineral metabolism. A variety of agents have been employed, including phosphate binders, vitamin D analogs (both native and active forms), calcimimetics, and bisphosphonates [62]. While these treatments are effective in correcting biochemical parameters, they have not shown sufficient impact on overall or cardiovascular mortality [62, 63]. Thus, although the association between disordered mineral metabolism in kidney failure and cardiovascular mortality is well established by cohort studies, pharmacological correction of these disturbances has yet to translate into improved clinical outcomes [63].

Inflammation

The progression of CKD is closely linked to systemic inflammation and oxidative stress, which contribute to a wide range of complications, including malnutrition, atherosclerosis, vascular calcification, heart failure, anemia, mineral and bone disorders, and increased cardiovascular mortality. Declining renal function leads to accumulation of advanced glycation end products and pro-oxidants, which promote oxidative damage, activate mononuclear cells, and stimulate chronic inflammatory pathways [64].

In patients with kidney failure, elevated levels of pro-inflammatory cytokines result not only from increased production but also from impaired clearance. The uremic state itself, together with comorbid conditions, genetic predisposition, and lifestyle factors, sustains a subacute inflammatory response. Additional dialysis-related factors further exacerbate inflammation, including the use of central venous catheters (CVCs), repeated contact of blood with dialysis membranes and extracorporeal circuit components, potential contamination of dialysate with bacterial endotoxins and backfiltration in the dialyzer, as well as infections such as catheter-related bacteremia and peritonitis in PD (Fig. 2) [65].

There is a clear positive correlation between creatinine clearance and concentrations of various pro-inflammatory cytokines, particularly interleukin (IL)-6, across different stages of CKD. Durlacher-Betzer et al. demonstrated that IL-6 plays a key role in stimulating FGF23 expression in uremia, with elevated FGF23 levels strongly associated with increased mortality [66].

Chronic hyperhydration, frequently observed in ESRD patients, further contributes to systemic inflammation. Intestinal wall edema promotes bacterial translocation and endotoxin leakage, which in turn activate the immune system and amplify cytokine production. Moreover, reduced renal clearance shifts the excretion of urea to the intestinal microbiota, leading to increased ammonium hydroxide formation and elevated intestinal pH. These changes disrupt the normal gut microbiome, favoring the growth of pathogenic species that drive persistent inflammatory processes [67].

Lipopolysaccharide-binding protein (LBP) is an acute-phase reactant that mediates immune responses triggered by microbial products. In patients undergoing maintenance HD, Paik Seong Lim et al. reported a significant positive correlation between circulating LBP levels and markers of systemic inflammation such as C-reactive protein (CRP), IL-6, and soluble CD14 [68]. Moreover, serum LBP level has been shown to independently predict the risk of cardiovascular events in this patient population, underscoring its role as both a biomarker and potential mediator of inflammation-driven cardiovascular injury [69].

Comorbidities such as congestive heart failure, diabetes, hypertension, and age-related changes in the immune response contribute to the development of chronic inflammation [70]. Patients with diabetes have elevated plasma levels of IL-1, IL-6, IL-18, tumor necrosis factor-alpha (TNF-α), ICAM-1, VCAM-1, and NF-κB [71]. Hypertension is associated with increased IL-6, VCAM and ICAM-1 levels [72]. Similarly, obesity drives the upregulation of IL-18, IL-1β, and TNF-α [73]. Acute and chronic infections, in particular periodontitis [74], viral hepatitis, and peritonitis in patients on peritoneal dialysis [75], play a separate role in stimulating the inflammatory response.

The pathophysiology of inflammation may vary among CKD patients depending on their genetic background. Losito et al. demonstrated a link between the IL-6-174G/C promoter polymorphism, arterial hypertension, and LVH in hemodialysis patients, particularly in those with diabetes [76]. Subsequently, Sharma et al. reported a link between polymorphisms in the promoter regions of proinflammatory cytokines (IL-6, TNF-α) and the regulatory monokine IL-10 with the development of ESRD, malnutrition-inflammation syndrome, comorbidities, and increased mortality risk in patients on maintenance hemodialysis [77].

Several studies have shown that vascular calcification is present in 30–70% of adult patients with CKD [78] and in nearly 15% of children with uremia [79]. ESRD patients are characterized by increased arterial stiffness,

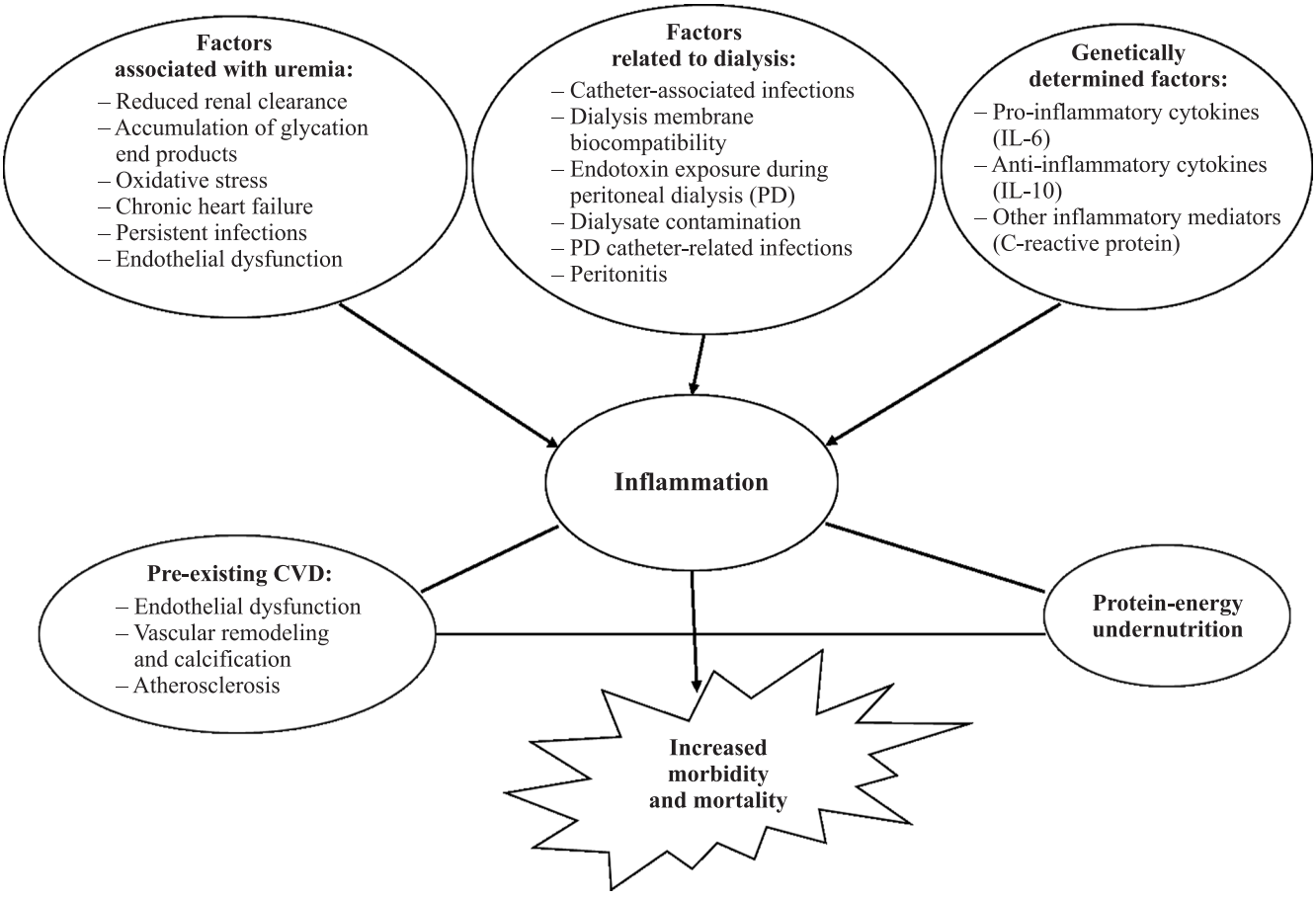

Fig. 2. Causes and consequences of inflammation in ESRD patients. Adapted from [65])

particularly in the aorta, common carotid artery, and cerebral vessels [80]. In addition, they frequently exhibit arterial dysfunction manifested by impaired nitric oxide–dependent vasodilation [81] and elevated pulse wave velocity [82].

Inflammatory cells accumulate within developing atherosclerotic plaques and in the aortic valve, underscoring the close link between systemic inflammation and vascular calcification. This process arises from deposition of calcium phosphate crystals in the arterial intima, resembling the mineralization seen in bone tissue. Nadra et al. [83] demonstrated that human macrophages exposed to calcium phosphate crystals *in vitro* internalize these crystals into vacuoles and subsequently release inflammatory cytokines (TNF-α, IL-1β, IL-8) through a protein kinase C–dependent mechanism. In addition, macrophages are able to secrete matrix vesicles enriched with annexin V and alkaline phosphatase, which possess strong calcifying potential [84]. The receptor activator of NF-κB ligand (RANKL) is a membrane-bound or soluble cytokine necessary for osteoclast differentiation, whereas osteoprotegerin masks the activity of RANKL. It can stimulate inflammation in atherosclerotic plaques, which in turn contributes to the further progression and complications of atherosclerosis, indicating a vicious circle of interrelated processes: inflammation and calcification of the arteries [85].

Fetuin-A, a glycoprotein of approximately 60 kDa synthesized by hepatocytes, is the most potent circulating inhibitor of calcification, preventing hydroxyapatite formation. Elevated levels of proinflammatory molecules can suppress fetuin-A production, leading to reduced serum levels, which are associated with increased cardiovascular risk and poorer outcomes in patients with CKD [86].

A substantial body of evidence highlights the role of inflammation in atherogenesis, demonstrating that the relationship between inflammation and CVD is evident not only in patients with renal failure but also in the general population [87]. For example, the JUPITER study showed that lowering high-sensitivity C-reactive protein (hs-CRP) levels with rosuvastatin significantly reduced the risk of cardiovascular complications, even in individuals with normal cholesterol levels [88]. Nishi et al. reported that pentraxin 3, hs-CRP, and tumor necrosis factor-α (TNF-α) were significantly elevated in patients with CKD and concomitant CVD compared to those without CVD. Jia Sun et al. identified circulating IL-6 and VCAM-1 as independent predictors of cardiovascular events and all-cause mortality in patients on maintenance HD [89].

All these studies demonstrate an undeniable link between inflammation and CVD in CKD patients. Following KT, restoration of renal function leads to significant changes in several inflammatory markers, which in turn influences cardiovascular risk. Yilmaz M.I. et al. reported that after transplantation, reductions in CRP and FGF23 levels were accompanied by a marked decrease in carotid intima–media thickness (–22%, 95% CI –24 to –20%, p = 0.001) [90]. A two-year study by Kensinger C. et al. showed that endothelial function improves after transplantation and remains stable for at least two years postoperatively [91].

Oxidative stress

Increased oxidative stress is closely associated with a higher risk of CVD in patients with kidney failure. Since the kidneys are one of the main sources of antioxidant enzymes, including glutathione peroxidase, their damage in ESRD leads to a reduction in these enzymes and a concomitant rise in prooxidants. Uremic toxins further contribute by activating polymorphonuclear leukocytes, monocytes/macrophages, lymphocytes, and antigen-presenting cells. The dialysis procedure itself can exacerbate oxidative stress by removing circulating antioxidants and stimulating leukocytes to produce reactive oxygen species. As a result, patients with ESRD develop a persistent imbalance between antioxidant defenses and prooxidant activity, ultimately promoting endothelial dysfunction, chronic inflammation, and progression of cardiac fibrosis [92].

Antioxidant therapy has been proposed as a potential strategy to improve cardiovascular outcomes in dialysis patients. Clinical studies suggest that N-acetylcysteine, a low-molecular-weight thiol with potent antioxidant properties, as well as β-carotene and vitamins A, C, and E, may reduce the risk of cardiovascular events in patients undergoing hemodialysis [92].

Electrolyte disturbances

The kidneys play a key role in maintaining homeostasis by continuously regulating the excretion and reabsorption of electrolytes and metabolic products. In CKD, impaired renal filtration, and in ESRD, the limited efficiency of dialysis, result in significant instability of electrolyte balance. Both hyperkalemia and hypokalemia have been independently linked to an increased risk of all-cause and cardiovascular mortality in patients with kidney failure [93].

Hyperkalemia is particularly common among ESRD patients receiving hemodialysis. It produces characteristic ECG changes, such as T-wave inversion, P-wave flattening, and widening of the QRS complex. Clinically, it can manifest as bradyarrhythmias, conduction disturbances, ventricular arrhythmias, and even asystole. Hyperkalemia may also drive a self-perpetuating cycle known as BRASH syndrome, which comprises bradycardia, renal failure, atrioventricular block, shock, and hyperkalemia. In this syndrome, both bradycardia and hyperkalemia may be drug-induced, particularly in elderly patients treated with β-blockers or calcium channel blockers for arrhythmias such as atrial fibrillation [94].

Hypokalemia occurs more frequently in patients with ESRD on peritoneal dialysis (PD). Ribeiro et al. demonstrated that serum potassium levels below 3.5–4 mmol/L were associated with an increased risk of all-cause and cardiovascular mortality, as well as with deaths from infectious diseases unrelated to PD [95].

Among the electrolyte disturbances characteristic of dialysis patients, hypomagnesemia is particularly important in the pathogenesis of vascular calcification. Reduced intracellular magnesium levels have been shown to promote proinflammatory and proatherogenic vascular injury by enhancing the production of reactive oxygen species, stimulating cytokine release, and activating endothelial cells. Magnesium supplementation has been shown to attenuate vascular calcification by disrupting calcium-phosphate crystal deposition within the vascular wall and by inhibiting the osteogenic transformation of vascular smooth muscle cells [96].

Immunosuppressive therapy

Standard immunosuppressive regimens for prevention of graft rejection typically combine calcineurin inhibitors (tacrolimus or cyclosporine) with either purine metabolism inhibitors (mycophenolate mofetil or azathioprine) or inhibitors of proliferative signal transduction (everolimus or sirolimus), often in conjunction with glucocorticosteroids (GCS) [97].

However, the adverse effects of these immunosuppressive drugs contribute to the development of CVD (Table 3). For example, post-transplant diabetes may occur with calcineurin inhibitors (CNIs), GCS, and proliferative response inhibitors, while anemia is often associated with mycophenolate mofetil and azathioprine [98]. CNIs can induce vascular remodeling and left ventricular hypertrophy, whereas proliferative response inhibitors and purine metabolism inhibitors have shown vasculoprotective and cardioprotective effects in certain studies.

Dyslipidemia is commonly linked to GCS, calcineurin inhibitors, and proliferative response inhibitors, but not to purine metabolism inhibitors. Arterial hypertension is promoted by CNIs and GCS, while some evidence suggests that proliferative response inhibitors and purine metabolism inhibitors may exert vasodilatory effects [99].

Kidney transplant dysfunction

Kidney transplant dysfunction is an important independent risk factor for CVD, primarily due to progression of hypertension, anemia, dyslipidemia, and hyperhomocysteinemia. According to published data, one year after KT, stage 3 CKD (estimated glomerular filtration rate, eGFR <60 mL/min/1.73 m^2) is observed in about 60% of recipients, while stage 4 CKD (eGFR <30 mL/min/1.73 m^2) develops in approximately 15% [100].

"Renal" risk factors for CVD become more pronounced as transplant function declines, particularly when eGFR falls below 60 mL/min/1.73 m^2 and even more so below 45 mL/min/1.73 m^2. Findings from the FAVORIT study demonstrated that CVD and all-cause mortality risks are significantly associated with eGFR <45 mL/min/1.73 m^2. In this group, each 5 mL/min/1.73 m^2 increase in eGFR corresponded to a 15% reduction in the risk of cardiovascular morbidity and mortality [101].

Proteinuria exceeding 1 g/day is observed in 20% of patients after KT [102]. In a study by Fernandez-Fresnedo et al., persistent proteinuria was shown to double the risk of CVD and overall mortality in KT recipients [103].

Although renin-angiotensin-aldosterone system (RAAS) blockers are widely used in patients with CKD and proteinuria, the evidence supporting their effectiveness in KT recipients remains inconclusive. A systematic review of 21 studies involving 1,549 patients demonstrated that RAAS blockade effectively reduced proteinuria after transplantation; however, the relatively short follow-up period (median 27 months) limited the ability to assess long-term outcomes for both graft and patient survival [104]. A subsequent systematic review of the same population found no significant effect of RAAS blockers on overall survival in KT recipients [105]. Similarly, a large retrospective study of 39,251 KT recipients showed that RAAS blockers did not reduce the risk of cardiovascular death compared with other classes of antihypertensive drugs [106]. Nevertheless, current clinical guidelines continue to recommend RAAS blockers for the management of proteinuria in KT recipients, given their demonstrated ability to reduce renal protein excretion [107].

Table 3

Side effects of immunosuppressive therapy [99]

Drug class	Hypertension	Dyslipidemia	Vascular remodeling, left ventricular hypertrophy	Diabetes	Anemia
Calcineurin inhibitors	+	+	+	+	
Proliferation signal inhibitors	–	+	–	+	
Purine metabolism inhibitors	–		–		+
Glucocorticosteroids (GCS)	+	+		+	

CONCLUSION

This review underscores the multifactorial nature of cardiovascular complications in patients with ESRD. Both renal pathology–related risk factors and the adverse effects of immunosuppressive therapy after KT play roles comparable in importance to traditional CVD risk factors. Early detection and targeted management of these factors are essential to reducing the burden of CVD in this patient population.

The authors declare no conflict of interest.

REFERENCES

1. *Jager KJ, Kovesdy C, Langham R, Rosenberg M, Jha V, Zoccali C.* A single number for advocacy and communication-worldwide more than 850 million individuals have kidney diseases. *Kidney international*. 2019 Nov 1; 96 (5): 1048–1050.
2. *Lv JC, Zhang LX.* Prevalence and Disease Burden of Chronic Kidney Disease. *Advances in experimental medicine and biology*. 2019; 1165: 3–15.
3. *Bikbov BT, Tomilina NA*. Status of renal replacement therapy in ESRD patients of Russian Federation in 1998–2009 Report of Russian RRT Register. *Nephrology and Dialysis*. 2011; 13 (3): 150–264. (In Russ.).
4. *Shilov EM, Shilova MM, Rumyantseva EI, Batyushin MM, Bevzenko AYu, Bel'skikh AN et al.* Nefrologicheskaya sluzhba Rossiyskoy Federatsii 2024: Chast' I. Zamestitel'naya pochechnaya terapiya. *Klinicheskaya nefrologiya [Clinical Nephrology]*. 2005; (1): 6–17.
5. Statista [Internet]. [cited 2023 Sep 15]. Kidney transplants worldwide by region 2021. Available from: https://www.statista.com/statistics/398657/kidney-transplants-by-world-region/.
6. *Gautier SV, Khomyakov SM*. Organ donation and transplantation in the Russian Federation in 2023. 16th Report from the Registry of the Russian Transplant Society. *Russian Journal of Transplantology and Artificial Organs*. 2024 Jul 19; 26 (3): 8–31.
7. *Mukhin NA, Fomin VV, Rogova IV, Damulin IV*. Khronicheskaya bolezn' pochek i sosudistaya dementsiya. *Terapevticheskiy arkhiv [Therapeutic Archive]*. 2014; 86 (6): 7–10.
8. *Visseren FLJ, Mach F, Smulders YM, Carballo D, Koskinas KC, Bäck M et al*. 2021 ESC Guidelines on cardiovascular disease prevention in clinical practice. *Eur Heart J*. 2021 Sep 7; 42 (34): 3227–3337.
9. *Dev Jegatheesan, Wenling Yang, Rathika Krishnasamy, Carmel M. Hawley, David W Johnson.* Cardiovascular Disease in Dialysis Patients. *Aspects in Dialysis*. 2017.
10. *Locatelli F, Pisoni RL, Combe C, Bommer J, Andreucci VE, Piera L et al.* Anaemia in haemodialysis patients of five European countries: association with morbidity and mortality in the Dialysis Outcomes and Practice Patterns Study (DOPPS). *Nephrology, dialysis, transplantation: official publication of the European Dialysis and Transplant Association – European Renal Association*. 2004 Jan; 19 (1): 121–132.
11. *Singh AK, Szczech L, Tang KL, Barnhart H, Sapp S, Wolfson M et al.* Correction of anemia with epoetin alfa in chronic kidney disease. *The New England journal of medicine*. 2006 Nov 16; 355 (20): 2085–2098.
12. *Palmer SC, Navaneethan SD, Craig JC, Johnson DW, Tonelli M, Garg AX et al.* Meta-analysis: erythropoiesis-stimulating agents in patients with chronic kidney disease. *Annals of internal medicine*. 2010 Jul 6; 153 (1): 23–33.
13. *Kliger AS, Foley RN, Goldfarb DS, Goldstein SL, Johansen K, Singh A et al.* KDOQI US commentary on the 2012 KDIGO Clinical Practice Guideline for Anemia in CKD. *American journal of kidney diseases: the official journal of the National Kidney Foundation*. 2013; 62 (5): 849–859.
14. *Coyne DW.* The KDOQI US commentary on KDIGO anemia guideline and quality of life. *American journal of kidney diseases: the official journal of the National Kidney Foundation*. 2014 Mar; 63 (3): 540.
15. Natsional'naya Assotsiatsiya nefrologov. Klinicheskie rekomendatsii. Khronicheskaya bolezn' pochek (KhBP). 2024. [National Association of Nephrologists. Clinical Guidelines. Chronic Kidney Disease (CKD)].
16. *Loncar D, Hodzic S*. Cardiovascular Diseases in Patients with Renal Transplantation. *Organ Donation and Transplantation*. 2018.
17. *Winkelmayer WC, Chandraker A*. Pottransplantation anemia: management and rationale. *Clin J Am Soc Nephrol*. 2008 Mar; 3 (Suppl 2): S49–S55.
18. *Borrows R, Loucaidou M, Chusney G, Borrows S, Tromp JV, Cairns T et al.* Anaemia and congestive heart failure early post-renal transplantation. *Nephrol Dial Transplant*. 2008 May; 23 (5): 1728–1734.
19. *Kalantar-Zadeh K, Regidor DL, Kovesdy CP, Van Wyck D, Bunnapradist S, Horwich TB et al.* Fluid retention is associated with cardiovascular mortality in patients undergoing long-term hemodialysis. *Circulation*. 2009 Feb 10; 119 (5): 671–679.
20. *Chazot C, Wabel P, Chamney P, Moissl U, Wieskotten S, Wizemann V*. Importance of normohydration for the long-term survival of haemodialysis patients. *Nephrol Dial Transplant*. 2012 Jun; 27 (6): 2404–2410.
21. *Moissl UM, Wabel P, Chamney PW, Bosaeus I, Levin NW, Bosy-Westphal A et al.* Body fluid volume determination via body composition spectroscopy in health and disease. *Physiol Meas*. 2006 Sep; 27 (9): 921–933.
22. *Woodrow G, Oldroyd B, Turney JH, Davies PS, Day JM, Smith MA.* Measurement of total body water by bioelectrical impedance in chronic renal failure. *Eur J Clin Nutr*. 1996 Oct; 50 (10): 676–681.
23. *Duan S, Ma Y, Lu F, Zhang C, Guo H, Zeng M et al.* High sodium intake and fluid overhydration predict cardiac structural and functional impairments in chronic kidney disease. *Front Nutr*. 2024; 11: 1388591.
24. *Vega A, Abad S, Macías N, Aragoncillo I, García-Prieto A, Linares T et al*. Any grade of relative overhydration is associated with long-term mortality in patients with Stages 4 and 5 non-dialysis chronic kidney disease. *Clin Kidney J*. 2018 Jun; 11 (3): 372–376.
25. *Tsai YC, Chiu YW, Tsai JC, Kuo HT, Hung CC, Hwang SJ et al.* Association of fluid overload with cardiovascular morbidity and all-cause mortality in stages 4 and 5 CKD. *Clin J Am Soc Nephrol*. 2015 Jan 7; 10 (1): 39–46.

26. *Tabinor M, Elphick E, Dudson M, Kwok CS, Lambie M, Davies SJ.* Bioimpedance-defined overhydration predicts survival in end stage kidney failure (ESKF): systematic review and subgroup meta-analysis. *Sci Rep*. 2018 Mar 13; 8 (1): 4441.
27. *Wang Y, Gu Z.* Effect of bioimpedance-defined overhydration parameters on mortality and cardiovascular events in patients undergoing dialysis: a systematic review and meta-analysis. *J Int Med Res*. 2021 Sep; 49 (9): 3000605211031063.
28. *Covic A, Ciumanghel AI, Siriopol D, Kanbay M, Dumea R, Gavrilovici C et al.* Value of bioimpedance analysis estimated "dry weight" in maintenance dialysis patients: a systematic review and meta-analysis. *Int Urol Nephrol*. 2017 Dec; 49 (12): 2231–2245.
29. *Onofriescu M, Siriopol D, Voroneanu L, Hogas S, Nistor I, Apetrii M et al.* Overhydration, Cardiac Function and Survival in Hemodialysis Patients. *PLoS One*. 2015; 10 (8): e0135691.
30. *Cheng L, Chang L, Tian R, Zhou J, Luo F, Zhang H.* The predictive value of bioimpedance-derived fluid parameters for cardiovascular events in patients undergoing hemodialysis. *Ren Fail*. 2022 Dec; 44 (1): 1192–1200.
31. *Reyes-Bahamonde J, Raimann JG, Thijssen S, Levin NW, Kotanko P*. Fluid overload and inflammation – a vicious cycle. *Semin Dial*. 2013; 26 (1): 31–35.
32. *Jotterand Drepper V, Kihm LP, Kälble F, Diekmann C, Seckinger J, Sommerer C et al.* Overhydration Is a Strong Predictor of Mortality in Peritoneal Dialysis Patients – Independently of Cardiac Failure. *PLoS One*. 2016; 11 (7): e0158741.
33. *Zoccali C, Moissl U, Chazot C, Mallamaci F, Tripepi G, Arkossy O et al*. Chronic Fluid Overload and Mortality in ESRD. *J Am Soc Nephrol*. 2017 Aug; 28 (8): 2491–2497.
34. *Koutroumbas G, Georgianos PI, Sarafidis PA, Protogerou A, Karpetas A, Vakianis P et al.* Ambulatory aortic blood pressure, wave reflections and pulse wave velocity are elevated during the third in comparison to the second interdialytic day of the long interval in chronic haemodialysis patients. *Nephrol Dial Transplant*. 2015 Dec; 30 (12): 2046–2053.
35. *Tsilonis K, Sarafidis PA, Kamperidis V, Loutradis C, Georgianos PI, Imprialos K et al.* Echocardiographic Parameters During Long and Short Interdialytic Intervals in Hemodialysis Patients. *Am J Kidney Dis*. 2016 Nov; 68 (5): 772–781.
36. *Wizemann V, Wabel P, Chamney P, Zaluska W, Moissl U, Rode C et al.* The mortality risk of overhydration in haemodialysis patients. *Nephrology, dialysis, transplantation: official publication of the European Dialysis and Transplant Association – European Renal Association*. 2009 May; 24 (5): 1574–1579.
37. *Movilli E, Gaggia P, Zubani R, Camerini C, Vizzardi V, Parrinello G et al.* Association between high ultrafiltration rates and mortality in uraemic patients on regular haemodialysis. A 5-year prospective observational multicentre study. *Nephrol Dial Transplant*. 2007 Dec; 22 (12): 3547–3552.
38. *McIntyre CW, Burton JO, Selby NM, Leccisotti L, Korsheed S, Baker CSR et al.* Hemodialysis-induced cardiac dysfunction is associated with an acute reduction in global and segmental myocardial blood flow. *Clin J Am Soc Nephrol*. 2008 Jan; 3 (1): 19–26.
39. *Burton JO, Jefferies HJ, Selby NM, McIntyre CW*. Hemodialysis-induced cardiac injury: determinants and associated outcomes. *Clin J Am Soc Nephrol*. 2009 May; 4 (5): 914–920.
40. *Voroneanu L, Gavrilovici C, Covic A*. Overhydration, underhydration, and total body sodium: A tricky "ménage a trois" in dialysis patients. *Semin Dial*. 2018 Jan; 31 (1): 21–25.
41. *Mallamaci F, Benedetto FA, Tripepi R, Rastelli S, Castellino P, Tripepi G et al.* Detection of pulmonary congestion by chest ultrasound in dialysis patients. *JACC Cardiovasc Imaging*. 2010 Jun; 3 (6): 586–594.
42. *Saad MM, Kamal J, Moussaly E, Karam B, Mansour W, Gobran E et al.* Relevance of B-Lines on Lung Ultrasound in Volume Overload and Pulmonary Congestion: Clinical Correlations and Outcomes in Patients on Hemodialysis. *Cardiorenal Med*. 2018; 8 (2): 83–91.
43. *Kim HR, Jeon JW, Bae HJ, Shin JA, Ham YR, Na KR et al.* Body Fat Plays an Important Role in of Bioimpedance Spectroscopy-Based Dry Weight Measurement Error for Patients with Hemodialysis. *Diagnostics (Basel)*. 2021 Oct 15; 11 (10): 1907.
44. *Panuccio V, Enia G, Tripepi R, Torino C, Garozzo M, Battaglia GG et al*. Chest ultrasound and hidden lung congestion in peritoneal dialysis patients. *Nephrol Dial Transplant*. 2012 Sep; 27 (9): 3601–3605.
45. *Freire-Filho WA, Dalboni MA, Elias RM*. Effects of aging on chronic kidney disease mineral and bone disorder. *Curr Opin Nephrol Hypertens*. 2025 May 2.
46. *Neyra JA, Hu MC, Moe OW*. Klotho in Clinical Nephrology: Diagnostic and Therapeutic Implications. *Clin J Am Soc Nephrol*. 2020 Dec 31; 16 (1): 162–176.
47. *Oliveira RB, Cancela ALE, Graciolli FG, Dos Reis LM, Draibe SA, Cuppari L et al.* Early control of PTH and FGF23 in normophosphatemic CKD patients: a new target in CKD-MBD therapy? *Clin J Am Soc Nephrol*. 2010 Feb; 5 (2): 286–291.
48. *Segawa H, Shiozaki Y, Kaneko I, Miyamoto K ichi*. The Role of Sodium-Dependent Phosphate Transporter in Phosphate Homeostasis. *J Nutr Sci Vitaminol (Tokyo)*. 2015; 61 Suppl: S119–S121.
49. *Hiyamuta H, Yamada S, Taniguchi M, Tokumoto M, Tsuruya K, Nakano T et al.* Association of hyperphosphatemia with an increased risk of sudden death in patients on hemodialysis: Ten-year outcomes of the Q-Cohort Study. *Atherosclerosis*. 2021 Jan; 316: 25–31.
50. *Shimamoto S, Yamada S, Hiyamuta H, Arase H, Taniguchi M, Tokumoto M et al.* Association of serum phosphate concentration with the incidence of intervention for peripheral artery disease in patients undergoing hemodialysis: 10-year outcomes of the Q-Cohort Study. *Atherosclerosis*. 2020 Jul; 304: 22–29.
51. *Aghagolzadeh P, Bachtler M, Bijarnia R, Jackson C, Smith ER, Odermatt A et al.* Calcification of vascular smooth muscle cells is induced by secondary calciprotein particles and enhanced by tumor necrosis factor-α. *Atherosclerosis*. 2016 Aug; 251: 404–414.
52. *Block GA, Kilpatrick RD, Lowe KA, Wang W, Danese MD.* CKD-mineral and bone disorder and risk of death and cardiovascular hospitalization in patients on

hemodialysis. *Clin J Am Soc Nephrol*. 2013 Dec; 8 (12): 2132–2140.
53. *Faul C, Amaral AP, Oskouei B, Hu MC, Sloan A, Isakova T et al.* FGF23 induces left ventricular hypertrophy. *J Clin Invest*. 2011 Nov; 121 (11): 4393–4408.
54. *Yamaguchi S, Hamano T, Doi Y, Oka T, Kajimoto S, Kubota K et al*. Hidden Hypocalcemia as a Risk Factor for Cardiovascular Events and All-Cause Mortality among Patients Undergoing Incident Hemodialysis. *Sci Rep*. 2020 Mar 10; 10 (1): 4418.
55. *Kim ED, Watt J, Tereshchenko LG, Jaar BG, Sozio SM, Kao WHL et al.* Associations of serum and dialysate electrolytes with QT interval and prolongation in incident hemodialysis: the Predictors of Arrhythmic and Cardiovascular Risk in End-Stage Renal Disease (PACE) study. *BMC Nephrol*. 2019 Apr 18; 20 (1): 133.
56. *Xu C, Smith ER, Tiong MK, Ruderman I, Toussaint ND.* Interventions To Attenuate Vascular Calcification Progression in Chronic Kidney Disease: A Systematic Review of Clinical Trials. *J Am Soc Nephrol*. 2022 May; 33 (5): 1011–1032.
57. *Charoenngam N, Ponvilawan B, Ungprasert P*. Lower circulating soluble Klotho level is associated with increased risk of all-cause mortality in chronic kidney disease patients: a systematic review and meta-analysis. *Int Urol Nephrol*. 2020 Aug; 52 (8): 1543–1550.
58. *Kaur G, Singh J, Kumar J*. Vitamin D and cardiovascular disease in chronic kidney disease. *Pediatr Nephrol*. 2019 Dec; 34 (12): 2509–2522.
59. *Vermeulen EA, Vervloet MG*. Magnesium Administration in Chronic Kidney Disease. *Nutrients*. 2023 Jan 20; 15 (3): 547.
60. *Blacher J, Guerin AP, Pannier B, Marchais SJ, London GM.* Arterial calcifications, arterial stiffness, and cardiovascular risk in end-stage renal disease. *Hypertension*. 2001 Oct; 38 (4): 938–942.
61. *Bonato FOB, Karohl C, Canziani MEF*. Diagnosis of vascular calcification related to mineral and bone metabolism disorders in chronic kidney disease. *J Bras Nefrol*. 2021; 43 (4 Suppl 1): 628–631.
62. *Palmer SC, Teixeira-Pinto A, Saglimbene V, Craig JC, Macaskill P, Tonelli M et al.* Association of Drug Effects on Serum Parathyroid Hormone, Phosphorus, and Calcium Levels With Mortality in CKD: A Meta-analysis. *American journal of kidney diseases: the official journal of the National Kidney Foundation*. 2015 Dec 1; 66 (6): 962–971.
63. *Palmer SC, Gardner S, Tonelli M, Mavridis D, Johnson DW, Craig JC et al.* Phosphate-Binding Agents in Adults With CKD: A Network Meta-analysis of Randomized Trials. *Am J Kidney Dis*. 2016 Nov; 68 (5): 691–702.
64. *Fujii H.* Is Oxidative Stress a Key Player for Progression of Cardiovascular Disease in Dialysis Patients? JOUR [Internet]. 2020 Oct 1 [cited 2025 Apr 29]; Available from: https://www.researchgate.net/publication/344439517_Is_Oxidative_Stress_a_Key_Player_for_Progression_of_Cardiovascular_Disease_in_Dialysis_Patients.
65. *Yao Q, Axelsson J, Stenvinkel P, Lindholm B.* Chronic systemic inflammation in dialysis patients: an update on causes and consequences. *ASAIO J*. 2004; 50 (6): lii–lvii.
66. *Durlacher-Betzer K, Hassan A, Levi R, Axelrod J, Silver J, Naveh-Many T.* Interleukin-6 contributes to the increase in fibroblast growth factor 23 expression in acute and chronic kidney disease. *Kidney Int*. 2018 Aug; 94 (2): 315–325.
67. *Chi M, Ma K, Wang J, Ding Z, Li Y, Zhu S et al.* The Immunomodulatory Effect of the Gut Microbiota in Kidney Disease. *J Immunol Res*. 2021; 2021: 5516035.
68. *Lim PS, Chang YK, Wu TK*. Serum Lipopolysaccharide-Binding Protein is Associated with Chronic Inflammation and Metabolic Syndrome in Hemodialysis Patients. *Blood Purif*. 2019; 47 (1–3): 28–36.
69. *Lin TY, Chang YK, Wu MY, Wu TK, Chen CH, Lim PS.* Serum lipopolysaccharide-binding protein levels and cardiovascular events in hemodialysis patients: A prospective cohort study. *Nephrology (Carlton)*. 2022 Nov; 27 (11): 877–85.
70. *Dai L, Golembiewska E, Lindholm B, Stenvinkel P.* End-Stage Renal Disease, Inflammation and Cardiovascular Outcomes. *Contrib Nephrol*. 2017; 191: 32–43.
71. *Donate-Correa J, Luis-Rodríguez D, Martín-Núñez E, Tagua VG, Hernández-Carballo C, Ferri C et al*. Inflammatory Targets in Diabetic Nephropathy. *J Clin Med*. 2020 Feb 7; 9 (2): 458.
72. *Topchieva LV, Korneva VA, Kurbatova IV*. Svyaz' nositel'stva allel'nykh variatsiy po rs2228145 (A>C) gena IL6R c urovnem transkriptov genov VCAM1 i ICAM1 pri essentsial'noy arterial'noy gipertenzii. *Vavilovskiy zhurnal genetiki i selektsii*. 2020 Mar 18; 24 (1): 96–101.
73. *Hall JE, Mouton AJ, da Silva AA, Omoto ACM, Wang Z, Li X et al*. Obesity, kidney dysfunction, and inflammation: interactions in hypertension. *Cardiovasc Res*. 2021 Jul 7; 117 (8): 1859–1876.
74. *Nascimento GG, Leite FRM, Mesquita CM, Vidigal MTC, Borges GH, Paranhos LR.* Confounding in observational studies evaluating the association between Alzheimer's disease and periodontal disease: A systematic review. *Heliyon*. 2023 Apr; 9 (4): e15402.
75. *Krediet RT, Parikova A*. Relative Contributions of Pseudohypoxia and Inflammation to Peritoneal Alterations with Long-Term Peritoneal Dialysis Patients. *Clin J Am Soc Nephrol*. 2022 Aug; 17 (8): 1259–1266.
76. *Losito A, Kalidas K, Santoni S, Jeffery S*. Association of interleukin-6 -174G/C promoter polymorphism with hypertension and left ventricular hypertrophy in dialysis patients. *Kidney Int*. 2003 Aug; 64 (2): 616–622.
77. *Sharma R, Agrawal S, Saxena A, Sharma RK*. Association of IL-6, IL-10, and TNF-α gene polymorphism with malnutrition inflammation syndrome and survival among end stage renal disease patients. *J Interferon Cytokine Res*. 2013 Jul; 33 (7): 384–391.
78. *Sigrist M, Bungay P, Taal MW, McIntyre CW*. Vascular calcification and cardiovascular function in chronic kidney disease. *Nephrol Dial Transplant*. 2006 Mar; 21 (3): 707–714.
79. *Civilibal M, Caliskan S, Adaletli I, Oflaz H, Sever L, Candan C et al.* Coronary artery calcifications in children with end-stage renal disease. *Pediatr Nephrol*. 2006 Oct; 21 (10): 1426–1433.

80. *Paré M, Obeid H, Labrecque L, Drapeau A, Brassard P, Agharazii M.* Cerebral blood flow pulsatility and cerebral artery stiffness acutely decrease during hemodialysis. *Physiol Rep*. 2023 Feb; 11 (4): e15595.
81. *Arefin S, Mudrovcic N, Hobson S, Pietrocola F, Ebert T, Ward LJ et al*. Early vascular aging in chronic kidney disease: focus on microvascular maintenance, senescence signature and potential therapeutics. *Transl Res*. 2025 Jan; 275: 32–47.
82. *Petrovic M, Baralic M, Brkovic V, Arsenovic A, Stojanov V, Lalic N et al.* Significance of acPWV for Survival of Hemodialysis Patients. *Medicina (Kaunas)*. 2020 Aug 28; 56 (9): 435.
83. *Nadra I, Mason JC, Philippidis P, Florey O, Smythe CDW, McCarthy GM et al.* Proinflammatory activation of macrophages by basic calcium phosphate crystals via protein kinase C and MAP kinase pathways: a vicious cycle of inflammation and arterial calcification? *Circ Res*. 2005 Jun 24; 96 (12): 1248–1256.
84. *New SEP, Goettsch C, Aikawa M, Marchini JF, Shibasaki M, Yabusaki K et al.* Macrophage-derived matrix vesicles: an alternative novel mechanism for microcalcification in atherosclerotic plaques. *Circ Res*. 2013 Jun 21; 113 (1): 72–77.
85. *Cafiero C, Gigante M, Brunetti G, Simone S, Chaoul N, Oranger A et al.* Inflammation induces osteoclast differentiation from peripheral mononuclear cells in chronic kidney disease patients: crosstalk between the immune and bone systems. *Nephrol Dial Transplant*. 2018 Jan 1; 33 (1): 65–75.
86. *Zhou Z, Ji Y, Ju H, Chen H, Sun M*. Circulating Fetuin-A and Risk of All-Cause Mortality in Patients With Chronic Kidney Disease: A Systematic Review and Meta-Analysis. *Front Physiol*. 2019; 10: 966.
87. *Raggi P, Genest J, Giles JT, Rayner KJ, Dwivedi G, Beanlands RS et al.* Role of inflammation in the pathogenesis of atherosclerosis and therapeutic interventions. *Atherosclerosis*. 2018 Sep; 276: 98–108.
88. *Kones R*. Rosuvastatin, inflammation, C-reactive protein, JUPITER, and primary prevention of cardiovascular disease – a perspective. *Drug Des Devel Ther*. 2010 Dec 9; 4: 383–413.
89. *Sun J, Axelsson J, Machowska A, Heimbürger O, Bárány P, Lindholm B et al.* Biomarkers of Cardiovascular Disease and Mortality Risk in Patients with Advanced CKD. *Clin J Am Soc Nephrol*. 2016 Jul 7; 11 (7): 1163–1172.
90. *Yilmaz MI, Sonmez A, Saglam M, Cayci T, Kilic S, Unal HU et al.* A longitudinal study of inflammation, CKD-mineral bone disorder, and carotid atherosclerosis after renal transplantation. *Clin J Am Soc Nephrol*. 2015 Mar 6; 10 (3): 471–479.
91. *Kensinger C, Bian A, Fairchild M, Chen G, Lipworth L, Ikizler TA et al.* Long term evolution of endothelial function during kidney transplantation. *BMC Nephrol*. 2016 Oct 22; 17 (1): 160.
92. *Rysz J, Franczyk B, Ławiński J, Gluba-Brzózka A*. Oxidative Stress in ESRD Patients on Dialysis and the Risk of Cardiovascular Diseases. *Antioxidants (Basel)*. 2020 Nov 3; 9 (11): 1079.
93. *Turakhia MP, Blankestijn PJ, Carrero JJ, Clase CM, Deo R, Herzog CA et al.* Chronic kidney disease and arrhythmias: conclusions from a Kidney Disease: Improving Global Outcomes (KDIGO) Controversies Conference. *European Heart Journal*. 2018 Jun 21; 39 (24): 2314–2325.
94. *Akhtar Z, Leung LW, Kontogiannis C, Chung I, Bin Waleed K, Gallagher MM.* Arrhythmias in Chronic Kidney Disease. *Eur Cardiol*. 2022 Mar 7; 17: e05.
95. *Ribeiro SC, Figueiredo AE, Barretti P, Pecoits-Filho R, de Moraes TP, all centers that contributed to BRAZPD II study*. Low Serum Potassium Levels Increase the Infectious-Caused Mortality in Peritoneal Dialysis Patients: A Propensity-Matched Score Study. *PLoS One*. 2015; 10 (6): e0127453.
96. *Ter Braake AD, Shanahan CM, De Baaij JHF*. Magnesium Counteracts Vascular Calcification: Passive Interference or Active Modulation? *Arteriosclerosis, thrombosis, and vascular biology*. 2017 Aug 1; 37 (8): 1431–1445.
97. *Kalluri HV, Hardinger KL*. Current state of renal transplant immunosuppression: Present and future. *World J Transplant*. 2012 Aug 24; 2 (4): 51–68.
98. *Birdwell KA, Park M*. Post-Transplant Cardiovascular Disease. *Clin J Am Soc Nephrol*. 2021 Dec; 16 (12): 1878–1889.
99. *Elezaby A, Dexheimer R, Sallam K*. Cardiovascular effects of immunosuppression agents. Frontiers in Cardiovascular Medicine [Internet]. 2022 [cited 2023 Apr 19]; 9. Available from: https://www.frontiersin.org/articles/10.3389/fcvm.2022.981838.
100. *Moreso F, Grinyo JM*. Graft dysfunction and cardiovascular risk – an un-holy alliance. *Nephrol Dial Transplant*. 2007 Mar; 22 (3): 699–702.
101. *Weiner DE, Carpenter MA, Levey AS, Ivanova A, Cole EH, Hunsicker L et al.* Kidney function and risk of cardiovascular disease and mortality in kidney transplant recipients: the FAVORIT trial. *Am J Transplant*. 2012 Sep; 12 (9): 2437–2445.
102. *Shamseddin MK, Knoll GA*. Posttransplantation proteinuria: an approach to diagnosis and management. *Clin J Am Soc Nephrol*. 2011 Jul; 6 (7): 1786–1793.
103. *Fernández-Fresnedo G, Escallada R, Rodrigo E, De Francisco ALM, Cotorruelo JG, Sanz De Castro S et al*. The risk of cardiovascular disease associated with proteinuria in renal transplant patients. *Transplantation*. 2002 Apr 27; 73 (8): 1345–1348.
104. *Hiremath S, Fergusson D, Doucette S, Mulay AV, Knoll GA*. Renin angiotensin system blockade in kidney transplantation: a systematic review of the evidence. *Am J Transplant*. 2007 Oct; 7 (10): 2350–2360.
105. *Hiremath S, Fergusson DA, Fergusson N, Bennett A, Knoll GA*. Renin-Angiotensin System Blockade and Long-term Clinical Outcomes in Kidney Transplant Recipients: A Meta-analysis of Randomized Controlled Trials. *Am J Kidney Dis*. 2017 Jan; 69 (1): 78–86.
106. *Opelz G, Döhler B*. Cardiovascular death in kidney recipients treated with renin-angiotensin system blockers. Transplantation. 2014 Feb 15; 97 (3): 310–315.
107. *Kasiske BL, Zeier MG, Chapman JR, Craig JC, Ekberg H, Garvey CA et al.* KDIGO clinical practice guideline for the care of kidney transplant recipients: a summary. *Kidney Int*. 2010 Feb; 77 (4): 299–311.

The article was submitted to the journal on 8.05.2025

DOI: 10.15825/1995-1191-2025-3-173-203

STATUS AND TRENDS IN CHRONIC KIDNEY DISEASE AND RENAL REPLACEMENT THERAPY IN THE RUSSIAN FEDERATION: 2024 REPORT

Annual monitoring by the Center for Excellence in Medical Care in Nephrology at Shumakov National Medical Research Center of Transplantology and Artificial Organs, Moscow, Russian Federation

S.V. Gautier[1, 2], S.M. Khomyakov[1, 2], O.M. Tsirulnikova[1, 2], N.V. Chebotareva[1, 2], D.N. Kruglov[1, 2]

[1] Shumakov National Medical Research Center of Transplantology and Artificial Organs, Moscow, Russian Federation
[2] Sechenov University, Moscow, Russian Federation

Objective: to establish and conduct annual monitoring of the status and development trends in nephrology care across the federal subjects of the Russian Federation for the year 2024. **Materials and methods.** A comprehensive set of indicators was developed, and a structured survey was administered among leading freelance nephrology specialists across the regions. The collected data were systematically analyzed. **Results.** In 2024, the Russian Federation operated 706 hemodialysis (HD) centers and 49 kidney transplant (KT) centers. A total of 73,483 patients were receiving renal replacement therapy (RRT), of whom 76.6% were on HD, 2.7% on peritoneal dialysis (PD), and 20.6% were being monitored with a functioning kidney transplant. During the year, 1,943 KTs were performed across 49 centers in 38 regions. The overall RRT availability in the Russian Federation was 503.2 patients per million population (pmp), with HD at 385.7 pmp, PD at 13.7 pmp, and KT at 103.8 pmp. Among patients receiving HD in 2024, 81.9% were treated via arteriovenous fistula, 12.1% through permanent central venous catheter, 3.6% via temporary catheter, and 2.4% using vascular prostheses. In 2024, the Russian Federation had 537 nephrology outpatient offices, staffed by 690 physicians providing specialized care. The ratio of outpatient nephrologists to the population was 0.24 per 50,000, significantly below the recommended standard for medical personnel. Inpatient care for patients with pre-dialysis stages of chronic kidney disease (CKD) was delivered through 263 departments, comprising a total of 5,039 beds (equivalent to 0.35 beds per 10,000 population). Morphological evaluation of kidney biopsies – an important indicator of inpatient nephrological care – was independently conducted in 38 regions. Kidney biopsies were performed in 2.5% of patients hospitalized in inpatient facilities, translating to an average of 32.8 biopsies per million population. **Conclusion.** An annual monitoring framework has been successfully developed, with active collaboration established across regional centers, enabling the collection of up-to-date data on nephrological care in the Russian Federation for 2024. There is no current shortage of dialysis facilities, and a significant proportion of patients receive RRT via HD, an approach that places considerable financial burden on the national healthcare system. The high proportion of working-age individuals (62.4%) among HD patients underscores the substantial socio-economic impact of CKD and its treatment on both the state and society. Although the number of KTs continues to rise annually, current transplant volumes remain insufficient to fully meet demand and only partially offset the growing costs associated with RRT. Expanding the use of PD, particularly in sparsely populated regions, may offer advantages over HD. Nonetheless, KT remains the optimal treatment modality for patients with end-stage CKD, supporting the need to further expand transplant infrastructure and increase access to this intervention. The continuation of annual monitoring across all stages of CKD will allow for data-driven improvements in care delivery, incorporating emerging recommendations and regional insights.

Keywords: nephrological care, chronic kidney disease, CKD patient monitoring, vascular access for dialysis, renal replacement therapy, hemodialysis, peritoneal dialysis, kidney transplantation, Shumakov National Medical Research Center of Transplantology and Artificial Organs.

Corresponding author: Sergey Khomyakov. Address: 1, Schukinskaya str., Moscow, 123182, Russian Federation. Phone: (903) 150-89-55. E-mail: profkom_transpl@mail.ru

INTRODUCTION

The presented overview of nephrological care in Russia, conducted in the form of monitoring, was carried out within the authority of the Center for the Improvement of Medical Care in the Field of Nephrology at Shumakov National Medical Research Center of Transplantology and Artificial Organs (Order of the Russian Ministry of Health, No. 73, February 28, 2023).

For monitoring purposes, a system of indicators characterizing nephrological care and renal replacement therapy (RRT) in the regions was developed, along with 45 standardized tables for data collection. The resulting monitoring reports include not only statistical data for the reporting period but also a systematic analysis assessing the current state of RRT in Russia, identifying trends, and outlining prospects for further development of this healthcare sector.

The monitoring data is used by the Center for the Improvement of Medical Care in the Field of Nephrology at Shumakov National Medical Research Center of Transplantology and Artificial Organs, to address organizational and methodological tasks assigned by the Russian Ministry of Health. This includes preparation of proposals for improving nephrological care and RRT in Russia.

In addition, the monitoring data is provided to the Russian Ministry of Health, the executive authorities of the federal subjects of the Russian Federation in the field of healthcare, and the chief freelance specialists of the Russian Ministry of Health in the federal districts for use in their activities.

Data for monitoring is collected through questionnaires completed by those in charge – chief freelance specialists in nephrology, dialysis, and transplantation in the federal subjects of the Russian Federation. A comparative dynamic analysis of the obtained data will be presented in the next report to ensure consistency and avoid distortions that may arise when comparing with data from other registries that use different methodological approaches.

The working group expresses its gratitude to the chief freelance specialists in nephrology, dialysis, as well as the chief freelance specialists in transplantation from the federal subjects of the Russian Federation, the heads of nephrology departments and dialysis centers, as well as regional health authorities for their contribution in providing data and supporting the organization and improvement of this monitoring protocol.

It should be noted that the monitoring data may differ from the results of similar studies due to the specific methodology applied in the collection, processing, and analysis of information.

MEDICAL ORGANIZATIONS PROVIDING NEPHROLOGY CARE AND STAFFING

Outpatient nephrology care

According to monitoring data for 2024, 537 nephrology offices were operating in the Russian Federation, staffed by 690 physicians providing outpatient care. This corresponds to a ratio of 0.24 outpatient nephrologists per 50,000 population, which is significantly lower than the established standard of 1 medical personnel per 50,000 registered population, as defined by the Procedure for the Provision of Medical Care to the Adult Population in the Field of Nephrology (Order of the Russian Ministry of Health and Social Development No. 17n of January 18, 2012, as amended on February 21, 2020).

There is a shortage of nephrologists across all regions of the Russian Federation, especially in the Komi Republic, the Republic of Dagestan, Udmurt Republic, Republic of Mordovia, Altai Krai, Tuva Republic, and Tomsk Oblast (Table 1).

In some medical organizations, outpatient consultations and follow-up of patients with CKD are performed by physicians from hospital-based nephrology units and hemodialysis departments. However, this practice does not substantially reduce the need for dedicated outpatient nephrologists at the regional level and results in insufficiently effective monitoring and treatment of CKD patients, particularly those at advanced stages (stages 3–5), who require continuous dispensary follow-up.

In 2024, patient registration at pre-dialysis stages of CKD (primarily stages 3–4) was carried out in 53 regions of the Russian Federation. The number of patients with CKD stages 3–5D under nephrologist supervision, excluding those on dialysis, totaled 167,389. The number of patients receiving dialysis therapy (CKD 5D) in these regions was 41,704, bringing the overall number of patients with CKD stages 3–5D to 208,623.

This figure is markedly lower than the expected prevalence of CKD in the Russian Federation, which is estimated at approximately 13.6 million patients across all stages, based on international registry data and large-scale epidemiological studies [1–3].

The shortage of personnel highlights the urgent need for more targeted training and retraining of physicians in the field of nephrology. At present, specialized nephrology training programs are available in only 25 regions of the Russian Federation. Among the 690 outpatient nephrologists currently practicing, only 89 specialists (12.9%) have received additional training in the management of patients with kidney transplants. Given that 15,162 patients with functioning kidney transplants require continuous monitoring, there is a significant shortage of qualified physicians. This shortage affects not only the quality of dynamic control over immunosuppressive therapy and graft function but also the management of patients on the kidney transplant waiting list.

Table 1

Availability of nephrology medical institutions and nephrologists across regions in the Russian Federation

	Population (thousand)	Outpatient care (nephrologist's office)			Inpatient care (nephrology departments)				Dialysis (dialysis department)			
		Number of offices	Number of nephrologists	Availability of nephrologists per 50,000 population	Number of departments	Number of nephrology beds	Number of nephrologists	Availability of nephrology beds per 10,000 population	Number of centers (departments)	Number of dialysis stations	Number of doctors	Availability of dialysis stations per million population
1	2	3	4	5	6	7	8	9	10	11	12	13
Russian Federation	**146028.3**	**537**	**690**	**0.236**	**263**	**5039**	**783**	**0.345**	**706**	**21 828**	**2774**	**149.48**
Central Federal District	**40263.7**	**149**	**180**	**0.224**	**57**	**1022**	**165**	**0.254**	**175**	**4894**	**724**	**121.55**
Belgorod Oblast	1481.1	3	3	0.101	2	37	6	0.250	7	149	24	100.60
Bryansk Oblast	1132.5	3	3	0.132	1	40	2	0.353	5	141	18	124.50
Vladimir Oblast	1295.9	7	10	0.386	4	36	5	0.278	10	592	19	456.83
Voronezh Oblast	2259.6	10	10	0.221	3	71	10	0.314	9	171	33	75.68
Ivanovo Oblast	897.9	3	3	0.167	1	21	3	0.234	4	88	13	98.01
Kaluga Oblast	1064.7	3	3	0.141	1	18	3	0.169	3	52	6	48.84
Kostroma Oblast	560.8	4	3	0.267	2	30	6	0.535	5	390	13	695.44
Kursk Oblast	1050.1	6	7	0.333	2	52	6	0.495	5	101	21	96.18
Lipetsk Oblast	1107.8	4	4	0.181	3	62	11	0.560	9	142	24	128.18
Moscow Oblast	8766.6	54	49	0.279	15	67	30	0.076	22	1069	165	121.94
Oryol Oblast	685.7	3	3	0.219	2	50	7	0.729	5	69	15	100.63
Ryazan Oblast	1074.0	2	2	0.093	2	43	7	0.400	9	93	26	86.59
Smolensk Oblast	857.8	2	2	0.117	2	35	7	0.408	7	97	17	113.08
Tambov Oblast	946.0	7	10	0.529	2	47	4	0.497	8	102	20	107.82
Tver Oblast	1189.7	7	10	0.420	3	73	6	0.614	5	93	20	78.17
Tula Oblast	1455.9	5	7	0.240	2	60	7	0.412	8	288	23	197.82
Yaroslavl Oblast	1179.3	2	2	0.085	1	30	3	0.254	4	73	21	61.90
Moscow	13258.3	24	49	0.185	9	250	42	0.189	50	1184	246	89.30
Northwestern Federal District	**13863.9**	**41**	**70**	**0.252**	**24**	**427**	**50**	**0.308**	**82**	**1552**	**356**	**111.95**
Republic of Karelia	518.6	1	1	0.096	1	43	5	0.829	4	49	18	94.49
Komi Republic	714.4	1	1	0.070	2	40	6	0.560	9	111	13	155.38
Nenets Autonomous Okrug	41.8	1	1	1.196	0	0	0	0.000	1	3	1	71.77
Arkhangelsk Oblast without autonomy	946.0	11	14	0.740	3	27	4	0.285	9	126	28	133.19
Vologda Oblast	1114.6	4	7	0.314	1	12	1	0.108	5	104	17	93.31
Kaliningrad Oblast	1033.1	1	2	0.097	1	35	3	0.339	4	89	23	86.15
Leningrad Oblast	2057.7	7	5	0.121	2	26	5	0.126	15	222	62	107.89
Murmansk Oblast	650.9	1	3	0.230	1	26	3	0.399	2	281	11	431.71
Novgorod Oblast	566.7	1	2	0.176	1	15	2	0.265	6	61	9	107.64
Pskov Oblast	574.2	1	2	0.174	1	20	3	0.348	3	48	9	83.59
St. Petersburg	5645.9	12	32	0.283	11	183	18	0.324	24	458	165	81.12
Southern Federal District	**16585.9**	**60**	**70**	**0.211**	**30**	**612**	**88**	**0.369**	**39**	**2123**	**169**	**128.00**
Republic of Adygea	501.0	2	2	0.200	2	27	3	0.539	4	67	9	133.73
Republic of Kalmykia	267.4	1	2	0.374	1	10	1	0.374	4	67	7	250.56
Republic of Crimea	1901.1	7	9	0.237	3	82	7	0.431	7	765	31	402.40
Krasnodar Krai	5841.8	10	14	0.120	5	138	20	0.236	5	385	17	65.90
Astrakhan Oblast	946.0	8	9	0.476	3	45	6	0.476	4	77	14	81.40
Volgograd Oblast	2435.4	22	22	0.452	7	135	18	0.554	5	92	26	37.78
Rostov Oblast	4135.0	9	11	0.133	7	144	30	0.348	7	606	53	146.55
Sevastopol	558.2	1	1	0.090	2	31	3	0.555	3	64	12	114.65

Continuation of Table 1

1	2	3	4	5	6	7	8	9	10	11	12	13
North Caucasian Federal District	**10307.6**	**31**	**40**	**0.194**	**23**	**407**	**69**	**0.395**	**60**	**1257**	**213**	**121.95**
Republic of Dagestan	3259.0	1	1	0.015	1	10	0	0.031	16	272	51	83.46
Republic of Ingushetia	534.2	1	2	0.187	1	15	2	0.281	3	25	8	46.80
Kabardino-Balkarian Republic	908.1	6	7	0.385	5	117	11	1.288	7	116	20	127.74
Karachay-Cherkess Republic	468.5	3	4	0.427	5	50	10	1.067	2	80	6	170.76
Republic of North Ossetia – Alania	678.5	4	3	0.221	3	59	31	0.870	5	121	31	178.33
Chechen Republic	1575.8	5	5	0.159	2	50	3	0.317	10	154	34	97.73
Stavropol Krai	2883.5	11	18	0.312	6	106	12	0.368	17	489	63	169.59
Volga Federal District	**28397.8**	**107**	**153**	**0.269**	**50**	**1168**	**166**	**0.411**	**126**	**4542**	**554**	**159.94**
Republic of Bashkortostan	4046.1	7	7	0.087	4	125	11	0.309	4	1622	89	400.88
Mari El Republic	666.0	2	4	0.300	2	65	6	0.976	5	72	14	108.11
Republic of Mordovia	758.4	1	1	0.066	1	30	3	0.396	5	98	12	129.22
Republic of Tatarstan	4016.6	8	14	0.174	4	69	10	0.172	23	329	58	81.91
Udmurt Republic	1427.0	2	2	0.070	3	70	8	0.491	15	178	31	124.74
Chuvash Republic	1159.8	2	4	0.172	2	43	6	0.371	2	98	13	84.50
Perm Krai	2482.1	26	28	0.564	6	136	21	0.548	11	646	48	260.26
Kirov Oblast	1120.2	8	7	0.312	2	54	1	0.482	5	131	29	116.94
Nizhny Novgorod Oblast	3037.8	9	9	0.148	6	95	27	0.313	16	361	87	118.84
Orenburg Oblast	1815.7	7	8	0.220	4	83	20	0.457	11	183	37	100.79
Penza Oblast	1226.0	7	7	0.285	2	60	5	0.489	4	122	20	99.51
Samara Oblast	3108.9	4	10	0.161	4	107	13	0.344	10	309	47	99.39
Saratov Oblast	2368.4	20	41	0.866	10	231	35	0.975	8	232	52	97.96
Ulyanovsk Oblast	1164.8	4	11	0.472	0	0	0	0.000	7	161	17	138.22
Ural Federal District	**11914.3**	**47**	**57**	**0.239**	**21**	**396**	**57**	**0.332**	**69**	**2712**	**228**	**227.63**
Kurgan Oblast	744.2	2	2	0.134	1	13	4	0.175	4	63	16	84.65
Sverdlovsk Oblast	4218.2	12	16	0.190	8	110	21	0.261	17	585	90	138.68
Khanty-Mansi Autonomous Okrug – Yugra	1779.5	12	12	0.337	6	101	14	0.568	17	194	51	109.02
Yamalo-Nenets Autonomous Okrug	521.7	4	5	0.479	0	0	0	0.000	6	43	14	82.42
Tyumen Oblast without autonomies	1267.5	4	6	0.237	2	70	4	0.552	6	61	16	48.13
Chelyabinsk Oblast	3383.2	13	16	0.236	4	102	14	0.301	19	1766	41	521.99
Siberian Federal District	**16482.8**	**62**	**73**	**0.221**	**32**	**465**	**101**	**0.282**	**88**	**3015**	**284**	**182.92**
Altai Republic	210.1	1	3	0.714	0	0	0	0.000	1	32	3	152.31
Tuva Republic	338.3	0	0	0.000	0	0	0	0.000	1	20	2	59.12
Republic of Khakassia	525.5	1	1	0.095	2	11	8	0.209	4	41	11	78.02
Altai Krai	2099.0	3	2	0.048	2	55	7	0.262	11	1156	42	550.74
Krasnoyarsk Krai	2837.4	7	7	0.123	3	83	9	0.293	20	254	58	89.52
Irkutsk Oblast	2316.6	10	10	0.216	11	60	32	0.259	13	79	26	34.10
Kemerovo (Kuzbass) Oblast	2526.4	18	30	0.594	7	98	19	0.388	17	323	53	127.85
Novosibirsk Oblast	2784.6	13	11	0.198	4	71	16	0.255	7	841	44	302.02
Omsk Oblast	1805.4	8	8	0.222	2	39	3	0.216	8	201	25	111.33
Tomsk Oblast	1039.5	1	1	0.048	1	48	7	0.462	6	68	20	65.42
Far Eastern Federal District	**7853.5**	**31**	**39**	**0.248**	**19**	**392**	**64**	**0.499**	**58**	**1571**	**218**	**200.04**
Republic of Buryatia	970.7	5	7	0.361	3	44	3	0.453	7	130	34	133.92
Sakha (Yakutia) Republic	1007.1	4	4	0.199	2	50	13	0.496	9	849	54	843.01
Zabaykalsky Krai	982.5	5	8	0.407	4	75	7	0.763	10	89	26	90.59
Kamchatka Krai	287.9	2	2	0.347	1	5	0	0.174	2	19	5	66.00
Primorsky Krai	1798.0	3	6	0.167	2	85	17	0.473	14	213	49	118.46
Khabarovsk Krai	1273.1	4	4	0.157	3	55	13	0.432	8	103	25	80.90
Amur Oblast	750.9	3	3	0.200	1	35	6	0.466	3	57	9	75.91
Magadan Oblast	134.2	1	1	0.373	1	22	3	1.639	1	60	3	447.09

End of Table 1

1	2	3	4	5	6	7	8	9	10	11	12	13
Sakhalin Oblast	456.8	3	3	0.328	1	15	1	0.328	2	27	6	59.11
Jewish Autonomous Oblast	144.4	1	1	0.346	1	6	1	0.416	2	24	7	166.20
Chukotka Autonomous Okrug	47.9	0	0	0.000	0	0	0	0.000	0	0	0	0.00
New territories		**9**	**8**		**7**	**150**	**23**		**9**	**162**	**28**	
Donetsk People's Republic		6	6		5	120	13		5	108	19	
Luhansk People's Republic		3	2		1	20	9		1	25	7	
Zaporizhzhya Oblast		0	0		1	10	1		3	29	2	
Kherson Oblast		0	0		0	0	0		1	10	0	

Note. Population figures, as well as the availability of specialists and hospital beds in the Russian Federation, were calculated excluding the newly incorporated territories, due to the inability to accurately estimate the permanent population in those regions.

Patient education plays a crucial role in improving adherence to therapy, prognosis, and awareness of kidney disease. To this end, schools for patients with kidney disease are functioning in 29 regions of the Russian Federation. Of these, 20 regions offer in-person classes for patients with CKD, 24 regions for patients on hemodialysis, and 14 regions for patients with kidney transplants. Nevertheless, the need to expand these educational programs nationwide underscores the importance of strengthening outpatient nephrology services through an increase in the number of trained specialists.

Inpatient care in nephrology

In 2024, inpatient treatment for patients with chronic kidney disease (CKD) in pre-dialysis stages was provided in 263 hospital departments with a total capacity of 5,039 beds, corresponding to 0.35 nephrology beds per 10,000 population across the Russian Federation. However, several regions – Nenets Autonomous Okrug, Chukotka Autonomous Okrug, Altai Republic, and Tuva Republic – still lack inpatient nephrology services for pre-dialysis patients (Table 1). Nationwide, 783 nephrologists work in nephrology hospital settings, of whom only 187 have specialized training in managing kidney transplant patients. This remains insufficient to adequately monitor this growing patient category.

One important quality indicator of inpatient nephrology care is the number of kidney biopsies performed per million population per year. In 2024, kidney biopsies were conducted in 3,734 patients (2.5%) out of 147,681 hospitalizations, which corresponds to an average of 32.8 biopsies per million population.

Morphological studies are independently performed in 38 regions, while biopsy material from 26 regions is sent to larger nephrology centers for expert evaluation. Biopsy activity in some regions approaches or exceeds the European average of 76 biopsies per million population [4–8]. Notable examples include Kemerovo Oblast – 209 biopsies (100 per million); Chelyabinsk Oblast – 268 (97.9 per million); Krasnoyarsk Krai – 167 (73.1 per million); Moscow – 705 (63.7 per million); Republic of Tatarstan – 190 (58.8 per million); Samara Oblast – 146 (56.4 per million); Irkutsk Oblast – 100 (54.8 per million); Novosibirsk Oblast – 121 (53.7 per million); St. Petersburg – 202 (42.5 per million).

To improve diagnosis, optimize treatment strategies, and reduce progression to end-stage CKD, it is necessary to expand nephrobiopsy coverage to all regions, aiming for an average national rate of at least 70 biopsies per million population. This requires not only ensuring the technical capacity to perform kidney biopsies (in urology and surgical departments) but also establishing pathways for sending biopsy material to larger centers where qualified morphological examination can be performed.

CHARACTERISTICS OF THE POPULATION OF CKD PATIENTS ON RRT IN THE RUSSIAN FEDERATION

Data on RRT in 2024 were obtained from 89 regions of the Russian Federation. In total, 73,483 patients with stage 5 CKD were receiving RRT: 56,324 (76.7%) on HD, 1,997 (2.7%) on PD, 15,162 (20.6%) living with a functioning kidney transplant (Fig. 2).

The age distribution of patients by treatment modality is shown in Fig. 3. Kidney transplantation (KT) is the predominant method of RRT among children (0–18 years), accounting for 70% of patients in this age group. In contrast, HD dominates among adults: more than 60% of patients under 50 years and over 80% of those older than 50 years receive this therapy.

The high proportion of working-age patients maintained on HD, the most expensive RRT modality, highlights the urgent need to further expand KT programs across Russian regions.

No significant gender differences were observed in the distribution of patients across RRT modalities (Fig. 4).

The structure of underlying diseases among patients receiving dialysis (HD and PD) is dominated by glomerulonephritis (25.2%), kidney damage in type 2 diabetes mellitus (13.9%), and arterial hypertension (13.4%), followed by polycystic kidney disease (10%), chronic

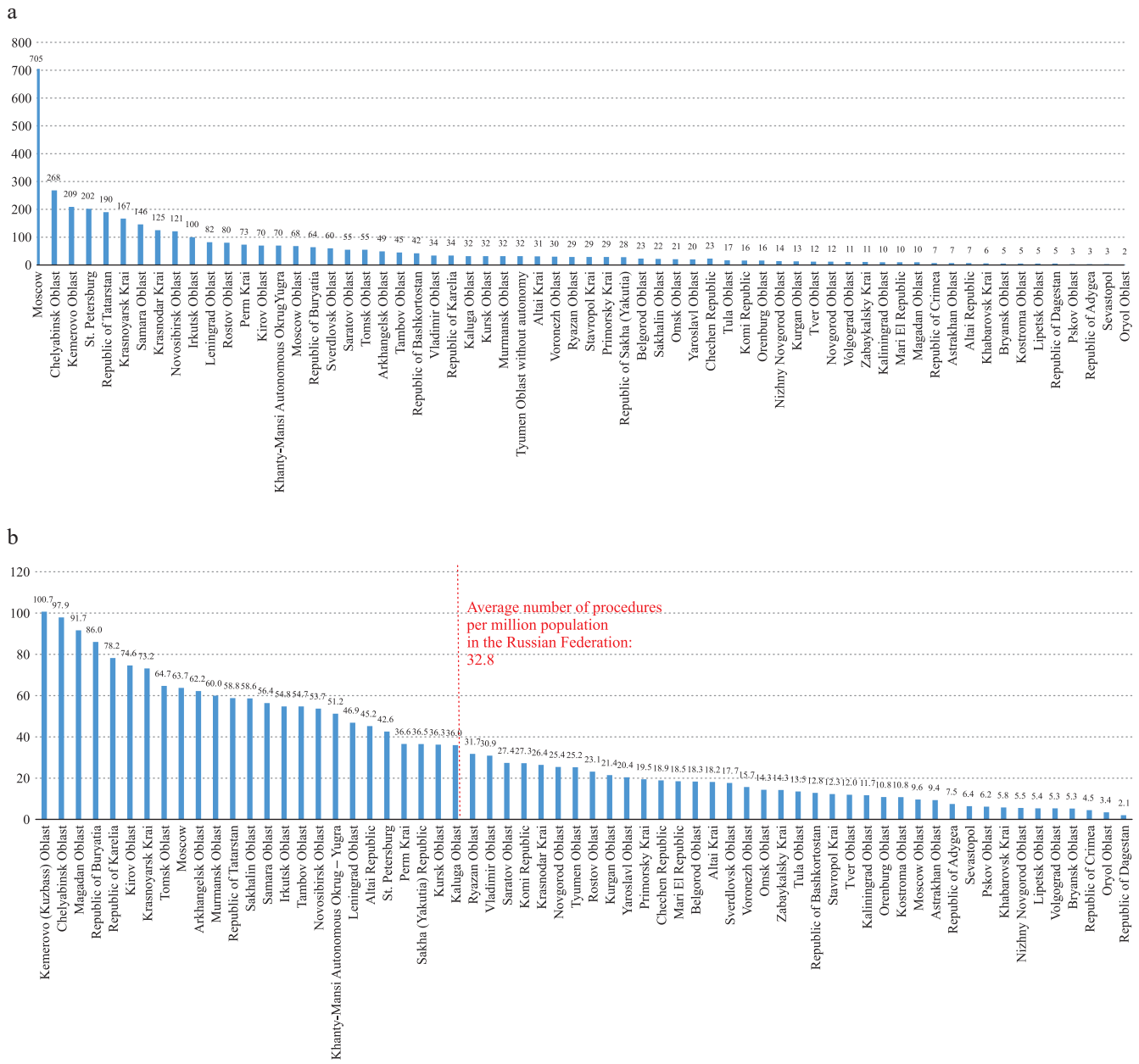

Fig. 1. Number of kidney biopsies performed across regions of the Russian Federation in 2024: a, total number of kidney biopsies; b, regional distribution of kidney biopsies per million population

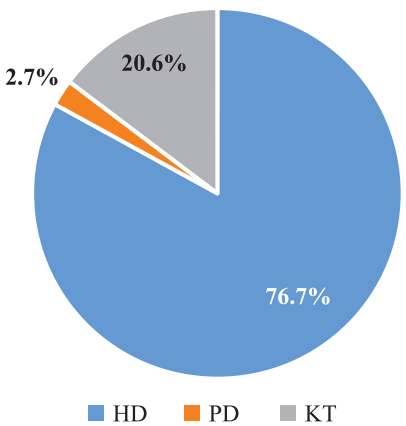

Fig. 2. Distribution of renal replacement therapy (RRT) modalities in the Russian Federation in 2024

pyelonephritis (8.8%), and tubulointerstitial kidney disease (6.8%) (Fig. 5).

The high prevalence of glomerulonephritis as a cause of end-stage CKD (esCKD) underscores the importance of timely kidney biopsy and accurate diagnosis of the underlying nosological form at earlier stages. This approach would facilitate the use of pathogenetic therapy, potentially slowing disease progression and reducing the burden of renal failure.

It should be noted that polycystic kidney disease (10%) and chronic pyelonephritis (8.8%) make a substantial contribution to the etiology of esCKD. Effective management of these conditions requires close collaboration between nephrologists and urologists.

The distribution of glomerulonephritis, diabetes mellitus, and polycystic kidney disease as causes of esCKD in Russia is broadly consistent with data from the international ERA Registry of dialysis patients. However, the relatively high frequency of arterial hypertension and chronic pyelonephritis as primary causes of esCKD in the Russian Federation is noteworthy [9]. Expanding the use of nephrobiopsy in patients with clinical indications will improve diagnostic accuracy.

RENAL REPLACEMENT THERAPY IN THE RUSSIAN FEDERATION IN 2024

In 2024, the overall RRT coverage rate in the Russian Federation was 503.2 patients per million population,

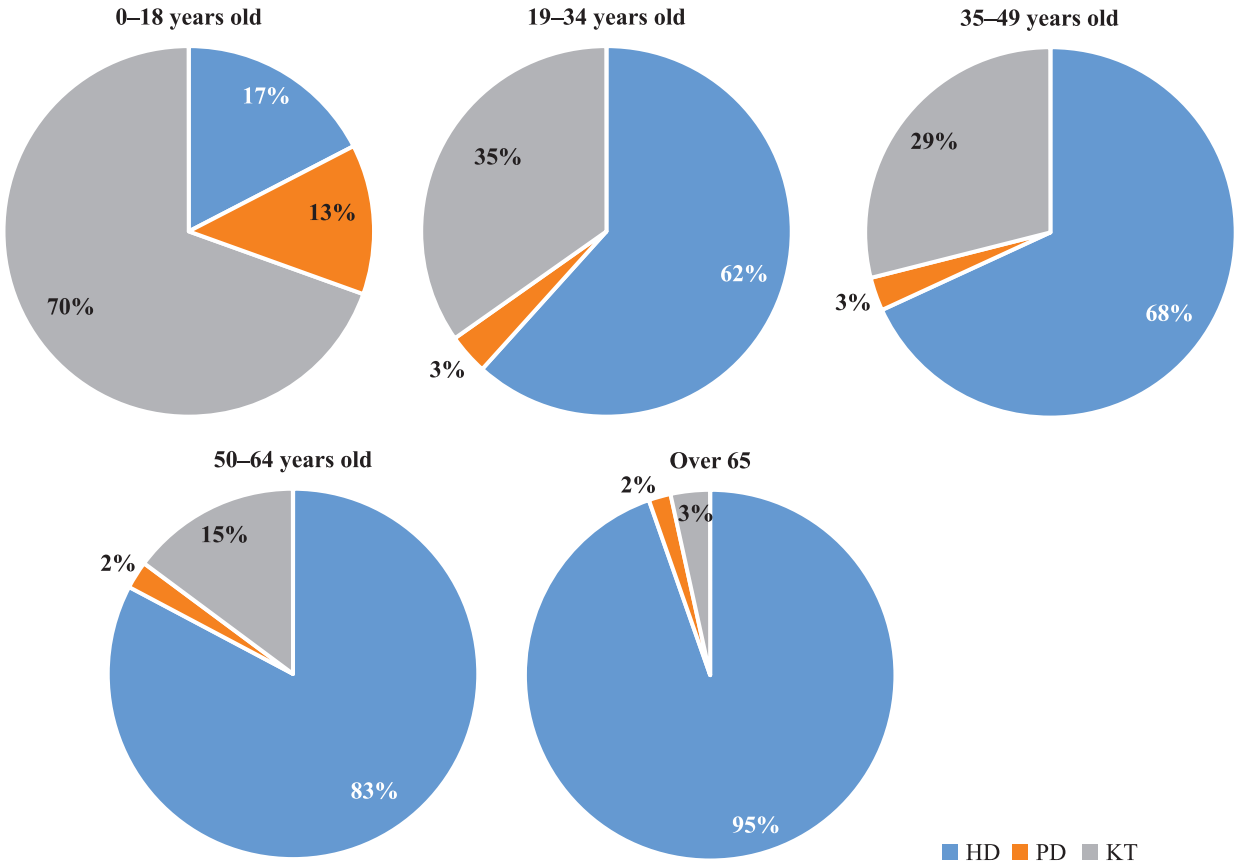

Fig. 3. Age distribution of patients with stage 5 chronic kidney diseasereceiving renal replacement therapy in the Russian Federation in 2024

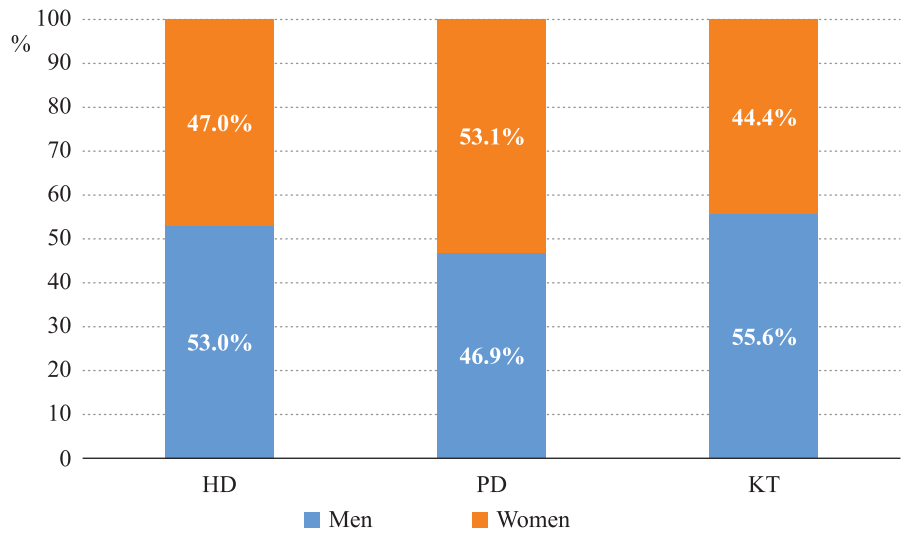

Fig. 4. Gender distribution of patients with stage 5 chronic kidney disease undergoing renal replacement therapy in the Russian Federation in 2024

including 385.7 per million on HD, 13.7 per million on PD, and 103.8 per million living with a functioning kidney transplant. Data on the availability of RRT in the newly incorporated regions are reported separately, taking into account changes in population size.

The number of dialysis patients, and consequently the financial burden on the national healthcare system, continues to rise in the Russian Federation [10]. In 2024, 14,426 patients initiated HD, 685 patients began PD, and 1,943 patients underwent KT. The indicators of RRT provision in the Russian Federation are presented in Table 2. In 2024, 6,995 patients on HD (9.8%) and 200 KT recipients (0.3%) died (Table 2). Mortality rates for HD varied slightly across regions but remained generally consistent with global data [11].

In 2024, a total of 706 dialysis centers were operating in the Russian Federation, of which 400 (56.7%) were privately or publicly owned. The total number of dialysis beds reached 21,828, corresponding to 149.5 per million population. Over the past five years, the number of centers increased by 18%, while the number of dialysis beds grew 2.4 times [12].

The staffing of dialysis units included 2,774 physicians and 5,966 nurses, resulting in an average of one nephrologist per 7.9 dialysis stations and one nurse per 3.7 stations per shift. These ratios meet the requirements established by the Procedure for the Provision of Medical Care to the Adult Population in the Field of Nephrology (Order of the Russian Ministry of Health and Social Development, January 18, 2012, No. 17n; as amended on February 21, 2020).

Across most regions of the Russian Federation, provision of HD per million population was comparable to the national average. However, some territories reported notable deviations: Krasnodar Krai, Republic of Buryatia, Republic of Kalmykia, Republic of North Ossetia, and Kabardino-Balkarian Republic had 1.5 times more patients on HD than the national mean. By contrast, Voronezh, Tomsk, Amur, and Volgograd regions, as well as the Altai Republic and Kaluga Oblast, reported lower-than-average HD prevalence. In several of these regions, reduced HD utilization was offset by higher rates of PD and KT (Figs. 6–8).

In Russia in 2024, vascular access for HD was distributed as follows: 81.9% of patients were treated via an arteriovenous fistula (AVF), 3.6% via a temporary central venous catheter, 12.1% via a permanent catheter, and 2.4% with a vascular prosthesis. AVF is the preferred vascular access method, as it provides the best outcomes. Overall, the proportion of patients receiving HD through AVF in the Russian Federation is sufficiently high, exceeding 80% in most regions, which is in line with international standards. In several regions, more than 90% of patients use AVF: Bryansk, Ryazan, the Republic of Karelia, the Republic of Mordovia, Chuvashia, Crimea, Republic of Dagestan, Zabaykalsky Krai, and Omsk Oblast.

However, in 10 regions, the proportion of patients undergoing HD via temporary catheters exceeds the national average. Reliance on temporary vascular access is associated with a significantly increased risk of infectious complications and mortality in HD patients.

In 2024, the Russian Federation reported a total of 15,030 HD machines, of which 14,188 (94.4%) were operational. In most regions, high-flux dialyzers – associated with greater efficiency compared to low-flux membranes – were predominantly used, accounting for 4,973,578 sessions (69%) out of the total 7,236,018 HD sessions performed.

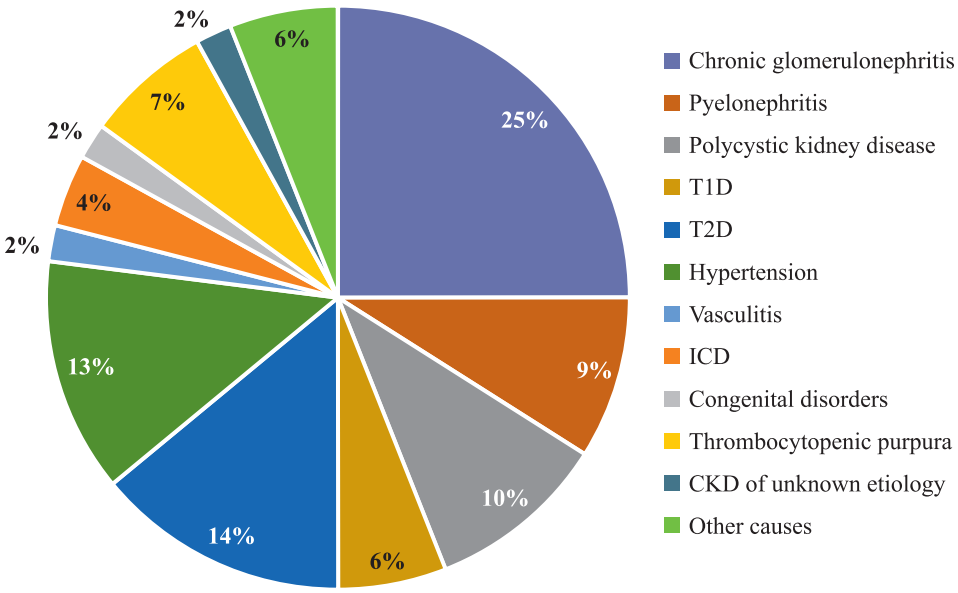

Fig. 5. Nosological structure of kidney disease in patients receiving renal replacement therapy in the Russian Federation

Table 2

Availability of renal replacement therapy for stage 5 CKD across regions of the Russian Federation. 2024

Federal Subjects of the Russian Federation	Population (thousand)	Number of HD patients (abs.)	Number of PD patients (abs.)	Number of KT recipients with functioning grafts (abs.)	Number of patients on the KT waitlist (abs.)	Total number of patients receiving RRT (abs.)	Availability of HD (patients per million population)	Availability of PD per million population	Availability of KT per million population	Availability of RRT per million population	Number of new HD patients (abs.)	Number of new PD patients (abs.)	Number of new KT recipients (abs.)	Number of new HD patients per million population	Number of new PD patients per million population	Number of new KT recipients per million population	Number of deaths among HD patients (abs.)	Number of deaths among PD patients (abs.)	Number of deaths among KT recipients (abs.)	Proportion of deaths on dialysis as a percentage of total RRT patients (%)	Proportion of among KT recipients as a percentage of total RRT patients (%)	Ratio of patients on HD/PD/KT		
																						HD	PD	KT
1	2	3	4	5	6	7	8	9	10	11	12	13	14	15	16	17	18	19	20	21	22	23	24	25
Russian Federation	**146028.3**	**56 324**	**1997**	**15 162**	**7331**	**73 483**	**385.7**	**13.7**	**103.8**	**503.2**	**14 426**	**685**	**1943**	**98.8**	**4.7**	**13.3**	**6995**	**215**	**200**	**9.8**	**0.3**	**76.6**	**2.7**	**20.6**
Central Federal District	**40263.7**	**14743**	**658**	**6032**	**2566**	**21433**	**366.2**	**16.3**	**149.8**	**532.3**	**4861**	**265**	**752**	**120.7**	**6.6**	**18.7**	**1816**	**50**	**73**	**8.7**	**0.3**	**68.8**	**3.1**	**28.1**
Belgorod Oblast	1481.1	689	0	113	81	802	465.2	0.0	76.3	541.5	151	0	8	102.0	0.0	5.4	121	0	2	15.1	0.2	85.9	0.0	14.1
Bryansk Oblast	1132.5	425	0	64	16	489	375.3	0.0	56.5	431.8	81	0	6	71.5	0.0	5.3	34	0	0	7.0	0.0	86.9	0.0	13.1
Vladimir Oblast	1295.9	468	5	131	78	604	361.1	3.9	101.1	466.1	121	2	12	93.4	1.5	9.3	60	0	0	9.9	0.0	77.5	0.8	21.7
Voronezh Oblast	2259.6	573	8	118	61	699	253.6	3.5	52.2	309.3	159	6	13	70.4	2.7	5.8	65	2	4	9.6	0.6	82.0	1.1	16.9
Ivanovo Oblast	897.9	313	0	53	14	366	348.6	0.0	59.0	407.6	68	0	10	75.7	0.0	11.1	27	0	0	7.4	0.0	85.5	0.0	14.5
Kaluga Oblast	1064.7	149	11	98	61	258	139.9	10.3	92.0	242.3	36	7	10	33.8	6.6	9.4	9	1	0	3.9	0.0	57.8	4.3	38.0
Kostroma Oblast	560.8	273	5	41	36	319	486.8	8.9	73.1	568.8	77	0	4	137.3	0.0	7.1	60	0	1	18.8	0.3	85.6	1.6	12.9
Kursk Oblast	1050.1	309	4	49	10	362	294.3	3.8	46.7	344.7	41	0	3	39.0	0.0	2.9	37	0	0	10.2	0.0	85.4	1.1	13.5
Lipetsk Oblast	1107.8	550	30	78	56	658	496.5	27.1	70.4	594.0	153	9	9	138.1	8.1	8.1	76	3	1	12.0	0.2	83.6	4.6	11.9
Moscow Oblast	8766.6	3352	96	958	765	4406	382.4	11.0	109.3	502.6	655	28	125	74.7	3.2	14.3	357	12	1	8.4	0.0	76.1	2.2	21.7
Oryol Oblast	685.7	292	0	49	23	341	425.8	0.0	71.5	497.3	74	0	7	107.9	0.0	10.2	37	0	0	10.9	0.0	85.6	0.0	14.4
Ryazan Oblast	1074.0	401	20	106	40	527	373.4	18.6	98.7	490.7	116	6	21	108.0	5.6	19.6	63	3	2	12.5	0.4	76.1	3.8	20.1
Smolensk Oblast	857.8	279	5	45	17	329	325.3	5.8	52.5	383.5	64	0	9	74.6	0.0	10.5	40	0	1	12.2	0.3	84.8	1.5	13.7
Tambov Oblast	946.0	392	5	44	14	441	414.4	5.3	46.5	466.2	111	3	2	117.3	3.2	2.1	51	1	3	11.8	0.7	88.9	1.1	10.0
Tver Oblast	1189.7	416	20	106	45	542	349.7	16.8	89.1	455.6	216	9	7	181.6	7.6	5.9	70	9	1	14.6	0.2	76.8	3.7	19.6
Tula Oblast	1455.9	436	18	136	44	590	299.5	12.4	93.4	405.2	88	6	10	60.4	4.1	6.9	54	4	5	9.8	0.8	73.9	3.1	23.1
Yaroslavl Oblast	1179.3	411	19	116	63	546	348.5	16.1	98.4	463.0	113	15	14	95.8	12.7	11.9	39	1	1	7.3	0.2	75.3	3.5	21.2
Moscow	13258.3	5015	412	3727	1142	9154	378.3	31.1	281.1	690.4	2537	174	482	191.4	13.1	36.4	616	14	51	6.9	0.6	54.8	4.5	40.7

Continuation of Table 2

1	2	3	4	5	6	7	8	9	10	11	12	13	14	15	16	17	18	19	20	21	22	23	24	25
Northwestern Federal District	**13863.9**	**5400**	**146**	**1449**	**507**	**6995**	**389.5**	**10.5**	**104.5**	**504.5**	**1112**	**64**	**234**	**80.2**	**4.6**	**16.9**	**573**	**5**	**18**	**8.3**	**0.3**	**77.2**	**2.1**	**20.7**
Republic of Karelia	518.6	214	7	31	21	252	412.6	13.5	59.8	485.9	57	1	2	109.9	1.9	3.9	27	2	0	11.5	0.0	84.9	2.8	12.3
Komi Republic	714.4	329	15	27	0	371	460.5	21.0	37.8	519.3	36	4	0	50.4	5.6	0.0	17	0	0	4.6	0.0	88.7	4.0	7.3
Nenets Autonomous Okrug	41.8	11	0	0	0	11	263.2	0.0	0.0	263.2	5	0	0	119.6	0.0	0.0	2	0	0	18.2	0.0	100.0	0.0	0.0
Arkhangelsk Oblast without autonomy	946.0	529	17	53	41	599	559.2	18.0	56.0	633.2	103	5	10	108.9	5.3	10.6	46	0	1	7.7	0.2	88.3	2.8	8.8
Vologda Oblast	1114.6	371	0	107	12	478	332.9	0.0	96.0	428.9	88	0	18	79.0	0.0	16.1	56	0	2	11.7	0.4	77.6	0.0	22.4
Kaliningrad Oblast	1033.1	366	4	49	0	419	354.3	3.9	47.4	405.6	58	0	3	56.1	0.0	2.9	32	0	2	7.6	0.5	87.4	1.0	11.7
Leningrad Oblast	2057.7	578	1	267	79	846	280.9	0.5	129.8	411.1	113	0	36	54.9	0.0	17.5	70	0	1	8.3	0.1	68.3	0.1	31.6
Murmansk Oblast	650.9	259	15	11	1	285	397.9	23.0	16.9	437.9	33	2	3	50.7	3.1	4.6	17	1	1	6.3	0.4	90.9	5.3	3.9
Novgorod Oblast	566.7	259	0	30	0	289	457.0	0.0	52.9	510.0	73	0	2	128.8	0.0	3.5	15	0	0	5.2	0.0	89.6	0.0	10.4
Pskov Oblast	574.2	209	0	23	7	232	364.0	0.0	40.1	404.0	34	0	7	59.2	0.0	12.2	26	0	0	11.2	0.0	90.1	0.0	9.9
St. Petersburg	5645.9	2275	87	851	346	3213	402.9	15.4	150.7	569.1	512	52	153	90.7	9.2	27.1	265	2	11	8.3	0.3	70.8	2.7	26.5
Southern Federal District	**16585.9**	**6545**	**217**	**1350**	**528**	**8112**	**394.6**	**13.1**	**81.4**	**489.1**	**1064**	**51**	**138**	**64.2**	**3.1**	**8.3**	**743**	**55**	**24**	**9.8**	**0.3**	**80.7**	**2.7**	**16.6**
Republic of Adygea	501.0	205	2	13	8	220	409.2	4.0	25.9	439.1	63	1	1	125.7	2.0	2.0	39	0	0	17.7	0.0	93.2	0.9	5.9
Republic of Kalmykia	267.4	179	1	36	0	216	669.4	3.7	134.6	807.8	28	0	4	104.7	0.0	15.0	25	0	0	11.6	0.0	82.9	0.5	16.7
Republic of Crimea	1901.1	692	15	110	41	817	364.0	7.9	57.9	429.8	213	8	12	112.0	4.2	6.3	78	1	4	9.7	0.5	84.7	1.8	13.5
Krasnodar Krai	5841.8	3253	97	550	35	3900	556.8	16.6	94.1	667.6	98	10	25	16.8	1.7	4.3	311	24	7	8.6	0.2	83.4	2.5	14.1
Astrakhan Oblast	946.0	371	2	78	31	451	392.2	2.1	82.5	476.7	101	0	21	106.8	0.0	22.2	65	1	1	14.6	0.2	82.3	0.4	17.3
Volgograd Oblast	2435.4	394	79	249	300	722	161.8	32.4	102.2	296.5	241	31	26	99.0	12.7	10.7	52	25	8	10.7	1.1	54.6	10.9	34.5
Rostov Oblast	4135.0	1233	20	301	108	1554	298.2	4.8	72.8	375.8	270	1	48	65.3	0.2	11.6	141	4	4	9.3	0.3	79.3	1.3	19.4
Sevastopol	558.2	218	1	13	5	232	390.5	1.8	23.3	415.6	50	0	1	89.6	0.0	1.8	32	0	0	13.8	0.0	94.0	0.4	5.6
North Caucasian Federal District	**10307.6**	**3960**	**36**	**457**	**133**	**4453**	**384.2**	**3.5**	**44.3**	**432.0**	**901**	**4**	**56**	**87.4**	**0.4**	**5.4**	**551**	**1**	**5**	**12.4**	**0.1**	**88.9**	**0.8**	**10.3**
Republic of Dagestan	3259.0	951	3	134	22	1088	291.8	0.9	41.1	333.8	226	2	17	69.3	0.6	5.2	133	0	2	12.2	0.2	87.4	0.3	12.3
Republic of Ingushetia	534.2	140	28	27	30	195	262.1	52.4	50.5	365.0	37	0	1	69.3	0.0	1.9	15	0	0	7.7	0.0	71.8	14.4	13.8
Kabardino-Balkarian Republic	908.1	496	3	17	3	516	546.2	3.3	18.7	568.2	110	2	2	121.1	2.2	2.2	59	0	0	11.4	0.0	96.1	0.6	3.3
Karachay-Cherkess Republic	468.5	203	0	22	3	225	433.3	0.0	47.0	480.3	21	0	1	44.8	0.0	2.1	27	0	0	12.0	0.0	90.2	0.0	9.8

Continuation of Table 2

1	2	3	4	5	6	7	8	9	10	11	12	13	14	15	16	17	18	19	20	21	22	23	24	25
Republic of North Ossetia – Alania	678.5	391	1	20	8	412	576.3	1.5	29.5	607.2	87	0	5	128.2	0.0	7.4	45	0	0	10.9	0.0	94.9	0.2	4.9
Chechen Republic	1575.8	629	0	123	7	752	399.2	0.0	78.1	477.2	164	0	13	104.1	0.0	8.2	99	0	0	13.2	0.0	83.6	0.0	16.4
Stavropol Krai	2883.5	1150	1	114	60	1265	398.8	0.3	39.5	438.7	256	0	17	88.8	0.0	5.9	173	1	3	13.8	0.2	90.9	0.1	9.0
Volga Federal District	**28397.8**	**10771**	**620**	**2530**	**1991**	**13921**	**379.3**	**21.8**	**89.1**	**490.2**	**2785**	**210**	**315**	**98.1**	**7.4**	**11.1**	**1616**	**69**	**30**	**12.1**	**0.2**	**77.4**	**4.5**	**18.2**
Republic of Bashkortostan	4046.1	1074	23	410	128	1507	265.4	5.7	101.3	372.5	375	16	40	92.7	4.0	9.9	236	2	0	15.8	0.0	71.3	1.5	27.2
Mari El Republic	666.0	245	4	42	40	291	367.9	6.0	63.1	436.9	57	2	5	85.6	3.0	7.5	26	0	1	8.9	0.3	84.2	1.4	14.4
Republic of Mordovia	758.4	308	17	46	109	371	406.1	22.4	60.7	489.2	43	1	4	56.7	1.3	5.3	37	0	0	10.0	0.0	83.0	4.6	12.4
Republic of Tatarstan	4016.6	1616	16	548	509	2180	402.3	4.0	136.4	542.7	469	4	101	116.8	1.0	25.1	234	2	8	10.8	0.4	74.1	0.7	25.1
Udmurt Republic	1427.0	720	38	94	79	852	504.6	26.6	65.9	597.1	173	6	9	121.2	4.2	6.3	87	5	2	10.8	0.2	84.5	4.5	11.0
Chuvash Republic	1159.8	370	0	72	47	442	319.0	0.0	62.1	381.1	92	0	5	79.3	0.0	4.3	64	0	0	14.5	0.0	83.7	0.0	16.3
Perm Krai	2482.1	1034	50	143	102	1227	416.6	20.1	57.6	494.3	178	19	11	71.7	7.7	4.4	139	1	1	11.4	0.1	84.3	4.1	11.7
Kirov Oblast	1120.2	494	14	50	22	558	441.0	12.5	44.6	498.1	86	2	3	76.8	1.8	2.7	45	1	1	8.2	0.2	88.5	2.5	9.0
Nizhny Novgorod Oblast	3037.8	1301	52	374	211	1727	428.3	17.1	123.1	568.5	319	14	26	105.0	4.6	8.6	188	7	0	11.3	0.0	75.3	3.0	21.7
Orenburg Oblast	1815.7	724	94	171	39	989	398.7	51.8	94.2	544.7	220	42	39	121.2	23.1	21.5	131	26	4	15.9	0.4	73.2	9.5	17.3
Penza Oblast	1226.0	475	63	47	241	585	387.4	51.4	38.3	477.2	86	12	6	70.1	9.8	4.9	69	5	0	12.6	0.0	81.2	10.8	8.0
Samara Oblast	3108.9	1197	144	265	109	1606	385.0	46.3	85.2	516.6	376	58	33	120.9	18.7	10.6	185	9	4	12.1	0.2	74.5	9.0	16.5
Saratov Oblast	2368.4	799	51	177	69	1027	337.4	21.5	74.7	433.6	183	21	24	77.3	8.9	10.1	116	7	6	12.0	0.6	77.8	5.0	17.2
Ulyanovsk Oblast	1164.8	414	54	91	286	559	355.4	46.4	78.1	479.9	128	13	9	109.9	11.2	7.7	59	4	3	11.3	0.5	74.1	9.7	16.3
Ural Federal District	**11914.3**	**5145**	**36**	**992**	**611**	**6173**	**431.8**	**3.0**	**83.3**	**518.1**	**1334**	**8**	**121**	**112.0**	**3.0**	**10.2**	**592**	**3**	**17**	**9.6**	**0.3**	**83.3**	**0.6**	**16.1**
Kurgan Oblast	744.2	334	0	27	8	361	448.8	0.0	36.3	485.1	177	0	3	237.8	0.0	4.0	65	0	0	18.0	0.0	92.5	0.0	7.5
Sverdlovsk Oblast	4218.2	2061	26	388	190	2475	488.6	6.2	92.0	586.7	587	2	38	139.2	0.5	9.0	296	2	6	12.0	0.2	83.3	1.1	15.7
Khanty-Mansi Autonomous Okrug – Yugra	1779.5	698	0	132	145	830	392.2	0.0	74.2	466.4	179	0	18	100.6	0.0	10.1	79	0	5	9.5	0.6	84.1	0.0	15.9
Yamalo-Nenets Autonomous Okrug	521.7	129	0	23	30	152	247.3	0.0	44.1	291.4	36	0	1	69.0	0.0	1.9	16	0	1	10.5	0.7	84.9	0.0	15.1
Tyumen Oblast without autonomies	1267.5	585	1	136	40	722	461.5	0.8	107.3	569.6	139	1	31	109.7	0.8	24.5	42	0	4	5.8	0.6	81.0	0.1	18.8
Chelyabinsk Oblast	3383.2	1338	9	286	198	1633	395.5	2.7	84.5	482.7	216	5	30	63.8	1.5	8.9	94	1	1	5.8	0.1	81.9	0.6	17.5
Siberian Federal District	**16482.8**	**6162**	**122**	**1636**	**685**	**7920**	**373.8**	**7.4**	**99.3**	**480.5**	**1478**	**32**	**230**	**89.7**	**1.9**	**14.0**	**736**	**18**	**28**	**9.5**	**0.4**	**77.8**	**1.5**	**20.7**
Altai Republic	210.1	11	0	8	11	19	52.4	0.0	38.1	90.4	4	0	3	19.0	0.0	14.3	4	0	0	21.1	0.0	57.9	0.0	42.1

End of Table 2

1	2	3	4	5	6	7	8	9	10	11	12	13	14	15	16	17	18	19	20	21	22	23	24	25
Tuva Republic	338.3	103	2	47	0	152	304.5	5.9	138.9	449.3	24	0	9	70.9	0.0	26.6	5	0	0	3.3	0.0	67.8	1.3	30.9
Republic of Khakassia	525.5	250	6	52	33	308	475.7	11.4	99.0	586.1	0	0	3	71.0	0.0	5.7	39	0	0	12.7	0.0	81.2	1.9	16.9
Altai Krai	2099.0	954	2	165	136	1121	454.5	1.0	78.6	534.1	322	0	16	153.4	0.0	7.6	169	0	1	15.1	0.1	85.1	0.2	14.7
Krasnoyarsk Krai	2837.4	1063	13	223	53	1299	374.6	4.6	78.6	457.8	294	1	42	103.6	0.4	14.8	96	0	3	7.4	0.2	81.8	1.0	17.2
Irkutsk Oblast	2316.6	1024	10	207	25	1241	442.0	4.3	89.4	535.7	162	2	36	69.9	0.9	15.5	72	0	4	5.8	0.3	82.5	0.8	16.7
Kemerovo (Kuzbass) Oblast	2526.4	908	17	454	135	1379	359.4	6.7	179.7	545.8	234	10	76	92.6	4.0	30.1	136	0	12	9.9	0.9	65.8	1.2	32.9
Novosibirsk Oblast	2784.6	868	48	300	57	1216	311.7	17.2	107.7	436.7	232	14	41	83.3	5.0	14.7	115	9	6	10.2	0.5	71.4	3.9	24.7
Omsk Oblast	1805.4	736	5	124	227	865	407.7	2.8	68.7	479.1	157	0	2	87.0	0.0	1.1	83	0	1	9.6	0.1	85.1	0.6	14.3
Tomsk Oblast	1039.5	245	19	56	8	320	235.7	18.3	53.9	307.8	49	5	2	47.1	4.8	1.9	17	9	1	8.1	0.3	76.6	5.9	17.5
Far Eastern Federal District	**7853.5**	**2975**	**151**	**583**	**254**	**3709**	**378.8**	**19.2**	**74.2**	**472.3**	**658**	**49**	**83**	**83.8**	**6.2**	**10.6**	**287**	**12**	**5**	**8.1**	**0.1**	**80.2**	**4.1**	**15.7**
Republic of Buryatia	970.7	558	5	116	17	679	574.8	5.2	119.5	699.5	87	5	10	89.6	5.2	10.3	52	2	0	8.0	0.0	82.2	0.7	17.1
Sakha (Yakutia) Republic	1007.1	618	16	194	50	828	613.6	15.9	192.6	822.2	270	3	27	268.1	3.0	26.8	55	0	0	6.6	0.0	74.6	1.9	23.4
Zabaykalsky Krai	982.5	353	16	34	0	403	359.3	16.3	34.6	410.2	10	2	13	10.2	2.0	13.2	18	0	0	4.5	0.0	87.6	4.0	8.4
Kamchatka Krai	287.9	81	0	17	0	98	281.3	0.0	59.0	340.4	25	0	1	86.8	0.0	3.5	9	0	0	9.2	0.0	82.7	0.0	17.3
Primorsky Krai	1798.0	499	64	80	126	643	277.5	35.6	44.5	357.6	146	20	14	81.2	11.1	7.8	62	3	2	10.1	0.3	77.6	10.0	12.4
Khabarovsk Krai	1273.1	422	14	48	46	484	331.5	11.0	37.7	380.2	32	3	11	25.1	2.4	8.6	36	7	1	8.9	0.2	87.2	2.9	9.9
Amur Oblast	750.9	148	30	48	7	226	197.1	40.0	63.9	301.0	51	11	4	67.9	14.6	5.3	23	0	2	10.2	0.9	65.5	13.3	21.2
Magadan Oblast	134.2	37	4	4	3	45	275.7	29.8	29.8	335.3	3	3	0	22.4	22.4	0.0	2	0	0	4.4	0.0	82.2	8.9	8.9
Sakhalin Oblast	456.8	206	1	38	5	245	451.0	2.2	83.2	536.3	26	2	3	56.9	4.4	6.6	18	0	0	7.3	0.0	84.1	0.4	15.5
Jewish Autonomous Oblast	144.4	53	1	3	0	57	367.0	6.9	20.8	394.7	8	0	0	55.4	0	0.0	12.0	0.0	0.0	21.1	0	93.0	1.8	5.3
Chukotka Autonomous Okrug	47.9	0	0	1	0	1	0.0	0.0	20.9	20.9	0	0	0	0.0	0	0.0	0	0	0	0.0	0	0.0	0.0	100.0
New territories	**3227.4**	**623**	**11**	**133**	**56**	**767**	**193.0**	**3.4**	**41.2**	**237.7**	**233**	**2**	**14**	**72.2**	**0.6**	**4.3**	**81**	**2**	**0**	**10.9**	**0**	**81.2**	**1.4**	**17.3**
Donetsk People's Republic		395	8	95	53	498					156	2	2				49	1	0	10.0	0	79.3	1.6	19.1
Luhansk People's Republic		155	3	30	3	188					43	0	5				27	1	0	14.9	0	82.4	1.6	16.0
Zaporizhzhya Oblast		73	0	7	0	80					34	0	6				5	0	0	6.3	0	91.3	0.0	8.8
Kherson Oblast		18	0	1	0	19					12	0	1				6	0	0	31.6	0	94.7	0.0	5.3

Note. Population figures and indicators per million population for the Russian Federation were calculated excluding the newly incorporated territories. due to the inability to accurately determine the permanent population in those regions.

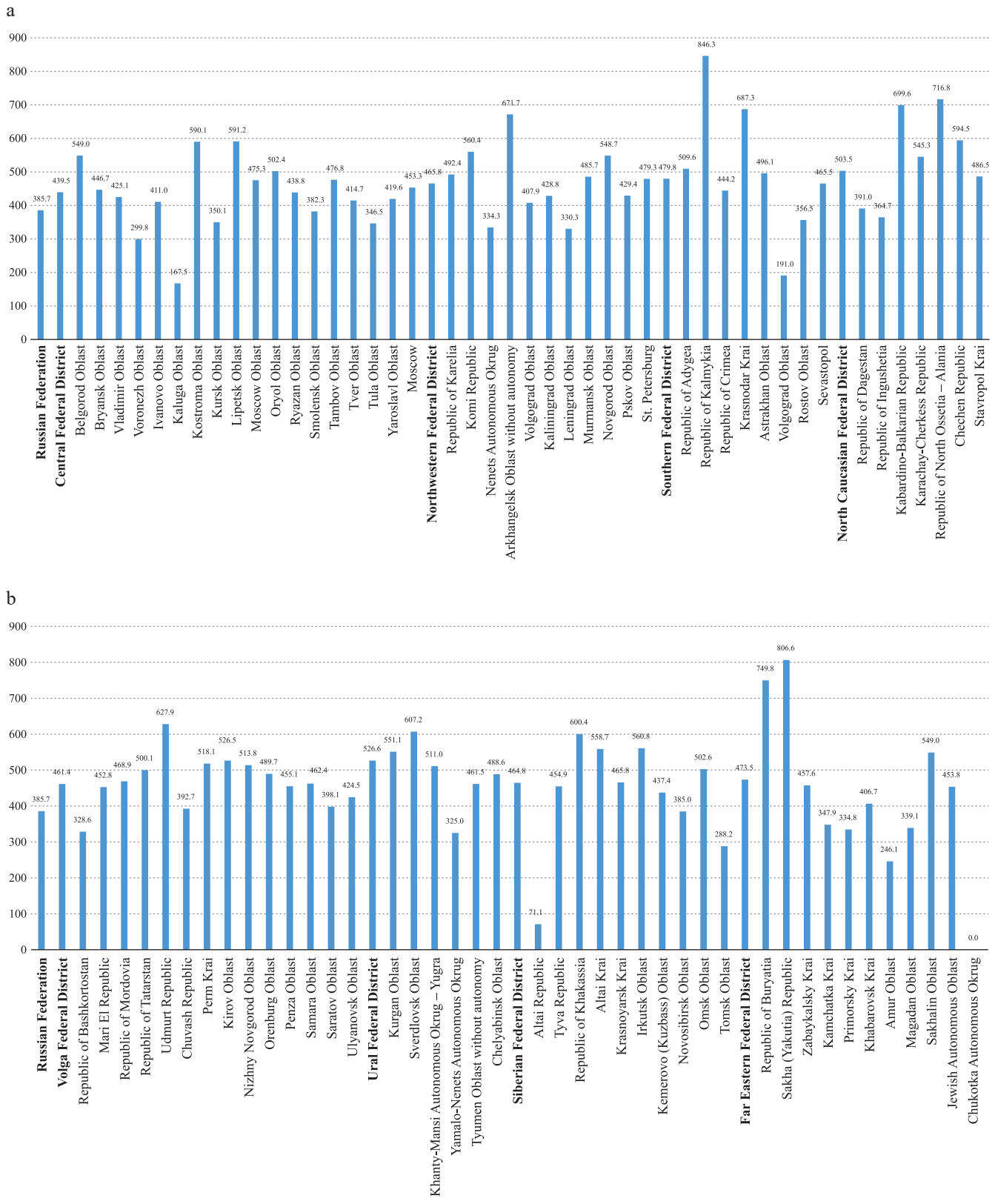

Fig. 6. Availability of hemodialysis per million population in regions of the Russian Federation: a, Central, Northwestern, Southern, and North Caucasian Federal Districts; b, Volga, Ural, Siberian, and Far Eastern Federal Districts

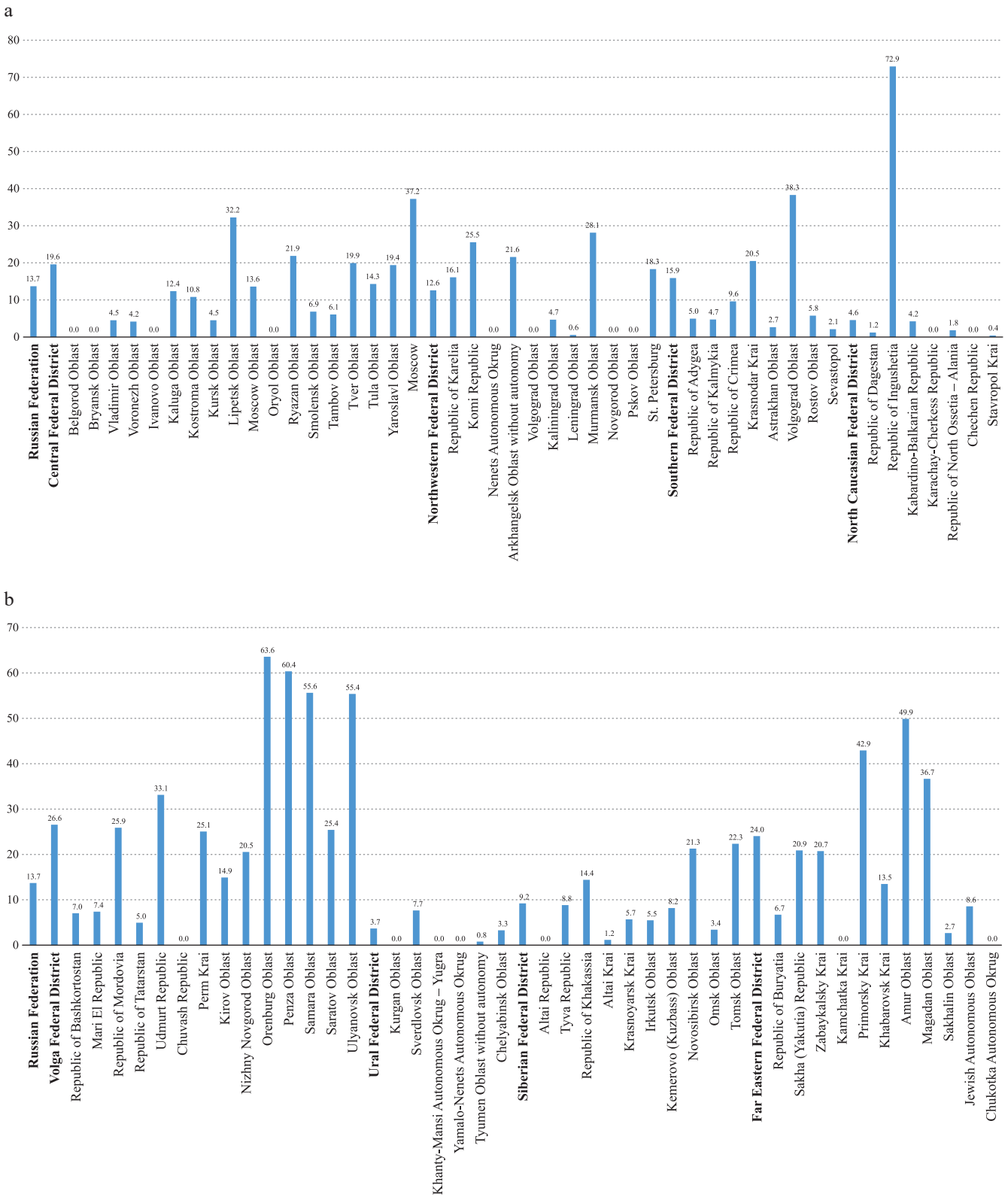

Fig. 7. Availability of peritoneal dialysis per million population in regions of the Russian Federation: a, Central, Northwestern, Southern, and North Caucasian Federal Districts; b, Volga, Ural, Siberian, and Far Eastern Federal Districts

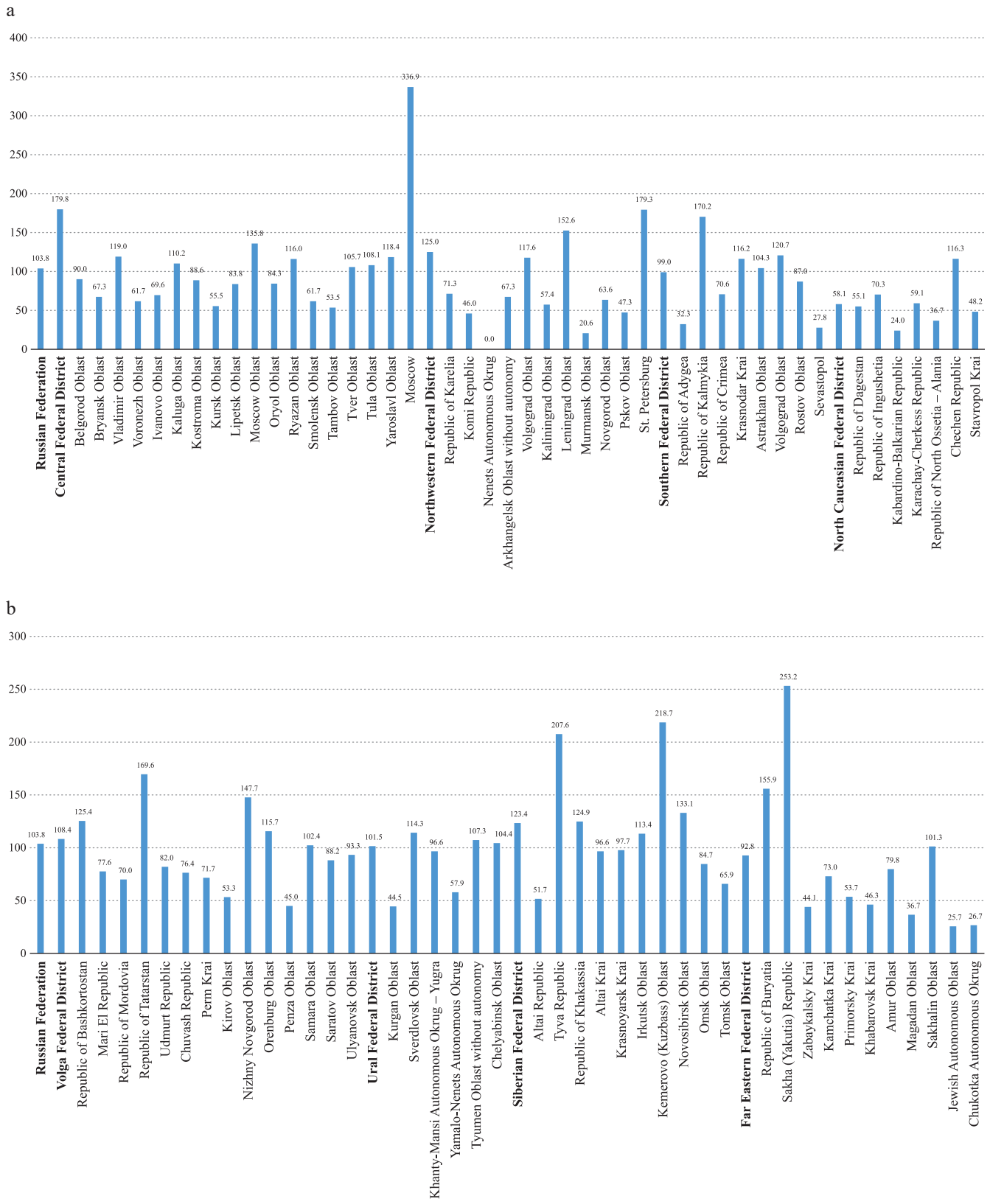

Fig. 8. Availability of kidney transplantation per million population in regions of the Russian Federation: a, Central, Northwestern, Southern, and North Caucasian Federal Districts; b, Volga, Ural, Siberian, and Far Eastern Federal Districts

The share of sessions conducted with low-flux membranes was 12%, which is consistent with global practice.

Hemodiafiltration (HDF), a more advanced modality compared to both low-flux and high-flux HD, accounted for 30% of all sessions (2,150,970), a frequency comparable to that observed in Europe [13]. Although the wider adoption of HDF in Russia appears to be constrained by its higher cost relative to high-flux HD, accumulating evidence highlights its long-term benefits, such as reduced mortality, fewer hospitalizations, reduced need for medication, and improved quality of life for patients [14, 15].

In Russia, 65.3% of HD patients have completed full vaccination against viral hepatitis B. The prevalence of infections among this population is as follows: 2.4% are infected with hepatitis B virus (HBV), 6.2% with hepatitis C virus (HCV), and 0.7% with human immunodeficiency virus (HIV). Notably, in several regions, including Kaluga, Kursk, Republic of Crimea, Republic of Dagestan, Kabardino-Balkarian Republic, Chechen Republic, Saratov, Khanty-Mansi Autonomous Okrug, Krasnoyarsk Krai, Kamchatka Krai, and Primorsky Krai, the proportion of HD patients with HCV exceeds 10%, significantly higher than the national average.

Peritoneal dialysis (PD) is available in 70 regions of the Russian Federation. In 2024, 1,997 patients were treated with PD, the majority (1,445; 72.4%) using continuous ambulatory peritoneal dialysis (CAPD). Automated peritoneal dialysis (APD) is also developing, with 552 patients (27.6%) receiving this modality, a distribution consistent with global practice. The availability of PD was more than twice the national average in several regions, including Moscow, Orenburg Oblast, Penza Oblast, Samara Oblast, Ulyanovsk Oblast, Amur Oblast, Primorsky Krai, Volgograd Oblast, Magadan Krai, Lipetsk Oblast, and Murmansk Oblast (Fig. 7).

ASSESSMENT OF THE EFFECTIVENESS AND QUALITY OF HEMODIALYSIS IN 2024

The effectiveness and quality of hemodialysis in the Russian Federation in 2024 were evaluated using the indicators presented in Table 3.

Target values were established in accordance with the 2024 clinical guidelines for CKD, except for hyperphosphatemia. Research evidence [16] shows that fewer than 50% of dialysis patients achieve a stable serum phosphate level below 1.78 mmol/L; therefore, this threshold was applied as the evaluation criterion.

Data were collected from 571 dialysis centers across the country. The target hemoglobin level was achieved in 80% of patients (95% CI: 71–87.5%), a result consistent with published global data [17]. Performance above the national average was reported in several regions of the Central Federal District, the Far Eastern Federal District, and multiple regions of the Ural Federal District (Fig. 9). By contrast, regions reporting results below the national average emphasized the need to improve access to essential medications for patients with CKD.

Target blood albumin levels were achieved in an average of 94% of HD patients in Russia in 2024 (95% CI: 89–98%) (Fig. 10). Serum albumin level is a key indicator of nutritional status in dialysis patients and is strongly associated with survival and hospitalization rates. Evidence from several large cohort studies demonstrates that albumin levels above 35 g/L are linked to reduced mortality, lower hospitalization rates, and improved quality of life in this patient population [18, 19].

Globally, approximately 10.5% of dialysis patients present with reduced serum albumin levels [16]. Clinical studies have shown that infusions of 25% albumin solution prior to HD can reduce the incidence of intradialytic hypotension in patients with hypoalbuminemia [20]. Dialysis centers reporting more than 10% of patients with hypoalbuminemia should therefore consider targeted interventions, including pre-dialysis albumin infusions and the use of specialized therapeutic nutrition, to correct hypoalbuminemia and improve outcomes.

Phosphorus–calcium metabolism indicators reflect the quality of medical care in patients receiving dialysis (Figs. 11–13). According to reports from dialysis centers, an average of 69% [95% CI: 58–79] of patients in Russia achieved target blood phosphate levels, and 71% [95% CI: 57–81] achieved target parathyroid hormone levels, figures that are consistent with global data [16].

Table 3

Indicators of hemodialysis efficiency and quality

S/N	Indicator	Value	Percentage of patients
1	Hemoglobin	≥100 ≤120	≥75
2	Albumin*	≥35	≥90
3	Calcium**	≥2.1 ≤2.5	≥75
4	Phosphorus	≤1.78	≥70
5	Parathyroid hormone	≥130 ≤325	≥70
6	Kt/V	≥1.4	≥90

Note. Hemodialysis efficiency and quality indicators are assessed as of December 31 of the reporting year; * Provided that serum albumin levels are measured using the bromocresol green (BCG) method; ** Calcium levels >2.1 mmol/L, excluding patients receiving calcimimetic therapy.

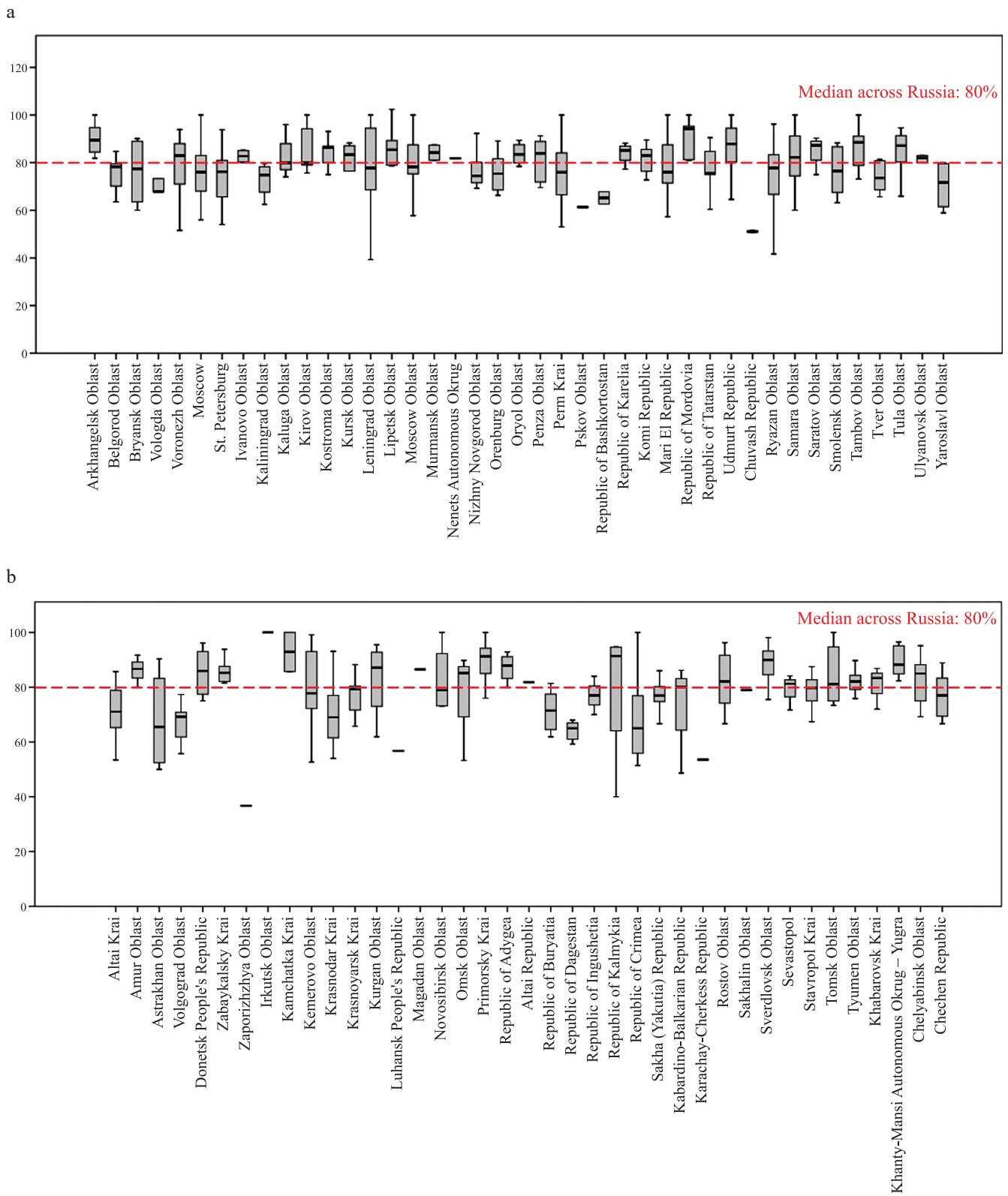

Fig. 9. Percentage of patients with target hemoglobin levels on dialysis in 2024: a, Central, Northwestern, and Volga Federal Districts; b, North Caucasian, Siberian, Far Eastern, Southern, Ural Federal Districts, and new territories. The figure shows medians and interquartile ranges [95% CI, 25–75%]

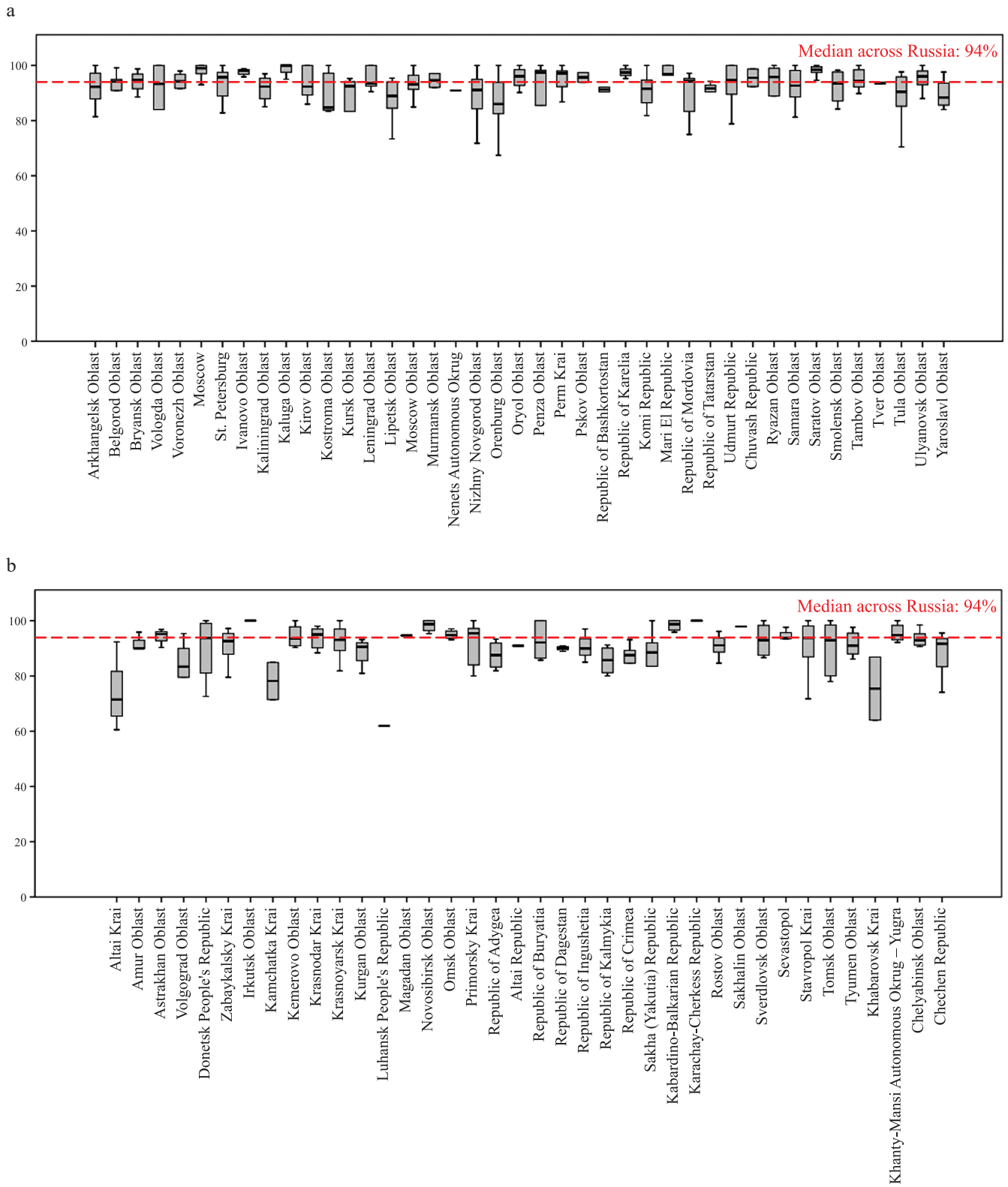

Fig. 10. Percentage of patients with target albumin levels on dialysis in 2024: a, Central, Northwestern, and Volga Federal Districts; b, North Caucasian, Siberian, Far Eastern, Southern, Ural Federal Districts, and new territories. The figure shows medians and interquartile ranges [95% CI, 25–75%]

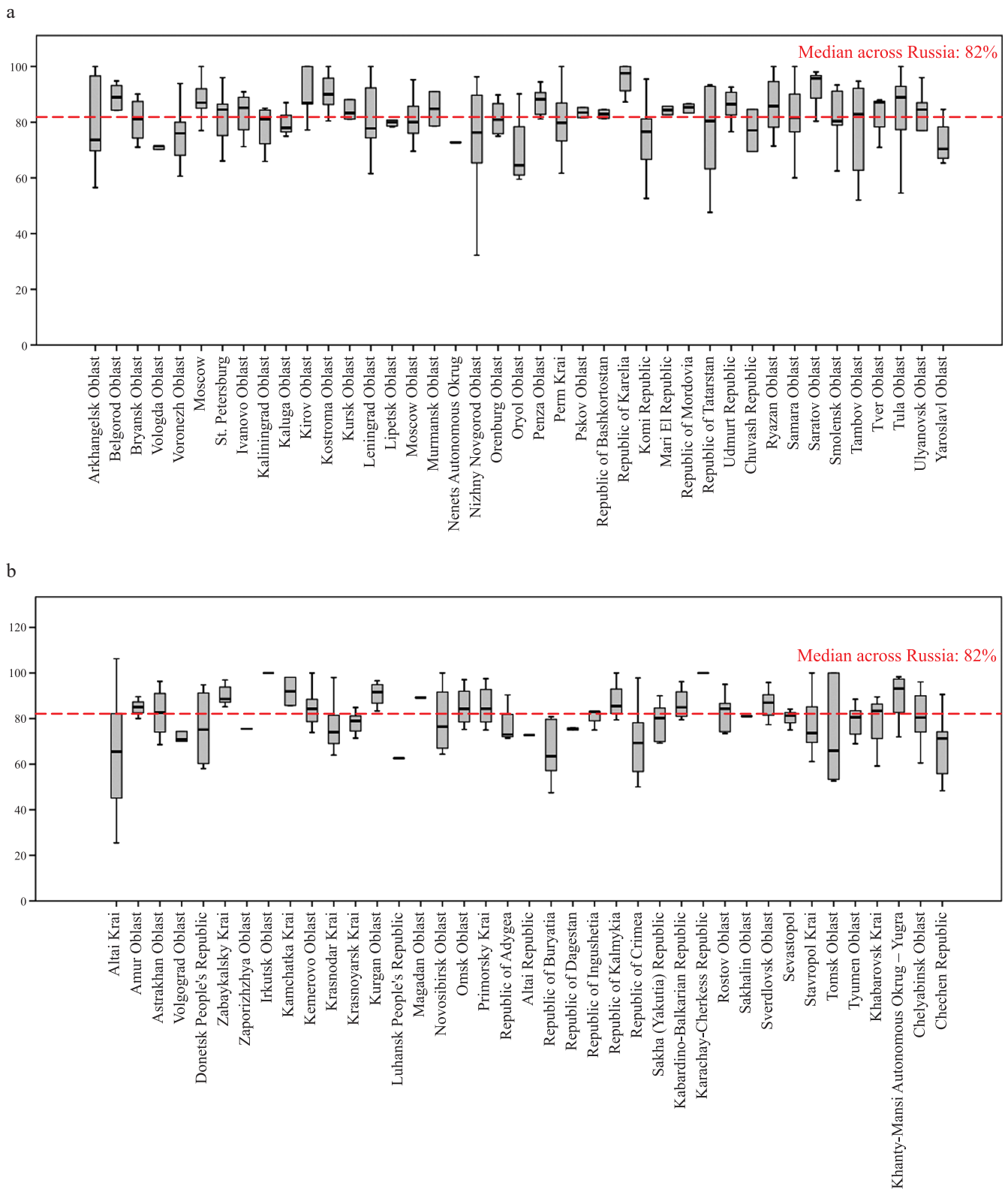

Fig. 11. Percentage of patients with target calcium levels on dialysis in 2024: a, Central, Northwestern, and Volga Federal Districts; b, North Caucasian, Siberian, Far Eastern, Southern, Ural Federal Districts, and new territories. The figure shows medians and interquartile ranges [95% CI, 25–75%]

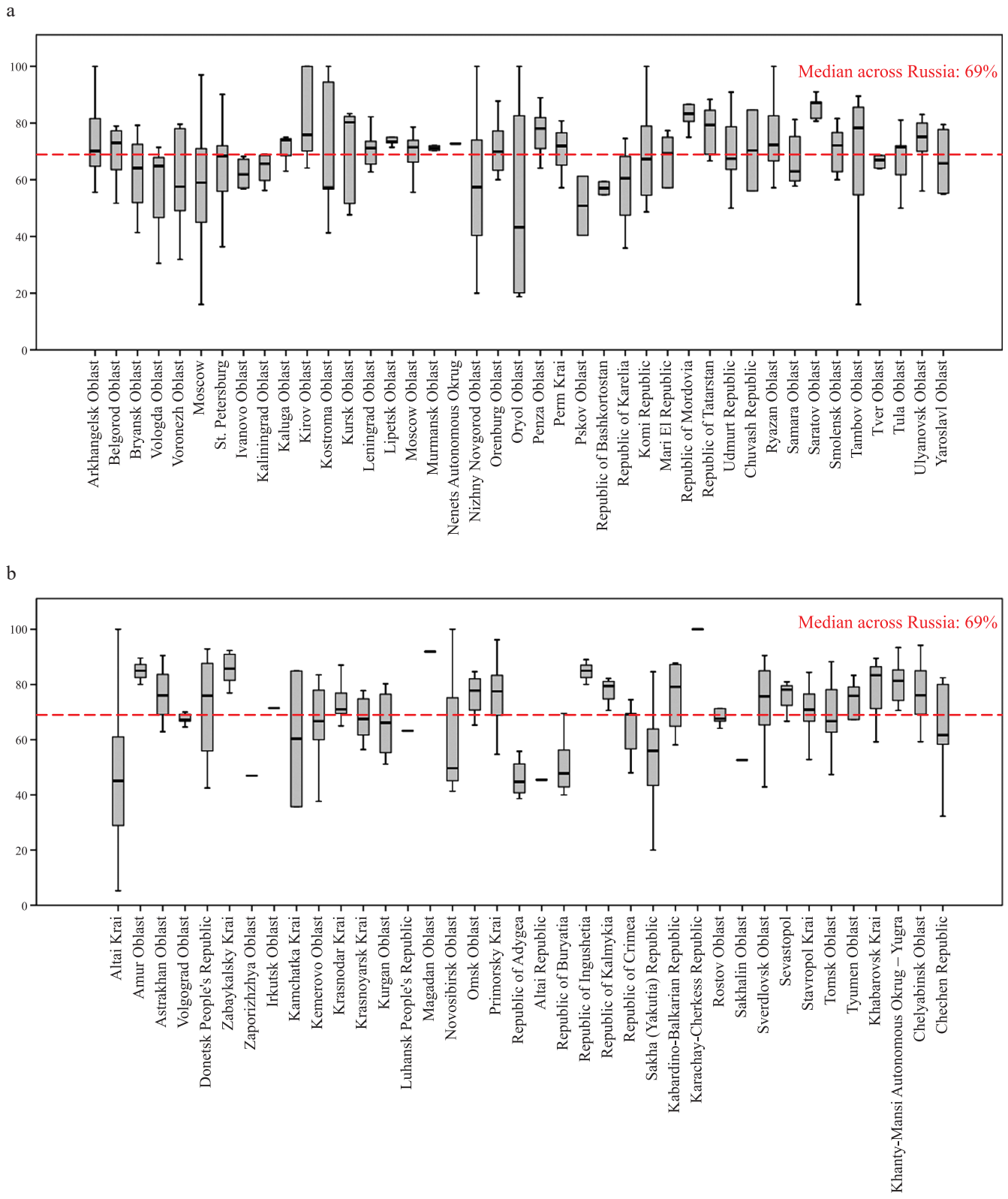

Fig. 12. Percentage of patients with target phosphorus levels on dialysis in 2024: a, Central, Northwestern, and Volga Federal Districts; b, North Caucasian, Siberian, Far Eastern, Southern, Ural Federal Districts, and new territories. The figure shows medians and interquartile ranges [95% CI, 25–75%]

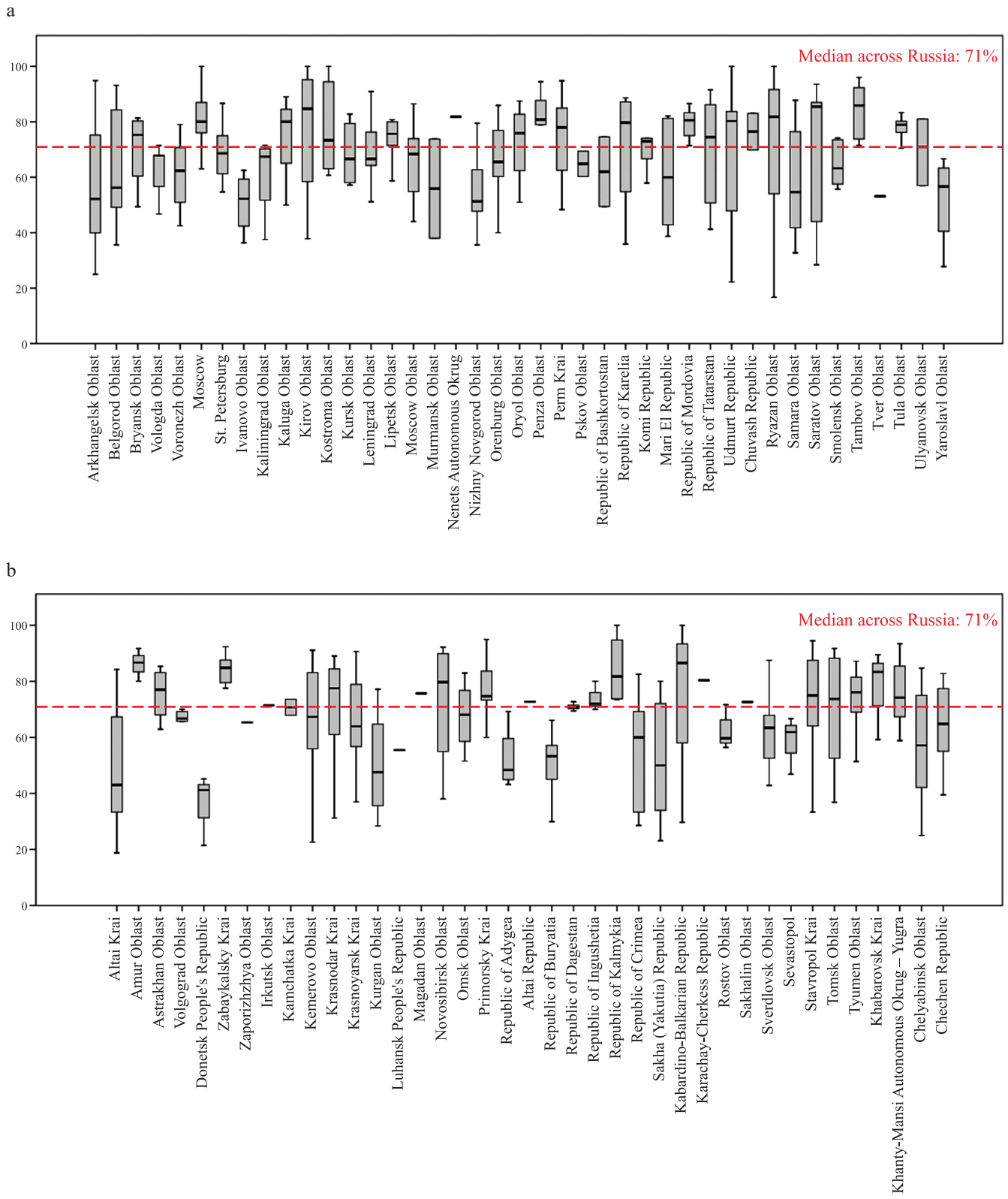

Fig. 13. Percentage of patients with target parathyroid hormone levels on dialysis in 2024: a, Central, Northwestern, and Volga Federal Districts; b, North Caucasian, Siberian, Far Eastern, Southern, Ural Federal Districts, and new territories. The figure shows medians and interquartile ranges [95% CI, 25–75%]

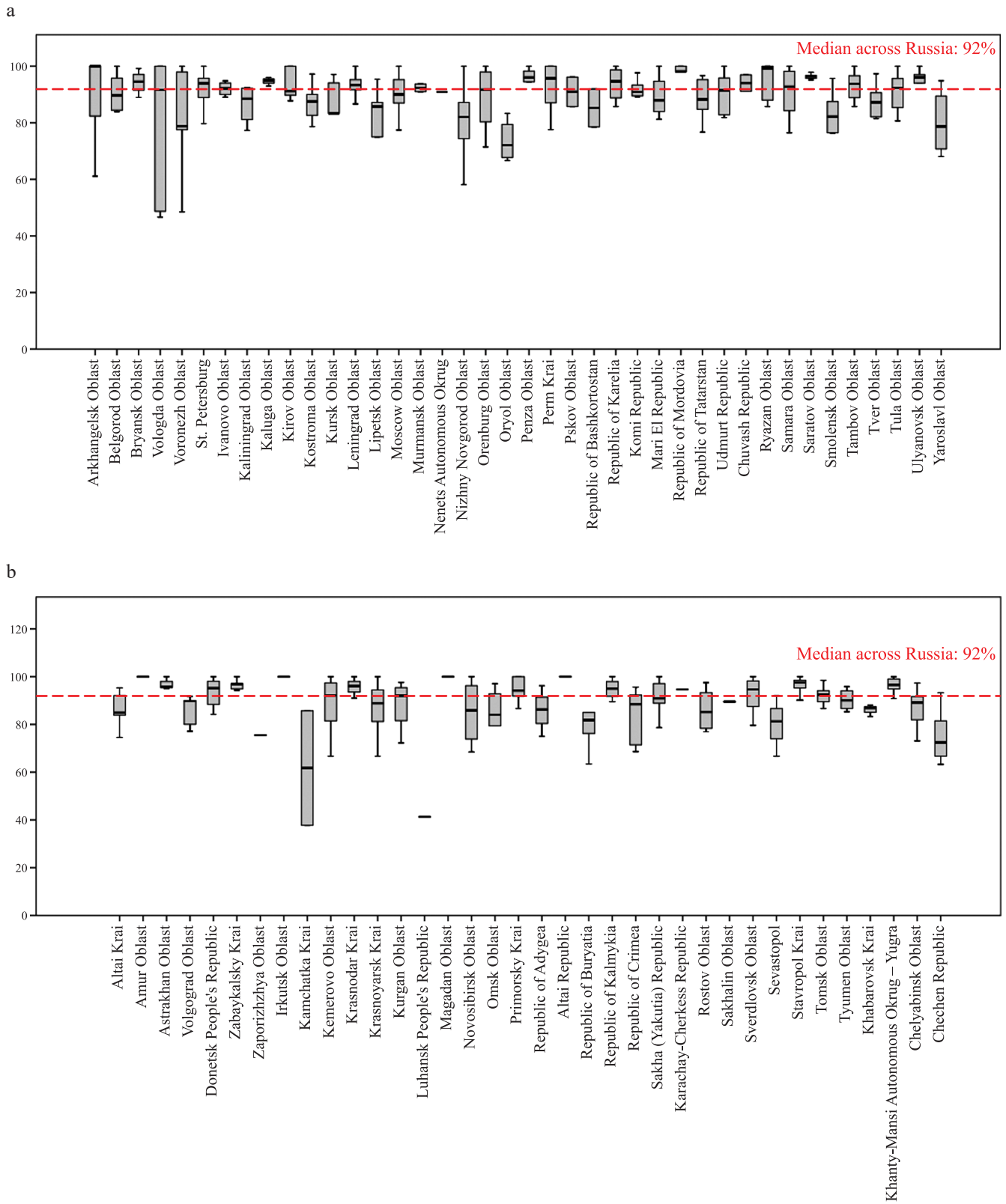

Fig. 14. Percentage of patients with target Kt/V levels on dialysis in 2024: a, Central, Northwestern, and Volga Federal Districts; b, North Caucasian, Siberian, Far Eastern, Southern, Ural Federal Districts, and new territories. The figure shows medians and interquartile ranges [95% CI, 25–75%]

Effectiveness indicators for a single HD session were also high: more than 90% of patients achieved the standard target Kt/V, with an overall average of 92% [95% CI: 84–97] (Fig. 14).

RENAL REPLACEMENT THERAPY IN PEDIATRIC PATIENTS

In 2024, 579 children with CKD stage 5 were on renal replacement therapy (RRT). Of these, 101 (17.4%) received HD, 76 (13.1%) underwent PD, and 402 (69.5%) had a functioning kidney transplant. Thus, kidney transplantation (KT) remains the predominant RRT modality in children in the Russian Federation, with other RRT modalities accounting for a considerably smaller proportion (Fig. 15).

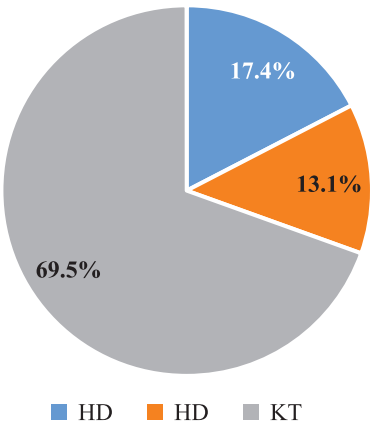

Fig. 15. Distribution of RRT types among children with stage 5 CKD in the Russian Federation in 2024

Across all pediatric patient groups, KT remains the predominant RRT modality, with the proportion of children living with a functioning transplanted kidney ranging from 76% to 81%. In the youngest age group (0–4 years), PD accounts for 44% of cases, whereas among older children (15–18 years), HD represents 19% of RRT, primarily as a preparatory stage before KT (Fig. 16). In 2024, a general trend was observed toward a higher proportion of male patients on RRT overall, particularly among those receiving HD and those with a functioning kidney transplant (Fig. 17).

Congenital malformations of the urinary system aaccount for more than half of the underlying diseases in children undergoing RRT (54.8% of cases), with glomerulonephritis (9.6%) and hemolytic-uremic syndrome (HUS, 10.3%) also contributing significantly. Approximately 5% of pediatric CKD cases are of unknown origin, likely reflecting undiagnosed genetic or other rare causes. This highlights the need to improve diagnostic

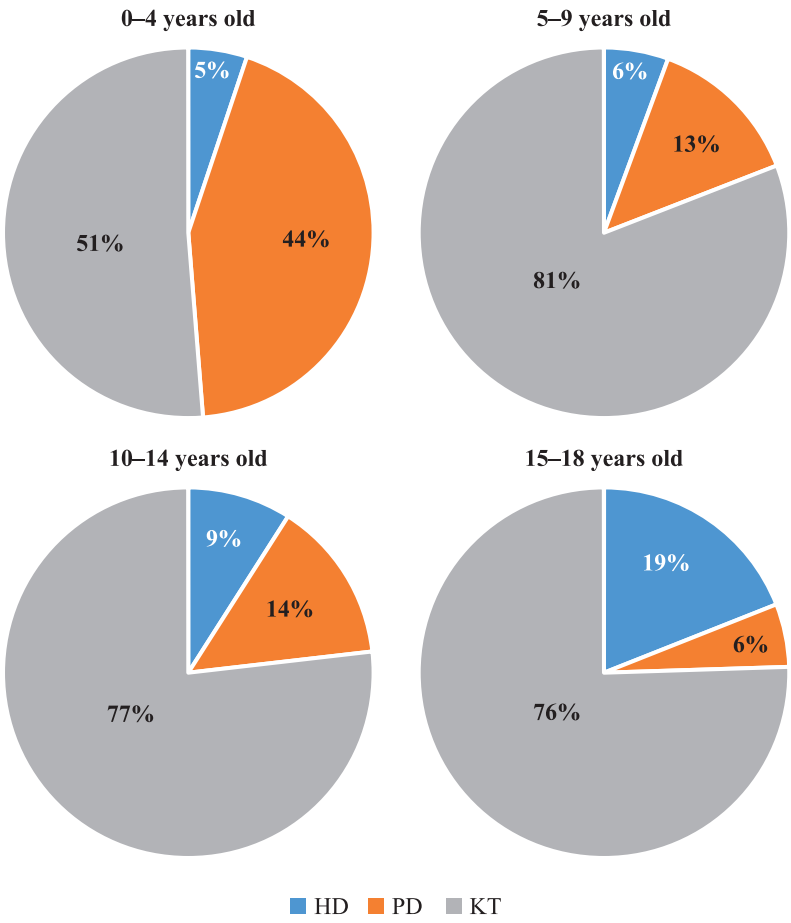

Fig. 16. Age distribution of children with stage 5 CKD receiving RRT in the Russian Federation in 2024

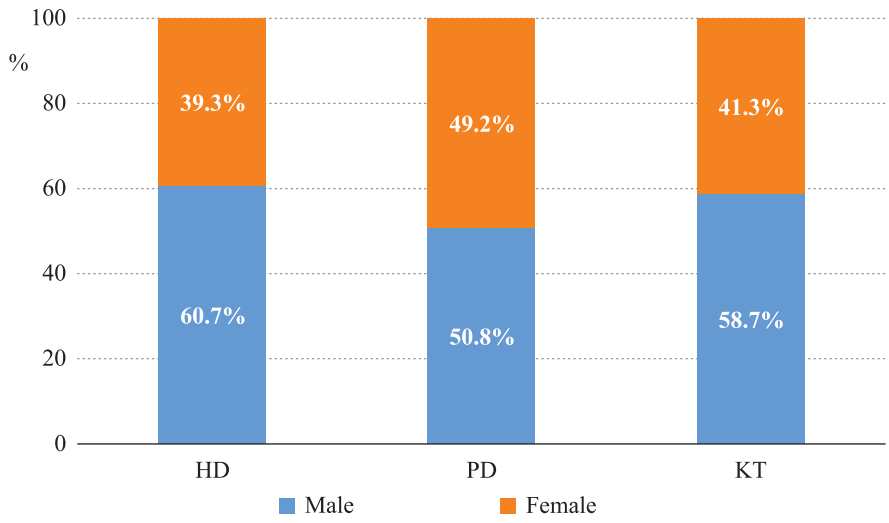

Fig. 17. Gender distribution of children with stage 5 CKD receiving RRT in the Russian Federation in 2024

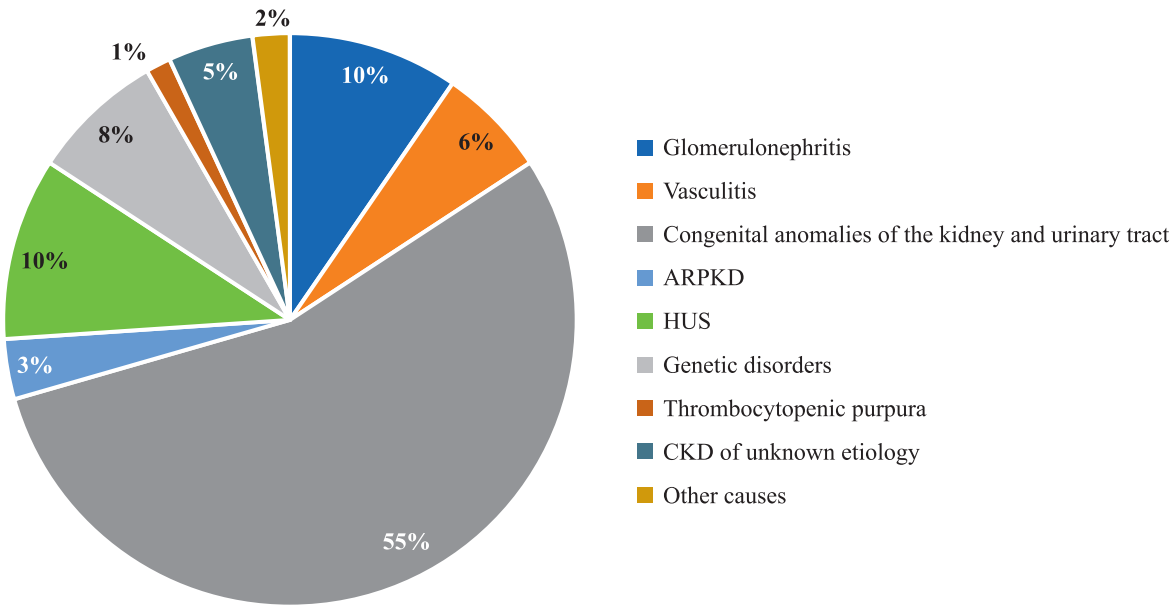

Fig. 18. Nosological structure of kidney disease in children receiving RRT in the Russian Federation

approaches, particularly through wider use of nephrobiopsy and expanded access to genetic testing, including molecular analysis of atypical HUS-associated genes and comprehensive kidney disease gene panels for pediatric patients (Fig. 18).

The availability of RRT for children in the Russian Federation is 24.7 per million of the pediatric population, of which KT accounts for 17.0 per million, PD for 3.2 per million, and HD for 4.3 per million. The highest numbers of children living with transplanted kidneys are observed in Moscow Oblast, Chelyabinsk Oblast, St. Petersburg, Krasnodar Krai, and Kemerovo Oblast.

CONCLUSION

The Center for Excellence in Medical Care in Nephrology at Shumakov National Medical Research Center of Transplantology and Artificial Organ has developed a framework for annual monitoring and established cooperation with regional health authorities, which has enabled the collection of data on the state of nephrology care and RRT across all regions of the Russian Federation. The set of monitoring indicators has been recommended for use by executive health authorities at federal subjects of the Russian Federation, as well as by regional chief freelance specialists in nephrology, dialysis, and transplantation.

However, it was noted that only 28 (31.5%) of 89 regions maintain records of patients in the pre-dialysis stages of CKD. This lack of systematic registration makes it difficult to accurately assess the prevalence of early CKD and to plan or organize appropriate nephrology care. Establishing comprehensive registries of patients in the pre-dialysis stages of CKD would provide more precise

epidemiological data, enable more effective planning of medical services, and improve the quality of nephrology care across the Russian Federation. This is particularly important given that patients with CKD already have a high or very high risk of cardiovascular mortality already in the pre-dialysis stages, starting from stage 3 of the disease [21].

The need to systematically register nephrology patients, conduct regular medical examinations for individuals with CKD, and establish patient education programs (such as kidney disease schools) underscores the importance of expanding outpatient nephrology services. Addressing the shortage of outpatient nephrologists requires not only intensified training of specialized nephrologists but also retraining and professional development of physicians from related specialties, including general internists, who are actively involved in the management of CKD patients. In many regions, there is also a shortage of nephrologists with expertise in managing kidney transplant recipients – a demand that will continue to grow in light of the steady annual increase in the number of transplant recipients.

One of the tools for tackling this issue is the Procedure for Dispensary Observation of Adults (Order of the Russian Ministry of Health, No. 168n, March 15, 2022), which mandates the dynamic follow-up of all patients with CKD stages 3b–5 as well as kidney transplant recipients. The proposal developed at Shumakov National Medical Research Center of Transplantology and Artificial Organ specifies the structure of follow-up medical care groups, recommended follow-up frequency, and the set of controlled clinical and laboratory indicators (Table 4). This decision will require regions to improve the staffing of outpatient clinics with nephrologists.

In 2024, HD remained the predominant RRT modality, with the distribution of patients across HD, PD, and KT in the Russian Federation being 76.7%, 2.7%, and 20.6%, respectively. Overall, the availability of HD remains consistently high across most regions. However, despite the generally high use of AVF access, some regions still report a substantial proportion of patients receiving HD through temporary central venous catheters. This is largely attributable to delays in the creation of permanent vascular access and highlights the need for enhanced training and continuing education of vascular surgeons, the establishment of specialized vascular access units, and the development of clear patient routing pathways in these regions.

Another important priority is to achieve universal coverage of HD patients with hepatitis B vaccination. One effective approach could be to recommend and implement vaccination already at the pre-dialysis stages of CKD, thereby improving both overall coverage and vaccine response rates, since patients with end-stage CKD often demonstrate a reduced immunologic response. This recommendation may be integrated into patient education programs such as CKD schools or included as part of structured follow-up medical care.

In regions where HCV prevalence among dialysis patients exceeds 10%, it is advisable to expand access to antiviral therapy. Broader treatment coverage will not only lower mortality but also improve eligibility for inclusion on the kidney transplant waiting list.

It is noteworthy that PD remains underutilized in the Russian Federation. Expanding PD services could be particularly valuable in regions with low population density and vast geographic areas, where access to dialysis centers is limited. Of special interest is the growing role of APD. Although APD is approximately 30% more expensive than CAPD) it offers clear advantages: improved quality of life due to greater daytime physical activity, increased ultrafiltration volume during nighttime exchanges, enhanced social participation, and particular suitability for children in the pre-transplant stage of RRT [22]. Prospects for further development of APD in Russia are favorable, as 60.2% of the total devices available (n = 917) are already in use.

In 2024, most indicators of dialysis effectiveness in the Russian Federation were consistent with global benchmarks, though the percentage of patients achieving target phosphorus and parathyroid hormone levels remained comparatively low. Given the importance of diet in maintaining target phosphorus levels, in addition to eliminating this trace element during dialysis or when taking medications, increasing patient adherence to treatment and compliance with dietary recommendations is a priority for education in schools for patients with end-stage CKD on dialysis.

Increasing the proportion of patients with functioning kidney transplants and those on PD, particularly in regions with low population density, remains a priority for the further development of nephrological care in the Russian Federation. Encouragingly, the number of kidney transplants has steadily increased over the past five years, and in several regions, the rise in the total number of patients on RRT has been primarily driven by an increase in transplant recipients. This trend can be regarded as a positive shift toward more effective and cost-efficient long-term treatment of end-stage CKD.

Ongoing monitoring of nephrological care and RRT across the Russian Federation will remain essential with an assessment of key indicators of medical care for patients at all stages of CKD and their dynamics. A summary of the main indicators reflecting the state of nephrological care and RRT in the Russian Federation in 2024 is presented in Table 5.

The authors declare no conflict of interest.

Table 4

Recommendations from the Shumakov National Medical Research Center of Transplantology and Artificial Organs on the organization of dispensary follow-up for patients with CKD stages 1–5 and kidney transplant recipients

S/N	ICD-10 Code	Chronic condition / functional disorder requiring regular medical follow-up	Minimum frequency of follow-up visits (examinations, consultations)	Health indicators monitored under regular medical follow-up	Follow-up duration	Remarks
Medical follow-up is carried out by a general practitioner						
1	N18.1, N18.2, N18.3	Chronic kidney disease (CKD) stages 1, 2, and 3a (glomerular filtration rate [GFR]: 45–60 mL/min)	At least twice a year, in accordance with clinical guidelines	Blood creatinine with GFR calculation (at least twice a year), albuminuria (at least twice a year), complete blood count (at least twice a year)	Lifelong, until initiation of renal replacement therapy	Appointment (examination or consultation) with a nephrologist as clinically indicated, in accordance with clinical guidelines
Medical follow-up is carried out by a nephrologist						
2	N18.3, N18.4	CKD stage 3b (GFR: 30–45 mL/min)	At least four times a year, in accordance with clinical guidelines	Blood creatinine with GFR calculation (at four times a year), blood potassium (at least 4 times a year), albuminuria (at least 4 times a year), complete blood count (at least twice a year)	Lifelong, until initiation of renal replacement therapy	
3	N18.5	CKD stage 5 prior to the initiation of renal replacement therapy (RRT)	At least once a month, in accordance with clinical guidelines	Blood creatinine with GFR calculation (at least 12 times a year), blood urea (at least 12 times a year), blood potassium (at least 12 times a year), complete blood count (at least twice a year)	Lifelong, until initiation of renal replacement therapy	
4	Z94.0	Presence of a functioning transplanted kidney	At least four times a year, in accordance with clinical guidelines	Complete blood count (at least 4 times a year), comprehensive metabolic panel (at least 4 times a year), drug level monitoring of tacrolimus/cyclosporine, everolimus (at least 4 times a year)	Lifelong, until graft failure or loss of function	

Note. The frequency of medical examinations (check-ups and consultations) is determined in accordance with the following clinical guidelines: "Chronic Kidney Disease (CKD)", Ministry of Health of the Russian Federation (URL: https://cr.minzdrav.gov.ru/recomend/469_2); KDIGO 2017 Clinical Practice Guideline Update for the Diagnosis, Evaluation, Prevention, and Treatment of Chronic Kidney Disease–Mineral and Bone Disorder (CKD-MBD). Kidney International Supplements (2017) 7, 1–59; KDIGO Clinical Practice Guideline for Anemia in Chronic Kidney Disease. Kidney International Supplements (2012) 2.

Table 5

Key indicators of nephrological care for patients with CKD and those receiving RRT in 2024 (based on data from 89 Federal Subjects of the Russian Federation)

Renal replacement therapy (RRT)	
Number of patients on RRT (abs.)	72,672
RRT coverage per million population	557.0
Number of patients on hemodialysis (HD, abs.)	56,134
HD coverage per million population	459.6
Number of patients on peritoneal dialysis (PD, abs.)	1,850
PD coverage per million population	12.7
Number of patients with functioning kidney transplant (KT, abs.)	14,688
KT coverage per million population	84.6
Number of KT centers	49

End of Table 5

Hemodialysis / HD centers	
Hemodialysis / HD centers *of which are state-owned*	674 274
Number of dialysis stations (abs.)	21,372
Availability of dialysis stations per million population	179.14
Number of doctors in dialysis centers/departments (abs.)	2,670
Number of nurses in dialysis centers/departments (abs.)	5,774
Number of hemodialysis machines	14,458
Outpatient nephrology services	
Number of nephrologists' offices in outpatient care	537
Number of nephrologists in outpatient care (abs.) *Of these, trained in managing patients with a transplanted kidney*	690 86
Availability of outpatient nephrologists per 50,000 registered population	0.27
Inpatient nephrology services (nephrology departments)	
Number of departments providing nephrology care (abs.)	263
Number of nephrology beds (abs.)	5,039
Number of nephrology beds per 10,000 population	0.35
Number of nephrologists in inpatient care (abs.) *Of which trained in the management of kidney recipients*	783 187
Total number of nephrologists	4,143

REFERENCES

1. *Hill NR, Fatoba ST, Oke JL, Hirst JA, O'Callaghan CA, Lasserson DS et al.* Global prevalence of chronic kidney disease – a systematic review and meta-analysis. *PloS One*. 2016; 11: e0158765. doi: 10.1371/journal.pone.0158765.
2. *Sundström J, Bodegard J, Bollmann A, Vervloet MG, Mark PB, Karasik A et al.* Prevalence, outcomes, and cost of chronic kidney disease in a contemporary population of 2·4 million patients from 11 countries: The CaReMe CKD study. *Lancet Reg Health Eur*. 2022 Jun 30; 20: 100438. doi: 10.1016/j.lanepe.2022.100438.
3. *Santos-Araújo C, Mendonça L, Carvalho DS, Bernardo F, Pardal M, Couceiro J et al.* Twenty years of real-world data to estimate chronic kidney disease prevalence and staging in an unselected population. *Clin Kidney J*. 2022. 12; 16 (1): 111–124. doi: 10.1093/ckj/sfac206.
4. *Heaf J.* The Danish Renal Biopsy Register. Kidney Int. 2004; 66 (3): 895–897. doi: 10.1111/j.1523-1755.2004.00832.x.
5. *Cunningham A, Benediktsson H, Muruve DA, Hildebrand AM, Ravani P.* Trends in Biopsy-Based Diagnosis of Kidney Disease: A Population Study. *Can J Kidney Health Dis*. 2018; 5: 2054358118799690. doi: 10.1177/2054358118799690.
6. *Fiorentino M, Bolignano D, Tesar V, Pisano A, Van Biesen W, D'Arrigo G et al.* Renal Biopsy in 2015 – From Epidemiology to Evidence-Based Indications. *Am J Nephrol*. 2016; 43 (1): 1–19. doi: 10.1159/000444026.
7. *Amodu A, Porteny T, Schmidt IM, Ladin K, Waikar SS.* Nephrologists' Attitudes Toward Native Kidney Biopsy: A Qualitative Study. *Kidney Med*. 2021; 3 (6): 1022–1031. doi: 10.1016/j.xkme.2021.06.014.
8. *Molnár A, Thomas MJ, Fintha A, Kardos M, Dobi D, Tislér A et al.* Kidney biopsy-based epidemiologic analysis shows growing biopsy rate among the elderly. *Sci Rep*. 2021; 11 (1): 24479. doi: 10.1038/s41598-021-04274-9.
9. ERA Registry Annual Report 2022; https://www.era-online.org/wp-content/uploads/2024/09/ERA-Registry-Annual-Report2022.pdf.
10. *Kotenko ON, Omelyanovsky VV, Ignatyeva VI, Yagnenkova EE, Rumyantseva EI.* The cost of chronic kidney disease in the Russian Federation. *Clinical nephrology*. 2021; 4: 30–38. doi: 10.18565/nephrology.2021.4.30-38.
11. *Bello AK, Okpechi IG, Osman MA, Cho Y, Htay H, Jha V et al*. Epidemiology of haemodialysis outcomes. *Nat Rev Nephrol*. 2022; 18 (6): 378–395. doi: 10.1038/s41581-022-00542-7.
12. *Andrusev AM, Tomilina NA, Peregudova NG, Shinkarev MB*. Kidney replacement therapy for end Stage Kidney Disease in Russian Federation, 2015–2019. Russian National Kidney Replacement Therapy Registry Report of Russian Public Organization of Nephrologists "Russian Dialysis Society". *Nephrology and Dialysis*. 2021; 23 (3): 255–329. doi: 10.28996/2618-9801-2021-3-255-329.
13. *Ficociello LH, Busink E, Sawin DA, Winter A*. Global real-world data on hemodiafiltration: An opportunity to complement clinical trial evidence. *Semin Dial*. 2022; 35 (5): 440–445. doi: 10.1111/sdi.13085.
14. *Vernooij RWM, Hockham C, Strippoli G, Green S, Hegbrant J, Davenport A et al.* Haemodiafiltration versus haemodialysis for kidney failure: an individual patient data meta-analysis of randomised controlled trials. *Lancet*. 2024 Oct 25: S0140-6736(24)01859-2. doi: 10.1016/s0140-6736(24)01859-2.

15. *Guimarães MGM, Tapioca FPM, Dos Santos NR, Tourinho Ferreira FPDC, Santana Passos LC, Rocha PN.* Hemodiafiltration versus Hemodialysis in End-Stage Kidney Disease: A Systematic Review and Meta-Analysis. *Kidney Med*. 2024; 6 (6): 100829. doi: 10.1016/j.xkme.2024.100829.
16. https://cr.minzdrav.gov.ru/preview-cr/469_3.
17. https://usrds-adr.niddk.nih.gov/2024/end-stage-renal-disease/3-clinical-indicators-and-preventive-care.
18. *Amaral S, Hwang W, Fivush B, Neu A, Frankenfield D, Furth S.* Serum albumin level and risk for mortality and hospitalization in adolescents on hemodialysis. *Clin J Am Soc Nephrol*. 2008; 3 (3): 759–767. doi: 10.2215/CJN.02720707.
19. *Leon JB, Albert JM, Gilchrist G, Kushner I, Lerner E, Mach S et al.* Improving albumin levels among hemodialysis patients: a community-based randomized controlled trial. *Am J Kidney Dis*. 2006; 48 (1): 28–36. doi: 10.1053/j.ajkd.2006.03.046.
20. *Macedo E, Karl B, Lee E, Mehta RL.* A randomized trial of albumin infusion to prevent intradialytic hypotension in hospitalized hypoalbuminemic patients. *Crit Care*. 2021; 25 (1): 18. doi: 10.1186/s13054-020-03441-0.
21. *Writing Group for the CKD Prognosis Consortium; Grams ME, Coresh J, Matsushita K, Ballew SH, Sang Y, Surapaneni A et al.* Estimated Glomerular Filtration Rate, Albuminuria, and Adverse Outcomes: An Individual-Participant Data Meta-Analysis. *JAMA*. 2023; 330 (13): 1266–1277. doi: 10.1001/jama.2023.17002.

The article was submitted to the journal on 27.06.2025

DOI: 10.15825/1995-1191-2025-3-204-215

SURGICAL ASPECTS OF TUNNELED CENTRAL VENOUS CATHETER IMPLANTATION FOR HEMODIALYSIS: A LITERATURE REVIEW

N.L. Shakhov, R.N. Trushkin, V.I. Vtorenko, O.N. Kotenko, N.F. Frolova, M.Yu. Bogodarov, E.S. Kudryavtseva, D.Z. Tazetdinov, A.S. Kiselev, A.A. Evdokimova
City Clinical Hospital No. 52, Moscow, Russian Federation

This review addresses a key issue in establishing vascular access for maintenance hemodialysis: the implantation of tunneled central venous catheters (TCVCs). Advances in catheter design and imaging technologies in recent years have significantly reduced the risk of complications associated with TCVC placement. Nevertheless, certain complex clinical scenarios still require individualized approaches during implantation. This review highlights the indications and contraindications for TCVC placement, examines the various catheter types and potential insertion sites, and discusses patient preparation, intraoperative considerations, and postoperative care. It also reviews early and late complications, along with strategies for their management. The use of additional imaging modalities to facilitate catheter placement is also presented. Currently, a standardized approach to TCVC implantation is employed, encapsulated in a standard operating procedure (SOP), which ensures adherence to aseptic techniques and provides a structured framework for training new clinical staff.

Keywords: tunneled central venous catheter, arteriovenous fistula, synthetic vascular graft, balloon angioplasty.

A joint statement by the American Society of Nephrology, the European Renal Association, and the International Society of Nephrology reported that by 2021, more than 850 million people worldwide had some form of kidney disease. This figure is nearly twice the global prevalence of diabetes (422 million) and about 20 times higher than the prevalence of malignant tumors (42 million) or the number of people living with HIV/AIDS (36.7 million). These estimates were derived from multiple international studies that applied varying definitions of chronic kidney disease (CKD); nevertheless, they remain the most reliable approximation of the global CKD burden [1].

Currently, the number of patients requiring renal replacement therapy (RRT) continues to grow, accompanied by the expansion of hemodialysis (HD) centers worldwide. Advances in dialysis technology and clinical practice have significantly improved the quality of HD, contributing to longer survival among patients with end-stage renal disease (ESRD). However, establishing and maintaining reliable vascular access remains a major clinical challenge. The three principal types of vascular access used in chronic HD are: native arteriovenous fistula (AVF), synthetic vascular graft (SVG), and tunneled (cuffed) central venous catheters [2].

According to the KDOQI (Kidney Disease Outcomes Quality Initiative) guidelines, arteriovenous access (AVF or SVG) is considered the preferred option for patients requiring HD, provided it aligns with the individual's life plan for ESRD and overall treatment goals. Nonetheless, under specific and justified clinical circumstances, KDOQI guidelines recognize the appropriateness of using tunneled central venous catheters (CVCs) as a long-term vascular access option in select patients [2].

Despite ongoing initiatives aimed at increasing the number of patients starting HD with AVF, data from the US Renal Data System (USRDS) show a persistent reliance on catheters. Between 2018 and 2022, the proportion of patients initiating HD with a catheter increased by 3.9%, reaching 84.7%, underscoring the challenges in achieving widespread early AVF placement [3].

INDICATIONS FOR TUNNELED CENTRAL VENOUS CATHETER IMPLANTATION

1 Failure of the fistula to mature sufficiently by the time HD is required, often due to delayed referral to a vascular surgeon or other specialists, resulting in late preventive AVF formation.
2 Inability to form an AVF or SVG due to the vascular anatomy (excessive vein depth (>6 mm), which does not allow for adequate puncture, or a scattered type).
3 Absence of superficial and deep veins of the required diameter for AVF or SVG formation.
4 Severe heart failure with significantly reduced left ventricular ejection fraction, where AVF creation

Corresponding author: Nikolay Shakhov. Address: 3, Pehotnaya str., Moscow, 123182, Russian Federation. Phone: (926) 212-81-14. E-mail: Nick-graft@rambler.ru

would impose additional myocardial stress and decompensation of chronic heart failure.
5 Patients undergoing peritoneal dialysis are temporarily implanted with tunneled CVCs for HD in the event of catheter-associated infection.
6 Limited life expectancy (<1 year), where short-term palliative dialysis is indicated.
7 Living-donor kidney transplantation planned within a relatively short period of time.
8 Uncertainty regarding renal function recovery in cases of acute kidney injury (AKI) [4].
9 Patient declines AVF or SVG formation [2].

CONTRAINDICATIONS TO TUNNELLED CENTRAL VENOUS CATHETER IMPLANTATION:

1 AKI requiring emergency HD.
2 Active infection involving an existing tunneled CVC (as bridge therapy/replacement).
3 Short-term bridge therapy (<2 weeks) during AVF reconstruction that does not require prolonged maturation.
4 Persistent bloodstream infection and the need for urgent HD treatment [4].

Elderly patients are a special group when it comes to choosing vascular access for HD. With advancing age, progression of kidney disease to an end stage influences multiple therapeutic decisions, including the choice of renal replacement therapy and individualized recommendations for dialysis access [5, 6]. In older individuals with significant comorbidities, such as severe heart failure, peritoneal dialysis or hemodialysis via tunneled CVCs are often considered the most practical and safest options [2, 7].

Currently used tunneled catheters vary in catheter tip design and insertion method [8].

THE THREE MAIN TYPES OF TUNNELED CATHETERS USED FOR HEMODIALYSIS ARE:

1. Retrograde catheters – inserted first into the central vein and then passed through a subcutaneous tunnel.
2. Antegrade catheters – passed initially through a subcutaneous tunnel and then inserted into a central vein.
3. Retroantegrade catheters – may be inserted using either approach, depending on the surgeon's preference.

Polyurethane double-lumen catheters are available in various lengths (tip-to-cuff: 24, 28, 32, 36, and 55 cm) and diameters (10, 12.5, 14.5, and 15 Fr). Their configuration can also differ, being either straight or pre-shaped (curved into a loop or set at a 90° angle).

LUMEN AND TIP DESIGN OF DIALYSIS CATHETERS

Five tip designs are commonly used in tunneled CVCs for hemodialysis: stepped, symmetrical, split, self-centering, and Y-shaped (Fig. 1) [9].

Catheters with a stepped tip have a narrowed arterial lumen facing the mediastinum (Fig. 1, a). Split-tip catheters have split lumens at their ends, designed primarily to reduce recirculation (Fig. 1, c). To further address this issue, manufacturers developed the symmetrical tip, in which the venous and arterial lumens terminate at the same level. This design incorporates an inclined spiral notch that diverts venous outflow away from arterial inflow (Fig. 1, b) [10]. The recirculation rate for symmetrical-tip catheters is approximately 1%, the lowest among available designs. In comparison, stepped and split-tip catheters demonstrate recirculation rates of about 7% during direct flow and 10–30% during reverse flow [11]. Although split-tip catheters tend to maintain patency longer than stepped-tip catheters, both designs provide comparable blood flow rates [10]. In comparison, symmetrical-tip catheters have demonstrated higher blood flow rates than stepped-tip catheters, while showing similar outcomes with respect to primary patency, infection, and thrombosis [12].

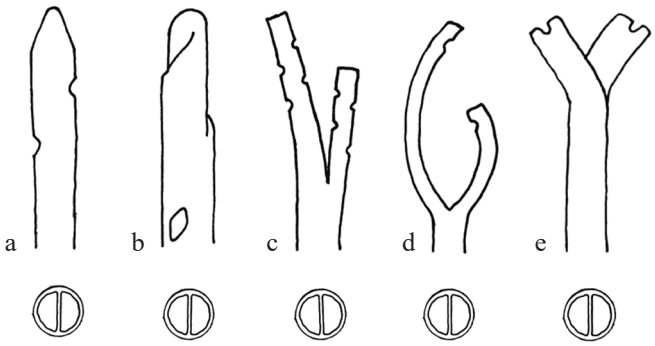

Fig. 1. Modern hemodialysis catheter designs: (a) step-tip catheter; (b) symmetrical-tip catheter; (c) split-tip catheter; (d) self-centering split-tip catheter; (e) Y-shaped catheter. Illustration by Yuri Bassuner [9]

A prospective randomized trial further reported that symmetrical-tip catheters not only maintain patency for a longer duration but also exhibit lower rates of dysfunction and reverse blood flow compared to stepped-tip designs [13]. Supporting these findings, a 4-year multicenter study in Australia involving 4,722 patients found that both symmetrical-tip and split-tip catheters were associated with a reduced risk of catheter dysfunction requiring removal when compared with stepped-tip catheters [14].

There is another symmetrical catheter tip design that places the distal lumens at an angle on opposite sides of the catheter. This configuration deflects blood exiting the venous port away from blood entering the arterial port, thereby reducing recirculation. In addition, the design generates a spiral laminar flow, which decreases platelet activation during dialysis and consequently prolongs catheter life [15]. A recent multicenter randomized study showed that both symmetrical tip catheters and spiral laminar flow catheters exhibit the same 90-day primary patency; however, Kt/V values were significantly higher in the spiral laminar flow group [16].

The self-centering catheter represents an improved modification of the bifurcated design. Its side ports are oriented inward, preventing contact with the vessel wall and thereby reducing the risk of fibrin sheath formation and port occlusion (Fig. 1, d). In a prospective multicenter study, self-centering catheters maintained a high blood flow rate (>300 ml/min) in 87% of patients during 26 weeks of follow-up. Throughout the study, no reduction in average dialysis flow rate or significant changes in hydraulic resistance of the arterial and venous lumens were observed [17].

Catheters with a Y-shaped tip have slits but no side ports (Fig. 1, e). This design is reported to prolong initial patency and decrease the incidence of catheter-related thrombosis and infections. Preliminary clinical data confirm good patency rates and a low incidence of complications [18].

Various coatings have been developed to enhance the efficiency of HD catheters. Heparin is commonly employed as an anti-adhesive coating to prevent the formation of blood clots and fibrin coats [19], while silver is utilized for its antimicrobial properties. An emerging and promising area of research involves microstructuring, which mimics natural surfaces such as shark skin (Sharklet) or lotus leaves. Through microstructuring technologies, catheter surfaces can be modified to inhibit the adhesion of bacteria and platelets, thereby reducing the risk of colonization and fibrin sheath formation [20]. Another innovative approach, the water infused surface protection (WISP) technology technology, provides protection for the inner surface of the catheter. This coating reduces protein adsorption, reducing protein adsorption and effectively (up to 96%) degrading adsorbed protein structures on the inner surface, compared to uncoated catheters [21].

According to KDOQI guidelines, the strategies for implanting tunneled CVCs and the choice of catheter insertion sites should be guided by the patient's life plan. This plan outlines the long-term strategy for providing vascular access for dialysis in individuals with chronic kidney disease and is developed jointly with the patient and a multidisciplinary team of specialists. The team typically includes a nephrologist, a surgeon, a radiologist, a nurse, and members of the patient's family.

The choice of catheter location is determined by several factors, including the patient's age, expected duration of tunneled CVC use (short-term, up to 3 months, or long-term, more than 3 months), the presence of an AVF or plans for AVF creation on the same side, as well as waiting for a kidney transplant, where preservation of the iliac vessels is necessary. Based on these criteria, the preferred order of sites for tunneled CVC placement is as follows:

1. Internal jugular vein.
2. External jugular vein.
3. Femoral vein.
4. Subclavian vein.
5. Iliac vein.

Whenever possible, tunneled CVCs should be implanted on the right side rather than the left, as the anatomy of the right-sided veins provides a more direct course to the right atrium. Exceptions include cases where preexisting pathology (e.g., central venous stenosis) or prior interventions (e.g., pacemaker implantation) preclude right-sided access. In situations where pathology on one side prevents the creation of arteriovenous access but still permits catheter placement, tunneled CVCs should be placed on that side in order to preserve the other side for future arteriovenous access [2].

A recent meta-analysis, however, found no association between unilateral placement of tunneled CVCs and AVFs with regard to fistula maturation time or dysfunction rates [22]. Despite this, dysfunction of tunneled CVCs implanted in the right internal jugular vein is consistently reported to be less frequent than in the left internal jugular vein. Left-sided placement is associated with a higher risk of intraoperative complications due to the longer and more tortuous venous course. Moreover, studies have shown higher rates of infection and dysfunction with left-sided catheters. For adequate performance of left-sided catheters, precise tip positioning within the right atrium is considered essential [9, 23].

If implantation in the jugular veins is not feasible, the femoral vein is recommended as the next option. However, this site is considered less favorable due to a higher incidence of infectious complications, attributable to its anatomical location, and thrombotic complications, particularly catheter lumen thrombosis.

Placement of tunneled CVCs in the right or left subclavian vein is generally not recommended, as it is frequently associated with vascular stenosis [2]. Nevertheless, in some patients, identifying a suitable site for tunneled CVC placement can be extremely challenging or even impossible. In such cases, alternative approaches have been reported in the literature, including tunneled CVC implantation in the external jugular vein [24, 25], placement in the inferior vena cava (IVC) at the confluence of the iliac veins in patients with exhausted vascular access [26], and transhepatic catheterization of the IVC in patients with both exhausted vascular access and a preexisting cava filter [9, 27].

TUNNELED CVC IMPLANTATION TECHNIQUE

Tunneled CVCs are inserted following a standard algorithm and are typically performed without systemic antibiotic prophylaxis. The rationale for not using prophylactic antibiotics routinely lies in the fact that the procedure is conducted under aseptic conditions. Routine administration of antibiotics may introduce unnecessary risks, such as allergic reactions or drug toxicity, and may contribute to the emergence of antibiotic-resistant microbial strains [28].

Retrograde tunneling catheter placement procedure begins with puncture of the vein using an 18 G needle under ultrasound guidance, followed by insertion of a metal guidewire advanced to the level of the right atrium (visualized in real time in the X-ray operating room). In the absence of intraoperative fluoroscopic control, correct guidewire placement can be verified by observing its characteristic reverse movement (rebound with cardiac contractions), performing Doppler ultrasound of the right subclavian vein (RSV) and left subclavian veins (LSV) and the left internal jugular vein (LIJV) to exclude misplacement, or by echocardiography to directly visualize the guidewire and subsequently the catheter tip in the right atrium (ensuring the catheter does not contact the tricuspid valve) [2, 29–31].

Next, a 1.0–1.5 cm skin incision is made at the guidewire entry site down to the platysma muscle. The vein is dilated sequentially along the guidewire, and a 16 Fr breakaway introducer with reverse-flow valve is advanced (Fig. 2). The chosen catheter is then inserted, after which the guidewire and introducer are removed. The catheter is checked for patency and temporarily clamped with a soft clamp. Since blood often leaks paracatheterically (sometimes significantly), a single suture is placed around the catheter through the platysma muscle using an atraumatic absorbable thread. This helps prevent complications such as hematoma formation in the catheter area or bleeding from postoperative wounds.

Next, the right supraclavicular region is anesthetized, a 0.5 cm skin incision is made, and a metal tunneling guide is passed through the subcutaneous tunnel. After dilation, the catheter is pulled through the tunnel and exteriorized, leaving approximately 2 cm of distance from the cuff to the exit site. A replaceable port block is then attached to the external end of the catheter (Fig. 3). Finally, the catheter is filled with heparin solution, and the skin is closed with sutures followed by an aseptic dressing [4, 32].

For antegrade tunneling catheter placement into the right internal jugular vein (RIJV), the procedure begins with ultrasound-guided puncture of the vein using an 18 G needle, followed by insertion of a metal guidewire advanced to the level of the right atrium. A 1.0–1.5 cm skin incision is then made at the guidewire entry site down to the platysma muscle.

Next, a 5–7 mm incision is created in the right shoulder region at the planned exit site, corresponding to the intended subcutaneous position of the catheter cuff (2–3 cm from the cuff location). Using a tunneler, the catheter is advanced subcutaneously toward the venous puncture site and brought out through the skin incision where the guidewire is located.

The vein is then dilated sequentially along the guidewire, and a 15 Fr breakaway introducer with valve is inserted. After removal of the guidewire, the selected catheter is introduced through the introducer (Fig. 4). The catheter is checked for patency, filled with heparin solution, and secured. The skin incisions are closed with sutures, and an aseptic dressing is applied.

Fig. 2. 16 Fr Peel-away introducer with integrated blood backflow valve

Fig. 3. Removable unit with ports

Fig. 4. Non-removable unit with ports

The diagram illustrating tunneled CVC placement through the right internal jugular vein, along with the external appearance of the catheter, is presented in Fig. 5.

Advantages of retrograde tunneling technology compared to the traditional antegrade insertion technique:

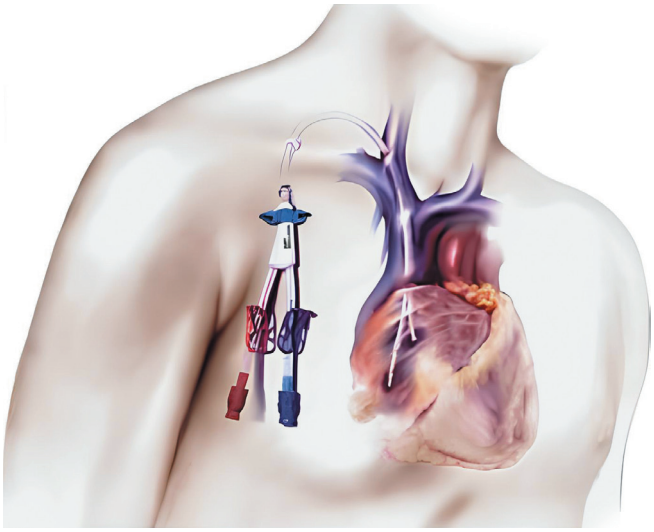

Fig. 5. Final positioning of the tunneled CVC following insertion into the right atrium via the right internal jugular vein

1. Retrograde tunneling allows the catheter tip to be accurately positioned before creating the subcutaneous tunnel, ensuring that the cuff is placed in the optimal location.
2. This technique eliminates the need to advance the catheter tips through the subcutaneous channel prior to venous insertion, thereby reducing the risk of infection.
3. The split V-shaped catheter tip minimizes the risk of occlusion and lowers the level of dialyzed blood recirculation to less than 5%.
4. The presence of a replaceable port block enables continued vascular access in cases where the external portion of the catheter is damaged, thereby extending its functional lifespan.
5. The density of the catheter's material allows it to maintain its bend angle after insertion, preventing breakage at physiological curves and ensuring stable HD flow compared with other catheters [32].

When using the antegrade technique, the catheter is first advanced subcutaneously to the puncture site of the central vein and then positioned in the right atrium. Even a slight deviation from the tunnel trajectory can significantly alter the final position of the catheter tip [33]. Accurate placement of the tip within the right atrium (RA) is a critical determinant of catheter longevity [34, 35]. However, mechanical irritation of the heart tissue by the guidewire or catheter can provoke clinically significant arrhythmias. For this reason, continuous electrocardiographic (ECG) monitoring during tunneled CVC placement is recommended [36].

ADDITIONAL DEVICES USED FOR TUNNELED CVC IMPLANTATION

The revised 2019 KDOQI vascular access guidelines recommend the use of radiographic imaging during tunneled CVC placement to improve procedural success and enhance patient safety [2]. Ultrasound-guided puncture of the jugular vein significantly reduces the risk of failed cannulation and associated complications [37]. Direct visualization of the guidewire in the IVC and fluoroscopic confirmation of catheter tip placement are considered the gold standard for tunneled CVC insertion. ***Fluoroscopy*** also enables early detection and timely management of procedural complications [38]. However, its use is limited by high costs and patient exposure to X-rays [39]. In addition, radiological landmarks such as the junction of the superior vena cava (SVC) with the RA or thoracic vertebrae are not always reliable, and extravascular catheter placement may be missed on frontal X-ray images. In uncertain cases, administration of a radiopaque contrast agent is required for precise tip localization. Transesophageal echocardiography can also be used to determine the exact location of the SVC/RA junction [40–42].

ECG monitoring is widely used during tunneled CVC implantation to verify correct catheter tip positioning. When the catheter is inserted from the upper shoulder girdle, a marked increase in P-wave amplitude is recorded on the ECG if the tip is located at the cavo-atrial junction [36]. A study using transesophageal echocardiography confirmed that the maximum P-wave amplitude corresponds precisely to this anatomical location [43]. When the catheter is introduced via the femoral vein, the sequence of ECG changes differs significantly [44]. ECG-assisted tip localization can also be applied in patients with atrial fibrillation [45].

Echocardiography (ECHO). ECHO-guided catheter placement provides direct visualization of the catheter tip in relation to key anatomical structures. This approach helps to avoid malpositioning in the IVC or near the tricuspid valve. Even in cases of low atrial filling, the optimal position within the right atrium can be confirmed by injecting saline into the catheter lumen [29, 30].

Although evidence on the use of ultrasound alone for tunneled CVC positioning remains limited, recent studies have reported promising results. In one series, the authors confirmed correct tip location by visualizing the guidewire within the RA or IVC [46, 47]. More recently, a prospective study of 134 patients undergoing sequential tunneled CVC implantation using an ultrasound-based technique demonstrated its feasibility and safety. The J-shaped tip of the guidewire, located directly at the distal end of the catheter, served as a reliable landmark for safe placement. In this cohort, ultrasound guidance alone was sufficient in 97% of cases; in the remaining 3%, inadequate visualization necessitated supplementary ECG monitoring and saline injection into the catheter lumen, ensuring accurate catheter tip positioning [31].

THE MOST COMMON COMPLICATIONS OF TUNNELED CVCS

The main complications associated with tunneled CVCs include infection, catheter lumen thrombosis, stenosis, and central vein occlusion. Despite advances in catheter design and biomaterials, infectious complications and consequences of central vein stenosis remain significant challenges.

Infectious complications may present as infection of the external catheter exit site, tunnel infection, or catheter-associated bloodstream infection (CABSI). Strategies to reduce infection rates include strict adherence to aseptic technique when connecting tunneled CVCs, education of both patients and dialysis staff, and implementation of local epidemiological surveillance programs [48].

When infection develops at the external catheter exit site, antiseptic dressings (most commonly with chlorhexidine) are applied, which has been shown to reduce the incidence of CABSI [49, 50]. The risk of bacteremia increases proportionally with catheter dwell time. In one study, 16.4% of patients developed CABSI within the first year after catheter insertion, with skin flora microorganisms such as Staphylococcus aureus and Staphylococcus epidermidis being the most frequently isolated pathogens. Importantly, hematogenous dissemination of these organisms can result in severe complications, including endocarditis, osteomyelitis, septic arthritis, epidural abscess, septic shock, and even death [51].

To reduce CABSI incidence, antimicrobial blocking solutions that inhibit colonization and biofilm formation, often in combination with anticoagulants, are widely used. A common formulation is gentamicin with 4% citrate [52]. Evidence indicates that antimicrobial–citrate combinations are more effective in preventing CABSI than antimicrobial–heparin formulations [53].

Non-antibiotic antimicrobial agents such as taurolidine have also shown benefit. When combined with 4% citrate – or with 4% citrate and weekly urokinase (25,000 units) – taurolidine improves catheter function and significantly reduces CABSI rates [54].

More recently, antimicrobial barrier caps have been introduced. These devices contain a rod impregnated with chlorhexidine acetate, which is inserted into the catheter hub. Chlorhexidine is gradually released into the locking solution, providing continuous antimicrobial activity. Clinical studies have demonstrated that such caps are superior to standard protective caps in reducing CABSI incidence [55, 56].

Catheter lumen thrombosis is among the most frequent complications of tunneled CVCs. It may be classified as internal (thrombus within the catheter lumen, thrombus at the catheter tip, or fibrin sheath formation) and external (thrombosis involving the vessel wall, such as the brachiocephalic trunk, internal jugular vein, subclavian vein; thrombosis of the central veins, including the SVC; or atrial thrombosis) [9].

The pathogenesis is linked to vascular endothelial trauma during catheter insertion and to turbulent blood flow around the catheter. Heparin locks remain the standard method of prevention. In the event of thrombosis, first-line management is local fibrinolytic therapy, most commonly with alteplase, to restore adequate blood flow. Thrombolytic agents have also been evaluated prophylactically as alternatives to heparin locks [57].

A randomized controlled trial demonstrated that a regimen combining taurolidine with heparin (twice weekly) and taurolidine with urokinase (once weekly) significantly reduced both infection and thrombosis compared with 4% citrate locking solution. The use of taurolidine was also associated with improved pharmacoeconomic outcomes, reducing total annual costs per patient [58].

The most serious manifestation is a catheter-related right atrial thrombus (CRAT). In HD patients, CRAT may present with fever, sepsis, or pulmonary embolism, though it is asymptomatic in more than 20% of cases. Optimal management remains debated. Options include catheter removal, anticoagulation, thrombolysis, and surgical thrombectomy [59]. Because premature catheter removal can precipitate pulmonary embolism, removal is generally performed only after initiation of therapeutic anticoagulation. A tailored approach has been proposed: for thrombi <6 cm, catheter removal combined with anticoagulation; for thrombi ≥6 cm, surgical thrombectomy is preferred. Thrombolysis is rarely successful, though it remains an option in cases of hemodynamically unstable thromboembolism [60, 61].

Recent clinical evidence supports these strategies. A prospective study of 178 patients with CRAT confirmed the role of anticoagulation with delayed catheter removal [62]. Similarly, a retrospective study of 20 patients suggested that catheter removal combined with anticoagulant/antiplatelet therapy is effective in HD patients with CRAT [63]. For patients with exhausted vascular access in whom catheter removal is not feasible, combining thrombolytic solution with systemic anticoagulation while retaining the catheter may be considered [64].

There is currently no strong evidence to support treatment of asymptomatic pulmonary embolism. Anticoagulant therapy is recommended only for patients with thromboembolism of the main, lobar, or segmental pulmonary arteries, in those with concomitant deep vein thrombosis, or in patients with cancer [65]. Despite available therapeutic options, mortality remains high: in chronic HD patients, CRAT-related mortality is approximately 18% [59], while pulmonary embolism leads to death within 3 months in approximately 15% of patients [65].

The formation of a fibrinous membrane, composed of smooth muscle cells within a collagen matrix and covered by endothelial cells, plays an important role in the development of venous stenosis. Within a few days, this

structure forms a cuff around the catheter at the vascular entry site and may function as a one-way valve [66, 67].

Central vein stenosis and occlusion are common and severe complications in patients receiving long-term HD, with a reported incidence of 20–50% [2]. In patients with a functioning AVF or SVG on the ipsilateral side, the condition is often associated with more pronounced symptoms than in the general population with this pathology [19].

According to KDOQI guidelines, the preferred first-line treatment is percutaneous transluminal angioplasty (PTA) with or without stent placement [2]. Technical success rates for PTA range from 70% to 90%. However, angioplasty alone can result in intimal rupture, predisposing to restenosis [68].

Stents correct vessel tortuosity, prevent elastic recoil following balloon dilation, eliminate dissections that impede blood flow, and help maintain long-term venous patency [2]. The use of high-pressure balloons coated with antiproliferative agents (paclitaxel) has further improved outcomes. Clinical studies demonstrate superior secondary patency at 6 and 12 months compared with conventional balloon angioplasty [69, 70].

In patients with central vein occlusion, a complex hybrid device, the HD Reliable Outflow (HeRo) graft, has been developed as an alternative. The device consists of a venous outflow component – a radiopaque silicone tube reinforced with braided nitinol (6.3 mm in diameter, 40 cm in length) – and an arterial component, a polytetrafluoroethylene (PTFE) vascular prosthesis (7.3 mm in diameter, 53 cm in length), connected via a titanium adapter. This design enables long-term HD access by bypassing the stenosed or occluded central venous segment [71].

REPLACEMENT OF TUNNELED CVCS

Catheter dysfunction is defined by KDOQI guidelines as the inability to sustain adequate blood flow for HD without significantly prolonging treatment duration. Causes of catheter dysfunction include mechanical problems such as kinking, fracture, twisting, migration, or malposition of the catheter tip. In such cases, catheter removal or replacement is indicated [2]. Replacement may be performed in two ways: creating a new tunnel and exit site or inserting a guidewire through the existing catheter with or without a new tunnel [72, 73].

STANDARDIZED APPROACH

To ensure the effective and safe implantation and maintenance of tunneled CVCs, adherence to a comprehensive set of measures is essential. Every step of the catheter placement and post-procedural care must follow a unified standard, typically outlined in a standard operating procedure (SOP). Such an SOP not only provides a framework for training new staff but also facilitates consistent monitoring of safety and quality indicators. Presented below is an example of a standardized protocol adapted in our practice to optimize both the implantation and long-term use of tunneled CVCs (Tables 1 and 2) [74].

Table 1

Key steps in the implantation of a tunneled central venous catheter

S/N	Implantation of a tunneled central venous catheter
1	Surgical asepsis: a) surgical hand disinfection b) use of sterile gloves, gown, and face mask c) establishment of a limited sterile surgical field
2	Use of a two-component aseptic solution consisting of alcohol and a residual antimicrobial agent (e.g., chlorhexidine, octenidine dihydrochloride)
3	Preferred site for catheter placement: right internal jugular vein a) catheter placement in the subclavian and femoral veins should be reserved for cases where access to the internal jugular veins is not possible due to occlusion
4	Central vein puncture only under ultrasound guidance
5	The correct catheter tip position (ideally located in the mid-right atrium) should be confirmed by: a) a second (additional) control method , such as ECG, echocardiography, or fluoroscopy) b) an aspiration test using a 20 ml syringe prior to final catheter placement
6	Use of sterile dressings for catheter site care, preferably semi-permeable transparent dressings)
7	Teaching patients the basics of asepsis: a) Hand hygiene b) Understanding the potential risks associated with catheter use c) Recognizing early signs of catheter infection d) Receiving clear instructions on how patients should behave with a catheter outside the dialysis unit e) Catheter site care f) Instructions on keeping the area around the catheter dry and clean, no showering for 3 days after catheter placement g) When resuming showering, always use a waterproof dressing

Table 2

Guidelines for the care and removal of a tunneled central venous catheter

S/N	Catheter care
1	Always follow strict aseptic technique when handling the catheter, including the use of sterile gloves and a gown a) Clean the catheter exit site using a chlorhexidine-based antiseptic solution
2	Dressing guidelines: a) Should protect against environmental contamination b) To further minimize infection risk, consider using a chlorhexidine-impregnated dressing c) Change the dressing regularly – at least once per week
3	Apply an antimicrobial locking solution (e.g., based on citrate or taurine)
4	If the patient is diagnosed with intranasal colonization by *S. aureus*, include mupirocin nasal ointment in the treatment protocol
5	Patient education
	Catheter removal
1	The tunneled catheter should be removed as planned no later than 2 weeks after its last use
2	In the event of thrombosis, the catheter must be promptly replaced with a new one
3	If catheter-associated bloodstream infection (CAIK) or sepsis is suspected, catheter removal should be strongly considered
4	Routine catheter exchange over a guidewire is not recommended

CONCLUSION

Tunneled CVCs have become an indispensable component in the management of patients receiving maintenance HD. Standardized implantation techniques are now well established and enable reliable vascular access in most cases. However, in complex scenarios such as patients with exhausted vascular access, an individualized approach is essential, often requiring the development of new surgical strategies [75].

The authors declare no conflict of interest.

REFERENCES

1. Kidney Disease: Improving Global Outcomes (KDIGO) CKD Work Group. KDIGO 2024 Clinical Practice Guideline for the Evaluation and Management of Chronic Kidney Disease. *Kidney Int*. 2024; 105 (4S): S117–S314.
2. *Lok CE, Huber TS Lee T et al.* KDOQI Clinical Practice Guideline for Vascular Access: 2019 Update. *Am J Kidney Dis.* 2020. 75 (4): S1–S164. doi: 10.1053/j.ajkd.2019.12.001.
3. United States Renal Data System. 2023 USRDS Annual Data Report: Epidemiology of Kidney Disease in the United States. Bethesda, MD: National Institute of Diabetes and Digestive and Kidney Diseases, 2023.
4. *Bernd Schröppel, Lucas Bettac, Lena Schulte-Kemna et al.* Placement of tunnelled haemodialysis catheters – interventional standard. *Nephrol Dial Transplant*. 2025; 40: 264–272. https://doi.org/10.1093/ndt/gfae181.
5. *O'Hare AM, Choi AI, Bertenthal D et al.* Age affects outcomes in chronic kidney disease. *J Am Soc Nephrol.* 2007; 18: 2758–2765. https://doi.org/10.1681/ASN.2007040422.
6. *Schulte-Kemna L, Künzig M, Dallmeier D et al.* [Frailty in renal diseases]. *Z Gerontol Geriatr.* 2021; 54: 708–716. https://doi.org/10.1007/s00391-021-01953-0.
7. *Lyu B, Chan MR, Yevzlin AS et al.* Catheter dependence after arteriovenous fistula or graft placement among elderly patients on hemodialysis. *Am J Kidney Dis.* 2021; 78: 399–408.e1. https://doi.org/10.1053/j.ajkd.2020.12.019.
8. *Boubes K, Shaikh A, Alsauskas Z et al.* New directions in ensuring catheter safety. *Adv Chronic Kidney Dis.* 2020; 27: 228–235. https://doi.org/10.1053/j.ackd.2020.02.004.
9. *Husameddin El Khudari, Merve Ozen, Bridget Kowalczyk et al.* Hemodialysis Catheters: Update on Types, Outcomes, Designs and Complications. *Semin Intervent Radiol.* 2022 Feb 18; 39 (1): 90–102. doi: 10.1055/s-0042-1742346.
10. *D M, Trerotola SO, Clark T.* Clinical and Regulatory Considerations for Central Venous Catheters for Hemodialysis. *Clin J Am Soc Nephrol.* 2018; 13 (12): 1924–1932. doi: 10.2215/CJN.14251217.
11. *Vesely T M, Ravenscroft A.* Hemodialysis catheter tip design: observations on fluid flow and recirculation. *J Vasc Access.* 2016; 17 (01): 29–39. doi: 10.5301/jva.5000463.
12. *Van Der Meersch H, De Bacquer D et al.* Hemodialysis catheter design and catheter performance: a randomized controlled trial [published correction appears in *Am J Kidney Dis.* 2015 May; 65 (5): 810]. doi: 10.1053/j.ajkd.2014.02.017.
13. *Hwang HS, Kang SH, Choi SR et al.* Comparison of the palindrome vs. step-tip tunneled hemodialysis catheter: a prospective randomized trial. *Semin Dial.* 2012; 25 (05): 587–591. doi: 10.1111/j.1525-139X.2012.01054.x.
14. *Benjamin Lazarus, Kevan R Polkinghorne, Martin Gallagher et al.* Tunneled Hemodialysis Catheter Tip Design and Risk of Catheter Dysfunction: An Australian Nationwide Cohort Study. *Am J Kidney Dis.* 2024 Apr; 83 (4): 445–455. doi: 10.1053/j.ajkd.2023.09.021.
15. *Clark TW, Redmond JW, Mantell MP.* Initial Clinical Experience: Symmetric-Tip Dialysis Catheter with Helical Flow Characteristics Improves Patient Outcomes. *J Vasc Interv Radiol.* 2015; 26 (10): 1501–1508. doi: 10.1016/j.jvir.2015.06.033.

16. *Nadolski GJ, Redmond J, Shin B.* Comparison of Clinical Performance of VectorFlow and Palindrome Symmetric-Tip Dialysis Catheters: A Multicenter, Randomized Trial. *J Vasc Interv Radiol.* 2020; 31 (07): 1148–1155. doi: 10.1016/j.jvir.2020.02.001.
17. *Anil K Agarwal, Stephen R Ash.* Maintenance of blood flow rate on dialysis with self-centering CentrosFLO catheter: A multicenter prospective study. *Hemodial Int.* 2016 Oct; 20 (4): 501–509. doi: 10.1111/hdi.12443.
18. *Tal MG, Peixoto AJ, Crowley ST et al.* Comparison of side hole versus non side hole high flow hemodialysis catheters. *Hemodial Int.* 2006; 10 (01): 63–67. doi: 10.1111/j.1542-4758.2006.01176.x.
19. *Bulent Arslan, Abdulrahman Masrani*. Patency and time to malfunction comparison of BioFlo Duramax to Equistream hemodialysis catheters. *Journal of Vascular and Interventional Radiology.* 2016; 27 (3): S199–S200. https://doi.org/10.1016/j.jvir.2015.12.514.
20. *May RM, Magin CM, Mann EE.* An engineered micropattern to reduce bacterial colonization, platelet adhesion and fibrin sheath formation for improved biocompatibility of central venous catheters. *Clin Transl Med.* 2015; 4: 9. doi: 10.1186/s40169-015-0050-9.
21. *David W Sutherland Jr, Zachary D Blanks, Xin Zhang*. Relationship Between Central Venous Catheter Protein Adsorption and Water Infused Surface Protection Mechanisms. *Artif Organs.* 2018 Nov; 42 (11): E369–E379. doi: 10.1111/aor.13274.
22. *Koudounas G, Giannopoulos S, Volteas P et al.* Arteriovenous fistula maturation in patients with ipsilateral versus contralateral tunneled dialysis catheter: a systematic review and metaanalysis. *Ann Vasc Surg.* 2024; 103: 14–21. doi: 10.1016/j.avsg.2023.11.048.
23. *Engstrom BI, Horvath JJ, Stewart JK et al.* Tunneled internal jugular hemodialysis catheters: impact of laterality and tip position on catheter dysfunction and infection rates. *J Vasc Interv Radiol.* 2013; 24: 1295–302. https://doi.org/10.1016/j.jvir.2013.05.035.
24. *Ali Akbar Beigi, Ali Sharifi, Hafez Gaheri et al.* Placement of long-term hemodialysis catheter (permcath) in patients with end-stage renal disease through external jugular vein. *Advanced Biomedical Research.* 2014 Dec; 3 (1): 252. doi: 10.4103/2277-9175.146381.
25. *Pei Wang, Yufei Wang, Yingjin Qiao et al.* Retrospective Study of Preferable Alternative Route to Right Internal Jugular Vein for Placing Tunneled Dialysis Catheters: Right External Jugular Vein versus Left Internal Jugular Vein. *PLoS One.* 2016; 11 (1): e0146411. doi: 10.1371/journal.pone.0146411.
26. *Yankovoy AG, Zulkarnaev AB*. Surgical implantation of a tunnel dialysis catheter into the inferior vena cava. Case report. *Nephrology and Dialysis*. 2023; 25 (1): 111–115. (In Russ.). doi: 10.28996/2618-9801-2023-1-111-115.
27. *Hieu M Vo, Raeeha Syeda, Mohammad Ali.* Inferior Vena Cava Placement of a Transhepatic Tunneled Dialysis Catheter in a Patient with Atypical Hepatic Venous Anatomy. *A Case Report*. 2024 Sep 13; 16 (9): e69365. doi: 10.7759/cureus.69365.
28. *Buetti N, Souweine B, Mermel L et al.* Concurrent systemic antibiotics at catheter insertion and intravascular catheter-related infection in the ICU: a post hoc analysis using individual data from five large RCTs. *Clin Microbiol Infect.* 2021; 27: 1279–1284. https://doi.org/10.1016/j.cmi.2020.10.026.
29. *Korsten P, Kuczera T, Wallbach M et al.* The rapid atrial swirl sign for ultrasound-guided tip positioning of retrogradetunneled hemodialysis catheters: a cross-sectional study from a single center. *J Clin Med.* 2021; 10: 3999. https://doi.org/10.3390/jcm10173999.
30. *Da Hora Passos R, Ribeiro M, da Conceição LFMR et al.* Agitated saline bubble – enhanced ultrasound for the positioning of cuffed, tunneled dialysis catheters in patients with end-stage renal disease. *J Vasc Access.* 2019; 20: 362–367. https://doi.org/10.1177/1129729818806121.
31. *Kächele M, Bettac L, Hofmann C et al*. Feasibility analysis of ultrasound-guided placement of tunneled hemodialysis catheters. *Kidney Int Rep.* 2023; 8: 2001–2007. https://doi.org/10.1016/j.ekir.2023.07.03.
32. *Bream PR.* Update on insertion and complications of central venous catheters for hemodialysis. *Semin Interv Radiol.* 2016; 33: 31–38. doi: 10.1055/s-0036-1572547.
33. *Sharma M, Tong WL, Thompson D et al.* Placing an appropriate tunneled dialysis catheter in an appropriate patient including the nonconventional sites. *Cardiovasc Diagn Ther.* 2023; 13: 28190–28290. https://doi.org/10.21037/cdt-22-426.
34. *Maggiani-Aguilera P, Chávez-Iñiguez JS, Navarro-Gallardo JG et al.* The impact of anatomical variables on haemodialysis tunnelled catheter replacement without fluoroscopy. *Nephrology (Carlton).* 2021; 26: 824–832. doi: 10.1111/nep.13909.
35. *Engstrom BI, Horvath JJ, Stewart JK et al.* Tunneled internal jugular hemodialysis catheters: impact of laterality and tip position on catheter dysfunction and infection rates. *J Vasc Interv Radiol.* 2013; 24: 1295–1302. https://doi.org/10.1016/j.jvir.2013.05.035.
36. Practice guidelines for central venous access 2020: an updated report by the American Society of Anesthesiologists Task Force on Central Venous Access. *Anesthesiology.* 2020; 132: 8–43. https://doi.org/10.1097/ALN.0000000000002864.
37. *Rabindranath KS, Kumar E, Shail R et al.* Use of real-time ultrasound guidance for the placement of hemodialysis catheters: a systematic review and meta-analysis of randomized controlled trials. *Am J Kidney Dis.* 2011; 58: 964–970. https://doi.org/10.1053/j.ajkd.2011.07.025.
38. *Prasad P, Vachharajani TJ.* Non-fluoroscopic techniques to insert a tunneled hemodialysis catheter. *Kidney Int Rep.* 2023; 8: 2191–2193. https://doi.org/10.1016/j.ekir.2023.09.023.
39. *Yevzlin AS, Song GU, Sanchez RJ et al.* Fluoroscopically guided *vs* modified traditional placement of tunneled hemodialysis catheters: clinical outcomes and cost analysis. *J Vasc Access.* 2007; 8: 245–251. https://doi.org/10.1177/112972980700800405.
40. *Hsu JH, Wang CK, Chu KS et al.* Comparison of radiographic landmarks and the echocardiographic SVC/RA junction in the positioning of long-term central venous catheters. *Acta Anaesthesiol Scand.* 2006; 50: 731–735. https://doi.org/10.1111/j.1399-6576.2006.01025.x.
41. *Schuepfer AC, Schuepfer G, Mauch J.* Three near fatal or fatal complications during implantation of tunnelled

hemodialysis catheters learning from experts. *Anaesthesiologie.* 2022; 71: 541–545.
42. *Rattka M, Rottbauer W, Markovic S.* Acute chest pain following parenteral infusion. *Dtsch Arzteblatt Int.* 2021; 118: 841. doi: 10.3238/arztebl.m2021.0094.
43. *Jeon Y, Ryu HG, Yoon SZ et al.* Transesophageal echocardiographic evaluation of ECG-guided central venous catheter placement. *Can J Anaesth.* 2006; 53: 978–983. https://doi.org/10.1007/BF03022525.
44. *Gibault P, Desruennes E, Bourgain JL.* Peroperative electrocardiographic control of catheter tip position during implantation of femoral venous ports. *J Vasc Access.* 2015; 16: 294–298. https://doi.org/10.5301/jva.5000386.
45. *Steinhagen F, Kanthak M, Kukuk G et al.* Electrocardiographycontrolled central venous catheter tip positioning in patients with atrial fibrillation. *J Vasc Access.* 2018; 19: 528–534. https://doi.org/10.1177/1129729818757976.
46. *Pereira Junior GM, Souza Alvarenga A, Almeida Felipe CR et al.* Use of ultrasound to confirm guidewire position in hemodialysis catheter implantation. *J Nephrol.* 2022; 35: 1515–1519. https://doi.org/10.1007/s40620-022-01346-5.
47. *Kairidibo, Pandey AR, Dwivedi V et al.* "Rapid Atrial Swirl Sign": A Better Tool Than the Landmark Technique for Ensuring Correct Depth of Insertion of Central Venous Catheters. *Cureus.* 2024 Jul 23; 16 (7): e65211. doi: 10.7759/cureus.65211.
48. *Fisher M, Golestaneh L, Allon M et al.* Prevention of bloodstream infections in patients undergoing hemodialysis. *Clin J Am Soc Nephrol.* 2020; 15: 132–151. https://doi.org/10.2215/CJN.06820619.
49. *Apata IW, Hanfelt J, Bailey JL et al.* Chlorhexidine-impregnated transparent dressings decrease catheter-related infections in hemodialysis patients: a quality improvement project. *J Vasc Access.* 2017; 18: 103–108. https://doi.org/10.5301/jva.5000658.
50. *Hou Y, Griffin L, Bernatchez SF et al.* Comparative Effectiveness of 2 Chlorhexidine Gluconate-Containing Dressings in Reducing Central Line-Associated Bloodstream Infections, Hospital Stay, and Costs. *Inquiry.* 2023 Jan-Dec; 60: 469580231214751. doi: 10.1177/00469580231214751.
51. *Gabriele Donati, Alessandra Spazzoli, Anna Laura Croci Chiocchini.* Bloodstream infections and patient survival with tunneled-cuffed catheters for hemodialysis: A single-center observational study. *Int J Artif Organs.* 2020 Dec; 43 (12): 767–773. doi: 10.1177/0391398820917148.
52. *Carol L Moore, Anatole Besarab, Marie Ajluni.* Comparative effectiveness of two catheter locking solutions to reduce catheter-related bloodstream infection in hemodialysis patients. *Clin J Am Soc Nephrol.* 2014 Jul; 9 (7): 1232–1239. doi: 10.2215/CJN.11291113.
53. *Hongxia Mai, Yuliang Zhao, Stephen Salerno et al.* Citrate versus heparin lock for prevention of hemodialysis catheter-related complications: updated systematic review and meta-analysis of randomized controlled trials. *Int Urol Nephrol.* 2019 Jun; 51 (6): 1019–1033. doi: 10.1007/s11255-019-02150-0.
54. *Fadwa Al-Ali, Ahmad F Hamdy, Abdullah Hamad et al.* Safety and efficacy of taurolidine/urokinase versus taurolidine/heparin as a tunneled catheter lock solution in hemodialysis patients: a prospective, randomized, controlled study. *Nephrol Dial Transplant.* 2018 Apr 1; 33 (4): 619–626. doi: 10.1093/ndt/gfx187.
55. *Jeffrey L Hymes, Ann Mooney, Carly Van Zandt et al.* Dialysis Catheter-Related Bloodstream Infections: A Cluster-Randomized Trial of the ClearGuard HD Antimicrobial Barrier Cap. *Am J Kidney Dis.* 2017 Feb; 69 (2): 220–227. doi: 10.1053/j.ajkd.2016.09.014.
56. *Amy Nau, Troy Richardson, Diana Cardwell et al.* Use of ClearGuard HD caps in pediatric hemodialysis patients. *Pediatr Nephrol.* 2024 Jul; 39 (7): 2171–2175. doi: 10.1007/s00467-023-06273-6.
57. *Hemmelgarn BR, Moist LM, Lok CE et al.* Prevention of dialysis catheter malfunction with recombinant tissue plasminogen activator. *N Engl J Med.* 2011; 364: 303–312. https://doi.org/10.1056/NEJMoa1011376.
58. *Winnicki W, Herkner H, Lorenz M et al.* Taurolidine-based catheter lock regimen significantly reduces overall costs, infection, and dysfunction rates of tunneled hemodialysis catheters. *Kidney Int.* 2018; 93: 753–760. https://doi.org/10.1016/j.kint.2017.06.026.
59. *Tran MH, Wilco T, Tran PN.* Cather-related right atrial thrombosis. *J Vasc Access.* 2020; 21 (3): 300–307. doi: 10.1177/1129729819873851.
60. *Stavroulopoulos A, Aresti V, Zounis C.* Right atrial thrombi complicating haemodialysis catheters. A meta-analysis of reported cases and a proposal of a management algorithm. *Nephrol Dial Transplant.* 2012; 27 (7): 2936–2944. doi: 10.1093/ndt/gfr739.
61. *Chen L, Chen B, Lai Q et al.* Management of catheter-related right atrial thrombus in hemodialysis: a systematic review. *BMC Cardiovasc Disord.* 2024 Nov 20; 24 (1): 656. https://doi.org/10.1186/s12872-024-04330-y.
62. *Sun J, Liu Y, Chen J et al.* Catheter replacement combined with antiplatelet therapy in hemodialysis catheter-related right atrial thrombus: a potential treatment approach. *BMC Cardiovasc Disord.* 2025 Jan 16; 25 (1): 26. https://doi.org/10.1186/s12872-025-04485-2.
63. *Yang H, Chen F, Jiao H et al.* Management of tunneled-cuffed catheter-related right atrial thrombosis in hemodialysis patients. *J Vasc Surg.* 2018; 68 (5): 1491–1498. doi: 10.1016/j.jvs.2018.02.039.
64. *Rossi L, Libutti P, Casucci F et al.* Is the removal of a central venous catheter always necessary in the context of catheter-related right atrial thrombosis? *J Vasc Access.* 2018; 20 (1): 98–101. doi: 10.1177/1129729818774438.
65. *Kruger PC, Eikelboom JW, Douketis JD et al.* Pulmonary embolism: update on diagnosis and management. *Med J Aust*. 2019 Jul; 211 (2): 82–87. doi: 10.5694/mja2.50233.
66. *Ahmed R, Chapman SA, Tantrige P et al.* TuLIP (Tunnelled Line Intraluminal Plasty): An Alternative Technique for Salvaging Haemodialysis Catheter Patency in Fibrin Sheath Formation. *Cardiovasc Intervent Radiol.* 2019; 42: 770–774. https://doi.org/10.1007/s00270-019-02189-7.
67. *Lizhu Jin, Hui Wang, Tianlei Cui et al.* [Catheter Replacement Methods in Hemodialysis Patients With Dysfunctional Tunneled-Cuffed Catheters With Fibrin Sheaths]. *Sichuan Da Xue Xue Bao Yi Xue Ban*. 2023 Nov 20; 54 (6): 1283–1287. doi: 10.12182/20231160201.

68. *Nayak-Rao S, Ramanna B, Subramanyam K et al*. Endovascular intervention for central venous stenosis in hemodialysis patients: A single-center experience. *Indian J Nephrol.* 2020; 0 (0): 0. doi: 10.4103/ijn.IJN_343_19.
69. *Kitrou PM, Papadimatos P, Spiliopoulos S et al.* Paclitaxel-Coated Balloons for the Treatment of Symptomatic Central Venous Stenosis in Dialysis Access: Results from a Randomized Controlled Trial. *J Vasc Interv Radiol.* 2017 Jun; 28 (6): 811–817. doi: 10.1016/j.jvir.2017.03.007.
70. *Panagiotis M Kitrou, Tobias Steinke, Rami El Hage et al.* Paclitaxel-Coated Balloons for the Treatment of Symptomatic Central Venous Stenosis in Vascular Access: Results from a European, Multicenter, Single-Arm Retrospective Analysis. *J Endovasc Ther.* 2021 Jun; 28 (3): 442–451. doi: 10.1177/15266028211007471.
71. *David M Tabriz, Bulent Arslan.* HeRO Graft: Indications, Technique, Outcomes, and Secondary Intervention. *Semin Intervent Radiol.* 2022 Feb 18; 39 (1): 82–89. doi: 10.1055/s-0042-1742391.
72. *Leclaire C, Lobbedez T, Henri P et al.* A new procedure for guidewire exchange of tunneled hemodialysis catheters in chronic hemodialysis patients: a pilot study. *Blood Purif.* 2023; 52: 91–100. https://doi.org/10.1159/000525436.
73. *Wang J, Nguyen TA, Chin AI et al.* Treatment of tunneled dialysis catheter malfunction: revision versus exchange. *J Vasc Access.* 2016; 17: 328–332. https://doi.org/10.5301/jva.5000533.
74. *Lazarus B, Kotwal S, Gallagher M et al.* Effect of a multifaceted intervention on the incidence of hemodialysis catheter dysfunction in a national stepped-wedge cluster randomized trial. *Kidney Int Rep.* 2023; 8: 1941–1950. https://doi.org/10.1016/j.ekir.2023.07.013.
75. *Niyyar VD, Beathard G.* Interventional nephrology: opportunities and challenges. *Adv Chronic Kidney Dis.* 2020; 27: 344–349.e1. https://doi.org/10.1053/j.ackd.2020.05.013.

The article was submitted to the journal on 20.02.2025

DOI: 10.15825/1995-1191-2025-3-216-224

OPTIMAL TEMPERATURE CONDITIONS FOR PROLONGED TRANSPORT OF DONOR HEARTS: AN EXPERIMENTAL STUDY

A.V. Fomichev[1], A.V. Protopopov[1], M.O. Zhulkov[1], A.G. Makaev[1], I.S. Zykov[1], A.R. Tarkova[1], K.N. Kaldar[1], M.N. Murtazaliev[1], Ya.M. Smirnov[1], A.D. Limanskiy[1], A.V. Guseva[1], D.A. Sirota[1, 2]

[1] Meshalkin National Medical Research Center, Novosibirsk, Russian Federation
[2] Novosibirsk State Medical University, Novosibirsk, Russian Federation

Objective: to compare the effectiveness of extended heart preservation (up to 6 hours) at a temperature of +4 to +8 °C with the standard method. **Materials and methods.** The study was conducted using male Landrace pigs weighing 40–60 kg (n = 6). The experimental group (n = 3) underwent heart preservation at an optimized temperature of +4 to +8 °C for 6 hours prior to transplantation. In the control group (n = 3), hearts were preserved using the standard method for the same duration. Following preservation, coronary perfusion was restored *ex vivo*, cardiac activity was reinitiated, and myocardial function was evaluated alongside biochemical markers of cardiac tissue injury. **Results.** Following the resumption of blood supply and cardiac activity, both groups showed a reduction in superoxide dismutase (SOD) and malondialdehyde (MDA) levels. In the experimental group (preserved at +4–8 °C), SOD and MDA levels decreased from 12.31 to 8.85 ng/mL per 1 g of protein, while in the control group (standard method), levels declined from 12.04 to 9.23 ng/mL per 1 g of protein. In the experimental group, the level of heart-type fatty acid-binding protein (H-FABP) remained stable, whereas in the control group, it declined from 1.42 to 1.06 ng/mL per 1 g of protein. After prolonged preservation, receptor-interacting protein (RIP) kinase concentrations increased more markedly in the control group (from 0.071 to 0.086 ng/mL) than in the experimental group (from 0.024 to 0.028 ng/mL per 1 g of protein). Additionally, caspase-8 levels in the experimental group significantly decreased from 0.04 to 0.013 ng/mL per 1 g of protein. No significant differences were observed in von Willebrand factor levels between the two groups. However, histological analysis in the control group revealed muscle fiber fragmentation and widespread coagulopathy in myocardial tissue following standard cold ("ice") preservation. **Conclusion.** This pilot experimental study indicates that long-term preservation of donor hearts at a controlled temperature of +4–8 °C is both effective and safe when compared to the conventional preservation method.

Keywords: preservation, heart transplantation, coronary perfusion, graft dysfunction.

INTRODUCTION

Progressive heart failure (HF) is a life-threatening, disabling condition and one of the leading causes of mortality worldwide. For patients with end-stage HF, heart transplantation (HT) remains the only definitive treatment. However, the demand for donor hearts continues to rise, while the supply of deceased donors remains insufficient, resulting in increased waitlist mortality [1]. The solution to the problem of donor organ shortage has been a subject of debate among transplantologists for many years. With conventional cold storage – using a triple-bag system placed in an ice container – the optimal cold ischemia time is approximately 4 hours [2, 3], with an absolute maximum of 6 hours [4]. Prolonged ischemia increases the risk of ischemia-reperfusion injury (IRI), which can lead to irreversible damage, most notably primary graft dysfunction [5]. Transporting the organ in an ice-filled thermal container causes uncontrolled and uneven cooling. When the temperature falls to +2 °C, there is a risk of cold-induced injury to cardiomyocytes; at 0 °C, these changes may become irreversible [2].

The combined challenges of IRI and the persistent shortage of donor organs underscore the need to optimize organ transport technologies and to develop both perfusion and non-perfusion preservation methods. The Paragonix SherpaPak® Cardiac Transport System (Paragonix Technologies, Cambridge, MA) is a portable device designed to maintain the heart graft at an optimal temperature regardless of external conditions, thereby eliminating the risk of cold-induced myocardial injury and reducing the likelihood of primary graft dysfunction. The system preserves the organ within a controlled temperature range of +4 to +8 °C for up to 24 hours, ensuring uniform cooling, reducing metabolic demands, and protecting against IRI. While clinical data exist for its use in short-duration transport (<4 hours), its effectiveness under conditions of prolonged ischemia remains unproven. Moreover, the high cost (~$20,000) and lack

Corresponding author: Andrey Protopopov. Address: 15, Rechkunovskaya str., 630055, Novosibirsk, Russian Federation. Phone: (914) 708-39-79. E-mail: andrew-uss@yandex.ru

of regulatory certification currently make it impossible to use the system in Russia [6, 7].

Published positive results on the use of the SherpaPak system for donor heart preservation of up to 4 hours, combined with the significant shortage of available heart transplants due to the underutilization of many donor centers, highlight the need to investigate longer preservation times under controlled cold ischemia. Extending safe preservation duration could expand the geographical reach of donor programs while reducing an IRI risk.

Objective of the study: To experimentally evaluate the feasibility of extended heart preservation for 6 hours at a controlled temperature of +4 to +8 °C compared with standard ice storage for the same duration.

MATERIALS AND METHODS

The study was conducted in compliance with the Rules for the Care and Use of Laboratory Animals. The experimental subjects were large laboratory animals – male mini-pigs weighing 40–60 kg (n = 6). Animals were randomly assigned to two groups: a control group (n = 3), in which hearts were preserved using the standard cold storage method, and an experimental group (n = 3), in which hearts were preserved under controlled cold ischemia conditions.

Animal housing, care, experimental procedures, observation, and euthanasia were carried out in accordance with the European Convention for the Protection of Vertebrate Animals Used for Experimental and Other Scientific Purposes (Strasbourg, March 18, 1986). Ethical approval for the study was obtained from the Bioethics Committee of Meshalkin National Medical Research Center (Minutes of the meeting dated June 8, 2023, No. 2, agenda item No. 1). During the experiments, continuous monitoring included invasive arterial pressure via catheterization of the left carotid artery, central venous pressure via catheterization of the left jugular vein, heart rhythm by electrocardiography, body temperature, blood gas composition, activated clotting time, and cardiac hemodynamics using transesophageal echocardiography and Swan–Ganz catheterization. Vital parameters were recorded with an IntelliVue MP70 monitor (Philips, Germany).

Following surgical access via median sternotomy and isolation of the major vessels, all required diagnostic procedures were performed in accordance with the study protocol, including echocardiography as well as collection of laboratory and morphological samples. After occlusion of the aorta as close as possible to the origin of the brachiocephalic trunk, 3 liters of Bretschneider cardioplegic solution (4 °C) were administered into the aortic root. The heart was then explanted and packaged using the standard triple-bag method. In the experimental group, the graft was placed in a medical refrigerator with continuous temperature monitoring at +4 to +8 °C; in the control group, it was placed in a transport container with ice and coolants. Both preservation methods were maintained for 6 hours.

After the preservation period, perfusion of the heart with oxygenated blood was initiated using a heart–lung machine, starting at an aortic pressure of 40–50 mmHg and gradually increasing to approximately 70 mmHg within 15 minutes. Upon restoration of coordinated myocardial contractions, tissue biopsies and diagnostic tests were performed for comparative analysis.

To assess left ventricular function by ultrasound, cardiac activity was restored under constant volume conditions using an autoperfused complex model (Fig. 1). In this setup, blood was pumped by the heart's own contractions through an oxygenator into a reservoir, from

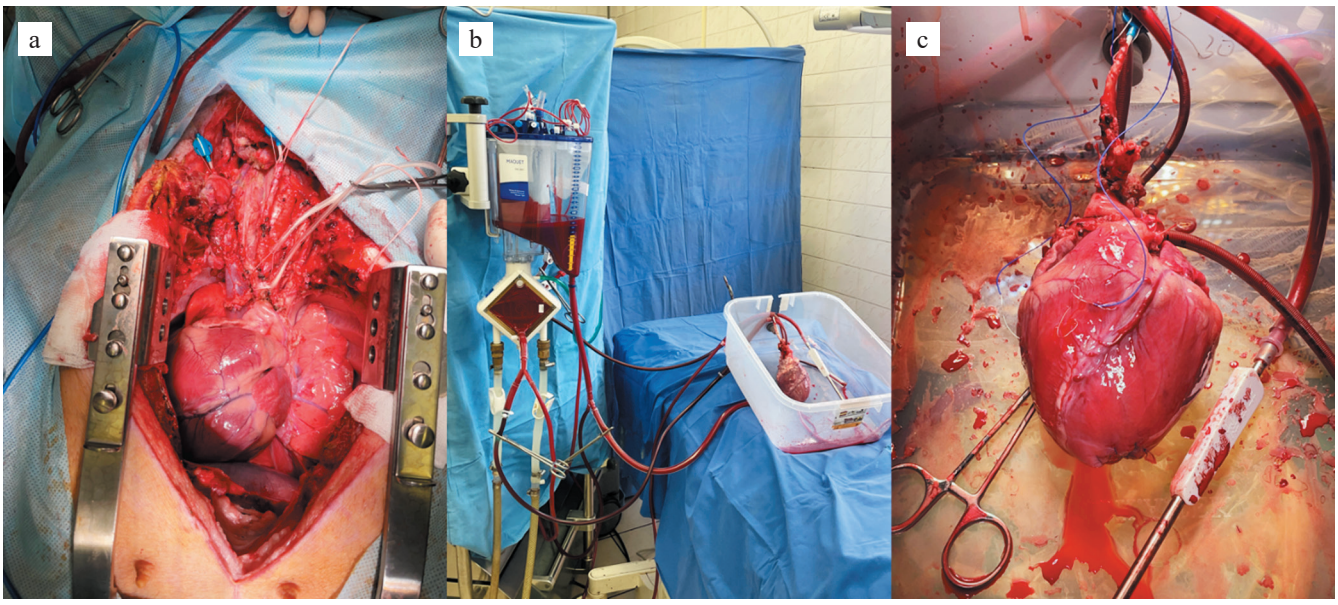

Fig. 1. Heart appearance: a, b – before preservation; c – after reperfusion

Fig. 2. Echocardiographic assessment of the heart during *ex vivo* perfusion

which it returned by gravity to the left atrium and right heart chambers. Perfusion and monitoring of the heart were performed for 1 hour after restoration of cardiac activity.

Echocardiography was performed using a portable multifunctional ultrasound system, the Philips CX50 (Philips Ultrasound, USA), with ECG synchronization and a sector phased-array transducer (S5-1). The transducer was placed *ex vivo* along the long axis of the left ventricle and in the apical four-chamber position, using a water-filled glove to enlarge the imaging window (Fig. 2). Cardiac function was assessed by determining the left ventricular ejection fraction (LVEF) and cardiac output (CO). The LVEF was calculated using Simpson's method in the apical four-chamber view according to the formula: LVEF (%) = (EDV – ESV) / EDV, where EDV is the left ventricular end-diastolic volume (mL), and ESV is the end-systolic volume (mL). Cardiac output was calculated using the formula: CO (L/min) = (π × (LVOTD/2)^2 × VTI × HR)/1000, where LVOTD is the Left Ventricular Outflow Tract Diameter (cm), VTI is the velocity time integral (cm), and HR is the heart rate (beats per minute).

During the experiment, a protocol was drawn up in accordance with which myocardial tissue samples were collected to determine the levels of caspase-8, RIP kinases, nitric oxide (NO), prostacyclin, prostaglandin H2, and von Willebrand factor. Blood samples were also obtained from the central vein to measure superoxide dismutase and heart-type fatty acid-binding protein (FABP-H) as biomarkers of oxidative stress. Sampling was conducted both before organ removal and after reperfusion of the heart in both study groups.

The objectives of the comparative study of myocardial morphology and tissue homeostasis after preservation at target temperature parameters (+4 to +8 °C) versus standard ice preservation for 6 hours – using atomic force microscopy and electron microscopy – were as follows:

1) To conduct an *in vitro* analysis of cardiomyocyte cell death (apoptosis and necrosis) after heart preservation at target temperature parameters (+4 to +8 °C) versus standard ice preservation for 6 hours, based on quantification of caspase-8 and RIP kinase levels in myocardial tissue extracts using enzyme-linked immunosorbent assay (ELISA) kits from specialized manufacturers.
2) To determine the extent of myocardial injury after preservation at +4 to +8 °C and standard ice preservation for 6 hours by measuring levels of cardiac FABP-H, troponin I, malondialdehyde, and superoxide dismutase in tissue extracts using ELISA-based kits.
3) To compare the preservation of total endothelial regulatory function under both temperature conditions by measuring stable NO, prostacyclin, prostaglandin H_2, and von Willebrand factor using ELISA kits from specialized manufacturers.

RESULTS

Data on the functional state of the myocardium were obtained through echocardiographic assessment following preservation at the specified temperature (+4–8 °C) and after standard ice preservation. Given the variability of cardiac functional and hemodynamic parameters among laboratory animals in both groups, direct comparison between the groups was not feasible. Nevertheless, it can be noted that within each individual group, after reperfusion and restoration of cardiac activity, myocardial function and hemodynamic parameters returned to baseline values and remained stable throughout the observation period (1 hour). A detailed comparative analysis of myocardial morphology after 6 hours of preservation at target temperatures (+4–8 °C) and standard ice preservation was also conducted.

Morphological changes in the myocardium in the study group (target temperature) were predominantly reversible and were characterized by Grade I–II contracture-type damage to the contractile apparatus, intracellular and interstitial edema, and mild coagulopathy. By contrast, in the standard cold ("ice") preservation group, a number of changes were largely irreversible,

with damage primarily of a lysosomal type, accompanied by fragmentation of muscle fibers and pronounced widespread coagulopathy in the muscle tissue (Figs. 3 and 4).

Immunoenzymatic assessment of ischemic myocardial injury included assessment of superoxide dismutase (SOD) and malondialdehyde (MDA) levels, which serve as markers of oxidative stress during and after ischemia. Interestingly, the results were paradoxical. After prolonged preservation, followed by reperfusion and restoration of cardiac activity, both groups demonstrated a decrease in SOD and MDA levels: from 12.31 to 8.85 ng/ml per 1 g of protein in the study group (+4–8 °C), and from 12.04 to 9.23 ng/ml per 1 g of protein in the control group (Figs. 5 and 6). A similar trend was noted for heart-type fatty acid-binding protein (H-FABP), which is localized in the cytoplasm of cardiomyocytes and is released rapidly into the systemic circulation in response to cellular damage due to its small molecular size and cytoplasmic localization. In the study group, H-FABP level remained unchanged, whereas in the control group it decreased from 1.42 to 1.06 ng/ml per 1 g of protein (Fig. 5).

An assessment of cell death mechanisms was also performed, with particular attention to regulated necrosis (necroptosis). Upon activation of necroptosis receptors, such as Toll-like receptors 3 and 4, autophosphorylation and activation of RIPK1 and RIPK3 occurs. Analysis of RIP kinase levels after prolonged preservation revealed a more pronounced increase in enzyme concentration in the control group compared with the study group – from 0.071 to 0.086 ng/mL per 1 g of protein in the control

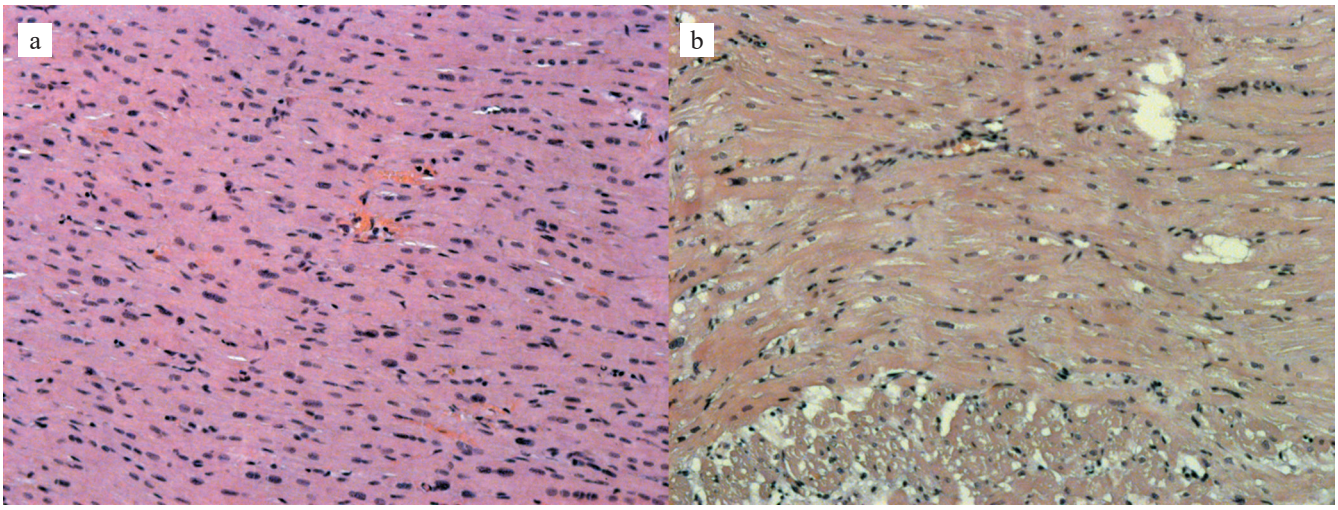

Fig. 3. Microscopic examination of the myocardium (Sample No. 1): a – control group: myocardial fibers are uniform in diameter and largely intact; moderate interstitial edema is observed in some areas, with isolated mononuclear cells present; b – experimental group: areas of perinuclear edema and signs of myofibril lysis are evident. Hematoxylin and eosin stain; 200× magnification

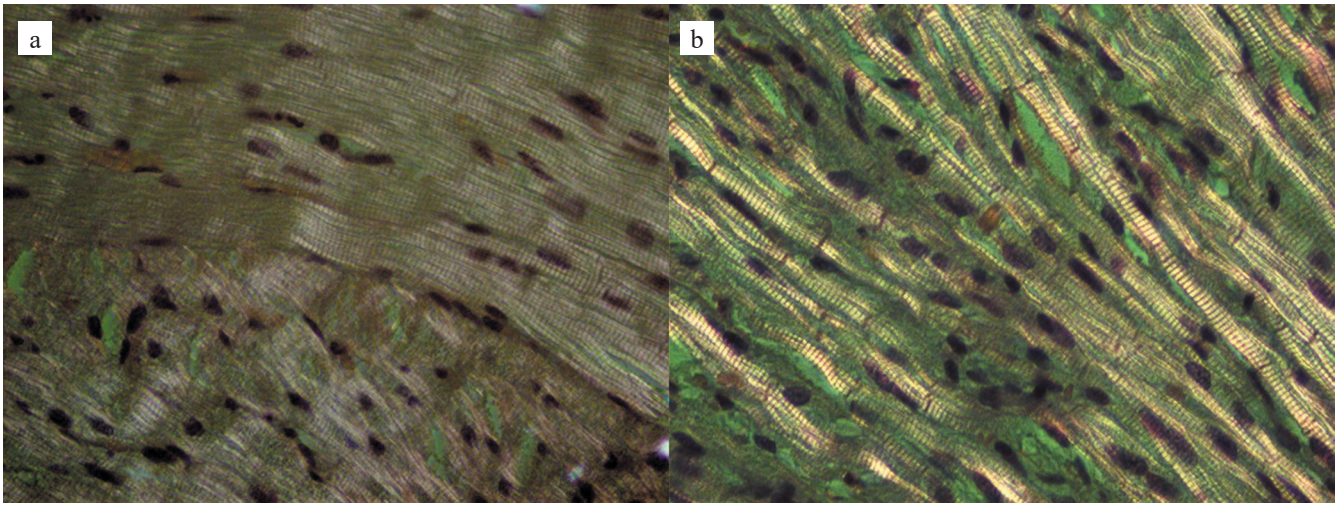

Fig. 4. Microscopic examination of myocardium (Sample No. 2): a – control group: preserved transverse striations of cardiomyocytes; areas of mild to moderate contracture are noted; b – experimental group: focal myofibril lysis with loss of transverse striations in cardiomyocytes. 630× magnification

group, and from 0.024 to 0.028 ng/mL in the study group (Fig. 6).

Apoptosis is a regulated form of cell death triggered by internal or external stimuli. Unlike necroptosis, where RIPK1, RIPK3, and MLKL play a central role, apoptosis is caspase-dependent and characterized by a decrease in cell volume, chromatin condensation (karyopyknosis), and subsequent chromatin fragmentation (karyorrhexis). Analysis of caspase-8 (Casp8) level in the study group revealed a decrease from 0.04 to 0.013 ng/ml per 1 g of protein (Fig. 7).

When von Willebrand factor was analyzed, no distinct changes were observed in either group after prolonged preservation. In the study group, levels were 4.17 and 3.99 ng/ml, and in the control group 7.07 and 6.84 ng/ml, respectively (Fig. 7), despite its initially higher baseline concentration in the control group.

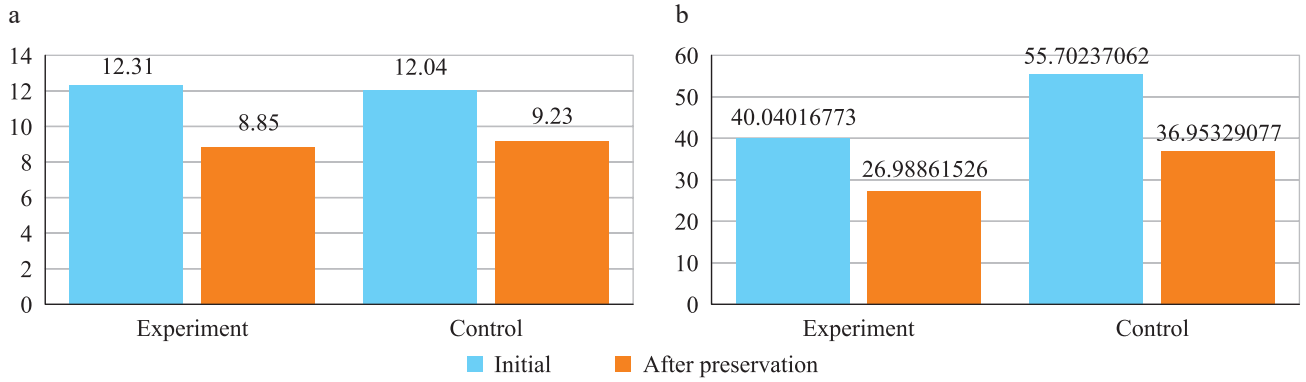

Fig. 5. Biochemical dynamics following reperfusion: a – changes in superoxide dismutase levels; b – changes in malondialdehyde levels

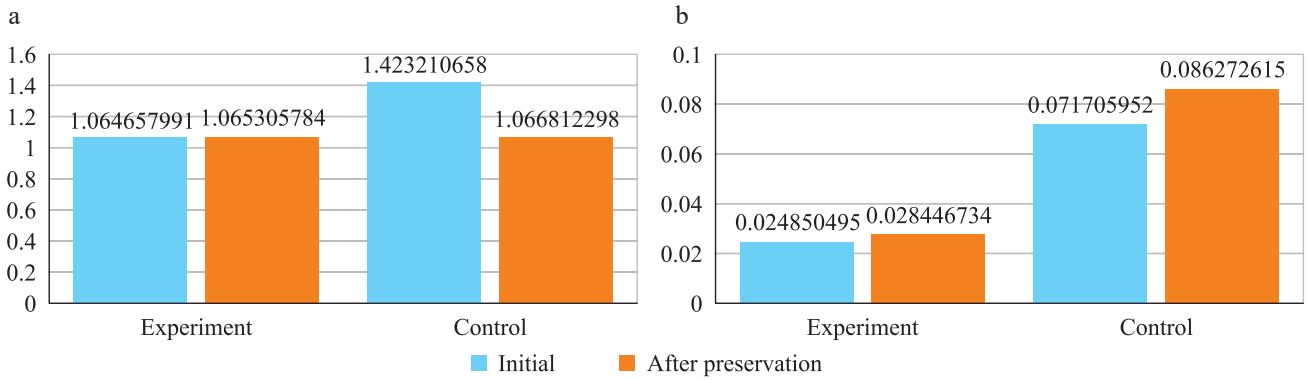

Fig. 6. Biochemical dynamics following reperfusion: a – changes in H-FABP levels; b – changes in RIP kinase levels, an indicator of necrosis

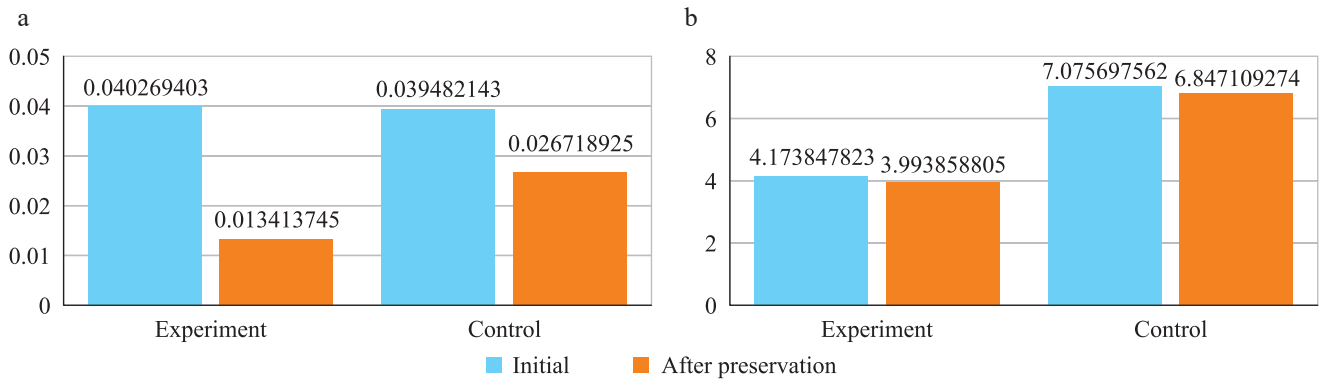

Fig. 7. Biochemical dynamics following reperfusion: a – changes in caspase 8 levels, an indicator of apoptosis; b – changes in von Willebrand factor levels, reflecting endothelial function

DISCUSSION

The optimal method for preserving heart transplants remains a cornerstone in addressing the problem of donor organ shortage. For decades, the standard method has involved classical static preservation of the graft in a thermal container filled with ice. However, this approach has begun to evolve due to the expansion of donor selection criteria and the development of both perfusion and non-perfusion preservation technologies, such as the Transmedics Organ Care System [8–10] and the Paragonix SherpaPak Cardiac Transport System. In this context, the development of a domestic method for static cold preservation of the heart – with controlled and uniform cooling – remains highly relevant for the Russian Federation, given the considerable geographical distances involved.

According to Van't Hoff's rule, a decrease in temperature by 10 °C reduces enzymatic activity by 1.5–2 times; however, the activity of the sodium–potassium pump also declines, leading to cellular edema during prolonged hypothermia [11]. Cold ischemia promotes anaerobic glycolysis and glycogenolysis, resulting in lactic acidosis. During reperfusion, reactive oxygen species are generated, contributing to irreversible cellular injury [12, 13]. Although high-energy phosphates may be preserved at donor organ temperatures between 0–4 °C, the risk of irreversible cold damage increases substantially, especially in the presence of uneven cooling of the graft [14, 15].

The ischemic heart is characterized by a state of oxidative stress, during which free oxygen radicals are released [16]. MDA serves as a key marker of lipid peroxidation and is produced as a result of the action of free radicals on polyunsaturated fatty acids [17]. An increase in MDA typically signifies damage to cardiomyocytes [18]. However, in our study, we observed a paradoxical decrease in MDA levels in both groups, as well as a concurrent reduction in SOD. SOD protects cells against oxidative stress by converting superoxide radicals into hydrogen peroxide, which is further degraded into water and oxygen by enzymes. It is noteworthy that under conditions of intense oxidative stress, the content of SOD itself may decrease [19]. Thus, SOD content plays a key role in regulating superoxide levels in tissues. As reported by Gheddouchi S. et al., SOD levels were significantly lower in patients with acute coronary syndrome, i.e., in conditions characterized by extremely high oxidative stress and myocardial ischemia.

A similar pattern was observed when analyzing the level of H-FABP, a cardiac fatty acid–binding protein that is essential for fatty acid metabolism in cardiomyocytes. Elevation of this biomarker generally reflects myocardial injury [20]. In this context, the absence of any change in H-FABP levels in the experimental group, along with a decrease in the control group, remains an open question and may warrant further investigation.

Another important indicator of acute myocardial injury is the family of RIP kinases (RIPK1 and RIPK3). These intracellular signaling proteins initiate necrotic pathways that result in rapid loss of plasma membrane integrity and release of pro-inflammatory cytokines [21, 22]. In our study, a more pronounced increase in RIP kinase levels was observed in the control group compared with the experimental group. Regarding von Willebrand factor, levels were initially elevated in both groups, and no statistically significant differences were detected after preservation. Since von Willebrand factor is stored in large amounts within Weibel–Palade bodies of endothelial cells, an increase in its concentration would typically indicate the onset of endothelial dysfunction [23].

Long-term preservation under controlled, uniform cold ischemia has the potential to extend the current 4-hour limit of graft viability by minimizing ischemia–reperfusion injury. This, in turn, could significantly expand the geographic reach of donor organ procurement and help alleviate the shortage of donor hearts.

CONCLUSION

Preservation under controlled hypothermia (+4 to +8 °C) demonstrates clear advantages over standard ice preservation, as evidenced by improved morphological findings and reduced activation of necroptotic pathways (RIP kinase), while showing no significant differences in contractile function, hemodynamic parameters, or biochemical markers of myocardial damage.

LIMITATIONS

The main limitations of this study include the small sample size of experimental animals, heterogeneity of baseline parameters, and the absence of a clear reference standard. In addition, the evaluation was based largely on changes in indicators relative to baseline values.

This work was supported by the Russian Science Foundation (project No. 24-25-00352).

The authors declare no conflict of interest.

REFERENCES

1. *Gautier SV, Khomyakov SM*. Organ donation and transplantation in the Russian Federation in 2023. 16th Report from the Registry of the Russian Transplant Society. *Russian Journal of Transplantology and Artificial Organs*. 2024; 26 (3): 8–31. [In Russ, English abstract]. https://doi.org/10.15825/1995-1191-2024-3-8-31.
2. *Radakovic D, Karimli S, Penov K et al*. First clinical experience with the novel cold storage SherpaPakTM system for donor heart transportation. *J Thorac Dis*. 2020; 12 (12): 7227–7235. https://doi.org/10.21037/jtd-20-1827.

3. *Fomichev AV, Poptsov VN, Sirota DA, Zhulkov MO, Edemskiy AG, Protopopov AV et al*. Mid-term and long-term outcomes following heart transplantation with prolonged cold ischemia. *Russian Journal of Transplantology and Artificial Organs*. 2023; 25 (1): 99–105. [In Russ, English abstract]. https://doi.org/10.15825/1995-1191-2023-1-99-105.
4. *Minasian SM, Galagudza MM, Dmitriev YV, Karpov AA, Vlasov TD*. Preservation of the donor heart: from basic science to clinical studies. *Interact Cardiovasc Thorac Surg*. 2015; 20 (4): 510–519. https://doi.org/10.1093/ICVTS/IVU432.
5. *Lee JC, Christie JD*. Primary graft dysfunction. *Proc Am Thorac Soc*. 2009; 6 (1): 39–46. https://doi.org/10.1513/PATS.200808-082GO.
6. *Bixby CE, Balsam LB.* Better Than Ice: Advancing the Technology of Donor Heart Storage with the Paragonix SherpaPak. *ASAIO J*. 2023; 69 (4): 350–351. https://doi.org/10.1097/MAT.0000000000001925.
7. *Severino P, D'amato A, Pucci M et al*. Ischemic Heart Disease Pathophysiology Paradigms Overview: From Plaque Activation to Microvascular Dysfunction. *Int J Mol Sci*. 2020; 21 (21): 1–30. https://doi.org/10.3390/IJMS21218118.
8. *Alomari M, Garg P, Yazji JH et al*. Is the Organ Care System (OCS) Still the First Choice With Emerging New Strategies for Donation After Circulatory Death (DCD) in Heart Transplant? *Cureus*. 2022; 14 (6). https://doi.org/10.7759/CUREUS.26281.
9. *Tarkova AR, Zykov IS, Zhulkov MO, Protopopov AV, Smirnov YaM, Makaev AG et al*. Normothermic *ex vivo* heart and lung autoperfusion: assessment of functional status and metabolism. *Russian Journal of Transplantology and Artificial Organs*. 2023; 25 (4): 150–159. [In Russ, English abstract]. https://doi.org/10.15825/1995-1191-2023-4-150-159.
10. *Zhul'kov M, Tarkova A, Zykov I, Makaev A, Protopopov A, Murtazaliev M et al*. Dlitel'naja normotermicheskaja autoperfuzija serdechno-legochnogo kompleksa *ex vivo* kak metod jeffektivnogo kondicionirovanija transplantata: jeksperimental'noe issledovanie. *Patologija krovoobrashhenija i kardiohirurgija*. 2023; 27 (4): 33–42. https://doi.org/10.21688/1681-3472-2023-4-33-42.
11. *Zhukov A, Karlsson R.* Statistical aspects of van't Hoff analysis: a simulation study. *J Mol Recognit*. 2007; 20 (5): 379–385. https://doi.org/10.1002/JMR.845.
12. *Belzer FO, Southard JH*. Principles of solid-organ preservation by cold storage. *Transplantation*. 1988; 45 (4): 673–676. https://doi.org/10.1097/00007890-198804000-00001.
13. *Smirnov YM, Zhulkov MO, Zykov IS, Sirota DA, Tarkova AR, Kliver EE et al.* Dynamics of the morphofunctional status of the isolated cardiopulmonary complex under conditions of normothermic autoperfusion *ex vivo*. *Clinical and Experimental Surgery*. 2024; 12 (3): 14–22. [In Russ, English abstract]. https://doi.org/10.33029/2308-1198-2024-12-3-14-22.
14. *Keon WJ, Hendry PJ, Taichman GC, Mainwood GW.* Cardiac transplantation: the ideal myocardial temperature for graft transport. *Ann Thorac Surg*. 1988; 46 (3): 337–341. https://doi.org/10.1016/S0003-4975(10)65939-5.
15. *Michel SG, II GML, Madariaga MLL, Anderson LM*. Innovative cold storage of donor organs using the Paragonix Sherpa Pak TM devices. *Heart Lung Vessel*. 2015; 7 (3): 246.
16. *Valko M, Leibfritz D, Moncol J, Cronin MTD, Mazur M, Telser J*. Free radicals and antioxidants in normal physiological functions and human disease. *Int J Biochem Cell Biol*. 2007; 39 (1): 44–84. https://doi.org/10.1016/J.BIOCEL.2006.07.001.
17. *Colak E, Pap D, Nikolić L, Vičković S*. The impact of obesity to antioxidant defense parameters in adolescents with increased cardiovascular risk. *J Med Biochem*. 2020; 39 (3): 346. https://doi.org/10.2478/JOMB-2019-0051.
18. *Amaki T, Suzuki T, Nakamura F et al*. Circulating malondialdehyde modified LDL is a biochemical risk marker for coronary artery disease. *Heart*. 2004; 90 (10): 1211–1213. https://doi.org/10.1136/HRT.2003.018226.
19. *Dhalla NS, Elmoselhi AB, Hata T, Makino N*. Status of myocardial antioxidants in ischemia-reperfusion injury. *Cardiovasc Res*. 2000; 47 (3): 446–456. https://doi.org/10.1016/S0008-6363(00)00078-X.
20. *Ye XD, He Y, Wang S, Wong GT, Irwin MG, Xia Z*. Heart-type fatty acid binding protein (H-FABP) as a biomarker for acute myocardial injury and long-term post-ischemic prognosis. *Acta Pharmacol Sin*. 2018; 39 (7): 1155. https://doi.org/10.1038/APS.2018.37.
21. *Deroo E, Zhou T, Liu B*. The Role of RIPK1 and RIPK3 in Cardiovascular Disease. *Int J Mol Sci*. 2020; 21 (21): 8174. https://doi.org/10.3390/IJMS21218174.
22. *Dhuriya YK, Sharma D*. Necroptosis: a regulated inflammatory mode of cell death. *Journal of Neuroinflammation*. 2018; 15 (1): 1–9. https://doi.org/10.1186/S12974-018-1235-0.
23. *Wang X, Zhao J, Zhang Y et al*. Kinetics of plasma von Willebrand factor in acute myocardial infarction patients: a meta-analysis. *Oncotarget*. 2017; 8 (52): 90371–90379. https://doi.org/10.18632/ONCOTARGET.20091.

The article was submitted to the journal on 8.02.2025

DOI: 10.15825/1995-1191-2025-3-225-231

PROTOCOL FOR ASSESSING THE EFFECTIVENESS OF LUNG PRESERVATION SOLUTIONS IN DONATION AFTER CIRCULATORY DEATH DONORS

N.S. Bunenkov[1–3], I.A. Zavjalov[6], A.L. Akopov[2], A.A. Karpov[1, 7], S.M. Minasyan[1, 2], A.A. Kutenkov[2], S.V. Popov[3–5], R.G. Gusejnov[3, 4], V.I. Pan[1], D.Yu. Ivkin[8], M.M. Galagudza[1, 2]

[1] Almazov National Medical Research Centre, St. Petersburg, Russian Federation
[2] Pavlov University, St. Petersburg, Russian Federation
[3] St. Luke's Clinical Hospital, St. Petersburg, Russian Federation
[4] St. Petersburg Medical and Social Institute, St. Petersburg, Russian Federation
[5] Kirov Military Medical Academy, St. Petersburg, Russian Federation
[6] St. Petersburg State University, St. Petersburg, Russian Federation
[7] St. Petersburg Electrotechnical University (LETI), St. Petersburg, Russian Federation
[8] St. Petersburg State Chemical and Pharmaceutical University, St. Petersburg, Russian Federation

Objective: to evaluate the effectiveness of lung preservation in donation after circulatory death (DCD) using a non-perfusion-based preservation method. **Materials and methods.** The study was conducted on eight healthy male Landrace pigs (weight range: 40–60 kg), divided into three groups based on the preservation solution used: Celsior group (n = 3), lungs preserved using a solution prepared according to the Celsior formulation.; NewSolution group (n = 3), lungs preserved using a custom-formulated solution developed in-house; NaCl group (n = 2), lungs preserved using saline (control group). **Results.** In the study groups (Celsior and NewSolution), the oxygenation index after reperfusion exceeded 350, while the control group (NaCl) exhibited an oxygenation index of less than 350. **Conclusions.** The method described for evaluating the effectiveness of new lung preservation solutions is technically simple and cost-effective, as it enables rapid experimentation with a sufficiently large number of observations. While this approach may not address all challenges in experimental transplantology, it provides a practical and efficient tool for preliminary screening of lung preservation strategies.

Keywords: lung transplantation model, non-perfusion method, lung preservation.

INTRODUCTION

Most end-stage chronic lung diseases are accompanied by progressive respiratory failure and systemic hypoxia. Lung diseases are among the leading causes of mortality worldwide [6, 11]. The COVID-19 pandemic, marked by pulmonary damage and high death rates, further underscored the urgent need for effective therapies and spurred global interest in advancing lung disease treatment methods.

In such a situation, lung transplantation (LT) represents a definitive treatment option. However, its widespread use is constrained by several factors, including the complexity and high cost of the procedure, shortage of donors, and the high vulnerability of donor lungs to injury [4]. Due to this vulnerability, only 15–20% of donor lungs are deemed suitable for transplantation – significantly lower than the acceptance rates for donor livers (69%) and kidneys (90%) [6]. Consequently, the mortality rate among patients on the transplant waiting list ranges from 20% to 40% within two years [6].

One promising direction to address this challenge is to develop a novel preservation solution with enhanced protective capabilities. Preclinical evaluation of such solutions requires the use of experimental animal models. While orthotopic LT in large animals (e.g., pigs, dogs, monkeys) offers the most compelling data, these experiments are technically demanding, resource-intensive, and expensive. The need to use a donor-recipient pair further increases logistical and financial burdens. Moreover, the postoperative care of recipient animals significantly adds to the cost.

Given these limitations, an alternative and more practical approach involves the preservation of donor lungs followed by *ex vivo* reperfusion with blood. This model allows for the assessment of graft viability by measuring the oxygenation capacity of blood collected from the pulmonary veins.

OBJECTIVE

To develop a model for preserving lungs from donation after circulatory death (DCD) donors, using *ex vivo*

Corresponding author: Nikolay Bunenkov. Address: 6-8, Lva Tolstogo str., St. Petersburg, 197022, Russian Federation. Phone: (812) 338-62-79. E-mail: bunenkov2006@gmail.com

perfusion of porcine lungs to assess the efficacy of a new preservation solution in preclinical studies.

MATERIALS AND METHODS

The study was conducted on 8 male Landrace pigs (weighing 40–60 kg), divided into three experimental groups based on the preservation solution used: Celsior group (n = 3, lungs preserved using a solution prepared according to the standard Celsior formulation), NewSolution group (n = 3, lungs preserved using a custom-formulated solution developed in-house, and NaCl group (n = 2, lungs preserved using a 0.9% saline as a control. Our in-house solution was prepared with changes in the components and concentrations of a previously presented recipe [9]. The animals were randomly allocated to the respective groups. All pigs were kept under standardized laboratory conditions with free access to complete feed and water ad libitum. The study protocol was reviewed and approved by the institutional local ethics committee.

All procedures were performed under aseptic conditions, with the animals under general anesthesia and mechanical ventilation (MV) using an inspired oxygen fraction (FiO_2) of 21%. Cannulation of the femoral vein was performed, and 2 liters of venous blood were collected into CPDA-containing blood bags for subsequent use. Intravenous heparin was administered at a dose of 300 IU/kg. This was followed by the administration of 10 mL of 2% lidocaine intravenously to induce cardiac arrest. Asystole was confirmed by continuous electrocardiographic (ECG) monitoring.

A median sternotomy was performed, and the pericardium was incised. The pulmonary trunk was cannulated, and the left atrial appendage was opened. Lung perfusion was initiated using a gravity-driven fluid column with a pressure of 180 cm H_2O. A total of 2 liters of cold preservative solution was administered over approximately 15 minutes. Perfusion was stopped upon the appearance of clear effluent from the left atrial appendage. The lungs were then explanted as an intact block.

On a separate sterile table, the lungs were further perfused with an additional 1 liter of the preservative solution for 10 minutes under aseptic conditions. Subsequently, the pulmonary veins were cannulated, and retrograde perfusion of the lung block was performed with 1 liter of the same solution.

Upon completion of lung perfusion, the explanted lungs and the collected blood (stored in CPDA-containing bags) were placed in a refrigerator and maintained at +4 °C for 4 hours. Following this cold ischemic period, both the lungs and the stored blood were removed from refrigeration and allowed to equilibrate at room temperature for 15 minutes to facilitate preliminary warming. Subsequently MV was initiated with an inspired oxygen fraction (FiO_2) of 21%, and *ex vivo* perfusion of the lungs was commenced using the stored autologous blood. Perfusion was carried out through the pulmonary trunk under a hydrostatic pressure of 180 cm H_2O. Once blood flow through the pulmonary veins was established, blood samples were collected to assess acid-base balance, including lactate concentration, as well as the partial pressures of oxygen (pO_2) and carbon dioxide (pCO_2). These parameters were analyzed using an ABL800 blood gas analyzer (Radiometer, Denmark). The oxygenation index (OI) was calculated as the ratio of pO_2 to FiO_2.

Measurements were obtained at three time points: prior to initiation of perfusion (baseline, T0), and at 10 minutes (T10) and 20 minutes (T20) after the onset of blood perfusion. An OI exceeding 350 following reperfusion was considered indicative of effective lung preservation.

At the conclusion of the experiment, lung tissue samples were fixed in 10% neutral buffered formalin for histopathological analysis. All quantitative data were statistically analyzed using Statistica 12 (StatSoft) and R statistical software.

RESULTS

At baseline (T0), prior to initiation of lung reperfusion, pO_2 in the venous blood did not exceed 53 mmHg across all groups (Table, Fig., c). Ten minutes after the onset of *ex vivo* reperfusion with blood, a marked increase in pO_2 was observed in the groups preserved with either the Celsior or NewSolution preservation solutions. In both groups, pO_2 levels in the pulmonary venous effluent approached 100 mmHg, while the OI neared 500 (Table, Fig., a).

In the control group preserved with saline solution, the OI consistently remained below 350 throughout the entire reperfusion period.

In contrast, both preservation solution groups demonstrated an increases in the OI, pO_2, and blood lactate concentration (Fig., a, c, d). Concurrently, pCO_2 exhibited a decreasing trend (Fig., b).

DISCUSSION

The shortage of donor organs and the vulnerability of grafts to ischemia-reperfusion injury (IRI) remain major challenges in modern transplantology [12, 14]. According to the Global Observatory on Donation and Transplantation, 102,090 kidney transplants were performed worldwide in 2023, while 361,197 patients remained on the waiting list [13]. Thus, less than one-third of patients in need were able to receive assistance.

A similar situation is observed in Russia, where only 2,555 of 8,378 patients requiring organ transplantation underwent the procedure in the same period [13]. In clinical practice, the ideal donor is a brain-dead donor; however, the number of such donors is extremely limited. In recent years, international transplant programs have begun to explore new approaches, including the use of organs from patients who have undergone euthanasia [13]. According to the literature, 2,966 cases of euthanasia were performed in Belgium in 2022, and

82,963 cases were reported in the Netherlands between 2002 and 2021. The presented data underscore the critical severity of the organ shortage problem. Even with recent efforts to expand the donor pool through inclusion of organs from patients who have undergone euthanasia, the current supply remains insufficient to meet clinical needs. Consequently, research into the utilization of suboptimal donor organs and the development of strategies to improve their functional viability is highly relevant.

One promising approach involves the application of new preservation solutions and *ex vivo* perfusion techniques to restore or enhance the function of donor organs that would otherwise be considered unsuitable for transplantation [1]. Experimental studies in animal models provide a controlled platform for investigating these strategies. By refining preservation methods and improving the functional status of marginal organs during *ex vivo* assessment, it may be possible to expand the criteria for organ acceptance and increase the number of viable transplants [5, 6, 11].

The issues outlined above are particularly critical in the context of LT. Both in Russia and globally, the current limitations in LT emphasize the pivotal role of preclinical and experimental studies in addressing key challenges in transplantology. The use of organs from DCD donors represents could somewhat alleviate the organ shortage problem [8, 10].

This paper presents experimental findings using a DCD donor model, which is essential for exploring techniques to procure and evaluate the suitability of lungs from non–heart-beating donors for transplantation. Developing and validating methods for assessing the effectiveness of lung preservation in such experimental large-animal models can provide valuable insights that are directly translatable to clinical practice.

Several experimental LT models and functional assessment techniques have been described reported.

A well-established approach for studying IRI in the lungs involves *ex vivo* or *in situ* lung isolation with continuous perfusion using a synthetic medium and temperature control via a heat exchanger. This model is widely recognized as an effective compromise between complex large-animal transplantation experiments and small-rodent studies [3, 5–7, 11].

In the present study, mechanical perfusion was not used. Instead, a non-perfusion lung preservation strategy was used, comparing three groups: lungs preserved in a standard commercial solution, lungs preserved in the authors' experimental solution, and a saline-preserved control group. The goal was not to investigate lung reconditioning, but rather to evaluate baseline preservation efficacy.

During subsequent reperfusion with autologous blood, a gradual improvement in functional parameters was observed in the two preservation solution groups. In contrast, the saline-preserved control group exhibited the absence of effective gas exchange.

Interestingly, histopathological analysis of lung tissue after reperfusion revealed no significant differences between the groups. All samples demonstrated a morphology consistent with that of viable lung tissue, which did not correlate with the partial pressures of respiratory gases. These findings suggest that histology alone is not an informative marker of the functional status of preserved lungs.

The findings from this study, conducted using an isolated lung model from DCD donors, are consistent with previously published data indicating that a progressive increase in oxygenation during reperfusion is a key marker of effective lung preservation and viability [2, 6, 11]. In both preservation solution groups, the post-reperfusion OI exceeded 350, indicating effective preservation.

Importantly, the study demonstrated that the experimental preservative solution developed by the authors was comparable in efficacy to the commercially available Celsior solution.

Nevertheless, the study has several limitations. First, the sample size was small, with no more than three ob-

Table

Lung gas exchange parameters after preservation and blood reperfusion following 4 hours of cold storage

Time (min)	Preservation solution	IO	pCO_2	pO_2	Lac
0	Celsior	225,2 [225,2; 225,2]	95,20 [95,2; 95,2]	47,30 [47,3; 47,3]	3,80 [3,8; 3,8]
0	NaCl	250,5 [250,0; 250,0]	94,9 [94,9; 94,9]	52,6 [52,6; 52,6]	4,0 [4,0; 4,0]
0	NewSolution	184,3 [175,2; 221,0]	83,6 [66,3; 83,6]	38,7 [36,8; 46,4]	3,6 [1,4; 5,9]
10	Celsior	504,8 [504,8; 504,8]	18,7 [18,7; 18,70]	106,0 [106,0; 106,0]	6,6 [6,6; 6,6]
10	NaCl	266,67 [249,5; 283,8]	56,4 [32,8; 79,9]	56,0 [52,4; 59,6]	5,1 [1,5; 8,7]
10	NewSolution	466,4 [432,9; 500,0]	36,05 [25,4; 46,7]	97,9 [90,9; 105,0]	5,2 [3,2; 7,2]
20	Celsior	590,5 [590,5; 590,5]	19,4 [19,4; 19,4]	124,0 [124,0; 124,0]	7,1 [7,1; 7,1]
20	NaCl	252,9 [252,9; 252,9]	50,0 [50,0; 50,0]	53,1 [53,1; 53,1]	5,4 [5,4; 5,4]
20	NewSolution	625,2 [384,5; 954,8]	36,6 [21,3; 60,2]	131,3 [80,8; 200,5]	6,2 [2,8; 11,1]

Abbreviations and definitions. NewSolution, a preservation solution developed in-house; Celsior, a preservation solution prepared according to the Celsior formula; NaCl, saline; OI, oxygenation index (measured at 21% oxygen fraction); pO_2, partial pressure of oxygen (at 21% oxygen fraction) in mmHg; pCO_2, partial pressure of carbon dioxide in mmHg; Lac, lactate level in mmol/L.

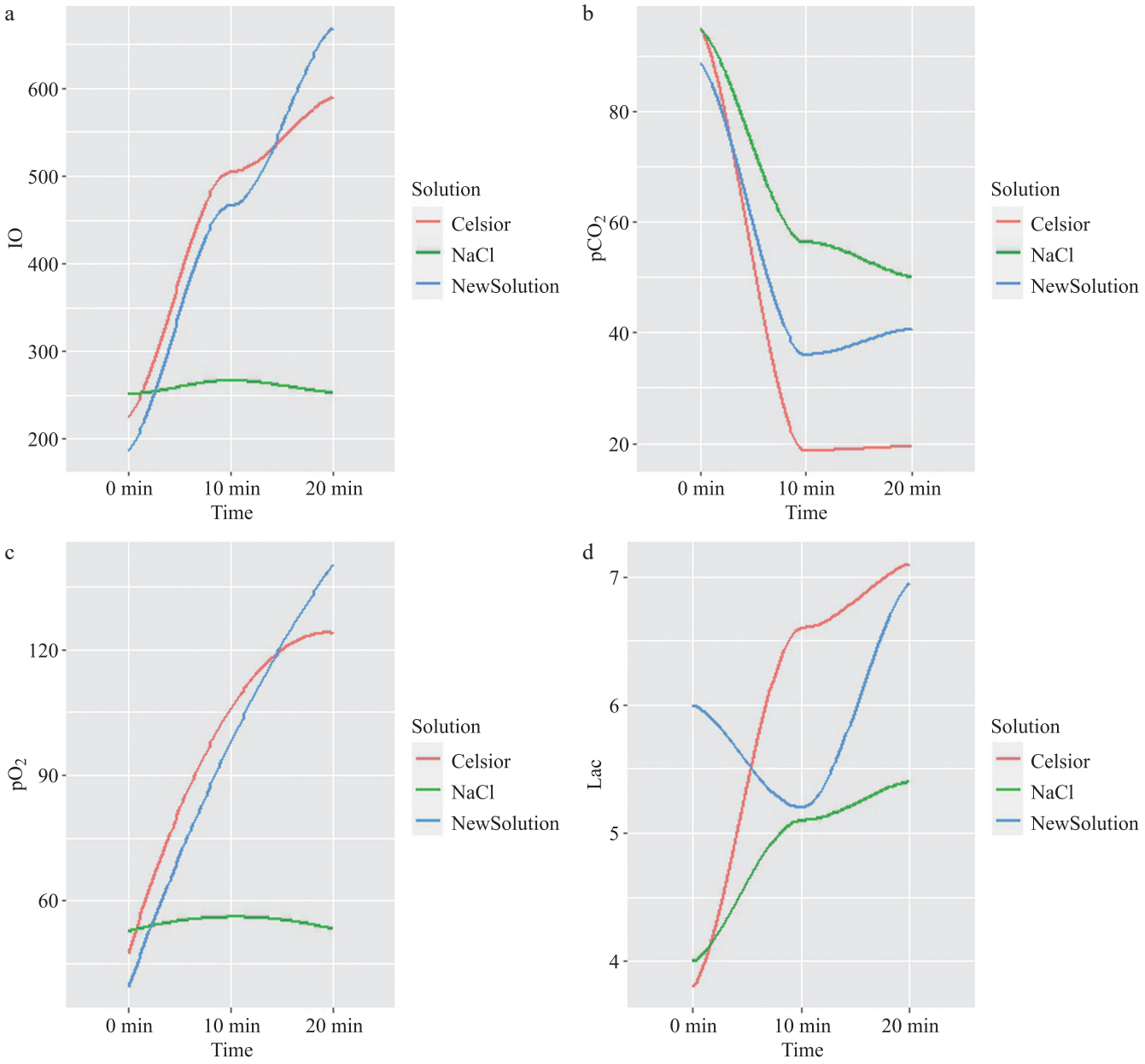

Fig. Lung function indicators after preservation during blood reperfusion after 4–10 hours of cold storage. Abbreviations and definitions: NewSolution, a preservation solution developed in-house; Celsior, a preservation solution prepared according to the Celsior formula; NaCl, saline; OI, oxygenation index (measured at 21% oxygen fraction); pO_2, partial pressure of oxygen (at 21% oxygen fraction) in mmHg; pCO_2, partial pressure of carbon dioxide in mmHg; Lac, lactate level in mmol/L

servations per group. Second, blood reperfusion was limited to 30 minutes. Finally, the preserved lungs were near-ideal donor organs, with minimal warm ischemic exposure, as explantation was performed immediately after circulatory arrest. These factors should be considered when extrapolating the results to clinical scenarios.

The experimental method described for evaluating the effectiveness of new lung preservation solutions is technically straightforward, cost-effective, and suitable for rapid implementation with a relatively large number of observations. While this approach does not fully address all the complexities of experimental transplantology, it can be used for the preliminary assessment of preservation strategies.

FINDINGS

1. The presented method for assessing the effectiveness of lung preservation in a DCD donor model using large animals – by measuring key gas exchange parameters during *ex vivo* blood perfusion – can serve as a first-stage approach in preclinical evaluation of novel preservation solutions. This model may be considered a practical alternative to orthotopic LT in long-term experimental studies.
2. For functional assessment of lungs in this experimental setting, pO_2 and pCO_2, along with OI, are the most informative indicators of preservation efficacy.

3. The histological picture of non-functioning lung tissue closely resembles that of functioning tissue. Therefore, histological examination alone is of limited diagnostic value in determining lung function following 4 hours of cold storage with isolated perfusion.

This study was conducted as part of the priority state task 720000F.99.1.BN62AB22000, titled "Development of a Universal Method for Multi-Organ Preservation of Donor Organs".

The authors declare no conflict of interest.

REFERENCES

1. *Akeely YY, Al Otaibi MM, Alesa SA, Bokhari NN, Alghamdi TA, Alahmari MS et al.* Organ Donation in the Emergency Department: Awareness and Opportunities. *Cureus*. 2023; 15 (11): e49746.
2. *Bribriesco AC*. Experimental models of lung transplantation. *Frontiers in Bioscience*. 2013; E5 (1): 266–272.
3. *Esipova OY, Bogdanov VK, Esipov AS, Kuleshov AP, Buchnev AS, Volkova EA.* Development of a new low-volume oxygenator and creation of a hydrodynamic test bench for *ex vivo* lung perfusion in small animals. *Russian Journal of Transplantology and Artificial Organs*. 2023; 25 (3): 106–112. https://doi.org/10.15825/1995-1191-2023-3-106-112.
4. *Gautier SV, Khomyakov SM.* Organ donation and transplantation in the Russian Federation in 2022. 15th Report from the Registry of the Russian Transplant Society. *Russian Journal of Transplantology and Artificial Organs.* 2023; 25 (3): 8–30. https://doi.org/10.15825/1995-1191-2023-3-8-30.
5. *Gautier SV, Tsirulnikova OM, Pashkov IV, Grudinin NV, Oleshkevich DO, Bondarenko DM.* Evaluation of the efficacy of a novel perfusion solution for normothermic *ex vivo* lung perfusion compared with Steen solution™ (animal experimental study). *Russian Journal of Transplantology and Artificial Organs.* 2021; 23 (3): 82–89. https://doi.org/10.15825/1995-1191-2021-3-82-89.
6. *Gautier SV, Tsirulnikova OM, Pashkov IV, Oleshkevich DO, Filatov IA, Bogdanov VK.* Normothermic *ex vivo* perfusion of isolated lungs in an experiment using a russian-made perfusion system. *Russian Journal of Transplantology and Artificial Organs*. 2022; 24 (2): 94–101. https://doi.org/10.15825/1995-1191-2022-2-94-101.
7. *Lama VN, Belperio JA, Christie JD, El-Chemaly S, Fishbein MC, Gelman AE.* Models of Lung Transplant Research: a consensus statement from the National Heart, Lung, and Blood Institute workshop. *JCI Insight*. 2017; 4 (2): 9.
8. *Louca JO, Manara A, Messer S, Ochsner M, McGiffin D, Austin I.* Getting out of the box: the future of the UK donation after circulatory determination of death heart programme. *EClinicalMedicine*. 2023; 66: 102320.
9. *Minasian SM, Galagudza MM, Dmitriev YV, Karpov AA, Vlasov TD.* Preservation of the donor heart: from basic science to clinical studies. *Interact Cardiovasc Thorac Surg*. 2015; 20 (4): 510–519.
10. *Morrison LJ, Sandroni C, Grunau B, Parr M, Macneil F, Perkins GD.* Organ Donation After Out-of-Hospital Cardiac Arrest: A Scientific Statement From the International Liaison Committee on Resuscitation. *Circulation*. 2023; 48 (10): e120–e146.
11. *Gautier SV, Pashkov IV, Bogdanov V K, Oleshkevich DO, Bondarenko DM, Mozheiko NP*. Normothermic *ex vivo* lung perfusion using a developed solution followed by orthotopic left lung transplantation (experimental study). *Russian Journal of Transplantology and Artificial Organs*. 2023; 25 (2): 158–166. https://doi.org/10.15825/1995-1191-2023-2-158-166.
12. *Qu Z, Oedingen C, Bartling T, Schrem H, Krauth C.* Factors influencing deceased organ donation rates in OECD countries: a panel data analysis. *BMJ Open*. 2024; 21 (14, 2): e077765.
13. *Reznik ON.* Organ donation after euthanasia. Review and criticism of foreign practice. *Russian Journal of Transplantology and Artificial Organs*. 2024; 26 (1): 149–159. https://doi.org/10.15825/1995-1191-2024-1-149-159.
14. *Semenova Y, Shaisultanova S, Beyembetova A, Asanova A, Sailybayeva A, Novikova S et al.* Examining a 12-year experience within Kazakhstan's national heart transplantation program. *Sci Rep.* 2024; 4 (14, 1): 10291.

The article was submitted to the journal on 22.09.2024

DOI: 10.15825/1995-1191-2025-3-232-237

C-REACTIVE PROTEIN AS AN INDICATOR OF INFLAMMATION AND INFECTION IN BRAIN-DEAD ORGAN DONORS

A.L. Lipnitski[1, 2], *A.V. Marochkov*[1, 2]

[1] Mogilev Regional Clinical Hospital, Mogilev, Belarus
[2] Vitebsk State Medical University, Vitebsk, Belarus

Elevated C-reactive protein (CRP) levels in brain-dead donors (BDDs) may indicate an underlying infectious process or may be related to the pathogenesis of the primary disease and brain death (BD) itself. The **objective** of this study was to assess the prognostic value of CRP levels in detecting infectious complications in BDDs prior to organ and/or tissue procurement. **Materials and methods.** This prospective pilot study included 345 BDDs. Median donor age was 54 years (IQR: 47–62); 218 (63.2%) were men and 127 (36.8%) women. The primary diagnoses leading to BD were: non-traumatic intracranial hemorrhage (n = 220; 63.8%), ischemic brain injury (n = 68; 19.7%), and traumatic brain injury (n = 57; 16.5%). **Results.** CRP levels measured after the first medical examination by the BD consultation were already significantly elevated above reference values, with a median of 176.2 mg/L (IQR: 100.5–276.4) after 18–24 hours. Following the second examination and confirmation of brain death, CRP levels increased further to a median of 271.1 (IQR: 174.1–365.0) mg/L ($\chi^2 = 35.79$, $p < 0.00001$). The most frequently diagnosed infection during donor conditioning was pneumonia, observed in 79 donors (22.9%). Receiver operating characteristic (ROC) analysis was conducted to evaluate the predictive value of CRP levels for pneumonia in potential donors: at stage 1, AUC = 0.633 (SE = 0.04; 95% CI: 0.57–0.69; p = 0.001), with a cutoff point of 295 mg/L (sensitivity 36.9%, specificity 86.3%). At stage 3, AUC = 0.630 (SE = 0.05; 95% CI: 0.55–0.71; p = 0.01), with a cutoff value of 348.6 mg/L (sensitivity 47.7%, specificity 79%). **Conclusion.** Analysis of CRP levels provides a useful tool for detecting pulmonary infections in potential BDDs.

Keywords: C-reactive protein, CRP, brain death, infection, organ donor, transplantation.

INTRODUCTION

Infectious complications in brain-dead organ donors (BDDs) remain a critical concern in transplantation medicine [1, 2]. Studies indicate that approximately 15% of organ transplant recipients develop infections transmitted from BDDs [3]. Such donor-derived infections can significantly compromise transplant outcomes, leading to reduced survival rates for both recipients and grafts [4, 5].

The most reliable approach to detecting infection in BDDs involves bacteriological analyses of suspected infection sites [6, 7]. However, these investigations are not routinely performed in donors who are not suspected of having infectious complications. Unfortunately, the results of such analyses often become available only after the organs have been transplanted to recipients.

A range of laboratory biomarkers, such as acute phase proteins, procalcitonin, and presepsin, are used to facilitate early detection of infection in BDDs [8]. Among these, C-reactive protein (CRP) is the most widely used in clinical practice [9]. CRP is a highly sensitive marker of acute-phase inflammation, capable of rapidly reflecting changes in the severity of inflammatory processes; however, its specificity remains low. Notably, elevated CRP levels in BDDs may result not only from infectious processes but also from destruction of brain cells [9].

At present, few studies have investigated the dynamics of CRP levels in potential BDDs and their relationship to active infection during intensive care management in anesthesiology and intensive care units (ICU) settings [10].

In this regard, the present study aimed to evaluate the prognostic value of CRP levels in detecting infectious complications in BDDs prior to organ and/or tissue procurement.

MATERIALS AND METHODS

This prospective study included 345 potential brain-dead organ and/or tissue donors who underwent intensive care and subsequent conditioning of functional systems in anesthesiology and ICU units between 2020 and 2023. The study protocol was reviewed and approved by the Regional Ethics Committee (Approval No. 1/2020).

The age of donors was 54 (47; 62) years (median and 25%–75% quartiles). Median body weight was 80 kg (IQR: 70–90), median height was 173 cm (IQR: 168–180), and median body mass index (BMI) was 26.3 kg/m^2 (IQR: 24.5–29.3). The study cohort comprised 218 male (63.2%) and 127 female donors (36.8%).

Corresponding author: Artur Lipnitski. Address: 12, Belynitskogo-Biruli str., Mogilev, 212016, Republic of Belarus. Phone: +375 (222) 62-75-95. E-mail: Lipnitski.al@gmail.com

Potential donors were eligible for inclusion if they met the following criteria:

1. Severe brain injury characterized by a Glasgow Coma Scale score of 3 and a Full Outline of UnResponsiveness (FOUR) scale score of 0, resulting from: nontraumatic intracranial hemorrhage (NICH), ischemic brain injury, including brain infarction (BI) or hypoxic brain injury, and traumatic brain injury (TBI)
2. Completion of a medical consultation confirming brain death.

The exclusion criteria were:

1. Presence of contraindications to organ and/or tissue procurement, including confirmed viral infectious diseases (hepatitis B, hepatitis C, or HIV), malignant neoplasms, or sepsis with evidence of multiple organ failure or dysfunction;
2. Existence of a written statement by the patient or their legal representative declining post-mortem organ donation.

Brain death was diagnosed by a medical council at the healthcare institution where the potential donor was hospitalized. The determination was made in accordance with generally recognized criteria and the applicable regulatory and legal provisions of the Republic of Belarus.

The main causes of brain death in the study cohort were: NICH (n = 220, 63.8%), ischemic BI (n = 53; 15.4%), hypoxic encephalopathy (n = 15, 4.3%), and TBI (n = 57, 16.5%).

The median time from hospital admission to the first medical consultation for confirmation of brain death (BD) was 60 hours (interquartile range: 34–118.3 hours). In 139 potential donors (40.3%), surgical procedures were performed to procure donor organs and/or tissues for transplantation. The median time from hospital admission to initiation of organ and/or tissue procurement surgery was 111 hours (interquartile range: 76.1–161 hours) (Fig. 1).

During intensive care and conditioning of functional systems, the condition of each potential donor was assessed using both laboratory and instrumental diagnostic methods. All donors underwent chest X-rays (at admission, upon BD confirmation, and upon suspicion of pulmonary pathology), abdominal and renal ultrasound, and echocardiography. All standard laboratory evaluations were performed daily, including complete blood count, urinalysis, biochemical profile test, coagulation tests, and electrolyte and arterial blood acid-base composition analysis. Additionally, CRP levels were measured daily using the immunoturbidimetric method, with reference serum values of 0–5 mg/L.

Laboratory and instrumental data were analyzed at three stages: stage 1 (after initial examination by the consultation committee to confirm BD), stage 2 (18–24 hours after the first examination), and stage 3 (after the second examination and the official confirmation of BD).

Statistical analysis was performed using Statistica 12.0 (StatSoft Inc., USA). Normality of data distribution was assessed using the Shapiro–Wilk test. For normally distributed data, results were expressed as mean ± standard deviation (M ± SD). For non-normally distributed data, results were presented as median with lower and upper quartiles (Me [LQ; UQ]).

Comparisons between independent groups were conducted using the Mann–Whitney U test, while comparisons between dependent groups employed the Wilcoxon matched pairs test or, for three or more groups, Friedman's test in conjunction with Kendall's coefficient of concordance. Where multiple comparisons were performed, p-values were adjusted using the Bonferroni correction.

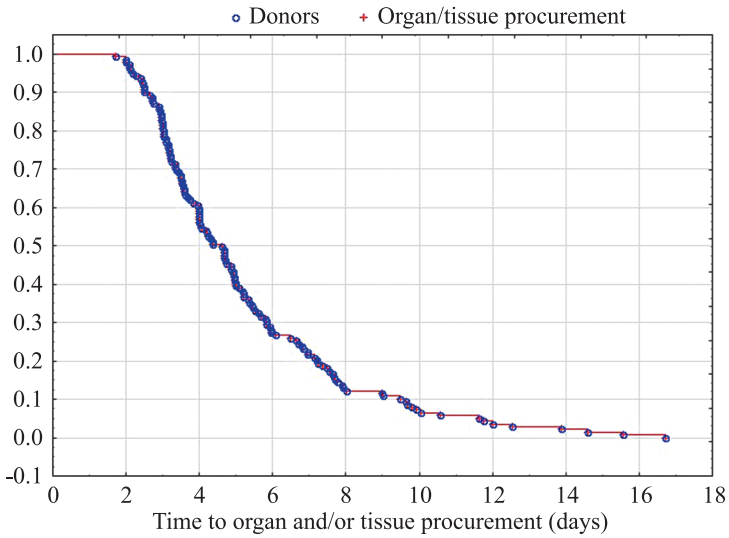

Fig. 1. Kaplan–Meier curve illustrating the time from donor arrival to the initiation of organ and/or tissue procurement in deceased donors

Correlation analysis was carried out using Spearman's rank correlation coefficient (R). Statistical significance was set at $p < 0.05$.

RESULTS

CRP values at all study stages are presented in Table 1. At stage 1, median CRP level was 176.2 (100.5–276.4) mg/L; at stage 2, it increased to 232.9 (137.2–329.0) mg/L; and at stage 3, it reached 271.1 (174.1–365.0) mg/L. This increase across stages was statistically significant ($\chi^2 = 35.79$, $p < 0.00001$; Friedman ANOVA with Kendall's coefficient of concordance). Pairwise comparisons revealed significant differences between all stages: stage 1 *vs* stage 2 ($p = 0.00001$), stage 2 *vs* stage 3 ($p = 0.0009$), and stage 1 *vs* stage 3 ($p = 0.00001$) (Wilcoxon matched pairs test).

When CRP levels were compared between brain-dead donors without organ or tissue procurement and those who underwent explantation, the following results were obtained: stage 1 – 173.2 (105.2–276.4) mg/L *vs* 184.2 (95.4–275.9) mg/L; stage 2 – 233.2 (169.5–324.4) mg/L *vs* 224.3 (132.5–330.0) mg/L; stage 3 – 303.4 (229.2–370.2) mg/L *vs* 267.8 (164.4–362.1) mg/L. These differences were not statistically significant at any stage ($p > 0.1$; Mann–Whitney U test).

We also analyzed laboratory markers of the inflammatory response, including procalcitonin levels, at each stage of the study (Table 1).

Correlation analysis between CRP levels and other laboratory markers of inflammatory response, including procalcitonin, showed the strongest positive correlation with erythrocyte sedimentation rate (ESR) at all stages of the study ($R = 0.38$, $p = 0.0004$; $R = 0.46$, $p < 0.00001$; and $R = 0.27$, $p = 0.01$ at stages 1, 2, and 3, respectively). A weak but statistically significant positive correlation was also observed between CRP and procalcitonin levels ($R = 0.30$, $p = 0.01$; $R = 0.38$, $p = 0.003$ at stages 1 and 2, respectively). No significant correlation was found between CRP levels and leukocyte differential parameters.

Pneumonia was the most common infectious complication among potential donors during conditioning, occurring in 79 cases (22.9%). Importantly, the presence of an infectious process does not preclude organ and tissue procurement, provided there is evidence of clinical improvement under antibacterial therapy and no signs suggestive of sepsis.

A comparison of leukocyte differential indicators and acute-phase protein levels between potential donors with and without pneumonia revealed no statistically significant differences, except for CRP values (Table 2). CRP levels were significantly higher in donors with pneumonia compared to those without, and this difference was observed at all stages of the study.

Receiver operating characteristic (ROC) analysis was conducted to evaluate the predictive value of CRP levels at stages 1 and 3 for the presence of pneumonia in potential donors (Fig. 2). At stage 1, the area under the curve (AUC) was 0.633 (SE = 0.04, 95% CI: 0.57–0.69, $p = 0.001$). The cutoff value for CRP at this stage was 295 mg/L, yielding a sensitivity of 36.9% and a specificity of 86.3% for predicting pneumonia after the first consultation to confirm BD.

At stage 3, after brain death was confirmed, the AUC was 0.63 (SE = 0.05, 95% CI: 0.55–0.71, $p = 0.01$). The CRP cutoff value at this stage was 348.6 mg/L, corresponding to a sensitivity of 47.7% and a specificity of 79%.

DISCUSSION

In this study, we evaluated CRP levels along with several other inflammatory response markers in BDDs across three stages of observation. A statistically significant increase in both CRP and ESR levels was observed at all stages, reflecting the extent of the non-infectious inflammatory response associated with cellular and tissue injury following severe brain injury and subsequent brain death. However, CRP levels did not influence the likelihood of organ or tissue procurement from potential donors.

Table 1

Leukocyte differential, ESR, and procalcitonin indicators at different stages of the study*

	Leukocytes ($\times 10^9$/L)	Neutrophils ($\times 10^9$/L)	Lymphocytes ($\times 10^9$/L)	Band neutrophils (%)	ESR (mm/h)	CRP (mg/mL)	Procalcitonin (ng/mL)
Stage 1	12.9 (9.8; 18)	10.5 (9.2; 14.8)	1.8 (1.2; 2.4)	8 (5; 14)	22 (12; 35)	176.2 (100.5; 276.4)	2.1 (0.6; 7.9)
Stage 2	15.1 (11; 18.6)	11.3 (8.1; 15.3)	1.5 (0.9; 2.2)	11 (6; 18.5)	30 (16; 45)	232.9 (137.2; 329)	2 (0.6; 5.1)
Stage 3	13.9 (10.1; 18.2)	10.5 (7.6; 14.6)	1.5 (1.1; 2.1)	13 (6; 21)	27 (16; 46)	271.1 (174.1; 365)	2.1 (0.7; 5.8)
ANOVA χ^2; p*	3.12; 0.21	3.15; 0.21	0.31; 0.86	3.06; 0.22	44.09; <0.00001	35.79; <0.00001	0.14; 0.93

* – comparison of indicators (Friedman ANOVA and Kendall Coeff). ESR, erythrocyte sedimentation rate; CRP, C-reactive protein.

Only a limited number of studies have investigated inflammatory response markers and acute-phase protein levels in patients with irreversible brain injury and in potential organ donors [10–12]. Consistent with our findings, these studies report a marked rise in CRP levels during the first 3–4 days after severe brain injury, with further elevation upon confirmation of BD [12]. The rapid surge in CRP may be attributed to its expression not only in hepatocytes but also in neurons and glial cells following brain injury [13].

In this study, we focused only on laboratory indicators of systemic inflammatory response syndrome , as clinical parameters such as heart rate and respiratory rate cannot be reliably interpreted in BD patients. Changes in leukocyte profile and procalcitonin levels across all study stages were not statistically significant. Notably, the study excluded BDDs with laboratory evidence of sepsis.

Given that CRP levels in BDDs are often dozens of times higher than reference values and continue to rise during conditioning, its diagnostic utility for identifying infectious complications remains uncertain. However, in our cohort, donors with pulmonary infections consistently demonstrated significantly higher CRP levels at all study stages. In contrast, procalcitonin and leukocyte profile changes did not reach statistical significance. Although the prognostic CRP thresholds determined by ROC analysis exhibited fairly low sensitivity, they may still serve as a useful tool for detecting localized infections in donors and for identifying cases warranting mandatory bacteriological testing.

Limitations of the study. It is important to acknowledge that CRP elevation in BDDs is influenced by several factors not examined in this study. These include duration of donor conditioning, interval since BD was confirmed, primary cause of brain injury (e.g., TBI), and any surgical interventions performed prior to organ procurement.

Therefore, CRP levels in potential organ and/or tissue donors may serve as a quantitative marker not only of systemic inflammatory response and organ injury fol-

Table 2

Leukocyte differential, ESR, and procalcitonin indicators in patients with and without pneumonia at different stages of the study*

		Leukocytes ($\times10^9$/L)	Neutrophils ($\times10^9$/L)	Lymphocytes ($\times10^9$/L)	Band neutrophils (%)	ESR (mm/h)	CRP (mg/mL)	Procalcitonin (ng/mL)
Without pneumonia, n = 266 (77.1%)	Stage 1	12.5 (9.7; 17.8)	11.1 (9.9; 14.8)	1.8 (1.3; 2.5)	8 (5; 12)	21 (11; 35)	164.7 (90.1; 255.5)	2.1 (0.7; 7.6)
	Stage 2	15.2 (11.4; 18.3)	12 (8.6; 15.3)	1.5 (1; 2)	10 (6; 18)	27.5 (15.5; 43)	215.5 (129.8; 294.1)	2.1 (0.5; 4.1)
	Stage 3	14 (10.5; 16.9)	10.8 (7.9; 13.8)	1.4 (1.1; 1.8)	11 (6; 19)	25 (16; 45)	244.2 (155.5; 335.6)	2.2 (0.7; 6.8)
With pneumonia, n = 79 (22.9%)	Stage 1	13.8 (10.8; 18.5)	9.7 (7.6; 16.3)	1.4 (0.9; 2.3)	11 (6; 19)	27.5 (15; 40)	235.5 (141; 350)	1 (0.2; 20)
	Stage 2	13.6 (10.4; 19.1)	9.9 (7.1; 16.1)	1.2 (0.9; 3.5)	14 (9; 21)	35 (16; 50)	297.4 (165.4; 386.4)	1.8 (0.9; 14.7)
	Stage 3	11.3 (9.8; 19.4)	9.8 (6.9; 14.7)	1.8 (0.8; 3)	16 (8; 22)	39 (17; 50)	314 (238.7; 393.2)	1.8 (1; 3.2)

* Comparison of CRP levels between two groups using the Mann–Whitney U test: Stage 1 – p = 0.0002; Stage 2 – p = 0.009; Stage 3 – p = 0.01. ESR, erythrocyte sedimentation rate; CRP, C-reactive protein.

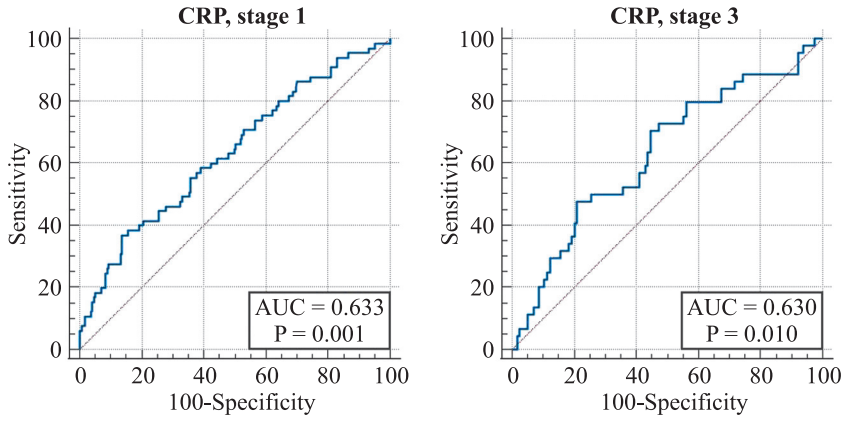

Fig. 2. ROC curves for CRP levels in relation to the presence of pneumonia in potential donors at different stages of the study

lowing severe brain damage and death, but also a criterion for the addition of an infectious process. Regular CRP monitoring during the conditioning period could aid in the early detection and management of infectious complications, improving transplant outcomes.

CONCLUSION

1. CRP levels in potential donors increases during brain death and conditioning of functional systems: stage 1 – 176.2 (100.5; 276.4) mg/L, stage 2 – 232.9 (137.2; 329) mg/L, and stage 3 – 271.1 (174.1; 365) mg/L ($\chi^2 = 35.79$, $p < 0.00001$).
2. Analysis of CRP levels allows the detection of an infectious process in the lungs of potential BDDs. Threshold values were >295 mg/L after the first consultation and >348.6 mg/L following BD confirmation, serving as potential cut-off points for infection screening.

The authors declare no conflict of interest.

REFERENCES

1. *Gautier SV.* Transplantology and artificial organs. M.: BKL Publishers, 2018; 320.
2. *Minina MG.* Infections in the pool of potential organ donors: is it always contraindication to donation? *Russian journal of transplantology and artificial organs*. 2011; 13 (1): 108–114. [In Russ]. doi: 10.15825/1995-1191-2011-1-108-114.
3. *Salimov UR, Shcherba AE, Rummo OO.* Bacterial complications after liver transplantation. Promising directions for further research. *The Russian Journal of Transplantation.* 2023; 15 (2): 238–250. [In Russ]. doi: 10.23873/2074-0506-2023-15-2-238-250.
4. *Kaul DR, Vece G, Blumberg E, La Hoz RM, Ison MG, Green M et al.* Ten years of donor-derived disease: A report of the disease transmission advisory committee. *Am J Transplant*. 2021 Feb; 21 (2): 689–702. doi: 10.1111/ajt.16178.
5. *Zhuravel SV, Kuznetsova NK, Chernenkaya TV, Utkina II.* Transmission of infectious agents from the donor to the recipient. Do we need change in the risk assessment? *The Russian Journal of Transplantation*. 2015; (1): 7–12.
6. *Shcherba AE, Kuzmenkova LL, Efimov DJ, Nosik AV, Prilutsky PS, Korotkov SV et al.* Risk factors and prediction of bacterial complications in liver transplantation. *Annaly khirurgicheskoy gepatologii.* 2023; 28 (3): 10–20. [In Russ]. doi: 10.16931/1995-5464.2023-3-10-20.
7. *Kirkovsky LV, Romanchuk KM, Shcherba AE, Rummo OO, Korytko AA, Spiridonov SV.* Causes of bacterial infection in liver and kidney donors. *Military Medicine.* 2016; (2): 44–48. [In Russ].
8. *Venkateswaran RV, Dronavalli V, Lambert PA, Steeds RP, Wilson IC, Thompson RD et al*. The proinflammatory environment in potential heart and lung donors: prevalence and impact of donor management and hormonal therapy. *Transplantation*. 2009; 88 (4): 582–588. doi: 10.1097/TP.0b013e3181b11e5d.
9. *Velkov VV.* Comprehensive laboratory system for diagnosing diseases and sepsis: C-reactive protein, procalcitonin, presepsin. M.: Diakon, 2015; 117. [In Russ].
10. *Lipnitski AL, Marochkov AV.* The analysis of the C-reactive protein dynamics in donors with brain death. *Vestnik VGMU.* 2024; 23 (4): 44–50. [In Russ]. doi: 10.22263/2312-4156.2024.4.44.
11. *Markevich DP, Viktorovich NE, Denisenko TV.* Ultrasound predictors of outcome of traumatic brain injury. *Health and Ecology Issues*. 2024; 21 (1): 42–48. [In Russ]. doi: 10.51523/2708-6011.2024-21-1-05.
12. *Lipnitski AL, Marochkov AV.* C-reactive protein as irreversible brain damage predictor. *Journal of the Grodno State Medical University*. 2024; 22 (5): 445–450. [In Russ]. doi: 10.25298/2221-8785-2024-22-5-445-450.
13. *Pathak A, Agrawal A.* Evolution of C-Reactive Protein. *Front Immunol*. 2019; 10: 943. doi: 10.3389/fimmu.2019.00943.

The article was submitted to the journal on 17.01.2025

DOI: 10.15825/1995-1191-2025-3-238-245

SODIUM FUMARATE IN THE PREVENTION OF ISCHEMIA-REPERFUSION INJURY IN RENAL SURGERY: OUTCOMES AND PROSPECTS

S.V. Popov[1, 2], R.G. Huseynov[1, 3], K.V. Sivak[1], A.H. Beshtoev[1], E.A. Malyshev[1], T.A. Lelyavina[1, 4]

[1] St. Luke's Clinical Hospital, St. Petersburg, Russian Federation
[2] Kirov Military Medical Academy, St. Petersburg, Russian Federation
[3] St. Petersburg Medical and Social Institute, St. Petersburg, Russian Federation
[4] Almazov National Medical Research Centre, St. Petersburg, Russian Federation

Objective: to review the current outcomes and future prospects of using sodium fumarate (SF) for the prevention of ischemia–reperfusion injury in renal surgery. **Materials and methods.** The drug used in the study was Konfumin, whose active ingredient is SF. The experimental sample consisted of 78 female Wistar rats. Renal warm ischemia (RWI) and reperfusion injury were modeled, involving either unilateral or bilateral kidney preservation. SF, administered as an infusion solution, was used to evaluate the effectiveness of infusion therapy in this renal injury model. It was administered as an intravenous infusion at doses of 1 mL/kg or 2 mL/kg. The infusion protocol included five administrations: one day prior to warm ischemia, on the day of the procedure, and over the subsequent three days. Clinical observation was then carried out. **Results.** Experimental therapy with SF led to a marked reduction in inflammation in the ischemic kidneys of rats, as evidenced by significant improvements in key markers of nephron function. The treatment also contributed to favorable pathomorphological changes associated with acute ischemia–reperfusion injury (IRI). Data from experimental models involving warm ischemia and reperfusion of a single kidney, as well as models with an intact contralateral kidney, demonstrated that SF, administered intravenously at doses ranging from 1 to 2.5 mL/kg, exerted a nephroprotective effect. This protective effect was reflected in the positive remodeling of ischemic renal infarction and its consequences, involving improvements across vascular, glomerular, tubular, and interstitial components of the renal parenchyma. **Conclusion.** SF, administered intravenously at doses of 1–2.5 mL/kg, demonstrated a clear nephroprotective effect. This was evidenced by favorable pathomorphological changes in ischemic renal infarction and its sequelae.

Keywords: sodium fumarate, intravenous infusion, ischemia-reperfusion, renal surgery, nephrectomy, RWI modeling.

INTRODUCTION

Ischemia and subsequent reperfusion of the organ activate pathological processes, notably the excessive production of reactive oxygen species and development of oxidative stress, leading to structural and functional tissue damage [1, 2]. In experimental nephrology, modeling various kidney pathologies is widely used to evaluate the efficacy of infusion drugs. The primary strategy for preventing post-ischemic kidney injury involves administration of pharmacological agents with anti-ischemic and antihypoxic properties [3]. One such agent is sodium fumarate (SF) [4]. In our study, we used the drug Konfumin, whose active ingredient is SF.

SF was selected for investigation because it is an effective antihypoxant. Exogenous fumarate is chemically identical to endogenous fumarate, making it indistinguishable when assessing intracellular substrate content. Its antihypoxic activity is mediated through participation in reversible oxidation–reduction reactions within the Krebs cycle, which facilitate adenosine triphosphate (ATP) synthesis essential for sustaining cellular function during hypoxia. Under oxygen deficiency, the pool of oxidation substrates, including fumarate ions, becomes depleted. Exogenous administration of Konfumin replenishes this pool, enhancing the reserve capacity of tissue respiratory systems and enabling continued ATP synthesis despite hypoxic conditions. This mechanism underlies the antihypoxic action of Konfumin.

Maintaining oxidative metabolism in tissues during oxygen deficiency prevents the formation and accumulation of under-oxidized metabolic products, thereby reducing acidosis. By promoting metabolic alkalization, Konfumin mitigates or eliminates acidosis through chemical neutralization of acidic metabolites.

The drug's positive effect on oxidative metabolism improves the functional state of vital organs, including

Corresponding author: Tatiana Lelyavina. Address: 6, Dekabristov, Strelna, St. Petersburg, 198515, Russian Federation. Phone: (981) 908-90-18. E-mail: tatianalelyavina@mail.ru

the heart, under hypoxic conditions. It supports myocardial contractility and exerts a cardiotonic effect. Furthermore, Konfumin reduces the concentration of lipid peroxidation products in the blood, demonstrating its antioxidant properties. These characteristics form the rationale for selecting Konfumin as a preventive agent against reperfusion syndrome.

The aim of this study is to evaluate the results and prospects of using SF for the prevention of ischemia-reperfusion injury (IRI) in kidney surgery.

Objective: to evaluate the results and prospects of using SF for the prevention of IRI in renal surgery.

MATERIALS AND METHODS

Study substance

The drug used was Konfumin, whose active ingredient is SF [5].

Sample characteristics

The study was conducted on 78 female Wistar rats. The animals were allocated into groups according to the extent of surgical intervention (right nephrectomy or no nephrectomy), duration of renal warm ischemia (45 minutes or 60 minutes), and administered SF dose (1 mL/kg or 2 mL/kg). At baseline, the rats were 6–8 weeks old and weighed 180–200 g. All animals were obtained from the laboratory animal breeding facility of the Kurchatov Institute – Rappolovo laboratory animal nursery, in Leningrad Oblast.

Study design: the experimental design is shown in Table 1.

Modeling methods

Renal warm ischemia (RWI) modeling and reperfusion injury were performed with either both kidneys or only one kidney preserved. RWI duration was set at either 45 or 60 minutes, depending on the experimental model. To evaluate the efficacy of the infusion drug in the induced kidney pathology, SF (solution for infusion) was administered at doses of 1 mL/kg or 2 mL/kg. Injections were given once daily for a total of 5 administrations – one day prior to warm ischemia, on the day of the procedure, and on the following 3 days.

Table 1

Study Design

Group	Sex	Sample size	Experimental procedure	Drug administration method and dose	Measured parameters
Intact	Female	6	None	None	Body weight, clinical condition, urine volume, density, protein content, creatinine levels, leukocyte and erythrocyte counts; blood urea, serum creatinine, lactate levels
RWI1	Female	6	Right nephrectomy followed by 45 minutes of renal ischemia and reperfusion	None	
RWI2	Female	6	Right nephrectomy followed by 60 minutes of renal ischemia and reperfusion	None	
RWI3	Female	6	Right nephrectomy with intravenous infusion of drug 1, followed by 45 minutes of renal ischemia and reperfusion	IV, 1.0 mL/kg sodium fumarate	
RWI4	Female	6	Right nephrectomy with intravenous infusion of drug 1, followed by 60 minutes of renal ischemia and reperfusion	IV, 1.0 mL/kg sodium fumarate	
RWI5	Female	6	Right nephrectomy with intravenous infusion of drug 2, followed by 45 minutes of renal ischemia and reperfusion	IV, 2.5 mL/kg sodium fumarate	
RWI6	Female	6	Right nephrectomy with intravenous infusion of drug 2, followed by 60 minutes of renal ischemia and reperfusion	IV, 2.5 mL/kg sodium fumarate	
RWI7	Female	6	Intravenous infusion of drug 1, followed by 45 minutes of renal ischemia and reperfusion	IV, 1.0 mL/kg sodium fumarate	
RWI8	Female	6	Intravenous infusion of drug 1, followed by 60 minutes of renal ischemia and reperfusion	IV, 1.0 mL/kg sodium fumarate	
RWI9	Female	6	Intravenous infusion of drug 2, followed by 45 minutes of renal ischemia and reperfusion	IV, 2.5 mL/kg sodium fumarate	
RWI10	Female	6	Intravenous infusion of drug 2, followed by 60 minutes of renal ischemia and reperfusion	IV, 2.5 mL/kg sodium fumarate	
RWI11	Female	6	Renal ischemia for 45 minutes followed by reperfusion	None	
RWI12	Female	6	Renal ischemia for 60 minutes followed by reperfusion	None	

Abbreviations: RWI, renal warm ischemia; IV, intravenous.

In some groups, a unilateral nephrectomy was performed to simulate acute kidney injury in a manner closely resembling clinical manifestations. RWI modeling, followed by reperfusion, was carried out two weeks after nephrectomy. At the end of the experiment, the rats were euthanized by decapitation under light anesthesia with diethyl ether.

Animal observation

General clinical monitoring of experimental animals was performed for 14 days after nephrectomy and for 21 days following RWI. Animal survival was assessed for 21 days after RWI modeling. Complete blood counts, urinalysis, clinical and biochemical parameters in blood and urine, biomarker measurements, and histological examinations were carried out. The degree of tissue damage was evaluated using a semi-quantitative method based on the EGTI scale for acute cortical necrosis of the kidney.

Data analysis was performed using Prism 8.0 (GraphPad Software, Inc.). All experimental procedures were approved by the institutional bioethics committee (protocol BEK No. 28, dated October 7, 2024).

RESULTS

Assessment of physiological and biochemical parameters in rats after nephrectomy and warm ischemia

The nephrectomy model in rats was successfully implemented without complications. On the day following surgery and throughout the subsequent 14-day follow-up period, all animals demonstrated normal coat condition, color of visible mucous membranes, respiratory rate, heart rhythm, response to stimuli, skeletal muscle tone, and fecal consistency. One animal in the RWI5 group died on postoperative day 3.

Following RWI surgery with reperfusion, most rats exhibited normal coat condition, mucous membrane color, respiratory rate, heart rhythm, reaction to stimuli, skeletal muscle tone, and fecal consistency on postoperative day 1. By day 3 after RWI, one animal in each of the RWI2, RWI5, and RWI6 groups died. The main indicators from the general urinalysis performed on day 7 after the procedures are presented in Table 2.

As shown by the data, body weight gain in animals subjected to nephrectomy (NE) followed by 45 minutes of RWI did not differ significantly from that of intact controls, with a slight positive trend observed in all rats. Extending the RWI duration to 60 minutes resulted in a significant decrease in body weight on day 7 after RWI in animals that received the drug at doses of 1 mL/kg or 2.5 mL/kg.

On day 7 after 45 minutes of RWI, a significant decrease in creatinine levels was observed compared with intact rats. In treated animals, the protein–creatinine ratio remained elevated. At the same time point after 60 minutes of RWI, a decrease in creatinine was noted only in rats receiving the 1 mL/kg dose. Other parameters remained within normal limits. Creatinine clearance did not differ between groups at any time during the study.

The results of blood biochemical analysis and measurement of renal injury biomarker levels are presented in Table 3.

On day 7 after 45 minutes of RWI, no significant changes were observed in most of the studied parameters. However, a significant increase in blood urea was noted in rats receiving both doses of the drug, with higher values recorded in the 2.5 mL/kg group. This group also demonstrated reduced lactate levels compared to intact controls, although the changes remained within the physiological range.

Following 60 minutes of RWI, rats in the pathology control group showed a significant increase in blood urea and creatinine levels. Elevated blood urea concentrations were also observed in animals receiving infusion therapy with the drug. Lactate levels did not differ significantly among the experimental groups.

Analysis of kidney injury biomarkers revealed no significant changes in serum or urinary cystatin C (Cys-C) on days 7 and 21 in any of the experimental groups.

On day 3 after RWI of 45 or 60 minutes, blood lipocalin-2 (NGAL) levels in the experimental groups were significantly elevated compared with intact animals, showing a 9–22-fold increase. Urinary NGAL concen-

Table 2

Results of general urine analysis on day 7

	Body weight (g)	Diuresis (mL/day/kg)	Urine protein (mg/dL)	Urine creatinine (mg/dL)	Protein/Creatinine ratio
Intact	217.4 ± 22.42	56.6 ± 33.0	23.6 ± 15.4	160.5 ± 76.8	0.139 ± 0.038
RWI1 / N + RWI 45 min	213.4 ± 7.35	93.7 ± 29.4	19.9 ± 9.2	87.2 ± 44.7	0.243 ± 0.126
RWI3 / N + RWI 45 min / SF, 1 mL/kg	198.4 ± 15.77	71.0 ± 35.5	33.6 ± 19.2	121.2 ± 56.9	0.285 ± 0.170
RWI5 / N + RWI 45 min / SF, 2.5 mL/kg	198.80 ± 16.43	106.9 ± 71.1	13.3 ± 12.4	93.4 ± 62.4	0.123 ± 0.044
RWI2 / N + RWI 60 min	193 ± 9.62	136.1 ± 62.9	24.3 ± 14.7	76.9 ± 64.2	0.446 ± 0.423
RWI4 / N + RWI 60 min / SF, 1 mL/kg	186.2 ± 11.47	139.3 ± 95.1	23.1 ± 14.2	72.6 ± 36.6	0.353 ± 0.192
RWI6 / N + RWI 60 min / SF, 2.5 mL/kg	1.81.6 ± 10.4	60.2 ± 25.9	28.5 ± 20.9	123.4 ± 74.8	0.220 ± 0.044

Abbreviations: RWI, renal warm ischemia; N, nephrectomy; SF, sodium fumarate.

tration after 45 minutes of RWI was also significantly higher than in intact controls; administration of the drug at both tested doses normalized this indicator.

RWI lasting 60 minutes resulted in a 2–3-fold increase in urinary NGAL in experimental animals compared with intact controls. Administration of SF at a dose of 2.5 mL/kg significantly reduced the elevated value compared with the pathology control group, although it remained higher than in intact animals.

On day 7 after 45 minutes of RWI, no significant differences in blood or urinary NGAL were observed between experimental groups. In contrast, at the same time point after 60 minutes of RWI, urinary NGAL concentrations in all experimental groups remained significantly elevated compared with intact controls – by approximately 4–6 times. In this case, therapy did not influence the changes in urinary NGAL levels.

On days 3 and 7 after RWI lasting 45 minutes, no significant changes were observed in blood MCP-1 levels in any of the experimental groups.

When ischemia time was extended to 60 minutes, a significant increase in blood MCP-1 was detected on day 3 in the pathology control group. SF therapy normalized this elevated parameter, with the higher dose of 2.5 mL/kg demonstrating greater efficacy. In treated rats, blood MCP-1 levels differed significantly from those in the pathology control group.

Urinary MCP-1 levels did not differ significantly among experimental groups overall. However, administration of SF at the maximum dose significantly reduced urinary MCP-1 levels in groups RWI5 and RWI6 compared with the pathology control. On day 7 after RWI, blood MCP-1 levels showed no significant differences between groups, while urinary MCP-1 was elevated in the pathology control group.

Assessment of physiological and biochemical indicators in rats after RWI

The main urinalysis parameters on day 7 after the procedures are presented in Table 4.

As can be seen from the data presented, therapy led to complete normalization of body weight by day 7. On day 3 after 45 minutes of RWI, rats in the pathology control group exhibited polyuria, decreased urine density, and reduced protein and creatinine levels. In rats treated with 1 mL/kg of the drug, urinary protein levels and diuresis returned to normal, while creatinine levels remained within the physiological range. In the group receiving 2.5 mL/kg, nearly all measured parameters matched those of healthy controls, except for creatinine, which remained elevated.

On day 7 after 45 minutes of RWI, only diuresis remained elevated in the pathology control group, whereas all urinary parameters in treated animals were within normal limits. Extending the RWI duration to 60 minutes led to increased diuresis and urinary pH, along with decreased creatinine levels. In treated animals, only the leukocyte count was elevated. Creatinine clearance

Table 3

Results of biochemical blood analysis and kidney damage biomarkers on day 7

	Urea (mmol/L)	Creatinine (mmol/L)	Lactate (mmol/L)
Intact	3.9 ± 0.5	65.4 ± 4.7	2.9 ± 0.4
RWI1 / N + RWI 45 min	6.2 ± 1.1	70.5 ± 2.7	2.7 ± 0.2
RWI3 / N + RWI 45 min / SF, 1 mL/kg	6.7 ± 1.2	68.6 ± 3.3	2.7 ± 0.4
RWI5 / N + RWI 45 min / SF, 2.5 mL/kg	9.3 ± 3.2	74.0 ± 13.0	2.1 ± 0.2
RWI2 / N + RWI 60 min	9.2 ± 5.0	92.3 ± 35.2	2.7 ± 0.3
RWI4 / N + RWI 60 min / SF, 1 mL/kg	15.4 ± 14.5	78.1 ± 31.3	2.2 ± 0.3
RWI6 / N + RWI 60 min / SF, 2.5 mL/kg	9.5 ± 4.4	63.2 ± 6.5	2.2 ± 0.2

Abbreviations: RWI, renal warm ischemia; N, nephrectomy; SF, sodium fumarate.

Table 4

Results of general urine analysis on day 7

	Body weight (g)	Diuresis (mL/day/kg)	Urine protein (mg/dL)	Urine creatinine (mg/dL)	Protein/Creatinine ratio
Intact	210.4 ± 18.46	43.6 ± 20.3	22.7 ± 9.4	153.2 ± 64.7	0.149 ± 0.014
RWI11 / 45 min	164.8 ± 16.2	120.7 ± 44.7	14.7 ± 5.9	74.9 ± 24	0.207 ± 0.114
RWI7 / RWI 45 min / SF, 1 mL/kg	186.9 ± 10.93	82 ± 22.5	10.0 ± 6.1	87.5 ± 26.4	0.106 ± 0.038
RWI9 / RWI 45 min / 60 min / SF, 1 mL/kg	184.6 ± 15.96	104.4 ± 67.4	18.1 ± 20.7	101.2 ± 104.0	0.162 ± 0.055
RWI12 / 60 min	161.1 ± 9.91	136.1 ± 62.9	22.7 ± 9.4	73.0 ± 23.3	0.244 ± 0.091
RWI8 / RWI 60 min / SF, 2.5 mL/kg	184.9 ± 16.49	139.3 ± 95.1	18.6 ± 11.1	163.8 ± 114.2	0.211 ± 0.132
RWI10 / RWI 45 min / SF, 2.5 mL/kg	187.2.6 ± 9.99	60.2 ± 25.9	37.2 ± 29.3	148 ± 53.9	0.185 ± 0.049

Abbreviations: RWI, renal warm ischemia; SF, sodium fumarate.

showed no significant differences between groups at any time point.

The results of biochemical blood analysis and kidney injury biomarker measurements are presented in Table 5.

On day 7 after 45 minutes of RWI, all parameters studied remained within normal limits. A slight decrease in lactate levels was observed in all rats after 60 minutes of RWI.

On day 7 following 60 minutes of RWI, a significant increase in Cys-C levels was detected in both blood and urine in all experimental groups, with values 4–5 times higher than those in intact controls. Administration of SF at a dose of 2.5 mL/kg had a positive effect, reducing Cys-C levels to values not significantly different from intact animals. Urinary Cys-C levels did not differ significantly among groups.

On day 3, all experimental groups exhibited a marked increase in blood NGAL concentrations after both 45 and 60 minutes of RWI, with values 50–90 times higher than those of intact controls. Urinary NGAL levels did not differ between groups. By days 7 and 21, NGAL concentrations in both blood and urine showed no significant differences among groups.

Calculation of the NGAL concentration index (CI) on day 3 after RWI revealed a significant decrease in all experimental groups compared with intact controls, except for the RWI11 pathology control group and the group receiving SF at a dose of 2.5 mL/kg. At later stages, no intergroup differences in CI were observed.

On day 7 after 45 minutes of RWI, MCP-1 levels in both blood and urine were elevated in the pathology control group and in animals receiving SF at a dose of 1 mL/kg. In contrast, rats treated with 2.5 mL/kg of the drug demonstrated MCP-1 levels within the normal range. A similar pattern was observed after 60 minutes of RWI, although in this case, therapy with 2.5 mL/kg reduced MCP-1 levels only in blood, while urinary levels remained pathologically high.

Calculation of the MCP-1 CI on day 7 revealed significant differences only in animals receiving 1 mL/kg of the drug. After 45 minutes of RWI, this group showed a modest but significant increase in CI compared with intact controls. Treatment with 2.5 mL/kg was more effective, significantly reducing CI. Extending the duration of RWI to 60 minutes resulted in a significant increase in CI in rats treated with both doses compared to intact controls.

RWI of 45 or 60 minutes did not affect Stat3 levels in blood or urine at any point in the experiment, and no statistically significant differences were observed among groups.

DISCUSSION

As a result of the study on Wistar rats, experimental models of RWI and reperfusion injury of a single kidney were developed. In some animals, right-sided nephrectomy was performed, followed by warm ischemia of the remaining kidney for 45 or 60 minutes. In others, warm ischemia of the kidney was induced for the same durations without prior nephrectomy (NE).

For both NE and RWI models of varying duration (45 and 60 minutes), as well as for RWI-only models (45 and 60 minutes), organ injury biomarkers were assessed, and the therapeutic efficacy of SF (15% injectable solution) at doses of 1 and 2.5 mL/kg was evaluated.

Analysis of the results demonstrates that administration of SF after nephrectomy and warm ischemia exerts a positive effect on the functional state of kidneys in experimental animals. The most pronounced therapeutic benefit was observed with the 2.5 mL/kg dose. This was reflected in lower urine protein levels (13.3 ± 12.4 mg/dL) compared with the non-SF group (19.9 ± 9.2 mg/dL), as well as a more favorable protein/creatinine ratio (0.123 ± 0.044 *vs* 0.243 ± 0.126 in the non-SF group).

Serum urea and creatinine levels in the group receiving SF at a dose of 2.5 mL/kg (9.3 ± 3.2 mmol/L and 74.0 ± 13.0 mmol/L, respectively) indicated a lesser degree of impairment in renal nitrogen excretion compared with groups receiving a lower dose or no SF at all.

Additionally, blood lactate levels in all SF–treated groups remained within normal limits (2.1–2.7 mmol/L), suggesting that adequate energy metabolism was preserved. Thus, in the nephrectomy + warm ischemia model, a dose of 2.5 mL/kg provided the most favorable balance between reducing proteinuria and preserving renal function. This was evidenced by lower urine protein levels (13.3 ± 12.4 mg/dL *vs* 19.9 ± 9.2 mg/dL in untreated animals) and an improved protein/creatinine

Table 5

Results of biochemical blood analysis and kidney damage biomarkers on day 7

	Urea (mmol/L)	Creatinine (mmol/L)	Lactate (mmol/L)
Intact	4.3 ± 0.3	65.5 ± 1.9	3.3 ± 0.5
RWI11 / disease control 45 minutes	4.5 ± 0.9	63.4 ± 2.0	2.5 ± 0.3
RWI7 / RWI 45 min / SF, 1 mL/kg	4.9 ± 0.6	64.8 ± 1.1	2.6 ± 0.2
RWI9 / RWI 45 min / 60 min / SF, 1 mL/kg	5.6 ± 0.9	64.0 ± 3.2	2.5 ± 0.5
RWI12 / disease control 60 minutes	23.6 ± 24.1	65.5 ± 1.9	2.4 ± 0.4
RWI8 / RWI 60 min / SF, 2.5 mL/kg	4.7 ± 0.8	61.1 ± 4.0	2.6 ± 0.3
RWI10 / RWI 45 min / SF, 2.5 mL/kg	7.7 ± 2.3	75.1 ± 12.9	2.2 ± 0.2

ratio (0.123 ± 0.044 *vs* 0.243 ± 0.126). In contrast, in the warm ischemia–only model, the most pronounced therapeutic effect was observed at a dose of 1 mL/kg. This group demonstrated the lowest proteinuria (10.0 ± 6.1 mg/dL) and the most favorable protein/creatinine ratio (0.106 ± 0.038), which closely approximated values in intact animals (0.149 ± 0.014).

Serum urea and creatinine levels in the group receiving SF at a dose of 1 mL/kg (4.9 ± 0.6 mmol/L and 64.8 ± 1.1 mmol/L, respectively) demonstrated the least impairment of renal nitrogen excretion compared with groups receiving other doses or no SF at all. Blood lactate levels in all SF–treated groups remained within the physiological range (2.2–2.6 mmol/L), indicating preserved energy metabolism. Overall, a comprehensive analysis of clinical and biochemical parameters suggests that a dose of 1 mL/kg SF is optimal for correcting renal dysfunction after warm ischemia, offering the most favorable balance between reducing proteinuria and preserving renal function.

CONCLUSION

The effectiveness of SF infusion was assessed in experimental models of RWI and reperfusion injury. The results demonstrated a pronounced therapeutic effect in mitigating renal dysfunction following nephrectomy and warm ischemia in experimental animals.

A dose-dependent response was observed: after nephrectomy and warm ischemia, the optimal dose was 2.5 mL/kg. This was evidenced by a marked reduction in proteinuria (13.3 ± 12.4 mg/dL) and a more favorable protein-to-creatinine ratio (0.123 ± 0.044), along with lower serum urea and creatinine levels (9.3 ± 3.2 mmol/L and 74.0 ± 13.0 mmol/L, respectively) compared with the control group.

After warm ischemia without nephrectomy, the most effective dose was 1 mL/kg, which yielded the lowest proteinuria level (10.0 ± 6.1 mg/dL) and a protein-to-creatinine ratio (0.106 ± 0.038) closest to that of the intact group. Corresponding serum urea and creatinine levels were 4.9 ± 0.6 mmol/L and 64.8 ± 1.1 mmol/L, respectively. A key indicator of therapeutic efficacy was the normalization of blood lactate levels (2.1–2.7 mmol/L), reflecting the preservation of adequate energy metabolism.

Overall, SF shows a significant nephroprotective effect, with the optimal dose varying according to the type of injury: 2.5 mL/kg for combined nephrectomy and ischemia, and 1 mL/kg for isolated warm ischemia. These conclusions are supported by a comprehensive set of biochemical markers of kidney function.

This article was completed as part of a government-funded project with the support of the St. Petersburg Health Care Committee under the program "High-Tech Medical Care not Included in the Compulsory Health Insurance Database", 2024–2025.

The authors declare no conflict of interest.

REFERENCES

1. *Plotnikov EY, Kazachenko AV, Vyssokikh MY, Vasileva AK, Tcvirkun DV, Isaev NK et al*. The role of mitochondria in oxidative and nitrosative stress during ischemia/reperfusion in the rat kidney. *Kidney Int*. 2007; 72 (12): 1493–1502.
2. *Goncharov RG, Rogov KA, Temnov AA, Novoselov VI, Sharapov MG*. Protective role of exogenous recombinant peroxiredoxin 6 under ischemia-reperfusion injury of kidney. *Cell Tissue Res*. 2019; 378 (2): 319–332.
3. *Grond J, van Goor H, Erkelens DW, Elema JD*. Glomerular sclerosis in Wistar rats: analysis of its variable occurrence after unilateral nephrectomy. *Br J Exp Pathol*. 1986 Aug; 67 (4): 473–479.
4. *Akinrinde AS, Oduwole O, Akinrinmade FJ, Bolaji-Alabi FB*. Nephroprotective effect of methanol extract of Moringa oleifera leaves on acute kidney injury induced by ischemia-reperfusion in rats. *Afr Health Sci*. 2020 Sep; 20 (3): 1382–1396.
5. *Khalid U et al*. Kidney ischaemia reperfusion injury in the rat: the EGTI scoring system as a valid and reliable tool for histological assessment. *J Histol Histopathol*. 2016; 3 (1): 1.

The article was submitted to the journal on 21.01.2025

INSTRUCTIONS TO AUTHORS

Articles should contain original information that has not been previously published and is not considered for publication in other editions. Fee for publication of manuscripts will not be charged.

The manuscript should be presented in Microsoft Word format A4, 1.5 spacing, and Times New Roman font size 12. Submit your article to the online submission system in accordance with the instructions on the journal's website https://journal.transpl.ru.

Structure of the article

The Title page should include:

– Initials (first name and patronymic) of the authors of the article should be specified before their respective last names.
– Author names (list the author's initials before listing his or her last name as when registering for ORCID, or Open Researcher and Contributor ID – a non-proprietary alphanumeric code that uniquely identifies scientific authors).
– Full official name of the institution, city and country.
– If authors from different institutions participated in writing of the manuscript, it is necessary to correlate those with the names of the authors by adding a digital index uppercase after last name, and right before the name of the institution.

Information about the authors

For each author fully specify the last and the first name, patronymic and position in the relevant department/institution.

For correspondence

Fully specify the last and the first name, patronymic of the author, who will be holding correspondence, address (including postal code), telephone, fax number, e-mail.

Abstract

Each article must be accompanied by an abstract. The amount of text for the abstract of the original article should be of no more than 300 words, for a literature review, clinical observation – no more than 200 words. The abstract must fully comply with the content of the work. The abstract should not use abbreviations without prior expansion.

Abstract of ***the original article*** should contain the following sections: ***Objective***, ***Materials and methods***, ***Results***, ***Conclusion***. The abstract should present the most important results of the research.

Do not write: "*A comparative analysis of the sensitivity and specificity was conducted …*"

Should write: "*The sensitivity was ... % and ...%, p = , specificity, respectively ...% and ...%, p =* ".

Keywords

At the end of the abstract keywords must be given. To select the keywords a thesaurus of U.S. National Library of Medicine should be used – Medical Subject Headings (MeSH) at https://www.ncbi.nlm.nih.gov/mesh.

Conflict of interest

The author should inform the editor about the factual or potential conflict of interest have included the information about such conflict into the respective section of an article.

If there is no conflict of interest, the author should say so in the form like the following: "Author declares unawareness of the conflict of interest".

This information is supposed to be placed before the article text.

Text of article

Original article should include the following sections:

- Introduction
- Materials and methods
- Results
- Discussion
- Conclusion
- References

Review article should include an analysis of the literature with the presentation of modern sources (mainly in the last 5 years).

Clinical observation should be well illustrated (to reflect the essence of the problem) and include discussion with the use of literature data.

References in the text are indicated by number in square brackets: [1], [2, 5], [14–18] and ***in the references section are presented in order of their appearance in the text.*** All values given in the article should be expressed or duplicated in **SI** units.

References

The author is solely responsible for the accuracy of the data included in the references section of the article. References to unpublished papers or papers in print works are not allowed.

References are presented on a separate page.

The names of journals can be contracted in accordance with an embodiment of reduction adopted by the specific journal.

If the article quoted has DOI (a digital object identifier) or/and PMID (Pub Med identifier) they must be specified after the description of the article. To compile descriptions in References section NLM bibliographic reference citation standard is used – U.S. National Library of Medicine (https://www.nlm.nih.gov/bsd/uniform_requirements.html). If the number of authors does not exceed 6, the bibliographic description includes all the authors. If the number of authors is more, only the first six authors should be indicated and then add et al.

Requirements for tables and figures

Tables should be placed into the text; they should have numbered heading and clearly labeled graphs, convenient and simple to read. Table's data must comply with the numbers in the text, but should not duplicate the information therein. Table references in the text are required.

Illustrations and drawings should be submitted in electronic format (JPEG or TIFF format with a resolution of at least 300 dpi and no smaller than 6 × 9 cm), in a volume of close to 1 MB. Drawings must include all copyright symbols – arrows, numbers, signs, etc. Figure captions should be submitted in a separate file with the extension *.doc. First, the name is given, then all arithmetic and alphabetical symbols (lettering) are explained.

Articles should be addressed
to the Russian Journal of Transplantology and Artificial Organs website:
https://journal.transpl.ru/vtio
E-mail: vestniktranspl@gmail.com

Издание зарегистрировано в Госкомпечати РФ, № 018616 от 23.03.99 г.

Подписано к печати 25.08.25.

Тираж 1000 экз.

ООО «Издательство «Триада».
ИД № 06059 от 16.10.01 г.
170034, г. Тверь, пр. Чайковского, 9, оф. 514,
тел.: +7 (915) 730-10-37, +7 (910) 647-49-85
E-mail: triadatver@yandex.ru
https://www.triada.tver.ru

Заказ 35252